



Provided by the author(s) and University of Galway in accordance with publisher policies. Please cite the published version when available.

Title	Cell wall immunocytochemistry and histology of hemiparasitism in <i>Rhinanthus minor</i> L. and <i>Odontites vernus</i> (Bellardi) Dumort: interactions at haustorial interfaces and implications for grassland biodiversity
Author(s)	Pielach, Anna
Publication Date	2013-11-21
Item record	http://hdl.handle.net/10379/3945

Downloaded 2024-05-14T06:22:52Z

Some rights reserved. For more information, please see the item record link above.



**Cell wall immunocytochemistry and histology
of hemiparasitism in *Rhinanthus minor* L. and *Odontites vernus*
(Bellardi) Dumort: interactions at haustorial interfaces
and implications for grassland biodiversity**

Anna Pielach

Supervisor: Dr Zoë A Popper

Botany and Plant Science
School of Natural Sciences
National University of Ireland, Galway



Submitted in April 2013



I certify that the thesis is all my own work and that I have not obtained a degree in this university or elsewhere on the basis of any of this work.

Summary of the contents

Parasitic plants develop specialised grafting organs called haustoria to attach to and infiltrate host plant organs to access nutrients. The outcome of the parasitic process is largely determined where cell walls of the host and parasite form the initial zone of contact at the haustorial interface. While haustorial cell walls show adaptation to virulence, host walls can be actively modified in response to attack.

A combination of field and analytical microscopy techniques were used to investigate haustoria of *Rhinanthus minor* and *Odontites vernus*, annual native Irish hemiparasites, and grassland community structure associated with parasitism. The two species were confirmed to be associated with species-rich grassland habitats.

In addition to lignified walls of haustorial xylem, required for solute uptake, other specialised wall types included; 1) unlignified flange-like thickenings of parenchyma adjacent to the xylem bridge, 2) thickened, unlignified walls of interfacial parenchyma and 3), primary cell walls of the hyaline body with associated paramural deposits. Arabinogalactan proteins (proteoglycans implicated in plant development) localised to the interfacial parenchyma and hyaline body and co-localised with extensins in partly differentiated xylem protoplasts suggesting roles in haustorial development and functioning.

Metahaustoria, attached to the pot surface rather than host roots, provided new insights into the derivation of phenolic substances typically found at the interfaces between hosts and parasitic plants and generally believed to be synthesised by hosts as a defence response. A phenolic-rich interfacial secretion complex was produced by metahaustoria which analytical methods, including histological staining and Raman spectroscopy, indicated are compositionally similar to the interfacial secretions between hosts and non-hosts. This suggests the interfacial lignin-like substances are not related to resistance but instead are produced by haustoria to facilitate the parasitic process. Parasitic plants might be the only organisms known to produce lignin to aid virulence.

Acknowledgements

I would like to acknowledge a number of people whose help and support were invaluable in the successful completion of this project.

Dr Zoë Popper, for her supervision and giving me the opportunity to work on this fascinating project, which allowed me to remain within the field of ecology and traditional botany while enabling me to explore advanced microscopy techniques

Dr Olivier Leroux, for invaluable advice on histochemistry, immunohistochemistry and microscopy as well as stimulating discussions fuelled with Belgian chocolate

Prof. David Domozych, for his suggestion on resin embedding, kind help and advice on various aspects histochemistry, immunohistochemistry and microscopy, introducing me to electron microscopy and donating secondary antibody-gold conjugates. Furthermore, David and his wife **Cathy**, for hosting me at their home while at Skidmore and **Amanda Andreas** for her assistance in the lab and fun after work.

Dr Gordon Allison, for hosting me in his lab in Aberystwyth and giving me the opportunity to learn Raman spectroscopy during the final stages of my PhD

Prof. Paul Knox from Centre for Plant Sciences, University of Leeds, for donating generous amounts of monoclonal antibodies and a very useful tip on quenching autofluorescence!

Dr Marie-Christine Ralet, INRA, Nantes, France for donating antibodies RU-I and RU-II against rhamnogalacturonan

Dr Katia Ruel from Centre de Recherches sur les Macromolécules Végétales for donating polyclonal antibodies against lignin

Prof. Michael G Hahn from Complex Carbohydrate Research Centre, The University of Georgia, for donating a variety of monoclonal antibodies

Dr Micheline Sheehy-Skeffington, **Dr Dagmar Stengel** and **Dr Maria Tuohy**, for their comments as members of my graduate research committee. I further thank **Dr Micheline Sheehy-Skeffington**, for ecological advice and familiarising me with the hot-spots of plant ecology in the wild Irish West

Centre for Microscopy and Imaging at Anatomy, School of Medicine, NUIG for facilitating my use of the ultramicrotome and the transmission electron microscope, without which a large part of this project would not have been possible. In particular, I would like to thank **Pierce Lalor** for always being positive and extremely helpful; **Mark Canney**; **Prof. Peter Dockery** and **Dr Eadaoin Timmins** are also thanked for their kind help.

Head of Botany and Plant Science, **Prof. Charles Spillane** for kindly allowing me to use his laboratory equipment and facilities

Dr Rory Hodd, for invaluable help with community analysis and for bryophyte forages

Dr Caroline Sullivan, for stats-chats and help with GPS data collection and processing

Alan Cookson at IBERS, University of Aberystwyth, for sharing his knowledge about haustorial ultrastructure

Jenny Beale at Brigit's Garden for providing an ecological survey site at Brigit's Garden

Paul Murphy at EirEco for providing an experimental blank canvas site in the beautiful Carron and cups of tea

Dr Deirdre Lynn at National Parks and Wildlife Service and **Dr Jim Martin at BEC Consultants** for their help in accessing the Irish Semi-natural Grassland Survey Data

Patrick O'Rafferty for technical help, fieldwork assistance and lifts to the college!

Michelle Donlon, Romain Castilleux and Quentin Coster, for help with tedious lab tasks

Chris Eschmann, Jonathan Kelly and Laoise Kelly for fieldwork assistance and trips to the Burren

Dr Joanne Denyer, for showing me that there is bryophyte life after hemiparasites

Dr Piotr Sikorski, Dr Marek Wierzba and Brian Mongan, for their help in organising the BotSoc trip to Poland

Dr David Bourke, Brendan Canning, Helen Carthy, Yvonne Cullivan, David Dempsey, Declan Doherty, Dorota Duszyńska, Chris Eschmann, Jonathan Kelly, Laoise Kelly, Michael Lydon, Caitriona Maher, James Owens and Kristine Tiltina for moral support, chatting, laughing, dancing, hiking, botanising and/or sharing the office with me.

I would particularly like to thank **Dr Simon Egan** for encouraging me to pursue a doctorate and his unfailing friendship and support.

I would also like to acknowledge the **Irish Research Council** for three years of funding under the EMBARK initiative. I acknowledge **NUI, Galway Thomas Crawford Hayes Fund**, for a three-month research award, which enabled me to continue work in 2013, as well as a travel award, which funded my attendance at Gordon Cell Wall Conference at Colby College and a research stay at Skidmore Microscopy Imaging Center in 2012.

Special thanks go to **Veronika Straberger** for collaborating with me on the wonderful Guerilla Science-Art project *Latch On!* (latch-on.blogspot.com) inspired by (and inspiring to) this research. NUI, Galway Research Office, Art Gallery and Community Knowledge Initiative (CKI) are thanked for funding the project.

Finally, I thank my mother and grandparents, for their moral and financial support.

This work is dedicated to the memory of my grandmother, Jadwiga Polak.



Contents:

1. General introduction	1
1.1 Hemiparasitic plants — definition and scientific interest	1
1.1.1 What are parasitic plants?	1
1.1.2 Structure and evolution of haustoria	2
1.1.3 Scientific interest	5
1.2 Cell walls and parasitism: biochemical determinants of ecological processes	7
1.2.1 Cell wall structure	7
1.2.2 Cell wall diversity and its possible consequences for parasitism	9
1.2.3 Cell wall constituents	12
1.2.3.1 Carbohydrates	12
Cellulose	13
Non-cellulosic carbohydrates (pectins and hemicelluloses)	13
Pectins	14
Hemicelluloses	15
Callose	17
1.2.3.2 Proteins and glycoproteins	17
Glycine-rich proteins (GRPs)	18
Glycoproteins and proteoglycans	18
Proline-Rich Proteins (PRPs)	18
Extensins	18
Arabinogalactan proteins (AGPs)	19
Cell wall active enzymes	20
1.2.3.3 Phenolics and lipid components	21
Phenolics	22
Lignin	22
Low molecular weight phenolics	23
Lipids	24
Suberin	24
Cutin, cutan and epicuticular waxes	24
1.2.3.4 Silica	25
1.3 Cell wall research tools, their potential and limitations for researching plant parasitism	25
1.4 Aims and outline of this project	28
2. Grassland communities of <i>Rhinanthus minor</i> and <i>Odontites vernus</i> in two limestone landscapes of the Irish West	29
2.1 Abstract	29
2.2 Introduction	30
2.3 Methods	36
2.3.1 Site selection and characteristics	36

2.3.2 Sampling.....	40
2.3.3 Data analysis	41
2.3.4 Vegetation classification	44
2.4 Results	45
2.4.1 Cluster analysis and indicator species analysis.....	45
2.4.2 NMS results	54
2.4.3 Correlations between secondary matrix variables	58
2.5 Discussion.....	60
3. Methods of processing and imaging haustorial material	65
3.1 Plant material.....	65
3.1.1 Species used	65
3.1.2 Seed germination	66
3.2 Pot cultures	69
3.2.1 Containers	69
3.2.2 Soil mix	69
3.2.3 Watering regime	70
3.2.4 Light and temperature regime	70
3.2.5 Fungicide treatment of plants	70
3.2.6 An overview of the plant material batches used in the project	70
3.3 Sample processing	72
3.3.1 Collection of haustoria	72
3.3.2 Fixation, dehydration and embedding.....	72
3.3.3 Slide preparation, sectioning and section mounting.....	75
3.4 Microscopic observations	77
3.4.1 Light microscopy	78
3.4.1.1 Histochemistry	78
3.4.1.2 Cross-polarised light microscopy	78
3.4.1.3 Epifluorescence microscopy	78
3.4.1.4 Raman spectroscopy	83
3.4.2 Electron microscopy.....	84
3.4.2.1 Scanning electron microscopy	84
3.4.2.2 Immunogold labelling and transmission electron microscopy...	84
4. Cell walls as contributors to virulence and defence in parasitic plant-host association.....	87
4.1 Abstract.....	87
4.2 Introduction	88
4.3 Cell walls are implicated in virulence and resistance — two inseparable elements of parasitism.....	89
4.4 The involvement of cell walls in virulence and defence at haustorial Interfaces	91
4.4.1 Cell wall as a dynamic interface	91
4.4.2 Wall-associated signals and receptors.....	93
4.4.3 Signalling in parasitic plant-host associations	96

4.4.4 Cell-wall localised enzymes in virulence and resistance.....	99
4.4.5 Protective components of the cell wall	103
4.4.6 Cell wall-localised barriers at different stages of parasitic plant intrusion	108
4.5 Closing remarks	110
5. Engineered for theft — an immunocytochemical study of specialized haustorial cell walls of <i>Rhinanthus minor</i> and <i>Odontites vernus</i>	113
5.1 Abstract	113
5.2 Introduction	114
5.3 Results	117
5.3.1 Tissue differentiation and establishment of vascular connections	117
5.3.1.1 Pre-attachment haustorial anatomy.....	117
5.3.1.2 Post-attachment haustorial anatomy	119
5.3.2 Immunolocalisation results.....	134
5.3.2.1 Hemicelluloses	134
5.3.2.2 Pectins	136
5.3.2.3 AGPs	146
5.3.2.4 Extensins	155
5.4 Discussion.....	157
5.4.1 Haustorial cell walls prior to attachment.....	157
5.4.2 Cell walls of endophyte parenchyma (post-attachment)	158
5.4.3 Xylogenesis.....	167
5.4.4 The hyaline body	170
5.4.5 Flange-like parenchyma	173
5.4.6 Haustorial AGPs.....	175
5.5 Conclusions	176
6. An extended menu or a physiological trap? — <i>Rhinanthus minor</i> forms xylem bridge connections with ‘bad hosts’	179
6.1 Abstract	179
6.2 Introduction	180
6.3 Results	182
6.3.1 Haustorial anatomy and immunocytochemistry in different parasite-host pairings.....	182
6.3.2 Histology and immunocytochemistry of host responses	189
6.3.3 Auto-parasitic haustoria.....	197
6.4 Discussion.....	199
6.5 Conclusions	210
7. Lignin as a contributor to virulence rather than defence? — novel-insights from metahaustoria	211
7.1 Abstract	211
7.2 Introduction	211
7.3 Results	214
7.3.1 Morphology and anatomy of metahaustoria	214

7.3.2 The architecture of the PhISC and contact parenchyma cell walls	217
7.4 Discussion.....	231
7.5 Conclusions	237
8. General discussion	239
9. Literature cited.....	249
10. Appendices.....	285

Abbreviation index:

ABA	abscisic acid
AGP	arabinogalactan protein
Avr	avirulence
CBM	carbohydrate binding module
CCRC	Complex Carbohydrate Research Centre
CWDE	cell wall-degrading enzymes
CWI	cell wall integrity
DAMPs	damage-associated molecular patterns
DH ₂ O	distilled water
DP	degree of polymerisation
DMBQ	2,6-dimethoxy-1,4-benzo-quinone
ECM	extracellular matrix
EMA	extrahaustorial matrix
ENOD	early nodulin
ENODL	early nodulin-like protein
ER	endoplasmic reticulum
ETI	effector-triggered immunity
EtOH	ethanol
FITC	fluorescein isothiocyanate (fluorochrome)
FT-IR	Fourier transform infrared spectroscopy
FLA	fasciclin-like arabinogalactan protein
GPI	glycosylphosphatidylinositol
GRP	glycine-rich protein
hpi	hours post inoculation
HAMPs	host-associated molecular patterns
HG	homogalacturonan
HIF	haustorial inducing factor
HRGP	hydroxyproline-rich protein

IDT	isodityrosine
IKI	iodine/potassium iodide reagent for starch
JA	jasmonic acid
JIM	John Innes monoclonal (antibody)
LM	Leeds monoclonal (antibody)
LRW	London Resin White
LTP	lipid transfer protein
mAb	monoclonal antibody
MAMPs	microbe-associated molecular patterns
MLG	mixed linkage glucan
PAMPs	pathogen-associated molecular patterns
PERK	Proline-rich Extensin-like Receptor Kinase
PhISC	phenolic-rich interfacial secretion complex
PME	pectin methylesterase
PRP	proline-rich protein
PRRs	pattern-recognition receptors
RG	rhamnogalacturonan
RLK	receptor-like kinase
RNS	reactive nitrogen species
ROS	reactive oxygen species
RT-PCR	real-time polymerise chain reaction
RP	resistance proteins
SA	salicylic acid
SSH	suppression subtractive hybridisation
SXSg	<i>Sorghum</i> xenognosin for <i>Striga</i> germination
TBO	toluidine blue O
WAK	wall-associated kinase

1 General introduction

1.1 Hemiparasitic plants — definition and scientific interest

1.1.1 What are parasitic plants?

Plants are predominantly photoautotrophic organisms capable of fixing inorganic carbon from carbon dioxide into organic forms, primarily carbohydrates which are a starting point for synthesis of other classes of organic compounds. However, certain plants display heterotrophic behaviour as either 1) mycotrophs or 2) haustorial parasites (Nickerent *et al.* 1998).

Mycoheterotrophs obtain their carbon from mycorrhizal fungi and those that use fungi as intermediators to obtain nutrients from other plants are known as epiparasites (Bidartondo *et al.*, 2002). Plants parasitic on fungi are represented by over 400 species in 87 genera and 10 families (Leake, 2004), and there are two epiparasites in the Irish flora; *Hypopitys monotropa* Crantz (Yellow Bird's nest) (Björkman, 1960; Yang & Pfister, 2006) and *Neottia nidus-avis* (L.) Rich. (Bird's-nest orchid), often mistakenly described in literature as a saprophytic species (Leake 2005).

The concept of parasitism has been addressed by many authors (Cheng, 1991; Zelmer, 1998; Poulin & Morand, 2000; Lafferty, 2008) and it is generally agreed that a parasitic organism derives nutrients from, and benefits at, the cost of another organism known as the host. While the difference between parasitism and other life strategies is not always clear-cut in other kingdoms, all non-mycotrophic parasitic plants are defined by the presence of haustoria — specialized organs facilitating attachment to the host, penetration of its tissues and uptake of nutrients (Kuijt, 1969; Press & Graves, 1995; Heide-Jørgensen, 2008). Haustoria can either be developed on a parasite's stems (*Cuscuta* sp., *Cassytha* sp.) or roots (*Striga* sp., *Rhinathus* sp.) and attach either to roots (*Striga* sp., *Rhinathus* sp.), stems (*Cuscuta* sp., *Cassytha* sp., *Viscum* sp.) or even the leaves (*Cuscuta* sp.) of its hosts. Conventionally the taxa parasitizing host shoots are known as shoot parasites and those parasitic on roots, root parasites (Fig. 1.1). Holoparasites are parasites that through the course of evolution have lost a significant proportion of their chlorophyll and plastid genome (Krause, 2011) or even leaves and, consequently, the ability to fix organic carbon. They are obligate parasites, i.e. are completely dependent on creating haustorial links with their hosts which provide them with all needed nutrients. Holoparasites are often confined to a small number of specific host taxa or in extreme cases, only one. Several *Rafflesia* species have adapted to parasitise single species of *Tetrastigma* (Barcelona *et al.*, 2009) while *Epifagus virginiana* (L.) Bart. lives only on *Fagus grandifolia* Ehrh. (Press & Phoenix, 2005). In contrast, hemiparasites have retained their photosynthetic ability

and therefore parasitise mainly to obtain water and inorganic nutrients while themselves fixing most of the carbon they need. Unlike all holoparasites, for which parasitism is always an obligatory life strategy, hemiparasites are less specialized, often have large host ranges and certain species (for instance *Rhinanthus minor* and *Odontites vernus*) display facultative dependence on hosts. They can often complete their life cycle without attaching to a host (Mutikainen *et al.*, 2000), although their performance is much poorer (Klaren & Janssen, 1978). In natural conditions, unattached hemiparasites are usually not able to compete with other plants and are, therefore, hard to find in the wild (Seel & Press, 1994). Some species can switch from holo- to hemiparasitism during their life cycle stage (Irving & Cameron, 2009). For example, *Striga* (Del.) Benth is holoparasitic during the subterranean stage of its life cycle and becomes hemiparasitic after emerging from the soil (Ejeta & Butler, 1993).

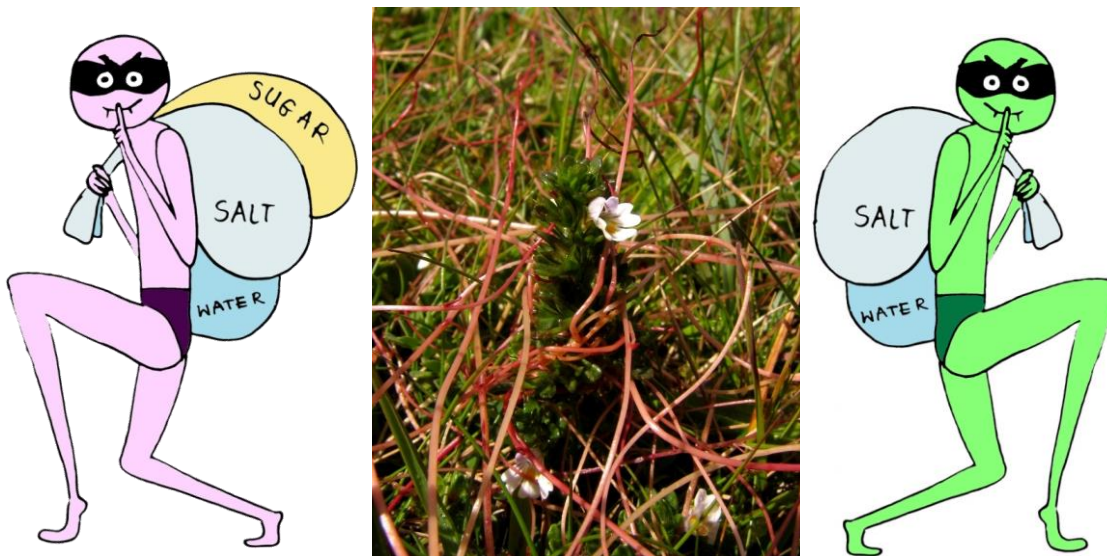


Figure 1.1: An unusual case of epiparasitism: the root hemiparasite *Euphrasia tetraquetra* (Bréb.) Arrond. parasitised by a twining stem holoparasite *Cuscuta epithymum* (L.) L. at Fanore sand dunes, Co. Clare. Hemiparasites are green as they have retained their photosynthetic ability and therefore “steal” mainly water and minerals whereas holoparasites are achlorophyllous (i.e. lack chlorophyll) and depend on their hosts for all nutrients. (author’s own images)

1.1.2 Structure and evolution of haustoria

A number of features can be observed in most mature haustoria (Fig. 1.2). From the functional point of view, the xylem bridge connecting the parasite and the host is perhaps the most prominent one and common to all parasitic species (Kuijt, 1969). It connects the vascular tissue of the parasite root with the vasculature of the host upon successful penetration by the multicellular scavenging portion of the haustorium

known as the endophyte. In contrast to the structure in some holoparasites, phloem is not present in hemiparasitic haustoria and the xylem bridge is surrounded by a parenchymateous core that can be of different structure in different species. In many Orobanchaceae, for example *Rhinanthus minor* L. or *Alectra voglii* Benth., this region is known as the hyaline body — a parenchymateous tissue composed of round cells with thin cell walls and high metabolic activity (Visser *et al.*, 1984; Rümer *et al.*, 2007). Certain species within the family, for example *Rhamphicarpa fistulosa* (Hochst.) Benth., do not possess hyaline bodies in their haustoria (Neumann *et al.*, 1999).

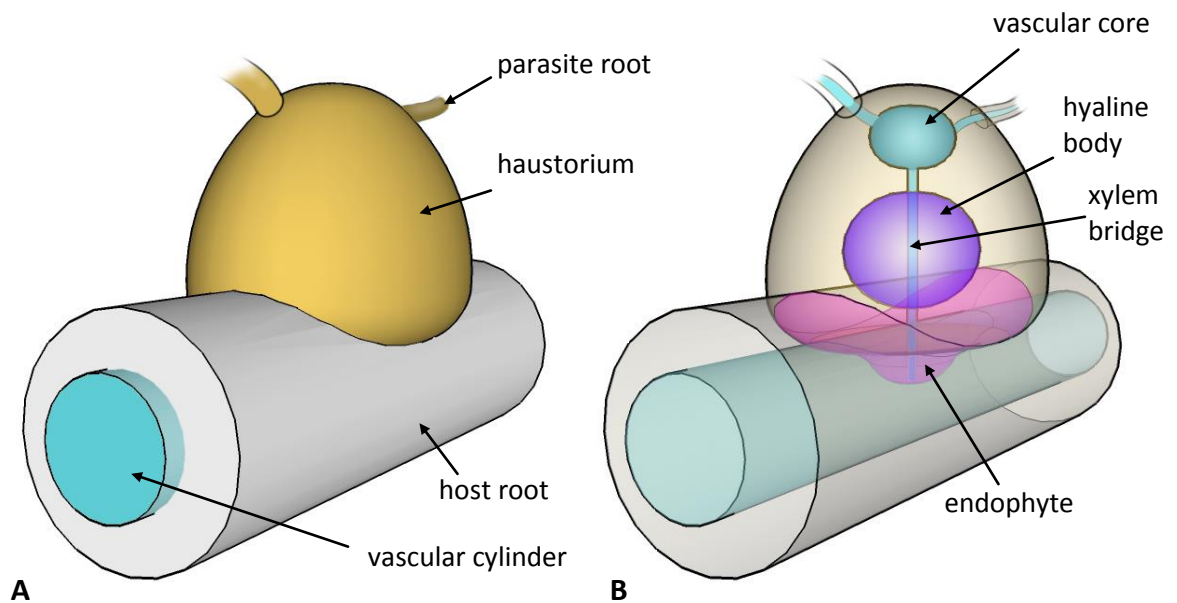


Figure 1.2: A 3D model of a haustorium typical of Orobanchaceae, attached to a host root. **A)** The haustorium develops laterally on a parasite's root and clasps around it. **B)** The central proportion of the haustorium within the host tissues is known as the endophyte and forms part of the interface (magenta). Vascular continuity (blue colour) develops between the haustorium and host root. Vasculature of the parasite in the upper haustorium forms so called vascular core, from which a narrower strand of the xylem bridge extends towards the host. The xylem bridge traverses the hyaline body — an ovoid tissue region of high metabolic activity. (author's own images)

The appearance of haustoria was the key evolutionary step to plant parasitism (Westwood *et al.*, 2010). Kuijt (1969) proposed that parasitic plants evolved from non-parasitic taxa and that haustoria were of exogenous, mycoheterotrophic origin whereby epiparasitic mycotrophs gradually lost the intermediary fungal component. Two general hypotheses explaining the evolutionary origins of haustoria are currently speculated (Yoder *et al.*, 2009):

1. endogenous modifications (duplication and neofunctionalisation) of genes of a non-parasitic ancestor plant that led to the appearance of haustoria

2. exogenous gene acquisition via endosymbiosis (when one organism lives inside the another) or horizontal gene transfer.

Yoder and colleagues (2009) point to nodule development genes in certain legumes that are homologous to genes with alternative functions in non-legumes. Homologous genes with different functions in different taxa could be the key to understanding novel functions of pre-existing genes that might have led to development of haustoria in plants. Endogenous gene modifications are further supported by lack of homologies between *Triphysaria* transcripts during haustorial development and known microbial or fungal sequences (Yoder *et al.*, 2009) as well as the fact that parasitic mechanisms in plants and fungi differ (Mayer, 2006).

A functional distinction between primary (terminal) and secondary (lateral) haustoria can be made. Secondary haustoria are believed to be the evolutionary predecessors of primary haustoria (Weber, 1987; Riopel & Timko, 1995; Westwood *et al.*, 2010). Primary haustoria are typically developed by obligate parasites, for example *Alectra* and *Striga*, and often form as large tubercles, followed by development of smaller secondary haustoria (Nwoke & Okonkwo, 1978; Okonkwo & Nwoke, 1978). The primary haustorium develops at the apex of the seedling radicle and its successful attachment determines the subsequent development of the shoot and root systems, followed by optional formation of lateral haustoria (Westwood *et al.*, 2010). Secondary haustoria of facultative parasites originate near the root tips of actively growing secondary roots. In response to biochemical and thigmotropic cues (Yoder *et al.*, 2009), the apical meristem of the root stops its growth and abundant proliferation of root hairs coupled with root swelling occurs in close proximity to the root tip. After the swelling has formed, the root tip resumes its growth and the swelling continues to differentiate laterally (Tomilov *et al.*, 2005).

In Ireland, there are twenty species of haustorial parasites which are placed in the genera *Cuscuta*, *Euphrasia*, *Lathraea*, *Orobancha*, *Parentucellia*, *Pedicularis*, *Rhinanthus* and *Viscum* (see chapter 7 for more details) (Parnell & Curtis, 2012). This constitutes a very small fraction of the world's parasitic taxa. According to a list managed by Nickerent (<http://www.parasiticplants.siu.edu/ParPlantNumbers.pdf>, last updated 6 March 2012) there are currently 4450 species known to supplement their diets by abstracting the resources (water, minerals and photosynthates) of other plants through haustoria. It is not clear why plant parasitism evolved and the common conception that it was an adaptation to nutrient-poor and arid environments is not supported by the fact that plant parasites occur in a wide range of habitats, some of which are very productive (Atsatt, 1973). Varying life strategies of parasitic plants (point of attachment, degree of dependence of hosts, etc.) reflect multiple origins of parasitism in plants. It has been established that plant parasitism in angiosperms evolved independently 12–13 times and currently characterises approximately

1% of taxa (Westwood *et al.*, 2010), all of which are eudicots, while *Parasitaxus usta* (Vieill.) de Laub. is the only parasitic gymnosperm currently known to science (Irving & Cameron, 2009). In comparison, parasitism of metazoans by other metazoans evolved at least 60 times (Poulin & Morand, 2000) and according to Price (1980) as quoted by Morand & Gonzalez (1997) “no animal species is free of parasites”. Although plant parasitism by other plants is less widespread, it is locally common with disastrous consequences for arable system productivity in developing parts of the world. One of the most infamous examples, *Striga hermonthica*, is a persistent pest in intensively managed cereal fields in sub-Saharan Africa (Schulz *et al.*, 2003) with recent estimates of up to 50 million hectares of agricultural land and 300 million farmers being affected by the genus, and resulting in potential economic losses in the region of \$US 7 billion annually (Parker, 2009; Atera & Itoh, 2011).

1.1.3 Scientific interest

The economic consequences of plant parasitism in agricultural systems and the development of prevention measures have been the primary focus areas in parasitic plant research. While most major lineages of parasitic plants display only one type of parasitic strategy, Orobanchaceae, the family which includes most parasitic species native to Ireland and some of the most notorious crop weeds, is the only taxonomic group representing all degrees of parasitism: facultative and obligate hemiparasitism as well as holoparasitism (Westwood *et al.*, 2010). Considerable effort is currently being directed at sequencing plant genomes of three parasitic plants from this family; *Orobanche aegyptiaca* (Pers.) Pomel (*syn. Phelipanche aegyptiaca* (Pers.) Pomel), a holoparasite; *Striga hermonthica*, an obligate hemiparasite, and, *Triphysaria versicolor* Fisch. & C.A. Mey., a facultative hemiparasite, with the hope of dissecting the molecular processes underlying development and host resistance (Westwood *et al.*, 2012). Furthermore, whole genome sequencing of *Striga asiatica*, *S. gesneroides* and *S. sermothica* is currently in progress (Yoshida & Shirasu, 2012).

Although agricultural weeds have received far more research attention than parasites in semi-natural systems (Štech & Wesselingh, 2010), elucidation of factors underlying the variation in host vulnerability is also of great importance to the less obvious aspect of parasitism, namely its impact on ecosystem biodiversity (Press & Phoenix, 2005; Watson, 2009). From the ecological point of view, the most important consequences of variable host resistance are the existence of host preference, host ranges and host functional groups of hosts (susceptible) and non-hosts (resistant). Parasites effect shifts in competitive balance in favour of non-hosts, often leading to increased species richness. This phenomenon has been particularly well documented (Gibson & Watkinson, 1991, 1992; Davies, 1997; Ameloot *et al.*, 2005; Ameloot, 2007) for *Rhinanthus* — a genus of annual hemiparasites native to northern temperate regions. *Rhinanthus* preferentially parasitises grasses and legumes and as

a consequence the fecundity of these functional groups of hosts is reduced while most eudicots increase in abundance, adding floral diversity to grass-dominated communities (Fig. 1.3). Furthermore, the overall biomass usually decreases (Ameloot *et al.*, 2005). These properties have been practically applied in restoration of grassland biodiversity, whereby introduction of *Rhinanthus minor* to grass-dominated, species-poor grasslands leads to an increase in floral diversity (Davies, 1997; Pywell *et al.*, 2004; Bullock & Pywell, 2005; Westbury *et al.*, 2006).

There is ample evidence that the outcome of a parasite-host interaction is largely determined at haustorial interfaces which are frequently sites of resistance expression. This has been demonstrated for *Rhinanthus minor* as well as a number of weed crops, for example *Alectra* (Visser *et al.*, 1990), *Orobanche* (Pérez-de-Luque *et al.*, 2005; Echevarría-Zomeño *et al.*, 2006) and *Striga* (Hood *et al.*, 1998). Several different defence mechanisms exist, including physical barriers resulting from reinforcement of host cell walls or cell necrosis (Cameron *et al.*, 2006); phytotoxic mechanisms aiming to inhibit haustorial development, for example secretion of coumarins (Serghini *et al.*, 2001) or phytoalexins (Lozano-Baena *et al.*, 2007). Evidence for barriers to haustorial development comes mainly from histological studies although there is accumulating molecular evidence to support the image-based approaches (see chapter 4).

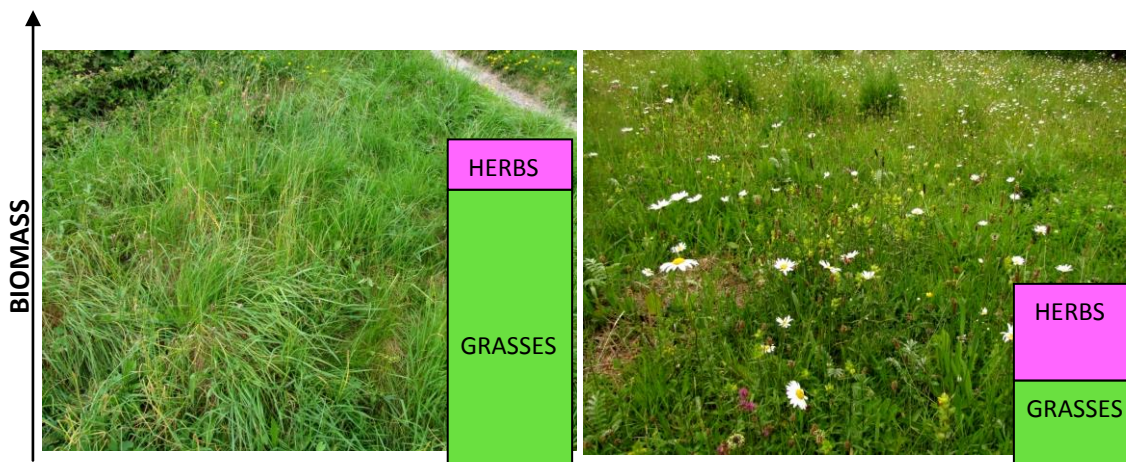


Figure 1.3: Changes in community structure effected by hemiparasites result from shifts in proportions between grasses and eudicot herbs (Gibson & Watkinson, 1991) as well as reduced overall biomass (Ameloot *et al.*, 2005). The image on the left illustrates a grassland dominated by a vigorous grass species *Dactylis glomerata*, while the image on the right depicts a species-rich hay meadow with more balanced proportions between grass and eudicot herb cover (including abundant *Leucanthemum vulgare*) and diversity. (author's own images)

Parasitic plants are also very interesting in terms of evolution and speciation. Holoparasites such as *Orobanche* are examples of extremely advanced adaptation (Thorogood *et al.*, 2009) while the parasitic genus *Rafflesia* produces the largest

flowers found on Earth resulting from a spectacular 79-fold increase in floral diameter which has been dated to have occurred in the Rafflesiaceae lineage over 46 million years (Barkman *et al.*, 2004; Davis *et al.*, 2007).

1.2 Cell walls and parasitism: biochemical determinants of ecological processes

1.2.1 Cell wall structure

A cellulose-rich wall surrounds the cells of most plants, with a few exceptions such as the tapetum of pollen grains and gametes (Albersheim *et al.*, 2011). Cell walls are of critical importance to plant cells as they play various physiological and structural roles. While previously believed to be rigid structures responsible merely for granting plant cells their shape, cell walls are now appreciated as complex and dynamic, spatio-temporally diverse structures forming a continuum with the protoplast (Brett, 1983; Roberts, 1994; Humphrey *et al.*, 2007). They display regional, cellular heterogeneity that changes with time. In addition to determining cell shape and firmness, they control cell growth, development and intercellular transport while allowing interactions with other cells and organisms, including pathogens (Hüchelhoven, 2007). During parasitism, the cell walls of the parasite and the host at the haustorial interface form a contact zone that is modified during infection. As a result of these dynamic properties, the term *extracellular matrix* (ECM) is often used interchangeably with cell wall (Bolwell, 1993; Roberts, 1994).

Where three cells meet, a three-way cell wall junction (Fig. 1.4) is preferentially created (Flanders *et al.*, 1990). These junctions are initially very small but expand with age, to eventually create a network of three-sided intercellular spaces (Harker & Hallett, 1992) (Fig. 1.4), analogically to spaces between glass balls in a bowl. The struts of three way junctions are responsible for most of the tissue's strength. Direct communication between protoplasts of neighbouring cells is possible via plasmodesmata (Robards & Lucas, 1990).

Typical, fully developed cell walls are composed of three layers (radial heterogeneity) (Fig. 1.4): middle lamella (~20 nm thick), primary cell wall (50–200 nm) and secondary cell wall. Adjacent cells in a tissue are held together by tight adhesion attributed to a pectin-rich middle lamella — the outermost layer deposited soon after mitosis between the daughter cells (Knox, 1992; Jarvis *et al.*, 2003). The primary cell wall is synthesised during expansive cell growth and the innermost secondary cell wall is typically deposited when cell growth has stopped and usually does not allow for further cell growth (Cosgrove, 1997; Albersheim *et al.*, 2011). Secondary cell walls of specialised tissues and cells, for example xylem (Oda & Fukuda, 2012; Schuetz *et al.*, 2013) or transfer cells (Pate & Gunning, 1972), are often considerably thickened and have very elaborate structures. Walls of certain tissues such as collenchyma may be primary while also being thickened non-uniformly (Leroux, 2012). However, in this

case the distinction between primary and secondary cell walls is not very clear, similar to helically thickened xylem elements which can elongate after the deposition of thickenings and in which the term secondary wall can be applied regionally to the thickenings (Leroux, 2012). A secondary cell wall does not always develop. For instance, parenchyma of meristem tissues is surrounded by primary cell walls to allow cell proliferation and subsequent elongation (Albersheim *et al.*, 2011).

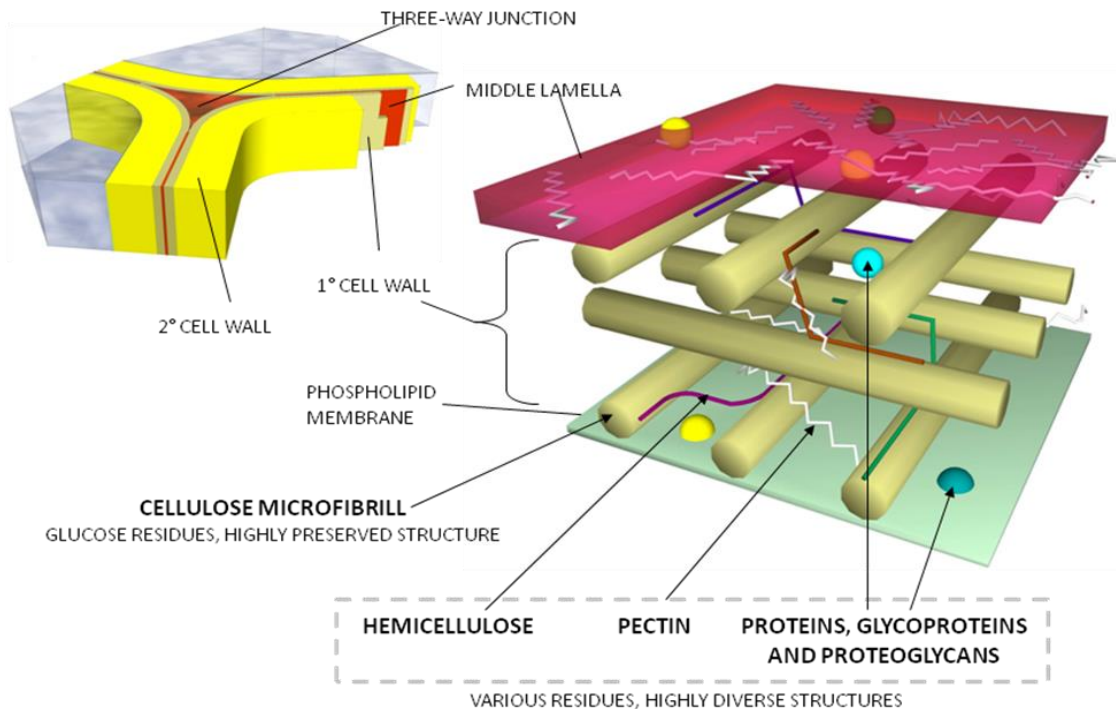


Figure 1.4: Simplified representation of cell wall structure. (author's own images)

Biochemically, all three layers of the cell wall are composed of cellulose microfibrils embedded in a matrix of hemicelluloses, pectins, glycoproteins, interlinked covalently and non-covalently (Fry, 2011), as well as water (Fig. 1.4). Cellulose and matrix polysaccharides form two major dynamic networks 1) a network of hydrogen-bonded cellulose and hemicelluloses (Carpita & Gibeaut, 1993) and 2) a pectin network held together with calcium crosslinks, borate diesters, covalent links with phenolics and hydrogen bonds (Caffall & Mohnen, 2009), and covalently bound to the hemicelluloses (Popper & Fry, 2005). Several models have been proposed to explain the architecture of cell walls (Keegstra *et al.*, 1973; McCann & Roberts, 1991; Carpita & Gibeaut, 1993; Somerville *et al.*, 2004; Baba, 2006) and constituent polymers, for example cellulose fibrils (Ding & Himmel, 2006). However, elucidation of the real nature of interactions between the main groups of polymers is one of the biggest challenges in cell wall research. The structure is somewhat analogous

to that of fiber composite materials whereby fibers (cellulose microfibrils non-covalently cross-linked by hemicelluloses) are the components resistant to stretching or tension (tensile strength) and are embedded in a matrix (pectins, proteins, water) resistant to compression (Albersheim *et al.*, 2011).

1.2.2 Cell wall diversity and its possible consequences for parasitism

The proportions of cell wall components differ between plant taxa, tissues, individual cells and cell wall layers and change as the tissue differentiates and matures (Knox, 2008). Middle lamellae are composed chiefly of pectins and proteins (Carpita & Gibeaut, 1993). The primary cell wall is characterised by relatively even proportions between different polymers and high water content of more than 70% of fresh weight (Albersheim *et al.*, 2011). Secondary walls display a range of differences to primary walls, from similar composition or decreased proportion of pectins and increased proportion of cellulose (collenchyma, phloem) to almost purely cellulosic composition (cotton fibers) or heavy impregnation with lignin (xylem vessels, fibers, sclereids) or suberin (cork tissue) (Albersheim *et al.*, 2011).

The biochemical composition of the cell wall reflects the evolution of different plant taxa and there are some significant differences between different systematic groups (Harris, 2005; Popper, 2008; Sørensen *et al.*, 2010; Popper *et al.*, 2011). While the microfibrillar structure is uniform across all higher plant taxa, the non-cellulosic molecules exhibit high diversity. This provides an interesting context for understanding plant parasitism, in particular differences in host susceptibility. It has been reported that many parasitic species discriminate between eudicot and monocot hosts and for several species, for example *Rhinanthus minor* or *Striga hermonthica*, grasses are the preferred hosts (Gibson & Watkinson, 1989; Mohamed *et al.*, 2001). The ability to recognise the host or host susceptibility could be associated with cell wall differences between dicots and Poales (Fig. 1.5). In eudicot cell walls the major hemicellulose is xyloglucan, which constitutes up to 25% w/w of their primary cell wall (Keegstra *et al.*, 1973), traditionally although decreasingly referred to as type I cell wall (Brett & Waldron, 1996; Albersheim *et al.*, 2011). However, xyloglucan only makes up approximately 4 % w/w of the Poales primary cell wall (Fry, 1988). Instead, Poales, which have type II primary cell walls, are characterised by the presence of the hemicelluloses mixed-linkage glucan and glucuronoarabinoxylan often crosslinked by esters of abundant phenolic substances, namely ferulic, hydroxycinnamic and *p*-coumaric acid (Carpita, 1996; Vogel, 2008). Furthermore, pectins can constitute approximately 35% of dry weight of primary cell wall of dicots compared with only 5% or indeed trace amounts in the Poales (Fry, 1988). Moreover, primary cell walls of the Poales are characterised by a much lower proportion of structural proteins such as extensins than other plant groups (Carpita 1996). These differences in composition may influence host recognition by parasitic

Chapter 1

plants and the infective process. Using histological techniques Rümer and colleagues (2007) found that the variable success of *Rhinanthus minor* (yellow rattle) on five different hosts was determined by resistance mechanisms in their cell walls. *Rhinanthus* managed to create xylem bridges to the root vasculature of grasses (*Hordeum vulgare* L. and *Phleum bertolonii* DC.) and legumes (*Vicia cracca* L.), whereas non-leguminous forbs (*Leucanthemum vulgare* Lam. and *Plantago lanceolata* L.) saturated their cell walls with lignin or suberin, thereby encapsulating the haustorium before it reached their xylem. Consequently, yellow rattle develops parasitically functional haustoria on grasses and legumes and reduces their biomass, whereas it does not affect the productivity of other plants. This is in agreement with the finding by Cameron and Seel (2007) that yellow rattle could gain 17% of ¹⁵N-labelled potassium nitrate from *Cynosurus cristatus* L., and only 2.5% and 0.2% from *Leucanthemum vulgare* and *Plantago lanceolata* respectively. Except for the defence mechanisms described by Rümer, Cameron and co-workers, not much is known about the interactive processes in the cell walls of hosts and *Rhinanthus minor*, or in fact other parasitic plants, during infection. However, as the ground work has been laid, yellow rattle is a convenient candidate for further investigations of cell-wall related virulence and resistance in ecologically important parasitic plants. Chapter 3 discusses implications of cell walls and their diversity in parasitism in more detail.

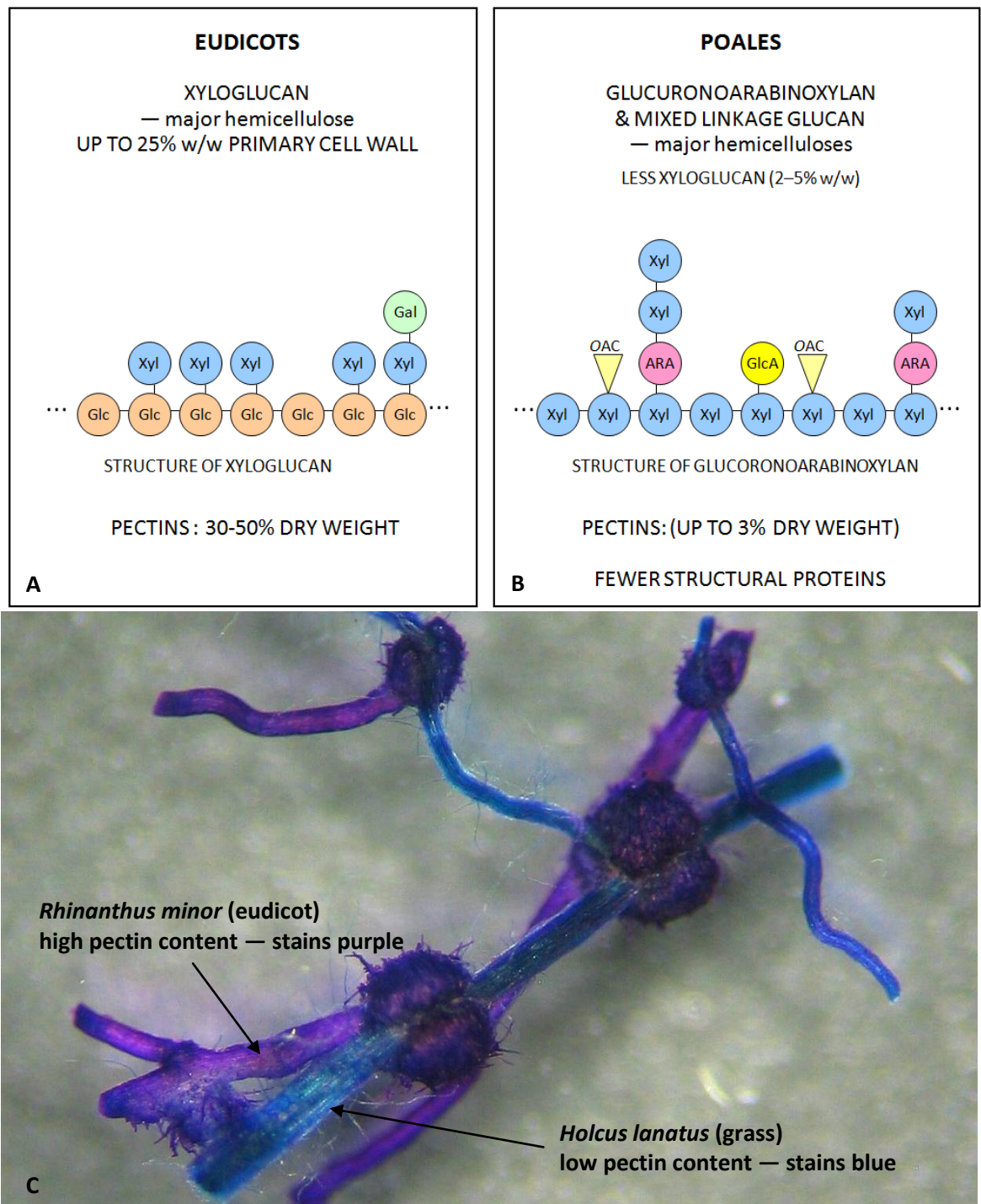


Figure 1.5: Major differences between cell wall constituents of eudicots (A) and Poales (B). The main distinction is in the types of hemicelluloses as well as abundance of pectins and structural proteins. C) Differences in pectin content result in clearly visible differential staining with the polychromatic dye Toluidine Blue O which stains cellulose blue, phenolics green-blue and pectin-enriched cell walls purple (O'Brien *et al.*, 1964). The roots and haustoria of hemiparasite *Rhinanthus minor* (eudicot) stain purple while the roots of a grass host (Poales) stain blue. (author's own images)

1.2.3 Cell wall constituents

1.2.3.1 Carbohydrates

There are 13 different building blocks available for cell wall carbohydrate synthesis (Table 1.1) (Brett & Waldron, 1996; Albersheim *et al.*, 2011). While cellulose is composed solely of glucose, all 13 sugars are incorporated into the non-cellulosic carbohydrates. Prior to polymerization they are activated as nucleotide sugars, mainly in the cytosol but also by Golgi membrane enzymes (Bar-Peled & O'Neill, 2011). Glycosyltransferases are membrane-localised enzymes that catalyse addition of individual monosaccharides to growing nascent polysaccharides as well as proteins and lipids. Therefore monosaccharides are activated in the cytosol, however they are transported to, and polymerised by, membrane-bound enzymes. The synthesis of xyloglucan, xylan and pectins occurs in Golgi compartments while cellulose and callose are synthesised by plasma membrane-localised enzyme rosette complexes (Cosgrove, 2005b). The carbohydrate components of proteoglycans and glycoproteins are carried from cytoplasm on lipid carriers known as dolichols to the protein moieties synthesised in the ER. The intermediates are then transported to and further modified in the Golgi cisternae. The individual monomers can undergo various modifications such as methyl-esterification of carboxyl groups or substitution of carboxyl groups with *O*-acetyl (CH₃CO) groups (*O*-acetylation) (Renard & Jarvis, 1999; Pauly & Scheller, 2000). This affects the properties of polymers that the modified monomers are incorporated in, notably availability to enzymes (Lionetti *et al.*, 2012).

Table 1.1: Monosaccharide monomers of cell wall carbohydrates

Monosaccharide	abbreviation	Classification (Albersheim <i>et al.</i> , 2011)
D-Glucose	Glc	hexoses
D-Galactose	Gal	
D-Mannose	Man	
L-Rhamnose	Rha	deoxy-hexoses
L-Fucose	Fuc	
L-Arabinose	Ara	pentoses
D-Xylose	Xyl	
D-Apiose	Api	
D-Galacturonic acid	GalA	acidic sugars
D-Glucuronic acid	GlcA	
L-Aceric acid	AceA	
3-deoxy-D-mannooctulosonic acid	KDO	
3-deoxy-D-lyxo-2 heptulosaric acid	DHA	

Cellulose

Cellulose is the most structurally conserved component of cell walls and is made of cellobiose, i.e. β -1 \rightarrow 4 linked glucopyranosyl dimer units. Cellulose is very stable and insoluble. Its content and degree of polymerisation (DP) differ between primary and secondary cell walls. In primary walls cellulose contributes 20–30% of the dry weight and its DP occurs in two fractions of 250–500 and 2500–4000 (Albersheim *et al.*, 2011). The cellulose content of secondary walls is up to 50% and its DP is much greater, typically 10,000–15,000. Between 30 and 50 individual β -1 \rightarrow 4-linked glucan chains hydrogen-bond (crystallise) to form microfibrils of 3–5 nm diameter. Cellulose in cell walls occurs in two forms; a highly organised crystalline form with considerable mechanical strength, and a paracrystalline amorphous form, which is important for its viscoelastic properties (Mazeau & Heux, 2003).

In the cell wall, the cellulose component is arranged in layers (lamellae) that are one microfibril thick (Evert, 2006). Plants can, to a certain extent, control the orientation of fibrils within and between layers, depending on the desired cell wall properties (Burgert & Fratzl, 2009). They are deposited perpendicularly to the direction of growth in elongating cells and are subsequently passively reorganised during cell elongation. On the other hand, cellulose microfibrils are deliberately arranged at alternating angles between the three different layers (S1, S2 and S3) in xylem thickenings, granting them high strength (Evert, 2006). This orientation does not subsequently change as the thickened walls do not continue to expand (Burgert & Fratzl, 2009). In certain thick walls, a conspicuous helicoidal texture can be observed when sectioned at an oblique angle. The consecutive lamellae are laid down by an as yet unexplained self-assembly mechanism and rotated by a small fixed angle resulting in the optical effect of light and dark bands (Roland & Reis, 1982; Albersheim *et al.*, 2011).

Non-cellulosic carbohydrates (pectins and hemicelluloses)

Pectins and hemicelluloses are the carbohydrate components of cell walls contributing to their biochemical diversity. They are composed of all 13 monosaccharide residues (Table 1.1), variously linked. The existence of D versus L enantiomers and α versus β -linked anomers further complicates carbohydrate structures, contributing to diversity. Pectins and hemicelluloses were traditionally distinguished by the methods employed in their extraction whereby pectins were first extracted using treatments with hot water, weak acid, weak alkali and ammonium oxalate or with chelating agents, such as EDTA or CDTA, and hemicelluloses were subsequently solubilised by treatment with aqueous alkali. This definition is now known to be inaccurate and therefore Albersheim and colleagues (2011) define pectins as polysaccharides with over 20 mol % content of D-galactosyluronic acid and hemicelluloses as polymers that form hydrogen bonds with cellulose.

Pectins: The biology of pectins has been reviewed by several authors (Willats *et al.*, 2006; Mohnen, 2008; Caffall & Mohnen, 2009; Harholt *et al.*, 2010). They can be subdivided into 3 types of polymers: homogalacturonan (HG), rhamnogalacturonan-I (RG-I) and rhamnogalacturonan-II (RG-II). The pectin network is no longer believed to be simply an amorphous jelly that fills the gaps between the fibrous elements of the wall. Instead, different types of pectin interact and play both structural and functional roles. Calcium cations (Ca^{2+}) cross-link free carboxyl groups where stretches of 10–15 non-esterified galactosyluronic acid residues of homogalacturonans occur, contributing to cell wall strength and adhesion. Additionally borate diester bridges form between RG-II molecules, resulting in RG-II dimers, which covalently link with other types of pectin. This pectin network intermeshes with and occludes pores in the cellulose-hemicellulose network to 4–13 nm diameter — the size range of medium-sized proteins. Therefore it controls accessibility of other polymers to enzymes, etc.

Homogalacturonans (HGs) are the pectins which have the simplest structure. HG contains exclusively α -D-galactosyluronic acid residues that are 4-linked. It is synthesised in methyl-esterified form and subsequently deesterified in the wall by pectin methylesterase (PME). Methyl-esterification of the pectin backbone decreases its availability to enzymes and prevents calcium cross-linking between carboxyl groups and aggregation into gels (Knox *et al.*, 1990). Therefore, deesterified pectins are often less abundant in the walls of dividing and expanding cells where the walls need to be more malleable (Dolan *et al.*, 1997; Palin & Geitmann, 2012). The non-esterified forms have been found mainly in the middle lamella and in cell corners while the esterified forms intermesh with the cellulose-hemicellulose network (Knox *et al.*, 1990).

Substituted galacturonans share a backbone of homogalacturonan with some of the residues substituted with side chains. Apiogalacturonan extracted from *Lemna minor* L. has side chains composed of apiosyl residues (Golovchenko *et al.*, 2002). The backbone of xylogalacturonan, a polymer found in pine pollen, apple fruit or bean cotyledons, is substituted with β -1→3-linked xylosyl residues (Zandleven *et al.*, 2007). The roles of substituted galacturonans are largely unexplored although immunohistochemical evidence shows that xylogalacturonan is specifically associated with areas of cell detachment at the root cap and seed testa of *Pisum sativum* L. (Willats *et al.*, 2004).

Rhamnogalacturonans (RGs) are more complex, branched polymers. **RG-I** backbone is composed of galacturonic acid-rhamnose dimers (4)- α -D-GalpA-(1→2)- α -L-Rhap-(1→). Galactosyluronic acid residues of RG-I backbone do not occur in esterified form and they all contain an acetyl group at C-2 or C-3. Between 25 and 80% of rhamnosyl residues are substituted at C-4 with approximately 40 types of side chains of mainly

L-arabinosyl and D-galactosyl as well as small amounts of L-fucosyl and D-glucosyluronic acid. The side chains are made of 1–30 residues, are often branched and account for the diversity as well as 70% of the size of RG-I molecules. Their structure has been well studied, however, their position on the backbone remains unresolved. The functions of RG-I are more obscure than those of HG and RG-II, although mediation of physical interactions between HG chains and transmission of stresses in the wall have been proposed (Harholt *et al.*, 2010). **RG-II** is composed of only 30 glycan residues yet surprisingly it is the most complex plant polysaccharide so far identified, with the highest diversity of glycan residues (11, no mannose or glucose) and glycosyl linkages (over 20). It is technically a substituted galacturonan and its HG-like backbone is made of 9 to 11 4-linked α -D-galactosyluronic acid residues with side chains composed of aldo- and ketosugars at C-2 and C-3. Some of the backbone residues can be methyl-esterified. The major components of RG-II: galactosyluronic acid and rhamnosyl residues constitute 30 and 14 mol % respectively. KDO and DHA are rare sugar residues found only in RG-II of land plants and charophycean green algae (Sørensen *et al.*, 2011). Co-occurring apiosyl, 2-O-methyl fucosyl, 2-O-methyl xylosyl and arabinopyranosyl residues are also characteristic of RG-II. RG-II is expected to play important structural, physical and mechanical roles due to the pectin cross linking via borate diesters (O'Neill *et al.*, 2004), which result in the formation of RG-II molecule dimers. Indeed, boron requirement is linked to pectin content and plants that have little pectin such as grasses need less boron than plants that have significantly more pectin in their walls (O'Neill *et al.*, 2004). It has also been proposed to form covalent linkages with both HG and RG-I and therefore might be responsible for the covalent binding and organisation within the whole pectin network (O'Neill *et al.*, 2004). Its complexity, high energetic cost of production (involving over 50 enzymes) and highly conserved structure across different plant groups point to important functional roles in primary cell walls (Albersheim *et al.*, 2011).

Hemicelluloses: Hemicelluloses form part of the cell wall matrix, where they coat and non-covalently cross link cellulose microfibrils. The cross links are of 20–30 nm length and through hydrogen bonds they hold microfibrils together and separate them at the same time, preventing collapse of microfibrils onto each other (Fry, 1989; Park & Cosgrove, 2012).

Xyloglucan is present in all higher plants but is much more abundant (approximately 25% of dry weight) in primary walls of eudicots than of non-gramonoid monocots (approximately 2–5 % dry weight) and conifers (10%) (Scheller & Ulvskov, 2010). It is made of a cellulose-like backbone where around 5% of glucosyl residues are substituted at C-2 with by β -D-xylosyl and 75% of are substituted at C6 with single α -D-xylosyl residues. Some of the latter can in turn have β -D-galactosyl or α -L-fucosyl-(1→2)- β -D-galactosyl units attached to C-2. Other substituents in sycamore include O-acetyl on 2-linked galactosyl residues or α -L-arabinosyl residues attached

to the backbone or β -D-xylosyl residues. Xyloglucans of grasses have few galactosyl residues and no fucosyl and arabinosyl residues, whereas members of the asteridae also exhibit structural diversity with regard to xyloglucan composition (Hoffman *et al.*, 2005). They are also less branched than in most dicots and most side chains are single α -D-xylosyl residues (Carpita & Gibeaut, 1993).

Arabinoxylan is the predominant hemicellulose of graminoid monocots where it contributes <40 % of dry weight, much more than in dicots and gymnosperms (<5%) (Albersheim *et al.*, 2011). Its backbone is made of β -1 \rightarrow 4-xylosyl residues, 10–90 % of which bear side chains of xylosyl, arabinosyl, glucosyluronic acid and 4-*O*-methyl glucosyluronic acid. Scarcely-branched arabinoxylans can hydrogen-bond to cellulose. The acidic residues account for a major difference between arabinoxylans and xyloglucans, which are neutral.

In the secondary walls of angiosperms **glucuronoxylans** and **glucomannans** are the major hemicelluloses (Zhong & Ye, 2009). **Glucomannans** are linear polymers of 1 \rightarrow 4-linked glucosyl and mannosyl residues at ratios varying between 1:1 and 2:1. They are most abundant in dicot walls (up to 5%), while being absent from conifer walls (Scheller & Ulvskov, 2010). **Galactoglucomannans** are substituted by side chains of galactan and are acetylated (Zhong & Ye, 2009). They account for up to 30% of dry weight of conifer walls and up to 3% of eudicot secondary walls. Their backbone of **glucuronoxylans** is the same as in arabinoxylan of primary walls with approximately 1 of every 10 residues substituted by single 4-*O*-methyl α -D-glucosyluronic acid residues attached to C-2 and around 70% of backbone residues having one *O*-acetyl group at C-2 or C-3. Arabinosyl residues have also been found but are not abundant. Glucuronoxylans take the place of xyloglucans in secondary walls of eudicots (Scheller & Ulvskov, 2010). On the other hand, **glucuronoarabinoxylans** are absent from secondary eudicot walls and are particularly abundant in cell walls of grasses, particularly their secondary cell walls (Carpita, 1996; Scheller & Ulvskov, 2010). They differ from glucuronoxylans in that they are partly substituted with arabinan on C-2 and/or C-3, and 4-*O*-methyl-substituted glucuronic acid on C-2 or C-3 (Carpita & Gibeaut, 1993).

(1 \rightarrow 3)(1 \rightarrow 4)- β -D-glucan, otherwise known as mixed-linkage glucans (MLGs) are similar to cellulose in that they are composed exclusively of glucosyl residues, however, they contain both 1 \rightarrow 3 and 1 \rightarrow 4-linkages (Woodward *et al.*, 1983). Once believed to be found exclusively in Poales, MLG has recently been discovered in *Equisetum* (Fry *et al.*, 2008; Sørensen *et al.*, 2008). Products of hydrolysis of MLG from Poales are the trisaccharide cellobiosyl-1 \rightarrow 3- β -D-glucose and tetrasaccharide cellotriosyl-1 \rightarrow 3- β -D-glucose present in a ratio of approximately 2:1 and constituting approximately 90% of the polysaccharide (Woodward *et al.*, 1983). In *Equisetum* sp., tetrasaccharide β -glucosyl-(1 \rightarrow 4)- β -glucosyl-(1 \rightarrow 4)- β -glucosyl-(1 \rightarrow 3)-glucose is a predominant product

(Fry *et al.*, 2008). Contiguous stretches of around ten β -1 \rightarrow 4-linked glucosyl residues that are believed to be responsible for hydrogen bonding between MLG chains as well as MLG and cellulose have been identified while irregularly interspersed β -1 \rightarrow 3-linked glucosyl residues give flexibility to the MLG backbone. It is not clear whether MLG is synthesised in the Golgi apparatus or the plasma membrane (Albersheim *et al.*, 2011). While glucuronoarabinoxylan is the main hemicellulose of secondary grass walls, MLG is present mainly in primary walls where it accounts for up to 15% w/w of the cell wall (Scheller & Ulvskov, 2010).

Callose: Callose, similar to cellulose and mixed linkage glucans, is a linear polymer of glucose, however, the residues are β 1 \rightarrow 3 linked. Callose is synthesised by enzyme rosettes at the plasma membrane in response to wounding or pathogen attack as well as in sieve plates of phloem, pollen tubes and plant styles (Chen & Kim, 2009). Unlike cellulose synthase that appears in membranes as needed, callose synthase is present in the membranes throughout a cell's life and can be activated when needed. Callose is insoluble and the β -1 \rightarrow 3-D-linkage causes the gel-forming helical conformation of the polymer and results in electron-lucent appearance of callose-rich cell walls (Dyakov *et al.*, 2007; Albersheim *et al.*, 2011).

1.2.3.2 Proteins and glycoproteins

Proteins constitute 1–10% of the dry weight of cell walls and can be divided into insoluble structural proteins and soluble proteins (Albersheim *et al.*, 2011). The most abundant and most studied examples of the former are extensins (hydroxyproline-rich), glycine-rich proteins (GRPs) and proline-rich proteins (PRPs) (Cassab, 1998). Soluble proteins include enzymes, transport proteins, defense proteins, lectins and AGPs (arabinogalactan proteins). AGPs, extensins, PRPs and an additional group of proteins known as solanaceous lectins form a superfamily of hydroxyproline-rich glycoproteins (HRGPs) (Sommer-Knudsen *et al.*, 1998). There are also chimeric molecules that possess the properties of more than one group of proteins. These include Fasciclin-Like AGPs (FLAs) that possess one or two fasciclin domains known to participate in cell adhesion in animals (Johnson *et al.*, 2003), Early nodulins (ENODLs) related to phytocyanins (Mashiguchi *et al.*, 2009), some non-specific lipid transfer proteins (*ns*-LTPs) (Mashiguchi *et al.*, 2004) — a group of molecules involved in plant defences (Wang *et al.*, 2004; Salcedo *et al.*, 2007), legume AGP-extensins (Brewin *et al.*, 2008; Reguera *et al.*, 2010) and other molecules with characteristics of both AGPs and extensins (Lind *et al.*, 1994; Bosch *et al.*, 2001).

Glycine-rich proteins (GRPs)

Cell wall glycine-rich proteins are non-glycosylated proteins that contain 50–70% glycine (Gly) residues and have a β -pleated sheet structure (Ringli *et al.*, 2001; Mangeon *et al.*, 2010). They are associated with xylem development and are produced

within the xylem elements, as well as in adjacent parenchyma from which they are then transported to modified cell walls of xylem (Keller *et al.*, 1989; Ryser *et al.*, 1997). They are speculated to contribute to cell wall integrity, elasticity and tensile strength or to act as nucleation sites for lignification during xylem differentiation. GRPs are also present in root cap mucilage (Matsuyama *et al.*, 1999). Furthermore, they can be upregulated in response to fungal elicitors (Brady *et al.*, 1993).

Glycoproteins and proteoglycans

This group of cell wall molecules includes proline/hydroxyproline-rich family comprising a range of molecules differing in levels of glycosylation, dependent on the protein backbone sequence as proposed in the hydroxyproline (Hyp) contiguity hypothesis (Kieliszewski & Lamport, 1994; Shpak *et al.*, 2001). The hypothesis predicts that contiguous Hyp residues are arabinosylated while clustered, non-contiguous Hyp residues are galactosylated. Proline rich proteins (PRPs) are not glycosylated or only weakly glycosylated. Hydroxyproline-rich proteins; extensins and arabinogalactan proteins (AGPs) are glycosylated. Extensins possess contiguous Hyp residues glycosylated with relatively short arabinose (Ara) oligosaccharides. Arabinogalactan proteins are most glycosylated and possess arabinogalactan II moieties attached to their non-contiguous Hyp residues (alanine (Ala)-Hyp, Serine (Ser)-Hyp).

Proline-Rich Proteins (PRPs): Proline rich proteins are made of equimolar quantities of hydroxyproline and proline (Pro), with the latter occurring in variously incorporated Pro-Pro repeats (Marcus *et al.*, 1991; Showalter, 1993). PRPs are often developmentally regulated (Wyatt *et al.*, 1992) and contribute to normal cell processes such as cell elongation (Dvoráková *et al.*, 2012) or secondary wall deposition (Vignols *et al.*, 1999) and often co-localise with GRPs in lignified cell walls (Ye *et al.*, 1991; Ryser *et al.*, 1997). They have also been shown to confer tolerance to abiotic stresses, for example cold (Gothandam *et al.*, 2010) and water deficit (Battaglia *et al.*, 2007), as well as wounding and pathogen elicitors (Sheng *et al.*, 1991; Bradley *et al.*, 1992). They are also important during nodulation as components of legume infection thread, nodule vascular bundle walls and intercellular spaces of nodule parenchyma (Sherrier & Vandenbosch, 1994; Bonilla *et al.*, 1997).

Extensins: Hydroxyproline-rich glycoproteins are rodlike molecules that owe their structure to characteristic repeat sequence motif X-Hyp-Hyp-(Hyp)_n (Kieliszewski & Lamport, 1994; Lamport *et al.*, 2011). Those repeated blocks determine inflexible left-handed polyproline II-helix conformation coated with mono- and oligo-saccharides. Extensins are basic HRGPs with multiple copies of Ser(Hyp)₄ sequence and abundant Val, Tyr, Lys and His residues. Glycosylation of most Hyp residues and Ser residues yields sugar-coated structures that are very resistant to proteolytic action.

Extensins contribute to cell wall strength and have been observed to accumulate and covalently cross-link under peroxidase control at sites of infection by pathogens, limiting or preventing pathogen ingress (Wei & Shirsat, 2006; Deepak *et al.*, 2010). However, they are also implicated in normal developmental phenomena, notably they self-assemble into scaffold-like precursors allowing normal cell wall formation (Cannon *et al.*, 2008; Lamport *et al.*, 2011).

Arabinogalactan proteins (AGPs): Some of the most cutting-edge cell wall research focuses on arabinogalactan proteins (AGPs), the most glycosylated of plant glycoproteins. As reviewed by several authors (Fincher & Stone, 1983; Chasan, 1994; Kreuger & van Holst, 1996; Du *et al.*, 1996; Schultz *et al.*, 1998; Serpe & Nothnagel, 1999; Cheung & Wu, 1999; Majewska-Sawka & Nothnagel, 2000; Showalter, 2001; Gaspar *et al.*, 2001; Seifert & Roberts, 2007; Ellis *et al.*, 2010; Tan *et al.*, 2012; Nguema-Ona *et al.*, 2012), AGPs are plasma membrane, cell wall and intercellular space-located proteoglycans of extremely complicated structure, which results from heterogeneity of both the protein and the glycan moieties. The name arabinogalactan proteins reflects their biochemical composition, with up to 98 % w/w of the molecule being made up of an arabinose- and galactose-rich carbohydrate moiety with the remaining proportion (up to 10 % w/w) consisting of a hydroxyproline-rich protein domain (Seifert & Roberts, 2007). Considering genetic and proteomic evidence including chimeric types of AGPs, Seifert and Roberts (2007) state that “any peptide sequence containing a secretion signal on their protein backbone and AG glycomodules can be considered AGP-like, pending experimental proof”. The backbones occur in a multitude of structures which additionally present in many different glycoforms. High carbohydrate content makes them thermo-tolerant and proteolysis-resistant (Albersheim *et al.*, 2011). They are also extremely hydroscopic and non-viscous even at high concentrations and therefore have emulsifying properties (Ellis *et al.*, 2010). On the other hand, peroxidase-catalysed cross-linking of AGPs might rigidify the cell wall (Kjellbom *et al.*, 1997). Consequently, they can grant contrasting properties to different cell wall domains, for example as pectin plasticisers and membrane stabilisers (Lamport *et al.*, 2006). Two models for their structural arrangement have been proposed: 1) twisted hairy rope, producing an elongated molecule and 2) wattle-blossom, resulting in an ellipsoidal molecule arrangement (Du *et al.*, 1996).

Traditionally, AGPs have been classified as classical or non-classical based on their structure and ability to bind to the synthetic dye, Yariv reagent (Yariv *et al.*, 1962). Classical AGPs originate as proteins anchored through a glycosylphosphatidylinositol (GPI) lipid moiety to the plasma membrane and can be subsequently released as soluble AGPs by phospholipase action (Schultz *et al.*, 1998). Non-classical AGPs do not always bind to Yariv reagent and often do not possess a GPI anchor. They have the characteristic hydroxyproline-rich domain but non-proline-rich regions

are incorporated into approximately 50% of the proteinaceous component of the particle (Schultz *et al.*, 1998).

AGPs are ubiquitous, i.e. they probably occur in all higher plants (Gaspar *et al.* 2001) or even plant cells (Majewska-Sawka & Nothnagel, 2000). Similar to polyphenolics and pectins, they are some of the most complex plant macromolecules (Ellis *et al.*, 2010). This complexity imposes many difficulties for researchers interested in their function. As a result, complete structure, specific function or a mode of action have not been assigned even to a single AGP so far. The major obstacles to recognising the biological roles of AGPs include high levels of glycosylation hampering production of backbone-specific antibodies, gene redundancy preventing characterisation of single-AGP mutants or poor characterisation of relevant glycosyl transferases responsible for their glycosylation (Tan *et al.*, 2012).

Nevertheless, AGPs show temporal-, spatial-, and species-specificity and various lines of evidence suggest that they control fundamental plant processes, (Majewska-Sawka & Nothnagel, 2000). Experiments involving treatments with Yariv reagents, specific antibodies and manipulations of culture media provide circumstantial evidence of involvement in somatic embryogenesis (McCabe *et al.*, 1997), cell proliferation (Langan & Nothnagel, 1997; Lu *et al.*, 2001) or elongation (Willats & Knox, 1996; Ding & Zhu, 1997). Numerous studies on pollen tubes have demonstrated AGPs' involvement in plant sexual reproduction, with putative functions including adhesion, growth, guidance, nutrition and rejection of pollen tubes (Nguema-Ona *et al.*, 2012). Some immunolabeling studies point to biological pattern formation by marking specific cell types or their precursors (Knox *et al.*, 1991; Dolan *et al.*, 1995). Unfortunately, it is not clear to what extent AGPs effect or only mark developmental processes (Showalter, 2001). GPI-anchored proteins including AGPs are likely to occur in lipid rafts and could form membrane microdomains interacting with microtubules (Nguema-Ona *et al.*, 2012). Links with the cytoskeleton would allow them to play roles in cell shape control.

AGPs are also known to be important during interactions with bacterial and fungal symbionts (Balestrini *et al.*, 1996; Brewin, 2004) and pathogens (Stark-Urnau & Mendgen, 1995; Vicré *et al.*, 2005; Cannesan *et al.*, 2012). That considered, and since they are thought to be involved in cell-cell communication, cell fate determination or adhesion, they are excellent candidate molecules for the regulation of haustorial development and its interactions with host tissues.

Cell wall-active enzymes

An incredibly diverse array of enzymes and respective inhibitors is necessary for synthesis and restructuring of cell walls, as many of them can handle only individual types of sugar residues and linkages (Albersheim *et al.*, 2011). One important group

includes the various carbohydrate-specific glycosyltransferases, that catalyse the transfer of specific glycan residues onto existing polysaccharide chains or glycoside hydrolases and lyases, with hydrolytic and non-hydrolytic modes of action, respectively (Fry, 1995). Another group of cell wall-associated proteins with enzyme-like functions known as expansins facilitate turgor-driven cell wall creep during cell elongation by disruption of non-covalent bonds between wall polysaccharides (Cosgrove, 2005a). Wall-modifying enzymes can also be produced by pathogens to modify the host cell wall during infection, while plants can defend themselves by producing enzymes specific for pathogen wall polymers, for example chitinases or β -1 \rightarrow 3-endo-glucanases (Jongedijk *et al.*, 1995). Cell wall carbohydrate-specific enzymes of both plant and microbial origin are grouped based on their sequence similarities in the Carbohydrate Active Enzymes (CAZY) database available online at <http://www.cazy.org/>.

Plant oxidative enzymes such as peroxidases and laccases are involved in lignin synthesis, while the same types of enzymes secreted by pathogens such as fungi contribute to lignolysis (Gavnholt & Larsen, 2002). The functions of peroxidases extend beyond lignin synthesis. Since they are capable of both generating and neutralising reactive oxygen species (ROS); $O_2^{\bullet-}$, H_2O_2 and $\bullet OH$, they enable toxification and detoxification of the cell wall (Passardi *et al.*, 2004). In addition to lignification, they catalyse suberisation, protein crosslinking, or crosslinking of carbohydrates through the coupling of wall-bound phenolic acids. These properties allow them to participate in normal plant development as well as plant defence (Passardi *et al.*, 2005). Together with nicotinamide adenine dinucleotide phosphate (NADPH) oxidases they mediate an oxidative burst of ROS during early plant responses to pathogens and the subsequent hypersensitive response (Bindschedler *et al.*, 2006; Almagro *et al.*, 2009).

While it is beyond the scope of this chapter and study to appreciably present the diversity of cell wall active enzymes, more specific examples of their implications in plant parasitism are outlined in the chapter 3.

1.2.3.3 Phenolic and lipid components

Phenolic and lipid constituents of cell walls are structurally and compositionally very complicated molecules that play important roles in mechanical reinforcement and/or waterproofing. Cell wall phenolics can occur in highly polymeric forms as lignins or as low molecular weight phenolics. They also form the aromatic part of suberins, in which they occur in addition to the aliphatic lipid fraction. Other cell wall lipids include cutin, cutan and epicuticular waxes.

Phenolics

Lignin: Lignin is an amorphous polyphenol which surrounds cell wall polysaccharides of certain secondary cell walls, typically in xylem and sclerenchyma. It renders tissues hydrophobic (Laschimke, 1989), increases rigidity and compressive strength and is a well known defence polymer in wounded and parasitized plant tissues (Vance *et al.*, 1980). Lignification starts when the protoplast is still functioning but is typically associated with eventual cessation in growth and programmed cell death, after which lignin monomers are delivered from surrounding parenchyma (Boerjan *et al.*, 2003). Lignin is extremely stable and degraded only by specific fungi, primarily Basidiomycetes or white-rot fungi (Haakka, 2001). Undecomposed lignin residues form soil humic components.

Lignin monomers; guaiacyl (G), *p*-hydroxyphenyl (H) and syringyl (S) units (Fig. 1.6), are synthesised in the cytoplasm from phenylalanine that is converted into phenylpropanoid precursors with a characteristic phenolic ring and a 3-carbon propane side chain (α , β & γ carbons) (Boerjan *et al.*, 2003). They are delivered to the cell wall through as yet unknown mechanisms in a soluble, non-toxic glycosylated form. Monolignol glucosides can also be stored in vacuoles before the onset of lignification (Whetten & Sederoff, 1995). Oxidative polymerisation occurs in the cell wall, first at the cell corners, then 'through and between the secondary walls'. It is a more random process than polymerisation of proteins and polysaccharides, with no fixed sequence of added monomers, which further complicates the structure. The monomers are connected via ester or carbon-carbon bonds. The resulting structure depends on available precursors and their concentration as well as other conditions in the lignifying region. The linkages between monomers are described by the number of the phenolic ring carbon and the letter of the propane chain carbon. The most common one is a β -O-4 linkage. The onset of lignification is associated with deposition of the first layer of secondary wall and enrichment of walls with xylan.

Lignin is a racemic polymer (Ralph *et al.*, 1999) which means that the larger the particle the more isomeric forms it can display and the less likely it is that two particles will be similar. For example a β -O-4 dimeric lignin particle can have 4 isomers while a particle of 20 monomers of structure observed in poplars with dominant β -O-4 linkages can have millions of alternative forms (Albersheim *et al.*, 2011). Biochemical diversity of lignin is spatio-temporally regulated. Early deposited lignin in middle lamellae can be, for example, enriched in *p*-hydroxyphenyl (H) in comparison to later deposited lignin (Fukushima & Terashima, 1990, 1991). Differences in lignin composition are also found between different taxa (Vanholme *et al.*, 2010; Novo-Uzal *et al.*, 2012). G units dominate in gymnosperms while lignins of angiosperms are rich in S and G. H units are virtually absent from woody angiosperms, while being present

in compression wood of gymnosperms and in grasses. Unusual monomers (Ralph, 1986; Chen *et al.*, 2012) and intermediates such as aldehydes (Kim *et al.*, 2003) can also be incorporated in small amounts, further contributing to diversity.

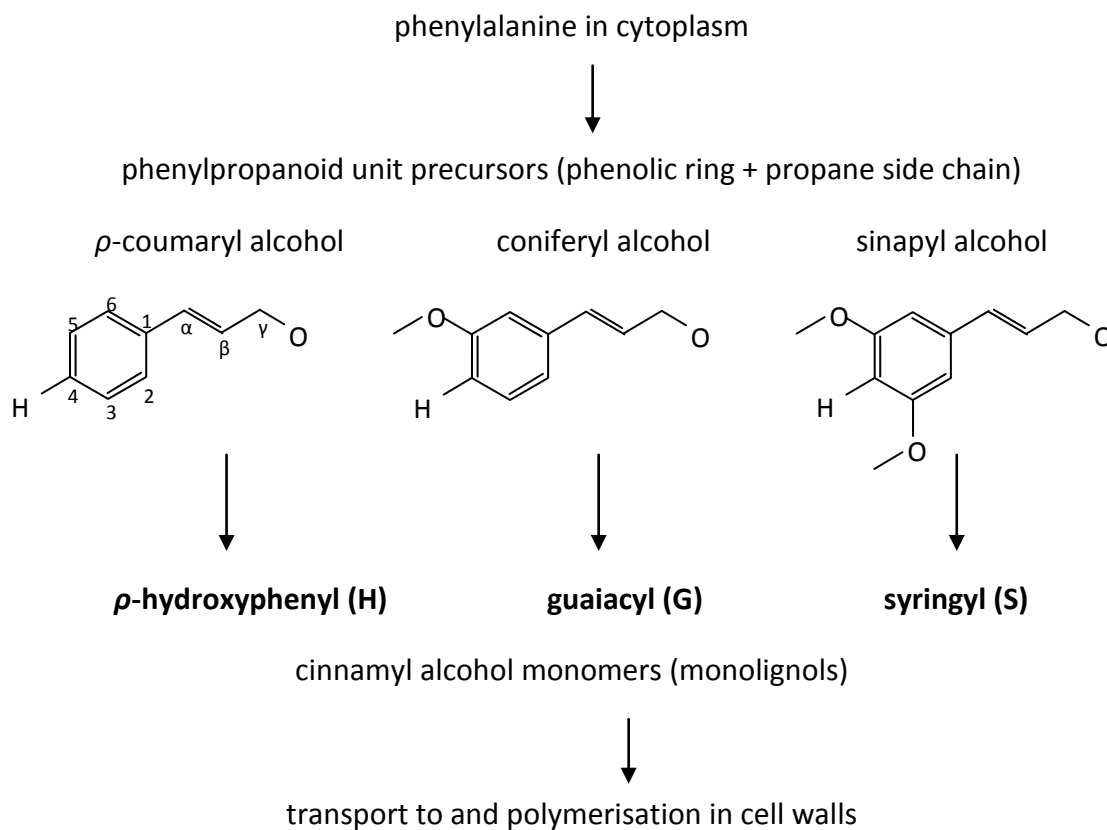


Figure 1.6: Major lignin monomers and their precursors. (author's own images)

The highly complex structure of lignin is largely unresolved as a result of an exponential diversity of linkages within lignin and between lignin residues and polysaccharides, which make it difficult to extract lignin for analysis (Hatakka, 2001). Through ester and ether linkages, they form complexes with cell wall carbohydrates (Jeffries *et al.*, 1990) that account for plant biomass resistance to decomposition, known as recalcitrance, which is one of the main obstacles to utilising the full potential of plant biomass in the biofuel industry (Himmel *et al.*, 2007) and contributes to the unavailability of lignified walls to pathogen enzymes.

Low molecular weight phenolic compounds: Phenolic acids, notably ferulic and *p*-coumaric acid, are also present in cell walls. While their presence is particularly prominent in grasses (Eraso & Hartley, 1990; Hartley & Morrison, 1991), they also occur in eudicots (Parr *et al.*, 1997; Harris & Trethewey, 2009). These phenolic acids are esterified to cell wall pectins (Fry, 1983) and hemicelluloses (Ishii & Hiroi, 1990)

and can be cross-linked, contributing to cell wall reinforcement (Kamisaka *et al.*, 1990). They also act as bridging molecules in lignin-carbohydrate complexes in grasses (Jeffries *et al.*, 1990).

Lipids

Suberin: Suberin is similar to lignin in that it is a complex, extremely stable, hydrophobic polymer (Bernards, 2002; Franke & Schreiber, 2007). However, it is composed mainly of aliphatic fatty acid monomers (predominantly C18 ω -hydroxy acids) with a relatively low proportion of phenylpropanoids (G and S subunits), ether-linked ferulic acid amides and other components. It occurs in two main forms: 1) as incrusting suberin in casparian strips of endodermis and exodermis or so called diffuse suberin appearing as striations within some epidermal walls as well as 2) adcrusting lamellae in endodermis, exodermis and cork (Peterson & Cholewa, 1998). The lamellar structure is formed when the aliphatic domains form translucent and phenolic domains form opaque layers (Bernards, 2002). In addition to preventing water loss (cork and epidermal suberin) or forming an important apoplastic barrier redirecting water and solute transfer to the protoplast (Casparian strips), suberin forms an intrinsic passive barrier for pathogens (Kamula *et al.*, 1994) and can be produced in response to wounding or infection (Lulai, 1998).

Cutin, cutan and epicuticular waxes: These three classes of lipid polymers are found cuticles of epidermis of all higher plants. Cuticles are composed of three distinctive layers; an innermost cuticular layer that contains a considerable amount of cell wall polysaccharides, the cuticle proper and epicuticular waxes (Jeffree, 2006). Cutin is an amorphous polymer of hydroxylated and esterified aliphatic acids and its monomers are typically C16–18 ω -hydroxy fatty acid chains (Pollard *et al.*, 2008). It incrusts carbohydrates of the cuticular layer and together with cutan forms the bulk of the cuticle proper. Waxes are formed by C24–34 chains and take on various crystalline morphologies on the external surfaces of cuticles or additionally incrust the cuticular layer and cuticle proper of cuticles (intracuticular wax) (Kunst & Samuels, 2003). While cutin and waxes can be removed, the remaining, resistant lipid material is formed by cutan, the structure of which is not well characterised (Pollard *et al.*, 2008).

Although the main function of the lipid polymers of cuticles is to form hydrophobic, protective layers preventing water loss, they also play roles in defence against herbivory (Eigenbrode & Espelie, 1995; Müller, 2008) and pathogen attack (Bessire *et al.*, 2007).

Cutin, wax and suberin building block synthesis starts in non-photosynthetic plastids and is continued in the endoplasmic reticulum (ER). The polymers are then assembled in the cell wall (Pollard *et al.*, 2008).

1.2.3.4 Silica

The biology of silica in plants was reviewed by Currie and Perry (2007). It is commonly associated with the epidermis but can also occur in the lumens of vessels or tracheid elements and in ray parenchyma of xylem where it is found in various forms including amorphous, crystalline, globular and sheet-like. Silica is implicated in alleviating abiotic and biotic stresses. Of particular relevance for the study presented in this thesis is the fact that proline-rich protein-mediated silica deposition was observed in *Cucumis sativa* cell walls at the site of attempted penetration by a fruit rot fungus *Colletotrichum lagenarium* (Kauss *et al.*, 2003)

1.3 Cell wall research tools, their potential and limitations for researching plant parasitism

Cell wall research tools include methods based on 1) extracting cell wall components and subsequent biochemical analysis (Fry, 1988) or 2) imaging methods whereby spatial distribution of cell wall components within tissues and individual cell walls is visualized via histological staining or, more specifically, labelling with antibodies raised against cell wall components (Hervé *et al.*, 2011; Avci *et al.*, 2012). Furthermore, genomics and proteomics enable researchers to gain insights into structure-function relationships. The first approach relies on a variety of methods, several of which are briefly mentioned here. Cell wall polysaccharides can be purified using ion-exchange chromatography and gel-permeation chromatography. They can subsequently be cleaved using either more specific cleavage by enzymes that target well recognised linkages, or using chemicals such as mild acid or base which result in breakage of a variety of linkages and a higher heterogeneity of released fragments. It is currently not possible to directly sequence polysaccharides and the available data comes from sequencing of enzyme or chemically released oligosaccharides (Albersheim *et al.*, 2011). Monosaccharides can be converted into volatile derivatives separated by gas chromatography (GC) and detected by mass spectrometry (MS). Methylation analysis is used for identifying glycosyl linkage composition, i.e. the carbons that participate in forming a linkage between residues and the types of residues. Alternatively, monosaccharides and oligosaccharides can be separated and detected by high pressure liquid chromatography (HPLC).

The second approach was chosen for this study, with a particular focus on immunocytochemistry which utilises monoclonal antibodies designed to recognise an array of cell wall components (Fig. 1.7) (Pattathil *et al.*, 2010; Lee *et al.*, 2011). Immunolocalisation is useful for researching interactions between haustoria and host tissues for several reasons. Firstly, as haustoria of many plants are relatively small structures (only up to several millimetres across in most cases), obtaining sufficient material for extraction or separating tissues of interest is often difficult. Secondly, extraction provides no information about the spatial localisation of molecules

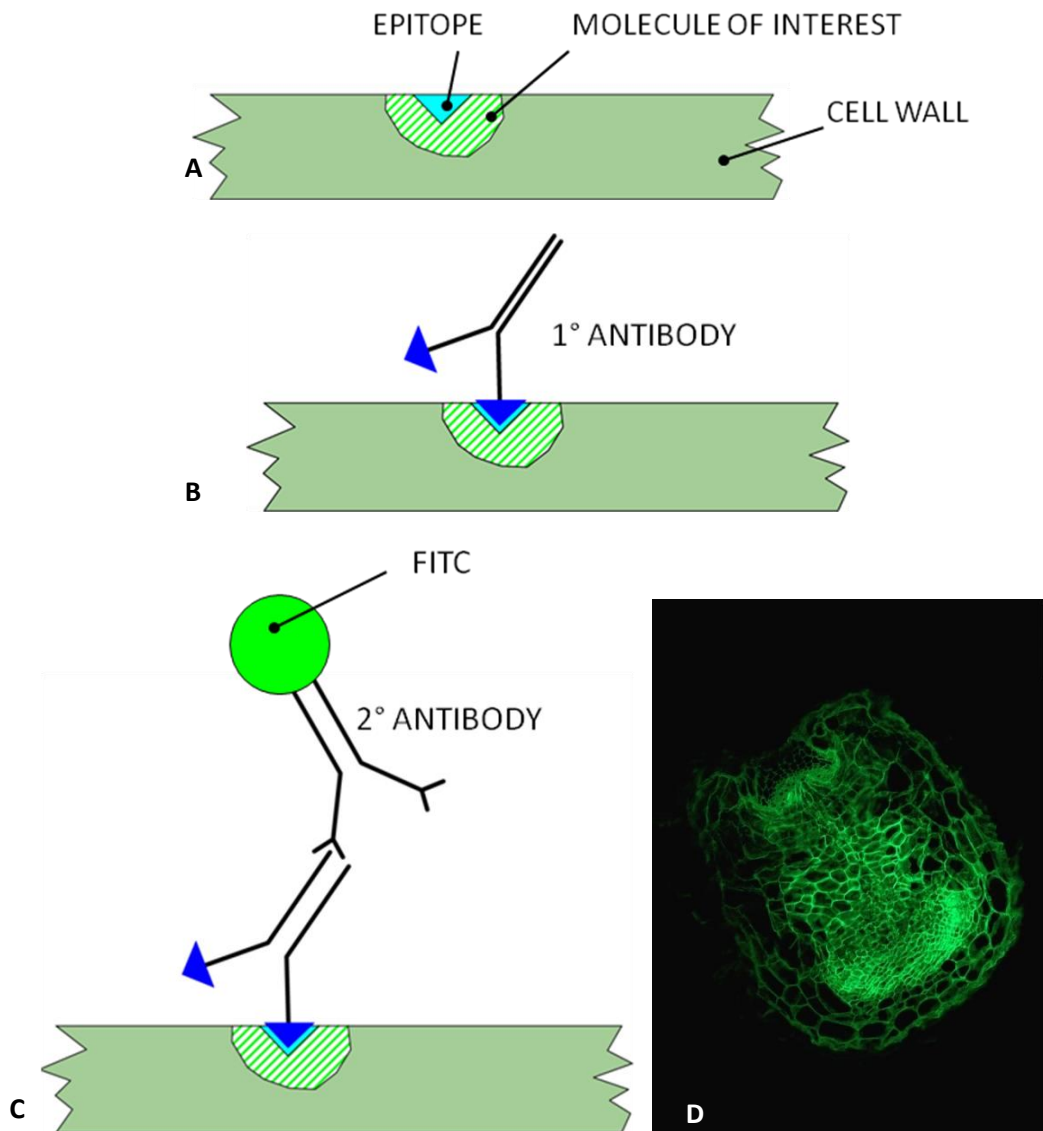


Figure 1.7: Schematic representation of the immunolabelling process. **A and B)** A section of plant material is probed with a primary antibody designed to recognize a characteristic sequence (epitope) present in the molecule of interest. **C)** Secondary antibody designed to bind to the primary antibody and conjugated to a fluorescent particle (here: fluorescein isothiocyanate, FITC) is then applied. **D)** The sample is viewed under UV light and the procedure results in the presence of fluorescence in those cell walls that possess the molecule of interest (here: chiefly de-esterified pectin localized using JIM7 mAb in this image). (author's own images)

in the tissues or individual cell walls, which is particularly important when investigating interactions and signalling between interfacial tissues of the host and parasite or digestion of host walls. On the other hand, immunolocalisation provides mainly qualitative information on certain fragments (epitopes) cell wall components, without precise quantitative data or full residue composition. Furthermore, immunolabelling produces only circumstantial evidence about the functions of detected components,

i.e. it allows correlation of molecule distribution and a type of cell at the time of material collection but does not explain their mode of action. Although genetic tools have great potential to reveal functions of cell wall constituents, this is easier achieved for proteins. Since cell wall carbohydrates are not directly coded by genes but instead are synthesised by a huge diversity of enzymes, study of their function through gene manipulation is more challenging. Nevertheless, image-based research will eventually require genetic verification, which is becoming more feasible as the Parasitic Genome Project is progressing (Westwood *et al.*, 2012).

1.4 Aims and outline of this project

This study was designed to contribute to better understanding of haustorial biology and ecology of two native Irish hemiparasites *Rhinanthus minor* L. and *Odontites vernus* (Bellardi) Dumort. using cell wall histology and immunocytochemistry. The primary aim was to immunocytochemically and histochemically characterise the cell wall biochemistry of haustorial interfaces of *Rhinanthus minor* and *Odontites vernus* with their hosts. This included two major lines of investigation:

- 1) mapping of cell wall epitopes in relation to tissue diversity within haustoria
- 2) changes in cell wall architecture related to host defence

A secondary objective was to compare local plant communities of *Rhinanthus minor* and *Odontites vernus* in terms of their floral diversity and associated hosts.

Chapter 2 summarises field-based research conducted in this study and includes the relevant methods. *Rhinanthus minor* is typically associated with higher floral diversity, higher eudicot to graminoid ratio and lower nitrogen values than *Odontites vernus*.

Chapter 3 describes laboratory methods relevant for result chapters 5 to 7, while **Chapter 4** is an elaboration on the multiple implications of cell walls in plant parasitism and provides detailed, cell wall-specific background for the subsequent chapters. **Chapter 5** presents a range of cell wall epitopes that are conspicuously upregulated throughout normal haustorial development. In particular, arabinogalactan proteins are strongly labelled in the interfacial part of the haustorium as well as the hyaline body, where they are associated with reduced detection of de-esterified pectin epitopes. Furthermore, extensins and AGPs are associated with xylem bridge differentiation. **Chapter 6** compares haustorial anatomy on a range of species, including some previously not investigated as hosts. The characteristic epitope distribution patterns described in chapter 4 do not differ with different hosts except extreme cases of bad hosts, suggesting that they are well preserved and fundamental to haustorial development and functioning. Furthermore, successful haustorial connections between *R. minor* and non-legume eudicot hosts are reported for the first time. **Chapter 7** focuses on extramural phenolic substances of the interfacial region, based on an unprecedented approach using so called meta-haustoria which attach to pot surface instead of host roots. Results suggest that phenolic substances generally believed to be synthesised by hosts as a form of defence are at least partly produced by and serve the parasite. Finally, **Chapter 8** discusses the possible relationship between and relevance of all of the above elements of this work.

2 Grassland communities of *Rhinanthus minor* and *Odontites vernus* in two limestone landscapes of the Irish West

2.1 Abstract

Rhinanthus minor and *Odontites vernus* are the two most common native Irish hemiparasites and both occur in grassland habitats. *Rhinanthus minor* is a species important for biodiversity and is primarily confined to semi-natural communities while *Odontites vernus* is a weed of arable systems and marginal communities such as road verges. A vegetation survey of grasslands rich in *Rhinanthus minor* and *Odontites vernus* was undertaken on three sites located in two major limestone landscapes in the West of Ireland: West Corrib landscape and the Burren. The aim was to compare stands abundant in either, both, or neither of these two hemiparasitic species and identify community traits associated with their presence. Sampling was targeted at grassland patches with high abundance of hemiparasites and control relevés without parasites in immediate vicinity were recorded for comparison. A total of 94 relevés were surveyed and grouped by means of cluster analysis which complimented NMS ordination.

Differences between hemiparasite-rich and control relevés were negligible and separation occurred mainly at site- and habitat-specific level. Six vegetation groups were identified within two phytosociological classes: *Molinio-Arrhenatheretea* (lowland meadows and pastures on neutral soils) and *Festuco-Brometea* (thermophilous species-rich grasslands on calcareous substrates). Both species were found within the two classes with notable differences in abundance between the six groups. Therefore, the groups were further classified within the 3 *Rhinanthus* groups, 2 *Odontites* groups and 1 *Rhinanthus/Odontites* group. A general positive association was seen between *Rhinanthus minor* abundance and high quality habitat parameters such as high species richness, high forb richness, high forb to graminoid ratio or bryophyte cover. *Odontites vernus* was generally associated with higher soil nutrient status as expressed by Ellenberg nitrogen indicator values and poorer habitat quality expressed in lower species richness and lower forb to graminoid cover ratio. However, under the conditions of disturbance in limestone grassland, *Odontites vernus* was associated with the highest species richness recorded in this study.

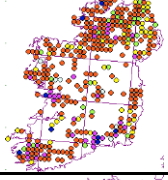
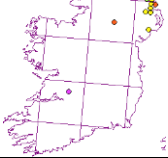
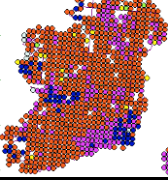
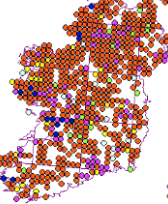
The results show that both *Rhinanthus minor* and *Odontites vernus* are associated with important, species-rich grassland habitats in Ireland and have the potential to impact their structure. This highlights the need to further compare the ecological dynamics of the two species and their effects on grassland habitats under different management regimes as well as potential cumulative or opposing effects in cases of distribution overlap.

2.2 Introduction

The parasitic flora of Ireland is relatively small and is represented by three genera of holoparasitic plants (*Cuscuta*, *Lathraea* and *Orobanche*) and seven genera of hemiparasites (*Euphrasia*, *Melampyrum*, *Odontites*, *Parentucellia*, *Pedicularis*, *Rhinanthus* and *Viscum*). Shoot parasites are represented by only two genera with only one species of each present in Ireland. The native holoparasite *Cuscuta epithymum* (dodder) occurs in coastal areas, while previous records of *Cuscuta epilinum* are now believed to be errors (Parnell & Curtis, 2012). A non-native hemiparasite *Viscum album*, which is the only non-herbaceous parasite in Ireland, is found in several scattered locations in the East and South-East, including the Botanic Gardens in Glasnevin, Dublin (Reynolds 2002). Similar to these two shoot holoparasites, *Lathraea squamaria*, a holoparasite growing on roots of trees and shrubs, notably *Corylus avellana* is the only example of its genus in Ireland. *Orobanche* is represented by 4 species: 1) *Orobanche alba*, parasitic on *Thymus*; 2) *Orobanche rapum-genistae*, parasitic on *Ulex* and *Cytisus* (both in the Fabaceae); 3) *Orobanche hederæ*, parasitic on *Hedera*; and 4) the non-native *Orobanche minor*, parasitizing a range of hosts, notably *Trifolium* and species of Asteraceae. *O. hederæ* and *O. minor* are most widespread while *O. alba* and *O. rapum-genistae* occur rather infrequently in scattered locations (Preston *et al.*, 2002).

Root hemiparasites feature by far the most prominently in Irish grasslands, with seven genera found on the island (Table 2.1). These are close relatives formerly classified within the Scrophulariaceae but since moved to a monophyletic clade within Orobanchaceae (Westwood *et al.*, 2010). *Pedicularis* is somewhat more distantly related and is classified within a separate clade that diverged earlier together with *Castilleja*, *Agalinis* and a few other taxa (Bennett & Mathews, 2006). The Orobanchaceae also includes *Lathraea squamaria* and, most obviously, *Orobanche* spp. and therefore most of the Irish parasitic taxa are found in this family. While classification of most Irish parasitic taxa within Orobanchaceae highlights the common general life strategy, only parasitism by the most widespread species are likely to have a marked effect on community ecology. *Rhinanthus minor* (yellow rattle) and *Odontites vernus* (red bartsia) are the most widespread. Distribution of *Euphrasia* treated as a genus or aggregate species *E. officinalis* also spans the entire island. However, the individual species can be much more restricted. The most distinctive of all, *Euphrasia salisburgensis*, for instance, is found only in the Mid-West and to the east of Sligo Bay (Preston *et al.*, 2002), where there is much outcropping limestone. *Pedicularis palustris* and *P. sylvatica* also occur throughout the country although they are found primarily in waterlogged areas and heathland or heathy grassland, respectively.

Table 2.1: Summary of the distribution and ecology of herbaceous hemiparasitic taxa found in Ireland. Distribution maps (Preston *et al.*, 2002) were obtained from the website of the Botanical Society of Britain and Ireland (bsbi.co.uk).

species	distribution in Ireland	Ellenberg values (Hill <i>et al.</i> , 1999)					Habitat (Parnell & Curtis, 2012)
		light (L)	moisture (F)	pH (R)	nitrogen (N)	salt (S)	
<i>Euphrasia</i> spp. (11 species) Eyebrights (distribution shown for <i>Euphrasia</i> agg.)		7–8	4–6	2–8	2–4	0; 3	Pastures, rough grassland, disturbed grassland, limestone grassland, meadows, heath, fens, roadside verges, field margins, stabilised dunes, mountain cliffs and exposed places near the sea
<i>Melampyrum pratense</i>		5	5	2	3	0	woods, bog margins, stony lake shores and mountain slopes
<i>Melampyrum sylvaticum</i>		4	5	2	2	0	woods and mountain glens in Antrim and Derry
<i>Odontites vernus</i>		7	5	6	5	0	pastures, roadsides and stony places
<i>Parentucellia viscosa</i>		7	7	7	5	0	damp grasslands
<i>Pedicularis palustris</i>		8	8	5	2	0	marshes, fens and meadows
<i>Pedicularis sylvatica</i>		8	8	3	2	0	damp or heathy upland pastures, moorland and drier parts of bogs
<i>Rhinanthus minor</i>		7	5	6	4	0	meadows and pastures

Colours indicate records by date: **blue** — up to 1930, **yellow** — 1930–1969, **green** — 1970–1986, **orange** — 1987–1999, **magenta** — 2000–2009, **navy** — 2010 onwards

Chapter 2

Parasitic plants are known to impact community structure by changing competitive interaction between their hosts and non-hosts (Press & Phoenix, 2005). As grasslands are the habitats for most Irish parasitic taxa (Table 2.1), including the most abundant ones, this is where their impact on community structure is likely to be most obvious. Currently, no Ireland-based studies on the impact of hemiparasites on grassland community structure exist. This is unfortunate as Irish grasslands are often quite different than their counterparts in Britain and continental Europe, with fewer species present often in unusual combinations (Pilcher & Hall, 2001). Therefore, they might respond differently to parasitism.

Furthermore, ecological studies on parasitism-associated grassland dynamics in Ireland would be beneficial for developing biodiversity management strategies as parasitic plants as well as species-rich grasslands that often host them have been subjected to the pressures of agricultural transformation and are disappearing. The survival of species-rich grassland communities depends on traditional, low-intensity management whereby grassland is cut for hay in July and grazed by cattle in the winter (Martin, 1991). Late cutting allows seeds to reach maturity while trampling by cattle in the winter time helps to mix the seeds with the soil. Regular removal of cut vegetation maintains low soil fertility. Agricultural intensification associated with the use of fertilizers, heavy grazing and early cutting for silage brings negative changes to grassland ecosystems (Plantureux 2005). It promotes vigorous and vegetatively reproducing species whereas taxa that depend on seed production or that do not tolerate high fertility are eliminated. Intermediate nutritional conditions usually allow the coexistence of many mesotrophic species with oligo- and eutrophic taxa and therefore contribute to high biodiversity (Plantureux 2005).

Agricultural intensification, which followed Ireland's accession to the European Union (Feehan, 2003), has been a major threat to grassland diversity in this country. McGough (1984) remarked in his work on the grasslands of the Burren that species-rich dry meadows were very rare and declining and could disappear within ten years if no conservation measures were undertaken. Martin (1991) expressed similar concern with regard to the hay meadows of the limestone area of West Corrib in County Galway. Unfortunately, species-rich grasslands continued to vanish and between 1996 and 2007, the area of hay meadows in Ireland decreased from 371,500 ha to 243,300 ha and areas under management for silage increased from 956,100 to 1,039,900 ha (O'Mara, 2008), reflecting the general trend of agricultural intensification. Most grassland habitats in Ireland exist currently as improved agricultural (GA1) and amenity grassland (GA2) (Fossitt 2000). Species-rich grasslands remain on grounds unfavourable for agriculture (Pilcher & Hall, 2001). Sullivan *et al.* (2010) found that only 10% of farmland grasslands studied in East Galway were of high nature value and most of them were found on wet sites. Similarly, wet grasslands were consistently the most frequent type of habitat recorded in the Irish Semi-natural Grassland Survey (Martin *et al.*, 2007, 2008; O'Neill *et al.*, 2009, 2010). Shannon

callows (seasonally flooded meadows) are one of the most important habitats for floristically-rich grasslands in Ireland (Heery, 1996). Dry species-rich grasslands occur mainly on sites which are not accessible to farmland machinery (Pilcher & Hall, 2001), for example esker ridges (Tubridy, 2006; Tubridy & Meehan, 2006a,b) or limestone grasslands of the Burren (Parr *et al.*, 2009).

The potential implications of grassland habitat loss cannot be ignored in a country where grasslands constitute over 60% of land cover. The value is approximate as no up-to-date, systematic record, with respect to distribution and classification, of Irish grassland habitats exists. While O'Sullivan (1982) estimated that various grasslands comprised over 70% of Ireland's area, Byrne (1996) discovered that 38% of grasslands surveyed by O'Sullivan were no longer semi-natural communities and total grassland cover had dropped to approximately 60%. Jeffrey *et al.* (1995) state that "Irish agriculture is dominated by grasslands, with approximately 16 million animals grazing 5.6 million ha, or 93% of agricultural land".

In terms of classification, the milestone phytosociological groundwork of Braun-Blanquet and Tüxen (1952) formed the basis for more focused studies, for instance on Irish lowland grasslands (O'Sullivan, 1982) or grasslands in locations of particular botanical interest such as the Burren (Ivimey-Cook & Proctor, 1966; McGough, 1984). The guide to Irish habitats by Fossitt (2000) is quite broad with grassland categories corresponding with phytosociological categories of more general level, ie. orders and alliances but not associations. On the other hand, the classification proposed in Rodwell's detailed volume on British grassland communities (Rodwell, 1992) is not always practical for Ireland, partly because of its reduced flora and unusual communities. Certain seminatural grasslands are classified within the Natura 2000 Habitats Directive Annex I, which lists vegetation types of conservation importance. Seven Annex I habitats are found in Ireland (Martin *et al.*, 2007): Calaminarian grasslands of the *Violetalia calaminariae* (6130), Semi-natural dry grasslands and scrubland facies on calcareous substrates (*Festuco- Brometalia*) (6210), Semi-natural dry grasslands and scrubland facies on calcareous substrates (*Festuco-Brometalia*) (important orchid sites) (6211), Species-rich *Nardus* grasslands, on siliceous substrates in mountain areas (and sub-mountain areas, in Continental Europe) (6230), *Molinia* meadows on calcareous, peaty or clayey-silt laden soils (*Molinion caerulea*) (6410), Hydrophilous tall herb fringe communities of plains and of the montane to alpine levels (6430) and lowland hay meadows (*Alopecurus pratensis*, *Sanguisorba officinalis*) (6510); priority status has been given to 6211 and 6230.

The very recently completed Irish Semi-natural Grassland Survey will provide an up-to-date overview of high value grassland habitats and a more comprehensive classification, as well as new data on the distribution of parasitic plants. While several annual reports have been published (Martin *et al.*, 2007, 2008; O'Neill *et al.*, 2009, 2010), the synopsis report is not yet available. Nevertheless, the latest of the reports

Chapter 2

divides Irish seminatural grasslands into 5 major vegetation groups, further subdivided into 34 vegetation types. These results are so far the most detailed in terms of classification. Sub-association *Centaureo-Cynosuretum galietosum*, for instance, which is one of the most common hay meadow associations is further subdivided into three vegetation types.

The focal species of this study, *Rhinanthus minor* and *Odontites vernus*, inhabit grasslands with different levels of diversity. *Rhinanthus minor* is typically associated with higher species richness, although the precise differences are not known as *Odontites vernus* has achieved disproportionately less research attention. While *Rhinanthus minor* has been under extensive scientific scrutiny for the past three decades, few references to *Odontites vernus* can be found in literature.

Rhinanthus minor, finds optimal growth conditions in moderate to low fertility grassland (Westbury 2004). While it used to occur in cereal fields (Long, 1924) it no longer does and it is considered a species primarily of semi-natural grasslands (Westbury, 2004). It does not have a permanent seed bank (seeds are viable for only one season) and does not reproduce vegetatively and therefore depends on annual seed production to survive (Westbury 2004). This has important implications from a conservation point of view as theoretically one year of unsuitable management, in particular an early cut before seed maturation, can wipe out a population of this species. Yellow rattle was classified as declining by Grime *et al.*, (1988). Although its status has not been systematically updated since, considering the general trend of farming intensification it is highly unlikely that it has improved.

As a facultative hemiparasite, *Rhinanthus minor* is quite generalist in its choice of hosts. Although their range is wide (Gibson & Watkinson, 1989), resistance varies. As a result grasses and legumes are parasitized more successfully than non-leguminous eudicots (Cameron *et al.*, 2006; Cameron & Seel, 2007; Rümer *et al.*, 2007). While the histological basis for differential resistance was mentioned briefly in chapter one and is further discussed in chapters 4–7, in this chapter I specifically remark on the ecological consequences of host preference. Biomass of good hosts is usually significantly reduced, which is the case particularly consistently with grasses, while legumes are not always affected in terms of vigour and cover (Joshi & Matthies, 2000; Cameron *et al.*, 2005). Since non-leguminous dicots are non-hosts i.e. they do not support infection, their biomass is not reduced. Therefore, in a grassland community yellow rattle typically weakens grasses more than forbs (non-leguminous perennial eudicots as defined by Cameron *et al.*, 2006 for *Rhinanthus minor* hosts and adopted in this study for consistency) and shifts the competitive balance in favour of the latter (Davies *et al.* 1997; Pywell *et al.* 2004). This has implications for biodiversity restoration. When *Rhinanthus* is sown into a grass-dominated community it can reduce the vigour of grasses and facilitate colonisation by less competitive flowering plants (Westbury and Dunnett 1997). Furthermore, parasitism by *Rhinanthus minor* leads to a general reduction in grassland productivity (Ameloot *et al.*, 2005). It can

consequently be applied in environmental management for increasing grassland biodiversity (Pywell *et al.* 2004) as a relatively easy and cheap complimentary or alternative technique to very labour-intensive and expensive means of reducing residual fertility, for example removal of topsoil.

Odontites vernus is native to Europe and Eurasia and occurs as an alien in North America (USDA, 2013). It is much less researched than *Rhinanthus minor*, and presumably as a result of this it did not sport a profile within Grime's renowned "Comparative Plant Ecology" (Grime *et al.*, 1988), while being mentioned only in the ecological attribute tables. The only dedicated works on the species are those on the physiology of its nutrition by Govier *et al.* (1967, 1968) and on the effect of different hosts on its growth by Snogerup (1982) as well as a recent publication on the genetics of its ecotypes by Koutecký *et al.* (2012). According to Stace (2010) there are three subspecies in the British Isles: the most common aestival subspecies *vernus* of grasslands, waysides as well as more disturbed habitats of arable and waste ground; aestival subspecies *litoralis* of saltmarshes and rocky sea-shores in Great Britain but not Ireland; and an autumnal subspecies *serotinus* occurring in the habitats of both of the other subspecies in Britain and Ireland. *Odontites vernus* is likely to be less sensitive to the increasing management pressures as it is much more tolerant of disturbance and is likely to take advantage of it (Hirst *et al.*, 2005). Furthermore, its seeds remain viable for up to 5 years, making it less vulnerable to elimination by early cutting. However, it should be noted that Albrecht *et al.* (2007) classified *Odontites vernus* as a rare arable weed in Germany and found that it was associated with organic but not conventional farming practices.

In this study, three species-rich grassland sites on limestone in the West of Ireland were surveyed. The aim was to characterise and compare the communities of *Odontites vernus* and *Rhinanthus minor* within and between these three locations and to identify community traits associated with the two species. Vegetation types that these hemiparasites occurred in were identified. Furthermore, it was investigated how hemiparasite cover related to species richness and proportions between three groups of plants: legumes, non-leguminous eudicots (referred to as forbs) and graminoids, i.e. functional groups of hosts.

2.3 Methods

2.3.1 Site selection and characteristics

Three species-rich grasslands of limestone landscapes near Galway City in the West of Ireland were surveyed in this study (Fig. 2.1).

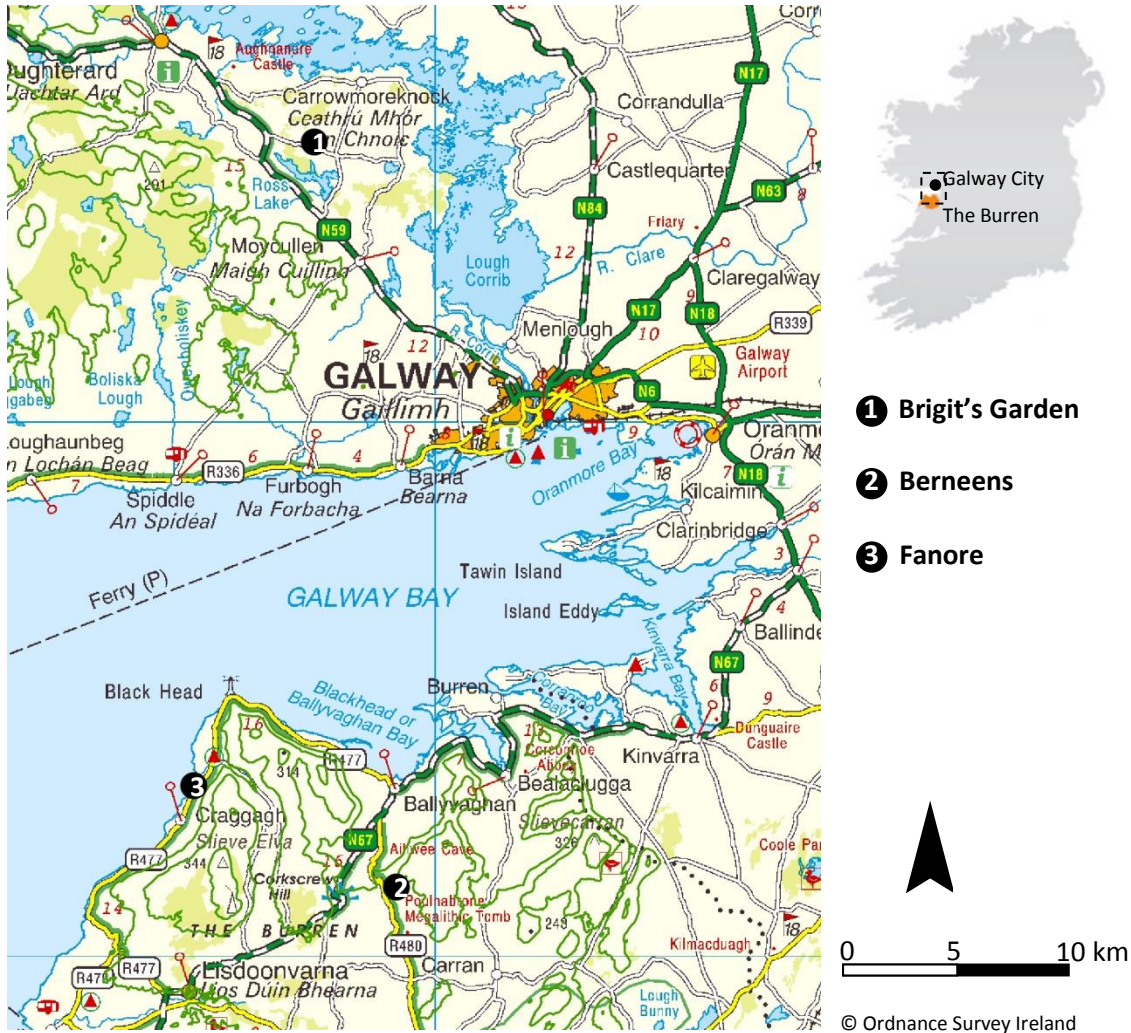


Figure 2.1: Approximate locations of the field sites (1, 2 and 3) and location of the Burren (small map inset). Green contour lines are isolines of 100 m above sea level.

Originally, Brigit's Garden (relevé code BG) in Roscahill, Co. Galway was chosen as the exclusive site for field research (Fig. 2.2). The site is located in the heart of the West Corrib limestone landscape (53°23'09 N, 9°12'42 W) — the only limestone area found to the west of Lough Corrib (McDonagh, 1992). Carboniferous limestone and calcareous shale form the bedrock of this flat area that typically does not rise above several metres above sea level. The area consists of small fields, poor pastures and meadows, contrasted with areas of bog, and the Killanin Esker which stretches from Roscahill Village to Tullykyne Village (west to east). Species-rich meadows used to be a common and well recognized component of this landscape but have declined dramatically as a result of intensive farming (Martin, 1991; Caitriona Carlin, *pers.*

comm.). *Rhinanthus minor* still grows locally on the grassy verge along the road running on top of the esker and in the remaining unimproved hay meadow fields.



0 20 40 80 Meters



© Ordnance Survey Ireland

Figure 2.2: Detail of site 1 (Brigit's Garden) location (white line). The extent of Little Meadow (the sampled meadow) is shown with a dashed yellow line. The road forming the southern boundary of the garden follows the direction of Killanin Esker.

Brigit's Garden was set up on formerly intensively farmed agricultural ground (Jenny Beale, *pers. comm.*). A part of the north slope of the esker including a fragment of dry grassland (Esker Meadow) with *Rhinanthus minor* is located in the garden. The site has been managed at low intensity to allow restoration of species-rich meadows typically found in this area. Brigit's Garden hosts a range of small grassland habitats that differ in their topography, management, plant communities and abundance of yellow rattle. A natural population of the hemiparasite grows in the Esker Meadow located on the esker slope. *Rhinanthus minor* shows great annual fluctuations of abundance

in this meadow and was very scarce during this study. Little Meadow (Fig. 2.2) was chosen for this study. It is located in the lower-lying parts of the garden. Although located in immediate vicinity to a waterlogged Rushy Meadow, it is better drained as it occupies part of a disjoint area of gravelly esker deposits (McDonagh, 1992). Nevertheless, soil in this part of the garden is classified as poorly drained mineral soils with peaty top soil (peaty gley) derived from carboniferous limestone till (EPA Envision, <http://gis.epa.ie/Envision/>). Yellow rattle seeds collected from the esker were sown here during winter 2007/08 and the species was already very abundant at the start of this project (2010).

The amenity character of the grassland did not allow very invasive experimental methodologies to be implemented. Therefore, a decision was made to expand the study to other sites in the second year of the project (2011). The remaining time of the study was too short to apply community manipulation experiments and therefore focus was placed on characterising differences between the communities of *Rhinanthus minor* and *Odontites vernus*, following the inclusion of the latter species into laboratory studies.

The additional two sites, both with *Rhinanthus minor* and *Odontites vernus* present, were selected within the Burren — an area of County Clare displaying unique geology and high botanical interest. Similar to the area to the west of Lough Corrib, the Burren's geology is dominated by limestone. The area is, however, of hilly character, rising up to 300 m above sea level (Ivimey-Cook & Proctor, 1966). The limestone is typically exposed forming pavement clints (blocks of limestone) and grykes (fissures, in which pockets of soil accumulate supporting vegetation). Numerous karstic features, including turloughs (lakes fed by ground water in the winter and drying out in the summer) are present. The Burren hosts an internationally unique congregation of plants, whereby arctic-alpine species such as *Dryas octopetala* and *Gentiana verna* grow unusually close to the sea level and co-occur with Mediterranean species, for instance *Neotinea maculata* and *Helianthemum canum* (Webb & Scannell, 1983).

A site in Berneens townland (relevé code B) (53°04'20.00" N, 9°09'06.00" W) on a plateau in the high Burren (approximately 155 m above sea level at the surveyed area) was selected as the second sampling location (Fig. 2.3). It falls within the Moneen Mountain Special Area of Conservation and National Heritage Area that protects extensive areas of limestone pavement and semi-natural dry grasslands and scrubland facies on calcareous substrates (*Festuco-Brometalia*), including important orchid sites (NPWS, 2011). It is characterised by shallow, well drained rendzinas and lithosols derived from calcareous materials underlain by karstified fossiliferous limestone bedrock which is frequently exposed (EPA Envision, <http://gis.epa.ie/Envision/>). Similar to many other grassland areas in the Burren, it is managed as a winterage grassland, i.e. it is grazed during the winter (October to March) and left ungrazed during the

summer months. *Odontites* is particularly abundant on this site and it co-occurs with less abundant *Rhinanthus minor* and *Euphrasia* spp.

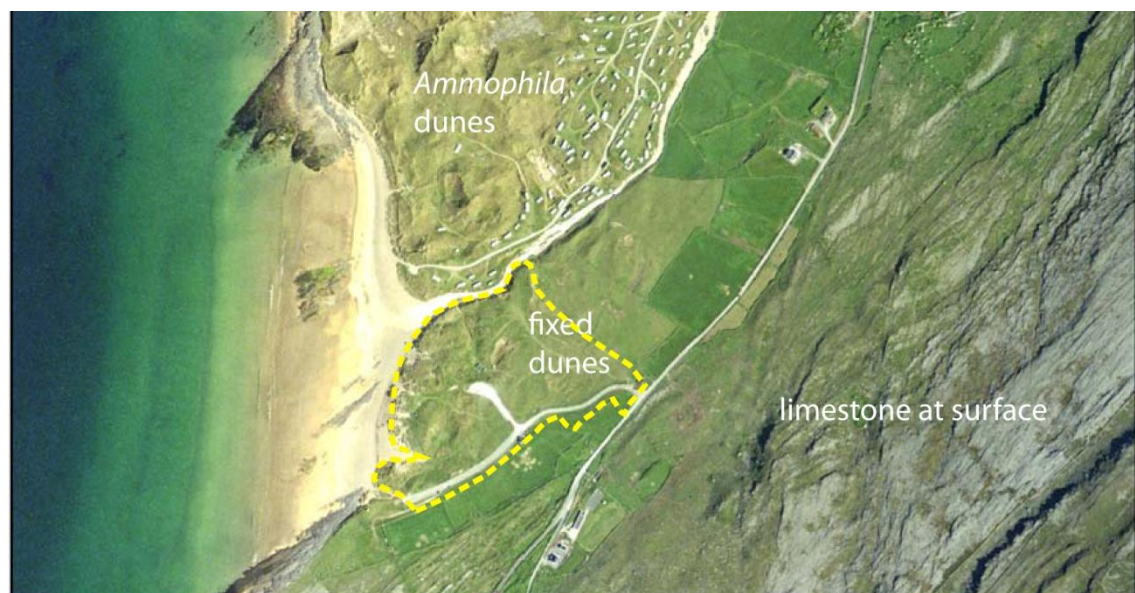


0 45 90 180 Meters



© Ordnance Survey Ireland

Figure 2.3: Detail of site 2 (Berneens) location. Yellow dashed line marks the extent of sampled community. Darker colouration of the delineated area is a result of disturbance and exposure of the soil. The general area is sloping towards the North-West and the sampled location is roughly flat.



0 100 200 400 Meters



© Ordnance Survey Ireland

Figure 2.4: Detail of site 3 (Fanore) location. Yellow dashed line marks the extent of sampled area. Shifting *Ammophila* dunes located along the shoreline occupy approximately two fifths of the area and gradually become fixed grey dunes. Further detail including relevé distribution is provided in the results section.

Chapter 2

Fanore (53°07'07.50" N, 9°17'02.50" W) sand dune system (relevé code F) was selected as the third sampling site. It forms part of the Burren coastline and is characterised by aeolian undifferentiated soils on carboniferous limestone tills and raised beach sands and gravels underlain by dolomitised limestone with shale (EPA Envision). The dune complex is under a conservation programme (Burrenconnect, http://www.burrenconnect.ie/environment/conservation_programme.html) as it forms part of the Blackhead-Poulsallagh Complex Special Area of Conservation. The sampled extent of the site does not contain any limestone pavement and can be subdivided into three distinctive areas: 1) a neglected, uncut grassy verge adjacent to silage fields to the south of the driveway, 2) a middle area of grey dunes with thermophilic grassland vegetation and 3) a complex of tall dunes dominated by *Ammophila arenaria* and dune slacks forming a wetter and more fertile habitat. These three areas are shown in more detail in figure 2.6 in the results section. The latter two correspond with Annex 1 habitats found within the site. These are “fixed coastal dunes with herbaceous vegetation (grey dunes)” — code 2130, embryonic shifting dunes — 2110, and “shifting dunes along the shoreline with *Ammophila arenaria* (white dunes) — 2120” (Burrenconnect). The site is grazed by cattle in the winter as well as by rabbits, as evidenced by numerous rabbit burrows and droppings and very low height of the sward all year round (personal observations).

All three sites are subject to a hyperoceanic climate and are located to the west of the '20' isoline on the oceanity index (a ratio between mean annual number of rain days and the range of mean monthly temperatures) of Averis *et al.* (2004). The climate is therefore milder and less extreme between summer and winter months than that of continental locations of the same latitude (Sweeney, 1997). High winter temperatures are a result of the influence of the Gulf Stream. The mean winter temperature for the study sites is 6°C and is only 7 degrees lower than the summer mean temperature (Walsh, 2012). The oceanic influence results not only in relatively cool summers but also in high annual rainfall. Mean annual precipitation is 1,200–1400 mm at Fanore, 1,600–1,800 mm at Berneens and 1,400–1,600 mm at Brigit's Garden (Walsh, 2012), with over 180 rain days for all three areas. The average annual temperature for all field sites is approximately 10°C (Walsh, 2012).

2.3.2 Sampling

Data were collected during the summer of 2011. The general approach was to compare patches of grassland with dense cover of *Rhinanthus minor* and/or *Odontites vernus* and adjacent patches free of parasites. A relevé size of 1 m × 1 m was selected and a timber frame quadrat subdivided with string into a 10 cm × 10 cm mesh was used to facilitate sampling. While this size is typically thought to be the minimum for grassland surveys and can result in considerable deviation of ordination results (Otypková & Chytrý, 2006), it was justified for the sampling approach applied in this study as it matched the size of densely-

parasitised grassland patches. Applying a larger size would likely have blurred the differences between parasitised and non-parasitised patches or the effects of extreme differences in parasite abundance.

At Fanore and Berneens *Rhinanthus minor* and *Odontites vernus* typically occurred in discrete patches, up to several metres across. The small size of these homogenous areas did not allow for stratified randomised sampling (randomised sampling within homogenous areas). Examples distributed across the two sites were therefore sampled by locating the relevés in the areas of locally highest density of the parasite. For each relevé with abundant *R. minor* or *O. vernus* a control relevé preferentially without parasites or otherwise with parasite cover below 1% was surveyed. Occasional areas occurred where the two species overlapped in distribution; these were sampled in the same manner (pairs of relevés with and without parasites). Relevé locations were chosen randomly within Little Meadow where *Rhinanthus minor* was distributed very uniformly and essentially no control relevés could be applied. The map of the site was overlain with a 2m × 2m grid. The nodes were numbered and a random number generator was used to select 20 relevés.

Percentage cover was estimated at approximately 1% precision and no generalised scale was used. Only those plants that were rooted within the relevé were included. Bryophyte, litter, bare ground and rock/stone cover were also recorded as percentage cover. To provide information on how evenly the hemiparasites were distributed within the relevés, a number of quadrat grid squares (10 cm × 10 cm) that hemiparasites were rooted in was also recorded as frequency.

2.3.3 Data analysis

Simple statistical computations such as a correlation coefficient calculation were carried out in Minitab 16. PC-ORD 5 (Grandin, 2006; McCune & Mefford, 2006) software was used for multivariate community analysis. Outlier relevés were first identified as those beyond 2 standard deviations from the mean (McCune & Grace, 2002). Five such relevés were found, as listed in table 2.2. While outliers are typically excluded from the analysis to increase result interpretability, comparison of autopilot results (not shown) showed no major effect on the results. Therefore, all relevés were included.

Table 2.2: Outlier relevés identified in this study

relevé ID	average distance	st.dev. from the mean
B8	0.94473	3.43783
F28	0.88501	2.27198
F52	0.87801	2.13536
F7	0.66463	-2.03057
F21	0.65710	-2.17769

Chapter 2

Using PC-ORD, the relevés were classified into groups and ordinated. Grouping results in discrete categories of relevés based on floristic similarities, while ordination arranges relevés spatially in a continuous manner along hypothetical axes representing theoretical gradients typically corresponding with environmental gradients. The grouping can be used as a categorical variable overlain with ordination results to help explain the results of the latter.

In order to group the relevés, hierarchical, polythetic, agglomerative cluster analysis was carried out. It is more suitable for community data analysis than other grouping techniques such as TWINSpan (McCune & Grace, 2002). Sørensen (Bray-Curtis) was the distance measure used and Flexible Beta ($\beta = -0.25$) was the linkage method applied. The cluster analysis procedure is carried out repeatedly starting with creation of two groups and each subsequent run returning one more group than the previous. The analysis can theoretically be repeated until all resultant groups include only 1 relevé. However, the aim is to reach a number of groups that best reflect ecological differences. While determination of a suitable number of groups has a subjective component, the choice is based on certain statistical parameters. To obtain these, the cluster analysis procedure is first carried out a number of times higher than what seems a reasonable number of groups (communities) for a particular data set. For the data set in this study the cluster analysis procedure was repeated 9 times (i.e. resulting in 9 clusters containing 2–10 groups). Subsequently a cut-off point for the number of groups is determined using Indicator Species Analysis (ISA) (Perrin *et al.*, 2006). ISA determines the affinity of all individual species for the output groups from cluster analysis. The more consistently and abundantly a species is found within the relevés in a group, the better indicator species it is. This is reflected in the indicator value for this species which can be in the range from 0 (non-indicator species) to 100 (perfect indicator species). In addition to indicator values, significance of individual species as indicator species can be calculated. *P* values are then averaged for all species in each group and subsequently plotted against the number of significant ($p \leq 0.05$) indicator species for each cluster. The number of groups is selected as the optimum balance between the highest number of indicator species and the lowest average *p* value. The Monte Carlo method was used to assess the significance of individual species in this study.

Multivariate community analysis was carried out using Non-Metric Multidimensional Scaling (NMS). The resultant ordination allows for establishment of links between relevés (primary matrix) and other, e.g. environmental variables (secondary matrix). The relevés are represented as points within a theoretical space. Distances between points reflect dissimilarities. The quantitative variables from the secondary matrix are represented as vectors of length positively correlated with significance while categorical data can be overlain with relevés and used as grouping variables. Length of the vectors informs about the strengths of correlation with relevés. The angle

between a vector and an axis reflects the correlation between both, i.e. the closer to parallel the two are, the higher the correlation.

Quantitative secondary matrix variables used in this study are summarised in table 2.3. While Ellenberg indicators (Hill *et al.*, 1999) are principally categorical with categories numbered from 1 to 9, they reflect environmental gradients and can be averaged for all species in a relevé, with resultant values used as a quantitative variable. Such surrogate variables allow inclusion of environmental factors into analysis without the data having to be physically obtained. In this study, this was carried out for three Ellenberg indicators: moisture (F), Nitrogen (N) and pH (R — reaction). A value of 1 represents the lowest, and 9, the highest moisture, nitrogen and pH.

Categorical variables used were vegetation group numbers from cluster analysis, and the presence of *Rhinanthus* and *Odontites* defined as:

- 0 — neither hemiparasite present
- 1 — only *Rhinanthus* present
- 2 — only *Odontites* present
- 3 — *Rhinanthus* and *Odontites* present

Table 2.3: Quantitative secondary matrix variables with units and value ranges

variable	unit	range
<i>Rhinanthus</i> frequency	number of quadrat mesh squares (10cm × 10cm) that the species was rooted in	0–100
<i>Odontites</i> frequency		
<i>Euphrasia</i> frequency		
<i>Rhinanthus</i> cover	%	0–100
<i>Odontites</i> cover		
<i>Euphrasia</i> cover		
<i>Cuscuta</i> cover		
total parasite cover	%	0+ (as a result of stratification)
bare ground cover	%	0–100
rock and stone cover	%	0–100
graminoid cover	%	0+
legume cover	%	0+
non-legume eudicot cover excl. parasites	%	0+
non-legume eudicot cover incl. parasites	%	0+
bryophyte cover	%	0–100
litter cover	%	0–100
cowpat cover	%	0–100
species richness	total number of species in a relevé	0+
total plant cover	%	0+
Ellenberg moisture indicator (F)	average for all species in a relevé	1–9
reaction (pH) Ellenberg indicator (R)		1–9
nitrogen Ellenberg indicator (N)		1–9

Chapter 2

An auto-pilot mode using Quantitative Sørensen (Bray Curtis) distance measure was initially used for NMS to determine the best parameter settings for the final analysis. Three axes were recommended for the final thorough run at stress value of 13.592. Reduction of stress was minimal with more than 3 axes. According to Kruskal's rule of thumb the obtained stress value provides a fair level of interpretability intermediate between good (5–10) and poor (>20) (McCune & Grace, 2002).

Secondary matrix variables were overlain on the ordination results. Subsequently, Pearson's correlation coefficient (r^2) values were calculated to assess the strength of the relationships between secondary matrix variables and ordination axes. A value of 0.2 was set as "significant" and therefore typically variables correlated at r^2 value of 0.2 or more with at least one of the axes were displayed as vectors.

2.3.4 Vegetation classification

Since classification of Irish grassland vegetation poses inherent problems resulting from the lack of a sufficiently detailed national system, description of vegetation types in this study was based on several publications. As the phytosociological classification based on the work of Braun-Blanquet and Tüxen (1952) and slightly modified by O'Sullivan (1982) is the most established and relatively detailed, it formed the basis for classifying the relevés. For Brigit's Garden, further confirmation of locally found phytosociological units was obtained from the work of Martin (1991). An approach more detailed than phytosociological association level classification was proposed for the Burren limestone grasslands by Parr *et al.* (2009) on the basis of TWINSpan analysis of 200 relevés recorded in this habitat. Therefore, the vegetation at Berneens was assigned to a phytosociological alliance and subsequently ascribed a vegetation type of Parr *et al.* (2009). Grey dune vegetation at Fanore was phytosociologically identified by Ivimey-Cook and Proctor (1966) as well as Doyle (1993) and therefore their findings were consulted. The level of detail of NVC classification units of Rodwell (1992, 2000) generally matches that of phytosociological associations. This classification was additionally suggested where appropriate. Finally, the most detailed vegetation classification proposed in the Irish Semi-natural Grassland Survey report of O'Neill *et al.* (2010) was consulted as it draws analogies with the remaining classifications while specifically being based on detailed Irish examples. However, this classification is likely to change when the data from the surveys conducted in 2011 and 2012 is incorporated and therefore it was used to compliment this study.

2.4 Results

2.4.1 Cluster analysis and indicator species analysis results

Ninety four relevés were surveyed on the three sites; 20 in Roscahill, 60 in Fanore and 14 in Berneens. Cluster analysis and indicator species analysis returned six major vegetation groups. Figure 2.5 shows that the balance between the mean p values and the number of significant indicator species was optimal for cluster 5. However, using 6 groups made more ecological sense while resulting in only a minimal increase of the p value from 0.160 to 0.173. As a result, floristically different relevés which were aggregated within one group for cluster 5, were separated into groups 1 and 2. Table 2.4 summarises the resultant groups and their indicator species. While a species can be an indicator for only one group, it can also occur in other groups. This was the case for the focal species in this study — *Rhinanthus minor* and *Odontites vernus* which were relatively abundant in more than one group. This is reflected in relatively high p values (low significance) when compared to other indicator species within the two groups, i.e. the two parasites were not the best indicator species for those groups.

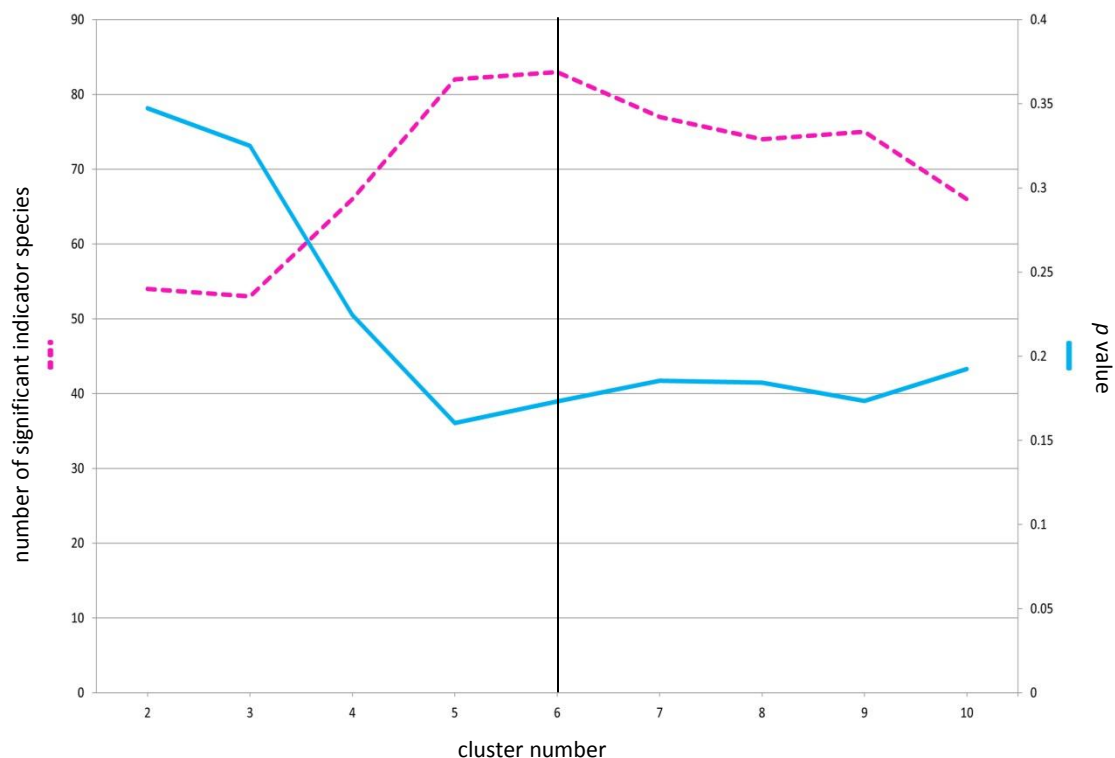


Figure 2.5: Graphical illustration of average p values and numbers of significant indicator species for different cluster numbers. The lowest p -value and the highest number of indicator species was achieved for 5 groups. However, 6 groups were found more appropriate for explaining the ecological differences.

The 6 groups were categorised as *Rhinanthus minor* groups (1, 4 and 5), *Odontites vernus* groups (2 and 3) and a *Rhinanthus minor/Odontites vernus* group (6). It must be highlighted that relevés with hemiparasites and control relevés without hemiparasites were not separated by the cluster analysis, with the exception of relevés 1–6. Running the analysis for up to 9 groups did not lead to separation of control relevés. Therefore, the *Rhinanthus minor* category, for instance, includes both the relevés with this species and the associated control relevés.

Site was an important grouping factor and therefore group 5 contains all Brigit’s Garden relevés representing a *Rhinanthus minor*-rich mesotrophic grassland from *Molinio-Arrhenatheretea* class and no other relevés. Cluster analysis for up to nine groups did not lead to subdivisions. Group 6 contains exclusively 11 out of 14 Berneens relevés representing a degenerated limestone pavement grassland with marked presence of ruderal species with both *Odontites vernus* and *Rhinanthus minor*. Fanore relevés were divided into 4 groups (1–4), two of which (1 and 2) represent thermophilous, species-rich communities from *Festuco-Brometea* while the other two (3 and 4) represent mesophilic grasslands of *Molinio-Arrhenatheretea*. This corresponds well with the marked presence and abundance of *Rhinanthus minor* and *Odontites vernus* in the first and the latter, respectively. Phytosociological classification of the groups is summarised in figure 2.6. Example images of vegetation within groups are presented in figure 2.7.

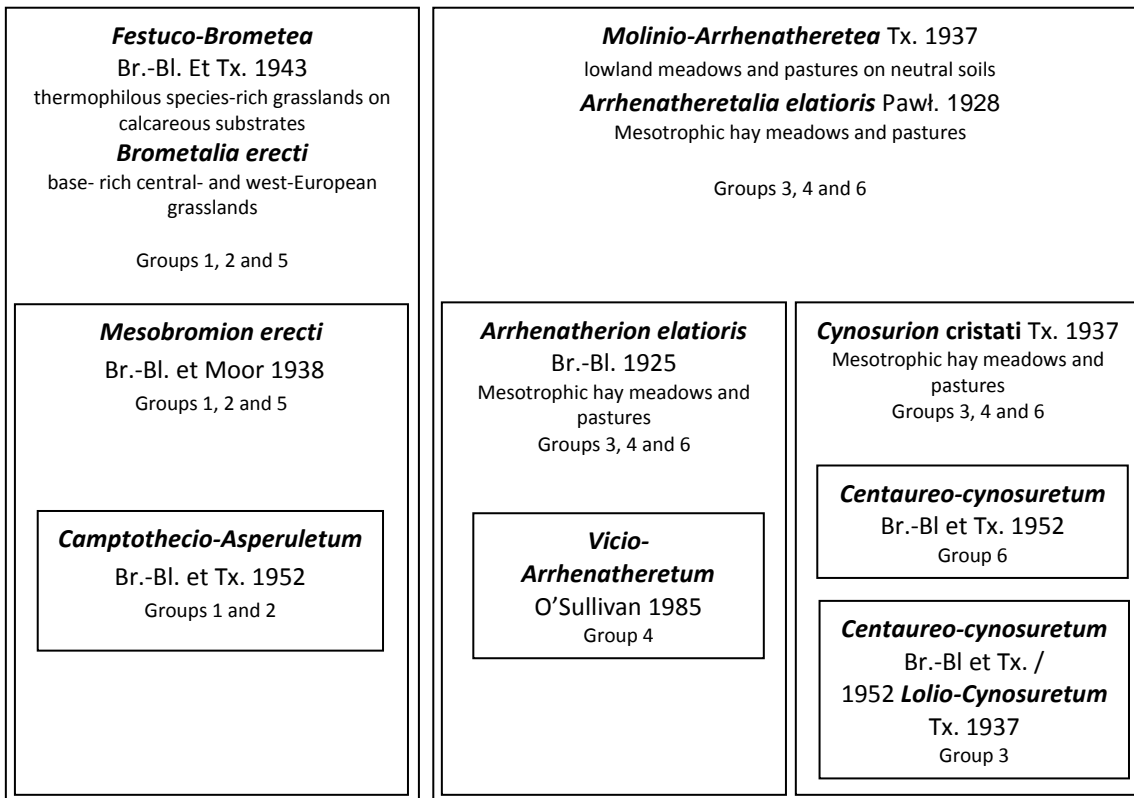


Figure 2.6: Summary of phytosociological classification of vegetation in this study.



Figure 2.7: Example photographs of representative areas of the six vegetation groups identified in this study. **A**—group 1: *Camptotecio-Asperuletum* (with *Rhinanthus minor*, Fanore sand dunes), **B**—group 2: *Camptotecio-Asperuletum*, variant with *Sesleria caerulea* (with *Rhinanthus minor*, Fanore sand dunes), **C**—group 3: *Centaureo-Cynosuretum/Lolio-Cynosuretum* intermediate (with *Odontites vernus*, Fanore dune slack), **D**—group 4: *Vicio-Arrhenatheretum* (with *Rhinanthus minor* and *Odontites vernus*, Fanore grassy verge), **E**—group 5: *Anthyllis vulneraria-Plantago maritima* subcommunity of *Sesleria caerulea-Breutelia chrysocoma* group (with *Rhinanthus minor* and *Odontites vernus*, Berneens winterage), **F**—group 6: *Centaureo-Cynosuretum* (with *Rhinanthus minor*, Brigit’s Garden hay meadow).

Table 2.4: ISA groups and their indicator species

P value is the primary sorting factor, followed by indicator value. Indicators included regardless of the insignificant *p* value on the basis of their marked presence or abundance are in brackets. Hemiparasites are indicated in bold.

group	relevés	mean species richness	indicator species	<i>p</i> value	indicator value	community classification and determining literature
1	F1, F3, F5, F7–10, F17–25, F27–28, B4, B6, B14	24.05	<i>Koeleria macrantha</i>	0.0002	65.9	<i>Camptothecio-Asperuletum</i> (Braun-Blanquet & Tüxen, 1952; Ivimey-Cook & Proctor, 1966)
			<i>Briza media</i>	0.0002	53.1	
			<i>Ranunculus bulbosus</i>	0.0038	36.8	
			<i>Leontodon saxatilis</i>	0.0064	27.8	
			<i>Euphrasia sp.</i>	0.0252	30.2	
			(<i>Anacamptis pyramidalis</i>)	0.0694	14.3	
			(<i>Prunella vulgaris</i>)	0.0742	24.5	
			(<i>Cuscuta epithimum</i>)	0.1398	14.2	
2	F11–16, F26	23.14	<i>Sesleria caerulea</i>	0.0002	95.1	<i>Camptothecio-Asperuletum</i> variant with <i>Sesleria caerulea</i>
			<i>Succisa pratensis</i>	0.0002	80.2	
			<i>Leontodon hispidus</i>	0.0002	64.3	
			<i>Asperula cynanchica</i>	0.0002	62.8	
			<i>Polygala vulgaris</i>	0.0002	59.1	
			<i>Dactylorrhiza fuchsii</i>	0.0002	53.6	
			<i>Carex caryophyllaea</i>	0.0002	46.7	
			<i>Gentiana verna</i>	0.0006	41.4	
			<i>Sherardia arvensis</i>	0.0016	33.4	
			<i>Thymus polytrichus</i>	0.0024	40.1	
			<i>Carex flacca</i>	0.0028	37.6	
			<i>Linum catharticum</i>	0.0128	30.7	
			<i>Anthyllis vulneraria</i>	0.0448	24.9	
(<i>Blackstonia perfoliata</i>)	0.0684	14.3				
(<i>Antennaria dioica</i>)	0.0758	14.3				
(<i>Danthonia decumbens</i>)	0.2	14.8				
3	F29–39, F46–48,	18.57	<i>Galium verum</i>	0.0002	80.2	Intermediate between <i>Centaureo-Cynosuretum</i> and <i>Lolio-Cynosuretum</i> (O'Sullivan, 1982)
			<i>Carex arenaria</i>	0.0002	68.9	
			<i>Lotus corniculatus</i>	0.0002	54	
			<i>Ammophila arenaria</i>	0.0002	50	
			<i>Poa humilis</i>	0.0002	48.3	
			<i>Festuca rubra</i>	0.002	33.2	
			<i>Odontites vernus</i>	0.0044	37.3	
			<i>Viola sp.</i>	0.0092	33.7	
<i>Bellis perennis</i>	0.0128	22.9				
4	F2, F4, F6, F40–45, F49–60	13.1	<i>Arrhenatherum elatius</i>	0.0002	72.1	<i>Vicio-Arrhenatheretum</i> (O'Sullivan, 1982) variant with abundant <i>Trifolium repens</i>
			<i>Dactylis glomerata</i>	0.0002	46.1	
			<i>Trifolium repens</i>	0.0006	44.4	
			<i>Avenula pubescens</i>	0.0028	32.2	
			<i>Lolium perenne</i>	0.0058	36.2	
			<i>Elytrygia repens</i>	0.0426	19.9	
			<i>Veronica persica</i>	0.045	17.9	
			(<i>Cirsium arvense</i>)	0.72	16.5	
			(<i>Trifolium pratense</i>)	0.1674	24.2	
			(<i>Heracleum sphondylium</i>)	0.4385	10	

5	B1–3, B5, B7–13	28.18	<i>Daucus carota</i>	0.0002	77.8	Anthyllis vulneraria- Plantago maritima subcommunity of <i>Sesleria</i> <i>caerulea</i> - <i>Breutelia</i> <i>chrysocoma</i> group (Parr <i>et al.</i> , 2009)
			<i>Leontodon autumnalis</i>	0.0002	76.2	
			<i>Ranunculus acris</i>	0.0002	70.8	
			<i>Poa pratensis</i>	0.0002	69.7	
			<i>Veronica arvensis</i>	0.0002	63.6	
			<i>Geranium sanguineum</i>	0.0002	50.4	
			<i>Sonchus asper</i>	0.0002	42.7	
			<i>Cynosurus cristatus</i>	0.0004	59.9	
			<i>Potentilla erecta</i>	0.0004	45.0	
			<i>Polygonum aviculare</i>	0.0006	36.4	
			<i>Agrostis stolonifera</i>	0.0012	43.2	
			<i>Myosotis arvensis</i>	0.0012	27.3	
			<i>Holcus lanatus</i>	0.002	43.4	
			<i>Euphrasia rostkoviana</i>	0.0022	27.3	
			<i>Sagina nodosa</i>	0.0044	23.2	
			<i>Stellaria media</i>	0.009	27.3	
			<i>Capsella bursa-pastoris</i>	0.016	18.2	
			<i>Alchemilla sp.</i>	0.021	18.2	
			(<i>Cardamine hirsuta</i>)	0.0222	18.2	
			(<i>Cerastium fontanum</i>)	0.0254	28.8	
(<i>Campanula rotundifolia</i>)	0.0478	16.7				
(<i>Medicago lupulina</i>)	0.048	25.3				
6	BG1–20	25.7	<i>Primula veris</i>	0.0002	89	<i>Centaureo</i> - <i>Cynosuretum</i> (O’Sullivan, 1982)
			<i>Anthoxanthum odoratum</i>	0.0002	83.7	
			<i>Fraxinus excelsior</i>	0.0002	75.0	
			<i>Stellaria graminea</i>	0.0002	75.0	
			<i>Achillea millefolium</i>	0.0002	70.2	
			<i>Lathyrus pratensis</i>	0.0002	65.0	
			<i>Rumex acetosa</i>	0.0002	63.9	
			<i>Centaurea nigra</i>	0.0002	55.1	
			<i>Plantago lanceolata</i>	0.0002	40.3	
			<i>Leucanthemum vulgare</i>	0.0004	56.1	
			<i>Agrostis capillaris</i>	0.0004	46.5	
			<i>Veronica chamaedrys</i>	0.001	40	
			<i>Knautia arvensis</i>	0.0014	45.0	
			<i>Origanum vulgare</i>	0.0018	35	
			<i>Luzula campestris</i>	0.002	40.3	
			<i>Rhinanthus minor</i>	0.0028	34.5	
			<i>Salix sp.</i>	0.003	25.0	
			<i>Taraxacum aggregatum</i>	0.0042	34.9	
			<i>Crepis capillaris</i>	0.0048	25.0	
			<i>Plantago major</i>	0.0064	37.7	
			<i>Ranunculus repens</i>	0.0176	26.1	
			<i>Hypericum perforatum</i>	0.0236	15.0	
			<i>Potentilla sp.</i>	0.0244	15.0	
<i>Epilobium sp.</i>	0.029	15.0				
<i>Lotus pedunculatus</i>	0.0384	15.0				
<i>Rubus fruticosus</i>	0.044	15.0				
<i>Lythrum salicaria</i>	0.043	15.4				

The first four groups are located at Fanore sand dunes. The distribution of relevés within these groups is illustrated in figure 2.8. Colour codes correspond with those in ordination plots for ease of reference and interpretation. As there was no intra-site grouping within Brigit’s Garden the exact locations of relevés on this site are not

shown. Similarly, the detail of relevé distribution at Berneens is not shown as most relevés fall within one group.



© Ordnance Survey Ireland

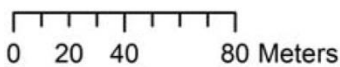


Figure 2.8: Distribution of Fanore site relevés grouped on the basis of cluster analysis. Colour codes are as follows:

● — group 1 (*Camptothecio-Asperuletum*), ● — group 2 (*Camptothecio-Asperuletum*, variant with *Sesleria caerulea*), ● — group 3 (*Centaureo-Cynosuretum/Lolio-Cynosuretum*), ● — group 4 (*Vicio-Arrhenatheretum*)

Group 1 is made of 21 relevés, most of which are located in Fanore, in addition to 3 relevés from the site at Berneens. These three relevés were not separated from the Fanore quadrats at higher levels of grouping.

Indicator species for the group include 2 graminoids, 5 non-legume eudicots including the holoparasite *Cuscuta epithymum* and hemiparasite *Euphrasia* sp.. *Cuscuta* and

Euphrasia were included regardless of their low statistical significance as they were most abundantly and consistently found within this group. This was also true for the only orchid indicator species — *Anacamptis pyramidalis*, which, together with *Asperula cynanchica* is an important diagnostic taxon for *Mesobromion* alliance of *Festuco-Brometea* class of thermophilous, species-rich grasslands on calcareous substrates. *Mesobromion* includes grasslands on limestone and established calcareous dunes (Shimwell, 1971). Indeed, the typical vegetation of grey sand dunes was previously described at the Fanore site by Ivimey-Cook and Proctor (1966) as *Galium verum-Asperula cynanchica* Nodum, which closely resembles *Camptothecio-Asperuletum cynanchicae* Br.-Bl. et Tx. 1952 of *Festuco-Brometea*. These findings were further confirmed by Doyle (1993).

Five relevés from this group contain *Sesleria caerulea*, which is also a strong indicator species for similar group 4. Originally a sub-association of *Camptothecio-Asperuletum* with *Sesleria* was recognised within *Eu-Mesobromenion* suballiance. However, it was moved to a new sub-alliance *Seslerio-Mesobromenion* as *Asperulo-Seslerietum* (Br.-Bl. et Tx. 1952) Shimwell 1968 by Shimwell (1971), who reserved *Eu-Mesobromenion* for analogous communities without this or other alpine species. However, the floral composition of the discussed group seems to match that of the original sub-association, as the character species of *Asperulo-Seslerietum*, namely *Dryas octopetala*, *Geranium sanguineum* and *Helianthemum canum*, are missing. Furthermore, *Asperulo-Seslerietum* is typically found on shallow soils over limestone pavement.

Group 2 is the group with the lowest number of relevés (7). It is similar to group 1 in its general physiognomy (compare Fig. 2.7A and B) and is likely to represent its variant with more abundant *Sesleria caerulea* and fewer species of nutrient-rich habitats. Indicator species for this group are mostly non-legume eudicots (12 species) in addition to 2 sedges, 1 grass and 1 orchid. *Sesleria caerulea* and *Succisa pratensis* are statistically very strong indicators and occur markedly abundantly in this group, with a cover of up to 20 and 45 % respectively. *Carex flacca* is also noticeably more abundant than in other groups, with a cover of up to 13%. All three species occur in group 1 as well, where they are also relatively abundant, with *Succisa pratensis* reaching the unusually high level of 50% in relevé F22. Other shared species include *Asperula cynanchica*, *Briza media*, *Linum catharticum*, *Plantago lanceolata*, *Rhinanthus minor*, *Sherardia arvensis* and *Thymus polytrichus*. The most notable differences between the two groups are the lower abundance of *Dactylis glomerata*, *Galium verum*, *Koeleria macrantha*, *Lotus corniculatus* and *Trifolium repens* in group 4. As all of these, except *Koeleria*, were indicative of more nutrient-rich and moister groups 3 and 4 (see below), most likely the difference between groups 1 and 2 result from slight topographic differences and associated hydrological variations. Association-level classification is further complicated by the fact that high constancy of *Briza media*, *Carex caryophyllea*, *Carex flacca*, *Linum catharticum*, *Lotus corniculatus* and *Polygala*

vulgaris is suggestive of *Antennarietum hibernicae* Br. Bl. et Tx. 1952 of *Eu-Mesobromenion* (O'Sullivan, 1982). *Antennaria dioica* was found only in relevé F16 with 22% cover.

Group 3 contains 14 relevés, mainly of dune slacks and three relevés of the grass verge adjacent to the car park. It includes *Odontites vernus* as an indicator species. Three other non-legume eudicots, 1 sedge and 3 grasses are also indicative of this group. Its indicator species are character species of two mesotrophic grassland associations: *Lolio-Cynosuretum* and *Centaureo-Cynosuretum* (O'Sullivan, 1982). *Plantago lanceolata* is a non-indicator species that is also consistently found within this group with a cover of 2 to 22%. *Agrostis stolonifera*, *Cerastium fontanum*, *Holcus lanatus* and *Hypochaeris radicata* are somewhat less consistent components.

Based on the classification of O'Sullivan (1982), this grassland belongs to *Cynosurion cristati* Tx 1937. alliance with an additional influence of shifting sand dune species. The community includes character and differential species of moderate quality pastures of *Centaureo-Cynosuretum* Br. Bl. et Tx. 1952, particularly *Lotus corniculatus* and *Hypochaeris radicata*. Species of *Lolio-Cynosuretum* (Br. Bl. et de Leeuw 1936) Tx. 1937 association found on more fertile soils, in particular abundant *Trifolium repens* but also non-abundant *Lolium perenne* are present as well. These are likely a result of trampling within the dune slacks and a more typical *Centaureo-Cynosuretum* would likely develop if the community was freed of this pressure. Rodwell (2000) distinguishes between the *Centaureo-Cynosuretum* of hay meadows (MG5) and a similar community in association with sand dunes. He classifies the latter as SD8 *Festuca rubra-Galium verum* fixed dune grassland which can develop in sheltered areas between shifting dunes.

Group 4 includes 20 relevés recorded in the neglected grass verge along the driveway and 1 dune slack quadrat. The verge is not mown or grazed in the summer and therefore supports relatively tall grassland vegetation, notably *Arrhenatherum elatius*. Five vigorous grass species are indicators for this group, in addition to *Trifolium repens* and *Trifolium pratense* as the only legume indicators. Non-leguminous eudicot indicators are *Cirsium arvense*, *Heracleum sphondylium* and *Veronica persica*. *Odontites vernus* is present in 18 relevés and reaches the highest recorded abundance of 40% in quadrat F53. *Rhinanthus minor* is present in 4 relevés, in 3 of which it co-occurs with *Odontites vernus*. A number of species are shared with group 3. *Festuca rubra*, *Lotus corniculatus* and *Plantago lanceolata* are important components although of somewhat lower constancy and less consistent abundance than in group 3. Similar to group 3, *Holcus lanatus* occurs relatively consistently at low cover, while inabundant *Cerastium fontanum* is found in 11 quadrats. The most notable difference is the much higher abundance in group 4 of indicator species *Arrhenatherum elatius*, and *Dactylis glomerata* and lower abundance of group 3 indicator species, *Galium verum*. Furthermore, *Agrostis stolonifera* and *Trifolium pratense* have a higher affinity for group 4, with the latter species present in 16 relevés at 0.5–20% cover, while being

present in only 5 quadrats from group 3. This is the floristically poorest group, with an average species richness of 13.1.

High contribution of *Arrhenatherum elatius* and *Dactylis glomerata* suggests *Arrhenatherion elatioris* W. Koch 1926 alliance, which according to O'Sullivan (1982) was poorly studied within Ireland. He proposed a *Vicio-Arrhenatheretum* as the association name. The analogous community of Rodwell (1992) is *Arrhenatherum elatius* grassland (MG1). The stands found within group four are likely atypical as character species of *Cynosurion cristati* are also present, notably *Trifolium repens* and differential species *Cirsium arvense* and *Odontites vernus*.

Group 5 includes 11 relevés, exclusively from the winterage site at Berneens. Indicator species for this group include 4 grasses, 18 non-leguminous dicots and 1 legume. Phytosociologically this groups appears to represent a degenerated version of a limestone grassland of *Mesobromion* alliance, as evidenced by the presence of *Geranium sanguineum*, with possible influence of limestone heath. Both of these habitats are found in the adjacent fields and the high level of disturbance is likely to blur subtle differences.

Parr *et al.* (2009) classified species rich limestone grasslands of the Burren into two major groups: *Sesleria caerulea-Breutelia chrysocoma* group indicated by *Thymus polytrichus* and the moss *Breutelia chrysocoma* as well as *Dactylis glomerata-Holcus lanatus* group indicated by *Dactylis glomerata* and *Holcus lanatus*. The authors draw a general analogy with *Mesobromion* alliance although no association-level comparisons are made.

Daucus carota, *Leontodon autumnalis* and *Leucanthemum vulgare* abundant in group 5 are indicative of *Anthyllis vulneraria-Plantago maritima* subcommunity of *Sesleria caerulea-Breutelia chrysocoma*, although *Sesleria caerulea* is not present. Lack of *Arrhenatherum elatius* indicative of *Achillea millefolium-Avenula pubescens* subcommunity and preferential species of *Solidago virgaurea-Hypericum pulchrum*, e.g. *Dryas octopetala*, *Hypericum pulchrum* or *Solidago virgaurea* further support this classification. Ruderal and arable annuals including, *Atriplex sp.*, *Capsella bursa-pastoris*, *Polygonum aviculare*, *Sonchus asper*, *Stellaria media* and *Veronica arvensis* are suggestive of negative changes induced by disturbance resulting from trampling by cattle. Regardless of these negative changes to community structure, this group contains relevés of exceptionally high species richness, with 36 vascular plant species recorded in one quadrat and 35 species in 2 quadrats.

Group 6 contains all 20 relevés from Little Meadow in Brigit's garden. It includes *Rhinanthus minor* and 19 other herbaceous non-leguminous eudicots as indicator species while only 2 legumes and 3 graminoid species are indicator species. Additionally, 3 woody species encroaching from the adjacent hedgerow are indicators.

This group represents association *Centaureo-Cynosuretum* Br.-Bl. Et Tx. 1952 (O'Sullivan 1982; Rodwell 1992) which is characterised by moderate fertility, presence of poor yielding grasses and presence of the following differential species: *Hypochaeris radicata*, *Carex flacca*, *Lotus corniculatus*, *Centaurea nigra*, *Luzula campestris* and *Rhytidiadelphus squarrosus*. High constancy and abundance of *Primula veris*, *Galium verum*, *Daucus carota* and *Medicago lupulina* suggest subassociation 'galietosum' characteristic of well-drained soils on carboniferous limestone and previously found in this area by Martin (1991). However, high abundance of the acidophilic moss *Pleurozium schreberii* in Esker Meadow (personal observations) indicates that the upper layer of calcareous esker gravel might be leached.

2.4.2 NMS results

Most variance was explained by axis 2 (31.5%), followed by axis 3 (28%) and axis 1 (21.6%). Overall, 81.1% of variance was represented by the three axes. Correlations of secondary matrix variables with the axes are presented in table 2.5. The most prominent correlation is that of Ellenberg value for nitrogen with axis 3. Data were chosen to be plotted against axes 2 and 3 as key variables and vegetation groups were most discernible in that configuration (Fig. 2.9 and 2.10). Categories of parasite presence were also most apparent and parasite abundance vectors were best defined. Grouping was also well represented in plots against axes 1 and 2 as well as 1 and 3 (not shown). However, presence and abundance of parasites were not.

Figure 2.9 shows that presence of *Rhinanthus* and *Odontites* is associated with two extreme positions in the plot, while relevés without parasites and with both parasites are located between these two extremes and opposite each other.

In figure 2.10, vegetation groups are distributed along a gradient, diagonally to the two axes. This is seen between sites but additionally, an intra-site gradient is observed at Fanore. This gradient (group 2, group 1, group 3, group 4) roughly corresponds with an increase in nitrogen values and follows a pattern of decrease in *Rhinanthus* cover, forb cover and richness and species richness, as well as increase in graminoid and legume cover and increase in *Odontites* abundance. Relevés from Brigit's Garden are located at the "*Rhinanthus* extreme" of the plot. Relevés from group 5 are located at an intermediate position along the gradient.

Table 2.5: Correlation between secondary matrix variables and NMS plot axes expressed as Pearson correlation co-efficient (r^2).

R^2 values are between 0 and 1. A correlation is negative (-) if the original r value was negative. Therefore (-) 1 expresses perfect negative correlation And (+) 1 shows a perfect positive correlation. "Significant" correlations ($r^2 > 0.2$) are in bold. Abbreviations for vectors displayed in ordination graphs are in brackets.

variable	Axis 1	Axis 2	Axis 3
<i>Rhinanthus</i> frequency (Rhin. fr.)	(+) 0.015	(-) 0.325	(-) 0.241
<i>Odontites</i> frequency (Odon fr.)	(-) 0.077	(+) 0.129	(+) 0.194
<i>Euphrasia</i> frequency (Euphr fr.)	(+) 0.203	(-) 0.002	(-) 0.111
<i>Rhinanthus</i> cover (Rhin. cov.)	(+) 0.027	(-) 0.168	(-) 0.109
<i>Odontites</i> cover (Odon. cov.)	(+) 0.081	(+) 0.142	(+) 0.202
<i>Euphrasia</i> cover (Euphr. cov.)	(-) 0.009	(-) 0.041	(+) 0.028
<i>Cuscuta</i> cover (Cusc. cov.)	(+) 0.000	(+) 0.000	(-) 0.000
total parasite cover	(+) 0.062	(-) 0.003	(+) 0.069
bare ground cover	(-) 0.004	(-) 0.085	(+) 0.087
rock and stone cover	(-) 0.016	(-) 0.022	(+) 0.016
graminoid cover (gram.)	(-) 0.084	(+) 0.291	(+) 0.202
graminoid richness (gram. rich.)	(-) 0.042	(+) 0.132	(+) 0.025
legume cover (legu.)	(+) 0.146	(+) 0.176	(+) 0.142
legume richness (legu. rich.)	(+) 0.000	(-) 0.062	(-) 0.017
non-legume eudicot cover excl. parasites (forb*)	(+) 0.026	(-) 0.467	(-) 0.253
non-legume eudicot richness excl. parasites (forb. rich.)	(-) 0.002	(-) 0.444	(-) 0.199
non-legume eudicot cover excl. parasites (forb inc. par.)	(+) 0.070	(-) 0.396	(-) 0.098
bryophyte cover (bryo.)	(+) 0.035	(-) 0.219	(-) 0.082
litter cover (litter)	(-) 0.284	(-) 0.007	(-) 0.131
cowpat cover	(-) 0.009	(+) 0.019	(+) 0.000
species richness (sp. rich.)	(-) 0.006	(-) 0.420	(-) 0.186
total plant cover	(+) 0.134	(+) 0.082	(+) 0.063
F mean (F)	(-) 0.031	(-) 0.023	(+) 0.258
R mean	(+) 0.140	(+) 0.065	(+) 0.102
N mean (N)	(+) 0.230	(+) 0.021	(+) 0.626

*the term forb is used here to mean non-leguminous dicots only, as it was previously applied for perennial eudicot hosts of *Rhinanthus minor* by (Cameron *et al.*, 2006). Additionally, annual eudicots are included.

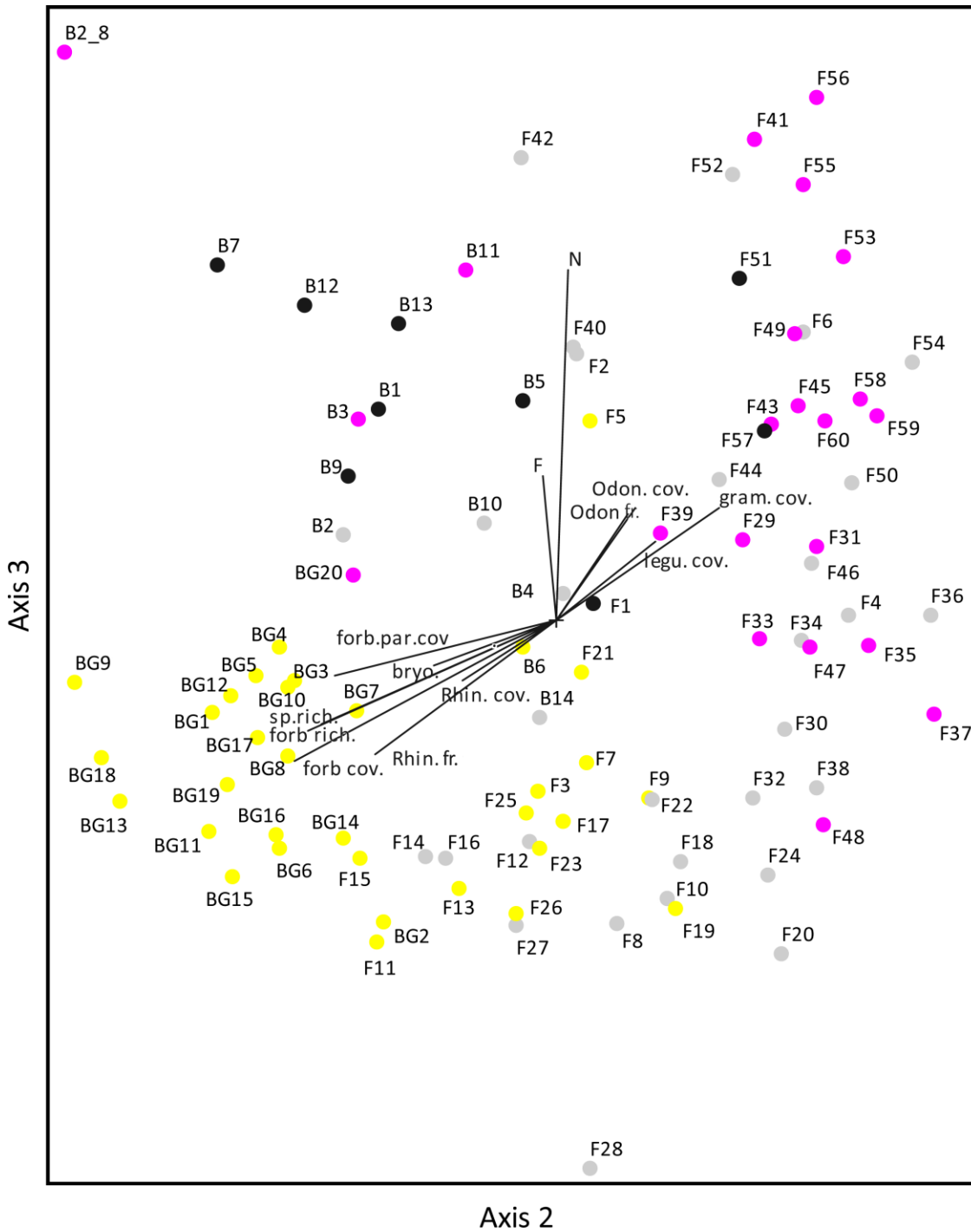


Figure 2.9: NMS ordination plot illustrating all relevés grouped by the presence of parasites *Rhinanthus minor* and *Odontites vernus*.

● — neither species present, ● — *R. minor* only present, ● — *O. vernus* only present, ● — both species present

F — Ellenberg’s indicator of moisture, **N** — Ellenberg’s indicator of nitrogen, **bryo** — bryophyte cover, **forb cov.** — forb cover excluding parasites, **forb par. cov.** — cover of forbs including parasites, **forb rich.** — forb species richness, **gram. cov.** — graminoid cover, **legu. cov.** — cover of legumes, **Odon. cov.** — cover of *Odontites vernus*, **Odon. freq.** — frequency of *Odontites vernus*, **Rhin. cov.** — cover of *Rhinanthus minor*, **Rhin. freq.** — frequency of *Rhinanthus minor*, **sp. rich.** — species richness

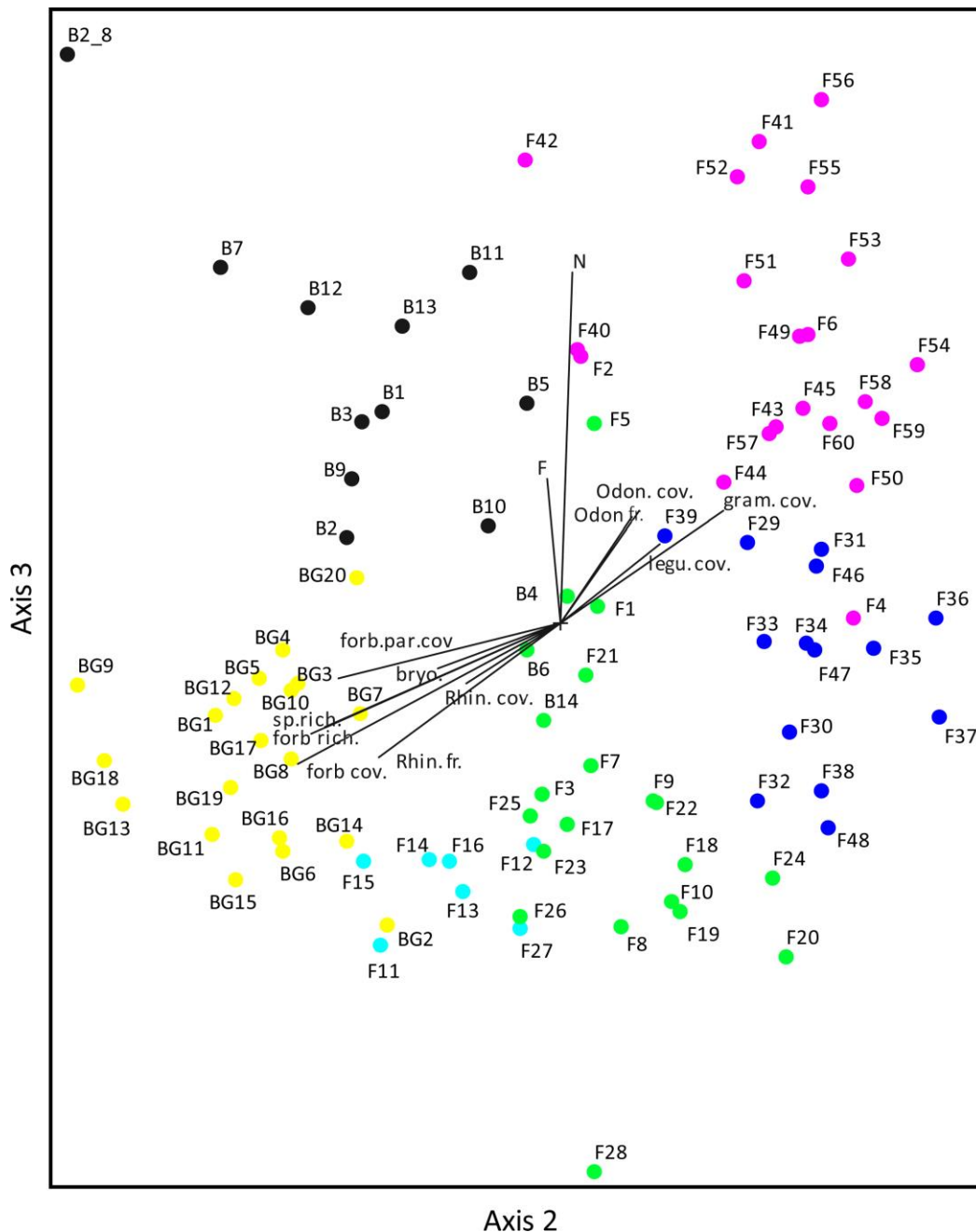


Figure 2.10: NMS ordination plot, illustrating all relevés grouped by vegetation groups obtained through cluster analysis and indicator species analysis.

● — group 1 (*Camptotecio-Asperuletum*), ● — group 2 (*Camptotecio-Asperuletum*, variant with *Sesleria caerulea*), ● — group 3 (*Centaureo-Cynosuretum/Lolio-Cynosuretum* intermediate), ● — group 4 (*Vicio-Arrhenatheretum*), ● — group 5 (*Anthyllis vulneraria-Plantago maritima* community), ● — group 6 (*Centaureo-Cynosuretum*) (see Table 2.4 for further detail)

F — Ellenberg's indicator of moisture, **N** — Ellenberg's indicator of nitrogen, **bryo** — bryophyte cover, **forb cov.** — forb cover excluding parasites, **forb par.cov.** — cover of forbs including parasites, **forb rich.** — forb species richness, **gram.** — graminoid cover, **legu.** — cover of legumes, **Odon. cov.** — cover of *Odontites vernus*, **Odon. freq.** — frequency of *Odontites vernus*, **Rhin. cov.** — cover of *Rhinanthus minor*, **Rhin. freq.** — frequency of *Rhinanthus minor*, **sp.rich.** — species richness

2.4.3 Correlations between secondary matrix variables

Table 2.6 summarises all correlations between secondary matrix variables calculated in Minitab 16. Strong significant correlations were observed between several variables within the secondary matrix and were in agreement with the general trends seen in the NMS plot, ie. species richness (Fig. 2.11) and higher forb to grass ratio being positively associated with *Rhinanthus minor* groups and negatively associated with *Odontites vernus* groups, which also show preference for higher fertility (N). Abundance of *Euphrasia* sp. showed similar positive relationship with forb richness and species richness as *R. minor* ($p=0.002$ and 0.004 respectively). The strongest of all relationships was found between forb richness and species richness ($r^2=0.937$, $p=0.000$), confirming similar results of the ordination.

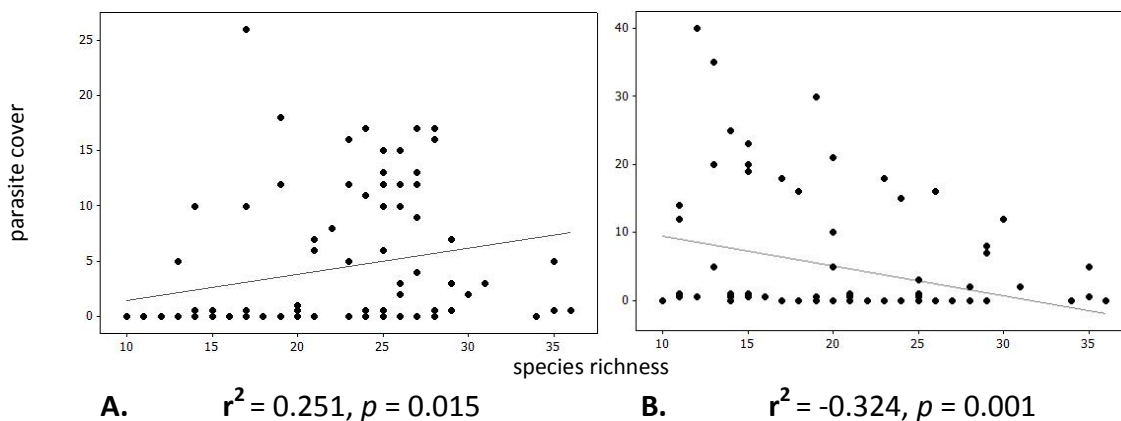


Figure 2.11: Scatter plots of correlations between parasite cover and species richness A) *Rhinanthus minor* cover and species richness, B) *Odontites vernus* cover and species richness

Several additional correlations with variables that were not included in the ordination plot are of particular interest. Total vascular plant cover is one of the variables that were not included in the ordination graph. While it was weakly positively correlated with *Odontites vernus* cover ($p=0.048$), no significant correlation with *Rhinanthus minor* cover ($p=0.437$) was found. However, it was negatively correlated with species richness ($p=0.002$).

A low number of significant correlations with total parasite cover was seen and is most likely a result of opposing effects of *Rhinanthus minor* and *Odontites vernus*. Total parasite cover was significantly correlated only with bare ground cover (positive correlation at $p=0.006$) and graminoid cover (negative at $p=0.014$).

Differences in correlation between abundance and richness within different plant groups were also seen. Forb cover and richness were strongly positively correlated ($r^2=0.686$, $p=0.000$). In contrast, no significant relationship between legume cover and richness was found ($p=0.738$). Litter cover showed significant negative correlations with legumes ($p=0.000$), total cover ($p=0.000$) and nitrogen values ($p=0.000$) while being positively correlated only with pH ($p=0.049$).

Table 2.6: Correlations between secondary matrix variables. Top values represent Pearson's correlation coefficient, bottom — p values.

Significant correlations ($p < 0.05$) are indicated in bold. Acronyms as in table 2.5. F, N, R — Ellenberg's indicators of moisture, nitrogen, and acidity, respectively, **bare gr.** — bare ground cover, **bryo** — bryophyte cover, **forb cov.** — forb cover excluding parasites, **forb par.cov.** — cover of forbs including parasites, **forb rich.** — forb species richness, **gram.** — graminoid cover, **gram. rich.** — graminoid richness, **legu.** — cover of legumes, **legu. rich.** — legume richness, **litter** — litter cover, **Euphr. cov.** — cover of *Euphrasia* spp., **Odon. cov.** — cover of *Odontites vernus*, **par. cov.** — parasite cover, **Rhin. cov.** — cover of *Rhinanthus minor*, **rock cov.** — rock cover **sp.rich.** — species richness, **tot. cov.** — total cover

	Rhin. cov.	Odon. cov.	Euphr. cov.	par. cov.	bare gr.	rock cov.	gram. cov.	legu. cov.	forb. cov.	forb. par. cov.	bryo.	litter	leg. rich.	gram. rich.	forb. rich.	sp. rich.	tot. cov.	F	R	
Odon. cov.	-0.264																			
	0.010																			
Euphr. cov.	-0.051	0.006																		
	0.628	0.952																		
par. cov.	0.307	0.624	0.586																	
	0.003	0.000	0.000																	
bare. gr.	-0.095	0.063	0.477	0.284																
	0.361	0.544	0.000	0.006																
rock. cov.	-0.125	-0.052	0.126	-0.031	0.210															
	0.232	0.618	0.226	0.768	0.043															
gram. cov.	-0.295	-0.039	-0.100	-0.253	-0.043	-0.054														
	0.004	0.707	0.338	0.014	0.678	0.604														
legu. cov.	-0.221	0.298	-0.051	0.075	-0.111	-0.002	-0.008													
	0.032	0.003	0.626	0.475	0.285	0.986	0.939													
forb. cov.	0.258	-0.311	0.131	-0.019	0.080	-0.000	-0.658	-0.435												
	0.012	0.002	0.209	0.856	0.442	0.999	0.000	0.000												
forb.par. cov.	0.378	0.033	0.403	0.475	0.210	-0.015	-0.704	-0.346	0.871											
	0.000	0.753	0.000	0.000	0.042	0.884	0.000	0.001	0.000											
bryo.	0.148	-0.253	-0.006	-0.114	-0.060	-0.046	-0.429	-0.158	0.396	0.292										
	0.155	0.014	0.958	0.273	0.567	0.661	0.000	0.129	0.000	0.004										
litter	0.016	-0.114	-0.068	-0.118	0.038	-0.080	-0.101	-0.379	0.048	-0.016	-0.035									
	0.879	0.274	0.517	0.257	0.716	0.441	0.333	0.000	0.649	0.877	0.738									
leg. rich.	0.057	-0.028	0.165	0.110	0.148	0.364	-0.244	-0.035	0.202	0.232	0.129	-0.116								
	0.587	0.792	0.111	0.293	0.154	0.000	0.018	0.738	0.051	0.025	0.216	0.264								
gram. rich.	-0.093	-0.005	0.168	0.047	0.002	0.271	0.383	0.045	-0.258	-0.204	-0.410	-0.092	0.177							
	0.371	0.963	0.106	0.650	0.982	0.008	0.000	0.669	0.012	0.049	0.000	0.379	0.087							
forb. rich.	0.198	-0.296	0.309	0.069	0.205	0.384	-0.565	-0.428	0.686	0.638	0.314	0.123	0.503	-0.103						
	0.056	0.004	0.002	0.506	0.047	0.000	0.000	0.000	0.000	0.000	0.002	0.236	0.000	0.325						
sp.rich.	0.251	-0.324	0.297	0.070	0.215	0.437	-0.491	-0.455	0.662	0.617	0.221	0.101	0.587	0.136	0.937					
	0.015	0.001	0.004	0.505	0.038	0.000	0.000	0.000	0.000	0.000	0.032	0.335	0.000	0.192	0.000					
tot. cov.	0.081	0.205	-0.054	0.163	-0.111	-0.213	0.271	0.432	0.002	0.082	-0.313	-0.465	-0.059	0.171	-0.317	-0.256				
	0.437	0.048	0.607	0.117	0.288	0.040	0.008	0.000	0.986	0.434	0.002	0.000	0.573	0.100	0.002	0.013				
F	0.075	-0.031	0.023	0.026	0.078	0.079	0.272	0.103	-0.122	-0.095	-0.005	-0.202	-0.068	0.052	-0.186	-0.110	0.213			
	0.475	0.764	0.828	0.806	0.456	0.446	0.008	0.325	0.242	0.364	0.965	0.051	0.513	0.620	0.073	0.291	0.039			
R	-0.266	0.206	-0.118	-0.067	0.072	-0.055	0.308	0.133	-0.470	-0.447	-0.334	0.204	-0.023	0.017	-0.380	-0.391	-0.096	0.147		
	0.009	0.046	0.255	0.519	0.488	0.599	0.002	0.203	0.000	0.000	0.001	0.049	0.828	0.871	0.000	0.000	0.358	0.156		
N	-0.109	0.317	-0.072	0.132	0.104	-0.052	0.410	0.381	-0.366	-0.257	-0.170	-0.479	-0.193	0.001	-0.505	-0.492	0.409	0.629	0.276	
	0.296	0.002	0.493	0.206	0.318	0.618	0.000	0.000	0.000	0.012	0.101	0.000	0.063	0.994	0.000	0.000	0.000	0.000	0.000	0.007

2.5 Discussion

In this study, three sites with different abundances of *Rhinanthus minor* and *Odontites vernus* were surveyed. The focus was placed on comparing community structure between 1) *Rhinanthus minor* and *Odontites vernus*-rich relevés, and 2) parasite-rich relevés with control relevés to establish community features associated with the two species. The main differences were expected to be seen in the balance between species richness, graminoid to forb cover ratio and total vegetal cover, which is an indirect measure of biomass production (Kent & Coker, 1994). To my best knowledge, this is the first habitat survey focused on hemiparasites in Ireland, while the habitats and the hosts of the holoparasite *Cuscuta epithymum* in the Burren limestone pavement and at Fanore sand dunes have been previously compared by Doyle (1993).

Results showed that differences between habitats had a stronger bearing on clustering and ordination than differences in parasite presence and absence. However, a distinction between the communities of the two hemiparasites was clear, with only one group displaying the presence of both.

Inconsiderable community differences between control and parasite-rich relevés could be a consequence of several factors. *Rhinanthus angustifolius* is known to form transient patches within grasslands as part of its population dynamics (Ameloot *et al.*, 2006). However, the patchy distribution of *Rhinanthus minor*, is likely to be a consequence of dry conditions during the spring of 2011 (Met Eireann) as it was absent from the driest parts of fixed dunes. In the previous year, it was distributed much more uniformly and therefore its possible impact would have been less localised. One year of more spatially restricted impact might have not been enough to result in community changes between parasitized and non-parasitized patches, especially in a long-established and species-rich community which is likely to display a significant buffering capacity. Watkinson and Davy (1985) found that *Rhinanthus minor* and *Euphrasia* spp. were found specifically in areas of sand dunes that had high eudicot cover but no such link was observed in this study.

In case of *Odontites vernus* groups in Fanore, the community is characterised by considerably lower species richness and therefore might be expected to be more susceptible to change; nevertheless, no considerable difference was seen. The distribution of this species was not investigated in the year preceding the survey and therefore it is not known if it was a new component in the surveyed patches of grassland or whether it persisted from previous years. It is possible that higher vigour of component species in group 3, which is characterised by high abundance of legumes, makes up for the deleterious effects of parasitism. Surplus of nitrogen resources in legumes was suggested as a mechanism of compensation for the abstracted nutrients (Govier *et al.*, 1967). As mentioned in the introduction, biomass and vigour of legumes are not always

Chapter 2

affected when subject to parasitism by *Rhinanthus minor* (Joshi & Matthies, 2000; Cameron *et al.*, 2005), therefore, this phenomenon might be quite common.

A clearer distinction was made between vegetation types characterised by pronounced presence of *Rhinanthus minor* and *Odontites vernus*. However, relevés from group 3 characterised by *Odontites vernus* as an indicator species were agglomerated with *Rhinanthus* group 1 when cluster analysis was tested for 5 groups. This leads to the conclusion that parasite presence may not compensate for or obscure the differences between the habitats of neglected grassland of group 4, where lack of summer grazing and trampling is a determining ecological factor, and group 3 which contains relevés located near paths and therefore is exposed to trampling. The very clear distinction seen between the patches occupied by *Rhinanthus minor* and *Odontites vernus* is therefore most likely a consequence of habitat differences and a reason for, rather than a consequence of, parasitism by these two different species. This is further supported by the fact that site was a very important factor in the grouping and ordination.

Plant communities in which the two hemiparasitic species were recorded do not deviate from previously published data. *Rhinanthus minor* finds its habitat optimum in hay meadows (Grime *et al.*, 1988; Westbury, 2004). This is further highlighted for the Irish flora by the fact that O'Neill *et al.* (2010) found it to be indicative of a *Trifolium pratense*-*Rhinanthus minor* meadow vegetation type during the semi-natural grassland survey. The example of *Centaureo-Cynosuretum galietosum* is well developed, with many character and differential species present. The presence of *Rhinanthus minor* in fixed sand dune vegetation (Watkinson & Davy, 1985; Rodwell, 2000) and in calcareous grassland (Rodwell, 1992) recorded in this study is not unusual either. However, *Rhinanthus* was not found in dune slacks, which have been previously recorded as a habitat for this species (Rodwell, 2000). This is interesting as the community found in group 3 has many species of *Centaureo-Cynosuretum* and could apparently support *Rhinanthus minor*. Why *R. minor* is absent is not clear, especially considering that *Rhinanthus* is water-limited in the fixed dune area, as evidenced by the purple colouration of the foliage. It is possible that the shifting dunes form a barrier for seed dispersal which is typically within 0.5m from the plant (Westbury, 2004). On the other hand, the presence of *Odontites vernus* in this community is not surprising as it has been previously found in the similar SD8 community (Rodwell, 2000).

Habitat overlap of *Rhinanthus minor* and *Odontites vernus* was seen within *Vicio-Arrhenatheretum* (3 out of 20 relevés) and *Anthyllis vulneraria-Plantago maritima* community (6 out of 14 relevés). *Arrhenatherum elatius*-rich communities often develop in marginal, ungrazed habitats such as cemeteries and road verges (Rodwell, 2000). Both species have been previously recorded in this type of habitat. *Odontites vernus* is most commonly found at road verges, in addition to wasteland and as a weed of pastures and

Chapter 2

arable fields (Snogerup, 1982; Grime *et al.*, 1988). *Rhinanthus minor* is found in one of the most common habitats of *Odontites*, i.e. grassy road verges (personal observations) and MG1 *Arrhenatheretum* grasslands at low constancy (Rodwell, 1992). Interestingly, Rodwell does not list *Odontites* as a species of MG1, although it was found in this community by Dunnett *et al.* (1998a).

The overlap was more obvious at the Berneens site. While *Rhinanthus* is a common and desirable component of calcareous grasslands, *Odontites* appears in this habitat opportunistically following sward and soil disturbance and indicating negative changes to the community (Hirst *et al.*, 2005). The two species can, therefore, co-occur, presumably until the habitat regenerates and *Odontites* declines. It is not known how these two species, directly or indirectly, affect each other during this time. Competition could potentially occur at different levels. First of all, the two species were seen as seedlings and young plants closely together early in the vegetative season (personal observations). Therefore, competition for resources such as light or soil nutrients might be of importance before establishment on hosts occurs. Secondly and more intriguingly, it is possible that the two species could compete for hosts. The generalist character of hemiparasitism might further contribute to the considerable overlap in the potential hosts for both species. Similar or opposite preferences could have cumulative or opposing effect on the mediation of competitive relationships between hosts. Although the co-occurrence is expected to be transient, it might potentially determine the speed of regeneration of the habitat after disturbance occurs. If that was the case, it is particularly important within the Burren, where overgrazing and associated soil disturbance are a known peril to heath and grassland biodiversity (Deenihan *et al.*, 2009). Identification of other habitats in which the distribution of these two hemiparasites is frequent and subsequent studies of their effect on community dynamics are necessary to answer these questions.

Presence of *Odontites vernus* on the fringes of species-rich habitats and much smaller seeds dispersed by wind (Fitter & Peat, 1994) make it easy for it to encroach on these habitats when disturbance is applied. Since moisture and fertility are limiting factors for *Odontites* more so than for *Rhinanthus*, exposed and very dry sites such as the driest parts of sand dunes are less vulnerable. However, dry springs have been found to promote *Odontites* along road verges in a study carried out in England (Dunnett *et al.*, 1998). This means that in a habitat that is not originally extremely water-limited, *Odontites vernus* can gain advantage if drought occurs. This could potentially be true for habitats in pockets of clayey soil found between the predominant skeletal soils in the Burren (Parr *et al.*, 2009). Overall, the Burren offers a range of sites that appear ideal for carrying out a time-course study of ecological dynamics of *Odontites vernus* populations and its impact on vegetation structure.

Chapter 2

Although *Odontites* occupied either more nutrient-rich and/or disturbed patches and was generally associated with lower species richness, its association with the latter was not consistent. Its habitat at Berneens was characterised by extremely high species richness (up to 36 vascular plant species in a 1 m × 1 m relevé). As many of the contributing species were ruderal annuals, the quality of the habitat did not reflect the high species richness. Therefore *Odontites vernus* cannot be universally used as an indicator of biodiversity decline but might be a good indicator of habitat quality decline.

Correlations of *Rhinanthus minor* abundance with grass and forb cover agreed with the general grass-legume-forb pattern of host quality and mediation of competition which are well characterised for this species (Cameron *et al.*, 2005). The fact that the correlations of forb and graminoid abundance with *Odontites vernus* are opposite indirectly suggests contrasting host preferences. However, this requires further determination via haustorial dissection and growth experiments. Preference for dicots would mean that in addition to negative changes to community structure resulting directly from disturbance, parasitism by *Odontites vernus* could further contribute to negative shifts floristic composition by decreasing abundance of eudicot herbs and encouraging grasses. However, previously reported hosts of *Odontites* are *Trifolium repens*, *Hordeum vulgare* and *Stellaria media* (Govier *et al.*, 1967, 1968) as well as *Secale cereale*, *Poa subcaerulea*, *Festuca arundinacea*, *Festuca rubra*, *Juncus gerardi*, *Plantago maritima*, *Spergula arvensis* and *Trifolium repens* (Snogerup, 1982). Reported non hosts were *Carex distans*, *Plantago lanceolata* and *Triglochin maritima* (Snogerup, 1982). *Secale cereale* was the most beneficial host reported by Snogerup (1982). Furthermore, Matthies (1998) reported that *Medicago sativa* was a better host than *Lolium perenne* for *Odontites vularis*, currently classified as *Odontites vernus* ssp. *serotinus* (Stace, 2010). Overall, the pattern of host preference is not as clearly defined as in the case of *Rhinanthus minor*.

Rhinanthus is not the sole genus known to benefit biodiversity. *Cuscuta salina* var. *major* was found to benefit rare species of a Californian salt marsh (Grewell, 2008) and *Triphysaria pusilla* and *T. eriantha* were important for maintaining a balance between grasses and forbs in a coastal prairie in California (Marvier, 1998). Although *Odontites vernus* is generally not expected to contribute to species richness, it might itself become of conservation value if agricultural intensification is not halted, in analogy with the German example (Albrecht *et al.*, 2007).

In conclusion, both *Rhinanthus minor* and *Odontites vernus* are associated with important grassland habitats in Ireland. Better understanding of their local host ranges and population dynamics in those systems would be of great value to grassland management for conservation.

3 Methods of processing and imaging haustorial material

3.1 Plant material

3.1.1 Species used

Two locally-growing native annual hemiparasites *Rhinanthus minor* L. (yellow rattle) and *Odontites vernus* (Bellardi) Dumort. (red bartsia) of the family *Orobanchaceae* were selected for this study. Anatomy and immunocytochemistry of their haustorial connections with roots of known and potential native hosts and non-hosts was compared. *Rhinanthus minor* is a species of species-rich semi-natural grasslands. Its ecology and physiology are well researched and a link between haustorial anatomy and the ecological impact of *R. minor* has been partly elucidated (see chapter 1). Therefore, this species offers a useful system for the investigation of cell wall level interactions with different hosts and the ecological implications of those interactions. *Odontites vernus*, a weed occurring in more disturbed and nutrient-rich communities, was chosen to determine if certain characteristic immunocytochemical features initially identified in *R. minor* are also present in this species and therefore are likely to occur in many other *Orobanchaceae*.

Based on previous studies (Cameron *et al.*, 2006; Cameron & Seel, 2007; Rümer *et al.*, 2007) which distinguished three functional groups of *Rhinanthus* hosts: 1) grasses and 2) legume herbs (good hosts) and 3) non-leguminous herbs (bad hosts), the following species were selected:

- known good hosts : grasses *Cynosurus cristatus* L. (crested dog's tail) and *Lolium perenne* L. (perennial rye-grass)
- potential good hosts: grasses *Agrostis stolonifera* L. (creeping bent), *Arrhenatherum elatius* (L.) P. Beauv. Ex J. & C. Presl var. *bulbosum* (Willd.) St-Amans (false oat-grass) and *Holcus lanatus* L. (Yorkshire-fog); legumes *Lathyrus pratensis* L. (meadow vetchling), *Anthyllis vulneraria* L. (kidney vetch), *Medicago lupulina* L. (black medick) and *Vicia sepium* L. (bush vetch)
- known eudicot partial host: *Daucus carota* L. (wild carrot)
- known non-leguminous eudicot non-host *Plantago lanceolata* L. (ribwort plantain)
- potential non-leguminous eudicot non-hosts: *Pimpinella major* L. (greater burnet-saxifrage) and *Prunella vulgaris* L. (selfheal)

As determined by the ecological research presented in chapter 2, the above species were found co-occurring with *Rhinanthus minor*. The species that had not previously been investigated as hosts (potential hosts and non-hosts) were chosen specifically to further explore the host range of *Rhinanthus minor*.

Latin nomenclature used in this study follows that of Stace (2010).

3.1.2 Seed germination

Germination of parasite seeds

Seeds of *Rhinanthus minor* were purchased from Emorsgate Seeds in England (<http://wildseed.co.uk/>) in the first year of the project and used to obtain the first batch of plants. They were subsequently collected in Ireland (see table 1 for details of collection sites). *Odontites vernus* seeds were collected from a neglected lawn located opposite the entrance to Corrib Village at Newcastle Road in Galway City and in Barneens townland in The Burren, County Clare (table 1). Seed provenance was always clearly indicated. Seeds were sterilised by immersion in 1% v/v Bravo500 fungicide or 30% v/v thick Domestos bleach (working concentration of sodium hypochlorite — 1.35% w/v) for 10 minutes, washed in several changes of distilled water and placed in Petri dishes on discs of filter paper (Whatman No. 1, 9 cm diameter) moistened with 0.1% Bravo500 fungicide (Sygenta) in distilled water (DH₂O) at a density of 25 seeds per dish for *Rhinanthus* and 50 seeds for *Odontites*. As the determining germination factor for *Rhinanthus minor* and *Odontites vernus* is cold stratification (Borg, 2005), the seeds were cold-treated for 8–12 weeks in the dark at a constant temperature of 4°C (in a fridge) or under a 4°C/0°C regime (12 h/12 h in a BINDER growth chamber model KBW720; www.binder-world.com). The 4/0°C regime resulted in more abundant and uniform germination than stratification in the fridge as presented in appendix 1.

Germination of host seeds

Seeds of hosts were sterilised as described in the paragraph above and germinated mostly in the same manner as the hemiparasites, with the exception of the first batch of grasses which were treated as described below. A range of grass, legume and non-leguminous eudicot herb species were initially used and those species which germinated readily and grew fast were selected. Seeds were sterilised and placed in Petri dishes as described for the parasite species. Differences included the densities of very fine seeds of *Agrostis stolonifera* and *Holcus lanatus*, which were sprinkled across the surface of the filter paper, and large seeds of legumes (10 to 20 per Petri dish).

A total of five species of grasses that co-occur naturally with *Rhinanthus minor* were used as its hosts. *Agrostis stolonifera*, *Cynosurus cristatus*, *Holcus lanatus* and *Lolium perenne* were germinated directly in seed trays filled with soil in a greenhouse or in Petri dishes in a constant 22°C/16 h light regime growth cabinet. *Arrhenatherum elatius* ssp. *bulbosum* was introduced in year two and germinated on filter paper only. Bare caryopses of *Arrhenatherum* were used as the husks were easily removable, while whole caryopses of other grass species were used. *Arrhenatherum elatius* ssp. *bulbosum* was selected for subsequent studies as it germinated within two to three days with a success rate of 99%, produced a dense root system and encouraged numerous haustorial connections on large and fine roots.

Germination methods for non-legume eudicots differed. *Daucus carota* and *Pimpinella major* seeds were cold-stratified (0°C/4°C) for 4 weeks and moved to a windowsill (natural light conditions and room temperature) where approximately 20 to 30% of them germinated after two to three weeks. *Plantago lanceolata* germinated readily within several days without stratification. A germination rate of 30% after three weeks was reached by *Prunella vulgaris*.

Thirty minute scarification in concentrated sulphuric acid (10276, BDH) was necessary for the germination of legume species *Anthyllis vulneraria*, *Lathyrus pratensis*, *Medicago lupulina* and *Vicia sepium*. No additional sterilisation was necessary in addition to this harsh treatment. *Anthyllis vulneraria* proved most difficult to maintain in the chamber showing chlorosis and poor growth and attracted very few haustorial connections (not more than five per pot). The remaining three species yielded many connections (numbers not recorded). *Vicia sepium* was the most robust legume species under the growth conditions used.

From *Rhinanthus* and *Odontites* seeds germinating on filter paper those from which the radicle but not the cotyledons had just emerged were used. This was to avoid any damage to cotyledons that might attract pathogens. Host plants were generally more resistant to infections and slightly more advanced in age (several days post germination) when lifted from Petri dishes.

Table 3.1 summarises data on seed provenance and germination requirements of all species used in this project.

TABLE 3.1: Seed provenance and germination requirements of species used in this study

	species	provenance	sterilisation	scarification	stratification	germination substrate	approximate germination rate	
grasses	<i>Agrostis stolonifera</i>	England (Emorsgate seeds)	1% v/v Bravo 500 or 30% bleach	-	none	directly in soil	abundant after several days (seeds too small to count exact numbers)	
	<i>Arrhenatherum elatius</i> ssp. <i>bulbosum</i>	Inis Mór ¹		husks removed		-	99% after 2–3 days	
	<i>Cynosurus cristatus</i>	England (Emorsgate seeds)		-		directly in soil	approximately 40% after 2–3 weeks	
	<i>Holcus lanatus</i>			-		abundant after several days		
	<i>Lolium perenne</i>			-		approximately 20% after 3–4 weeks		
legumes	<i>Anthyllis vulneraria</i>	Esker Meadow ² at Brigit's Garden	same as scarification	incubation in 100% (18.1 M) sulphuric acid for 30 min	Parafilm® M-sealed Petri dish lined with moist filter paper	-	99% after 2–3 days	
	<i>Lathyrus pratensis</i>	winterage site in the Burren ³				-	80% after 4–5 days	
	<i>Medicago lupulina</i>	Little Meadow ⁴ at Brigit's Garden				-	30% 3 weeks after first break in dormancy	
	<i>Vicia sepium</i>	winterage site in the Burren ³				-	20% 3 weeks after first break in dormancy	
non-legume forbs	<i>Daucus carota</i>	Inis Mór ¹	1% Bravo 500 or 30% bleach	none	1 month at 0/4°C	-	95% within 1 week	
	<i>Pimpinella major</i>	Little Meadow ⁴ at Brigit's Garden				-	30% after 3 weeks	
	<i>Plantago lanceolata</i>					-	80% 3–4 weeks after first break in dormancy was observed	
	<i>Prunella vulgaris</i>					-	90% 3–4 weeks after first break in dormancy was observed	
	<i>Odontites vernus</i>	winterage site in the Burren ³ , Newcastle Road in Galway City ⁵				8–12 weeks at 12 h 0°C / 12 h 4°C	-	90% 3–4 weeks after first break in dormancy was observed
	<i>Rhinanthus minor</i>	Emorsgate Seeds (England); Killanin Esker, Roscahill, Co. Galway ⁶ ; Fanore Sand Dunes, Co. Clare ⁷ ; Shannon Callows near Lusmagh ⁸				-	-	-

1. Inis Mór 53°07'53.25" N, 9°40'45.20" W
2. Esker Meadow, Brigit's Garden 53°23'07.00" N, 9°12'38.55" W
3. winterage site in the Burren 53°04'20.00" N, 9°09'06.00" W
4. Little Meadow, Brigit's Garden 53°23'11.50" N, 9°12'39.50" W
5. Newcastle Road, Galway City 53°17'16.51" N, 9°04'13.12" W
6. Killanin Esker, Roscahill, Co. Galway 53°22'56.20" N, 9°12'00.00" W
7. Fanore Sand Dunes, Co. Clare 53°07'07.50" N, 9°17'02.50" W
8. Callow meadow near Lusmagh, Co. Offaly 53°09'01.50" N, 8°01'02.50" W

3.2 Pot cultures

3.2.1 Containers

The following types of containers were used to grow plants:

- full size seed trays, 38 cm × 25 cm × 5 cm, were used to grow the first batch of grasses only
- half size seed propagators, 23 cm × 17 cm × 7 cm with translucent plastic covers (7cm high), were used to grow *Odontites vernus* without hosts, *Daucus carota* with *Rhinanthus minor*, *Pimpinella major* with *Rhinanthus minor*, *Prunella vulgaris* with *Rhinanthus minor*, *Plantago lanceolata* with *Rhinanthus minor*, *Plantago lanceolata* with *Odontites vernus* (one container each)
- cavity inserts for seedling propagation, 2 cm × 2.5 cm (bottom of cavity) to 3 cm × 3.5 cm (top of cavity) × 5 cm height, were used to grow the first batch of *Rhinanthus minor* without hosts only
- 7.6 cm round plastic pots (Stewart Company) were used for the remaining growth experiments

All pots used had drainage holes and were used together with matching drainage trays. Prior to use, containers were soaked in thick bleach in tap water (200 ml in 5 litres, 0.0018 g of sodium hypochlorite in 100 ml H₂O) for 30 minutes, rinsed with DH₂O and dried in an oven at 60°C.

3.2.2 Soil mix

Initially, John Innes No. 1 compost for seedlings or a mixture of John Innes No. 3 for mature plants with sharp sand (1:1) was used. This provided unsatisfactory results as the soil was too rich in coarse organic fibrous fractions, became compacted and waterlogged fast and proved very difficult to remove from plant roots. An optimal soil mix was obtained by mixing 3 parts of well mineralised, dark garden soil (collected in Woodquay, Galway City 53°16'38.50" N, 9°03'05.35" W) with 3 parts of B&Q kiln-dried sand and 1 part of heavy calcareous clay (collected from a cliff in Silverstrand, Co. Galway 53°15'04.70" N, 9°07'24.50" W). This mixture provided sufficient nutrition and water retention while remaining easy to wash from the roots after soaking in water for several minutes.

To eliminate bacterial and fungal pathogens, small invertebrates and unwanted plant propagules, the soil was heated to 70°C in an oven and left at that temperature for 30 minutes after which it was left to cool. Higher temperatures were avoided as they can result in the presence of toxic compounds (Sonneveld & Voogt, 2009).

3.2.3 Watering regime

The saucers or drainage trays were filled with distilled water when the surface of the soil became dry (daily to once per week) and any excess water was removed after 30 minutes to prevent waterlogging.

3.2.4 Light and temperature regime

The first batch of plants was grown in a glass house with no temperature or light regulation. This proved unsatisfactory and subsequently plants were grown in a temperature control chamber (Binder) programmed to a cycle of 16 h light (approximately $100 \mu\text{mol} \times \text{m}^{-2} \times \text{s}^{-1}$ when measured at 10 cm away from the light source) and 22°C, followed by 8 h dark, 16°C regime. Daytime temperatures tended to rise up to 25°C on warm days as a result of the cabinet overheating.

3.2.5 Fungicide treatment of plants

Bravo500 (Sygenta) in DH_2O was used at 1:1000 v/v concentration for preventive treatment of plants against fungal pathogens. The diluted suspension was applied as a fine mist with a spray bottle once a week. Any plants that showed signs of pathogen infection were immediately removed and destroyed.

3.2.6 An overview of the plant material batches used in the project

The host-parasite mixes were grown for haustorial material in several batches which are described briefly below. More detail on the relevant batches is provided in chapters 4–6. Both *Odontites vernus* and *Rhinanthus minor* were grown with hosts, to obtain normal attached haustoria, and without hosts to stimulate development of metahaustoria. However, metahaustoria formed on plants grown with hosts and were also used in this study.

The first batch of haustorial samples (summer 2010) was grown in a glass house and comprised of full size seed trays sown with the grasses; *Agrostis stolonifera*, *Cynosurus cristatus*, *Holcus lanatus* and *Lolium perenne* (Emorsgate, UK) on 12.03.10 in No. 1 John Innes compost for seedlings in a greenhouse at natural light and non-controlled temperature conditions. Plants germinated within a week and several-day old *Rhinanthus* seedlings (Emorsgate) were added on 13.05.10 and thinned to 4 strong specimens per tray after 4 weeks. *Rhinanthus* haustoria attached to grasses were harvested on the 20th and 21st of June 2010 (*Rhinanthus* in flower). Additionally, *Rhinanthus* seedlings were planted in cavity inserts for seedling propagation on the 13th of March 2010, grown without hosts and harvested on the 25th of May 2010. Numerous metahaustoria were immediately processed for wax embedding. This batch of material was fixed in 4% formaldehyde in PEM buffer and embedded in Steedman's wax as described in section 3.3.2.

The second batch of haustorial material (summer 2011) comprised only of native material, mainly *Rhinanthus minor* (seeds collected at Killanin Esker, Roscahill) and *Odontites vernus* (Newcastle Rd, Galway) planted on 27.03.11 and parasitising *Arrhenatherum elatius* ssp. *bulbosum* and *Anthyllis vulneraria* (planted on 18.03.11). *Daucus carota*, *Medicago lupulina*, *Plantago lanceolata* and *Vicia sepium* were also tested as hosts in several additional pots. Plants were grown in round plastic pots (except *Daucus carota* grown with *Rhinanthus minor* in a half-size propagator), 2 parasite plants (both of the same species or one of each species) and two host plants (of the same species) per pot and harvested between the 11th and 18th of June 2011. These samples were fixed in 4% formaldehyde in PEM buffer and embedded in London Resin White (R1281, Agar Scientific, UK) and Steedman's wax.

During the spring and summer of 2012, the final samples were harvested and fixed using all of the fixing protocols described except for 4% formaldehyde in PEM and embedded in LRW and Spurr's resin (14300, Electron Microscopy Sciences, USA). The following parasite-host combinations were grown:

Half-size trays:

- *Daucus carota* planted 11.10.11 + *Rhinanthus minor* added 17.05.12, harvested 13.07.12
- *Odontites vernus* (Newcastle Rd) planted 11.11.11 with no hosts, harvested on 31.03.12
- *Pimpinella major* planted 04.11.11 + *Rhinanthus minor* added on 17.05.12, harvested 18.06.12
- *Plantago lanceolata* planted 12.10.11 + *Rhinanthus minor* and *Odontites vernus* added to a different tray each on 11.11.11
- *Prunella vulgaris* planted 15.10.11 + *Rhinanthus minor* added on 11.11.11, harvested 27.01.12

Round pots:

- *Arrhenatherum elatius* ssp. *bulbosum* planted 01.03.12 + *Rhinanthus minor* 18.04.12 and 17.05.12, harvested 14.06.12–24.07.12
- *Arrhenatherum elatius* ssp. *bulbosum* 01.03.12 + *Odontites vernus* 03.05.12, harvested 15.06.12–27.07.12
- *Lathyrus pratensis* planted 22.04.12 + *Rhinanthus minor* 2.05.12, harvested 24.07.12
- *Plantago lanceolata* planted 22.04.12 + *Rhinanthus minor* added 25.04.12,
- *Plantago lanceolata* planted 22.04.12 + *Rhinanthus minor* added 2.05.12, harvested 09.07.12
- *Vicia sepium* planted 22.04.12 + *Rhinanthus minor* added 25.04.12, harvested 30.06.12
- *Vicia sepium* planted 15.05.12 + *Odontites vernus* added 18.05.12, harvested 27.07.12

Cavity inserts:

- *Rhinanthus minor* planted 13.03.2010 with no hosts, harvested on 25.05.2010

3.3 Sample processing

3.3.1 Collection of haustoria

Plants were watered before harvesting and root balls were lifted from the pots carefully. Metahaustoria were collected first, as they had formed on the outside of the root ball where they had been adhering to the walls of the pot. Subsequently, the rest of the root system was removed in portions. Soil was removed from each portion immediately before it was examined while the remaining part of the root ball was kept in water with ice to minimise tissue degeneration. Each harvested part was washed of soil in a bucket with water, placed in water with ice and observed under a Leica M26 Stereo Microscope for normal attached haustoria. Haustoria were removed with parasitized pieces of host roots using scissors followed by precise cuts made with razor blades in a Petri dish with water to prevent air from entering the tissue. All collected samples were immediately plunged into fixative on ice. Obtaining samples of haustoria from each individual pot typically took about 30 minutes but could take up to two hours if various developmental stages were sought.

In addition to haustoria, unparasitised host roots were harvested and processed in the same way.

3.3.2 Fixation, dehydration and embedding

Fixative preparation and fixation procedure

Haustoria were fixed under vacuum for 30 min to one hour to remove trapped air. Two conventional fixatives for proteins, formaldehyde and glutaraldehyde, were used. The fixation by formaldehyde is weaker and partially reversible, yielding better access to epitopes and higher antigenicity (Ruzin, 1999). Glutaraldehyde fixation is irreversible and yields stronger cross-linking. This leads to better ultrastructure preservation, however, it may result in decreased antigenicity as the access to epitopes is more difficult in a densely cross-linked network (Ruzin, 1999). For good preservation of phospholipid membranes, particularly for ultrastructural investigations, postfixation in osmium tetroxide was applied. Depending on the type of investigations, different combinations of the three fixatives were applied, as listed in figure 3.1.

PEM and Sorensen's buffer were used for the preparation of fixatives.

PEM buffer: PEM buffer was made at double strength and stored frozen. Double strength PEM buffer consisted of 100mM (3.024 g in 100 ml of DH₂O) PIPES (piperazine-N,N'-bis[2-ethanesulfonic acid], P-6757, Sigma), 10mM (0.38 g in 100 ml of DH₂O) EGTA (ethylene glycol-bis(2-aminoethylether)-N,N,N',N'-tetraacetic acid, 03777, Sigma) and 10mM (0.246 g in 100 ml of DH₂O) MgSO₄ (magnesium sulphate, M7506, sigma) at pH 6.9 (adjusted with 1M NaOH and 1M HCl to allow PIPES to dissolve).

Sorensen's buffer: To make 1 litre of Sorensen's buffer at pH 7.2 140 ml of 0.2M (3.335 g in 140 ml of DH₂O) monosodium phosphate (NaH₂PO₄) were mixed with 360 ml of 0.2M (10.22 g in 360 ml of DH₂O) disodium phosphate (Na₂HPO₄) and 500 ml of DH₂O were added. The pH was checked and adjusted if necessary.

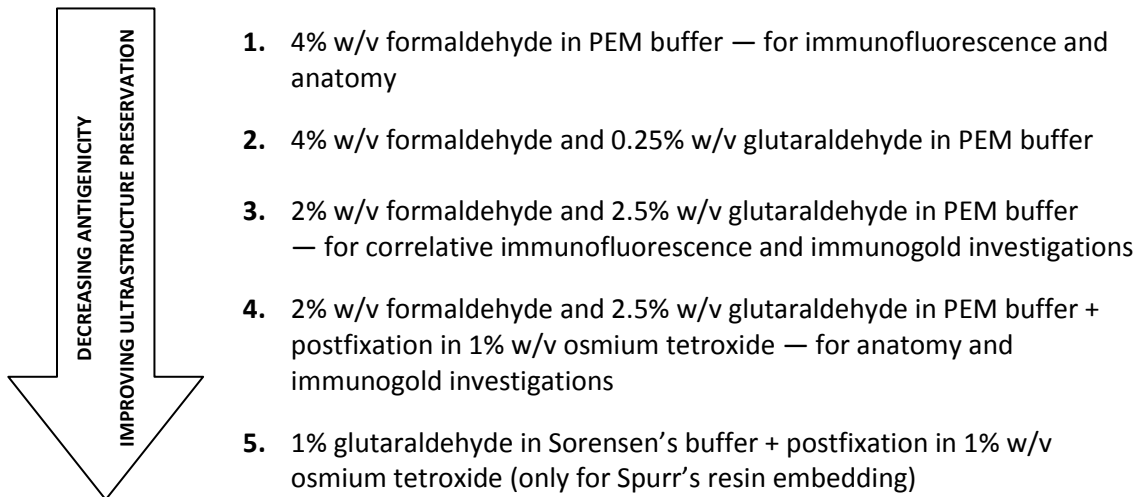


Figure 3.1: Fixatives used in this study in relation to antigenicity and ultrastructure preservation

Fixatives were prepared from stock solutions of 36.5% formaldehyde for molecular biology (F8775 Sigma) and 25% glutaraldehyde EM grade (R1010 Agar). To obtain 40 ml of a given fixative, 20 ml of double strength PEM buffer was mixed with 10 ml of DH₂O and 10 ml of one of the following fixative solutions:

- 10 ml of 16% formaldehyde (4.38 ml of stock + 5.62 ml of DH₂O) — to obtain 4% formaldehyde working solution
- 10 ml of 16% formaldehyde and 1% glutaraldehyde (4.38 ml of formaldehyde + 400 µl of glutaraldehyde stock + 5.22 ml DH₂O) — to obtain 4% formaldehyde/0.25% glutaraldehyde working solution
- 10 ml of 8% formaldehyde and 10% glutaraldehyde (2.19 ml of formaldehyde stock + 4 ml of glutaraldehyde stock + 3.81 ml of DH₂O)

For obtaining 1% glutaraldehyde in Sorensen's buffer, 4 ml of 25% stock (R1010, Agar) was diluted in 96 ml of the buffer.

The fixatives were aliquoted in 1 ml Eppendorf tubes, stored in a freezer and thawed only immediately before use.

Osmium tetroxide 4% w/v stock solution in 2 ml ampules (R1023, Agar Scientific) was diluted to a 2% concentration in DH₂O and could be stored in that form for several weeks (until the clear solution started turning grey/black) in a fridge in a tightly closed

glass bottle further sealed for air-tightness with Parafilm® M (P7543-1EA, Sigma). A working solution of 1% w/v was obtained by diluting the 2% stock in double strength PEM buffer.

Dehydration and embedding

Fixation and infiltration were carried out entirely in microcentrifuge tubes. After fixation in minimum tenfold volume of fixative, samples were washed in PBS buffer (3 times for 5 minutes) and dehydrated. The dehydration method depended on the embedding medium used (summarised in table 3.2). Steedman's wax (a low melting point wax which yields good antigenicity preservation, table 3.2) and London Resin White medium grade (Agar Scientific) required prior dehydration of plant material in ethanol. Samples prepared for Spurr's resin embedding (good for electron microscopy-based ultrastructural investigations) were dehydrated in acetone as ethanol (EtOH), which is normally also recommended, caused resin curdling. Gradual dehydration series of 30, 50, 70, 90, 100 and 100% of EtOH or acetone in DH₂O were applied. After reaching the 70% dehydration stage samples were left overnight. When the procedure had to be interrupted for several days, material was also incubated in 70%. This was generally avoided for samples intended for immunodetection to avoid potential epitope loss. Typically, dehydration was completed the following day and followed by infiltration with wax or resin. Steedman's wax infiltration was carried out at 37°C in three steps: 50% of molten wax in EtOH, 100% wax overnight and 100% wax for minimum 2 hours. Samples were then transferred to paper or silicon molds and left to set overnight at room temperature. Samples were stored in paper bags at room temperature. Resin infiltration was carried out on ice on a shaker and followed in more steps: 30%, 50%, 70%, 90%, 100%, 100%, 100% (in EtOH or acetone, London Resin White and Spurr's respectively), minimum 2 hours per step. Resin infiltrated samples were left in the second change of 100% resin overnight, and in the third change for at least one subsequent day or up to several months. Resin samples were cured for two days at 60°C (LRW) and 70°C (Spurr's) and stored in resealable plastic bags at room temperature.

TABLE 3.2: Comparison between the different properties of embedding media used in this project

medium property	Steedman's wax	London Resin White medium grade	Spurr's resin
method of preparation and storage	800 g of polyethylene glycol 400 distearate (305413, Sigma) and 100g of 1-hexadecanol (258741, Sigma) melted at 65°C, mixed and left to set at room temperature; stored in a closed container to exclude moisture	purchased as liquid from Agar Scientific and used without addition of optional accelerator; stored in the fridge for several months	ingredients purchased from Electron Microscopy Sciences (14300) and mixed in the following proportions: 10 g ERL, 8 g DER, 25 g NSA, 0.3 g DMAE; stored in the fridge for up to several days
melting/polymerisation temperature	melting point 37°C	polymerises at 60°C in anoxic conditions	polymerises at 70°C
solvent	ethanol	ethanol or acetone; in our study acetone caused curdling of resin	acetone
viscosity when pure (without solvent), Water: 1 centipoise (cp)	no published data but 28–30 cps at 55°C for a similar wax (Steedman 1960)	8 cps	60 cps (Spurr, 1969)
embedding molds used	paper or silicone molds	gelatine capsules or polyethylene molding cups (6×12×15 mm, Polysciences) with cavities covered with circles of Aclar embedding film (Electron Microscopy Sciences)	any plastic molds for microscopy
sectioning thickness	semi-thin (8–12 µm)	Semithin (0.5 µm, thicker sections do not stretch well) to ultrathin	semithin to ultrathin
affinity for water	hydrophobic	hydrophilic	hydrophobic
stability under the EM beam	n/a	Lower than Spurr's	higher than LRW
preservation of antigenicity	best	good	poorest
main applications	immunofluorescence (particularly when protein epitopes are a priority), alcohol-soluble dyes as resin samples often become dislodged from slides by alcohol	immunofluorescence, serial sectioning for anatomy at light microscopy level, immunogold labelling (for better antigenicity than Spurr's samples)	anatomy at ultra-structural level (TEM), Immunogold labelling of carbohydrates
summary of advantages and disadvantages	well preserved immunogenicity, cheaper sectioning equipment, allows detection of epitopes in the entire sample thickness	intermediate immunogenicity preservation, detection of epitopes on the sample surface mainly	reduced penetrability by antibodies (hydrophobic)

3.3.3 Slide preparation, sectioning and section mounting

For short and simple histological procedures such as toluidine blue O staining, plain pre-cleaned Corning® micro glass slides were used. For immunolocalisation studies, plain slides were treated with Vectabond™ (Vector Labs), to help sections adhere to the slides during several-hour long incubation times. Vectabond changes the properties of glass by etching as opposed to coating (De Mesy Jensen & Di Sant'Agnes, 1992). The solution was prepared by adding 7 ml stock solution into 350

Chapter 3

ml of acetone. Slides were cleaned in soapy water, rinsed with DH₂O and soaked in acetone for 5 minutes immediately before to immersing in Vectabond solution for 5 minutes. The slides were subsequently moved to DH₂O to remove excess of the solution. Moving from solution to solution was always carried out carefully to avoid creating bubbles. Slides were air dried after treatment. Polysine® Thermo Scientific slides were used interchangeably with Vectabond-treated slides.

Sectioning was carried out in two planes — transverse and longitudinal (Fig. 3.2). Wax-embedded samples were sectioned into ribbons with disposable microtome blades (Edge-Rite®, Richard-Allan Scientific®) at approximately 10 µm on a Leica RM2125RT microtome, mounted on drops of water on Vectabond™-treated slides or Polysine® slides and allowed to flatten and dry at room temperature. Samples were subsequently warmed on a hot plate heated to 40°C (for immunodetection) or 60°C (for histology) to increase section adhesion. However, the material often did not adhere sufficiently to either Vectabond-treated or Polysine® slides resulting in a large proportion of samples dislodging, with Vectabond-treated slides giving somewhat better results. Samples of haustoria attached to host roots proved particularly difficult to adhere to the slides and most sections were lost during dewaxing and dehydration. Samples of metahaustoria and healthy host roots adhered better but some loss of material also occurred. Alternatively, wax samples were sectioned and placed in small Petri dishes in which they were dewaxed and rehydrated and stained. Sections were then lifted with care using a Pasteur pipette and mounted on slides in water or a staining solution (see Table 3.3 for details).

Resin-embedded samples were sectioned on Reichert-Jung Ultracut microtome using a histo-diamond knife (Diatome, USA) as glass knives did not provide satisfactory results. Initially sections of 1 µm thickness were cut. However, the resultant sections did not adhere uniformly to slides. Sections of 0.5 µm were found to adhere better and this thickness was chosen for remaining sections. Polysine® and Vectabond™ slides worked equally well for resin-embedded material. Sections were mounted on drops of double distilled water on slides and dried in the oven at 60°C.

Resin samples for permanent preparations were stained with Toluidine Blue O, covered with a drop of Eukitt® quick-hardening mounting medium (Sigma) and a cover slip and left overnight for the medium to set.

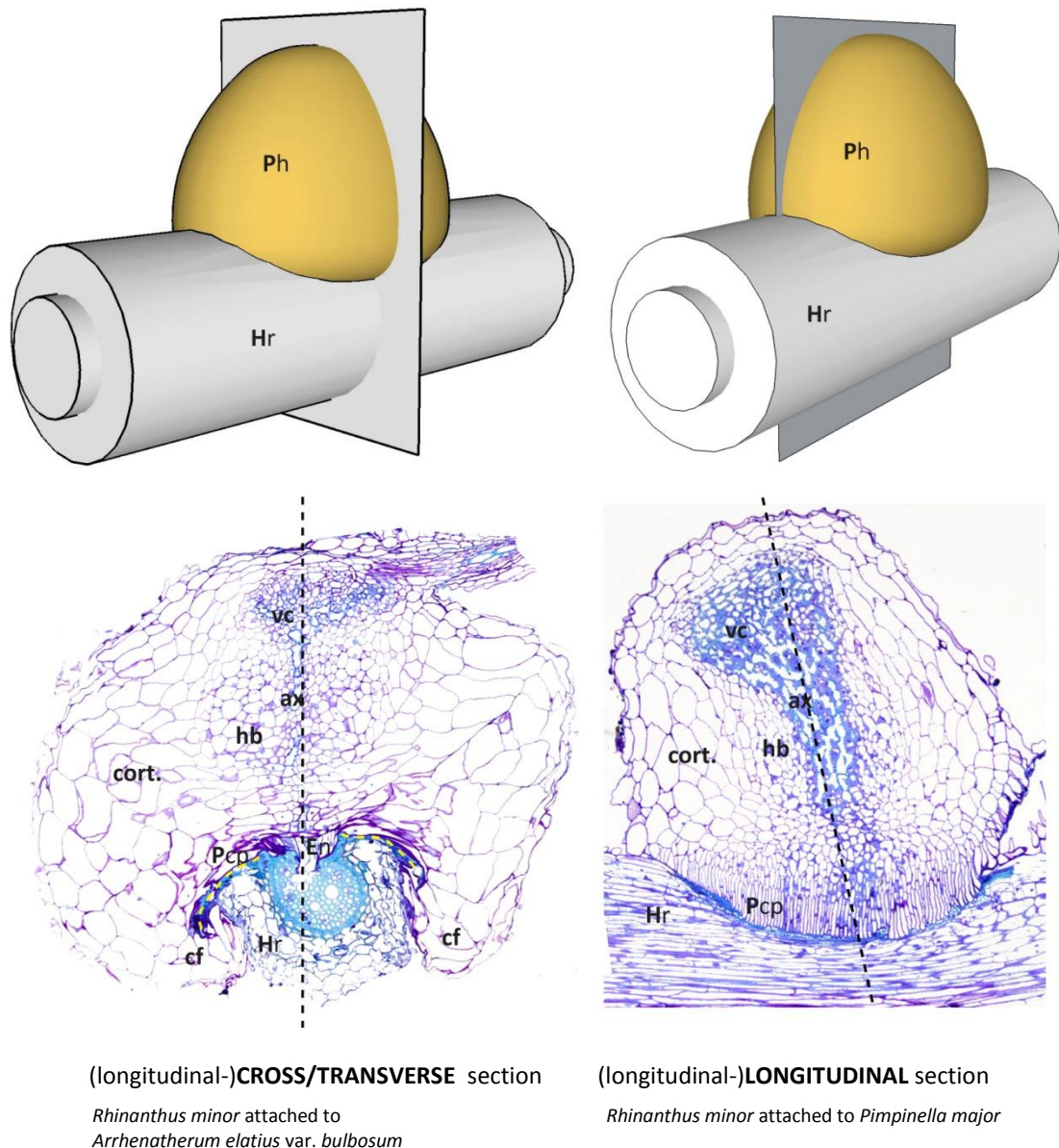


Figure 3.2: Haustorial section planes through parasitic plant haustoria (Ph) attached to host roots (Hr). All sections taken in this study were parallel to the xylem bridge axis (dashed line) and therefore longitudinal if the haustorium is considered separately. However, these sections were either perpendicular or parallel to the host root axis. These perpendicular to host root axis are referred to as cross or transverse sections and the ones parallel to host root axis are referred to as longitudinal sections. In a cross section, the axial strand of xylem bridge is typically one vessel thick. Parasite contact parenchyma (Pcp) is visible at lateral interface (yellow dashed line) and at the central interface, where it forms a narrow wedge of the endophyte (En). In a longitudinal section, the axial strand is often more than one vessel wide and the entire length of the endophyte wedge is visible. The elongated morphology of parasite's contact parenchyma (Pcp) cells forming the endophyte is very apparent in this view. (author's own images)

3.4 Microscopic observations

Bright field, fluorescence and electron microscopy were used in this project. A stereo microscope and an environmental scanning electron microscope were used to look at the morphology of whole haustoria. A compound epifluorescent microscope was

Chapter 3

used to look at the anatomy and histology of sectioned material and correlative immunofluorescence patterns. Ultrastructure was investigated using electron microscopy.

3.4.1 Light microscopy

Several whole haustoria and metahaustoria were observed using a Leica M26 Stereo Microscope immediately after harvesting. A number of haustoria were subsequently stained with Toluidine Blue O, Weisner reagent and Sudan IV and observed in the same way. Photographs were taken using a Canon PowerShot S50 camera.

Olympus BX51 epifluorescent microscope with x-Cite[®] 120Q mercury lamp and an Olympus XC10 digital camera (1376 × 1032 resolution) and Cell[^]B image acquisition software were used for histological and fluorescence-based investigations. Figure 3.3 summarises the wavelength specifications of the channels relevant to this study.

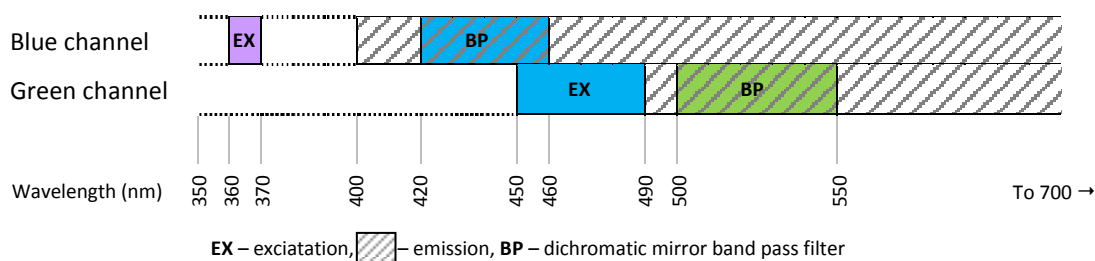


Figure 3.3: Blue and green channel wavelength specifications for the Olympus BX51 microscope used in this study

3.4.1.1 Histochemistry

The variety of stains and fluorochromes were used in this project and are summarised in table 3.3.

3.4.1.2 Cross-polarised light microscopy

Samples were observed for cell wall birefringence in cross-polarised light on the Olympus Olympus BX51 microscope. Samples in London Resin (unstained and stained with Toluidine Blue) as well as dewaxed and rehydrated samples were investigated.

3.4.1.3 Epifluorescence microscopy

Fluorescence microscopy was used to detect autofluorescence as well as cell wall compounds stained with fluorescent histological stains or labelled with fluorochrome-tagged secondary antibodies.

Table 3.3: Stains and fluorochromes used in this study (excluding antibodies)

stain	protocol	working solutions	staining procedure, mounting and observation	staining pattern	compatible embedding medium*
aniline blue fluorochrome (BioSupplies 100-1)		stock solution of 0.1 mg/ml diluted 1:5 in DH ₂ O before use	stain for 30 minutes, wash with DH ₂ O, counterstain with Toluidine Blue O (TBO) for 2 minutes, wash and mount in an antifade reagent AF2 (R1321, Agar)	callose fluoresces green in GFP channel	wax, resin
auramine O		0.01% w/v in 0.05M Tris-HCl buffer at pH 7.2	mount for 10 minutes and observe in GFP channel	unsaturated waxes fluoresce yellow	wax, resin
calcofluor fluorochrome		2.5g in 1ml H ₂ O for stock diluted 1:100 before use	stain for several minutes, rinse and mount in water or glycerol; not compatible with TBO post-staining	cellulose fluoresces blue	wax, resin
IKI		2% w/v KI in DH ₂ O + 0.2 g of iodine	stain for a minute, wash with DH ₂ O and mount in water or glycerol	starch stains purple/blue to black	wax, resin
Maüle reagent		1% w/v KMnO ₄ (potassium permanaganate), 3% HCl, conc. NH ₄ OH (ammonium hydroxide)	stain with KMnO ₄ for 20 minutes, rinse in DH ₂ O, differentiate in 3% HCl, rinse in DH ₂ O, count in conc. NH ₄ OH. rinse in DH ₂ O, mount in glycerol	syringil-rich lignin stains reddish brown, G and H lignins stain pale brown	wax
oil blue N		filtered, saturated stock in Isopropanol diluted 6:4 with DH ₂ O before use	stain for 30 minutes, rinse in 60% isobutanol and mount in water	lipids stain blue	wax
oil red O		filtered, saturated stock in Isopropanol diluted 6:4 with DH ₂ O before use	stain for 30 minutes, rinse in 60% isobutanol and mount in water	lipids stain red	wax
rhodamine B		0.1% w/v, aq.	stain for 30 minutes, wash in DH ₂ O and mount in water or glycerol	lipids fluoresce white pink under UV excitation	wax
ruthenium red		2% w/v, aq.	stain for 5 minutes, rinse with water and mount in water or glycerol	de-esterified pectins stain red/pink	wax
sudan III sudan IV		freshly made 1% w/v in 70% aqueous EtOH	incubate sections in 70% EtOH for a few seconds, Stain for 10 minutes, rinse with 70% EtOH and mount in water or glycerol	lipids stain red	wax
sudan black		0.4% w/v in 70% aq. EtOH	stain in a sealed container for at 60°C for 1h, briefly wash in 70% EtOH and mount in water or glycerol	lipids stain black	wax
toluidine blue O (TBO)		0.2% in 1% aq. borax** (sodium tetraborate decahydrate)	stain for several minutes and repeat if colours to weak, mount in water or glycerol	lignins stain greenish blue to bright blue, pectins stain purple pink	wax, resin
Weisner reagent			sections mounted in a solution of 1% w/v phloroglucinol in 95% EtOH mixed 5:1 with concentrated HCl immediately before use; solution may be blotted off after the colours have developed and replaced with water to avoid contact of acid from the slide with the microscope stage	lignin stains magenta/red	wax;
Yariv reagent			incubate dewaxed and rehydrated samples for 1 hour in β-D-glucosyl Yariv reagent in 0.15 M NaCl on a rocking platform. Use α-D-glucosyl Yariv reagent as control	AGPs stain orange	wax

* Incompatibility of resin results from faint staining as well as dislodgement of samples during staining when alcohol-based dye solutions are used.

** Addition of Borax results in high 9.2 pH of the solution for better penetration into epoxy resin-embedded (Spurr's) samples (Berlyn & Miksche, 1976; Ruzin, 1999) without affecting the polychromatic effect which is achieved in a range of pH from 5 to 9 (O'Brien *et al.*, 1964).

Fluorescence quenching

A number of components that auto-fluoresce when excited at 365 nm and above are present in plants (Rost, 1995). The cell walls of examined plants contain lignin, suberin (in which the phenylpropanoid component is autofluorescent), ferulic acids, coumarin and potentially cutin or wax. The autofluorescence emission spectra are only partly characterised and some data is presented in table 3.4. The intrinsic fluorescence of tissues overlapped with the immunofluorescence from the FITC fluorophore used as the tag of the secondary antibodies. To eliminate this problem, Toluidine Blue O was applied as a quenching stain after immunolabelling (Fig. 3.4).

Table 3.4: Natural fluorochromes present in investigated plant material

fluorochrome	Excitation	Emission
lignin	240–320 nm	peak at \approx 360 nm (Albinsson <i>et al.</i> , 1999)
phenylpropanoids of suberin	UV	blue and green
ferulic acid,	UV	blue; green in alkaline conditions (Harris <i>et al.</i> , 1997)
<i>p</i> -coumaric acid	UV	blue (Rost, 1995)
cutin	UV	whitish (Rost, 1995)

Toluidine blue O binds to samples through ionic interactions. It is a cationic (“basic”) dye attracted to acidic (negatively charged) components (Ruzin, 1999). It is polychromatic which means that different colours develop when it binds to different components (O’Brien *et al.*, 1964; Parker *et al.*, 1982), e.g. pectins stain pink purple while lignin stains light/turquoise blue. The exact mechanism of binding is not yet known although ionic interactions are believed to form the basis of the interaction (Ruzin, 1999) and the polychromatic effect is highly reliable for the detection of lignins and pectins when compared to a range of other techniques (Parker *et al.*, 1982). Similarly, the mechanism of autofluorescence quenching is not well understood. However, formation of ground-state complexes of TBO with bovine serum albumin (BSA) and bacterial fluorophores in *Pseudomonas aeruginosa* has been previously described (Usacheva *et al.*, 2008).

Immunolabelling for light microscopy

A total of 32 monoclonal (for glycan and protein epitope detection) and 4 polyclonal (for lignin epitope detection) antibodies were used in this project and are summarised in table 3.5. PBST — PBS (P5493, Agar) with 0.1% v/v Tween[®] 20 (P1379, Sigma) detergent aiding penetration of solutions into the resin) was used for block and antibody/block solutions as well as for washing between incubation steps. Dewaxed semi-thin sections and semi-thin sections of LRW-embedded material were first incubated in 3% w/v non-fat milk protein (dried skimmed milk) or Bovine serum albumin (BSA; A4503, Sigma) in 1× PBST for 30 minutes to 1 hour to block unspecific

binding. Following blocking, the sections were washed in PBST three times for at least 5 minutes per step and incubated in primary antibody in the BSA/PBST blocking solution for 1–2 hours at room temperature or overnight at 4°C. Controls were performed by excluding the primary antibody from the blocking solution to assess if the secondary antibody was binding unspecifically to the samples. The sections were then washed 3 times in PBST and incubated in secondary antibody; anti-rat (F6258, Sigma) or anti-mouse (F0257, Sigma) conjugated to fluorochrome fluorescein isothiocyanate (FITC) for 1–2 hours. They were subsequently stained with Toluidine Blue O to quench autofluorescence. No unspecific binding was seen throughout this project as exemplified in figure 3.4F and residual autofluorescence was seen only in the host *Daucus carota*.

Sections were mounted in glycerol-based anti-fade mounting medium Citifluor AF2 (R1321, Agar) or in distilled water with a drop of PBS-based Citifluor AF3 (R1322, Agar).

Masking of hemicelluloses by pectins (Marcus *et al.*, 2008, 2010; Hervé *et al.*, 2011), AGPs by pectins (Jauh & Lord, 1996) and hemicelluloses by hemicelluloses (Paul Knox, *pers. com.*) whereby one abundant polymer prevents access of antibodies to epitopes of another polymer has been previously described for other species. Unmasking by means of enzymatic removal of pectins was therefore carried out prior to hemicelluloses immunolabelling to test whether the signal would improve. Sections were incubated in 0.1 M sodium carbonate (S7795, Sigma) at pH 11.4 for 2 hours to remove methyl groups and make the polymers more vulnerable to the action of unmasking enzymes. The slides were subsequently washed in PBS and treated with Pectinex®UltraSPL (pectinase from *Aspergillus aculeatus*, P2611, Sigma) in *N*-cyclohexyl-3-aminopropanesulfonic acid (CAPS) buffer (50 mM CAPS, 2 mM CaCl₂, pH 10) at 1000 units of enzyme/ml (264 µl of stock solution topped up to 1 ml with CAPS buffer) or pectate lyase in CAPS buffer at 10 mg/mL (1 in 75 v/v) for 2 hours.

Table 3.5: List of antibodies used in this study, their sources, specificities and working concentrations

antibody	relevant publications	immunogen	reactivity	epitope structure	dilution of 1 st mAb stock	2 nd	supplier
400-2	Meikle <i>et al.</i> , 1991	laminarin-haemocyanin conjugate	(1→3)β-glucan, callose	five (1→3)β-linked	1:125	Mouse	Biosupplies biosupplies.com.au
Anti-MLG	Meikle <i>et al.</i> , 1994	<i>Hordeum vulgare</i> L.	(1→3)(1→4)β-glucan (MLG)	βGlc(1→3)βGlc(1→4)βGlc(1→4)βGlc(1→4)βGlc(1→4)Glc	1:100	Mouse	
CCRC-M1	Puhmann <i>et al.</i> , 1994	rhamnogalacturonan I-ME	xyloglucan, RGI	αFuc(1→2)βGal	1.5 or 1:10	Mouse	CarboSource http://www.ccrcc.uga.edu/~carb
CCRC-M7	Puhmann <i>et al.</i> , 1994	BSA complex	RGI, AGP	trimer or larger of β(1→6)Gal carrying one or more Ara residues of unknown linkage	1.5 or 1:10	Mouse	osource/CSS_home.html
INRA-RU1	Ralet <i>et al.</i> , 2010	oligorhamnogalacturonan-ovalbumin	RGI	at least 6 backbone disaccharide Rha(1→4)GalA(1→2) repeats	1.5 or 1:10	Mouse	Prof. Marie-Christine Ralet
INRA-RU2	Ralet <i>et al.</i> , 2010		RGI	at least 2 and optimally 7 backbone disaccharide Rha(1→4)GalA(1→2) repeats	1.5 or 1:10	Mouse	INRA, Not available commercially
JIM4	Knox <i>et al.</i> , 1989; Yates <i>et al.</i> , 1996		AGP	βGlcA(1→3)αGalA(1→2)Rha	1.5 or 1:10	Rat	
JIM5	Clausen <i>et al.</i> , 2003	<i>Daucus carota</i> L. protoplasts from suspension culture	partially Me-HG/no ester	MeαGalA(1→4)αGalA(1→4)αGalA(1→4)αGalA(1→4)αGalA(1→4)αGalA	1.5 or 1:10	Rat	
JIM7	Clausen <i>et al.</i> , 2003		partially Me-HG	GalA(1→4)MeGalA(1→4)MeGalA(1→4)MeGalA(1→4)GalA	1.5 or 1:10	Rat	
JIM8	Pennell <i>et al.</i> , 1991	<i>Beta vulgaris</i> L. protoplasts from suspension culture	AGP	unknown	1.5 or 1:10	Rat	
JIM12	Smallwood <i>et al.</i> , 1994	<i>Daucus carota</i> nuclear matrix protein extract	extensin	unknown	1.5 or 1:10	Rat	
JIM13	Knox <i>et al.</i> , 1991; Yates <i>et al.</i> , 1996	<i>Daucus carota</i> AGP2	(1→5)α-L-arabinan	βGlcA(1→3)αGalA(1→2)Rha	1.5 or 1:10	Rat	
JIM14	Knox <i>et al.</i> , 1991; Yates <i>et al.</i> , 1996		AGP	unknown	1.5 or 1:10	Rat	
JIM15	Knox <i>et al.</i> , 1991; Yates <i>et al.</i> , 1996	<i>Daucus carota</i> AGP1	AGP	unknown	1.5 or 1:10	Rat	
JIM16	Knox <i>et al.</i> , 1991; Yates <i>et al.</i> , 1996		AGP	unknown	1.5 or 1:10	Rat	
JIM19	Smallwood <i>et al.</i> , 1994	<i>Pisum sativum</i> L. guard cell protoplast	extensin	unknown	1.5 or 1:10	Rat	
JIM20	Smallwood <i>et al.</i> , 1994		extensin	unknown	1.5 or 1:10	Rat	
LM1	Smallwood <i>et al.</i> , 1995		HRGP	unknown	1.5 or 1:10	Rat	
LM2	Smallwood <i>et al.</i> , 1996; Yates <i>et al.</i> , 1996	rice cell wall material	AGP (GlcA)	beta-linked glucuronic acid	1.5 or 1:10	Rat	
LM5	Jones <i>et al.</i> , 1997	neoglycoprotein	(1→4)β-D-arabinan of RGI	(1→4)β-D-galactose oligomers	1.5 or 1:10	Rat	PlantProbes
LM6	Willats <i>et al.</i> , 1998		(1→5)α-L-arabinan of RGI and AGPs	(1→5)α-L-arabinose oligomers	1.5 or 1:10	Rat	
LM7	Willats <i>et al.</i> , 2001; Clausen <i>et al.</i> , 2003	rice pectin	partially Me-HG/non-blockwise	unknown	1.5 or 1:10	Rat	
LM8	Willats <i>et al.</i> , 2004	xylogalacturonan	xylogalacturonan	unknown	1.5 or 1:10	Rat	
LM10	McCartney <i>et al.</i> , 2005	xylopentaose-BSA	(1→4)β-D-xylan	βXyl(1→4)βXyl	1.5 or 1:10	Rat	
LM11	McCartney <i>et al.</i> , 2005		(1→4)β-D-xylan/arabinoxylan	βXyl(1→4)βXyl(1→4)βXyl(1→4)βXyl	1.5 or 1:10	Rat	
LM15	Marcus <i>et al.</i> , 2008	XXXG-BSA	xyloglucan	XXXG	1.5 or 1:10	Rat	
LM18	Verherbruggen <i>et al.</i> , 2009	seed mucilage	partially Me-HG/no ester	αGalA(1→4)αGalA(1→4)αGalA	1.5 or 1:10	Rat	
LM19	Verherbruggen <i>et al.</i> , 2009	fruit pectic galacturonan	partially Me-HG/no ester	αGalA(1→4)αGalA(1→4)αGalA(1→4)αGalA	1.5 or 1:10	Rat	
LM20	Verherbruggen <i>et al.</i> , 2009	seed mucilage	partially Me-HG	αMeGalA(1→4)αMeGalA(1→4)αMeGalA	1.5 or 1:10	Rat	
LM21	Marcus <i>et al.</i> , 2010	mannopentaose-BSA	mannan, glucomannan, galactomannan	unknown	1.5 or 1:10	Rat	
LM22	Marcus <i>et al.</i> , 2010	digalactosylmannopentaose-BSA	mannan, glucomannan	unknown	1.5 or 1:10	Rat	
LM25	Pedersen <i>et al.</i> , 2012	peribacteroid membrane	xyloglucan, unsubstituted β-glucan	galactosylated xyloglucan	1.5 or 1:10	Rat	
MAC207	Pennell <i>et al.</i> , 1989	from <i>Pisum sativum</i> nodules	AGP	βGlcA(1→3)αGalA(1→2)Rha	1.5 or 1:10	Rat	
anti-G lignin	Ruel <i>et al.</i> , 1994; Joseleau & Ruel, 1997; Zeier <i>et al.</i> , 1999	synthetic guaiacyl dehydrogenation polymer (DHP)	guaiacyl lignin	unknown	1:100	rabbit	
anti-H lignin	Ruel <i>et al.</i> , 1994; Joseleau & Ruel, 1997; Zeier <i>et al.</i> , 1999	p-hydroxyphenyl DHP	p-hydroxyphenyl lignin	unknown	1:100	rabbit	Prof. Katia Ruel CERMAV-CNRS, not available commercially
anti-GS lignin	Ruel <i>et al.</i> , 1994; Joseleau & Ruel, 1997; Misel <i>et al.</i> , 1997; Zeier <i>et al.</i> , 1999	mixed guaiacyl/syringil DHP	mixed guaiacyl/syringil lignin	unknown	1:100	rabbit	
anti-S lignin	Joseleau, 2004	syringil DHP	syringil lignin	minimum 2 contiguous syringil residues	1:100	rabbit	

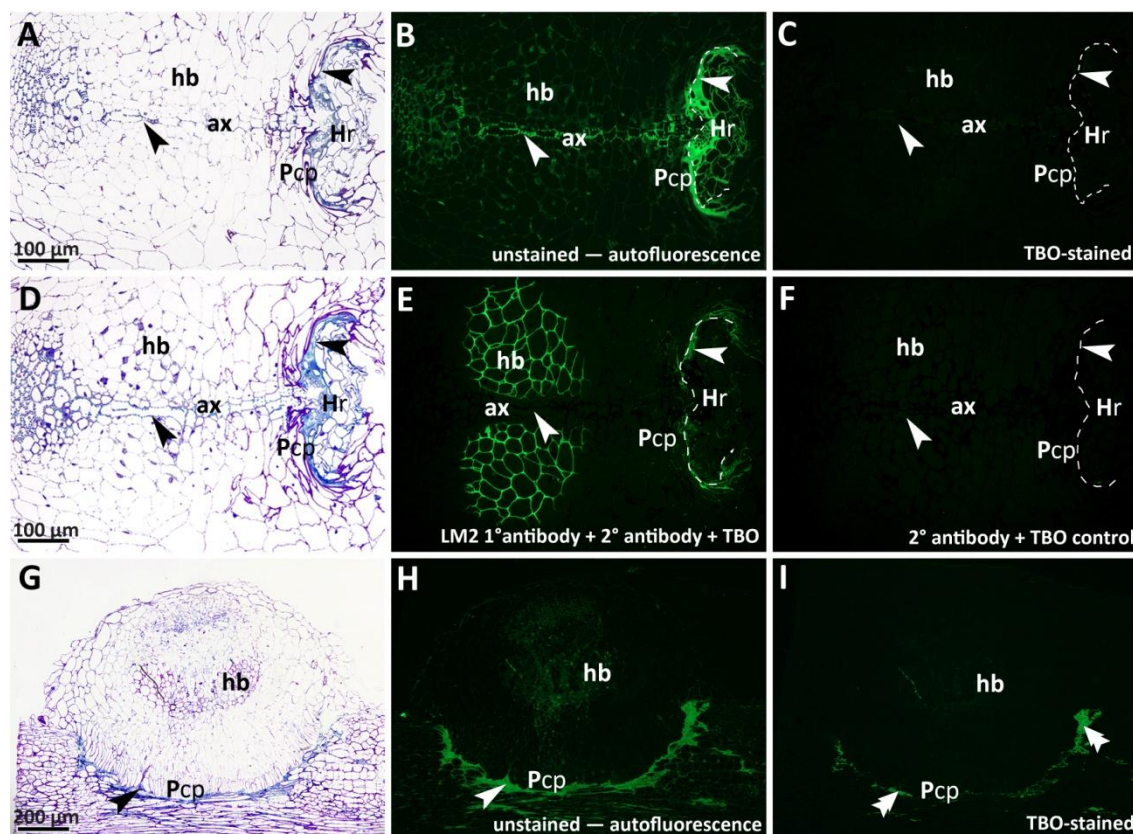


Figure 3.4: Autofluorescence quenching and control images. **A–C)** Serial cross sections through a haustorium of *Rhinanthus minor* attached to *Arrhenatherum elatius* var. *bulbosum*. Images A–C are of the same section. Images D and E also illustrate one section, different to that in A–C. Image F is of a section different to those in A–E. **G–I)** longitudinal sections through haustoria of *Rhinanthus minor* attached to *Daucus carota*. Unstained samples show high strong autofluorescence (**B** and **H**) in green channel, where FITC-conjugated secondary antibody labelling is also observed (**E**). Xylem (**ax**) and the phenolic-rich interfacial region between parasite contact parenchyma (**Pcp**) and host root (**Hr**) are most autofluorescent. Post-immunolabelling staining with toluidine blue O (TBO) quenched autofluorescence in a vast majority of examined samples, as exemplified in image **C**. Figure **F** shows a control image where the primary antibody was not applied to assess potential unspecific binding of the secondary antibody. Neither autofluorescence, nor unspecific binding are present. Interfacial phenolic compounds of *Daucus carota* are not quenched by toluidine blue O (**H** and **I**). As unspecific binding was never seen in this study and autofluorescence was almost always fully quenched, control images are not shown throughout this thesis. Localised areas of residual autofluorescence in *Daucus carota* are indicated with double white arrowheads.

3.4.1.4 Raman spectroscopy

Renishaw® InVia Raman spectrometer coupled with a Leica microscope equipped with a motorized xyz stage was used. Green laser (514 nm) was used and prior to sample measurements calibration on a silica sheet at 520 wavenumbers cm^{-1} was carried out. Point test measurements were taken from samples for a range of published bands characteristics of lignin/phenolics, aliphatic domain of suberin and cellulose (Prinsloo *et al.*, 2004; Schmidt *et al.*, 2010; Busch *et al.*, 2010). As the obtained peaks were distinctive only for lignin, mapping in the relevant range (1300–1700 wavenumbers cm^{-1}) only was continued. Mapping was carried out at $\times 50$ magnification, at 1 μm resolution and 100% power and with cosmic ray removal. Wax-embedded samples

were extremely autofluorescent under the green laser, which was expressed in a noisy spectrum. Therefore, wax-embedded samples were not mapped. Resin quenched the green laser-induced autofluorescence but required longer exposure time (10s), resulting in longer mapping times and smaller mapping areas. 1 μm thick sections were most suitable, whereas 0.5 μm sections produced a much weaker signal.

Data was analysed in MATLAB R2012a. Principle Component Analysis (PCA) and Multivariate Curve Resolution (MCR) were employed for chemometric analysis. Spectral data was pre-processed by normalisation and smoothing (Savitzky-Golay). Additionally, data was mean-centred for PCA and baseline-corrected with classical least squares for MCR. PCA was mostly useful in assessing the number of components applied in MCR analysis as well as detecting correlation (both positive and negative) between different parts of the spectrum. Loadings from MCR corresponded more tightly with spectra of individual biochemical components and were therefore more chemically significant.

3.4.2 Electron microscopy

3.4.2.1 Scanning electron microscopy

Environmental SEM images of metahaustoria were taken using Hitachi S-2600N Variable Pressure Scanning Electron Microscope at the Centre for Microscopy and Imaging, NUI Galway. Fresh samples were used without prior processing.

3.4.2.2 Immunogold labelling and transmission electron microscopy

Material fixed according to methods B–E (Fig. 3.1) was used for ultrastructural investigations. Nickel grids were used for immunogold labelling and copper grids were used for anatomical observations. Nickel grids can become magnetised under the electron beam and cause stigmatism during observations. Copper grids do not become magnetised, however, they produce precipitates in contact with buffers used during immunolabelling and possibly affect antigen-antibody reactions (Osafune & Schwartzbach, 2010). Grid coating was carried out in a room dehumidified by heating up for several hours to prevent occurrence of holes in the Formvar support film which reacts with moisture in the air during the drying process. Formvar solution (0.4% w/v) was prepared by dissolving Formvar powder (R1202, Agar) in pure chloroform (25690, Sigma). Plain slides (Corning) were cleaned with butyl acetate (287725, Sigma), dipped in the Formvar solution for 10 seconds and left to dry for 5 minutes in a chamber with silica gel. The edges of the film covering the slides were scored with a razor blade and Formvar was floated from slides onto the surface of water by slowly immersing the slide in distilled water vertically. Grids were slightly bevelled with a round-tipped glass rod and carefully placed on the floating Formvar film, convex side down. They were subsequently lifted on sheets of Parafilm[®] M and left to dry overnight in a covered Petri dish.

Ultrathin sections of silver to gold colour were obtained using Reichert-Jung Ultracut microtome and collected on Formvar-coated slot and 75 mesh grids.

Sections of osmicated samples for immunogold labelling were incubated in freshly made 5% hydrogen peroxide in DH_2O for 5 minutes to remove excess osmium, rinsed in distilled water and incubated in freshly prepared ammonium chloride (0.13 g in 50 ml DI, 48.6 mM) for 15 minutes to block aldehydes from fixative. The above steps were skipped for sections analysed only for anatomy.

Sections for immunogold labelling with monoclonal antibodies were blocked in 1% BSA in PBST (centrifuged to remove undissolved particles before use) and those intended for incubation with polyclonal antibodies against lignin were blocked with 3% v/v goat normal serum (G9023, Sigma) in PBST. Grids were then washed by placing them on drops of PBST on Parafilm® M (3 changes, 5 minutes each) and rinsed by running PBST down forceps onto the grid. Primary antibodies were applied for 2 hours at 37°C or room temperature in a simple moisture chamber (plastic box with moist filter paper, covered with a lid). This was followed by rinsing in PBST in the same manner as described above and subsequently appropriate secondary antibodies (mouse, rat or rabbit) were applied at dilutions indicated in table 3.5. Grids were thoroughly washed on drops and under running distilled water as above and either dried for future staining or stained immediately with uranyl acetate and lead citrate. Staining was carried out manually or in an automatic contrasting system (Leica EM AC20). During the manual procedure, uranyl acetate was applied by placing grids on drops of the stain on Parafilm® M for up to 30 minutes. Samples were washed with DH_2O and stained in lead citrate for 3 minutes in a glass Petri dish filled with sodium hydroxide pellets to absorb carbon dioxide and prevent carbonate precipitation. Boiled DH_2O water (CO_2 removed during boiling) was used for rinsing the grids before and after lead citrate staining to further reduce carbonate precipitates. Grids were air dried for several hours before observations.

The stains were prepared according to the following protocols and stored in the fridge with the screw top caps sealed with Parafilm® M:

- Uranyl acetate — 1% w/v in DH_2O , centrifuged for 2 minutes before use
- Lead citrate — 0.1–0.3 g in 100ml of DH_2O + 1 ml of 10 M sodium hydroxide mixed with 10 μl of detergent into 10 ml of stain before use

TEM images were taken using Zeiss Libra®120 (120 kV) with a slow scan CCD digital camera (Albert Tröndle Restlichtverstärkersysteme) at Skidmore Microscopy and Imaging Center (USA) as well as HitachiH7000 (75 kV working voltage) with Hamamatsu 1K digital camera and AMT image acquisition software at Centre for Microscopy and Imaging, NUI Galway.

4 Cell walls as contributors to virulence and defence in parasitic plant-host associations

4.1 Abstract

Virulence and defence are two counterforces acting in host-pathogen, as well as parasitic, plant-host associations. Cell walls at haustorial interfaces are the sites of initial contact between the opponents. Many early responses are triggered and implemented within the extracellular matrix (ECM). Therefore, cell walls contribute to both virulence and defence. However, parasitism between angiosperms is not characterised as fully as interactions between plants and microbial pathogens.

A range of receptors necessary for exchange of signals between the parasite and the host are localised at the plasma membrane-cell wall interfaces. These include receptor like kinases (RLKs) and other putative receptor molecules, for example GPI-anchored arabinogalactan proteins (AGPs). The ECM is also a source of signalling ligands, for example elicitors of host defence responses or haustorium inducing factors (HIFs). Furthermore, cell walls constitute intrinsic physical barriers protecting the host from the invader and shielding the parasite from host responses. Further reinforcement with structural proteins and phenolics often contributes to resistance. A range of cell wall degrading enzymes (CWDEs) are employed by the parasites to facilitate intrusive growth, while pathogenesis-related proteins (PRPs) including inhibitors of parasite's enzymes or enzymes directed at the parasite's wall components are part of the host's defence arsenal.

Cell wall diversity is likely to affect the processes at haustorial interfaces with different hosts as differences in wall composition result in differences in digestibility or released signalling molecules. As cell walls are implicated in all stages of infection, from haustorial initiation to complete penetration, they offer a wide range of research targets for better understanding of parasitism and engineering of host resistance. While further scientific progress is needed to achieve this, several studies have shown that cell wall-focused approaches have the potential to identify factors crucial in haustorial development as well as host resistance.

4.2 Introduction

If plants were sentient organisms and awards for the most uncanny vegetal life strategy were being presented, parasitic angiosperms would stand a very good chance of winning the title. The members of this fascinating group of plants have the ability to rob nutrients directly from organs of other plants known as hosts. For that purpose, parasitic angiosperms have evolved haustoria — specialised grafting organs responsible for attachment to, and solute flow from, host tissues (Kuijt, 1969). It is therefore not surprising that the success of infection and the invader's well-being are determined by the functionality of these structures. In anatomically mature, fully developed haustoria of most species, contact between vasculatures of the host and the parasite is developed to facilitate the flow of water and mineral nutrients. It is at the site of contact known as the interface that cell walls of the victim (host) and its perpetrator (parasite) physically interact. As a natural consequence, cell-wall localised processes contribute to the failure or success of the contestants in what has previously been described as “a shifting balance of power” (Timko *et al.* 2012) or “arms race” (Irving and Cameron 2009). The overall outcome of plant parasitism is a counterpoise between parasite virulence and host resistance — two inseparable and complex components of the interaction that continuously evolve in an attempt to gain advantage over each other. Cell walls play an integral role in this battle as they are the site of initial contact and mounting of early responses (Humphrey *et al.*, 2007). In addition to having mechanical functions, they can be the source of perception molecules, a barrier that needs to be crossed by them, and a site of receptor domains of receptor proteins located at the membrane-wall interfaces. To better understand how the extracellular matrix is and might be implicated in both “defence and offence” (Kim *et al.*, 1998), and to help interpret the results presented in subsequent chapters of this thesis, an overview of the function of the cell wall in virulence versus defence mechanisms is presented in this chapter. Plant defence mechanisms against parasitic plants have not been identified as clearly as those directed against herbivores or pathogens (Runyon *et al.*, 2010) despite huge economic (Parker, 2009, 2012; Rubiales & Fernández-Aparicio, 2012) and ecological (Press & Phoenix, 2005; Watson, 2009) implications of plant parasitism. While some fundamental elements of responses to parasitic plant ingress are likely to be similar to those during other biotic interactions, physiological similarity between parasitic plants and their hosts is likely result in certain mechanisms being specific to this type of interaction. As cell wall-localised responses to pathogens are relatively well understood (Hückelhoven, 2007), comparisons with bacterial and fungal pathogens are drawn and suggestions on possible analogies are made where no data for equivalent processes in parasitic angiosperms exists.

4.3 Cell walls are implicated in virulence and resistance — two inseparable elements of parasitism

Toft and Aeschlimann (1991) define virulence as “the net harm that parasites do to the host”, where the word “net” highlights the inseparability of virulence and resistance. It is therefore important to note that the overall impact of parasitic plants on host plants is the combined result of the host plant defence mechanisms and the parasite’s virulence acting against each other to produce a synergetic effect, further modified by environmental factors (Fig. 4.1). Virulence of parasitic plants is not well defined and if loosely treated as the ability to invade host tissues and abstract nutrients, it is partly determined by the hosts resistance levels. This creates a terminological and functional loop. Virulence mechanisms tamper with and modify defence mechanisms and vice versa. A parasite can secrete host cell wall-degrading enzymes while the host plant may fight back by synthesising and releasing protein inhibitors (Juge, 2006; Misas-Villamil & van der Hoorn, 2008).

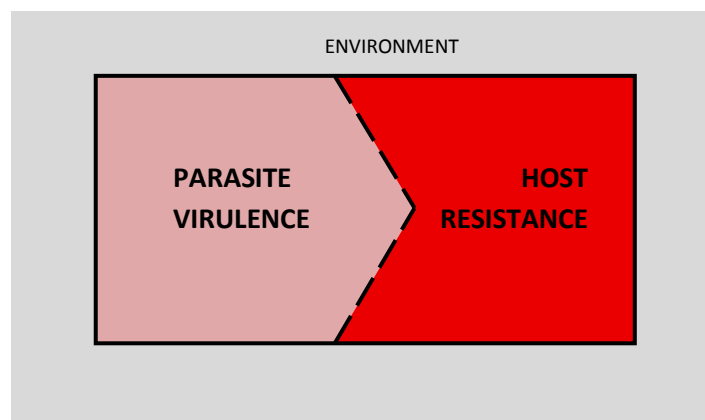


Figure 4.1: A schematic representation of parasite-host associations. The net outcome (area within a solid black line) results from the shifting balance of parasite’s virulence and host’s defence abilities (dashed line) and is further modified by environmental factors. (author’s own image)

Both virulence and defence are commonly used and researched themes of the interactions between plants and their bacterial and fungal antagonists. Contrastingly, defence responses in parasitic plant-host associations tend to be defined more tangibly than virulence, the latter remaining relatively undefined. While host defences have been demonstrated by molecular, anatomical, physiological and ecological techniques as referenced throughout this thesis, the term *virulence* appears very rarely in parasitic plant-related literature. In his classical text book on parasitic angiosperms, Kuijt (1969) refers to virulence and, while acknowledging that it is superimposed on resistance, he gives examples only for the latter. In the majority of relevant publications the term “virulence” does not appear even when the described factor (for example host

cell wall-degrading enzymes) is an obvious contributor to the invader's success. An exception from this is the work by Veronesi and co-workers (2005) who looked into links between the virulence of *Orobanche cumana* Wallr. and pectinolytic enzymes secreted by it into the interface. Several studies consider virulence only in terms of overall outcomes rather than mechanisms. Mutikainen and co-workers (2000) expressed the virulence-resistance balance between *Rhinanthus serotinus* (Schönh.) Oborny and *Agrostis capillaris* L. as vegetative and generative biomass of the two species. Similarly, Rowntree *et al.* (2011) used biomass and reproductive output of *Rhinanthus minor* L. and *Hordeum vulgare* L. to measure the effects of intraspecific genetic variation of the opponents. Virulence was specifically defined as the difference in seed production in parasitized and non-parasitized barley plants. Prior to that, genetic variation in the virulence-tolerance relationship between *Cuscuta europaea* L. and *Urtica dioica* L. was researched, also using a biomass-focused approach (Koskela *et al.*, 2002). A recent review by Timko *et al.* (2012) is an important addition providing a theoretical model of gene-for-gene resistance to parasitic plants, based on the existing knowledge of plant interactions with microbial pathogens.

The apparent absence of the term *virulence* from the relevant literature might result in an under-appreciation of its role when dissecting and interpreting the effectiveness of the various components of defence mechanisms, which constitute only a piece of a very complicated and dynamic antagonistic system. While virulence is not clearly defined for parasitic plants, it is safe to say that its contributors at haustorial level comprise all the mechanisms required for recognition of the host organ, attachment to it, recognition of the entry point and subsequent penetration using mechanical pressure coupled with intrusive growth aided by enzymatic and signalling machinery.

In addition to being counteracted by virulence, resistance is not the only element within the host defence arsenal as host defences can be divided into resistance and tolerance (Mauricio *et al.*, 1997; Roy & Kirchner, 2000). Resistance either prevents (qualitative resistance) or limits (quantitative resistance) infection and reduces parasite fecundity. If resistance is not sufficient to stop the invasion (in that case termed *host resistance*), tolerance can act by mitigating the pathogenic consequences of successful infection for host fecundity, while maintaining parasite's fitness. When resistance is successful and prevents parasite establishment this is termed *non-host resistance*. The two share some components in terms of signalling pathway (Thordal-Christensen, 2003) and therefore certain fundamental responses overlap in the host and non-host responses. *Solanum* host and non-hosts to *Phytophthora infestans* (Mont.) de Bary shared hypersensitive response expression, with quantitative (number of dead cells) and timing differences (time of induction after inoculation) accounting for the overall outcome (Vleeshouwers *et al.*, 2000).

Resistance and tolerance behave differently in co-evolutionary terms. Roy and Kirchner (2000) explain that the advantage of carrying resistance genes decreases with evolutionary time. As the resistance acts on the pathogen, the incidence of disease decreases and resistance is no longer selected for. A steady equilibrium is reached before the pathogen is eliminated. Tolerance genes are generally of greater fitness advantage to hosts because they allow co-existence of host and parasite and therefore tolerance is selected for. Consequently, resistance genes do not tend to become fixed whereas tolerance genes do. Additionally, while hosts continue to evolve towards full resistance, parasites continue to evolve mechanisms to overcome those barriers, making fixation of ultimate resistance difficult (Schneider & Ayres, 2008). However, full resistance (Pérez-de-Luque *et al.*, 2005; Gurney *et al.*, 2006; Echevarría-Zomeño *et al.*, 2006) and tolerance (Gurney *et al.*, 2002) have both been found in parasitic plant hosts. Moreover both strategies have been demonstrated to co-exist (Medel, 2001). The need to include tolerance in parasitic plant hosts as a mechanism complimentary to resistance was explored by Rodenburg & Bastiaans (2011) for parasitism by *Striga*. Similar to defense versus virulence considerations it is important to bear in mind how resistance and tolerance within the host might modify each other. Can lack of mechanical resistance be a consequence of well developed tolerance or will lack of resistance eventually lead to the evolution of tolerance? To what extent do tolerant plants attempt to resist parasitic attack before giving in?

A further point worth noticing is that in addition to species-to-species co-evolution resulting from close interactions between two individual taxa, full resistance may develop as a result of so called diffuse co-evolution — evolution between groups of organisms, in this case — plants and pathogens. An example of this phenomenon in parasitic plant-host interactions was provided by Hood and co-workers (1998) who pointed out that lettuce (*Lactuca sativa* L. cv. Bibb) and marigold (*Tagetes erecta* L. cv. Crackerjack) were resistant to *Striga asiatica* (L.) Kuntze even though they do not naturally co-occur with the parasite.

4.4 The involvement of cell walls in virulence and defence at haustorial interfaces

4.4.1 Cell wall as a dynamic interface

As structures external to the protoplast, cell walls play active roles in communication and development of all plant cells. They are the site of initial contact and signalling between plants and pathogens. Haustorial and host cells also sense each other and “talk” across cell walls, which continue to form not only the physical but also the physiological interface in a maturing graft. Just as host cell walls need to remain vigilant to parasitic attack, the parasite cell walls at the contact zone must specialise to aid penetration and resource uptake in the hostile environment of the host tissue. The extracellular matrix

is implicated in signalling, attachment to the host and penetrative growth into its tissues, recognition by the host and subsequent defence mechanisms (Hückelhoven, 2007; Cantu *et al.*, 2008). Intensive trafficking of molecules from and into the apoplast is associated with the infection (Yun & Kwon, 2012). To allow this array of functions, cell wall architecture must facilitate the flow of molecules between the two organisms. These molecules include germination cues, haustorial inducing factors (HIFs), elicitors, enzymes and other pathogenesis related proteins such as enzyme inhibitors, abstracted nutrients and many more.

Theoretically, the flow of substances between the protoplasts of adjacent cells could be achieved through plasmodesmata. As haustorial endophytes primarily grow intercellularly following decomposition of the host middle lamellae (see Joel & Losner-Goshen, 1994 and chapter 5), intraspecific plasmodesmata are theoretically possible. However, fully functional, plasmodesmal connections have been reported only transiently between *Cuscuta* (dodder) penetrative cells termed searching hyphae and host cortex cells (Kuijt, 1977; Vaughn, 2003; Birschwilks *et al.*, 2007) as well as between *Orobanche* and its host, preceding interspecific sieve pore differentiation (Dörr & Kollman, 1995). Half plasmodesmata have also been recorded for *Arceuthobium*-host associations, some of which were aligned yet without a confirmed symplastic link (Alosi, 1980; Carol & Calvin, 1985; Calvin & Wilson, 1996). Considering the lack of plasmodesmal links and the fact that many signals are perceived before physical contact occurs, it is more likely that the majority of information travels across the extracellular matrix (ECM).

The ability of the extracellular matrix to expand and/or enable transport is a function of its biochemical and physical properties. Rheological properties such as porosity compliment active means of perception and transport, i.e. receptor and transport molecules discussed in the section 4.4.2. Pectins are one of the “usual suspects” when considering rheological properties as they are amongst to the most mobile components of the extracellular polysaccharide matrix (Bootten *et al.*, 2011). The relative proportions of their methylated and non-methylated forms lead to shifts from sol to gel and affect porosity (Baron-Epel *et al.*, 1988; Willats *et al.*, 2001). This affects diffusion of substances across the wall as well as growth and intrusion-enabling physical properties of walls. Vaughn (2006) demonstrated cell wall loosening through reduction of cellulose and xyloglucans and enrichment in pectins in phloic searching cells of *Cuscuta pentagona* Engelm. These changes were proposed to facilitate apoplastic transport of carbohydrates from the host as well as to increase malleability which is necessary for the scavenging growth. During the intrusive growth of the endophyte, the cell walls of the penetrative cells are subjected to rapid elongation and remodelling until they reach the host cell of destination. While being pliable enough to allow this, the cell wall needs to remain coherent to avoid shear damage when the parasite pushes its way through host cells.

Other potential modes of trans-wall transport between the parasite and host exist. One of the most intriguing and virtually unexplored possibilities to consider is trans-wall vesicle transport such as that found in fungal hyphae (Casadevall *et al.*, 2009).

4.4.2 Wall-associated signals and receptors

Transport and communication across the wall is by no means limited to passive diffusion of molecules. There are several groups of receptors dedicated to sensing signals in the apoplast and transferring the information to the cell interior. The nature of both receptor and signal molecules is outlined below. The extent to which they participate in plant parasite-host interactions is not well understood, although considering their role in many other fundamental processes, they are likely to be important in haustorial differentiation, host defences and exchange of information between the two organisms. While future research has yet to identify wall-associated receptors important specifically during parasitism by angiosperms, the known examples of their up-regulation and functions are mentioned below.

Receptor-Like Kinases (RLKs)

Physical and signalling continuity between the cell wall and the protoplast is achieved through certain groups of proteins found at the interface between the plasmalemma and cell wall called the periplasmic space (Lampert & Kieliszewski, 2005). They are known as receptor-like kinases (RLKs) and possess three domains necessary for reception of signals and their transduction to the cell: 1) an extracellular signal binding domain, 2) a transmembrane moiety and 3) a cytosolic kinase domain that allows transduction of the signal into the protoplast. In addition to enabling fundamental processes such as growth and development (Becraft, 2002) some RLKs have been found to be involved in plant interactions with symbionts as well as in responses to insect attack or microbial and fungal pathogen invasion (Morris & Walker, 2003; Afzal *et al.*, 2008) and have been suggested to participate in responses to parasitic nematodes (Wieczorek & Seifert, 2012). Amongst RLKs is a subfamily of **wall-associated kinases (WAKs)**. WAKs are the most characterised wall receptors associated with perceiving external danger signals (Seifert & Blaukopf, 2010; Kohorn & Kohorn, 2012; Wieczorek & Seifert, 2012). WAK1 of *Arabidopsis*, for example, has been identified as a pathogenesis-related (PR) protein (He *et al.*, 1998). Similar to most receptor proteins, WAKs have the 3 crucial domains. The WAK receptor domain is covalently (Anderson *et al.*, 2001; Wagner & Kohorn, 2001) and/or non-covalently (Decreux & Messiaen, 2005) bound to cell wall pectin as well as to glycine-rich proteins (GRPs) (Anderson *et al.*, 2001; Kohorn, 2001). This link creates an opportunity for perceiving cues from a changing cell wall and modulation of WAK activity during pectin modification (de-esterification or depolymerisation) by the parasite (Decreux & Messiaen, 2005). *Lycopersicon esculentum* Mill. wall associated kinase

(LeWAK) has indeed been found to be involved in the recognition of signals found in exudates of germinating *Orobanche ramosa* L. although the specificity of the signal was not demonstrated (Lejeune *et al.*, 2006).

Receptor kinases with an extensin-like extracellular domain are termed **Proline-rich Extensin-like Receptor Kinases (PERKs)**. PERK1 of *Brassica napus* L. is upregulated during wounding and fungal infection (Silva & Goring, 2002) while a PERK-like receptor kinase of *Arabidopsis* facilitates viral infection (Florentino *et al.*, 2006). Similar to some WAKs, PERK4 of *Arabidopsis* was bound to pectins (Bai *et al.*, 2009). It was proposed to be a receptor of abscisic acid (ABA), controlling Ca²⁺ fluxes in signalling crucial for ceasing cell elongation during root growth (Bai *et al.*, 2009). Curiously, ABA is a hormone strongly upregulated in the roots and, particularly, the haustoria of *Rhinanthus minor* after attachment to *Hordeum vulgare* where it was suggested to control lignification and suberisation of cell walls (Jiang *et al.*, 2004).

Leucine-Rich Repeat Receptor Like Kinases (LRR-RLKs); BAK1/SERK3 and BKK1/SERK4 have been shown to contribute to resistance of *Arabidopsis* against a bacterium and an oomycete (Roux *et al.*, 2011). A bioinformatics approach showed that BAK1 is indeed an element responsible for *Arabidopsis* immunity (Postel *et al.*, 2010) and is upregulated in *Orobanche*-infected *Medicago truncatula* Gaertn. (Die *et al.*, 2007; Dita *et al.*, 2009).

GPI-anchored proteins (GAPs)

GPI-anchored proteins (GAPs) are proteins that are post-translationally modified at their C-terminus by the addition of a glycosylphosphatidylinositol (GPI) anchor moiety in the ER (Ikezawa, 2002; Fujita & Kinoshita, 2012). GPIs anchor GAPs to the plasma membrane without traversing it fully, while the ability to signal between the cell interior and exterior is achieved through interactions with other proteins (Fujita & Kinoshita, 2012). GPI anchors may be putative analogues to WAK trans-membrane domains as they are known to enable or increase mobility in the membranes, polarised transport or exclusion from endocytotic clathrin-coated pits in mammals (Hooper, 1997)

Arabinogalactan proteins (AGPs): GPI-anchored AGPs are a group of both putative signal source and receptor molecules (Schultz *et al.*, 1998). Signals might be created by the release of the soluble proteoglycan from its anchor into the intercellular space via phospholipase-effected cleavage or oligosaccharide messengers could be produced by endoglycanases acting on the carbohydrate side chains (Seifert & Roberts, 2007). It is also possible that the GPI anchors are a source of intracellular signalling molecules (Showalter, 2001) although the more likely mechanism of downstream signalling involves interactions with proteins that possess cytosolic domains, for example with WAKs (Schultz *et al.*, 1998). A particularly intriguing association between AGPs and WAKs was presented

by Gens and co-workers (2000) in cultured tobacco cells where the CCRC-M7 antibody against AG epitopes of AGPs labelled the external face of the protoplast in a polyhedral pattern and an anti-WAK polyclonal antibody localised to the vertices of the formation. The structure, named plasmalemmal reticulum, binds the cell wall, plasmalemma and cytoskeleton, and is believed to play roles in regulation of mechanosensory Ca^{2+} -selective cation channels (Pickard & Fujiki, 2005). There is currently no evidence available for the involvement of mechanosensors during infection by parasitic plants. Calcium peaks induced by a proteinaceous or volatile compounds rather than tactile stimuli from *Cuscuta reflexa* Roxb. haustoria were found in tomato during infection (Albert *et al.*, 2010). However, this field remains largely unexplored and the involvement of mechanosensors might yet be discovered.

Similar to WAKs and PERKs, AGPs can interact with pectins. Immerzeel and co-workers (2006) found high amounts of GalA and some Rha residues in AGP fractions isolated from carrot and suggested that the AG moiety might be esterified to homogalacturonan and perhaps rhamnogalacturonan. Prior to that, a Hyp-deficient AGP was found associated with pectins extracted from carrot and onion, possibly in a Ca^{2+} -dependent manner (Baldwin *et al.*, 1993). It is therefore possible that, for example, changes to the pectin-AGP network of the host effected by the advancing haustorium can be sensed and elicit a GPI anchor-mediated response.

While precise functions of AGPs remain elusive, accumulating evidence suggests their involvement in plant interactions with symbionts (Balestrini *et al.*, 1996; van Buuren *et al.*, 1999), microbial pathogens (Stark-Urnau & Mendgen, 1995) and parasitic plants (Vaughn, 2003; Albert *et al.*, 2006; Li *et al.*, 2009; Rehker *et al.*, 2012), manifested at various stages and components of the interactions. A mutation in *atAGP17*, the gene coding for a lysine-rich AGP of *Arabidopsis*, rendered it resistant to transformation with *Agrobacterium* (Gaspar *et al.*, 2004). One of the mechanisms proposed to be disturbed in the mutants was signalling necessary for bacterial attachment to the root surface. Similarly, Albert and co-workers (2006) found a positive correlation between attachment force of *Cuscuta* haustoria and transcript levels of tomato host attAGP — an AGP expressed specifically during the infection, predicted to be GPI-anchored and proposed to bind pectins secreted by the parasite, facilitating attachment. It was later found that attAGP is also expressed during parasitism by a root holoparasite *Phelipanche aegyptiaca* (Pers.) Pomel (Rehker *et al.*, 2012). Fasciclin-like AGP (FLA) transcripts were upregulated in *Mikania micrantha* Kunth during infection by *Cuscuta campestris* Yunck. (Li *et al.*, 2009). FLAs are regulated by stress and development and the fasciclin protein domains are known to participate in cell adhesion in humans and proposed to fulfil the same role in plants as components of lipid raft AGPs (Johnson *et al.*, 2003).

In addition to AGPs, **other GPI-anchored proteins** have been identified in *Arabidopsis* and they may play roles in signalling in plants (Borner *et al.*, 2003). Nodulins, typically confined to legume root nodules (Sanchez *et al.*, 1991) are predicted to possess GPI anchors (Frühling *et al.*, 2000). The *MtENOD11* gene encoding an early nodulin (ENOD) is induced during an association between *Medicago truncatula* and arbuscular fungi (Kosuta *et al.*, 2003). Similarly, *Orobancha crenata* Forsk. tubercle formation on the same species of medick induced expression of early nodulin genes in this host (Dita *et al.*, 2009). Therefore, the relevant nodulins may form a shared component of the signalling pathways during nodulation and haustorial attachment. Interestingly, a homolog of ENODs has also been identified in a parasitic plant rather than a host, namely, germinated and haustorially induced seedlings of *Striga hermonthica* (Del.) express a sha-39 protein gene, in addition to a lipid transfer protein (LTP) gene being expressed specifically during the haustorial stage (Stranger *et al.*, 1999). As true ENODs are restricted to legumes, the sha-39 gene might in fact encode part of an early nodulin-like protein (ENODL), many of which are known to form chimeras with AGPs (Mashiguchi *et al.*, 2009). The involvement of **other proteins localised at the plasma membrane** e.g. the plasma membrane intrinsic protein (PIP) family of aquaporins in plant interactions with pathogens and symbionts (Roussel *et al.*, 1997; Keller *et al.*, 1998; Uehlein *et al.*, 2007), as well as parasitic plants (Werner *et al.*, 2001), continue to be discovered.

Cell wall integrity sensors

Perturbations to cell wall structural integrity or shape can be detected by mechano-sensitive ion channels which open when plasma membrane is distorted. They are well characterised in fungi and have been proposed to aid recognition of the host surface by fungal hyphae and induce formation of appressoria upon contact (Zhou *et al.*, 1991). Emerging evidence suggests that a plant cell wall integrity (CWI) maintenance system fed by turgor pressure, mechano-receptors and cell wall damage sensors also exists (Hamann & Denness 2011; Hamann 2012, Nuhse 2012). Although this has been an area of research for some plant-pathogen interactions including CWI of the fungal perpetrator *Magnaporthe* (Skamnioti *et al.*, 2007; Jeon *et al.*, 2008), the potential of this type of surveillance in host recognition by parasitic plants or host sensing of wall disruption during the attack provides a new unexplored field for parasitic plant research.

4.4.3 Signalling in parasitic plant-host associations

Signalling specifically in parasitic plant-host associations was most recently reviewed by Yoder (2001) and Yoder *et al.* (2009). Host-derived signalling molecules include those that stimulate germination (germination cues) as well as those that subsequently induce haustorial development (haustorium inducing factors or HIFs). Strigol (Fig. 4.2a) was the first extracted germination stimulant (Cook *et al.*, 1966; Mescher *et al.*, 2009).

The source plant, cotton, was, *nota bene*, a non-host. Many other non-hosts have since been found to produce strigol and induce germination of incompatible parasites, i.e. without subsequent initiation of haustoria (Yoder *et al.*, 2009). Different related compounds known collectively as strigolactones have been discovered since and shown to play roles beyond parasitic plant-host interactions, for example in mycorrhizal associations or plant development (Bouwmeester *et al.*, 2007; Ruyter-Spira *et al.*, 2012 and references therein). Strigolactones are protoplast-derived products of the carotenoid pathway and their putative receptors at the plasma membrane have not been identified (Matusova *et al.*, 2005).

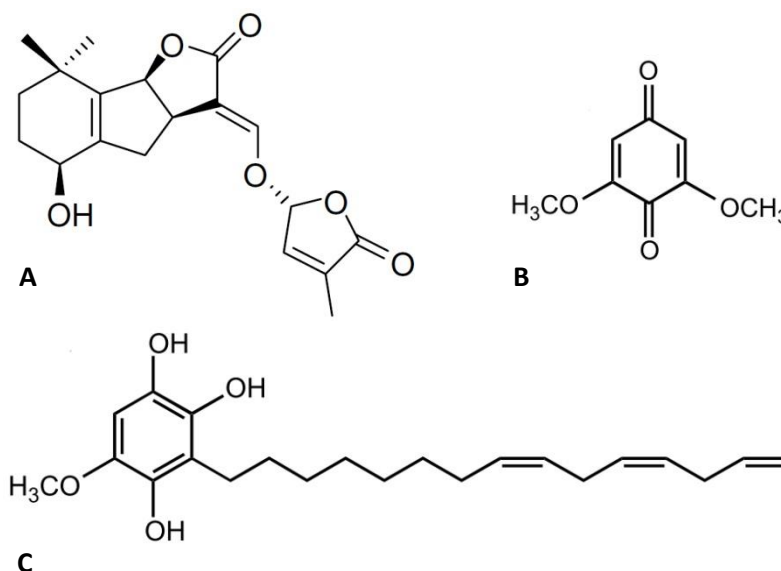


Figure 4.2: Host-derived molecules implicated in signalling during parasite germination and haustorial induction. **A** — strigol germination stimulant, **B** — 2,6-dimethoxy-1,4-benzo-quinone (DMBQ) haustorial inducing factor (HIF), **C** — *Sorghum* xenognosin for *Striga* germination (SXSg) — dihydrosorgoleone (Yoder, 2001)

Mescher *et al.* (2009) point out some inconsistencies in the data regarding germination stimulants, namely, conflicting information on the roles of strigolactones and a class of phenolic-derivatives called hydroquinones (mainly *Sorghum* xenognosin for *Striga* germination (SXSg) — Fig. 4.2C). Different authors present apparently convincing data that either one or the other is “the” stimulant. For example Estabrook and Yoder (1998) omit strigolactones from their review of parasitic plant-host signalling, while focusing on SXSg. Conversely, Zwanenburg and co-workers (2009) are of the opinion that SXSg is of little or no importance as a germination signal. Nevertheless, SXSg is important to mention in this work as it is a phenolic derivative, potentially originating from the cell wall and many other cyclic substances are used as signalling molecules between roots of plants and other soil inhabitants (Hirsch *et al.*, 2003). The possibility of a role in parasite

germination-specific signalling cannot therefore be neglected until more conclusive data is available. On the other hand, there is consensus about the role of phenolic derivatives in haustorial initiation. The first isolated inducing factor is 2,6-dimethoxy-1,4-benzoquinone (DMBQ) (Fig. 4.2B) present in cell walls (Chang & Lynn, 1986; Yoder *et al.*, 2009). It is believed that the redox cycling between its forms catalysed by two antagonistic quinone oxidoreductases induces haustorial development (Yoder *et al.*, 2009). As the host cell wall is digested during endophytic penetration, more HIFs are likely to be released to further stimulate and guide the developing haustorium (Estabrook and Yoder 1998).

Interestingly, oligosaccharins — a class of long-recognised signalling molecules derived from plant cell walls (Albersheim & Darvill, 1985; Albersheim *et al.*, 1992), are seemingly absent from the literature on parasitic plants. These cell wall carbohydrate fragments are derived via enzymatic action as part of normal development or during pathogenesis and act via membrane polarisation mechanisms or receptor-specific recognition (Field, 2009). Defence-related plant oligosaccharins identified so far are derived from pectins (oligogalacturonides) (Reymond *et al.*, 1995) and xyloglucans (Pavlova *et al.*, 1996), both of which are more abundant in eudicots than in grasses (Scheller & Ulvskov, 2010).

In addition to HIFs, other substances, for example hormones control haustorial development (Ramasubramanian *et al.*, 1988; Löffler *et al.*, 1999; Tomilov *et al.*, 2005; Zhang *et al.*, 2012). Yet again, the interception of these signals is partly dependent on wall-localised receptors. Some known receptors of auxins, PIN-FORMED proteins, are localised in the plasma membrane (Ganguly *et al.*, 2010) and histidine kinases responsible for perception of cytokinin signals are also located in the plasmalemma and possess extracellular ligand-binding CHASE domains (Kakimoto, 2003; Higuchi *et al.*, 2004). A leucine-rich repeat receptor-like kinase1 (RLK1) is involved in early perception of ABA in *Arabidopsis* (Osakabe *et al.*, 2005).

Invasion of host tissues by the haustorium shares characteristics of wounding and a pathogenic attack. Pathogen-directed resistance is generally dependent on the salicylic acid (SA) signaling pathway while systemic wound response is associated with the jasmonic acid (JA) pathway, both of which play a role in plant parasitism by parasitic plants (Smith *et al.*, 2009). However, the relative contribution is likely to vary between parasite-host pairings and requires further investigation. Salicylate-induced pathways, for example, have been shown to result in resistance of *Trifolium pretense* to *Orobancha minor* whereas jasmonate-induced resistance is insufficient to prevent parasitism, although a haustorial endophyte moves through host tissue through what is effectively a wound (Kusumoto *et al.*, 2007). However, application of both methyl salicylate and methyl jasmonate to *Arabidopsis* seedlings reduced formation of *Orobancha aegyptiaca* tubercles by 90% (Bar-Nun & Mayer, 2008; Bar Nun & Mayer, 2009).

Signaling in virulence and resistance in *Striga* species-host associations has been recently reviewed by Timko *et al.* (2012). The authors suggested a “zigzag” model for effector triggered immunity in hosts that bears resemblance to general mechanisms applied at the cell-wall plasmalemma interface during attack by bacteria or fungi. In a zigzag model, the individual “nodes” of the zigzag represent alternating steps of host and pathogen responses. In typical pathogenesis, signals effected by the pathogen, so called pathogen-associated molecular patterns (PAMPs) or microbe-associated molecular patterns (MAMPs) are sensed by plasma membrane-located pattern-recognition receptors (PRRs) that switch on immunity (Hématy *et al.*, 2009). These signals can come from the parasite (for example fragments of chitin from fungal hyphae) or can be produced as a result of host cell wall fragmentation by enzymes secreted by pathogens. In the latter case they are termed damage-associated molecular patterns (DAMPs) or host-associated molecular patterns (HAMPs) (Seifert & Blaukopf, 2010). Examples include oligosaccharins (oligosaccharides such as oligogalacturonides) and cutin monomers (when the cuticle is compromised). Both types of molecular patterns (MAMPs and DAMPs) trigger a common signaling pathway leading to activation of defense responses known as pattern-triggered immunity. This immunity can be blocked by effectors called avirulence (Avr) factors produced by the parasite, which in turn can be recognized by primarily (although not exclusively) intracellular resistance proteins (R), leading to another level of immunity, termed effector-triggered immunity (ETI) or gene-for-gene resistance (i.e. resistance gene for avirulence gene). Avr and R-genes constantly co-evolve. The term avirulence genes (Avr) may be confusing as they code effectors produced by the parasite to facilitate infection. However, if they are recognized by host receptors they inevitably trigger defence responses, hence the use of the term (Yin & Hulbert 2011; Timko *et al.* 2012).

4.4.4 Cell-wall localised enzymes in virulence and resistance

Enzymes secreted by the parasite and host at haustorial interfaces contribute to virulence and resistance alike by generating signals as well as both weakening of the opponent’s and strengthening of own cell walls. While the wall is often digested to generate germination cues and HIFs or to gain access to target tissues, a possibility exists that products of cell wall digestion can serve as nutrition to the parasite. This has been previously described for several fungi utilizing wall-derived pectins as sole source of carbon (Dean & Timberlake, 1989; Green III *et al.*, 1996).

Peroxidases are an important class of cell-wall localised oxidative enzymes that can serve both the parasite and the host. In a typical situation, host peroxidases catalyse the production of reactive oxygen species (ROS) that trigger physiological responses signalled by the jasmonic and salicylic acid pathways, resembling mechanisms of response to herbivores and pathogens (Runyon *et al.*, 2010). This leads to the expression of physical

Chapter 4

reinforcement mechanisms such as protein cross-linking (Brisson *et al.*, 1994), lignification and suberisation, catalysed by peroxidases in the cell wall (Almagro *et al.*, 2009). To generate phenolic-derived bezoquinone signals, polyphenol oxidases such as peroxidases are also needed. Kim *et al.* (1998) suggested that rather than secrete its own enzymes, *Striga asiatica* provides the oxidant (hydrogen peroxide, H₂O₂) for the reaction which is then catalysed by the host's peroxidases. Keyes *et al.* (2000) specify the source of phenolics as the phenolic esters of host pectins, which they found to be converted into DMBQ in the presence of hydrogen peroxide derived from the parasite. Peroxidases, which are normally used in host defence are in this case functionally adopted to perform a job to the parasite's benefit. Contrastingly, peroxidases localized in the cell walls of a different parasite, *Cuscuta jalapensis* Schltdl., were proposed to be involved in haustorial development by facilitating parasite's cell wall restructuring, in addition to host wall reorganization during infection (López-Curto *et al.*, 2006).

During penetration by fungal hyphae or the angiosperm haustorial endophyte, host cell walls need to be loosened. While fungi such as *Magnaporthe grisea* often enter their hosts intracellularly by a pressure-based mechanism implemented by appressoria (Goriely & Tabor, 2006), multicellular endophytes of parasitic plants typically move between host cells, therefore targeting mainly the middle lamellae. Both modes apply an array of cell wall degrading enzymes (CWDEs) directed against different wall components (Annis & Goodwin, 1997). Cell wall structure and composition affects its digestibility by the parasite's enzymes and the types of signalling molecules that are subsequently released.

Pectins are the most mobile component surrounding the cellulose-hemicellulose network and are therefore digested first, increasing availability of other polymers in the wall to CWDEs (Collmer and Keen 1986; Hématy *et al.* 2009). Methyl esters substituting varying patterns of homogalacturonan residues act as obstructions to pectolytic enzymes. Pectin methyl esterases (PMEs) are therefore a crucial component of the CWDE cocktail as they facilitate digestion of pectins by pectate lyases and polygalacturonases (Lionetti *et al.*, 2012).

Evidence for enzymatic depletion of pectins by parasitic plants in their host tissues was presented by Losner-Goshen (1998) for *Orobanchae*. Immunogold labeling of pectin methyl esterase (PME) revealed its presence in parasite cell walls, the adhesive substance between the parasite and host and in some adjacent host walls. Additionally, JIM5 mAb-recognised epitopes of low-esterified homogalacturonan were more abundant in walls close to the infection site, most likely as a result of PME activity. Pérez-de-Luque *et al.* (2006) localised low-methyl esterified pectins in *Pisum sativum* L. (pea) roots attacked by *Orobanchae crenata* using the histological stain ruthenium red.

A rich enzyme cocktail is required to target the entire diversity of cell wall components (Gilbert, 2010). In addition to pectinases — xylanases, xyloglucanases and cellulases are some of the other enzymes known to be secreted by pathogens and parasitic plants. As certain side chains are known to hamper degradation by backbone-cleaving enzymes polymers typically require groups of enzymes working in concert (Gilbert *et al.*, 2008). For instance, before endo-xylanases can start acting on glucuronoarabinoxylan, arabinofuranosyl side chains need to be removed by α -L-arabinofuranosidase (Wood & McCrae, 1996). As wall carbohydrate-degrading enzymes target specific linkages and considering that the diversity of substrates, the variety of corresponding enzymes, their products and possible physiological functions are immense.

Only a handful of studies focused on the cell wall degrading enzymes present in, or secreted by, parasitic plants exists. A study of *Cuscuta reflexa* demonstrated activities of a range of CWDEs, exo-1,4- β -D-glucosidase, xylanase, pectylhydrolase and polygalacturonase, to be considerably upregulated in haustoria when compared to surrounding tissues (50, 100 and 2–4 times higher respectively) (Nagar *et al.*, 1984). Curiously polymethylgalacturonase, cellulase or cellobiase were not upregulated. An array of parasite-secreted enzymes was extracted from 1-week-old *Orobancha aegyptiaca* and included polygalacturonase, PME, β -glucosidase, ligninase and endocellulase in addition to peroxidases (Shomer-Ilan, 1994). Cellulase activity was also indirectly demonstrated by host cellulose depletion studies in which the parasites *Cassytha filiformis* L. (Reddy *et al.* 1980) and *Striga hermonthica* (Olivier *et al.*, 1991) were found to reduce the cellulose content of their hosts. In the case of *Striga* it appeared as if the putative enzymes were able to diffuse within the walls of susceptible *Sorghum* strains, which was visualised as a reduction of labelling with an exoglucanase-gold complex some distance away from the parasite. No such depletion was noted in resistant strains.

Host plants are not defenceless in their battle against parasites' enzymes. CWDEs can be inhibited by plant proteins (Esquerré-Tugayé *et al.*, 2000; Juge, 2006). Polygalacturonase-inhibitor proteins are commonly secreted into the apoplast in response to fungal infection (Federici *et al.*, 2006). This was also demonstrated by (Singh & Singh, 1997) in an association of *Cuscuta* with two non-hosts *Ipomoea batatas* L. and *Lycopersicon esculentum*. Epidermal peel of these non-hosts contained inhibitors of cellulose, polygalacturonase and xylanase. Tannins, polyphenolics capable of precipitating proteins and known to decrease cell wall digestion by ruminants (Robbins *et al.*, 1987; Silanikove *et al.*, 1994), might also be released from dying host cells at the interface and bind to parasite's enzymes. Inhibitory effects of tannins on herbivore digestive enzymes including cellulase and β -glucanase have been previously reported (Schofield *et al.*, 2001). Furthermore, tannins might form indigestible complexes with wall polysaccharides (Reed, 1995 and references therein).

Chapter 4

Several wall degrading/restructuring enzymes were also upregulated in certain hosts during infection by parasitic plants. Although they were proposed to play roles in defence, it was not tested whether they were targeted at the parasite walls or acted on the host's own walls. Examples include xyloglucan endotransglycosylase/hydrolase up-regulated in an incompatible *Lycopersicon esculentum* host of *Cuscuta reflexa* (Albert *et al.*, 2004) as well as β -galactosidase, polygalacturonase and expansin A10 of *Mikania micrantha* parasitized by *Cuscuta campestris* (Li *et al.*, 2009). On the other hand, O'Malley and Lynn (2000) correlated expansin up-regulation specifically with hypertrophy of the haustorial initials of *Striga asiatica*.

While the parasite secretes enzymes aimed at digesting host walls, a mechanism preventing self-inflicted enzymatic damage must also be in place. Evidence for the existence of such mechanisms was shown in a study on cuscutain (Bleischwitz *et al.*, 2010). This cysteine protease of *Cuscuta reflexa* initially possesses a pre-peptide module responsible for directing the enzyme into the extracellular matrix, as well as an inhibitor pro-peptide module which is cleaved off in the cell wall, rendering the enzyme active. The authors suggested that a gradient of enzyme activation (decreasing towards the parasite) in addition to high pectic content of the parasite's contact secretion could contribute to mechanisms of auto-digestion prevention. Furthermore, polygalacturonase inhibitors were found in *Orobanche aegyptiaca* calli (Ben-Hod *et al.*, 1997) and suggested to have a similar self-protective role although no experimental evidence was provided for the latter. These studies show potential of cell wall science to deliver solutions to the parasitic weed problem. In the study on cuscutain (Bleischwitz *et al.*, 2010), simple application of the inhibitor solution with a spray bottle reduced successful infestation rate from 65% to 15%.

It is also important to note that parasites often pair with hosts from taxonomically distant groups, which therefore possess cell walls which have different composition and are digestible by different enzymes. There are, for example, no known monocot or legume parasites and only one gymnosperm parasite (Irving & Cameron, 2009) while species of these three groups are often preferred hosts (Mohamed *et al.*, 2001; Rümer *et al.*, 2007). The fact that known oligosaccharins come from pectins and xyloglucans, which are more abundant in eudicots than graminoids, would further suggest that such distinction may be based on wall composition. However, the possible protective implications of pairing unrelated taxa must be somewhat limited as associations with non-leguminous eudicot hosts are also well known. While most *Striga* species prefer grasses, *Striga gesneroides* (Willd.) Vatke parasitizes dicots (Mohamed *et al.*, 2001). In a study carried out by Yoder (1997), frequency of conspecific and congeneric haustoria of *Triphysaria versicolor* Fisch. & C.A.Mey. and *T. eriantha* (Benth.) T.I.Chuang & Heckard and haustoria developed on *Arabidopsis* were investigated. In this case, *Arabidopsis*

encouraged more haustoria than other *Triphysaria* species or the same species. This suggests that a gradient of susceptibility correlated with the degree of relatedness within eudicots exists. Whether this is partly attributed to cell wall diversity remains to be tested.

An additional consideration is that parasite-derived enzymes might not only release signals by digesting walls but that they could also themselves act as signals as previously demonstrated for fungal xylanases (Enkerli *et al.*, 1999; Beliën *et al.*, 2006; Noda *et al.*, 2010).

4.4.5 Protective components of the cell wall

During interactions of plants with pathogens, hormones including salicylic acid, jasmonic acid and ethylene, induce expression of so called pathogenesis-related proteins (PRPs) that accumulate in the apoplast and in the vacuole (Stintzi *et al.*, 1993; van Loon *et al.*, 2006). They are currently classified within 17 families (Van Loon *et al.*, 2006) including chitinases and glucanases directed at parasites' cell walls, endoproteinases, proteinase inhibitors, lipid transfer proteins or defensins and thionins. The modes of action of the latter two are only partly understood although inhibition of enzymes, ion channels and translation or disruption of host plasma membrane have been shown to contribute to their broad antibacterial and antifungal properties (Lay & Anderson, 2005; Pelegriani & Franco, 2005; van Loon *et al.*, 2006). In addition to PRPs *sensu stricto*, i.e. those that are induced during defence while otherwise being undetectable (Van Loon *et al.*, 2006), other PR proteins normally present in the wall are upregulated during pathogenesis. The most important of those are peroxidases (Prxs). They are crucial in the metabolism of reactive oxygen species (ROS) and reactive nitrogen species (RNS) during so called oxidative bursts that lead to toxification of the apoplast as well as enabling implementation of programmed cell death (Almagro *et al.*, 2009). Furthermore, their oxidative properties allow them to catalyse cross-linking of extensins or synthesis of lignins and suberins — compounds crucial in cell wall reinforcement. These peroxidase-mediated responses have many examples in parasitic plant-host interactions and are quoted throughout the remaining part of this chapter and thesis.

There is accumulating molecular evidence, obtained mainly through suppression subtractive hybridisation (SSH) and quantitative real time PCR (RT-PCR), for the involvement of wall-related PRPs in interactions between parasitic plants and their hosts. Genes of PRPs family PR-1 of unknown mode of action (Van Loon *et al.*, 2006) were expressed in roots of tobacco susceptible to *Orobanchae aegyptiaca* (Joel & Portnoy, 1998). In *Tagetes erecta* L. parasitized by *Striga asiatica*, cortical resistance in a form of necrosis of cells and thickening of the interface walls surrounding the penetrating endophyte was combined with increased expression of NRSA-1 encoding a protein with significant homology to known PRPs (Gowda *et al.* 1999). At least seven PRP genes were induced

in *Arabidopsis* by *Orobancha ramosa* attack: PR-3 encoding chitinase, *thi2.1* encoding thionin, a defensin gene *pdf1.2*, and a PME inhibitor as well as three genes encoding proteins known to play roles in detoxification of ROS, namely *gst1*, *gst11* and methionine sulfoxide reductase gene (Vieira Dos Santos *et al.*, 2003b,a). Detoxifying factors were also upregulated in *Helianthus annuus* L. infected by *Orobancha cumana* (Letousey *et al.*, 2007b). A β -1 \rightarrow 3-glucanase (an antifungal hydrolase) and a peroxidase were up-regulated in *Pisum sativum* during *Orobancha crenata* infection (Ángeles Castillejo *et al.*, 2004). In *Medicago truncatula*-*Orobancha crenata* interactions, genes and corresponding transcripts of caffeoyl-CoA *O*-methyltransferase and cinnamoyl-CoA reductase — enzymes involved in wall reinforcement through lignification, were identified in addition to an expansin-like protein and an early nodulin precursor (Die *et al.*, 2007). Defensins secreted to the apoplast have been demonstrated as a successful resistance factor against *Orobancha cumana* in *Helianthus annuus*, and proposed to interfere with parasite membrane sphingolipids (De Zélicourt *et al.*, 2007). A gene determining resistance of cowpea to a specific race of *S. gesneroides* is an R-protein gene (Li and Timko 2009). Chitinase, NHL1, glycolate oxidase and peroxidase were some of the PRPs identified in *Mikania micrantha* parasitized by *Cuscuta campestris* in addition to expansin A10, β -galactosidase and polygalacturonase mentioned earlier (Li *et al.*, 2009, 2010).

As briefly mentioned earlier, cell walls can be either constitutively resistant to infection or physically reinforced in response to haustorial intrusion. A secondary cell wall, tightly packed with carbohydrate polymers and less hydrated as a result of lower pectin content and, often, the presence of hydrophobic phenolic compounds and cross-linked proteins is an intrinsically more difficult substrate for degrading enzymes to work on than a looser and more hydrated primary wall (Hervé *et al.*, 2009). It also forms a stronger and more resistant passive barrier to penetration by the endophyte when, in concert with enzymatic modification, it is subjected to the mechanical pressure exerted by the haustorium (Joel & Losner-Goshen, 1994). A number of molecules typically associated with strengthening of cell walls after wounding and during pathogenic attack appear or increase in the affected host organs to further reinforce secondary walls and increase resistance of primary walls.

An important group of substances that may lead to impregnation and strengthening of cell walls are the products of phenylpropanoid and isopropanoid pathways, in particular lignins and suberins. While these components aid resistance as regular constituents of xylem, endodermis or cork, lignification (Vance *et al.*, 1980; Nicholson & Hammerschmidt, 1992; Bhuiyan *et al.*, 2009) and suberisation (O'Brien & Leach, 1983; Lulai, 1998; Thomas *et al.*, 2007; Ranathunge *et al.*, 2008) have been shown to be increased or induced in hosts during pathogenesis. Defences involving suberin, lignin and other phenolics have also been commonly observed in parasitic plant hosts

at the sites of haustorial intrusion. Wound periderm was induced in *Eucalyptus oleosa* F. Muell. ex Miq. infected by *Amyema preissii* (Miq.) Tieghem and in *Heterodendrum oleifolium* Desf. infected by *Lysiana exocarpi* (Behr.) Tieghem ssp. *exocarpi* (Yan, 1993) while *Leucantherum vulgare* Lam. appeared to encapsulate haustoria of *Rhinanthus minor* in a layer of suberised cells (Rümer *et al.*, 2007). Suberisation coupled with lignification of cortex in resistant *Helianthus* prevented *Orobanche cumana* from further ingress (Echevarría-Zomeño *et al.*, 2006). Lignification is one of the most common histological responses reported from hosts, although it does not always grant resistance. While lignification of endodermis and pericycle were main determinants of legume resistance to *Orobanche cranata* (Pérez-de-Luque *et al.*, 2005, 2007) or *Sorghum* to *Striga asiatica* (Maiti *et al.*, 1984), lignification of *Phleum bertolonii* DC. stele was not sufficient in stopping *Rhinanthus minor* endophyte penetration (Rümer *et al.*, 2007). It is important to note that, with the exception of one study where Fourier transform infrared spectroscopy (FT-IR) was applied (Cameron *et al.*, 2006), lignin at haustorial interfaces has been identified only using histological staining, which might not discriminate between lignin and other wall-bound or secreted phenolics. Phenolic acids such as ferulic or *p*-coumaric acid which intrinsically present in cell walls, and are particularly abundant in, but not limited to grasses (Harris & Hartley, 1976) may also become cross linked. Dimers of pre-existing ferulic acid increased in leaves of resistant oat at the sites of infection by *Puccinia coronata* f.sp. *avenae* P. Syd. & Syd (Ikegawa *et al.*, 1996). Such cross-linked phenolic acids and lignin-like substances might be detected by general stains such as safranin or acridine red, used in several anatomical studies of haustoria (Echevarría-Zomeño *et al.*, 2006; Pérez-de-Luque *et al.*, 2007; Rümer *et al.*, 2007). Chapter 6 discusses new data obtained in the course of this study that suggests the implications of interfacial extramural lignin-like substances in parasites' virulence as opposed to host resistance.

In addition to lignins and other wall-bound phenolics, other products of the phenylpropanoid pathway such as certain phytoalexins (Daayf *et al.*, 1997) can accumulate in the apoplast, as in the cortex of *Helianthus annuus* and the vascular cylinder of *Medicago truncatula* (Echevarría-Zomeño *et al.*, 2006; Lozano-Baena *et al.*, 2007) attacked by *Orobanche*.

Structural proteins including extensins, proline-rich proteins and glycine rich proteins can be immobilized in the cell wall via cross-linking. This leads to increased physical strength and decreased digestibility of the cell wall (Brisson *et al.*, 1994; Deepak *et al.*, 2010). HRGP and PRP cross-linking is best understood, as reviewed by (Deepak *et al.*, 2010). Covalent isodityrosine (IDT) bridge formation catalysed by peroxidases accounts for this process. Although GRPs have been proposed to act in an analogical way, the precise mechanism of cross-linking has not yet been elucidated (Ringli *et al.*, 2001; Mangeon *et al.*, 2010).

While Deepak (2010) provides multiple examples for HRGP involvement in plant defences, it is worth pointing out that cross-linking of pre-existing HRGPs can be a rapid form of defence preceding transcriptional changes (Bradley *et al.*, 1992; Brisson *et al.*, 1994) and that it often acts specifically at the site of pathogen intrusion (O'Connell *et al.*, 1990).

HRGPs and, more specifically, AGPs have been found in the interfacial substance called extrahaustorial matrix (EMA) present between fungal haustoria and invaginated host membranes. A remarkable example of a highly organized, sequentially deposited EMA was presented by Stark-Urnau and Mendgen (1995). *Uromyces vignae* Barclay M-haustoria (haustoria resembling undifferentiated hyphae) were encased in a three layered structure with the two layers, adjacent to haustorial and host plasma membrane each, being enriched in CCRC-M8-detected AGPs and HRGPs detected by HRGP_{2b} polyclonal antibody. These two layers were separated by a layer enriched in fucosylated xyloglucans and pectins and a layer of callose. On the other hand Balestrini (1996) showed that the interfacial material reflected the original composition of host cell wall in four species at the site of intrusion by arbuscular fungi and therefore CCRC-M7-recognised AGP/RG epitopes were not up-regulated specifically at the interface. Contrasting results were more recently obtained by Micali (2011) as well as Xie *et al.* (2011). The former localized AGPs specifically at the site of infection of *Arabidopsis* with *Golovinomyces orontii* (Castagne) V.P. Heluta (1988) using CCRC-M7. Curiously, extensins were not detected in the same study using the mAb JIM20. Xie *et al.* (2011) applied an extensive screen of 20 antibodies directed against extensins and AGPs to two cultivars of wax gourd (a resistant and a susceptible one) inoculated with *Fusarium oxysporum* f. sp. *Benincasaev* W.C. Snyder & H.N Hansen (1940). They found a correlation between CCRC-M7 specific epitopes and resistance, in addition to a range of other epitopes being differentially up-regulated during the infection. Immunogold labeling of EMA performed during some of the above studies shows that AGPs were present within the interfacial material as opposed to being confined to the membranes (Stark-Urnau & Mendgen, 1995). A structural role is therefore possible although the exact mechanism by which AGPs fulfill it has not been established. Evidence for possible structural reinforcement by AGPs was also provided by Wydra & Beri (2007). A tomato strain resistant to a wilt fungus *Ralstonia solanaceum* Smith (1896) displayed higher pre-inoculation content of AGPs in vessel walls and more blockwise esterification of HG in tissues in general than the susceptible host, while RG-I branching in vessel walls increased after inoculation. AGPs were also up-regulated in both strains post inoculation. The authors concluded that constitutive AGPs might contribute to resistance by strengthen the wall while induced AGPs might further reinforce this effect. Perhaps in addition to the well known phenomenon of pathogenesis-related extensin cross-linking, AGPs play a similar role, to that previously found during leaf excision (Kjellbom *et al.*, 1997). It has also been suggested that AGP cross-linking could trigger signaling cascades (Mashiguchi *et al.*, 2008). Widespread

occurrence of AGPs at the interfaces between plants and their symbionts and pathogens is also likely to reflect more than structural functions. Recently, AGPs secreted by border cells protecting root meristems of *Pisum sativum* L and *Brassica napus* L. were found to prevent root infection by pathogenic oomycete zoospores of *Aphanomyces euteiches* (Cannesan *et al.*, 2012). The proposed role was attraction and immobilization of the zoospores. Furthermore, AGPs are very abundant in wound exudates of *Acacia senegal* (Clarke *et al.*, 1979; Qi *et al.*, 1991) where they possess some glycomodules characteristic of extensins (Goodrum *et al.*, 2000).

Curiously, AGPs appear to be a substrate for chitinases, which are typically associated with antifungal activities (Domon *et al.*, 2000). AGPs have also been shown to possess N-acetylglucosamine and glucosamine residues and their chitinase-effected modification is important in somatic embryogenesis (Van Hengel *et al.*, 2001). It has not yet been investigated whether concomitant AGP and chitinase up-regulation during plant defence expression are a coincidence or whether an interaction related to resistance is in place.

Legume-specific root nodule extensins (RNEs) with characteristics of both extensins and AGPs play a role in infection thread morphogenesis by participating in gradual hardening of the infection thread (Brewin, 2004). Therefore, in addition to the earlier mentioned findings that some early nodulin-like proteins are upregulated during pathogenesis, HRGPs are another component of host response to nodulation and pathogen attack. The MAC265 monoclonal antibody recognizing RNE (Vandenbosch *et al.*, 1989) labeled regions of protein cross-linking in a highly resistant pearl millet host of downy mildew *Sclerospora graminopora* (Sacc.) J. Schröt. (Shailasree *et al.*, 2004). Together, these results suggest that there might be more parallels between the cell wall aspect of nodulation and pathogenesis. Exploring these similarities might have important implications for the theory of haustorial evolution.

Detection of AGPs and extensins in parasitic plant hosts is limited to just a handful of studies. Using the antibody LM1 against extensin, Neumann *et al.* (1999) found that it was accumulating at the haustorial interface of parasitic Orobanchaceae. HRGPs were detected on the host side suggesting their defensive role, while within haustoria they were confined to differentiating xylem elements, which implies spatio-temporal regulation of haustorial development. Using JIM8, CCRC-M7 and an anti-AGP mouse monoclonal antibody reported as being sourced from BioSystems, Australia (Vaughn, 2003) localised AGP epitopes in a chimeric wall formed at the *Cuscuta pentagona* Engelm.-*Impatiens sultanii* Hook. f. interface although it was not clarified whether the surrounding tissues also labelled or if the labelling was interface-specific. Furthermore, AGPs with a putative attachment-promoting function were up-regulated in hosts of *Cuscuta* and *Phelipanche* (Albert *et al.*, 2006; Rehker *et al.*, 2012) and an AGP of the fasciclin-like type proposed

to have attachment-facilitating functions (Johnson *et al.*, 2003) was upregulated in *Mikania micrantha* parasitized by *Cuscuta campestris* (Li *et al.*, 2009).

Callose is another important reinforcing component of cell walls, typically deposited at the interface between the plasma membrane and the cell wall (Chen & Kim, 2009). Deposition of callose-rich papillae and encasements are well known mechanisms of resistance to fungi which penetrate host cell walls (Smart *et al.*, 1986; Brown *et al.*, 1998; Albersheim *et al.*, 2011). Angiosperm haustoria are multicellular and therefore papillae have little potential to encapsulate them, although callose-enriched cell wall appositions were identified along the cell walls of *Impatiens sultanii* in contact with the cells of *Cuscuta pentagona* (Vaughn, 2003). Wall-reinforcement through callose deposition along the interfacial region played an important part in *Pisum sativum* and *Helianthus annuus* defence against *Orobanche crenata* and *O. cumana*, respectively (Pérez-de-Luque *et al.*, 2006; Letousey *et al.*, 2007a).

4.4.6 Cell wall-localised barriers at different stages of parasitic plant intrusion

Many host plants have developed resistance based on physically blocking the penetrating endophyte and thereby preventing parasite-host vasculature contact and nutrient translocation to the parasite. Although supporting molecular data is accumulating, knowledge of such host responses comes mainly from histological studies of haustorial intrusion into host tissues. Depending on how soon the signals from the parasite are recognised by the host, different defence mechanisms can be switched on at different stages of haustorial formation: 1) initiation of the primordium, 2) attachment, 3) penetration and 4) maturation (Musselman and Dickison 1975; Heide-Jørgensen and Kuijt 1995). Cell-wall localised barriers are induced as part of post-attachment resistance and are associated with other histological responses such as cell death that are triggered in the apoplast.

Pre-attachment resistance is sufficient in some species. Certain plants escape parasitic attack by lowering the levels of parasite-directed germination stimulants in their root exudates (Fernández-Aparicio *et al.*, 2012). If the requirement for biochemical cues from the host (obligate parasites) or environmental factors (facultative parasites) is fulfilled and successful germination does occur, the parasite can be stopped at the initial signalling stage. Cues from hosts occur in root exudates (Bouwmeester *et al.*, 2003; Yoneyama *et al.*, 2008) and can be either naturally absent (Rubiales *et al.*, 2003; Fernández-Aparicio *et al.*, 2012) in incompatible hosts or can be rendered absent or inabundant through cultivar selection and breeding (Jamil *et al.*, 2011). Additionally, the germinating parasite can be attacked by toxic secondary metabolites synthesised by the host. Phytoalexins and coumarins were produced by *Helianthus annuus* in response to germinating *Orobanche cumana* attack, resulting in the parasite's death (Serghini *et al.* 2001;

Echevarría-Zomeño et al. 2006). Facultative, generalistic parasites generally do not require germination cues from their hosts and pre-attachment resistance mechanisms do not play a significant role. In the case of *Rhinanthus minor*, for example, cold stratification is the factor determining germination (Ter Borg, 2005) and post-attachment histological responses underlie the variable host resistance (Cameron et al., 2006; Rümer et al., 2007).

Post-germination, certain physical barriers can act to prevent the parasite from reaching host outer surface. Glandular epidermal trichomes of *Solanum lycopersicum* proved to be an effective barrier to attachment of *Cuscuta pentagona* (Runyon et al., 2010). However, cacti spines, on which seeds of *Tristerix aphyllus* (Miers ex DC.) Barlow & Wiens are deposited by birds, are not a sufficient barrier as the radicles of this particular parasite are extremely long (Martinez Del Rio et al., 1995). Arrival at the host surface is followed by attachment. Parasite-derived extramural deposits of cell wall material play an important role during early attachment. Extensins and pectins were found to aid attachment of *Cuscuta* (Vaughn, 2002) whereas a cuticle-like secretion complex is produced by *Viscum minimum* Harv. (Heide-Jørgensen, 1988).

Stem parasites need to overcome the host cuticle barrier before entering its tissues. There is little information available on how this is achieved by parasitic plants. A combination of enzymatic and mechanical action is assumed, although no direct evidence of cutinase activity is available (Heide-Jørgensen, 2008). *Tristerix aphyllus* haustorium mechanically strips the host cuticle and epidermis off from a small area at the endophyte tip (Mauseth et al., 1985).

Much of the evidence behind spatio-temporal expression of post-attachment resistance comes from research on the economically and socially important *Striga* and *Orobanche*. Roots of *Orobanche minor* (Kusumoto et al., 2007) hosts block the progress of the endophyte at 3 points of penetration also found in other parasite-host combinations and were effected by a variety of mechanisms; 1) the cortex (through hypersensitive response and cell death or cell wall reinforcement); 2) endodermis (through lignification) or 3) xylem (by occlusion with secretions and tyloses). The effectiveness of these barriers varies. The suberised and lignified endodermis is an effective obstruction for *Orobanche aegyptiaca* in roots of resistant *Vicia* genotypes (Goldwasser et al., 2000) or for *Striga* in the NERICA (New Rice for Africa) rice cultivar (Cissoko et al., 2011) but does not prevent *Rhinanthus minor* from invading grass roots (Cameron et al., 2006; Cameron & Seel, 2007; Rümer et al., 2007).

While most physical barrier-based defences are initiated through cell-wall signalling, not all of the final products are localised in the wall. The hypersensitive response resulting in host cell necrosis around the penetration site leads to the early arrest and death of *Striga gesneroides* parasitizing cowpea (Lane et al., 1993) and *Orobanche aegyptiaca*

attacking vetch (Goldwasser *et al.*, 2000). Cell death has been reported on both host and endophyte sides of the haustorium. Hood *et al.* (1998) found that in associations with non-hosts; lettuce and marigold, the cytoplasm of the palisade interfacial tissue of *Striga asiatica* appeared degenerated, endophyte cell walls were thickened and the endophyte did not reach the endodermis or stele, except in less than 1% of the connections examined. Histological changes in host tissues included lettuce cortex cell necrosis at late stages of infection 120 hours post inoculation (hpi), increase in cytoplasm density in marigold cortex cells, 72 hpi, intracellular, electron dense wall appositions, 144 hpi, and subsequent necrosis of those cells as well as green staining of the cells with Toluidine Blue O, indicating abundance of phenolics.

Even when physical barriers fail and the parasite connects to the host's xylem, other defences can be mounted to prevent the parasite from succeeding. In haustoria of *Striga hermonthica* attached to *Tripsacum dactyloides* (L.) L. differentiation stopped after the xylem connection had been established suggesting that creation of a vascular connection is not the final step in haustorial development and that late, post-penetrational defence mechanisms can occur (Gurney *et al.*, 2001, 2003). Addition of primary HIFs did not induce further development of *Striga* haustoria which lacked well differentiated hyaline bodies (Gurney *et al.*, 2003). and the parasites did not make it beyond the tubercle stage. *Striga hermonthica* plants that had successfully attached to *Zea mays* (good host) and were subsequently manipulated to attach to *Tripsacum dactyloides* (bad host) not only developed poorly differentiated haustoria on *Tripsacum* but any haustoria that subsequently developed on *Zea* were also poorly differentiated (Gurney *et al.*, 2003). This suggests that inhibitory/toxic compounds from *Tripsacum* were exuded into the soil or taken up and transported within the parasite-graminoid root system. Conversely, cytotoxic compounds from *Alectra* and *Striga* have been hypothesised to poison cereal hosts as the reduced host yield cannot be accounted for solely by resource loss (Rank *et al.*, 2004).

4.5 Closing remarks

The aim of this chapter was to familiarize the reader with the complex roles played by cell walls in parasite virulence and host defence. Whereas cell wall architecture (composition and structure) has obvious mechanical implications for the interaction, its physiological implications are also extremely important and start acting first, through facilitation of signalling. Therefore, most mounted responses, wall-localised or not, depend on signalling molecule perception in or transport across the wall.

More research is needed to elucidate the elements of signalling pathways and defence mechanisms specific for plant parasitism by other plants as opposed to pathogens.

However, in the light of the multiple roles of the extracellular matrix in parasitism, cell wall research has the potential to offer key insights into avirulence and resistance, with important implications for crop science and ecology.

5 Engineered for theft: structural and immunocytochemical diversity of haustorial cell walls in *Rhinanthus minor* and *Odontites vernus*

5.1 Abstract

Structure and immunocytochemistry of the cell walls in *Rhinanthus minor* and *Odontites vernus* haustoria at different developmental stages were investigated. An extensive monoclonal antibody screen was carried out with 32 monoclonal antibodies. Distribution maps of a range of cell wall polymers were obtained for the whole haustoria.

Cell wall types and distribution of glycan and extensin epitopes were very similar in both species. Interfacial cell walls possessed considerably thickened, although apparently primary walls from early penetration stages until transition into xylem. Primary walls of the hyaline body walls were associated with paramural deposits. Xylem-associated, flange-like parenchyma with cell walls thickened in contact with vessel elements was for the first time observed in *Rhinanthus minor* and *Odontites vernus*.

The most novel immunolocalisation results concerned the presence of arabinogalactan protein (AGP) glycan epitopes in the hyaline body, interfacial parenchyma and partly-differentiated xylem bridges. This distribution was highly conserved in both species. AGPs first appeared in the interfacial parenchyma prior to attachment. LM2 antibody directed against β -linked glucuronic acid epitopes of AGP glycan side chains was the most consistent marker of their presence. Presence of AGPs in the hyaline body was associated with a decrease in de-esterified pectin labelling (JIM5, LM18 and LM19) in this tissue, while esterified homogalacturonans (JIM7, LM20) were present in all haustorial parenchyma. Rhamnogalacturonan I (RU-I, RU-II, LM5 and LM6 mAbs) occurred variably in haustorial parenchyma. Xyloglucans (LM15 and LM25) were rarely seen and were typically concentrated in the hyaline body walls and paramural deposits. Mannans were not detected. Flange-like thickenings were composed of layers which showed different textures and affinities for anti-pectin and anti-xyloglucan mAbs, while AGPs were not detected.

Partly-disintegrated protoplasts of xylem bridges labelled strongly with anti-AGP (LM2, JIM4, JIM8, JIM14) and anti-extensin (LM1, JIM12, JIM20) mAbs. Labelling was typically absent from the lignified thickenings, suggesting a role of these molecules in programmed cell death rather than wall deposition. Xylem thickenings were rich in xylans and LM5-detected epitopes of RG-I galactan side chains. Bands of very dense RU-II labelling were present in the lumen-facing parts of the thickenings in the vascular core but not the axial strand of the xylem bridge.

This is the first study to demonstrate presence of AGPs in angiosperm haustoria throughout their development and within the strategically important parts of the haustorium, i.e. interfacial parenchyma responsible for penetration and signalling with the host; xylem bridge, necessary for nutrient transfer; and, the hyaline body which is a likely site of nutrient processing and storage. This evidence strongly suggests that AGPs play fundamental, yet diverse functions in haustorial development and functioning.

5.2 Introduction

Cell wall composition has been sampled across different plant groups revealing its phylogenetic (Sørensen *et al.*, 2010; Popper *et al.*, 2011) as well as structural and functional diversity (Knox, 2008). However, no cell wall-focused, comprehensive studies of the highly specialised structures of angiosperm haustoria, encompassing both structure and composition exist in the literature. Although many anatomy-based journal articles (Visser *et al.*, 1984; Heide-Jørgensen, 1988; Kuo *et al.*, 1989; Fineran & Calvin, 2000) and key textbooks (Kuijt, 1969; Press & Graves, 1995; Heide-Jørgensen, 2008) discuss some aspects of haustorial cell wall architecture, our understanding of this aspect of haustorial structure and its implications in the infection process are far from exhaustive. This is not only a result of a low number of relevant studies focusing specifically on cell walls, but also a consequence of the techniques applied. Histochemistry has been by far the most widely used method of investigating changes in host cell walls during haustorial ingress as well as some specialised cell walls in haustoria of several species (Visser *et al.*, 1990; Hood *et al.*, 1998; Pérez-de-Luque *et al.*, 2006a, 2007; Echevarría-Zomeño *et al.*, 2006). However, the potential of histochemical studies for investigating cell wall architecture is limited by the relatively low specificity of histochemical dyes. Conveniently for parasitic plant research, some of the highest specificities are provided by dyes for defence-related cell wall components. Weisner reagent can produce relatively reliable information about the location of lignins, although also not without limitations (see discussion in chapter 7); aniline blue is commonly used in the detection of callose, and, Sudan dyes can be used to visualise the distribution of lipids, including the aliphatic fraction of suberins. Another commonly used dye, safranin, stains both lipids and phenolics (Ruzin, 1999) and can provide only a general overview of “defence compounds”. Only very general information on the localisation of cellulose (using for example calcofluor) and pectins (using toluidine blue O or Ruthenium Red) and virtually no information about hemicelluloses can be obtained through histological staining.

Immunolocalisation with monoclonal antibodies (mAbs) or carbohydrate binding modules (CBMs) is arguably the best tool allowing highly specific localisation of cell wall polymer epitopes *in muro* (Knox, 1997; Lee *et al.*, 2011) and is particularly important for localising glycan epitopes, the diversity of which is not directly encoded

by genes and therefore difficult or impossible to investigate through genetic sequencing and subsequent manipulation (Fangel *et al.*, 2012). Antibody probes have been successfully applied to study signalling, adhesion or histogenesis (Knox, 1997; McCann & Knox, 2011), i.e. topics that beg to be investigated when one considers the development and functioning of a haustorium. It is therefore surprising that only a handful of studies have applied immunocytochemistry to investigate haustorial connections between angiosperms (Olivier *et al.*, 1991; Reiss & Bailey, 1998; Losner-Goshen, 1998; Neumann *et al.*, 1999; Vaughn, 2003, 2006). This technique has provided some preliminary information about the changes in cell wall structure during parasitism, revealing some remarkable modifications, for example a relative increase in arabinose side chains of RG-I in a chimeric wall formed at the interfaces between *Cuscuta* searching parenchyma cells and its hosts (Vaughn, 2003). This modification appears, however, to be restricted to *Cuscuta* interfaces and parasitic plants typically grow between host cells. Our knowledge of how this is achieved is scarce and fragmented, although both host and parasite walls are likely to be rendered appropriately to their functions (defence and virulence, respectively) during penetration. Immunodetection of pectin methylesterase (PME) and de-esterified pectins (Losner-Goshen, 1998) as well as localisation of cellulose using an exocellulase-gold complex (Olivier *et al.*, 1991) showed, that pectins as well as celluloses are depleted in host tissues at the interfaces with haustoria.

Overall, investigations of cell wall structural elements and enzymes during parasitism have been restricted by a limited selection of probes used, focus on the interfacial region and exclusion or brief mention of early developmental stages. Little focus has been placed on mapping the spatio-temporal distribution of molecules that might have roles in parasite-host signalling or regulation of haustorial development. Extensins and AGPs in particular are groups of molecules implicated in xylem differentiation and signalling — processes crucial in establishing functional haustorial links with hosts. Several monoclonal antibodies directed against a range of these potential regulators of haustorial development exist, in addition to probes recognising typically, although not exclusively, structural cell wall components, namely pectins, hemicelluloses and cellulose (Pattathil *et al.*, 2010). Therefore, cell wall immunocytochemistry has great potential for increasing our understanding of how haustorial walls are adapted to and how host cell walls are modified during attachment and penetration.

While relatively few studies have been carried out on haustoria of parasitic plants which are not economically important as crop weeds (Štech & Wesselingh, 2010), good research foundations have been laid for *Rhinanthus minor*, owing to its practical applications in grassland biodiversity restoration (Davies, 1997; Pywell *et al.*, 2004; Bullock & Pywell, 2005; Westbury *et al.*, 2006). It has been previously demonstrated that its haustoria develop differently depending on the quality of the host, with non-hosts using cell wall-associated reinforcements in the host such as lignification

and suberisation to separate their vasculature from the haustorium (Cameron *et al.*, 2006; Cameron & Seel, 2007; Rümer *et al.*, 2007). However, similar to studies of different parasite-host associations that demonstrated analogous mechanisms of resistance (Visser *et al.*, 1990; Hood *et al.*, 1998; Pérez-de-Luque *et al.*, 2006a; Echevarría-Zomeño *et al.*, 2006), histochemistry techniques were only applied to *Rhinanthus haustoria* and a comprehensive developmental progression was not presented.

The introductory chapter of this thesis outlines the already well known general anatomy of haustoria in *Orobanchaceae*, which is also true for *Rhinanthus*. Rather than being simple grafting organs limited to establishing a xylem link, haustoria also appear to have a possible role in nutrient processing and storage, which has been suggested to be fulfilled by the distinctive central parenchymateous region called the hyaline body. This element of the haustorium must, indeed, be crucial in its functioning as its development has been shown to be severely limited during parasitism on non-hosts (Gurney *et al.*, 2003). While the focus of previously published works on haustorial anatomy at the level of detail allowing to make conclusions about cell wall structure has been typically placed on the interfacial region, the hyaline body has received surprisingly little attention. Only one publication to date focuses on the structure of this intriguing tissue, showing that extracellular deposits form a distinctive element of hyaline body apoplast in *Alectra vogelii* (Visser *et al.*, 1984). There are also reports of other distinct cell wall modifications in parenchyma associated with haustorial xylem, notably flange cells and flange-walled transfer cells, displaying characteristic lignified thickenings (Fineran, 1996; Fineran & Calvin, 2000), or xylem bridge-associated parenchyma in *Triphysaria*, with non-lignified thickenings abutting xylem cells (Heide-Jørgensen, 1995). The proposed function of these cell walls is to form additional sites of apoplastic transport and exchange of solutes between the modified cells and the xylem bridge to allow processing and, speculatively, their subsequent return into the xylem bridge (Fineran, 1996; Fineran & Calvin, 2000). Anatomical diversity within haustoria is likely to be reflected in cell wall composition, with consequences for cell wall and tissue physiology.

The main aim of research presented in this chapter was to characterise haustorial cell wall structure and composition in *Rhinanthus minor* and its close relative *Odontites vernus*, and identify cell wall components likely to play key roles in the functioning of haustoria. An *in-situ* analysis of cell wall components was carried out using an extensive immunocytochemical screen with 32 glycan- and extensin-directed monoclonal antibodies (listed in table 3.5) to identify spatial variation in epitope distribution. Aspects of developmental variation were investigated by including haustoria at early developmental stages.

5.3 Results

Unless indicated otherwise, the results concern both *Rhinanthus minor* and *Odontites vernus*. Similarly, unless otherwise stated, the results were obtained from samples collected from compatible grass and legume hosts. The differences in anatomy and immunocytochemistry of mature connections on a wider range of hosts and non-hosts are described in more detail in chapter 6. Sections were obtained from London Resin-embedded samples and stained with toluidine blue, unless indicated otherwise. Details are presented in chapter 3. Each immunofluorescence image taken in the green channel is presented to the right of a light micrograph of the same section for anatomical reference.

5.3.1 Tissue differentiation and establishment of vascular connections

5.3.1.1 Pre-attachment haustorial anatomy

It was confirmed that haustoria of *Rhinanthus minor* and *Odontites vernus* develop near the root tip, which continues to grow and may produce more haustoria. As a result, multiple haustoria attached to one root were commonly found. However, it was very difficult to obtain a series of haustoria that included early developmental stages which remained attached to host roots. Harvesting young plants (2 and 4 weeks old) did not yield the desired samples, as collected haustoria were either already at advanced developmental stages or, conversely, no connections had developed. Immature haustoria were therefore uncommon and most dislodged from the host root during collection. Furthermore, some haustoria were small and possessed no clasping folds, appearing to be immature. Careful examination with a stereomicroscope revealed that these apparently early-stage haustoria already possessed xylem bridges. In many cases when no xylem bridge was observed under a stereomicroscope, its presence became apparent during sectioning. Ultimately, few early stage samples were found. They were obtained from plants that were already flowering. Collected samples included 3 haustorial initials before contact with the host, 5 samples of haustoria that were at early stages of cortex penetration (4 of which dislodged during collection), 1 sample during early endodermal and pericycle penetration and many samples with partly-differentiated xylem, i.e. still possessing protoplast in the vessel elements. No samples at early attachment/adhesion stages were found intact.

The youngest haustoria found in this study had developed past the cortex hypertrophy stage of an early haustorial initial and had already expanded by means of some cortical divisions, as illustrated in figure 5.1A. All cells were strongly vacuolated at that stage, i.e. filled with single large vacuoles and small amounts of protoplast, which were not visible at light microscopy level. The epidermal cells in the distal part of the haustorial initial were slightly elongated. This part of epidermis is further referred to as contact

parenchyma or interfacial parenchyma. During penetrative stages of development, endophyte parenchyma is another term used interchangeably.

In addition to haustorial initials collected from pot-grown plants, a haustorium developed in contact with a Petri dish wall was harvested when it was several days old. It was likely to represent anatomy similar to that of early stages of contact with host root as the contact parenchyma displayed the cytoplasmically-rich appearance characteristic of early contact with a host (Riopel & Musselman, 1979) and its tissue differentiation was more advanced than in the initials (Fig. 5.1B). Strands of regularly stacked cells in the axial region indicated that cortical divisions had progressed. Additionally, the vacuoles of cells in the distal region were more fragmented, cytoplasmic staining was increased and large nuclei had appeared. The epidermis in proximal and median parts of haustoria appeared collapsed but some cells remained functional and produced haustorial hairs, which are not visible in the micrographs in figure 5.1.

Figure 5.1 also depicts a cross section through a root of *Arrhenatherum elatius* var. *bulbosum* (image C) — the main host used to obtain results illustrated in this chapter. No constitutive reinforcements are localised in the cortex, except thickened walls of its innermost cell layer. Most cells of the stele are, however, lignified and a tertiary endodermis is present.

Image 5.1D shows simplified anatomy of the haustorial initial and host root. The grey fill colour indicates the parasite (P) and the host (H) is indicated in white. This colour scheme is continued in graphs accompanying later developmental stages. Capital letters **P** and **H** indicate the parasite and host in image annotations, particularly at the interfacial regions.

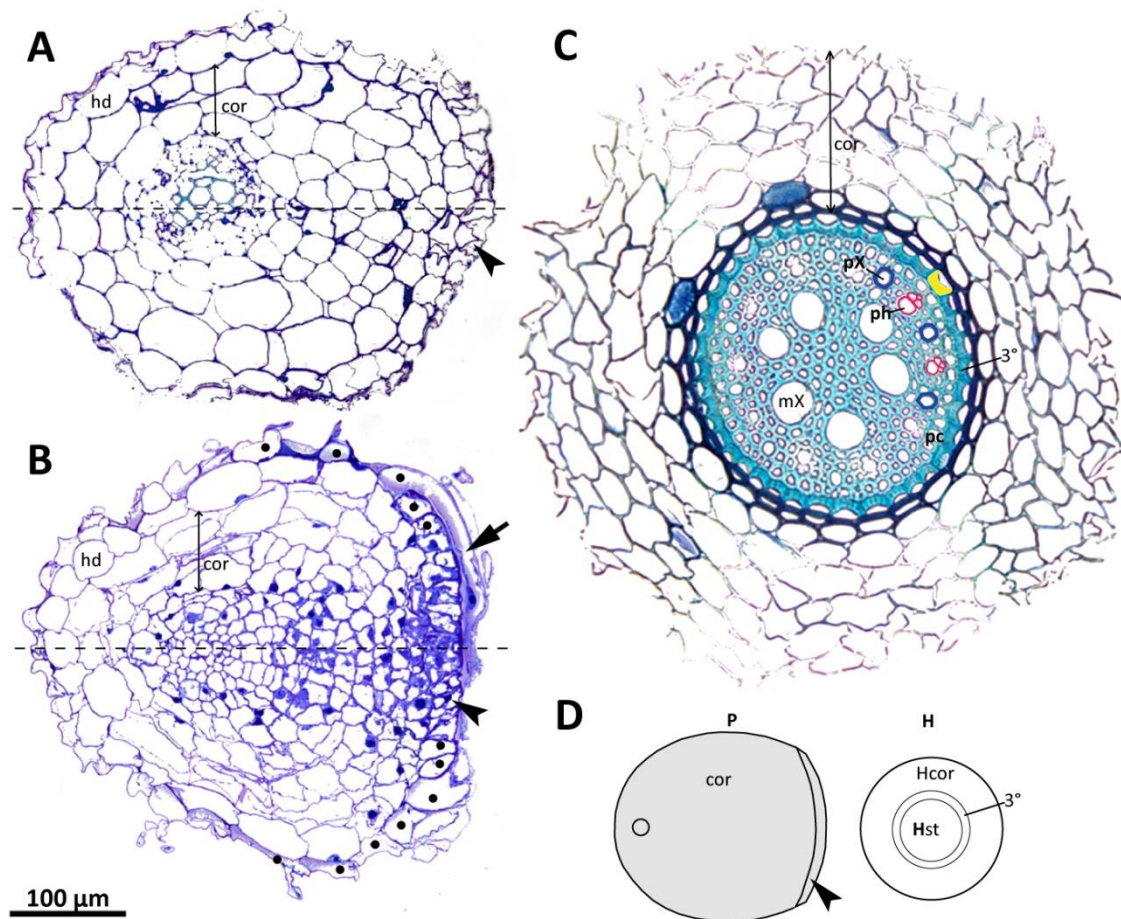


Figure 5.1: Pre-attachment anatomy of *Rhinanthus minor* haustoria (**A** and **B**) and of an uninfected root of host *Arrhenatherum elatius* var. *bulbosum* (**C**). **A**) Earliest-stage haustorium examined in this study shows directionality, with proliferated cortex (**cor**) cells and slightly elongated epidermal (\blacktriangleleft) cells present on the partly-differentiated side. Longitudinal axis is indicated with a dashed line. Hypodermis (**hd**) is exposed at the surface in some places. **B**) Haustorium collected from a Petri dish wall that shows a more advanced stage of development with further divided cortex cells with large nuclei and a more protoplasmic contact parenchyma (\blacktriangleleft), Dots (\bullet) mark epidermal cells and highlight their continuity with contact parenchyma. An exceptionally long epidermal cell (\blacktriangleleft) can also be observed at the contact face. **C**) Uninfected root of *Arrhenatherum elatius* var. *bulbosum* has a clearly differentiated tertiary endodermis (3°) with strongly thickened inner periclinal and anticlinal walls (indicated in yellow) which are lignified, as evidenced by turquoise staining with toluidine blue O. The innermost layer of the cortex (**cor**) is also considerably thickened, but not lignified. Within the stele, most cells, including pericycle (**pc**), are lignified. Phloem (**ph**) is the only non-lignified tissue. Large metaxylem (**mX**) vessels and smaller protoxylem (**px**) vessels are present. **D**) Diagram of haustorial initial and host root prior to infection. Grey fill colour and capital letter **P** are used to indicate the parasite in other diagrams, while white colour and capital letter **H** indicate the host, therefore, **Hcor** — host cortex, **Hst** — host stele.

5.3.1.2 Post-attachment haustorial anatomy

Haustorial anatomy during cortical penetration

At the next developmental stage analysed, the regular tissue patterns observed in the Petri dish-collected sample had been replaced by two tissue regions of highly-protoplasmic cells with large nuclei: 1) an ovoid, central tissue composed

of isodiametric cells in a region where a hyaline body is typically found in mature haustoria of Orobanchaceae and 2) a distal, smaller cluster of similar cells arranged in layers parallel to the interface (Fig. 5.2A).

An axial strand of somewhat smaller cells, presumably an initial stage of xylem bridge differentiation, was seen (Fig. 5.2B). The cell walls of the central protoplasmic tissue region were approximately 100 nm (Fig. 5.2C) and some of them labelled with the anti callose antibody (data not shown), suggesting that cell plates were forming during sample collection, and, further highlighting the proliferous character of this tissue. Parasite contact epidermis had formed a wide and blunt wedge of the early endophyte and had begun to penetrate the host root cortex (Fig. 5.2D). Endophyte cells, which spanned a considerable width of the interface, had started growing towards the host stele. No rupture of parasite tissues in the distal region of the haustorium occurred during endophyte formation, consistently with previously published findings that this organ is formed by epidermal cells (Heide-Jørgensen & Kuijt, 1993). Penetration was mechanically facilitated by clasping folds and, as a consequence, parasite contact parenchyma was adjacent to a layer of crushed host parenchyma cells at the lateral part of the interface (Fig. 5.2A and D). Contact between functional host parenchyma and parasite cells was therefore possible mainly at the central interface. No interspecific plasmodesmata were observed at any stage of haustorial development.

During early penetration of cortex, distal periclinal (parallel to the interface) and anticlinal (perpendicular to the interface) walls of parasite contact parenchyma became thickened (Fig. 5.2 E–G). Ultrastructural images showed that while cell walls of parenchyma cells behind the interface were at that stage approximately 0.1 μm wide, the periclinal contact wall was up to 1 μm thick and displayed a very loosely fibrillar structure, contrasting with tightly packed walls of the host (Fig. 5.2G). In several places within the central interface, this wall produced small outgrowths which coincided with what appeared to be dissolution of host wall and extramural material sandwiched between the parasite and the host (Fig. 5.2F and 5.2G). The anticlinal walls gradually thickened towards the interface, reaching up to 3 μm across, with the fibrils aligned chiefly parallel to the interface and displaying a somewhat tormented, sinuous structure (Fig. 5.2E).

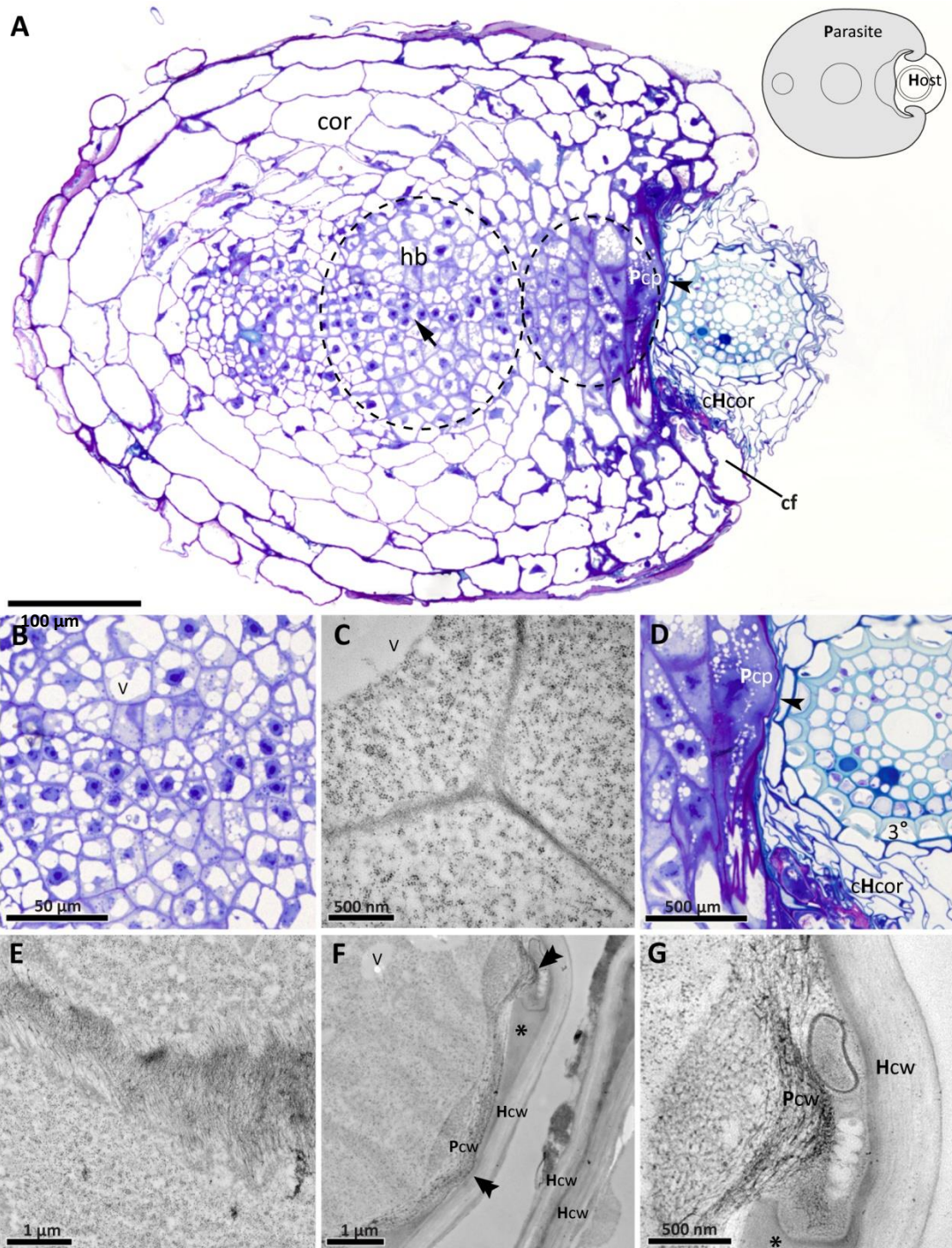


Figure 5.2: Haustorium of *Rhinanthus minor* collected during penetration of *Arrhenatherum elatius* var. *bulbosum* cortex. **A)** The haustorium is clamping around the host root (parasite and host indicated in the inset diagram) using clamping folds (**cf**). Host cortex is crushed (**cHcor**). Parasite contact parenchyma (**Pcp**) has reached the innermost later of host root cortex (**◄**), before the tertiary endodermis (**3°**) (**A, D**). Two distinct regions, with large nuclei and more protoplasmic than the haustorial cortex (**cor**), are present, as indicated by the dashed lines. An axial strand (**◄**) of slightly smaller, isodiametric cells is also present. **B)** Detail of the central region showing cytoplasmically-rich, vacuolated (**v**) cells with large nuclei, and the axial strand. Cells adhere tightly and no intercellular spaces are visible. **C)** TEM micrograph showing the thin (≈ 100 nm) cell walls of the central region shown in **B**. The grains within the cytoplasm are numerous ribosomes. **D)** Detail of the central interface (arrowhead) and lateral interface with crushed host cortex (**cHcor**). Parasite contact parenchyma spans the central interface and part of the lateral interface. Abundant cytoplasm of haustorial cells in this region stain purple and small but numerous vacuoles are present. **E)** TEM image of a sinuous, thickened periclinal wall of parasite contact parenchyma, made of fibrils aligned parallel to the interface. **F and G)** detail of the central interface (arrowhead in **D**) showing loosely fibrillar parasite wall (**Pcw**) producing outgrowths (**◄**) associated with apparent dissolution of extramural interfacial deposits (*****) and host wall (**Hcw**).

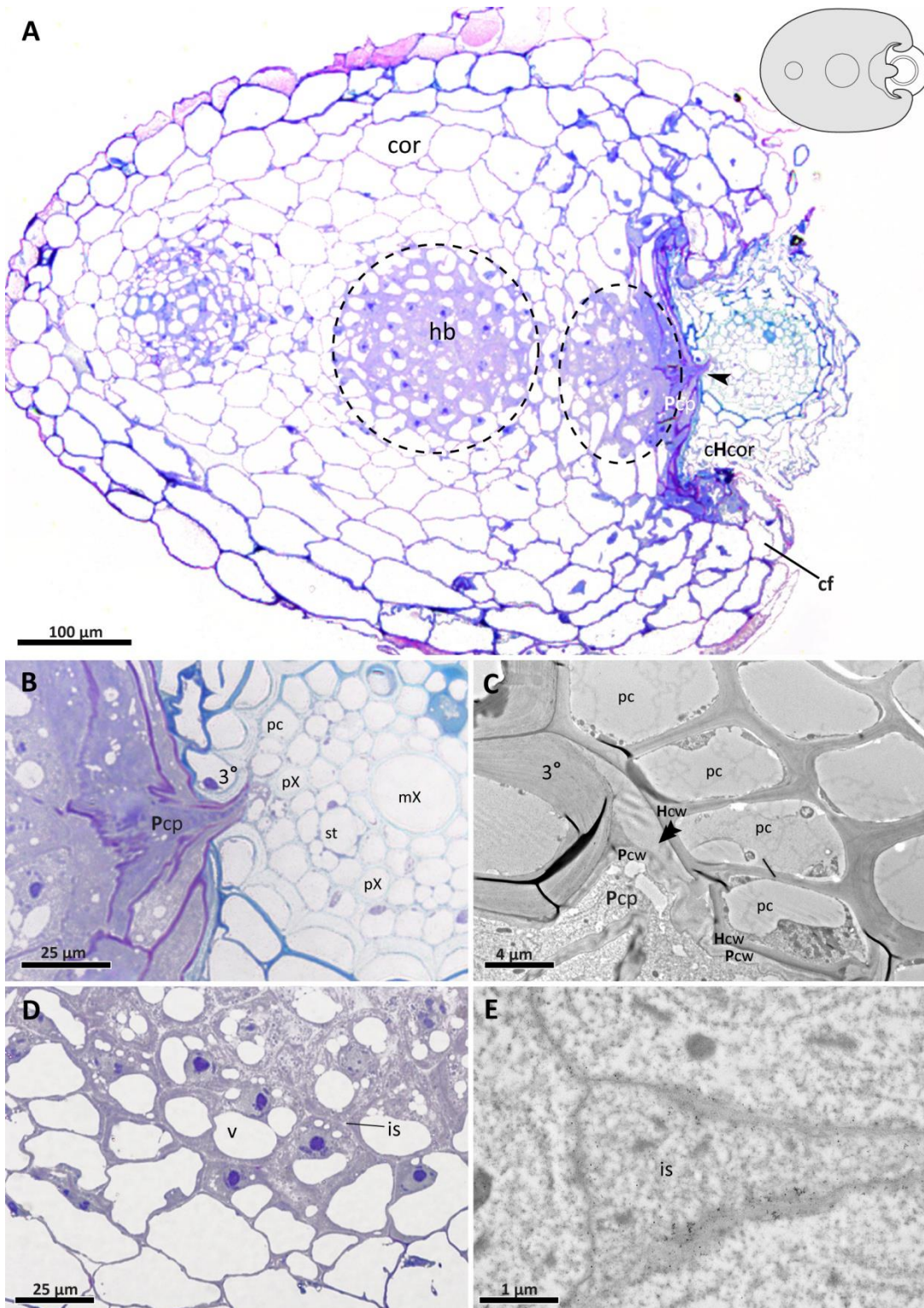


Figure 5.3: Haustorium of *Rhinanthus minor* collected during early penetration of the stele of *Arrhenatherum elatius* var. *bulbosum*. **A)** Two cytoplasmically-rich tissue regions, a central one and a distal one, are still present. **A, B and C)** Parasite contact parenchyma (**Pcp**) has begun separating (◄) two cells of the tertiary endodermis (**3°**) and penetrating between the cells of its pericycle (**pc**). **C)** TEM micrograph of the parasite contact parenchyma having partly separated host endodermis from pericycle. Cell walls of the parasite are thick ($\geq 1 \mu\text{m}$) but malleable and follow the shape of host walls (**Hcw**). The space between the endodermal and pericycle wall is filled with material of smooth appearance (◄). **D)** Detailed image of the central parenchymateous tissue shows that it is of similar structure as during cortical penetration although **E)** intercellular spaces filled with loose material are now present.

Haustorial anatomy during early penetration of the stele

During early penetration of the host stele, the two highly protoplasmic tissue regions were still present (Fig. 5.3A). Cells of the interfacial parenchyma had begun separation of endodermis and pericycle cells by intrusive intercellular growth (Fig. 5.3B). Cell walls of the penetrating cell tips were thickened but apparently malleable as they followed the shape of host walls tightly (Fig. 5.3C). The central tissue was of similar appearance as before (Fig. 5.3D) but intercellular spaces had become apparent (Fig. 5.3E).

Haustorial anatomy during xylem bridge development

Access to the stele was associated with maturation of the hyaline body and development of the xylem bridge composed of three main parts: 1) the vascular core, below the original parasite root vasculature (rx); 2) the axial strand and 3) the endophyte xylem. Longitudinal extent of all three parts is indicated in figure 5.4A. Although the first possible sign of xylem bridge initiation was observed in the form of a central meristematic strand during cortical penetration, the early stage of xylogenesis was not captured. All examined haustoria that had established within the stele had also developed a continuous xylem bridge with characteristically thickened walls. It was therefore not possible to anatomically determine the initiation point (or points) and direction of xylem bridge differentiation. The vessels in many samples still possessed protoplasts, which, in several cases, showed evidence of acropetal degradation progressing from the vascular core (no protoplast remnants), through the axial strand (grainy protoplast remnants) to the endophyte xylem (intact protoplast with nuclei and large vacuoles). However, local variations were also seen and no gradient of wall thickening could be identified in these partly differentiated xylem bridges as the secondary lignified thickenings appeared developed to the same degree along the entire length of the xylem. In the haustorium illustrated in figure 5.4, protoplast remnants were present in the axial vessel (Fig. 5.4B) and endophyte xylem (Fig. 5.4A) but not in some of the vascular core xylem cells (Fig. 5.4A). The central parenchymateous tissue in the same haustorium was more vacuolated than during earlier developmental stages. Its cells were also larger and possessed thicker cell walls ($\approx 0.5 \mu\text{m}$). However, organelle-rich cytoplasm was still present with prominent endoplasmic reticulum (ER). Scavenging parenchyma of the endophyte remained thick-walled during penetration of the stele as illustrated in Fig. 5.4E. Cell walls of contact parenchyma abutting the lateral interface were thickened in the same manner (data not shown). The thickening was never labyrinth-like and therefore it did not contribute to increasing the surface area of the plasmalemma.

Complete protoplast loss was observed in most haustoria examined. For practical reasons, these haustoria are referred to as “mature”. Non-protoplasmic inclusions were common in the lumina of both the axial strand and vascular core xylem of mature haustoria (Fig. 5.5). They formed grains of two types: 1) starchy grains (Fig. 5.5C and E)

and 2) grains of unidentified material (Fig. 5.5A, B and D). Starchy grains stained with IKI reagent for starch but not with toluidine blue O, which does not stain starch. The other type of grains stained purple or dark blue with toluidine blue O, but not with iodine in potassium iodide. It is therefore likely that non-starchy carbohydrates and, possibly, proteins might be involved although further study is required to confirm this.

In haustoria with complete xylem bridges, endophyte parenchyma and xylem co-occurred in varying proportions. Figure 5.6 illustrates endophyte cells at different stages of differentiation and inflicting various levels of damage to host cells, providing indirect information about the mode of penetration. Endophyte growth appears to have occurred chiefly intercellularly, whereby separation of host walls by the tip of the organ was achieved at the level of host middle lamellae. The intercellular mode of growth was particularly clear at the level of host endodermis. Typically, two cells of thickened grass endodermis were separated by meandering tips of the endophyte (Fig. 5.6A and B). These sloughed cells were often crushed to a varying degree and their content stained blue with toluidine blue O (Fig. 5.6A, B and C). Figure 5.6C illustrates a rare instance where a tip of a parasite cell was found sandwiched between separated layers of an endodermal cell wall.

Within the stele, the path of ingress was often very clean, with the cellulosic parts of lignified host walls left largely intact by the penetrating endophyte cells. This was mainly true for cells with lignified walls and is illustrated in figure 5.6B which shows parasite cells which have tightly followed the shape of host cells. Host cell damage is in such cases minimised to cell walls near three-way junctions which appear “snapped” when examined at ultrastructural level (Fig. 5.6E), suggesting that a strong mechanical force had been applied by the endophyte. However, in some samples even the cells reinforced by lignification were crushed and interrupted during the course of endophyte progression (Fig. 5.6D). Additionally, phloem cells, which possess unlignified walls, were often crushed (Fig. 5.6E) and in some cases it appeared that they were invaded by the narrow tips of endophyte parenchyma (Fig. 5.6C). Otherwise, protoplasts of host cells were rarely targeted.

Host wall dissolution was apparent only at the lateral interface with host cortex, where partly dissolved host walls were embedded in the extramural deposit layer. This is further discussed and illustrated in chapter 7, which deals specifically with these deposits. It could not be determined whether the dissolution was merely a consequence of the cells being crushed and subsequently subjected to further degradation or whether partial enzymatic dissolution preceded and partly facilitated the compression by clasping folds and endophyte. No clear evidence of host wall dissolution that might facilitate endophyte ingress was observed at the central interface. Furthermore, parasite cells were rarely seen entering host vessels.

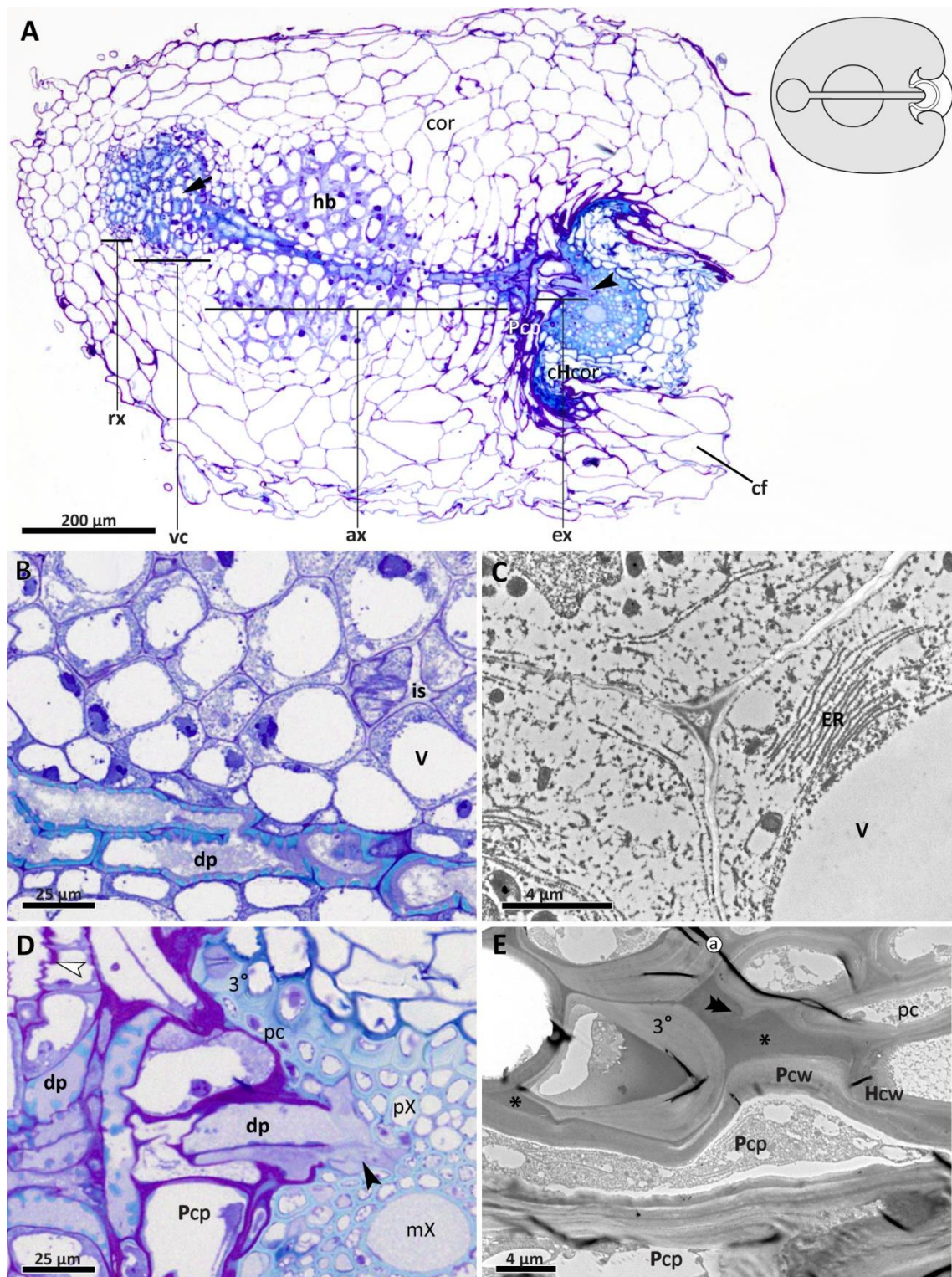


Figure 5.4: Haustorium of *Rhinanthus minor* attached to host *Arrhenatherum elatius* var. *bulbosum* collected during xylem bridge maturation (after the onset of thickening deposition and during cell death). **A)** The complete xylem bridge composed of a vascular core (**vc**), axial strand and endophyte xylem (**ex**) is present. Purple staining of partly-disintegrated protoplasts is present in xylem cells with some exceptions (\blackleftarrow) within the vascular core. Arrowhead (\blacktriangleleft) indicates the tip of the endophyte, which has reached the centre of the host stele. Clasp folds (**cf**) are well developed, securing parasite to the host root. **B)** Disintegrated protoplast (**dp**) fills the cells of the vasculature which has already developed secondary lignified thickenings, stained light blue. The hyaline body cells possess large intercellular spaces (**is**) and vacuoles (**v**). **C)** TEM micrograph of a three-way junction in the hyaline body the hyaline body from the same sample as in **B**. Abundant ER is present. **D)** Penetrating cell tips are in the vicinity of host protoxylem (**pX**) and metaxylem (**mX**) and have partly dissolved (see figure 5.6 for more detail).

Chapter 5

The hyaline body is still strongly protoplasmic, with darkly stained, large nuclei. Behind the parasite contact parenchyma (**Pcp**), a cluster of xylem cells with disintegrating protoplasts (**dp**), including a perpendicular one is present. Sinuous parenchyma cell walls are also present ($\langle \rangle$). **E**) A scavenging cell (**Pcp**) of the endophyte with a thick, malleable cell wall (**Pcw**), following the shape of the cell walls (**Hcw**) of host tertiary endodermis (**3°**) and pericycle (**pc**). Snapped host walls (\blacktriangleleft) are embedded in extramural secretion which fills the gap between the cells of the two plants.

The only clear example of a parasite cell entering host vessels through previously documented structures called osculi (Dörr, 1997) was found in a sample of *R. minor* parasitizing *Pimpinella major*. This is illustrated in figure 6.4D in chapter 6, which deals with the anatomy of haustoria in association with a diversity of hosts. What is however important to mention here is that penetration of *P. major* by osculi occurred via existing pits rather than following dissolution of the lignified wall. When the uncommon cases of host xylem wall disruption were observed (Fig. 5.6G), mechanical factors appeared more likely. This could be concluded on the basis that walls were interrupted but did not appear loosened as would be expected if they had been enzymatically digested.

This apparent scarcity of anatomical evidence for host wall dissolution is highlighted when contrasted with the clear examples of this phenomenon observed at the tips of parasite contact parenchyma cells during their conversion into xylem (Fig. 5.6D and F). Their thick walls stained purple with toluidine blue O prior to differentiation but in partly-differentiated cells, the cell wall in the tip region stained extremely pale pink, suggesting that depectinisation had occurred in preparation for cell opening at the tip (Fig. 5.6D). TEM images confirmed that the walls in this region were considerably loosened (Fig. 5.6F). In samples from more mature haustoria only extremely faintly-stained residual wall material was seen (Fig. 5.6H). As a result, a gap was often created between the ends of the lignified portion of the parasite xylem walls and host walls. This gap was not located specifically at host pits but instead several vessels opened to a relatively large common interfacial space which was in contact with numerous host pits (Fig. 5.6H). Most xylem cells abutted host vessels in this way as opposed to entering them, suggesting that indirect exploitation of pits might be a common means of infiltrating host xylem.

Parenchyma cells (Fig. 5.6H) and cells with secondary lignified thickenings and living protoplasts (Fig. 5.6G) often co-occurred with dead xylem cells. It could not be determined whether all of these living cells were simply at earlier stages of differentiation or whether the protoplasmic state was essential for their functions. In some haustoria, derivatives of the distal meristem also differentiated into xylem elements which were often perpendicular to the main xylem axis (Fig. 5.4D). The parenchyma cells in this region often possessed conspicuously sinuous walls. At least in some haustoria these curves marked the site of xylem wall lignification (data not shown) although in a number of samples the cells did not differentiate, while retaining the conspicuous wall shape (Fig. 5.4D).

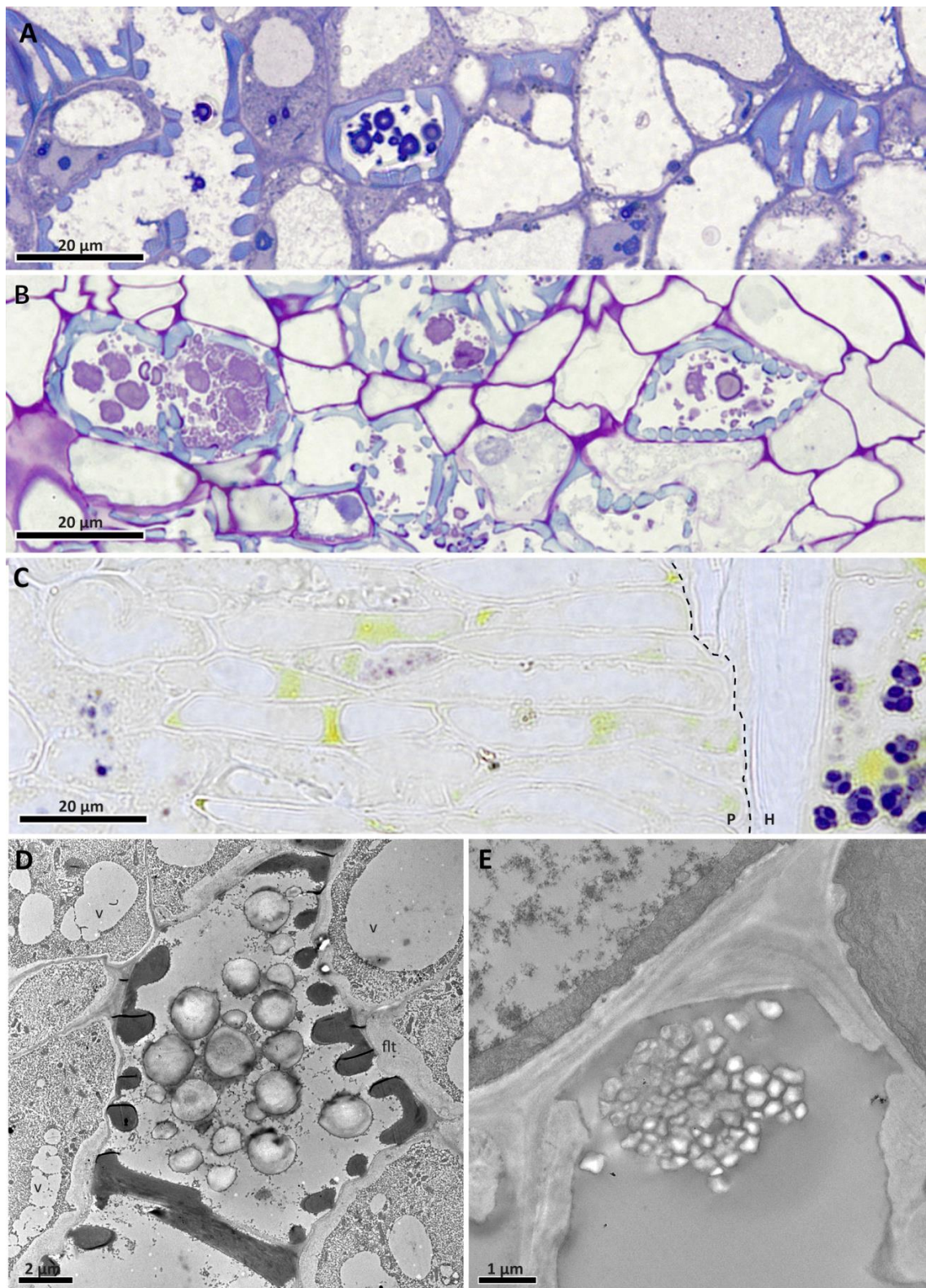


Figure 5.5: Graniferous xylem of *Rhinanthus minor* (**A**, **D** and **E**) and *Odontites vernus* (**B** and **C**). Light micrographs show sections stained with Toluidine Blue O (**A** and **B**) and IKI reagent for starch (**C**). **A)** Granules in the axial strand of *R. minor* stained dark blue. This colour is indicative of carbohydrates other than starch. IKI did not stain this material (data not shown). **B)** Light purple-stained granules in the vascular core of *Odontites vernus*. Material shown in the electron micrographs (**D** and **E**) is unstained.

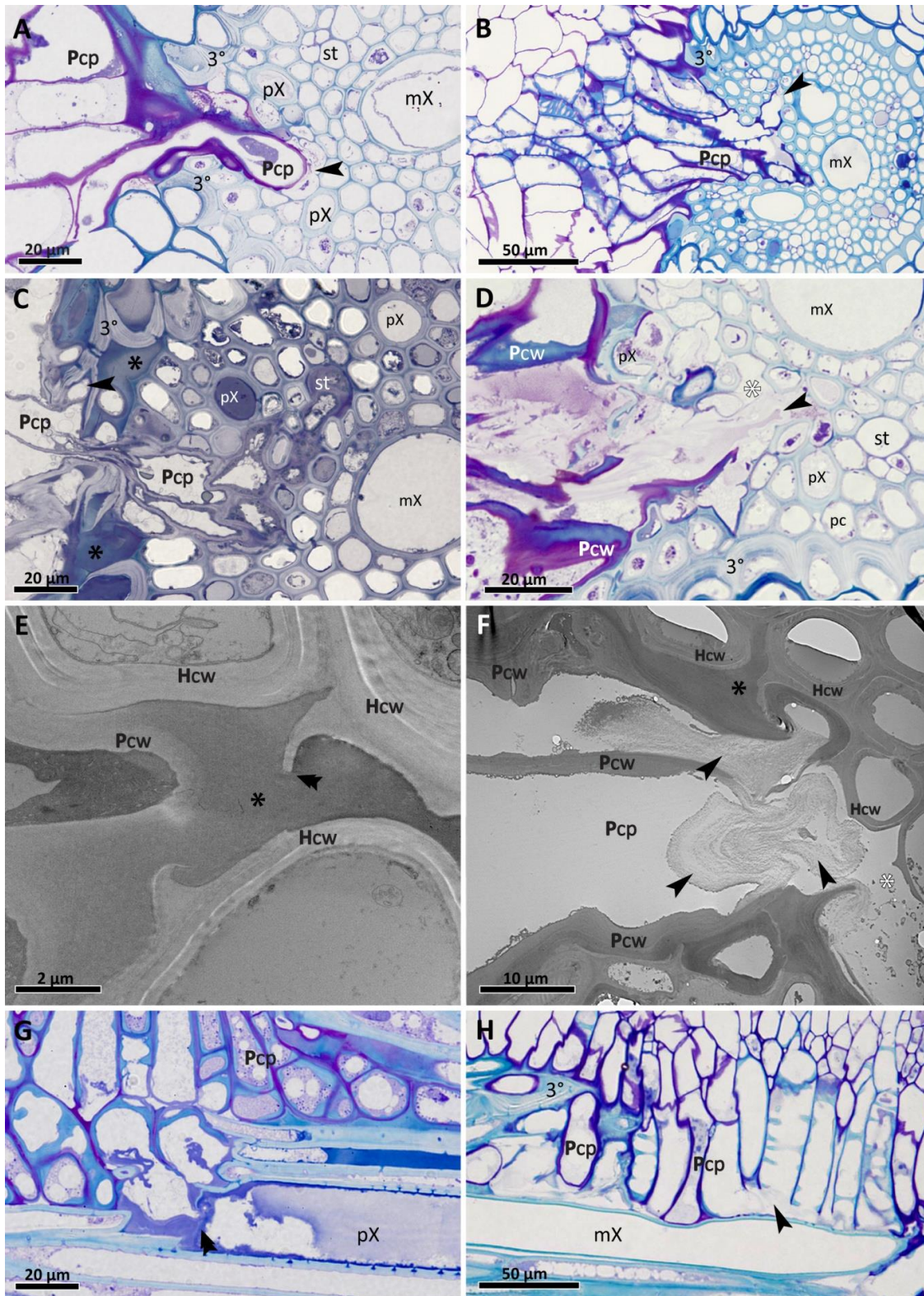


Figure 5.6 Types of contact between endophyte cell and host tissues. All images illustrate *Rhinanthus minor* attached to host *Arrhenatherum elatius* var. *bulbosum*. Arrowheads (◄) indicate endophyte cell (Pcp) tips, which have reached the centre of the host stele, crushing phloem (A), growing into a sieve tube (st) and between tertiary endodermis (3°) wall layers, abutting lignified stele cells (B), interrupting lignified host cells, for instance protoxylem (pX) (D and G) and producing intercellular cracks unfilled with material (*) or filled with extramural secretion (*). Snapped host walls (◄◄) are embedded in the secretion. Dissolved parasite cell wall is of much looser structure and is more electron-lucent (F). It stains very weakly pink with toluidine blue when the protoplast is still present (D) while appearing pale grayish-blue in more advanced cells (H). A common interfacial gap (◄) created in contact with host metaxylem (mX) after tip wall dissolution can be seen in image H. Living cells of parasite contact parenchyma (Pcp) co-occur with dead xylem cells (G and H). Oblique cross walls are common in these cells (G).

Although maturation of the xylem bridge correlated with that of the hyaline body, the link was not always very straightforward. Protoplast-containing xylem was typically, but not always, associated with a densely-cytoplasmic hyaline body (Fig. 5.4A). Figure 5.7 illustrates a range of sections through hyaline bodies from different samples. In older haustoria of *Rhinanthus minor*, hyaline body cells were typically strongly vacuolated, with thin layers of protoplasts appressed against the primary cell walls with prominent intercellular spaces (Fig. 5.7A, B and F). These protoplasts included large nuclei and were rich in mitochondria and dictyosomes, suggesting high metabolic activity of this tissue. Paramural deposits (deposits located between the cell wall and the plasmalemma) were often seen within the hyaline bodies, regardless of the level of their vacuolation. They were not always apparent at light microscopy level although in some samples their presence was clearly indicated by purple staining with toluidine blue O (Fig. 5.7A), suggesting carbohydrates such as pectins to be an important component. TEM micrographs showed that the deposits were more electron-opaque in osmicated material than the regular primary cell wall (Fig. 5.7B and C). Their deposition appeared to be associated with an endomembrane system, most likely smooth ER. Image 5.7C illustrates these deposits partly filling a membrane cistern which is fused with the plasmalemma. In addition to these cell-wall associated deposits, ovoid granules of material stained blue with toluidine blue O were often seen (Fig. 5.67A). These inclusions were found in non-osmicated material, suggesting that membrane fixation granted by osmium tetroxide was not crucial to the preservation of their shape. Similar, but much larger granules of toluidine blue O-stained material were exceptionally striking in some hyaline bodies of *Odontites vernus*, where they commonly occupied a large proportion of the cell volume (Fig. 5.7D). TEM image 5.7E shows the grainy structure of this material and its co-occurrence with another type of inclusion frequently seen in the hyaline body cells, namely spherical osmiophilic bodies. They appeared light grey-brown at light microscopy level (Fig. 5.7F) and black in TEM micrographs (Fig. 5.7G and H). Strongly osmiophilic properties suggest that oily substances might be the main component of these structures.

Generally, the central parenchymateous tissue region of *O. vernus* differed from that of *R. minor*. It was often wedge shaped in cross-longitudinal section in contrast with the round to oval shape found in *Rhinanthus* and remained cytoplasm-rich, meristem-like at late stages of xylem differentiation. No staining with anti-callose was observed in these cytoplasm-rich cells (data not shown). Therefore, this highly protoplasmic state was not directly related to cell proliferative activity. Figure 5.8 shows haustoria which have developed continuous xylem bridges. The central parenchymateous core of *Odontites* stains much darker and is narrower in comparison with the oval outline of the central parenchymateous tissue in *Rhinanthus minor*.

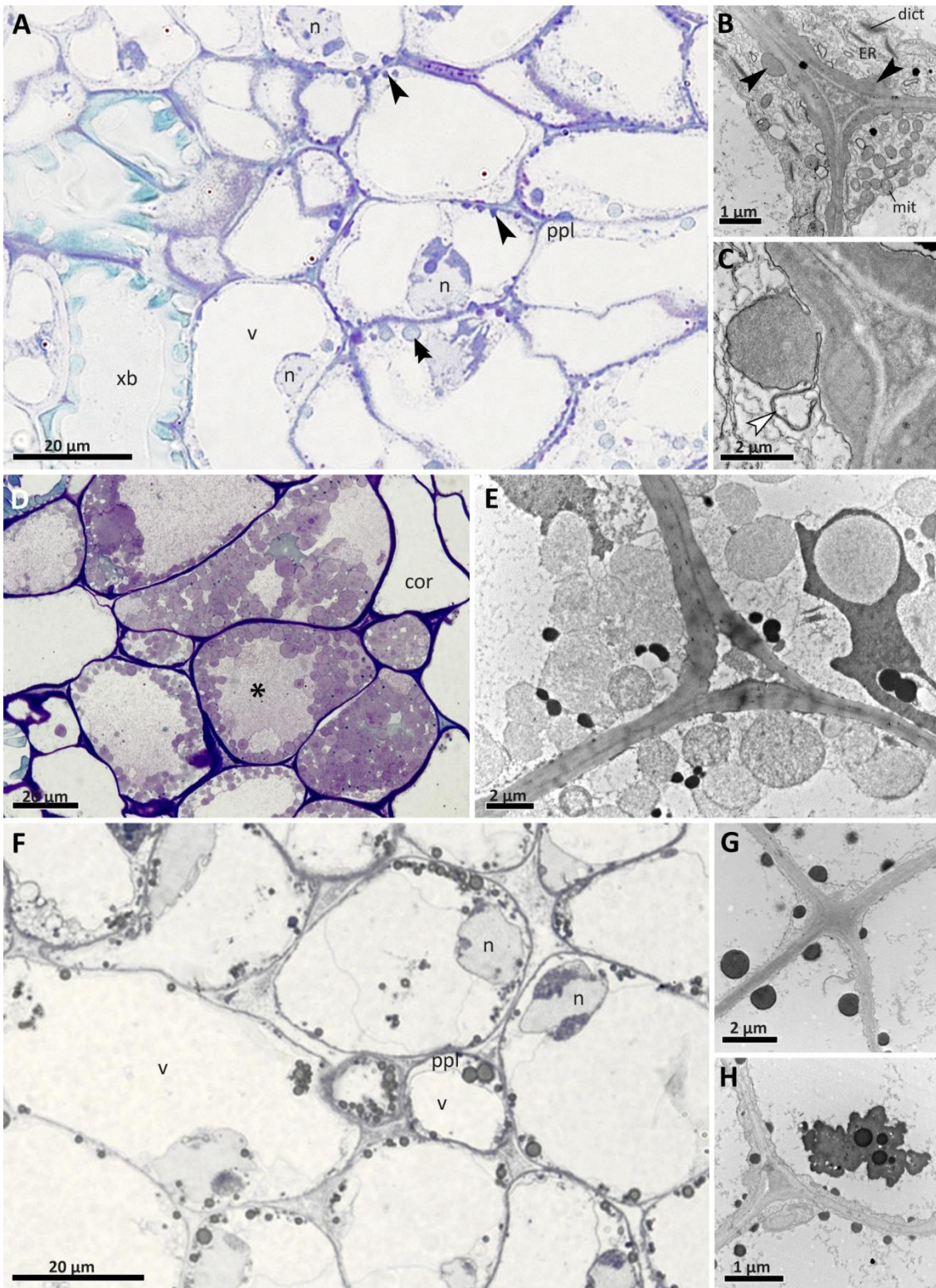


Figure 5.7 Structure of the hyaline bodies of *Rhinanthus minor* (A–C, F–H) and *Odontites vernus* (D, E) and ergastic materials found within them. **A)** *R. minor* hyaline body cells located near the xylem bridge (xb). Large vacuoles (v) fill the bulk of the cells, having pushed the protoplast (ppl) to cell peripheries. Large nuclei (n) with darkly stained nucleoli suggest high metabolic activity. Paramural deposits (◄) and ergastic inclusions (◄◄) of round outline are present. Dark purple staining of the former suggests abundant pectin component. **B and C)** Detail of a three way junction with paramural deposits in a hyaline body cell from an osmicated sample. Numerous mitochondria (mit) and dictyosomes (dict) and abundant ER suggest high metabolism and intensive trafficking. Paramural deposits, filling an otherwise narrow membranous cistern (◄◄), and partly merged with the wall, can be seen. **D and E)**

Ergastic materials of *O. vernus* are larger and display a grainy structure organised in round bodies and filling spaces between them (*). Whole hyaline body cells are commonly filled, in contrast with the cells of the cortex (**cor**). They are found in association with osmiophilic particles (black). **F, G and H**) Osmiophilic particles in *R. minor* hyaline body (**F and H**) and cortex (**G**). These, most likely lipidic, inclusions are typically round in outline although irregular masses of osmiophilic material are also found (**H**).

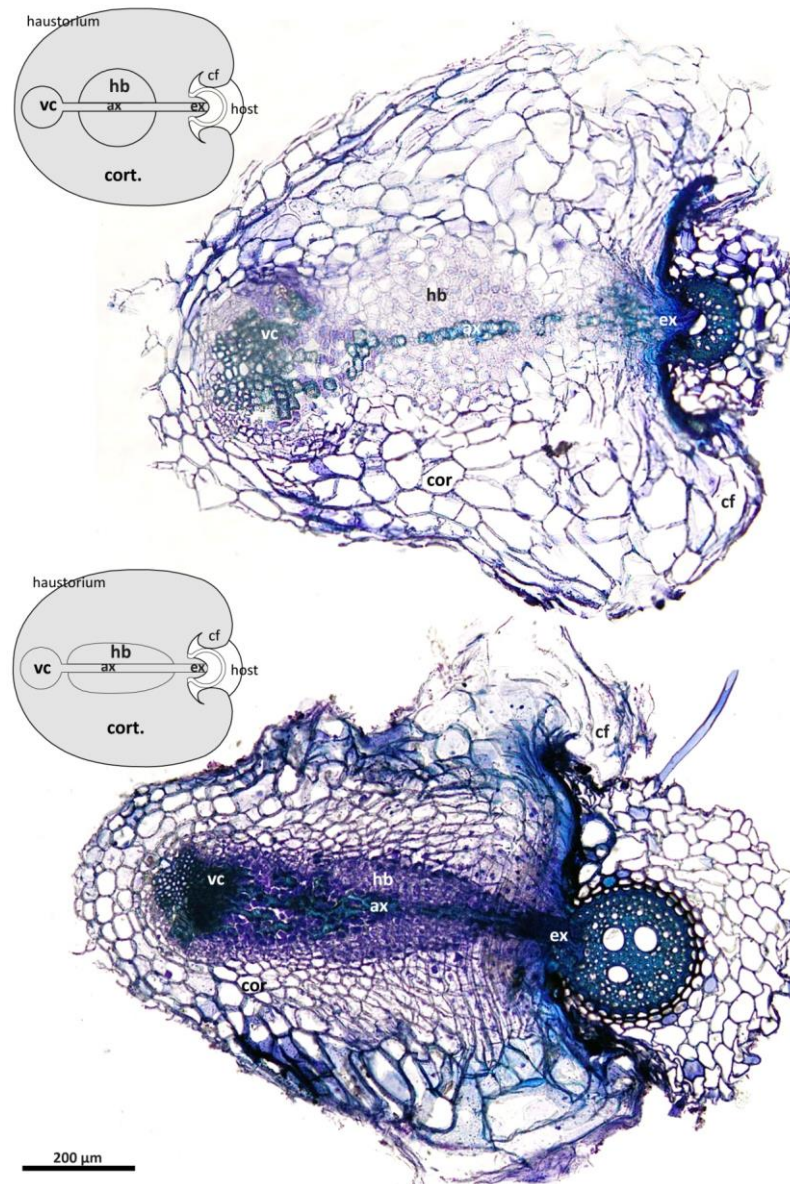


Figure 5.8: Mature haustoria of *Rhinanthus minor* (top) and *Odontites vernus* (bottom) attached to *Arrhenatherum elatius* var. *bulbosum*. Sections $\approx 10\mu\text{m}$ thick were taken from wax-embedded samples. All main structural elements are present. These include xylem bridge composed of a vascular core (**vc**), an axial strand (**ax**) and endophyte xylem (**ex**); hyaline body (**hb**) surrounded by the cortex (**cor**) and clasp folds (**cf**). The main difference can be seen in the more elongated shape and darker staining of the hyaline body in *O. vernus*.

A type of specialised parenchyma tissue was associated with the axial strands and vascular cores (but not endophyte tracheary elements) of xylem bridges (Fig. 5.9). Xylem-abutting walls of these highly protoplasmic cells were considerably thickened (up to several μm), in a uniform manner (Fig. 5.9A and B) very closely resembling that seen

in the analogous tissue of *Triphysaria* (Heide-Jørgensen, 1995) and *Euphrasia* (Fineran, 1987). As these authors did not propose a name for this little researched tissue, a working name *flange-like parenchyma* is adopted for the purpose of this study, based on some similarities to the flange cells defined by Fineran (Fineran, 1996; Fineran & Calvin, 2000), described in the discussion section of this chapter.

No labyrinth cell wall structure known from transfer cells was seen in flange-like parenchyma. However, in one haustorium of *Odontites vernus*, some cells with more elaborate thickenings intermediate between a flange and a transfer labyrinth wall were found (Fig. 5.9C). In some extreme cases, the thickenings filled almost the entire parenchyma cell (Fig. 5.9D). The thickened parts of the walls between xylem thickenings were in direct contact with vessel lumina.

The staining of the thickened wall was usually light pink or lilac and often washed out quicker than from other cell walls. This colour of staining suggests the presence of carbohydrates, but not lignin. Occasionally thin “veins” of dark purple staining, characteristic of pectins, were seen within the pale-stained bulk of the wall with relevant examples shown in section 5.3.2.2. The thickenings were not autofluorescent or birefringent, further suggesting lack of lignin (data not shown). However, differentiation of these cells into xylem was seen in several samples, in which case lignified thickenings had developed (Fig. 5.9 D, F and G).

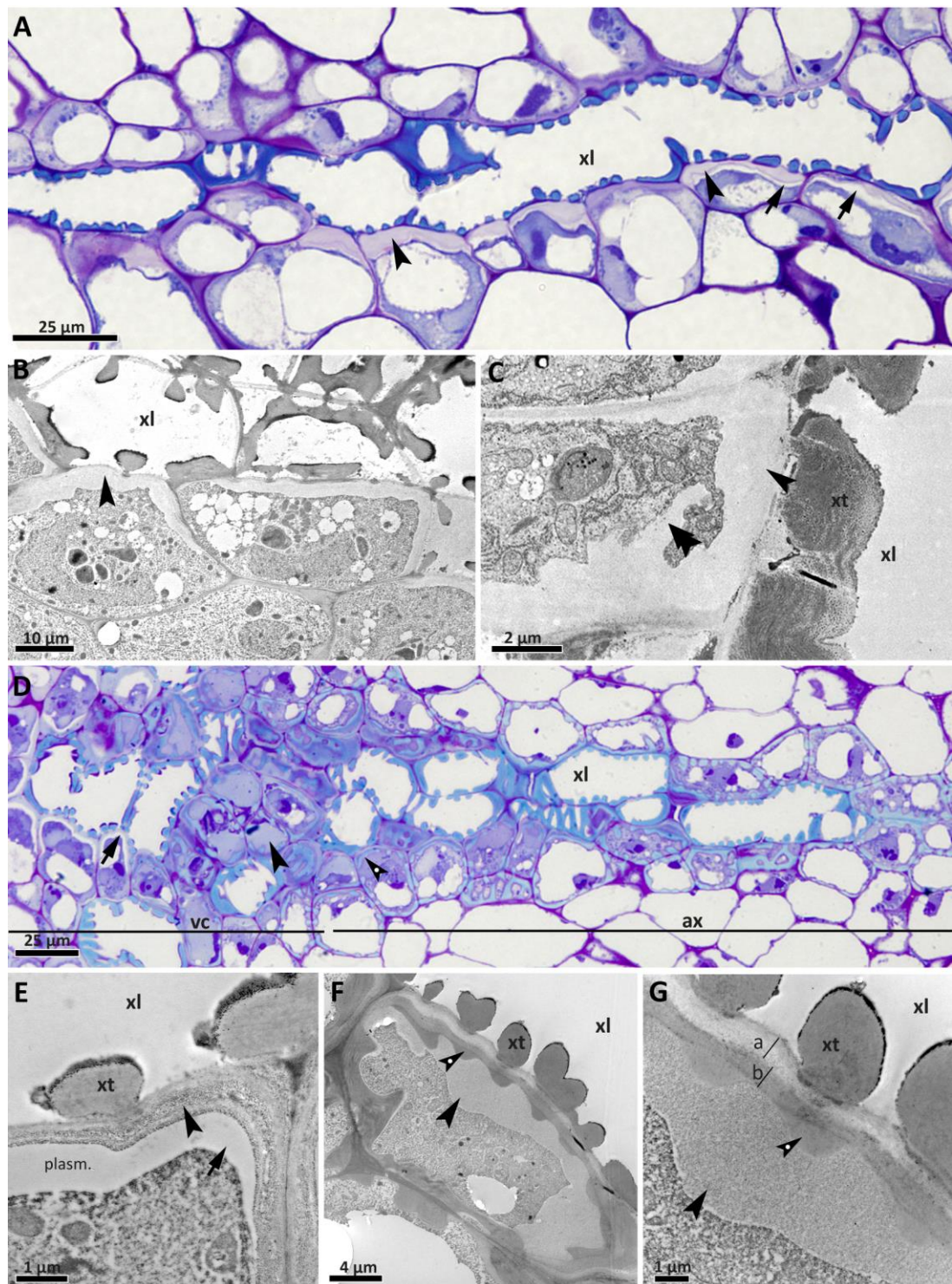


Figure 5.9: Flange-like parenchyma in haustoria of *Rhinanthus minor* (A, D–G) and *Odontites vernus* (B, C). Relatively uniformly thickened walls (◄) are typically seen in contact with xylem bridge cells, directly facing xylem lumina (xl) between xylem thickenings (xt). In some instances, the thickenings fill the entire volume of the cells (D—arrowhead). More complicated, transfer cell-like wall outgrowths (◄◄) are rarely present. Flange-like thickenings typically stain light purple (A), indicating that they are partly composed of pectins and are not lignified. In several association with the vascular core (vc) and axial strand (ax). An unstained layer (◄) at the inner face of the cell walls in some flange-like cells is a gap resulting from Plasmolysis (plasm.). This was only seen where the thickening was relatively narrow (E). The most elaborate thickenings found (F and G) possessed an unligified innermost layer characterised by grainy texture (◄), lignified thickenings (◄◄) embedded within it, and two narrower layers — a more electron lucent layer (a) in direct contact with the xylem and a more electron-opaque layer (b) in contact with all three remaining layers.

5.3.2 Immunolocalisation results

5.3.2.1 Hemicelluloses

Antibodies LM15, LM25 and CCRC-M1 against xyloglucan epitopes produced surprisingly little labelling for a eudicot organ. The stained sections rarely exhibited more than a faint immunofluorescence signal. In all cases, CCRC-M1 did not bind to any cell walls at light microscopy level (data not shown). Detection with LM15 produced no or little immunofluorescence in most tested samples. Pectinase pre-treatment aiming to remove pectins that might have been obscuring xyloglucan epitopes did not alter the labelling (data not shown).

Figure 5.10B (and the corresponding reference image 5.10A) show the most ubiquitous distribution detected throughout this study, with strongest LM15 binding in the epidermis, including the interfacial parenchyma, somewhat weaker binding in the hyaline body and least pronounced immunodetection in the cortex. In contrast with this sample, the hyaline body typically labelled most intensely and most frequently. The signal was distributed in two different ways; in the cellulosic cell walls, where it was concentrated in the struts of cell junctions and in paramural deposits (Fig. 5.10C and D). Labelling of endophyte parenchyma (Fig. 5.10E and F) and flange-like parenchyma (Fig. 5.10G and H) was seen least frequently of all labelled tissues. LM25 labelling overlapped with that of LM15 binding but often produced a stronger signal (data not shown).

Xyloglucan labelling was absent from lignified xylem thickenings in which LM10 and LM11-labelled xylans were the only hemicelluloses detected (Fig. 5.11). Binding was observed in all samples examined and no other cell wall type within haustoria labelled. The labelling of thickenings was confined to those parts that stained light blue with toluidine blue O and was absent from middle lamellae as well as purple-stained bands often seen on the lumen-facing side of xylem thickenings within the vascular core.

MAbs directed against mannans, LM21 and LM22, labelled only 2 samples, localising mainly to the hyaline body and outer cortex and producing an extremely weak signal (data not shown).

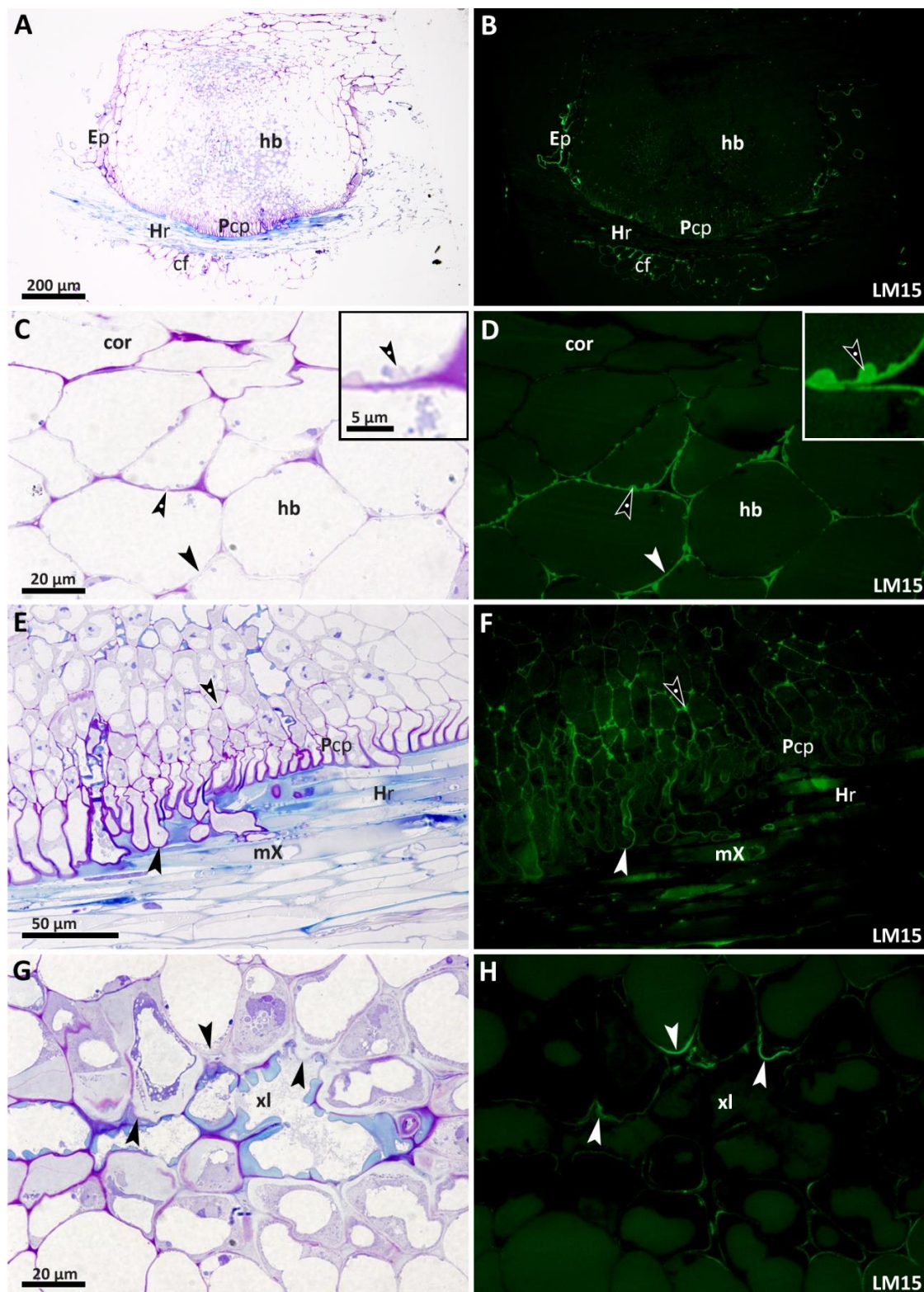


Figure 5.10: LM15 labelling of xyloglucan in haustoria of *Rhinanthus minor* attached to *Arrhenatherum elatius* var. *bulbosum*. Figures A and B illustrate a sample with the most widespread xyloglucan labelling found in this study. Immunofluorescence is seen in the walls of haustorial epidermis (Ep.), contact parenchyma (Pcp), hyaline body (hb) and claspings folds (cf). Within the hyaline body (images C and D), labelling is found in the cell walls (◄) and paramural deposits (◄), which are also found near the interface (E and F). Some labelling in the occluded cells of the host root (Hr), for example in the metaxylem cell (mX) is also seen. In the flange-like thickenings, labelling appears to be confined to the outermost wall layers, including the instances where the thickened wall has grown into the xylem lumen (G and H).

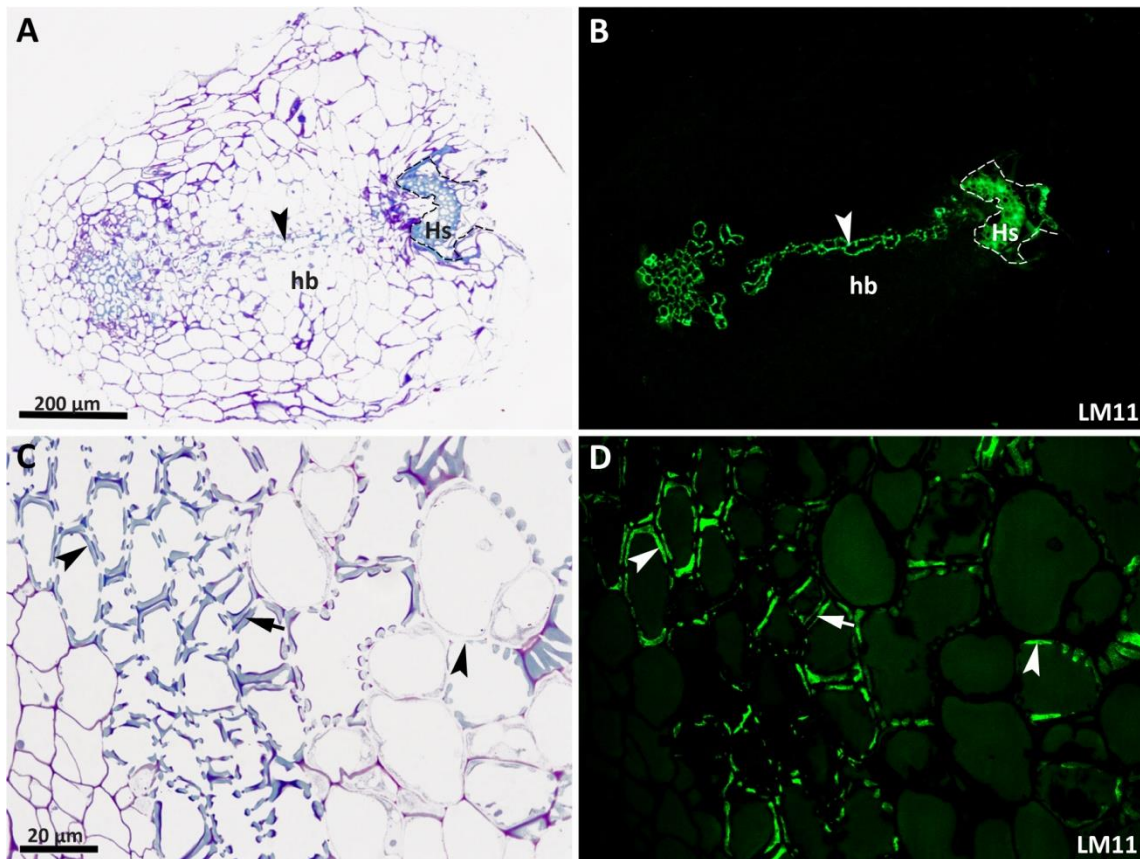


Figure 5.11: LM11 labelling of xylans in haustorial xylem bridge and in the root of host *Arrhenatherum elatius* var. *bulbosum*. **A)** Within the haustorium, LM11 labelled only xylem. Binding within the host root (interface indicated with a dashed line) is particularly strong within the stele (**Hs**). **B)** High magnification light micrograph shows that only the lignified thickenings label (◄), whereas the antibody does not bind to the middle lamellae (◄◄).

5.3.2.2 Pectins

Homogalacturonans

A difference in labelling was observed between probes directed against esterified and de-esterified homogalacturonans. Labelling with antibodies JIM7 and LM20 showed that esterified homogalacturonans were the most ubiquitous pectic polymers detected in the haustoria of *Rhinanthus minor* and *Odontites vernus*. Fluorescence was strong in parenchyma cell walls of the cortex, hyaline body, clasping folds and the endophyte. Strong labelling was observed at all developmental stages examined (Fig. 5.12). Labelling produced by JIM5, an antibody directed against chiefly de-esterified homogalacturonan, differed in that it was absent from, or considerably weaker in, the hyaline body cell walls (Fig. 5.13). Out of 30 mature haustoria labelled with JIM5, 25 showed no or only very weak labelling in the hyaline body contrasting with strong labelling of the adjacent cortex. In 2 remaining haustoria, one of which was still very protoplasmic, the hyaline body labelled stronger than the surrounding tissue

but this labelling was relatively weak when compared with labelling of the cortex in other samples (data not shown). Labelling remained undetermined in 3 haustoria where mounting artifacts made interpretation impossible. JIM5-detected epitopes were also absent from the hyaline body region before xylem bridge development, suggesting that absence or unavailability of this epitope in the cell walls of this tissue might be maintained throughout its development. However, LM18 and LM19, which are specific for homogalacturonans with slightly different levels and patterns of de-esterification (Verhertbruggen *et al.*, 2009), did label this region in the sample of the cortex-penetrating haustorium while being absent in the more advanced stage of passage between the endodermal cells. At later stages of development, LM18 and LM19, typically overlapped with the labelling by JIM5 although differences in intensity were often noticeable (data not shown). JIM19, for instance, often showed stronger labelling than JIM5, while displaying the same distribution. Figure 5.14 compares JIM5 and JIM7 labelling of mature haustoria and shows that the elongated, central parenchyma region of *Odontites vernus* haustoria does not label in an analogous fashion to the ovoid hyaline body of *Rhinanthus minor*.

In the hyaline body — cellulosic cell walls, paramural deposits and spherical inclusions within the protoplast labelled with JIM7 and LM20 (Fig. 5.15A–D). Although JIM5 did not label paramural deposits at light microscopy level, it produced appreciable immunogold labelling of these structures (Fig. 5.15E). Additionally, regions of swollen middle lamellae which were occasionally seen in parenchyma layers near the interface, showed dense immunogold labelling with JIM5 (Fig. 5.15 F).

Within the flange-like parenchyma cells, binding was generally weaker when compared to hyaline body cells and present mainly in the unthickened walls. This was particularly true for antibodies against de-esterified homogalacturonans; JIM5, LM18 and LM19, which bound only to unthickened walls, and the darkly purple-stained thin strands within the flange-like thickenings. However, JIM7 (but not LM20) often labelled thick bands within the flange-like thickenings (Fig. 5.15 A and B). Xylem thickenings and the dissolved tips of endophyte cells (Fig. 5.16) did not label with these or any other anti-pectin antibodies.

The LM8 antibody against xylogalacturonan, a type of homogalacturonan substituted with xylose residues (Zandleven *et al.*, 2007), produced no labelling (data not shown).

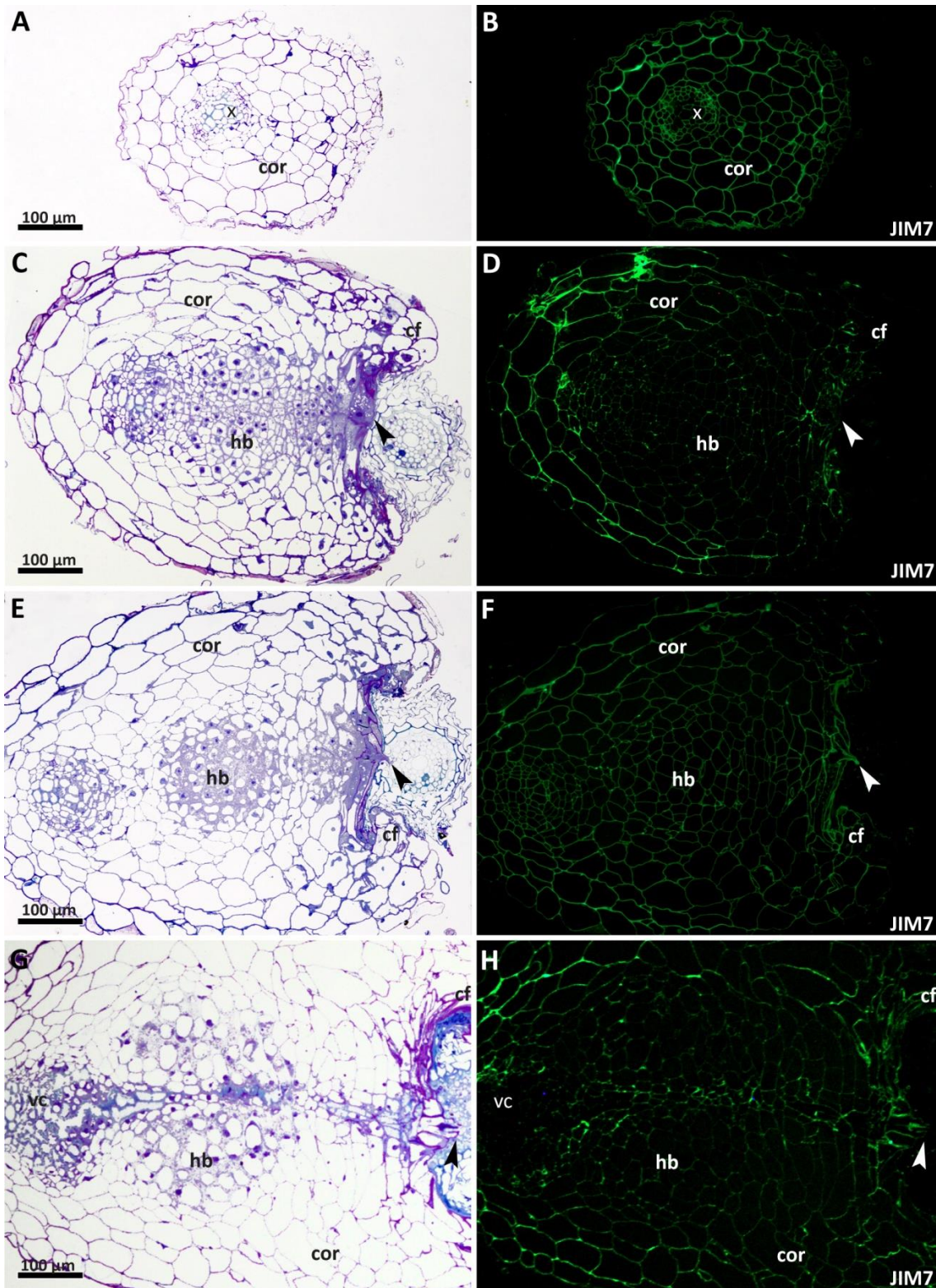


Figure 5.12: JIM7 labelling of esterified homogalacturonans in *Rhinanthus minor* haustoria at different stages of development, attached to host *Arrhenatherum elatius* var. *bulbosum*; prior to attachment (**A and B**), during cortical penetration (**C and D**), endodermal and early stele penetration (**E and F**) and xylem bridge maturation (**G and H**). Labelling is present in all parenchymateous haustorial tissues at all four developmental stages. No binding to the vascular core (**vc**) xylem is seen. **hb** — hyaline body; **cor** — cortex; **cf** — clasp fold

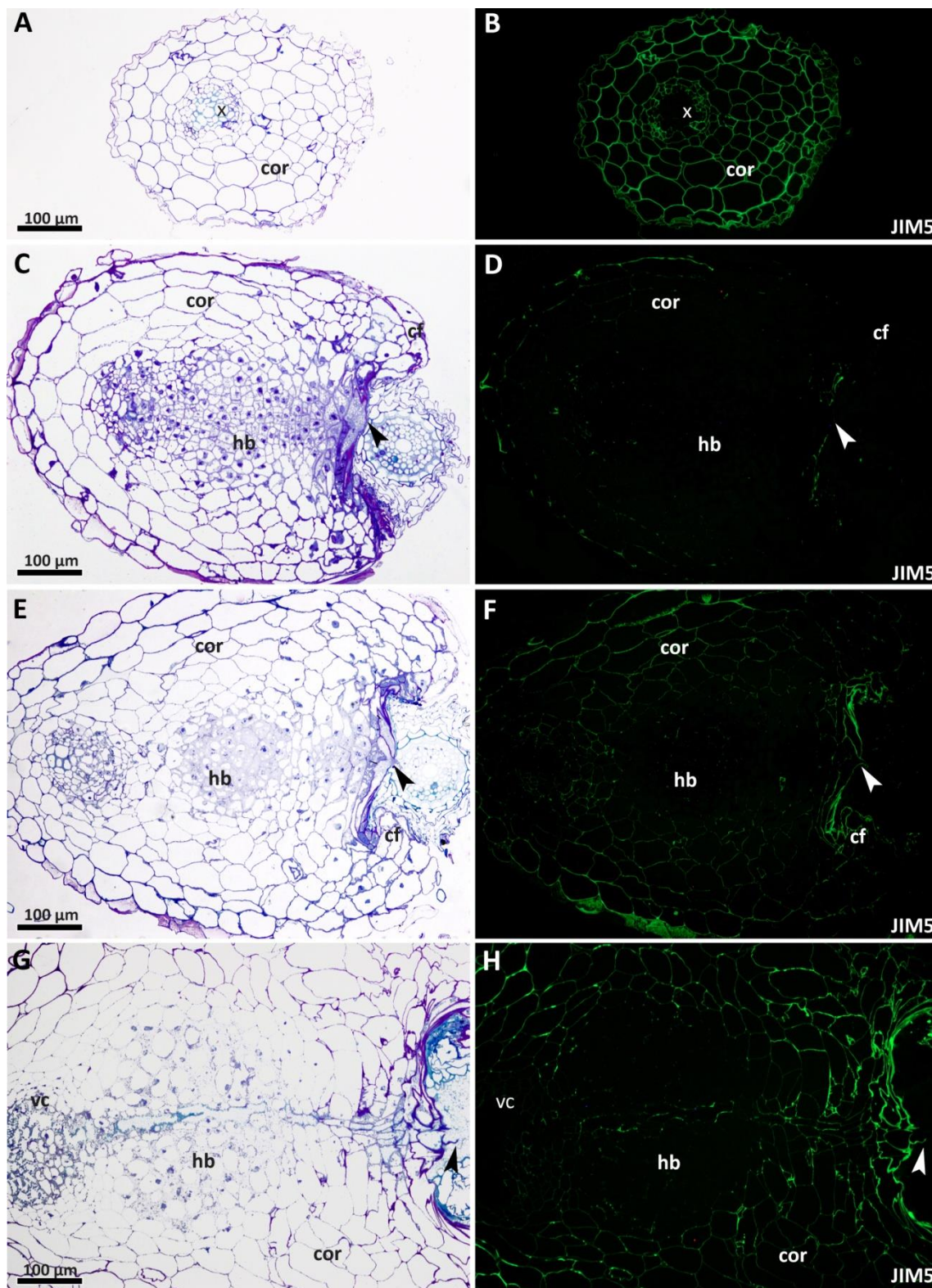


Figure 5.13: JIM5 labelling of de-esterified homogalacturonans in *Rhinanthus minor* haustoria at different stages of development, attached to host *Arrhenatherum elatius* var. *bulbosum*; prior to attachment (**A and B**), during cortical penetration (**C and D**), endodermal and early stele penetration (**E and F**) and xylem bridge maturation (**C and H**). Distribution of labelling differs from that with JIM7 mainly in the hyaline body (**hb**) region (**G and H**) and in its cell initials at early stages of differentiation (**C–F**), which show considerably lower intensity of JIM5-related immunofluorescence than the surrounding parenchyma. **hb** — hyaline body; **cor** — cortex; **cf** — clasp fold

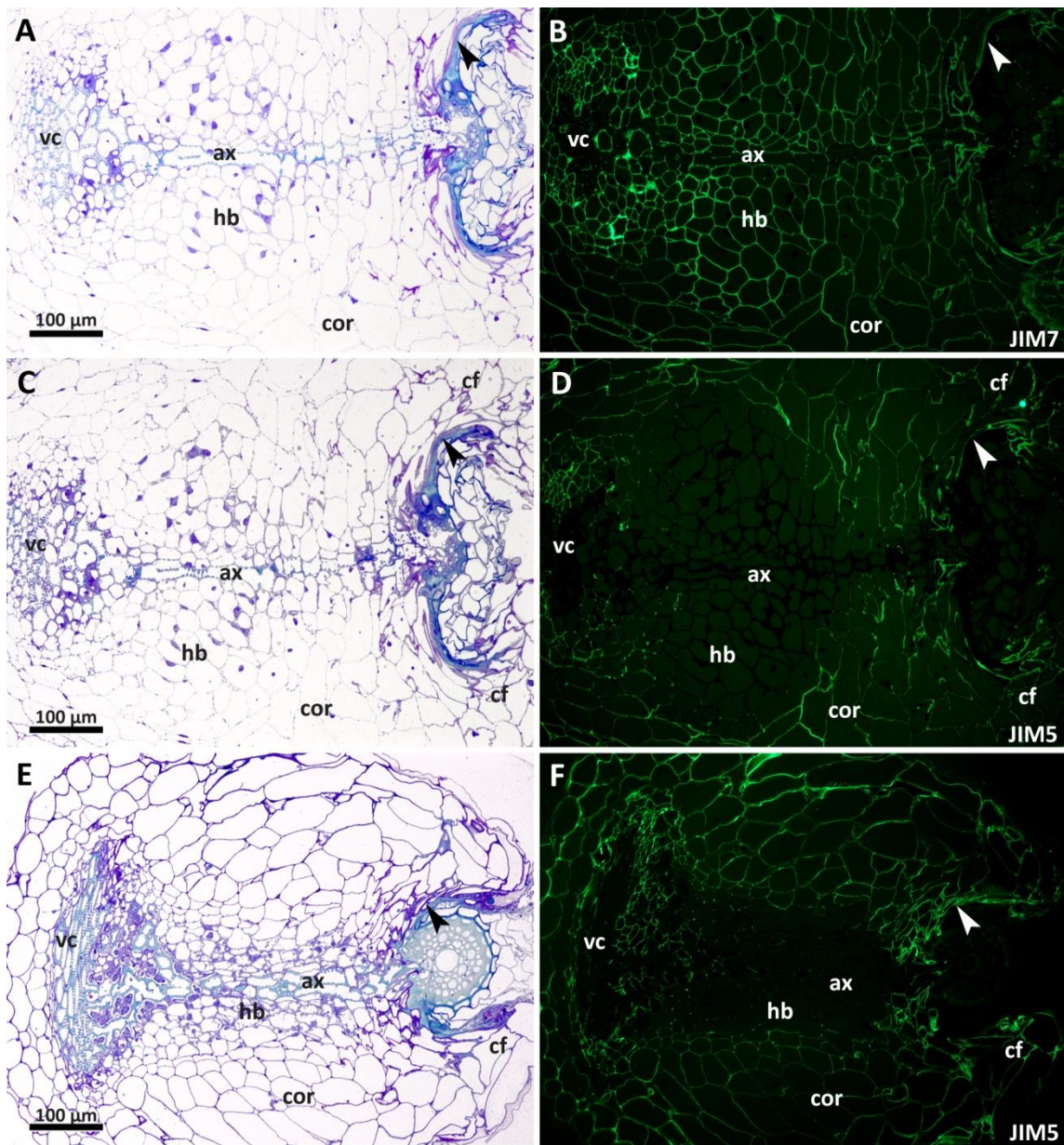


Figure 5.14: JIM5 and JIM7 labelling of homogalacturonans in *Rhinanthus minor* and *Odontites vernus* haustoria attached to host *Arrhenatherum elatius* var. *bulbosum*. Lack of de-esterified pectin immunodetection with JIM5 mAb (**C and D**) in the hyaline body contrasted with the presence of JIM7-recognised esterified pectins (**A and B**) continues during haustorial maturity (i.e. after full differentiation of the xylem bridge). The narrow, hyaline body of *Odontites vernus* does not label with JIM5, either (**E and F**). **ax** — axial strand of the xylem bridge; **cf** — claspings fold; **cor** — cortex; **hb** — hyaline body, **vc** — vascular core

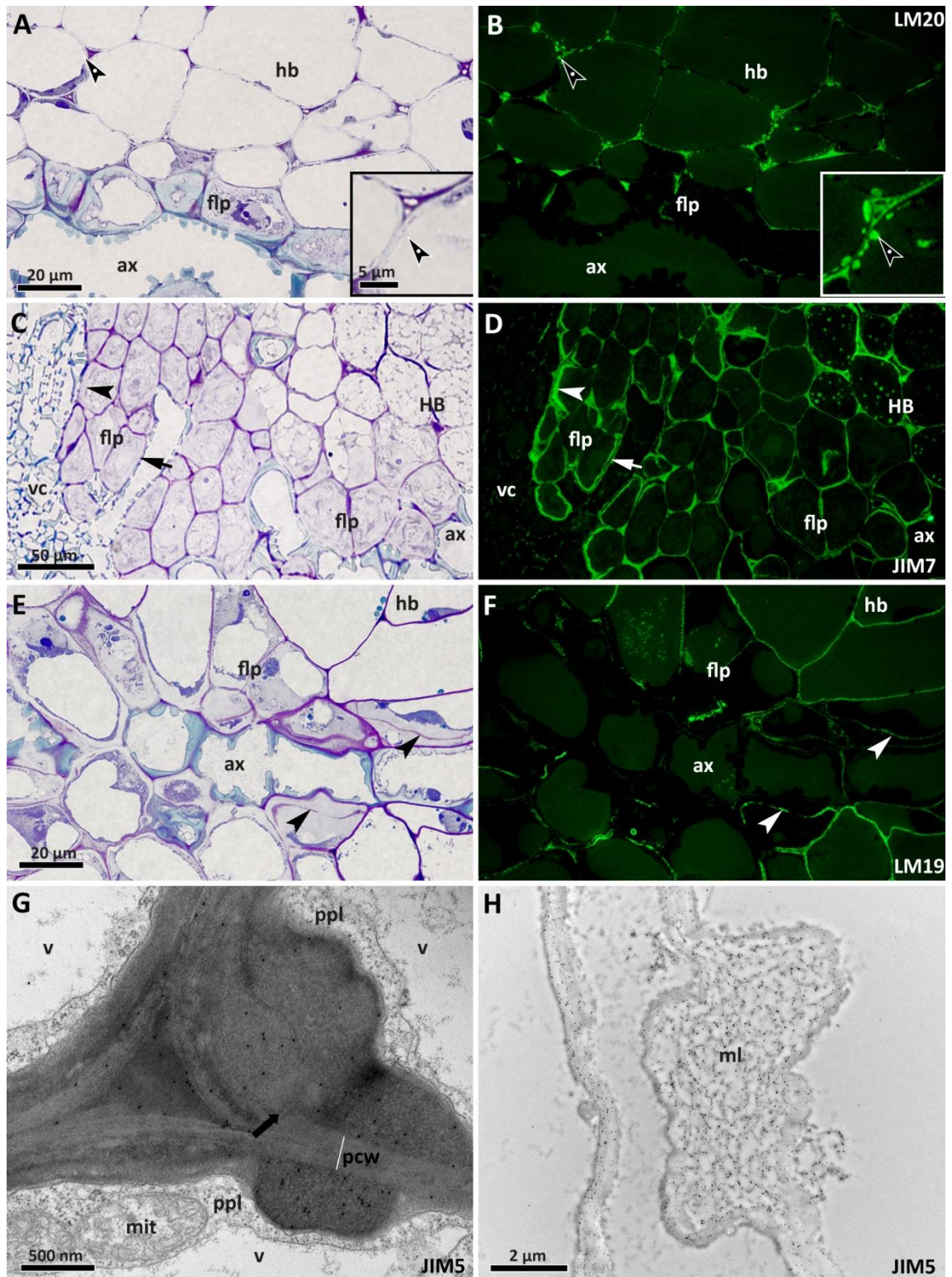


Figure 5.15: Detail of labelling of haustorial cell walls with mAbs against esterified (LM20 and JIM7) and de-esterified (LM19) homogalacturonans in *R. minor* (A, B, E–H) and *O. vernus* (C and D). **A and B)** hyaline body (HB) cell wall (◄) and paramural deposit (◄◄) labelling with LM20 antibody is contrasted with the lack of labelling in the xylem of the axial strand (ax) and restriction of labelling to intercellular spaces of flange-like parenchyma (flp). **C and D)** Labelling with JIM7 is present in most parenchyma cell walls, with unlabelled bands (◄◄) present between labelled cell walls. Flange-like thickenings often label across their entire thickness (◄◄). The antibody also binds to the hyaline body (hb) protoplasts in a speckled pattern. Labelling in the vascular core (vc) is restricted to primary walls between thickenings. **E and F)** In flange-like parenchyma (flp), LM19 labelling is absent from the thickenings, except in thin, purple-stained strands (◄◄). **G)** Immunogold labelling of an osmicated sample with JIM5 shows presence of de-esterified homogalacturonans in the paramural deposits. It is less abundant in what appears to be

the primary cell wall (**pcw**), which merges with the deposits in places (**←**). A thin layer of ribosome-rich protoplast (**ppl**) with mitochondria (**mit**) is sandwiched between the vacuoles (**v**) and the cell walls. **H**) Swollen middle lamellae (**ml**) occasionally seen near the interface label densely with JIM5 in the more electron-opaque, fibril-shaped areas.

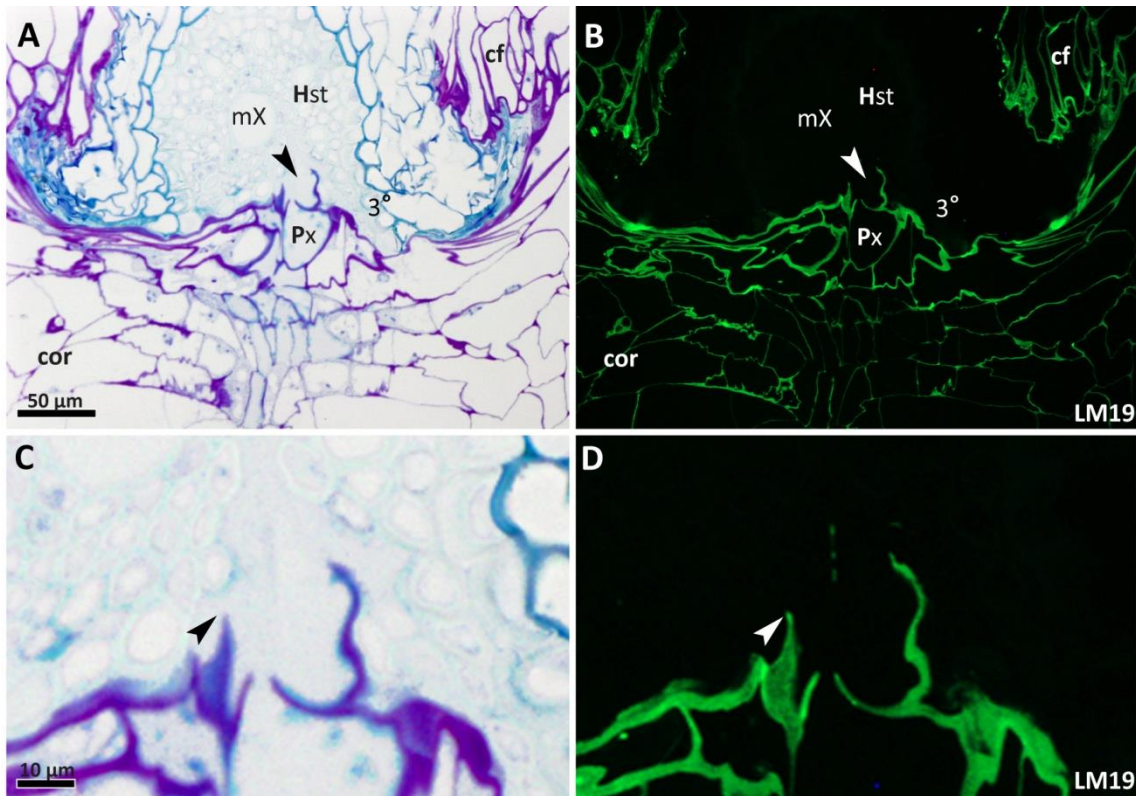


Figure 5.16: LM19 labelling of the interfacial region of *R. minor* haustorium attached to host *Arrhenatherum elatius* var. *bulbosum* from the same haustorium as illustrated in figure 5.4 i.e. during xylem bridge maturation associated with wall dissolution and protoplast disintegration. All parasite cells label, except in the lignified thickenings of the xylem (**Px**) and the dissolved tips of the endophyte cells within the host stele (**Hst**). No binding to the host root is seen.

Rhamnogalacturonan I

Rhamnogalacturonan I backbone labelling with mAbs RU-I and RU-II showed that this polymer was consistently associated with xylem wall thickenings as well as parenchyma in different regions of the haustorium. The latter displayed a great deal of inter- and intraspecific variation. The two antibodies provided overlapping distribution patterns, with RU-II typically resulting in stronger signal. Therefore RU-II labelling only is presented. Overall, rhamnogalacturonan backbone epitopes in haustorial parenchymateous tissues were not detected as consistently as those of homogalacturonan. Therefore the range of distributions included: 1) labelling in the cortex, hyaline body, endophyte parenchyma and xylem thickenings; 2) labelling in the cortex, hyaline body and xylem thickenings only; 3) labelling in the cortex, endophyte parenchyma and xylem thickenings only; 4) labelling in the cortex and xylem thickenings only. These patterns showed no apparent developmental preference.

Figure 5.17 illustrates the most ubiquitous distribution found, i.e. as described in point 1. It exemplifies a typical situation whereby cortex labelling is present mainly in the outer cell layers, except the hypodermis. The intensity is highest in the proximal part of the haustorium and gradually decreases towards the clasping folds as well as towards and around the hyaline body. While labelling within the hyaline bodies was typically concentrated in the struts of the 3-way junctions (Fig. 5.17C and D), the adhering parts of walls labelled more strongly in the outer cortex. In flange parenchyma cells the labelling was typically present in the unthickened walls but was occasionally seen in the flange-like thickenings (5.17E and F).

In contrast with the highly variable labelling of parenchyma, RU-I and II bound very strikingly and consistently to haustorial xylem thickenings, with different distribution patterns in the vascular core and the xylem bridge (Fig. 5.17E–H). In the vascular core, the labelling was detected at both light and electron microscopy level. Immunofluorescent bands within the lumen-facing parts of the thickenings overlapped with purple staining from toluidine blue O. No co-distribution of homogalacturonan was observed (Fig. 5.15A–F). Immunogold labelling revealed that the band was, in fact, formed by two parallel layers of labelling separated by a thin, unlabelled strand of higher electron-lucence than the remaining part of the thickening (Fig. 5.17G). Curiously, the signal did not always decrease after removal of pectin by Pectinex treatment (data not shown). No labelling of xylem thickenings with RU-I or RU-II was detected by immunofluorescence in the axial strand or endophyte xylem (Fig. 5.17E and F). However, immunogold labelling was positive across the entire thickenings, although less abundant than in the labelled bands of the vascular core (Fig. 5.17H), suggesting that detection levels might have been too low to result in immunofluorescence.

The LM6 antibody which recognises arabinan side chains of RG-I, but also of AGPs (Willats *et al.*, 1998), labelled the hyaline body very weakly while producing strong labelling of the contact parenchyma (Fig. 5.18A and B). Occasional areas of middle lamella swelling near the hyaline body also labelled strongly (Fig. 5.18A and B, inset). No labelling was noted in xylem thickenings.

LM5, which is specific for galactan epitopes of RG-I side chains, labelled the hyaline body strongly but did not label the contact parenchyma (Fig. 5.18C and D). Furthermore, it bound to xylem thickenings, within the axial strand (Fig. 5.18E and F), vascular core and original parasite root xylem (Fig. 5.18G and H). Interestingly, it was often absent from the bands darkly-stained with toluidine blue O, which typically labelled with RU-II (Fig. 5.18G and H, inset). Outer layers of flange-like thickenings also labelled (Fig. 5.18G and H, inset).

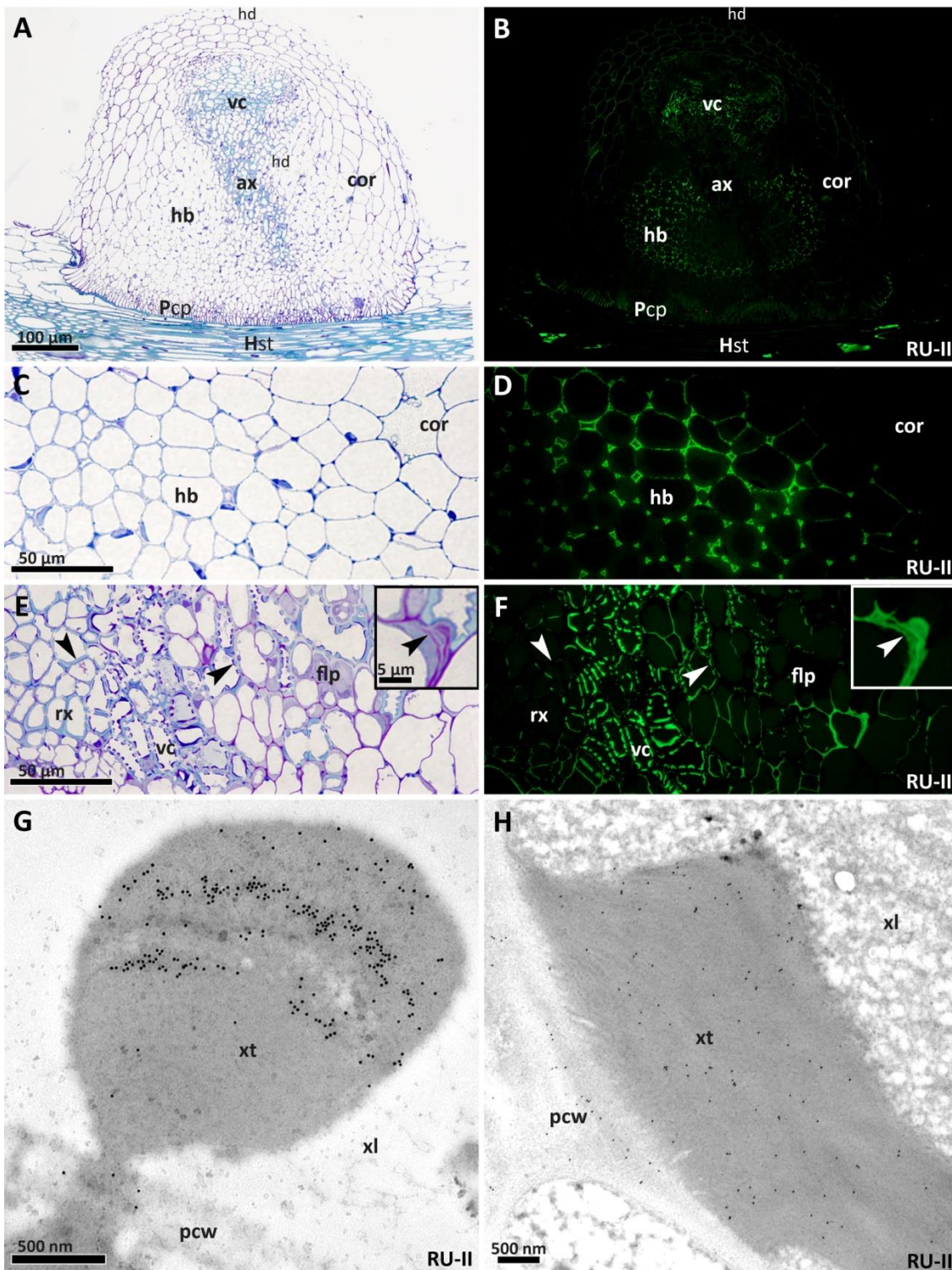


Figure 5.17: Labelling of *Rhinanthus minor* haustoria attached to host *Arrhenatherum elatius* var. *bulbosum*, with RU-II mAb against the backbone of rhamnogalacturonan-I. **A and B)** In the most widely labelled samples, immunofluorescence was detected in the vascular core (vc) parenchyma, proximal part (away from the interface) of the cortex (cor), with the exception of the hypodermis (hd); hyaline body (hb), and, to a lesser extent, parasite contact parenchyma (Pcp). Several cell lumina within the host stele (Hst) also labeled. **C and D)** Detail of hyaline body labelling from sample shown in images A and B. Labelling is the strongest at the three-way junctions of the hyaline body cells while being absent from the adjacent part of the cortex. **E and F)** labelling of xylem thickenings and flange-like parenchyma within the vascular core. Binding is much stronger in the thickenings within the vascular core than in the adjacent root xylem (rx). This labelling overlaps with purple staining, indicating that this region is not lignified. Flange-like thickening shows radial heterogeneity in labelling, with immunofluorescence present in the outer half of the wall thickness, including part of the thickening penetrating xylem of the upper axial

strand (inset). Immunogold labelling of xylem thickenings shows clear radial heterogeneity within the vascular core (G) with distribution of the label across the entire thickening within the axial strand (ax) of the xylem bridge (image H). xl — xylem lumen

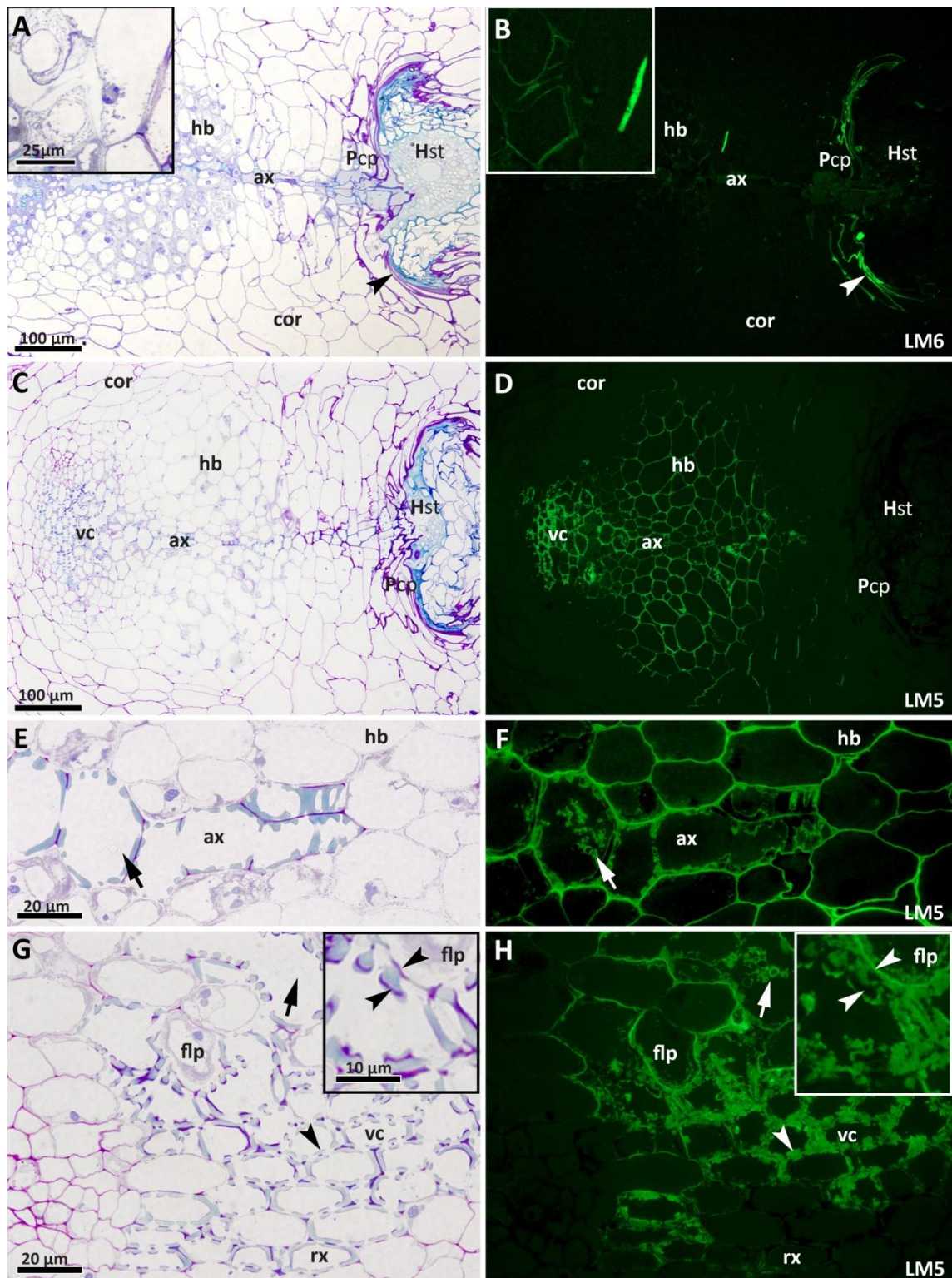


Figure 5.18: Labelling of *Rhinanthus minor* haustoria attached to host *Arrhenatherum elatius* var. *bulbosum* with antibodies LM5 and LM6 against galactan and arabinan side chains of RG-I, respectively. **A and B)** LM6 binds abundantly to the contact parenchyma of the parasite (**Pcp**), while only weakly labelling the hyaline body cells. Strong immunofluorescence was also seen in an area of cell wall swelling shown in the inset image. **C and D)** Galactan side chains are not detected at the interface but appear to

Chapter 5

be abundant within the hyaline body (**hb**), axial strand (**ax**) and vascular core (**vc**). **E and F**) In contrast with RU-II, LM5 often localises to the entire thickness of the lignified walls in the axial strand at light microscopy level. **G and H**) Within the vascular core, binding is seen in the xylem and flange like parenchyma (**flp**). Immunofluorescence is often absent from the darkly stained bands (inset) which label with RU-II, as shown in figure 5.17 E and F. Labelling is also concentrated around starch grains (◀, unstained with toluidine blue) in xylem lumina.

5.3.2.3 AGPs

Nine anti-AGP probes were used in this study: LM2, JIM4, JIM8, JIM13–16, CCRC-M7 and MAC207 (see: table 3.5). JIM15 and JIM16 resulted in no epitope recognition in any parts of the haustoria. MAC207 labelled very weakly the hyaline bodies and interfacial parenchyma of only two haustoria (data not shown). JIM4 produced barely detectable labelling in only one sample (data not shown). The LM2-recognised epitope of β -linked glucuronic acid (GlcA) was most consistently present and produced the strongest labelling. Antibodies JIM8, JIM13, JIM14, and CCRC-M7 produced more variable results, i.e. labelling was sometimes absent or weaker, although generally these probes labelled the same tissues as LM2. Overall, various combinations of between 2 and 5 anti-AGP antibodies produced overlapping signal within different haustoria.

Enrichment with a diversity of arabinogalactan protein epitopes was very apparent in three distinct regions of the haustorium: the hyaline body, the interfacial parenchyma and the differentiating xylem bridge. All three features are illustrated in image h of figure 5.19, which depicts AGP labelling at key developmental stages. Figure 5.20 shows sections taken from the same mature haustorium as that shown in figure 5.14, and labelled with three different anti-AGP mAbs.

The labelling of the hyaline body and interfacial parenchyma was observed in a vast majority (39 out of 40) of examined, normally developed haustoria of *Rhinanthus minor* attached to grasses and legumes (see chapter 6 for host-dependent variation). Lack of AGP labelling in the interfacial parenchyma of *Odontites vernus* was more frequent (3 out of 7 haustoria) and was not related to developmental stage or host species.

The walls of contact parenchyma were enriched from pre-contact stages (Fig 5.19A and B) until transition into xylem (Fig 5.19G and H), although binding was considerably weaker prior to attachment. The labelling often extended into the extramural interfacial deposits. This is illustrated and discussed in chapters 6 and 7. The distal cell cluster behind the interfacial parenchyma also labelled (Fig. 5.19C–F).

AGPs in the hyaline bodies appeared developmentally later than in the contact parenchyma, but labelled stronger, more consistently (including all examined haustoria of *Odontites vernus*) and with a greater number of anti-AGP probes. The high concentration of AGPs in this tissue was observed after penetration of the cortex had

occurred (Fig 5.19E and F) and separation of endodermal cells had begun. At that stage of development protoplasts and intercellular spaces labelled strongly (Fig. 5.21C and D), which was in contrast with the tightly adhering cells in this region at earlier developmental stages that did not label (Fig. 5.21A and B).

Labelling of cytoplasm and structures within it was not restricted to early stage hyaline bodies. Globular inclusions and, to a lesser extent, paramural bodies often labelled (Fig. 5.21E and F). Labelling of cell content was extremely pronounced in some haustoria of *Odontites vernus*, in which hyaline body cells were filled with grainy storage materials (Fig. 5.22). Nuclear labelling was also occasionally seen although it might have been non-specific as it was found across the entire thickness of the nuclei rather than being confined to the outer envelope or ER, where the presence of AGP epitopes would be more plausible.

At the cell wall level, AGPs were detected across the entire extent of the wall (Fig. 5.23). Although immunofluorescence results suggested that JIM8-recognised epitopes in the hyaline body and interfacial parenchyma might have been in several cases associated with the plasma membrane (data not shown), concentration near the plasmalemma was never observed after immunogold labelling, even in osmicated samples which granted better membrane preservation.

While no radial heterogeneity was observed, a polar type of cellular heterogeneity was observed within the outermost cell layer of the hyaline body (Fig. 5.24). The walls facing the centre of the hyaline body labelled in the same way as the walls of adjacent cells, while the signal gradually faded within the radial walls and eventually disappeared in the outer walls (Fig. 5.24A and B). Curiously, this cellular heterogeneity was also shown for de-esterified pectin epitopes although in an opposite direction, i.e. AGP labelling increased as that of de-esterified pectin decreased (Fig. 5.24C and D). Pectinase treatment did not alter AGP labelling, i.e. it was not increased in the cortex after pectin removal (data not shown).

In most cases, flange-like parenchyma did not label for AGPs (Fig. 5.22C and D). When labelling was observed, it was absent from the thickenings (Fig. 5.24B).

Within partly-differentiated xylem, LM2, JIM8 and, to a lesser extent, JIM4 bound to the disintegrated protoplasts but not the secondary lignified thickenings. Intensity differed slightly between probes and different parts of the xylem bridge (data not shown). The protoplast was often present in two distinctive forms: denser, more intensely labelled material of cell peripheries and a looser and more weakly labelled inner region. This is illustrated in image F of figure 5.25 which also depicts similar labelling with anti-extensin probe LM1. Immunogold labelling resulted in binding to some lignified thickenings (data not shown), suggesting that they are present in amounts below immunofluorescence detection level (Fig. 5.25H).

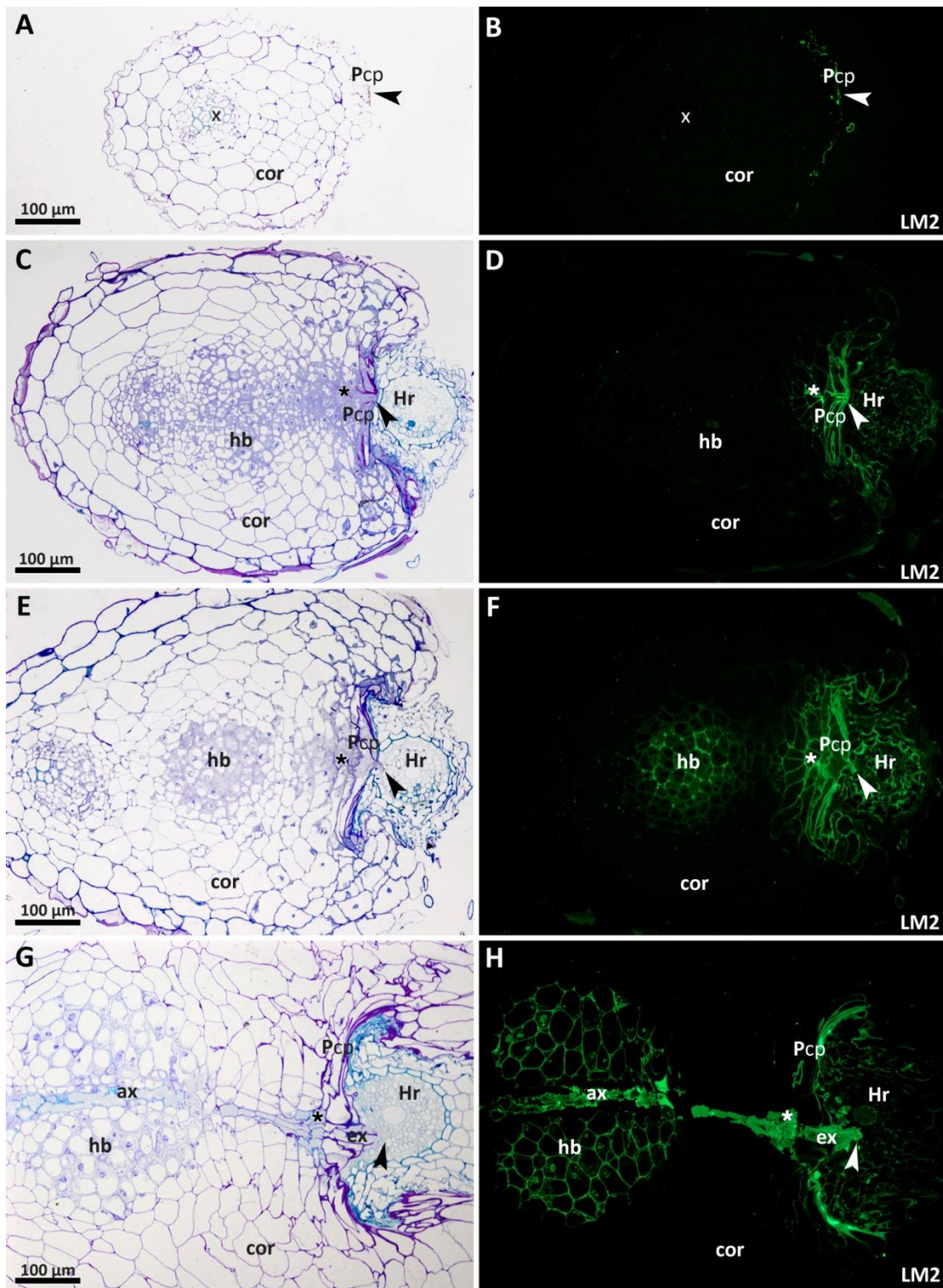


Figure 5.19: LM2 labelling of beta-linked glucuronic acid epitopes of AGPs in *Rhinanthus minor* haustoria at different stages of development: attached to host *Arrhenatherum elatius* var. *bulbosum*; prior to attachment (**A and B**), during cortical penetration (**C and D**), endodermal and early stele penetration (**E and F**) and xylem bridge maturation (**G and H**). **A and B**) The earliest appearance of AGPs was observed in the contact parenchyma (**Pcp**) of haustorial initials. **C and D**) Cortical penetration was associated with the spread of binding into the distal cluster of cells (*****) behind the interface. No labelling was seen in the young hyaline body (**hb**). **E and F**) LM2 binding appeared in the hyaline body during early penetration of the stele. **G and H**) In haustoria with maturing xylem bridges, labelling was

additionally seen in the disintegrating protoplasts of the axial strand (**ax**) and endophyte xylem (**ex**). Xylem derivatives of the distal cell cluster (*****) also labelled. Extensive binding to the host root seen in these samples was not present in all haustorial connections examined.

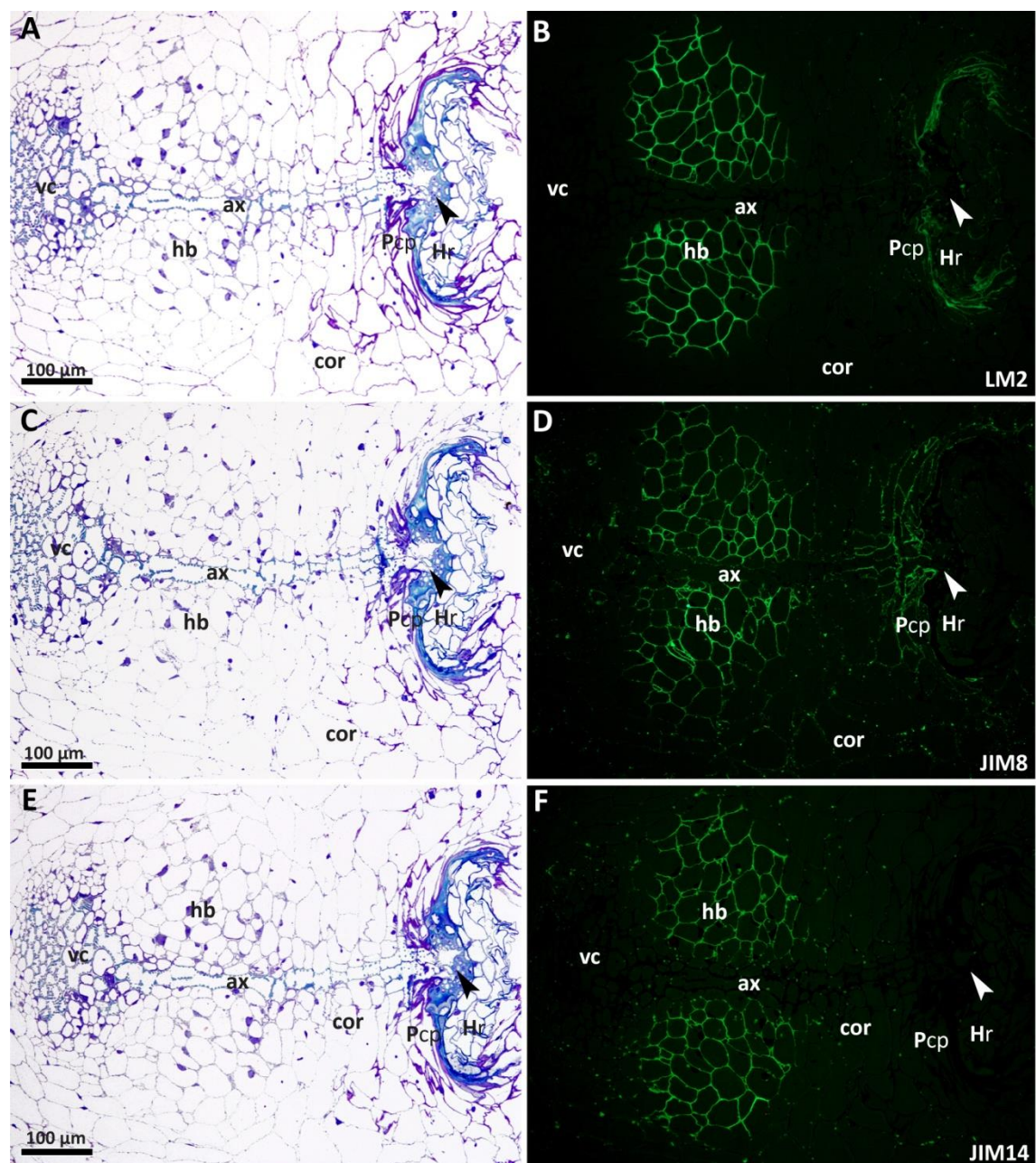


Figure 5.20: Labelling of AGPs in sections from the same *Rhinanthus minor* haustorium attached to *Arrhenatherum elatius* var. *bulbosum* as in figures 5.14A–D, i.e. a mature haustorium with a fully differentiated xylem bridge. **A and B)** LM2 binds to the hyaline body and parasite's contact parenchyma (**Pcp**). Labelling is not present in the xylem bridge. **C and D)** JIM8 labelling shows similar distribution, in addition to binding in the distal cell cluster (*****) and weak binding to the walls within the cortex (**cor**). **E and F)** JIM4 localises to the walls of the hyaline body but not the contact parenchyma. Speckled labelling is also present throughout the cortex.

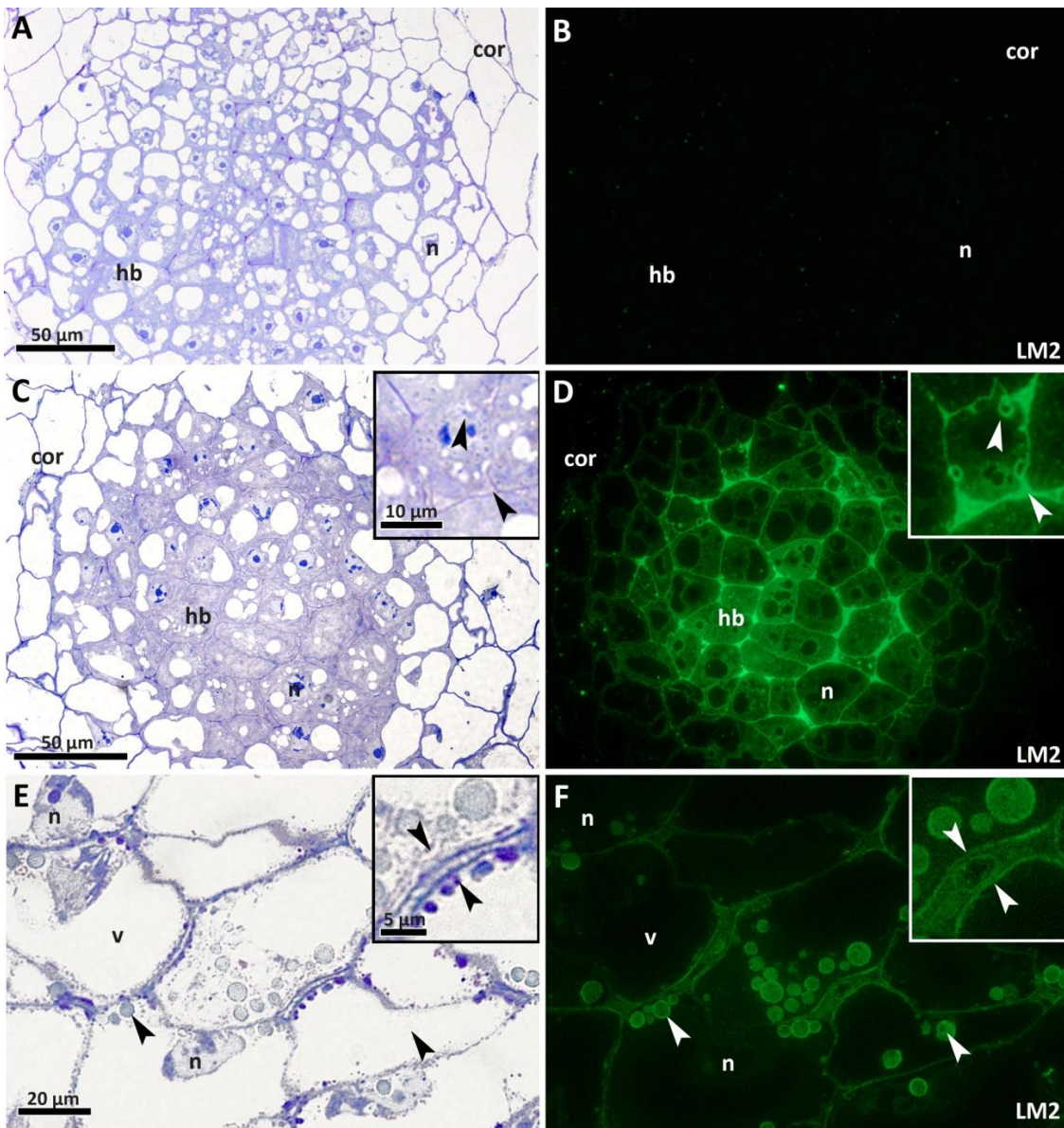


Figure 5.21: Detail of AGP labelling in the hyaline bodies of *Rhinanthus minor* haustoria attached to *Arrhenatherum elatius* var. *bulbosum* (A–D) and *Vicia sepium* (E and F). **A and B)** only extremely weak and speckled labelling is present in a sample collected during cortical penetration. **C and D)** Labelling during early stele penetration is very intense and includes intercellular spaces, cytoplasm and outer surfaces of vesicle-like structures (top arrowhead within the inset). **E and F)** Within a mature hyaline body, cell walls are labelled together with the associated paramural deposits (inset), in addition to globular ergastic inclusions. **v** — vacuole, **n** — nucleus, **hb** — hyaline body

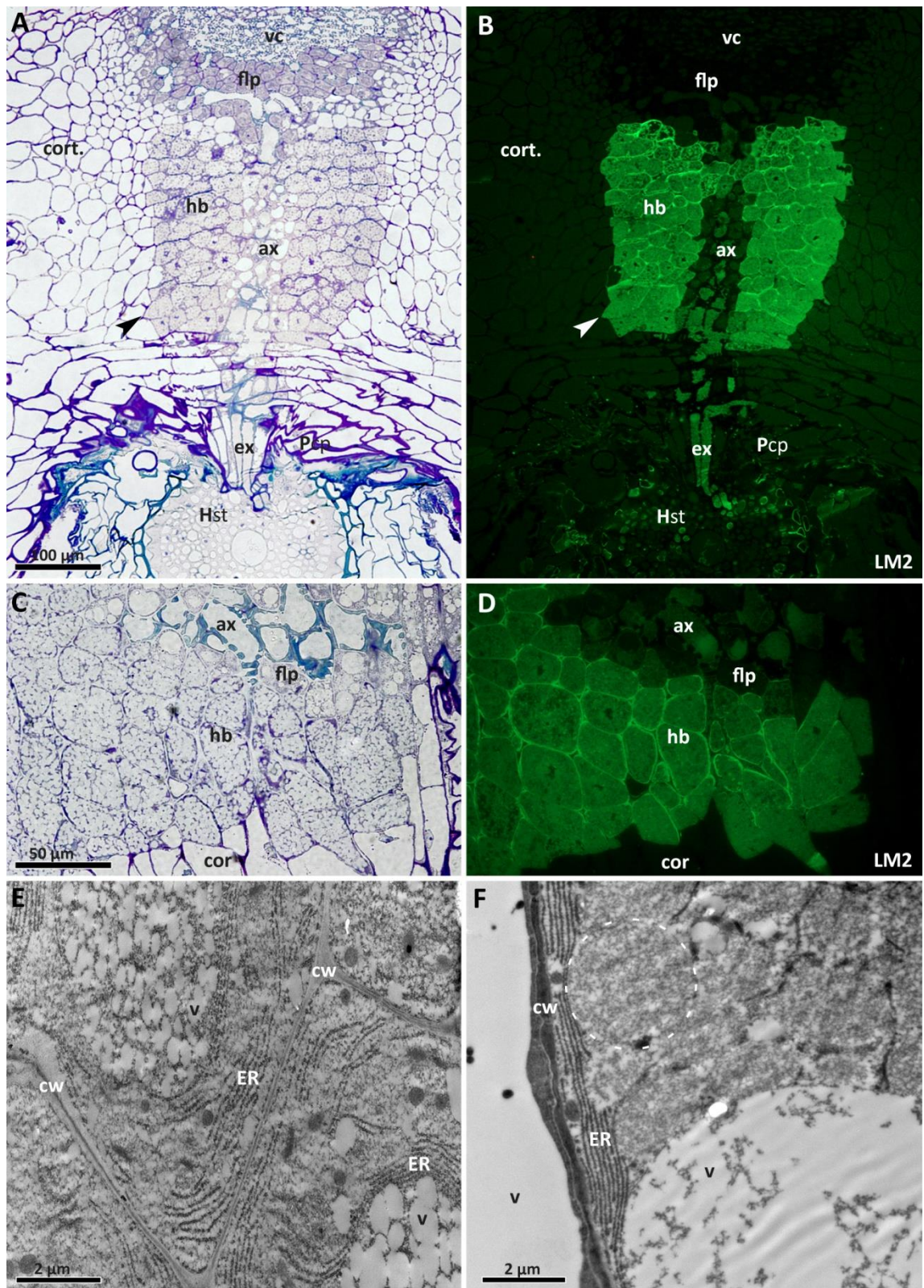


Figure 5.22: Extensive labelling of hyaline body cell contents in *Odontites vernus* haustorium attached to *Arrhenatherum elatius* var. *bulbom*. **A and B)** AGP labelling is weak in contact parenchyma (**Pcp**) in comparison with the extremely intense labelling of the hyaline body (**hb**). Immunofluorescence spans across the cell contents. The boundary between the hyaline body and cortex (**◄**) is very sharp. Labelling is also seen in the partly-differentiated xylem of the axial strand (**ax**) and endophyte xylem (**ex**), but not vascular core (**vc**) or associated flange-like parenchyma (**flp**). **C and D)** Magnified hyaline body region from the same haustorium as in A and B. Cell contents are filled with very lightly stained oval structures. **E)** TEM micrograph of flange-like parenchyma cells from the axial strand region. Abundant endoplasmic reticulum (**ER**) and clusters of small vacuoles (**v**) are present within

Chapter 5

the protoplast, which appears grainy. **F)** TEM micrograph of a hyaline body cell at the boundary with a cortex cell (to the left of the cell wall — **cw**). Dashed line delineates one of the numerous oval bodies filled with grainy material.

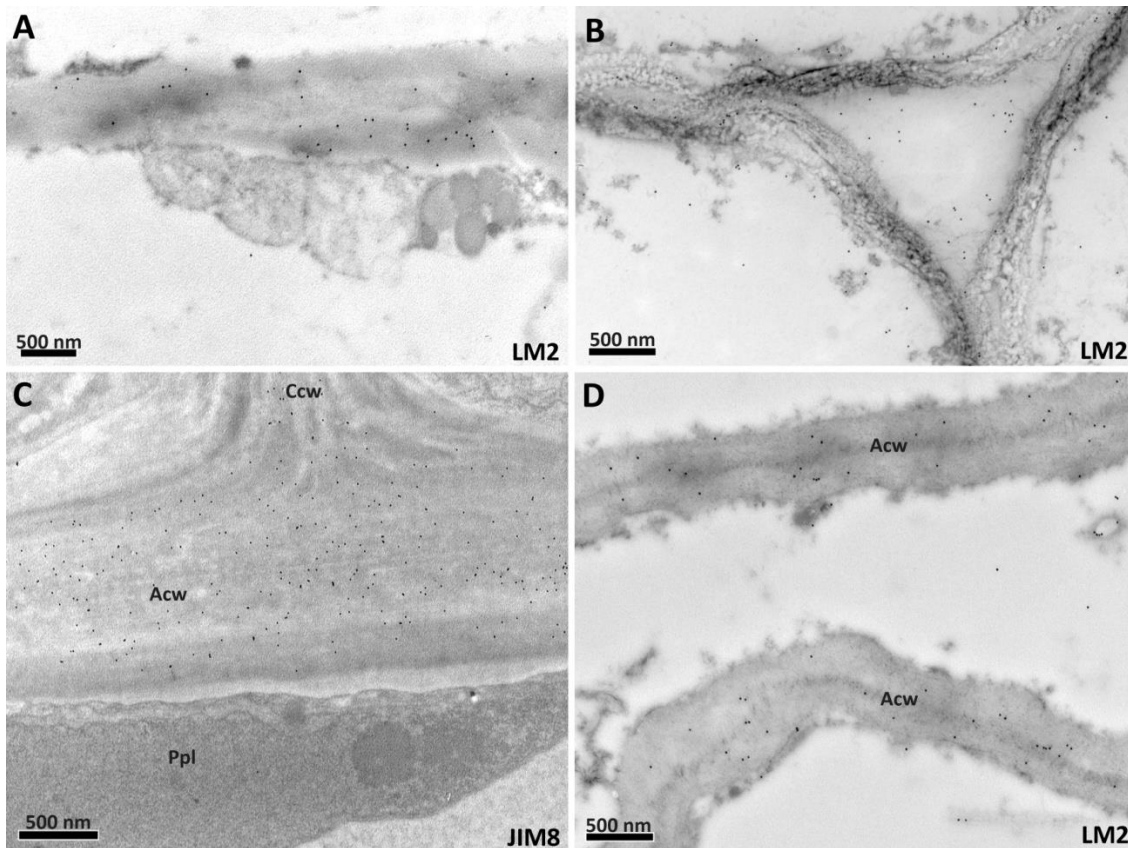


Figure 5.23: Distribution of AGPs across the entire extent of *Rhinanthus minor* cell walls and not at the plasma membrane. LM2 immunogold label is present within the walls (**A**) and intercellular spaces (**B**) of the hyaline body, and in anticlinal cell walls (**Acw**) of parasite's interfacial parenchyma (**D**). JIM8 also labels anticlinal, and cross cell walls (**Ccw**) within contact parenchyma, while the protoplast does not label (**C**). Samples shown in images A, B and D were not osmicated.

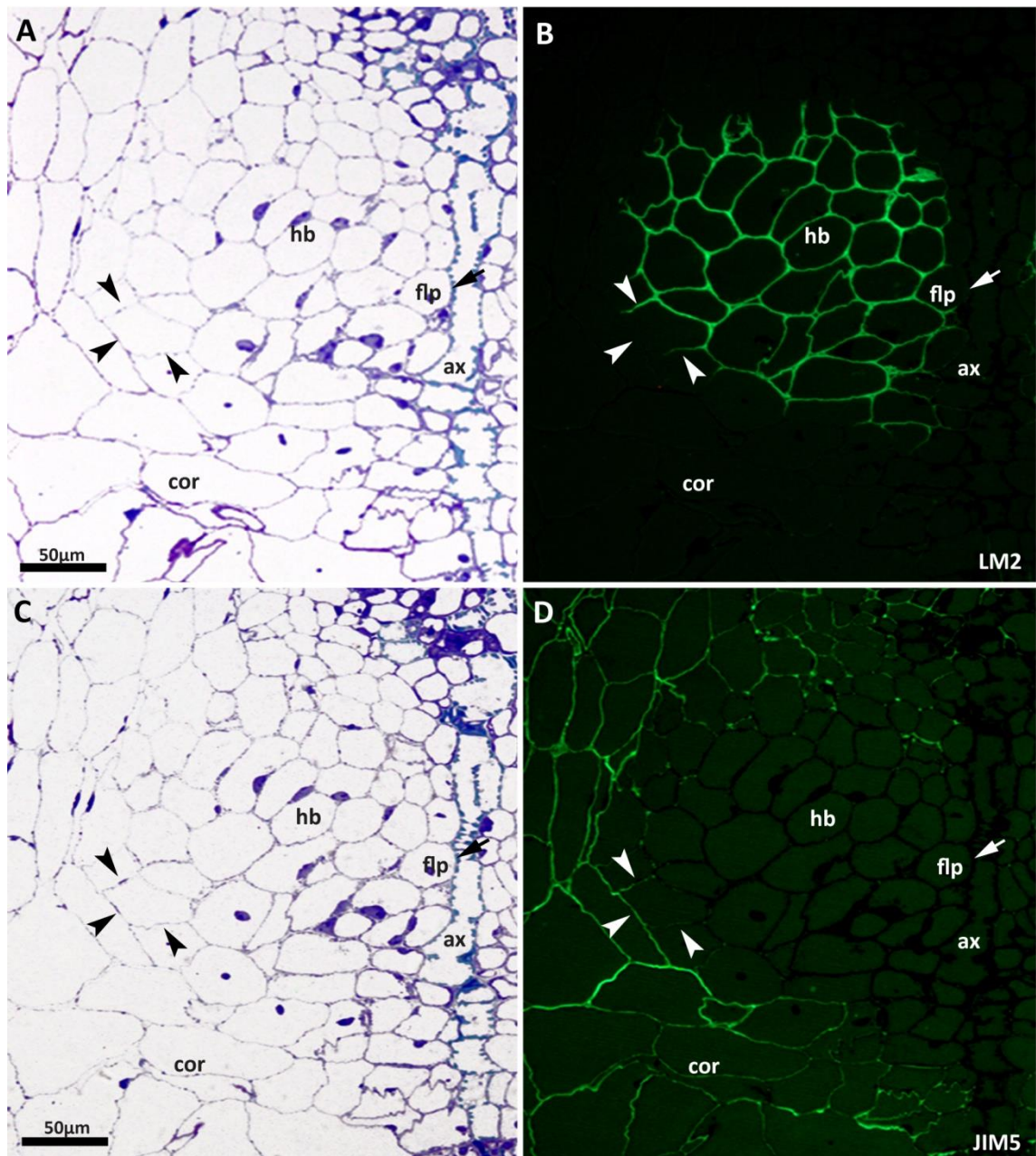


Figure 5.24: Polar heterogeneity in the distribution of JIM5 and LM2-recognised epitopes in the outermost layer of the hyaline body (**hb**). Arrowheads (\blacktriangleleft) indicate cell walls within the same cells in two serial sections. JIM5 and LM2 show affinity for the opposite sides of the outer hyaline body cells. Where LM2 labelling is absent, JIM5 labelling is most intense. Conversely, JIM5 binding is absent in the walls labelled with LM2. In the flange-like parenchyma (**flp**) adjacent to the axial xylem strand (**ax**), JIM5 labelling is absent and LM2 labelling gradually decreases towards the xylem (\blacktriangleleft).

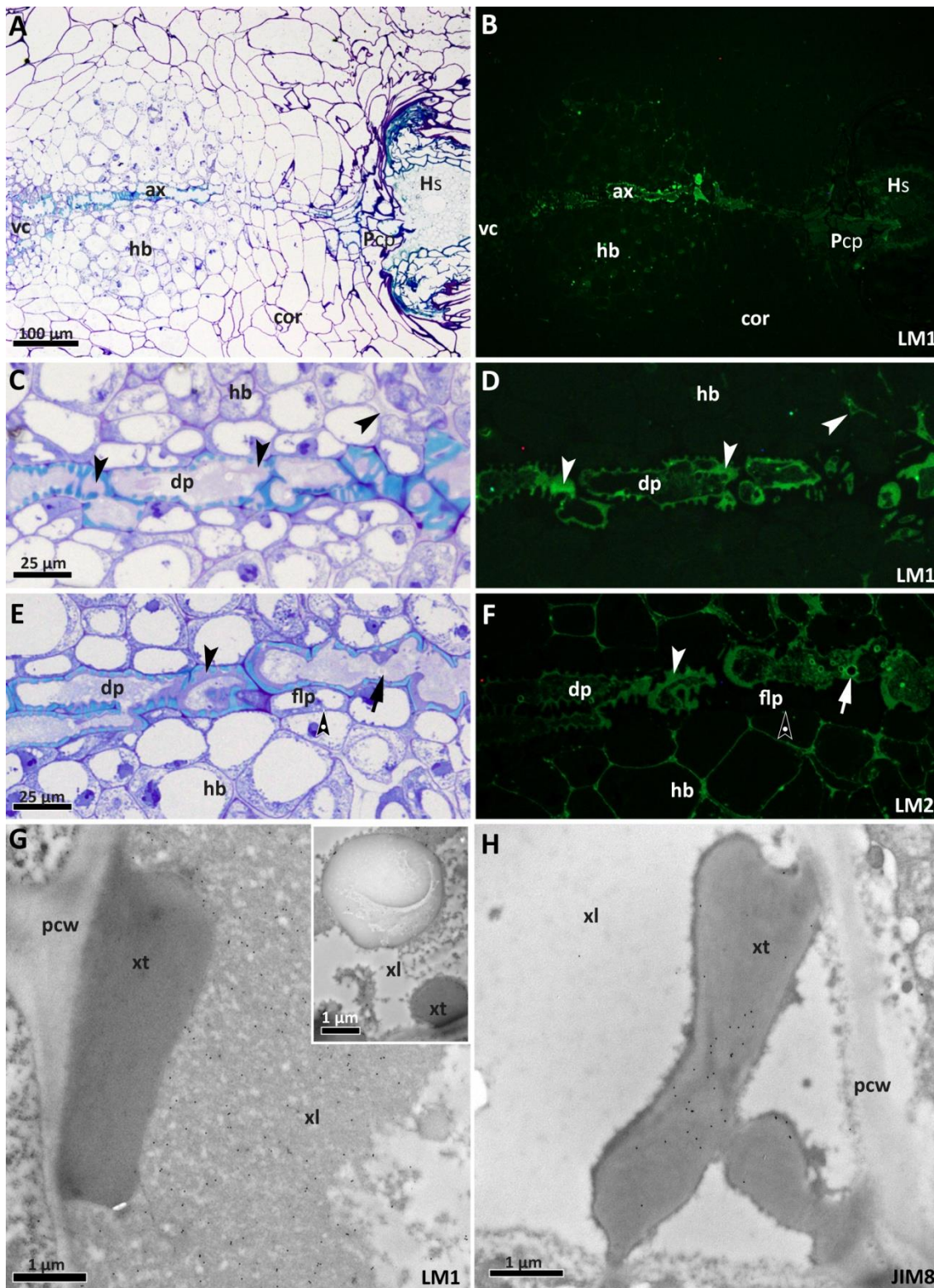


Figure 5.25: Immunolocalisation of extensin (LM1) and AGP (LM2) epitopes in the xylem bridge of *R. minor*. Sections were taken from the same haustorium as those illustrated in images 5.25G and H. **A and B)** Distribution of LM1-detected extensins in the partly-differentiated xylem bridge shows similar distribution to that of LM2 labelling, although the intensity is highest in the portion of the axial strand (ax) traversing the hyaline body (hb). **C and D)** Detail of LM1 labelling shown in A and B. Degenerating protoplast (dp) of the axial strand is exceptionally dense on the cell peripheries, where the labelling is the strongest. Labelling of the hyaline body is weak and restricted to several cell junctions. **E and F)** Labelling of xylem with LM2 is very similar to that with LM1. Grains within xylem lumina (←) do not label. The antibody binds to the hyaline body walls. Early stage flange-like parenchyma (flp) does not label and neither do xylem facing walls of the adjacent hyaline body cells.

G) Immunogold LM1 labelling of the axial strand of the same haustorium as in A–F. Gold particles are present in the densely grainy protoplast remnants in the xylem lumen (**xl**), corresponding to the strongly immunofluorescent region seen in images C and D. No labelling is seen in the lignified xylem thickening (**xt**), xylem granule (inset) or primary cell wall (**pcw**). **H)** JIM8 labelling of a xylem thickening.

5.3.2.4 Extensins

Figure 5.25 illustrates the distribution of extensins and AGPs. The most consistently observed pattern of extensin localisation was that of co-localisation with AGPs in the partly-differentiated xylem bridges (compare figures 5.19H and 5.25B as well as 5.26D and F). Similar to AGP distribution, extensin labelling was present in a layer of dense cytoplasm coating the thickenings (LM1, JIM12 and JIM20) and, at lower intensity, in the remaining part of the protoplast (LM1, JIM20) with no labelling of the cell walls, also when immunogold-labelled. Associated faint labelling of the hyaline body was confined to cell junctions (Fig. 5.26D). No labelling of extensins (or AGPs) was observed in any cells of the distal xylem initial cluster and therefore any putative axial strand initials. In rare instances, parenchyma in the cortex and mature hyaline body also labelled for extensins (data not shown).

Labelling of haustoria with anti-AGP, anti-homogalacturonan and anti-extensin mAbs is summarised in a diagram in figure 5.26. It is important to highlight that the highly protoplasmic, narrow region in the centre of *Odontites* haustoria labelled in the same manner as the hyaline body of *Rhinanthus*, further supporting the homology of these two tissues in both species.

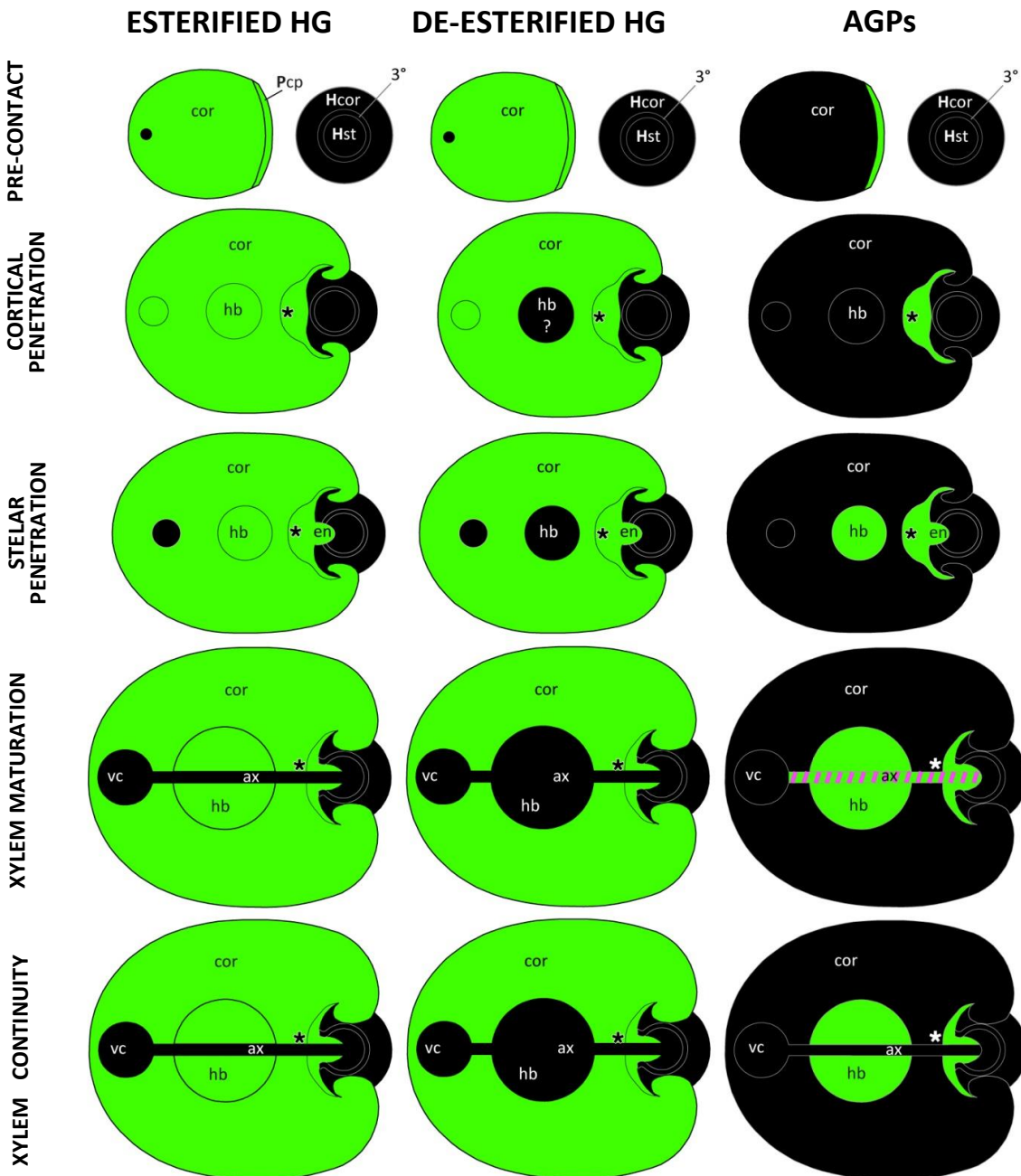


Figure 5.26: Diagram summarising homogalacturonan (HG) and AGP glycan epitope distribution in haustoria during key developmental stages. Green fill colour indicates labelling. AGPs and pectins are present in the cells of parasite contact parenchyma (**Pcp**) from pre-attachment stages and remain in xylogenic endophyte (**en**) cells until the onset of differentiation. A distal cell cluster (*****) behind the endophyte is also enriched in AGPs, but labeling disappears from this region during xylem maturation. Binding of anti-AGP probed in the host root is not indicated as it was not seen consistently. The hyaline body becomes enriched in AGPs approximately at the time of early stelar (**Hst**) penetration and maintains AGP-rich walls at maturity. This coincides with decreased detection of de-esterified HG epitopes in this tissue. The question mark indicates that presence of de-esterified pectins in the hyaline body initials during cortical penetration is not clear as JIM5 labelling is absent but LM18 and LM19 do label this tissue. Disintegrating xylem protoplasts of the xylem bridge axial strand are also AGP-rich while no labelling is seen in fully differentiated xylem bridges. AGP labelling in the xylem bridge overlaps with extensin epitope distribution (-----). **cor** — cortex of the haustorium, **vc** — vascular core, **ax** — axial strand, **hb** — hyaline body, **Hcor** — host cortex, **Hst** — host stele, **3°** — tertiary endodermis in the host root

5.4 Discussion

In this study, 32 monoclonal antibodies against cell wall components were applied to investigate cell wall composition of *Rhinanthus minor* and *Odontites vernus* haustoria. In addition to being the first study of angiosperm haustoria employing such a diversity of antibodies, at light and electron microscopy level, it is one of the very few illustrating different developmental stages. It is also the first immunohistochemical study of *Rhinanthus minor* and *Odontites vernus* and the most detailed structural account of their haustoria.

The most striking and novel finding of this project is that of arabinogalactan protein (AGP) epitope concentration in the hyaline body and contact parenchyma cell walls as well as in the protoplasts of partly-differentiated xylem bridges. Although AGPs are thought to occur in relatively low amounts (Fry, 1988; McCann & Knox, 2011), the intensity of their labelling matched only that of pectins, suggesting relatively high abundance or that the epitopes were easily accessible to labelling. The pronounced presence of arabinogalactan proteins and pectins was in striking contrast with scarce detection of xyloglucans — hemicelluloses typically abundant in eudicots (Scheller & Ulvskov, 2010). Cell wall polymers can mask and render each other undetectable to antibodies. So far, xylans (Hervé *et al.*, 2009), xyloglucans (Marcus *et al.*, 2008; Hervé *et al.*, 2011) and mannans (Marcus *et al.*, 2010b) have been reported to be masked by pectins. The occurrence of apparently abundant homogalacturonans within most haustorial cell walls observed in this study suggests that a masking interaction could occur. However, unmasking treatment with Pectinex® and pectate lyase did not result in signal increase in this study, even though homogalacturonans were removed. Interestingly, removal of pectins did not affect AGP detection either, suggesting that the lack of anti-AGP mAb binding observed in the haustorial cortex is not a consequence of masking.

The distribution of AGPs and pectins in haustoria was ubiquitous in spatial and temporal terms. Therefore, they are likely to fulfil a very wide array of functions. Possible implications of cell wall components, with a particular focus on these two abundant classes of molecules, are further discussed following a developmental progression and specific tissue types.

5.4.1 Haustorial cell walls prior to attachment

To gain insights into cell wall changes during haustorial development, a range of samples at different stages of development was analysed. Haustorial initials of parasitic plants formerly classified within the Scrophulariaceae develop laterally, near the growing tips of parasite roots by hypertrophy of root cortex, followed by periclinal divisions of the epidermis in the distal region (Musselman & Dickison, 1975). Hypertrophy is believed to be a less costly means of increasing haustorial volume

in comparison with cell division (Riopel & Musselman, 1979). Three expansin genes have previously been reported to be upregulated during hypertrophy in *Striga asiatica*, although the precise location of the proteins was not investigated (O'Malley & Lynn, 2000). As no commercially available anti-expansin antibodies exist, it is impossible to confirm their presence in hypertrophied cells via immunodetection. They are, however, likely to be localised in the cell walls of cells undergoing swelling and may facilitate the process. As AGPs are localised in strategic areas of *Rhinanthus minor* and *Odontites vernus* haustoria, it would be interesting to see whether they occur in the walls of hypertrophied cells. However, in this study, the youngest haustoria examined had developed beyond the hypertrophy stage and some cortical divisions had already occurred. No immunolocalisation specific to the derivatives of the hypertrophied cortical cells was observed. In fact, homogalacturonans were the only type of polymer detected abundantly in the haustorial initials and they were present in all parenchyma walls. AGPs were, however, found in contact parenchyma, which was the site of the developmentally earliest occurrence of these proteoglycans. Their presence in this tissue prior to attachment suggests a possible role in signalling and/or attachment. Attachment arabinogalactan proteins (attAGPs) have previously been found to be upregulated in hosts rather than the parasites (Albert *et al.*, 2006; Rehker *et al.*, 2012). AttAGP transcript levels in the *Lycopersicon esculentum* host were positively correlated with attachment force of *Cuscuta* haustoria and the attAGP itself was proposed to bind parasite-secreted pectins (Albert *et al.*, 2006). Vaughn (2003) detected JIM8-tagged epitopes in dodder searching cells and CCRC-M7 as well as MAC207-tagged epitopes in both the parasite and host cell walls and at their plasma membranes. However, he did not specify whether this distribution was confined strictly to the interfacial region, what developmental stage the labelling appeared at, or what the function of those AGPs might have been. Of further interest with regard to the early appearance of AGPs in the contact epidermis is the fact that they have also been proposed to control epidermal expansion (Ding & Zhu, 1997). Therefore, they might determine cell fate as markers of contact cell elongation during early attachment and continue to facilitate the process during the formation and penetration of the endophyte.

5.4.2 Cell walls of endophyte parenchyma (post-attachment)

Samples of young attached haustoria prior to advanced stelar penetration were rare and it is important at this point to elaborate on the reasons behind it, as it might help interpret the immunodetection results seen in this study. Early stage haustoria are notoriously scarce in collected samples and this has been ascribed to their fast development and weak adhesion at the initial stages of development (Musselman & Dickison, 1975; Heide-Jørgensen, 1995, 2008). Musselman & Dickison (1975) examined approximately 1000 haustoria collected in the field, only 25 of which were classified within young/early development stages. Neumann and colleagues (1998)

used a culture tube *in vitro* system for studying *Rhamphicarpa fistulosa* and still found it very difficult to obtain early stage haustoria penetrating pearl millet root cortices. Heide-Jørgensen (2008) suggests that it is specifically the penetrative phase that proceeds very fast and is difficult to capture. The “window of opportunity” for collecting some of the key stages of development is indeed quite narrow as evidenced by time course studies on *Striga* and *Triphysaria*. *Striga* is an obligate hemiparasite, seeds of which can be stimulated to germinate in unison and used to infect host roots. In such a system, development of primary haustoria at the tips of seedling radicles can be relatively easily monitored and collections performed at specific times post inoculation (pi) for comparison. This was carried out for *S. asiatica* by Ramaiah *et al.* (1991) who sampled haustorial development at 12 hour intervals. They found that attachment started approximately 36 hours after inoculation, followed by a minimum of 36 hours to enter the cortex and further 12 hours to reach the endodermis. Establishing contact with the host stele took an additional 24–60 hours and therefore 108 h post inoculation (including germination time) was the minimum time required for full penetration; only 17% of attached haustoria reached the endodermis and 14.8% of all attached haustoria established contact with the stele. Other authors suggest similar times for haustorial development. A subsequent study of *S. asiatica* determined that the endodermis of *Sorghum* was reached 48–72 hours pi but stelar penetration was delayed for a subsequent 72–96 hours (Hood *et al.*, 1998). The authors interpreted this as a possible sign of minimal partial resistance — a factor that is likely to contribute to variance in timing on different hosts. An *in vitro* root culture system developed for *Triphysaria versicolor* (Tomilov *et al.*, 2004) provided evidence that the time scale is similar for secondary haustoria of this species, although the minimum time for full establishment was even shorter. Examination of cleared haustoria obtained with this technique showed that xylem bridge occasionally connected the parasite with its maize host root within no more than 24 hours from initial contact. Penetration and maturation are, presumably, also very fast in *R. minor* and *O. vernus*. If this is the case, cell wall restructuring associated with cell growth and differentiation also occurs rapidly. Abundant AGPs might be important in directing these processes and alleviating the associated intramural stresses.

An important aspect of haustorial development that might be regulated by AGPs is not only the growth of the endophyte, but also the subsequent xylogenesis. Although an axial strand could be distinguished in the hyaline body meristem prior to the penetration of the endodermis, no xylem bridge elements were observed in the samples of haustoria before they reached the host stele. Therefore, differentiation must occur upon contact with host xylem as previously suggested (Musselman & Dickison, 1975; Riopel & Musselman, 1979). This contact is achieved via the penetrative action of the endophyte. The layer of elongated endophyte cells of *Rhinanthus minor* and *Odontites vernus* could be traced back to the epidermis

of the parent root and the individual cells often had divided via oblique periclinal divisions. Therefore, this palisade of interfacial parenchyma cells seems to form in a manner closely resembling that in *Triphysaria* (Heide-Jørgensen & Kuijt, 1993) and many other former Scrophulariaceae (Musselman & Dickison, 1975). This means that the AGP-labelled contact parenchyma of pre-attachment haustoria becomes the endophyte and, as a consequence, its original putative function in host signal perception is further accompanied by other roles, for example in attachment or penetration, with the ultimate fate being differentiation into xylem.

In all post-attachment samples examined, cell walls of interfacial parenchyma were considerably thickened during and after cell elongation and until their transition into xylem. This is not surprising, as it has been noted in a number of taxa that contact cells possess thickened, un lignified walls (Condon & Kuijt, 1994; Neumann *et al.*, 1998; Reiss & Bailey, 1998; Hood *et al.*, 1998). The thickenings are particularly sophisticated in *Orobanch*e (Heide-Jørgensen, 2008), where they resemble the labyrinth cell walls of transfer cells, and, to a lesser extent, in *Ola*x *phyllanthi* (Kuo *et al.*, 1989) where they form transfer-type wall ingrowths. In both cases these thickened walls are implicated in apoplastic transport of nutrients from the host. The walls of interfacial parenchyma in *Rhinanthus* and *Odontites* represent a simpler, uniform type of thickening which does not contribute to increased surface area of plasma membrane. However, it might contribute to apoplastic transport through transient storage of ions facilitating maintenance of osmotic standing gradients that allow passive flow of water. This additional function was proposed to be fulfilled by labyrinth transfer cell walls which act primarily by increasing plasmalemma surface (Pate & Gunning, 1972). However, it was impossible to determine, in this study, if parenchyma takes part in nutrient abstraction and/or processing before differentiation into xylem and if those cells that remain parenchymateous continue to play the same role as parenchyma cells before the transition. It is also not clear how AGPs might facilitate such possible functions. Apparently high AGP content across the entire thickness of the wall as opposed to localisation at the plasma membrane-wall interface indicates that they might play structural roles or modify rheological properties of the cell wall. Lamport *et al.* (2006) proposed that AGPs contribute to increased porosity of the pectin network by decreasing alignment and cross-linking of pectins. Modification of wall rheology could have important implications for apoplastic transfer of solutes although this is a purely theoretical suggestion. Uptake, of substances by interfacial cells is also possible and a previously published experiment shows that changes to wall AGPs affect uptake of water (Lu *et al.*, 2001). Treatment of tomato seedlings with Yariv reagent, which binds AGPs, inhibited water abstraction. This could reflect the putative role of AGPs as humectants (Fincher & Stone, 1983) or contributors of normal membrane functioning but the possibility of the reagent-AGP complexes physically impeding water uptake cannot be ruled out.

AGP distribution across the entire wall thickness persists until xylem thickenings develop, after which labelling for AGPs is associated with the protoplast. This suggests that the possible roles of AGPs in contact parenchyma ontogenesis are likely to be many-fold. Putative plasticising, structural or signalling functions of AGPs are likely to be crucial for cell wall remodelling during endophyte elongation. The specific functions of AGPs could vary depending on the precise mode of host tissue penetration and interfacial cell expansion. In comparison with fungi, these processes are generally poorly researched for parasitic plants (Mayer, 2006), although literature and data obtained in this project provide some information on how they occur in parasitic angiosperms.

Joel and Losner-Goshen (1994) hypothesised about the three main mechanisms of haustorial penetration: 1) between host cells, 2) perpendicular to host cell wall and 3) coordinated. The first mode of penetration might theoretically be executed purely by mechanical means or be facilitated by the action of cell wall degrading enzymes (CWDEs). In the exclusively mechanical mode, hydrostatic pressure of searching cells would be the main mechanical aid to penetration through the host middle lamellae. This is likely to be typically associated with vacuolation which allows for faster volume increase than meristematic growth (Cosgrove, 2000, 2005a). Vacuolation of, initially, highly protoplasmic contact cells, characteristic of early developmental stages (Neumann *et al.*, 1998), was observed during advanced stelar penetration by *Rhinanthus minor* and *Odontites vernus*. Claspings folds, which are well developed in some, although not all, haustoria, are likely to additionally facilitate mechanical opening of the root resulting in the presence of crushed host cells at the lateral interface. It was proposed that mechanical penetration between host cells would result in irregularly shaped remnants of middle lamellae along the separated walls (Joel & Losner-Goshen, 1994a). It is also more likely to be associated with increased shear stress within the endophyte walls, as a result of the high hydrostatic pressure, combined with movement through a constricted space. Enzymatic digestion should result in a smoother path of penetration with various degrees of host middle lamella, primary and secondary wall modification or dissolution, including complete disintegration in the most extreme case (Joel & Losner-Goshen, 1994a). Enzymatic dissolution of pectic middle lamellae has been previously indirectly demonstrated through immunodetection of PME and de-esterified pectins at the site intrusion of *Orobancha* into eudicot hosts *Helianthus annuus* and *Lycopersicon esculentum* (Losner-Goshen, 1998).

Joel and Losner-Goshen (1994) propose that in the case of the second, perpendicular mode of penetration, the host wall can be ruptured, allowing access to the protoplast; stretched, coating the parasite's wall or, alternatively; the cell may become crushed. This second mode is well documented for *Cuscuta*, where a chimeric wall is formed from the stretched host's wall and parasite's wall (Vaughn, 2003). This stretching was

suggested to be orchestrated by the parasite, by stimulating the host to synthesise new wall material. The non-haphazard nature of this process is highlighted by the fact that it is associated with one transient appearance of interspecific plasmodesmata (Vaughn, 2003). Host cell walls of stretched appearance were also found during invasion by *Striga gesneroides* (Joel & Losner-Goshen, 1994a). Although other reports of apparently intracellular growth exist (for example Visser *et al.*, 1990), they are likely to be the random result of pressure exerted by the searching cells rather than an intended mode of progression.

In coordinated penetration, host cells are stimulated by the parasite to proliferate in a way which facilitates endophyte progression, preventing damage to walls or protoplasts. This has been previously described for *Striga gesneroides* which induce hyperplasia in the root pericycle of *Vigna unguiculata*, allowing easier penetration of its endodermis (Smith & Stewart, 1987).

Overall, parasitic plant haustoria are currently thought to grow chiefly intercellularly, pushing host cells to the side and crushing them during this process (Heide-Jørgensen, 2008). Results of this study agree with this notion. It appears that the parasites attempt to grow between host cells rather than through them, although loss of host cells effected by the mechanical pressure exerted by the endophyte is unavoidable where host cells cannot withstand the resulting forces.

The mechanical aspect of penetration was clear in *Rhinanthus* and *Odontites*. The symptoms included cracks unfilled with material ahead of the tip of the advancing endophyte and “snapped” host walls seen between the parasite and host cells. No host wall loosening similar to that seen at differentiating endophyte tips was observed and neither were other signs of enzyme-inflicted damage, for instance loss of electron opacity (Heller & Thines, 2009). However, the narrow space between the parasite and host walls was tightly filled by smooth material, rather than irregular remnants of the middle lamellae which would suggest their mechanical disruption. Similar material was observed at the interface between *Striga gesneroides* and tobacco (Joel & Losner-Goshen, 1994a). No loosely fibrillar material indicative of enzymatic dissolution was seen in this study, except, occasionally, where endodermal cells were peeled from the pericycle. However, this space was also typically filled with the extramural material. The smooth, dense appearance of the interfacial material suggests that it is actively secreted during penetration, sealing off the narrow space, as opposed to representing pre-existing material. It is most likely the parasite that has the ability to produce it, as the highly protoplasmic cells of the endophyte are more suited for synthesis and secretion than the heavily lignified cells of host stele. Apparent dissolution of this material seen during cortical penetration (Fig 5.2F and G) was otherwise not seen and it is not clear what it signifies. Its localisation at the central

interface prior to formation of a penetrating tip might mean that that it represents a mechanism of secretion remodelling in anticipation for rapid intrusion the host stele.

Remnants of host middle lamellae resulting from enzymatic loosening or mechanical disruption must become embedded in the secretion as they are not visible. Cell walls of dissolved appearance belonging to crushed host cells were rarely seen embedded in the interfacial deposits at the central interface. It is not known if dissolution occurred as a result of mechanical disruption or whether it contributed to it. It is possible that the damage is a consequence of the cells being crushed as opposed to the cell walls being specifically targeted by enzymes secreted by the parasite and designed to facilitate penetration. Walls could be digested after becoming interrupted, provided that the extramural secretion contains enzymes. Enrichment of endophyte walls in AGPs and pectins might render them particularly well suited as a pathway for transport of the interfacial material. This, once again, highlights their possible role in creating suitable apoplastic environment associated with cross-wall transfer of substances. This seems to be further supported by the fact that their high concentration in the wall is maintained after the growth has most likely ceased (i.e. the cells have reached the centre of the vascular core), when a function in growth facilitation is no longer to be expected.

Although the mode of host tissue separation by parasitic plant haustoria is partly understood and factors such as CWDEs are documented (Reddy *et al.*, 1980, 1981; Nagar *et al.*, 1984; Olivier *et al.*, 1991; Shomer-Ilan, 1994; Losner-Goshen, 1998), this field of parasitic plant research requires further work. In particular, it would be important to elucidate the mechanisms of host vessel recognition and entry, as well as factors that make the parasite “decide” between indirectly using pits via abutment, exploit them directly by producing osculi or breaking host cell walls to create luminal continuity. All three modes were observed in this study, with the first being apparently most common. Exploitation of host pits has been previously demonstrated in *Olx phyllanthi* (Kuo *et al.*, 1989) and *Cuscuta pentagona* (Vaughn, 2006 – Fig.2c). In *Olx*, where parenchyma constitutes the majority of the contact tissue, its thickened cell walls display localised thinning abutting host xylem pits. Similar thinning of a xylic hypha of *Cuscuta pentagona* in a region abutting a xylem pit was observed. Apoplast tracer experiments, where the host was fed lanthanum nitrate or uranyl acetate, confirmed that host pits were the main gates for nutrient extraction by *Olx* and that they were subsequently transported via the apoplast of parenchyma into haustorial xylem (Kuo *et al.*, 1989). Mechanical disruption of vessel walls was proposed for *Rhamphicarpa fistulosa* although its exact nature was not explained (Neumann *et al.*, 1998).

Condon and Kuijt (1994) remarked that there was “no ultrastructural evidence of large scale enzymatic digestion of host or parasite tissues” at the interface between

Ileostylus micranthus and *Chamaecytisus palmensis*. Similar observations were made in this study although others have reported host wall thinning. Cell walls of host cortex cells pushed aside by the endophyte of *Striga gesneroides* were thinner but not disintegrated (Joel & Losner-Goshen, 1994a). Meanwhile, enzymatic penetration associated with host wall swelling or thinning was found in the host vascular cylinder (Olivier *et al.*, 1991; Joel & Losner-Goshen, 1994a). Similarly, wall thinning without disruption was observed in sorghum parasitized by *Striga hermonthica* (Olivier *et al.*, 1991).

Even less is known about the precise mechanism of interfacial cell elongation and wall remodelling than about the path of movement through host tissues. Since the initial function of the endophyte is intercellular penetration directed by cues from the host, polarised tip growth analogous to that of fungal hyphae, pollen tubes and rhizoids, rather than homotropic anisotropic growth characteristic of vascular tissues (Geitmann & Ortega, 2009) can be expected in these cells.

Searching cells of *R. minor* and *O. vernus* were observed to have grown between and around host cells. In this respect, they undoubtedly, resemble fungal hyphae and pollen tubes, which display meandering, chemotropic growth (Sbrana & Giovannetti, 2005; Johnson & Lord, 2006). In tip growth, reaction to directional cues is improved and the area of friction is reduced (Geitmann, 2010) — traits very much desired in fast growing, meandering cells of a scavenging endophyte. Indeed, dodder searching cells are termed hyphae and Vaughn (2003) describes them as “tip growing cells” similar to fungal hyphae and pollen tubes. However, this statement is not supported by sufficient evidence to demonstrate the real contribution of tip versus diffuse expansion, as no studies focused on the precise mechanism of expansion in growing endophyte cells exist. Mayer (2006) expresses his concern about using the term “hypha” to describe parasitic angiosperm cells although he does not back it by any evidence specific to wall expansion mechanisms, either.

A number of localised, growth-promoting cell wall modifications that were not observed in this study are known to occur in tip growing cells. Wall synthesis itself is not sufficient to effect expansion which is caused by a combination of wall relaxation and turgor (Cosgrove, 1993). Cell wall relaxation results in a drop in turgor pressure and water potential which, in turn, cause passive water influx, leading to irreversible deformation of the loosened wall. In polarised growth, localised cell wall loosening is necessary as turgor is a non-vectorial force acting evenly on the entire surface of a cell (Geitmann, 2011; Winship *et al.*, 2011). Three main load-bearing networks of 1) pectins, 2) cellulose-hemicelluloses and 3) proteins determine the extensibility of walls (Cosgrove, 1993). In the polarised tip growth exhibited by pollen tubes, highly esterified (non-jellified) pectins allow localised extension while the growth in distal

parts of the tube cylinder (behind the tip) ceases after wall enrichment in cellulose and callose (Palin & Geitmann, 2012).

Tip-specific polarity was not seen in this or other studies, and a pattern of callose deposition opposite to that in pollen tubes was seen in *Cuscuta*. Cell wall modification did not involve incorporation of callose into the cell walls of dodder during attachment (Vaughn, 2002) but the tips of searching hyphae were enriched in callose (Vaughn, 2003). This is an unexpected result considering callose absence from tips of growing pollen tubes and its presence behind the elongation zone, contributing to stabilisation of cell wall structure (Taylor & Hepler, 1997). No depletion in de-esterified pectin which is seen in pollen tubes (Chebli *et al.*, 2012) was observed at the tips of contact parenchyma until dissolution occurred, and neither was any tip-specific heterogeneity with regard to AGP epitope distribution, as previously found for pollen tubes (Li *et al.*, 1995; Jauh & Lord, 1996; Mollet *et al.*, 2002). However, the former does not necessarily mean that pectin network was not restructured to aid tip growth. As de-esterification renders pectin more prone to the action of backbone-acting pectinases, restructuring might still occur via enzymatic means (Palin & Geitmann, 2012). While this might be the case, it is interesting that, again, no localised enrichment occurs within the cells, despite evidence of such enrichment being seen during formation of primordia in shoot apical meristems of *Arabidopsis* (Peaucelle *et al.*, 2008).

Although the results of this project provided no evidence for tip wall composition being different than in the remaining cell walls before conversion into xylem, this warrants further, more detailed study with the involvement of different developmental stages. Such differences might be easier to capture in cells that produce osculi, which are created as a result of very localised expansion at the tip (Dörr, 1997), resembling penetration of host pits by fungal hyphae (Sachs *et al.*, 1970). Overall, wall restructuring in endophyte parenchyma is likely to display elements characteristic of both, tip growth and diffuse growth. The latter must be present to some extent as, in contrast with pollen tubes and fungal hyphae which expand in only one direction, the cells within the endophyte also expand laterally behind the tip, increasing the volume of the endophyte. Indeed, intrusive intercellular growth in plant cells does not need to be confined to tips. Lactifers display both diffuse growth in their lateral walls and tip growth when branching into organs (Serpe *et al.*, 2002 and references therein).

Regardless of the mode of expansion and penetration, endophyte searching cells are likely to be the fastest growing cells in the haustorium and possess the most dynamically remodelled cell walls and the presence of AGP glycans is likely to be somehow implicated. Pollen tubes are known to grow at 250 nm/s and root hairs at 10–40 nm/s (Hepler *et al.*, 2001). This means that at the growth rate of a pollen tube, a cell length of 200 μm (the approximate length of the longest endophyte cells

seen in this study) can be reached in less than 15 minutes. While cell walls of haustorial searching cells differ in that they are thicker-walled, connected to each other via middle lamellae and need to overcome host surveillance and defence systems, this value gives an upper limit to how fast growth might occur. This order of speed is not unlikely considering how difficult it is to obtain early stage haustoria. Therefore, the viscoelastic properties of endophyte cell walls can be expected to differ from those of other haustorial cells. They have to exert sufficient penetrative force while withstanding turgor pressure and shear stress, in addition to being sufficiently malleable to allow expansion and adjustment to the shape of separated host cells. These needs might be partly met by the enrichment in pectins and arabinogalactan proteins seen in this study. Pectins, which are an important component of the matrix surrounding the cellulose-hemicellulose network (Mohnen, 2008) contribute to cell wall mechanical properties (Braybrook *et al.*, 2012) and control expansion by affecting the interactions between cellulosic lamellae (Cosgrove, 2000; Palin & Geitmann, 2012). Implications of AGPs in restructuring of the wall are much more mysterious although there is evidence suggesting that their possible roles in wall expansion are particularly plausible. Schopfer (1990) hypothesised that AGPs secreted into the wall hydrate and form a gel contributing to easier sliding of microfibrils in an expanding wall. However, he localised AGPs only at the plasma membrane of the outer epidermal walls of maize coleoptiles at the start of the elongation process, using MAC207, while JIM13 epitopes were restricted to sclerenchyma and tracheids, and JIM14 to sclerenchyma. Although a putative role during expansion requires further research, the mode of action might be via intramural lubrication or loosening of pectin network (Lampert *et al.*, 2006). Such lubricative function of AGPs would be highly desirable in the fast growing cells of the endophyte and the resultant plasticity would not only allow cell expansion, but also adaptation to host wall shape seen in this study. Furthermore, AGPs may act as a periplasmic cushion and stabilize plasma membranes which are subjected to high turgor pressures in growing cells (Serpe & Nothnagel, 1999; Lampert *et al.*, 2006) during fast growth.

Wall-associated osmiophilic particles detected in this study were much larger than those seen by Schopfer (1990). However, all osmicated samples investigated were close to maturity and, hence, expansion might have ceased. Cell expansion in *Cuscuta* was aided by cell-wall loosening complexes secreted into the walls in a form of osmiophilic particles including expansins (Vaughn, 2002; Lee, 2008). More detailed studies of the composition of wall-associated osmiophilic particles in parasitic plant haustoria might provide some important information about cell wall expansion within the penetrative parts of these organs.

It is important to note that AGP and RG-I-associated arabinan side chains, which are thought to be important in terms of granting plasticity (Moore *et al.*, 2013a), were labelled strongly with LM6 specifically in the interfacial parenchyma in this study.

Curiously, Vaughn (2003) found that the LM6 epitope was restricted to the chimeric wall formed during penetration by *Cuscuta*. It would, therefore, be of interest to see if presence of arabinan epitopes in endophyte cells is highly conserved amongst various parasitic angiosperms.

In addition to plasticisation, AGPs can increase wall rigidity when they become oxidative cross-linked (Kjellbom *et al.*, 1997). Such contrasting functions could theoretically allow high malleability of endophyte cell walls at the tips, while cross-linking behind them could help stabilise the quickly expanding wall. Implications of AGP-related molecules in such stabilisation process have been shown for legume-specific root nodule extensins (RNEs) with characteristics of both extensins and AGPs. RNEs aid gradual hardening of the infection thread where they become deglycosylated, revealing the extensin modules, which subsequently become oxidatively cross-linked (Brewin, 2004b). Lack of polarity in AGP distribution seen in this study, does not, therefore, necessarily mean that they do not participate in polar growth. Instead, they might display different functions in different regions of the cell. However, it is difficult to make any suggestions about how these potential localised differences might be regulated.

5.4.3 Xylogenesis

AGPs remain in endophytic cells during differentiation into xylem although their localisation shifts from the cell-walls to the protoplast, where they are co-localised with extensins. Labelling of protoplasts of differentiating xylem bridges with anti-AGP and anti-extensin mAbs can be explained either by an influx of weakly bound epitopes from the wall during fixation or actual presence of those specific glycosyl sequences in the protoplasts of the developing tissue. The very strong labelling even at the centre of the protoplast, coupled with lack of detection in the walls, makes the first possibility rather unlikely. Cytoplasmic labelling was also present in the hyaline body and the interfacial parenchyma. However, these tissues contained living cytoplasm which might have been synthesising and trafficking the epitope-containing glycans. LM1 (Smallwood *et al.*, 1995) and LM2 (Šamaj *et al.*, 2000; Dahiya & Brewin, 2000; Konieczny *et al.*, 2007) have been previously found to label living cytoplasm and localisation in tonoplast membrane has been previously noted with MAC207 (Pennell *et al.*, 1989) and LM2 (Šamaj *et al.*, 2000). As extensins and AGPs are synthesised in and transported within the cytoplasm, these results are not surprising. However, it is not clear how these molecules find their way into the disintegrated protoplasts of dying cells. It is possible that AGPs originally present in parenchyma walls are transported back into the protoplast before vacuolar death.

AGPs have previously been associated with xylem differentiation (Loopstra & Sederoff, 1995; Casero *et al.*, 1998; No & Loopstra, 2000) or simply localised within the vasculature (Liu & Mehdy, 2007; Bossy *et al.*, 2009) of non-parasitic plants

and suggested to be involved in cell fate determination, deposition of thickenings and programmed cell death. Dolan *et al.* (1995) showed a remarkable example of AGP epitope correlation with early stage initiation of xylogenesis in *Arabidopsis* roots, where JIM13-recognised epitopes marked the pathway of xylem differentiation from the central xylem initial at the root apex. Analogical observations were not possible in this study as a result of the scarcity of early developmental stage material. Obvious xylem initials were not identified and it was impossible to ascertain if extensin epitopes might also act as tags for meristematic cell fate for this portion of the xylem bridge. However, the sections that were labelled had been cut very close to the centre of the hyaline body meristem and were likely to contain some xylem initials. Nevertheless, no cells in the hyaline body meristem labelled with anti-extensin or AGP probes but walls of the distal meristem did label with CCRC-M7, LM2, JIM8 and JIM13. These cells, as well as contact epidermis cells which also labelled, often differentiated into xylem. This suggests that the relevant proteoglycans might be tags of cell fate at least in these parts of the haustorium.

AGP presence was strongly marked in the protoplasts of developing haustorial xylem. While AGPs have been previously immunolocalised in xylem thickenings (Schindler *et al.*, 1995; Stacey *et al.*, 1995; Gao *et al.*, 1999; Gao & Showalter, 2000), only scarce immunogold localisation was observed in the thickenings of *R. minor* in this study. In *Pinus taeda* L., classical AGP (PtaAGP6) epitopes were present in differentiating xylem shortly before, and during, deposition of secondary thickenings but disappeared before the onset of lignification (Zhang *et al.*, 2003). A non-classical AGP xylogen has been demonstrated as a hormonally (auxin and cytokinin)-regulated factor mediating local intercellular communication in vascular cell differentiation (Motose *et al.*, 2001b, 2004; Fukuda, 2004). Similar to PtaAGP, xylogen was present before the appearance of thickenings and appeared to be responsible for development of xylem continuity rather than wall deposition (Stacey *et al.*, 1995; Motose *et al.*, 2001a).

Labelling of AGPs and extensins in the disintegrating protoplast, but not lignified thickenings, points to a role in programmed cell death (PCD) rather than cell wall deposition. The protoplasts that labelled with anti HRGP probes were devoid of vacuoles and displayed relatively uniform, pale purple, grainy staining with toluidine blue O. As lysis of vacuoles is associated with PCD during xylogenesis (Fukuda, 1997), their absence in these cells in parallel with the presence of thickenings might indicate early stages of PCD, more precisely — vacuolar cell death (Van Doorn *et al.*, 2011).

A functional relationship between AGPs and extensins in the differentiating xylem is a possibility although literature does not provide examples of specific types of interactions between these two classes of molecules. However, hybrid AGP-extensin molecules are known (Lind *et al.*, 1994; Bosch *et al.*, 2001), also from legume nodules

(Brewin *et al.*, 2008; Reguera *et al.*, 2010). AGPs and extensins have been observed to be co-expressed (Showalter *et al.*, 2010) but I am not aware of any co-localisation studies. Certainly, no such observations made in parasitic plants are published. Extensins, but not AGPs, have previously been associated with haustorial xylem formation. LM1-recognised extensin epitopes were localised in differentiating haustorial xylem of *Buchnera hispida*, *Rhamphicarpa fistulosa* and *Striga hermonthica* (Neumann *et al.*, 1999). The authors indicate that the labelling lined the thickenings in those xylem elements that possessed remnants of cytoplasm but do not specify if the labelling was confined to a cytoplasmic lining or peripheral parts of the actual thickenings. Figure 18 in Neumann *et al.*, 1999 is not sufficiently detailed to determine this. Vasculature of dodder and its host was also extensin-rich although the developmental stage was not indicated (Vaughn, 2003).

In addition to xylans, which are typically localised within xylem thickenings (McCartney *et al.*, 2005), RG-I backbone and arabinan side chain epitopes were found in the lignified thickenings of the xylem bridge. The striking binding of RU antibodies to a narrow outer band has not been previously reported although radial heterogeneity involving rhamnogalacturonan-I (1→4)-β-D-galactan side chains has been described, whereby the epitope was concentrated at the base of xylem thickenings (Fig. 6.37 in Albersheim *et al.*, 2011). It is not known what the purpose of this heterogeneity is and why the RU-labelled band within the vascular core xylem does not appear to lignify. Lack of this highly localised binding within the axial strand or endophytic xylem might be suggestive of differences in differentiation mode between the vascular core and the remaining part of the xylem bridge.

Since the differences in RG-I backbone epitope distribution are seen strictly between the vascular core and axial strand without displaying a gradient, no conclusions about the direction of differentiation can be made. The only apparent gradient seen in this study was that of acropetal protoplast degeneration. This direction of differentiation was also suggested by Cameron and Seel (2007) although the relevant diagram (Fig. 2a) is not backed with micrographs and illustrates xylem bridge differentiation occurring before endodermal penetration, for which no evidence was found in this study. Acropetal and basipetal xylem differentiation alike were found to occur in haustoria of *Striga asiatica* (Hood *et al.*, 1998). Unfortunately, the authors did not specify if this was with regard to the individual cells (and in which region) or the entire xylem bridge. In *Rhamphicarpa fistulosa* there were two points of initiation — one at the parent root stele and one in the centre of the haustorium (Neumann *et al.*, 1998).

Work with an antibody against antigen CN 8 (most likely belonging to a hemicellulose) specific to developing xylem and xylem parenchyma revealed that the recognised epitope was distributed in a polarised pattern in immature xylem elements in *Zinnia*

cell cultures (Shinohara *et al.*, 2000). This is another reason why it is somewhat surprising that the battery of probes applied in this study did not produce any clear polarised patterns of AGP, pectin or hemicellulose distribution in contact parenchyma.

5.4.4 The hyaline body

Immunolocalisation results presented in this study highlight the distinctiveness of the hyaline body from the parenchyma of the cortex. Known also as the central parenchymateous core (Kuijt, 1977) or haustorial nucleus (Nwoke, 1982), the hyaline body is a feature of many Orobanchaceae that were formerly classified within the Scrophulariaceae. Reports exist of the hyaline body being absent from haustoria of some species within this clade, for example *Striga gesneroides* (Ba, 1983) and *R. fistulosa* (Neumann *et al.*, 1998).

Hyaline bodies have been proposed to play important physiological roles although few specific functions have been suggested and none have been experimentally proven. Nutrient translocation and storage (Visser *et al.*, 1984) or synthesis of abscisic acid (ABA) — a hormone found abundantly in this tissue and proposed to control cell wall thickening and lignification in *Rhinanthus minor* haustoria (Jiang *et al.*, 2004; Rümer *et al.*, 2007) were suggested. For *Striga asiatica* hyaline bodies, Mallaburn and Stewart (1987) suggested a role in protein synthesis and starch storage as evidenced by abundant rough endoplasmic reticulum and amyloplasts respectively. Modification of nutrients derived from the host was also considered (Mallaburn & Stewart, 1987). This is in agreement with the enrichment of haustorial xylem fluid in amino acids versus inorganic nitrogen in comparison with host xylem fluid (O'Brien *et al.*, 1964).

The novel immunocytochemical findings in this project concern the cell walls of the hyaline body as well as paramural deposits and ergastic globules made of cell wall material and likely to have a storage function. Once again, AGPs were demonstrated to be ubiquitous, showing localisation within all these structures. Comparison of mature and early stage haustoria revealed that enrichment of walls in AGPs corresponded with low detection of de-esterified pectin epitopes, while esterified homogalacturinans were apparently abundant. Although the hyaline bodies of *Rhinanthus minor* and *Odontites vernus* differed in shape and density of organelles, this pattern was conserved in both, highlighting the homology of these two tissues and suggesting that the biochemical distinctiveness of hyaline body cell walls has an important, universal function in haustoria. This is an interesting observation in the light of the previous findings by Neumann *et al.* (1999) who found no differences in the distribution of JIM5 and JIM7 labelling of *Buchnera hispida*, *Rhamphicarpa fistulosa* and *Striga hermonthica* (Orobanchaceae).

Pectins are secreted in a highly methyl-esterified form and, if required, are de-esterified by PME at the cell wall, becoming prone to aggregation into gels

(Jarvis, 1984; Willats *et al.*, 2001b; Wolf *et al.*, 2009). Therefore, cell walls of young cells and tissues are often rich in highly methylated pectins. As the hyaline body cells remain protoplasmic longer than the surrounding cells, it could be argued that lack of de-esterified pectins is a consequence of this tissue being young. While JIM5 labelling results support this theory in that no labelling is present in the hyaline body meristem, presence of deesterified pectins is indicated in this tissue in the same sample by LM18 and JIM19. Nevertheless, low or lack of labelling with all three mAbs against de-esterified pectins was consistent in older samples, including the one during endodermal penetration. However, reduced de-esterification cannot be assumed to be the reason behind decreased labelling. It is possible that low-methylated pectins are not detected because they interact with the co-occurring AGPs immediately after de-esterification or might even be linked together during vesicular transport into the wall (Immerzeel *et al.*, 2006). Interestingly, AGP labelling was not sensitive to unmasking. Therefore, the hypothetical link between the two molecules requires further investigation.

The striking pattern of opposite localisation of de-esterified pectins and AGPs seen in this study has no apparent counterparts in the literature. Co-localisation of these wall components has not been a major focus of immunocytochemical studies, either. JIM5-detected homogalacturonan epitopes and MAC207-recognised AGP epitopes have been previously co-localised in *Arabidopsis* pollen grain intine where they were concentrated near the plasma membrane (Van Aelst & Van Went, 1992) although no interpretation of this was presented. Additionally, an association between JIM13 detected AGPs at pollen cell plasma membrane as well as walls and plasma membranes of transmitting-tract epidermal cells, where the pollen tubes adhered, and JIM5-detected deesterified pectins was proposed to participate in the adhesive interactions between and pollen tube walls in the styles of *Lilium longitorum*.

As the degree of esterification has implications for pectin gelling properties in that deesterified pectins can be calcium-crosslinked to form gels (Jarvis, 1984), their lower content could mean increased fluidity of the pectin matrix in the hyaline body cells. Additionally, AGPs, which are present across the hyaline body wall thickness and can act to loosen the pectin network (Lamport *et al.*, 2006; Moore *et al.*, 2013a), could further affect wall rheology. Altogether, these findings suggest that in comparison with the surrounding tissues, wall permeability might be altered in the hyaline body. If this is the case, it might have important consequences for apoplastic transport and, therefore, nutrient translocation through the haustorium.

The outermost layer of hyaline body cells that label with anti-AGP probes differ from those of the inner part of the tissue in that the distribution of JIM5 and AGP epitopes is polarised. This type of heterogeneity is quite unusual as it is typically associated with developmental directionality in embryogenic or differentiating cells (McCabe *et al.*,

1997; Motose *et al.*, 2004) and/or may correspond with structural heterogeneity (Konieczny *et al.*, 2007). For instance, in the latter example, polarity of JIM7 labelling of surface cells in wheat callus overlapped with differences in cell wall thickness. Labelling with JIM8 and JIM15 in pre-division state B cells of carrot in an embryogenic suspension culture demonstrated planar polarity of AGP epitope distribution which was not related to differences in cell wall structure but determined cell fate during somatic embryogenesis (McCabe *et al.*, 1997). The labelled and non-labelled “halves” of B cells gave rise to non-embryogenic (state F) and embryogenic (state C) cells respectively. In differentiating xylem elements of *Zinnia elegans*, *in vitro* and *in planta*, xylogen concentrates in cell walls of the tips of differentiating tracheary elements (Motose *et al.*, 2004). This polarity mediates inductive interactions between differentiating cells allowing structural continuity of the xylem strand. Polarisation in AGP/de-esterified homogalacturonan distribution in the outer cells of the hyaline body is related neither to any apparent structural differences at light or electron microscopy level, nor to proliferation. It is a mystery how this state is achieved and maintained and what its function might be. However, the fact that these biochemically distinctive walls are in contact only with each other, and not with walls of the cortex, suggests that the apoplastic system within the hyaline body might be, to at least some extent, functionally isolated from that of the cortex or that communication between the cells of this tissue is particularly important.

The paramural deposits and globular inclusions within the cytoplasm found in this study are most likely storage materials. While xyloglucan is a known cell wall storage compound in seeds (Reid, 1985; Hoch, 2007), it is somewhat surprising that these bodies are also rich in AGPs and pectins, suggesting functions beyond storage. Although the paramural deposits were not as extensive as those found in *Alectra*, where they filled large volumes of the cells (Visser *et al.*, 1984), they were seen in many haustoria and were numerous. The reason for storage of wall materials in the hyaline body is not known. It might be simply that these carbohydrates are deposited when the plant’s demand for carbon is higher than the amounts taken up from the host or that they form part of a system of osmotic gradients regulation important in the flow of substances into the parasite (Jiang *et al.*, 2010). Although hemiparasites photosynthesise, abstraction of xylem-mobile organic carbon from the host has been documented for both, *Odontites vernus* (Govier *et al.*, 1967) and *Rhinanthus minor*. The latter has been shown to gain as much as 50% of carbon from the host (Tesitel *et al.*, 2010), abstracted mainly as amino acids (Jiang *et al.*, 2010) and very little carbohydrates (Irving & Cameron, 2009). Dominance of amino acids in the abstracted carbon was also the case for *Odontites* (Govier *et al.*, 1967). This suggests that if the carbohydrate-based paramural deposits seen in this study are a means of storing host-derived carbon, processing must occur somewhere between abstraction and deposition and this is most likely achieved within the metabolically active hyaline body itself.

5.4.5 Flange-like parenchyma

Specialised cells with thickened walls adjacent to the xylem bridges and provisionally termed flange-like cells were identified in this study. They appear to be of the same structure as in *Orobanche crenata* (Dörr & Kollmann, 1976), *Euphrasia cuneata* (Fineran, 1987) and *Triphysaria versicolor* (Heide-Jørgensen, 1995). The main similarities are uniform thickening in contact with xylem cells and structural similarity to the unthickened primary cell wall, with no evidence of lignification, as well as organelle-rich cytoplasm. So far, no name has been proposed for these distinctive cells.

A similar type of thickening was seen in *Striga hermonthica* and *S. asiatica*. In these species, highly protoplasmic cells without any transfer cell-like wall modifications surrounded the xylem bridge (Mallaburn & Stewart, 1987). However, thickenings were found in their highly protoplasmic hyaline bodies where they occurred in a polarised manner, as described in this study. The thickenings were composed of an outer, pale fibrillar layer, and an inner dark granular layer, with the two often interdigitating. Figures 5.9F and G show the existence of as many as three non-lignified layers of different electron-lucence, in addition to lignified thickenings. Similar to the findings of Mallaburn & Stewart, 1987, the innermost layer is darker and appears more grainy. Immunodetection results suggest that enrichment of the individual layer in different types of pectins and hemicelluloses is a common feature, while the bulk of the thickened wall generally shows different binding than the unthickened walls. Furthermore, walls of flange-like parenchyma in general often show none or weaker labelling with anti-AGP probes. If AGPs modify the rheological properties of hyaline body walls, possibly contributing to nutrient translocation within this structure, it is difficult to explain why flange-like cells, which are even more obvious candidates for non-vascular apoplastic (as well as symplastic) transport in the haustorium, do not label with the anti-AGP probes.

These immunolocalisation findings are important as little is known about cell wall composition of transfer walls except the rather general information that cellulose and pectins are the main constituents (Offler *et al.*, 2003). DeWitt *et al.* (1999) quantified the relative abundance of different wall components in transfer and non-transfer walls of two endosperm lines of *Zea mays*, one of which exhibited transfer cell morphology. No differences in bulk proportions between cellulose, hemicelluloses and pectin were found, which is in contrast with the qualitative and spatial diversity seen in this project. Dahiya and Brewin (2000) immunogold-localised callose, xyloglucans, pectins and extensins in the labyrinth thickenings of *Pisum sativum* nodule transfer cells and AGPs were localised at the plasma membrane lining the thickenings. Transfer cell ingrowths of *Vicia faba* cotyledons showed positive labelling for all of the above wall components in an extensive immunocytochemical study carried out by Vaughn *et al.* (2007).

Lignified, xylem-like thickenings surrounded by non-lignified material were seen in flange-like cells in some haustoria. The presence of lignified thickenings in cells with living protoplasts is a feature of *flange cells* previously described in association with the xylem of penetrative structures of *Korthalsella* and *Phoradendron* (Fineran, 1996; Fineran & Calvin, 2000). These cells are believed to be specific to parasitic plants (Offler *et al.*, 2003) although they resemble *transfer cells with flange ingrowths* (Offler *et al.*, 2003; Evert, 2006) which are narrow and rib-shaped but not lignified. Flange cells possess a reticulate system of lignified thickenings, closely resembling xylem, while retaining protoplasts. It was impossible to determine in this study whether similar cells with lignified thickenings in *Rhinanthus minor* eventually lose their protoplasts and start functioning as xylem, since no such cells with disintegrating protoplasts were seen. The fact that the lignified thickenings are embedded within the extremely thickened, non-lignified, granular wall could suggest that they are deposited before this abundant material is added. However, lignified thickenings of endophyte xylem in *Orobanche crenata* haustoria are deposited within elaborately thickened, non-lignified transfer walls, which subsequently disintegrate (Dörr & Kollmann, 1976). In either case, the cell cannot function as xylem unless all wall material except the lignified thickenings is dissolved. The energetically-demanding deposition of thickened walls before lignification must be warranted by additional functions of this tissue. A possibility that the cells of flange-like parenchyma remain protoplasmic after the deposition of lignified thickenings and function in analogy to the flange cells of sinkers and suckers of *Korthalsella* and *Phoradendron* cannot be ruled out. If that was the case, it might also be true in some of the interfacial parasite cells with both xylem thickenings and protoplasts present.

Typical transfer cells of plants possess labyrinth ingrowths which increase the surface of plasma membrane, contributing to increased trafficking at the cell surface (Pate & Ireland, 1969; Talbot *et al.*, 2002; Offler *et al.*, 2003). As the thickenings present in flange-like parenchyma do not contribute to increase plasmalemma surface, another function seems more plausible, although even ordinary type parenchyma may perform transfer functions via invaginations of plasmalemma known as plasmatabules (Fineran, 1987). Flanges of *Phoradendron* were demonstrated to form an apoplastic pathway for lanthanum tracers (Fineran & Calvin, 2000) and were proposed to function in apoplastic translocation of nutrients from the host. An increase in apoplastic space necessary for the maintenance of osmotic standing gradients allowing the flow xylem sap was proposed as an additional function (Fineran, 1996; Fineran & Calvin, 2000). However, it is not understood how lignification of the flanges might facilitate these functions. In *Nuytsia floribunda* specialised thickened walls with similar proposed functions in loading and unloading of parasite xylem were present in association with haustorial vessels near the interface (Fineran, 1987). They displayed more pronounced thickening opposite the pit membranes. This resembles the situations seen in *Rhinanthus minor* and *Odontites vernus*, whereby flange-like ingrowths had

penetrated between xylem thickenings and entered xylem lumina, and might be associated with a similar function. Flange-like cells could also form a pathway of symplastic transport to parasite phloem, as suggested by Heide-Jørgensen (1995). It is unlikely that they represent a form of compensation mechanism in response to unfavourable conditions, as previously proposed for *Cuscuta reflexa*, which was found to produce transfer cell-like labyrinth ingrowths on its walls adjacent to xylem when grown on an incompatible host (Christensen *et al.*, 2003). In fact, flange-like parenchyma was absent from haustoria of *R. minor* attached to roots of *Plantago lanceolata* which is an incompatible host (data not shown). This further suggests that it forms an integral element of functional haustoria.

Flange parenchyma is currently the only term found in literature to describe a type of haustorial parenchyma cells that display a range of peculiar wall modifications with putative transfer functions. Therefore, the term *flange-like parenchyma* seems to be an appropriate temporary name for the tissue observed in this study. However, the family of such modified parenchyma cells in haustoria seems quite diverse. The discovery of their presence in the commonly found parasitic species investigated in this study implies that such cells are commonly found in haustoria and are likely to play important roles in their functioning. This will require further study. It would be of particular importance to investigate if, and how, these cells participate in the transfer of solutes between xylem bridges and hyaline bodies and what precise functions are granted by the conspicuous wall modifications.

5.4.6 Haustorial AGPs

AGPs were the most striking feature of the haustorial epitome investigated in this study. Their high concentration in the hyaline body, contact parenchyma and differentiating xylem bridges suggests fundamental, yet ubiquitous functions. As AGPs always co-localised with homogalacturonans, it is very likely that the two classes of molecules interact. AGPs of the hyaline body could interact with pectins differently than those of interfacial parenchyma, rendering de-esterified pectins inaccessible to antibodies in the walls of the former. It would, therefore, be of interest to investigate these potential differences in terms of intermolecular links. Laser microdissection and extractions of AGPs from these two distinctive regions could reveal whether a tighter connection between AGPs and homogalacturonans exists in the hyaline body than in the endophyte.

Although the presence in the hyaline body and contact parenchyma was seen from early developmental stages, it could not be determined whether AGPs accumulated over time and remained stable in the wall or were continuously synthesised and recycled. This is particularly interesting considering that AGPs were previously thought to be turned over between the cytoplasm and cell wall at extremely fast rates

(Gibeaut & Carpita, 1991), but are now believed to be turned over in a less rapid, non-degradative manner within the membrane-periplasm-wall system (Lamport & Kieliszewski, 2005). This possibility seems more metabolically feasible considering the continuous AGP presence in haustoria. Further research into this aspect of haustorial AGP biology could be important for distinguishing between their signalling and structural functions.

Arabinogalactan proteins are an extremely diverse group of membrane and wall-associated, as well as secreted, proteoglycans. They undeniably play important roles in plant structure and functioning although the precise modes of action are yet to be fully elucidated (Seifert & Roberts, 2007; Nguema-Ona *et al.*, 2012). Considering the ubiquitous distribution and fundamental functions of AGPs, one can postulate that they are likely to be present in most, if not all, plant cells. It is, therefore, the qualitative or quantitative differences of specific elements of AGPs (glycan side chains or protein backbone) that determine cell physiology.

From the variety of fundamental roles assigned to AGPs, a number appear particularly relevant to the structure and functioning of a haustorium. These include marking cell fate and control of differentiation, inter and intra-cellular signalling, cell extension or modification of rheological properties and permeability. The variety of these putative functions multiplied by the number of tissues and key developmental stages of haustoria provide an extensive array of possibilities which make interpretation of even the most distinct distribution patterns difficult.

5.5 Conclusions

The most comprehensive immunocytochemical study of parasitic angiosperm haustoria to date was presented in this chapter. It was also the first immunocytochemical, cell wall-focused study of *Rhinanthus* and *Odontites* haustoria and their most detailed anatomical account. Cell wall compositional and structural diversity was related to the main tissue regions within the haustoria, namely the hyaline body, interfacial parenchyma, flange-like parenchyma and xylem. However, examples of distinct cellular heterogeneity were also found in vascular core xylem, outermost cell layer of the hyaline body and in flange-like parenchyma.

The immunocytochemical results presented here demonstrate an apparently high abundance of arabinogalactan protein glycan epitopes in three haustorial regions strategic in the development and functioning of haustoria, namely; contact parenchyma, the hyaline body and differentiating xylem bridge. Despite the difficulties with obtaining early stage haustoria, some light was shed on the approximate stages of development that these characteristic composition patterns are initiated at. The marked presence of AGPs from pre-attachment developmental stages suggests

that this part of haustorial cell wall epitome is very important in the proper functioning of haustoria.

Although interpretation of these results is restricted by the limited understanding of arabinogalactan protein biology, this study is the first to demonstrate AGP presence in important haustorial tissues at several key stages of development. Since LM2-detected epitopes of β -linked glucuronic acid were most ubiquitous, this antibody might prove particularly useful in future studies.

6 An extended menu or a physiological trap? — *Rhinanthus minor* forms haustorial connections with eudicot herbs

6.1 Abstract

Histology and immunocytochemistry of haustorial connections between *Rhinanthus minor* and a range of potential hosts and non-hosts was investigated. Pairings with eleven species, eight of which had not been previously examined as *R. minor* hosts, were analysed for 1) the presence of vascular continuity between the parasite and host, 2) presence of AGPs in the haustorial hyaline body and interfacial parenchyma as well as 3) histological host responses to haustorial invasion.

In contrast to other studies, histological responses were of similar magnitude in all examined hosts and no particular modification of host tissues was identified as a consistent contributor to resistance. Consistently with published data, grasses and legumes were good hosts for *R. minor*. They supported vigorous growth and attracted numerous, fully differentiated haustoria with continuous xylem bridges and well-defined hyaline bodies. However, non-leguminous eudicot hosts showed a higher degree of haustorial penetration than expected from the literature. Development of complete, although most likely non-functional, xylem bridges in haustoria attached to *Plantago lanceolata*, a host formerly classified as resistant, is reported here for the first time. Parasitic growth was poor on this host, suggesting a multi-layered character of resistance with post-penetration mechanisms being in place. Parasite growth on *Prunella vulgaris* was similar to that on *P. lanceolata* roots although xylem bridges were more commonly formed and better developed. *Daucus carota* and *Pimpinella major* allowed development of numerous and fully differentiated haustoria and supported good growth of the parasite.

The characteristic localisation of AGP glycan epitopes detected by LM2 in the hyaline body and interfacial haustorial parenchyma was conserved in good hosts. Non-hosts *Plantago lanceolata* and *Prunella vulgaris* showed considerably weaker labelling of the poorly developed hyaline bodies. Labelling was also absent from the interfacial parenchyma when attached to *Prunella*. Lower concentrations of AGP epitopes in the hyaline body and poor differentiation of the xylem bridge were the most consistent features of haustoria attached to non-hosts. However, presence of AGPs at the interface was not consistently related to host quality.

These results show that host specificity is not absolute within the three functional host groups and that the haustorial AGP distribution described in chapter 4 is important to haustorial functioning and severely affected only in the cases of extremely bad host quality.

6.2 Introduction

Knowledge of haustorial structure is crucial to the understanding of parasite-host interactions at the ecological level and confident determination of host ranges. Non-resistant hosts allow successful haustorial development and subsequent nutrient transfer. As a consequence, they support parasite growth while suffering negative consequences, for instance reduction in biomass and reproductive output. On the other hand, resistant hosts (non-hosts) mount effective defences in response to parasitism, limiting or preventing damage. These differences in susceptibility result in 1) selective damage followed by 2) shifts in competitive abilities in favour of non-hosts leading to changes in community structure (Press & Phoenix, 2005; Watson, 2009). It is therefore essential to know the host ranges of parasitic angiosperms when predicting their impact on agrisystems as well as semi-natural communities. Knowledge of host ranges is also important for the conservation of declining parasitic species, even in case of generalist parasites (Marvier & Smith, 1997), which often utilise hosts disproportionately to their availability, depending on the degree of compatibility (Kelly *et al.*, 1988; Gibson & Watkinson, 1989; Lemaitre *et al.*, 2012).

Definition and confident establishment of a host range can be problematic as ecological factors often lead to exclusion of species that prove to be hosts under experimental conditions (Heide-Jørgensen, 2008). Nevertheless, examination of haustorial connections must form an important part of a successful approach. Although several authors have determined host ranges by looking simply at the presence or absence of haustorial connections (Gibson & Watkinson, 1989; Tennakoon *et al.*, 1997; Suetsugu *et al.*, 2008), superficially similar haustoria on different hosts may differ in their anatomy, depending on the degree of compatibility with the parasitized species. Therefore, clearing or sectioning of haustorial material need to be carried out to confirm presence of xylem continuity between the parasite and the host. In addition to xylem bridge anatomy, the structure of a haustorial hyaline body — central parenchymateous region of high metabolic activity found in many species, has been shown to be a better indicator of host quality than the presence of a vascular link (Gurney *et al.*, 2003). Nevertheless, comparative histological studies of haustorial anatomy on different hosts are limited in number, concern predominantly economically important crop weed species of parasites, and have involved only small numbers of host species. While species from the genera *Striga* (Dörr, 1997; Gurney *et al.*, 2003, 2006; Vasey *et al.*, 2005; Yoshida & Shirasu, 2009; Cissoko *et al.*, 2011; Jamil *et al.*, 2011) or *Orobancha* (Dörr & Kollman, 1995; Losner-Goshen, 1998; Goldwasser *et al.*, 2000; Pérez-de-Luque *et al.*, 2006, 2007, 2008) have been subjects of several anatomical studies, the time-consuming character of the work results in researchers tackling small numbers of hosts at a time. Examples include interactions of *Alectra vogelii* with one host and two non-hosts (Visser *et al.*,

1990), *Viscum album* with one host and one non-host (Hariri *et al.*, 1991), *Striga asiatica* with one host and three non-hosts (Hood *et al.*, 1998).

The subject of this study, *Rhinanthus minor*, is species of semi-natural grassland ecosystems of the northern hemisphere (Westbury, 2004) and the most extensively studied parasitic angiosperm not related to crop loss. This is a consequence of its ability to mediate competition in grassland communities through reduction of grass growth and allowing forbs to compete more successfully (Gibson & Watkinson, 1991). The varying impact on different groups of grassland species has been practically applied in grassland biodiversity restoration (Davies, 1997; Pywell *et al.*, 2004; Bullock & Pywell, 2005; Westbury *et al.*, 2006). The influence of *R. minor* on semi-natural grassland structure has been the subject of numerous ecological studies complimented by physiology and biomass-focused growth experiments. The former included measurements of host and parasite photosynthetic rates (Seel, 1996; Cameron *et al.*, 2008), water and solute transfer (Seel & Parsons, 1993; Seel & Jeschke, 1999; Jiang *et al.*, 2003, 2005, 2008a,b; Jiang, 2004; Cameron & Seel, 2007) including hormone abscisic acid (ABA) fluxes (Jiang, 2004; Jiang *et al.*, 2004), effect of light on the parasite (Hwangbo & Seel, 2002) and effects of CO₂ availability on the parasite (Hwangbo *et al.*, 2003). Effects on host biomass from different studies were meta-analysed by Ameloot and colleagues (2005), showing a general trend to reduce host and overall vegetation biomass reduction in the occupied communities. A number of studies of *Rhinanthus* show that the outcome of parasitism is a function of ecological factors such as host and parasite density (Van Hulst *et al.*, 1987; Pywell *et al.*, 2004; Ameloot *et al.*, 2006; Westbury & Dunnett, 2007), distance from each other (Keith *et al.*, 2004), soil nutritional status (Salonen & Puustinen, 1996; Cameron *et al.*, 2005) or host defoliation (Salonen & Puustinen, 1996), as well as physiological factors, mainly host resistance mechanisms at haustorial interfaces (Cameron *et al.*, 2006; Cameron & Seel, 2007; Rümer *et al.*, 2007). Anatomical accounts of the *Rhinanthus minor* haustorial structure on 4 hosts (grasses *Cynosurus cristatus*, *Hordeum vulgare* and *Phleum bertolonii* and a legume *Vicia cracca*) and 2 non-hosts (non-legume eudicots *Leucanthemum vulgare* and *Plantago lanceolata*) exist. Furthermore, anatomical barriers in the form of encapsulation in lignin, suberin or dead cells resulting from hypersensitive response induced in the interfaced tissues of non-hosts were proposed as the main determinants of their resistance (Cameron *et al.*, 2006; Rümer *et al.*, 2007) and correlated with the ability of the parasite to abstract nutrients from the host (Cameron & Seel, 2007). Together with the results of ecological studies, this formed the basis for the distinction of three main functional host groups: 1) grasses (good hosts), 2) herbaceous legumes (good hosts) and 3) non-leguminous eudicots (bad hosts), with some authors (Ameloot *et al.*, 2005, 2006) additionally distinguishing other graminoids in biomass studies without histological verification of their hosting quality. The histological approach was a break-through in understanding the basis for this way of grouping and yielded interesting preliminary results in terms of cell wall involvement in physical barrier formation in parasitized hosts. However, evidence

for cell wall lignification and/or suberisation was not followed up in terms of different cell wall molecules, for example glycoproteins or pectins, a wider range of hosts or more precise and specific localisation techniques such as immunocytochemistry. While this might not be very surprising considering the general crop-weed focus of parasitic plant research, immunocytochemical studies of haustorial connections in general are very scarce (Olivier *et al.*, 1991; Reiss & Bailey, 1998; Losner-Goshen, 1998; Neumann *et al.*, 1999; Vaughn, 2003, 2006).

As presented in chapter 4, AGP glycan epitopes are concentrated in the walls of haustorial contact parenchyma and the hyaline body of *Rhinanthus minor* haustoria. The monoclonal antibody (mAb) LM2 directed against beta-linked glucuronic acid of the glycan side chains of AGPs labelled epitopes present in the haustorium particularly strongly and consistently. Other AGP epitopes of uncharacterised structure, e.g. as recognised by the mAbs JIM8 and JIM14 often co-localised with LM2 labelling, suggesting the presence of multiple epitopes associated with AGPs either co-occurring in a single type of glycan chain or in multiple side chains. Furthermore, de-esterified pectin labelling with antibodies JIM5, LM18 and LM19 was absent or considerably weaker in the hyaline body, overlapping precisely with AGP labelling (Fig. 5.24). The aim of research presented in this chapter was to investigate whether this pattern of epitope distribution was conserved between haustoria of *Rhinanthus minor* growing on hosts and non hosts and if it is, therefore, related to host quality. To achieve this, twelve species occurring locally with *Rhinanthus minor* were examined histologically to determine if successful haustorial connections were established. Eight species were subsequently selected for immunohistochemical studies. The criteria were the ease of germination and growth, although *Pimpinella major* and *Prunella vulgaris*, which were difficult to germinate, were used as it was important to further investigate as many eudicot hosts as possible. The selected species included a grass (*Arrhenatherum elatius* var. *bulbosum*), legumes (*Anthyllis vulneraria*, *Lathyrus pratensis* and *Vicia sepium*) and eudicots (*Daucus carota*, *Pimpinella major*, *Plantago lanceolata* and *Prunella vulgaris*) were selected. It was also investigated whether any particular histological responses in the selected hosts related to host resistance and altered AGP distribution in the haustoria. Details of immunolabelling and histological staining are described in chapter 3.

6.3 Results

6.3.1 Haustorial anatomy and immunocytochemistry in different parasite-host pairings

All *Rhinanthus minor* planted with *Plantago lanceolata* pre-grown for one month failed to develop properly. Seedlings stopped growth after the first pair of leaves emerged, remained at that stage for up to four weeks and died. No haustoria were developed by this lot of plants. All other parasite-host pairings, including those where *R. minor* was planted with three-day old *Plantago lanceolata*, yielded attached haustoria.

However, the growth of *Rhinanthus minor* was particularly good on legumes *Vicia sepium* and *Lathyrus pratensis* and grasses and exceptionally bad on *Plantago lanceolata* and *Prunella vulgaris*. *Daucus carota* was also a good host in terms of biomass produced by the host although growth was slower. Figure 6.1 compares

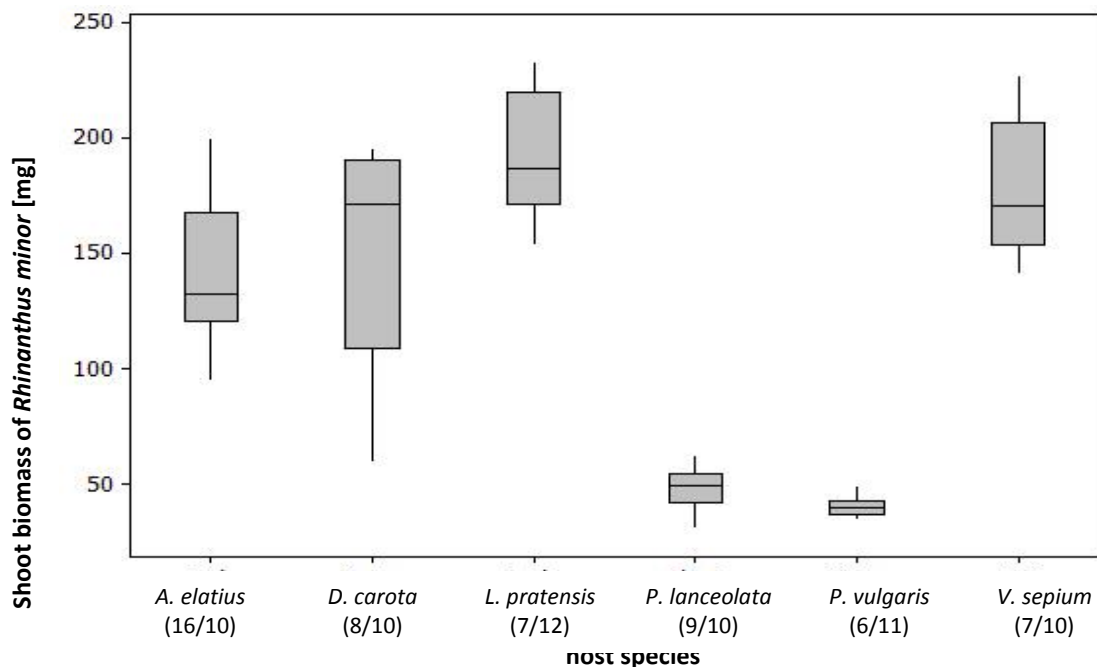


Figure 6.1: Boxplot of shoot biomass of *Rhinanthus minor* grown with different hosts. Numbers in brackets: number of replicates/age of the parasite in weeks when harvested. Parasitism on *P. lanceolata* and *P. vulgaris* resulted in considerably lower parasite biomass than when attached to good hosts.

Table 6.1: Morphology of *Rhinanthus minor* grown with different hosts

Host species	Morphological features of <i>R. minor</i>		
	leaf colour	branching	mean number of flowers per plant
<i>Lathyrus pratensis</i> ⁴ <i>Vicia sepium</i> ⁴	very dark green	1 st degree branching present at 2 nodes	3.2 (7 plants) 3.4 (7 plants)
<i>Arrhenatherum elatius</i> ssp. <i>bulbosum</i> ⁴	dark green	no branching	2.7 (20 plants)
<i>Cynosurus cristatus</i> ¹ <i>Holcus lanatus</i> ³ <i>Lolium perenne</i> ³	dark green	no branching	flowering present but numbers not recorded
<i>Daucus carota</i> ³	dark green	no branching	1.8 (8 plants)
<i>Plantago lanceolata</i> ²	pale green, 2 youngest pairs of leaves yellow-green	no branching	flowers never present (9 plants grown with young <i>P. lanceolata</i>)
<i>Prunella vulgaris</i> ⁴	pale green	no branching	flowers never present (6 plants)
<i>Anthyllis vulneraria</i> ⁴ <i>Medicago lupulina</i> ³ <i>Pimpinella major</i> ⁴	dark green	not applicable: plants attacked by a fungus and harvested prematurely, developed well prior to infection	

1 — species previously determined as a good host based on haustorial anatomy and growth experiments Cameron *et al.*, 2006; Cameron & Seel, 2007

2 — species previously determined as a non-host based on haustorial anatomy and growth experiments Cameron *et al.*, 2006; Cameron & Seel, 2007; Rümer *et al.*, 2007

3 — species previously recorded as a host through sward excavation (Gibson & Watkinson, 1989) but not examined anatomically

4 — species previously not recorded as a host and not examined anatomically

biomass of the parasite grown with *Arrhenatherum elatius* var. *bulbosum*, *Daucus carota*, *Lathyrus pratensis*, *Plantago lanceolata*, *Prunella vulgaris* and *Vicia sepium*. Measurements were not taken for hosts infected by fungi and harvested prematurely, i.e. *Anthyllis vulneraria*, *Medicago lupulina* and *Pimpinella major*. Table 6.1 summarises the morphology of *R. minor* grown with different hosts.

The differences in growth of *R. minor* were related to differences in haustorial anatomy. However, the differences in haustorial structure between non-hosts *Plantago lanceolata* and *Prunella vulgaris* and good hosts were not always very clear.

Figure 6.2 illustrates anatomy and LM2 labelling of haustorial connections with *A. elatius* and the three legume species; *Anthyllis vulneraria*, *Lathyrus pratensis* and *Vicia sepium*. Haustoria on these hosts developed as expected for potential good hosts, penetrating host stele, accessing its xylem and showing clear differentiation of the hyaline body. Immunolocalisation of AGPs yielded distributions as described in chapter 4, i.e. the hyaline body and interfacial contact parenchyma (called parasite contact parenchyma — Pcp for easy identification of parasite versus host (H) cells at the interface) of the endophyte labelled with the anti AGP mAb LM2. Vessel cytoplasm of partly differentiated xylem bridges also labelled with LM2 (Fig. 6.2G). More surprisingly, penetration of the stele was also achieved in all non-legume eudicot hosts, i.e. the potential non-hosts (Fig. 6.3B, D, F and H). Their steles were penetrated by the endophytes with contact parenchyma cells differentiating into xylem and forming part of continuous xylem bridges. Clear contact between the endophytic xylem and xylem of all examined eudicots was seen (Fig. 6.4).

Differences in parasite growth were correlated with differences in general robustness of haustoria, particularly the anatomy of hyaline body and xylem bridge as well as AGP immunolocalisation patterns. *Daucus carota* and *Pimpinella major* supported good haustorial development (Fig. 6.3A–D) associated with good growth of the parasite (Fig. 6.1 and table 6.1). The latter was monitored until flowering on *D. carota*. As *R. minor* growing with *P. major* was infected by a fungus four weeks post inoculation and had to be harvested in the fifth week, flowering was not observed although growth prior to infection was good. Endophyte xylem in haustoria of these two eudicots was abundant and the vessels were large (Fig. 6.4A–D). Open ducts were formed via dissolution of parasite xylem cell tips in contact with host vessels. Direct lumen-lumen contact was usually achieved via abutment although in one haustorium attached to *Pimpinella major* early stage osculi were present as well (Fig. 6.4D). Interfacial parenchyma labelled with anti-AGP probes although the labelling with LM2 was often absent or weak on *D. carota* (Fig. 6.3C). However, JIM8 or JIM14 detection usually yielded weak labelling in those cases (data not shown). Well-marked hyaline bodies labelled intensely with LM2 on both hosts (Fig. 6.3C and E).

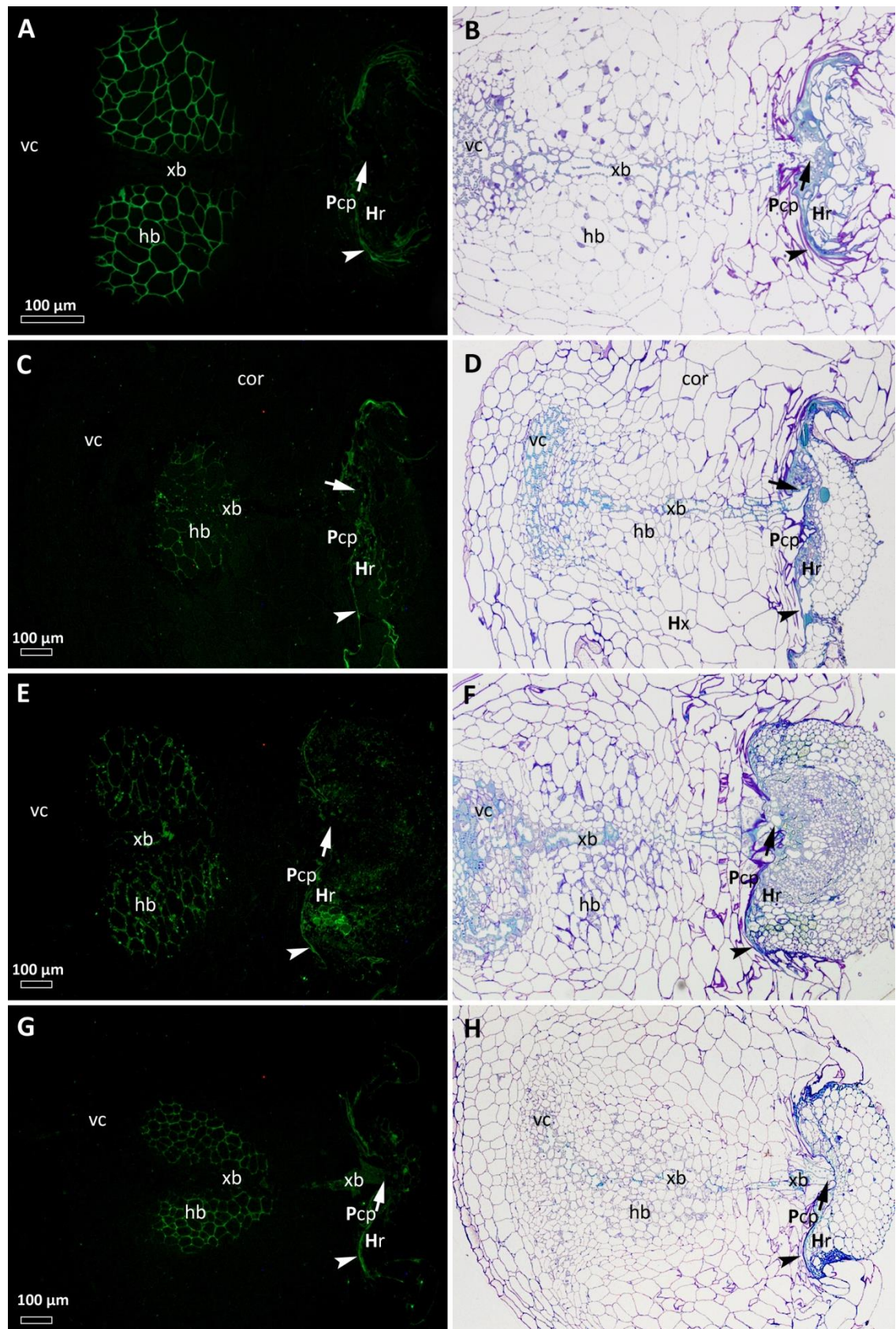


Figure 6.2: Haustorial connections of *R. minor* with *A. elatius* (A–B), *Anthyllis vulneraria* (C–D), *Vicia sepium* (E–F) and *Lathyrus pratensis* (G–H) immunolabelled with an anti-AGP mAb LM2 (A, C, E and G) and stained with toluidine blue O (B, D, G and H). A continuous xylem bridge (xb) is present in all pairings and contact between parasite and host root (Hr) vessels is indicated (◄). There is strong labelling of the hyaline body (hb) as well as parasite contact parenchyma (Pcp) along the parasite-host interface (◄). Cytoplasm of a partly differentiated xylem bridge is also visible (G). Host root labelling is also visible but is not concentrated near the parasite's endophyte parenchyma. Note that host roots also label.

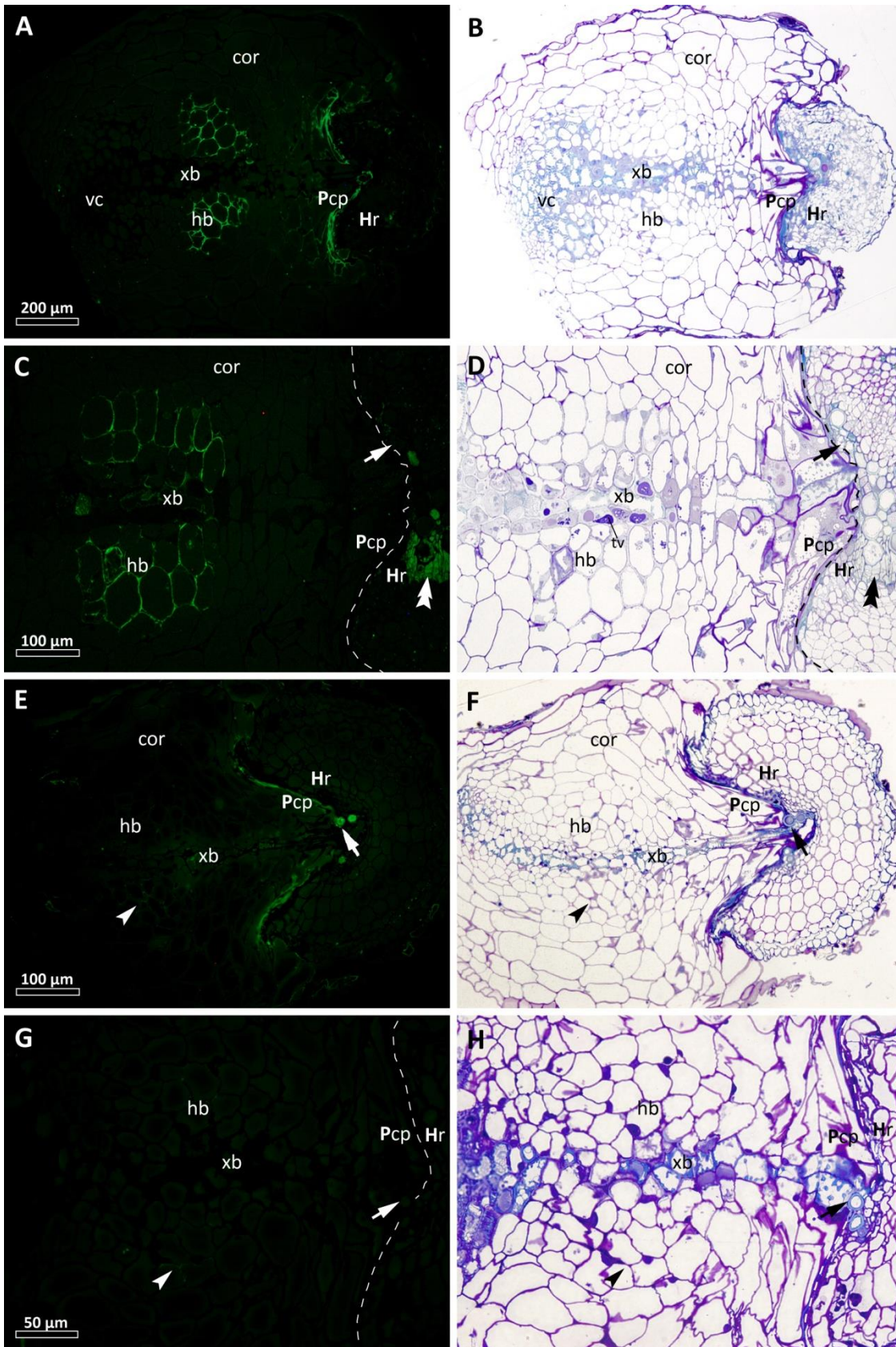


Figure 6.3: Haustorial connections of *R. minor* with *P. major* (A–B), *D. carota* (C–D), *P. lanceolata* (E–F) and *P. vulgaris* (G–H) immunolabelled with an anti-AGP mAb LM2 (A, C, E and G) and stained with toluidine blue O (B, D, G and H). Continuous xylem bridge (xb) is present in all pairings with intraspecific vessel contact indicated (◄). Hyaline body (hb) labelling is extremely weak (◄) in haustoria attached to roots (Hr) of *P. lanceolata* (E) and *P. vulgaris* (G) and strong on the other two hosts. Labelling is absent from parasite contact parenchyma (Pcp) at interfaces (dashed line) with *D. carota* and *P. vulgaris*. ◄— autofluorescent tissue region unquenched by toluidine blue staining. Note that *P. lanceolata* vessel lumina also label.

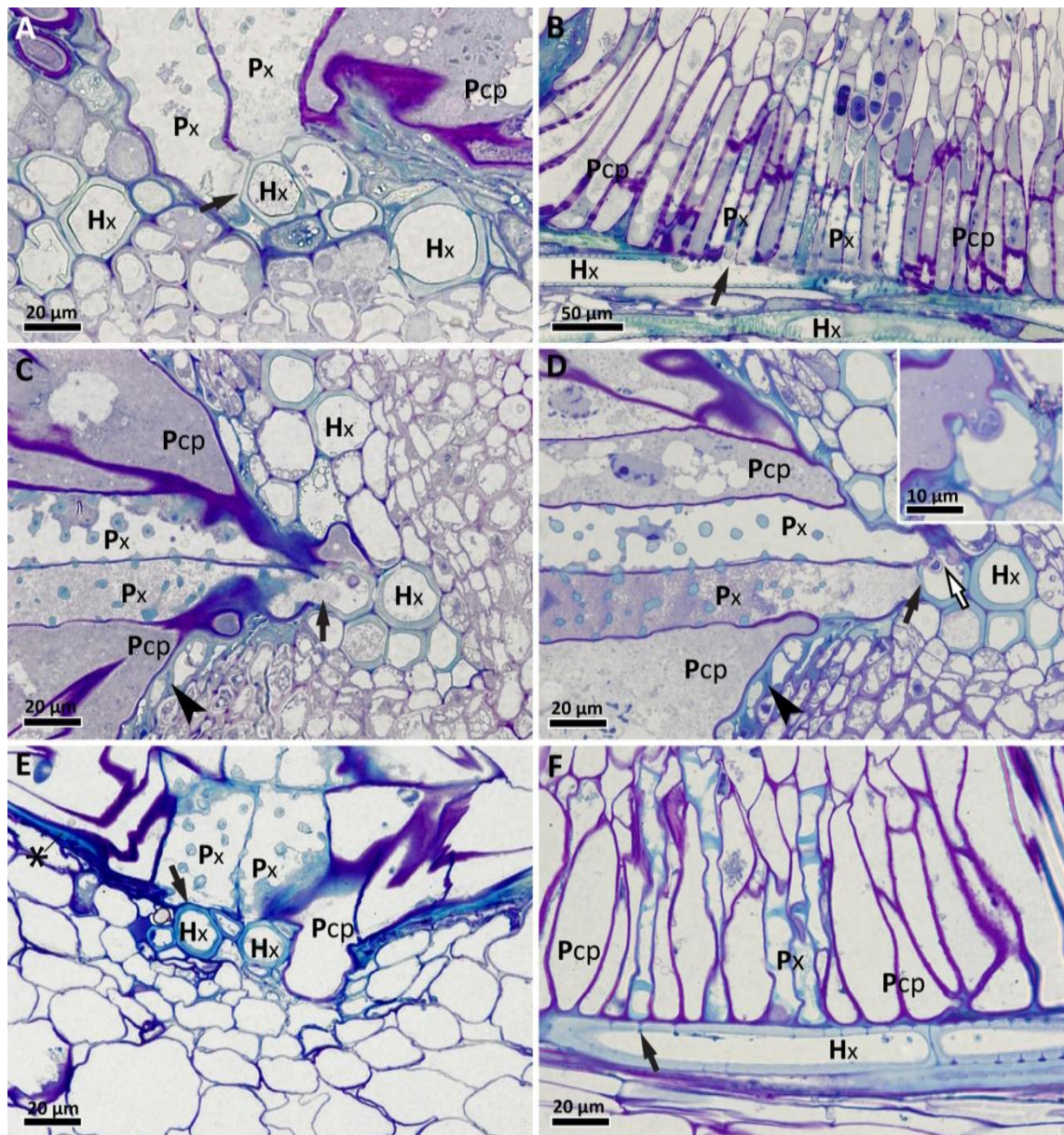


Figure 6.4: Detail of host xylem in haustorial connections of *R. minor* with eudicots *D. carota* (A,B), *P. major* (C,D), *P. vulgaris* (E) and *P. lanceolata* (F) stained with toluidine blue O. Direct contact between parasite's xylem (Px) and contact parenchyma (Pcp) and host xylem (Hx) is achieved through abutment (←) or formation of osculi (↔). Dissolution of the parasite xylem wall in contact with the vessels of all hosts except *P. lanceolata* is apparent from a considerable reduction in staining. Lumen-lumen continuity is apparent in figures B, C and D and results of host xylem wall dissolution (B) or penetration of pits (C and D). One vessel can be abutted by parasite's xylem (C) or penetrated by osculi (D). Note that the osculum wall is not lignified while the remaining portion of the cell already displays the lignified secondary thickenings characteristic of xylem. Some thickened and lignified parenchyma walls (◄) are present in *P. major* cortex (C and D). Phenolic-rich, extramural interfacial deposits (*) are visible at the interface with *P. vulgaris* (E).

In contrast with haustoria attached to *D. carota* and *P. major*, endophyte xylem at the interfaces with *Plantago lanceolata* was clearly less abundant, the cells were considerably narrower than on other hosts and direct openings were never observed (Fig. 6.4F and 6.5F). Xylem was either absent (Fig. 6.5D) or very scarce (Fig. 6.5F) in haustoria attached to *Plantago* roots with secondary growth. In one case, the axial strand was connected to only one xylem cell in the endophyte and this cell did not

appear to have gained lumen-lumen continuity with the abutted host vessel (data not shown). While there were no cases of endophytic xylem presence without the axial strand having also developed in any of the examined haustoria, one haustorium attached to *Plantago* possessed no endophytic xylem while the axial xylem strand was present (data not shown). Therefore, the range of haustoria formed on *Plantago* included those with 1) no xylem bridge, 2) an axial strand but no endophytic xylem (only on roots with secondary growth) and 3) a continuous xylem bridge with one or several terminal endophytic xylem elements (mainly on roots with primary growth). Flange-like cells associated with the xylem bridge, such as those seen on good hosts (chapter 5, Fig. 5.9) were never seen at light microscopy level on *Plantago* and electron microscopy revealed only very slight thickening of walls in these cells (data not shown). All haustoria attached to *Prunella vulgaris* had developed well marked xylem bridges with endophytic xylem (Fig. 6.3H). Vessels of the endophyte were at least in some cases able to develop similar to vessels in contact with good hosts (Fig. 6.4E) although vessels similar to those in *R. minor* parasitizing *Plantago* were also observed and no clear lumen-lumen continuity was seen (data not shown).

In addition to scarcer haustorial xylem, haustoria attached to *Prunella* showed no labelling with LM2 in the interfacial parenchyma (Fig. 6.3G), although the tissue always labelled strongly when attached to *Plantago* (Fig. 6.3E and 6.5A, C and E). Consistently, attachment to these two species resulted in less differentiated hyaline bodies, which never possessed dense cytoplasm or storage materials seen during attachment to good hosts and were strongly vacuolated (Fig. 6.3H and 6.6H). Nuclei could usually be seen (Fig. 6.6H) although they were never as large as in the hyaline bodies on good hosts. The most notable difference appeared to be in the strength of labelling with anti-AGP probes. Labelling with the LM2 mAb was typically much weaker in haustoria attached to *Plantago* and *Prunella*, often did not become visible until x40 magnification was applied, and exposure times approximately twice as long (in the range of 1000 to 2000 ms), as for good hosts were used. Furthermore, de-esterified pectin epitopes were present as shown for *Plantago lanceolata* in figure 6.5G. this was in contrast with haustoria attached to good hosts, where labelling for de-esterified pectins with the mAb JIM5 was absent or much weaker in the hyaline bodies (chapter 5, Fig. 5.13, 5.14 and 5.24).

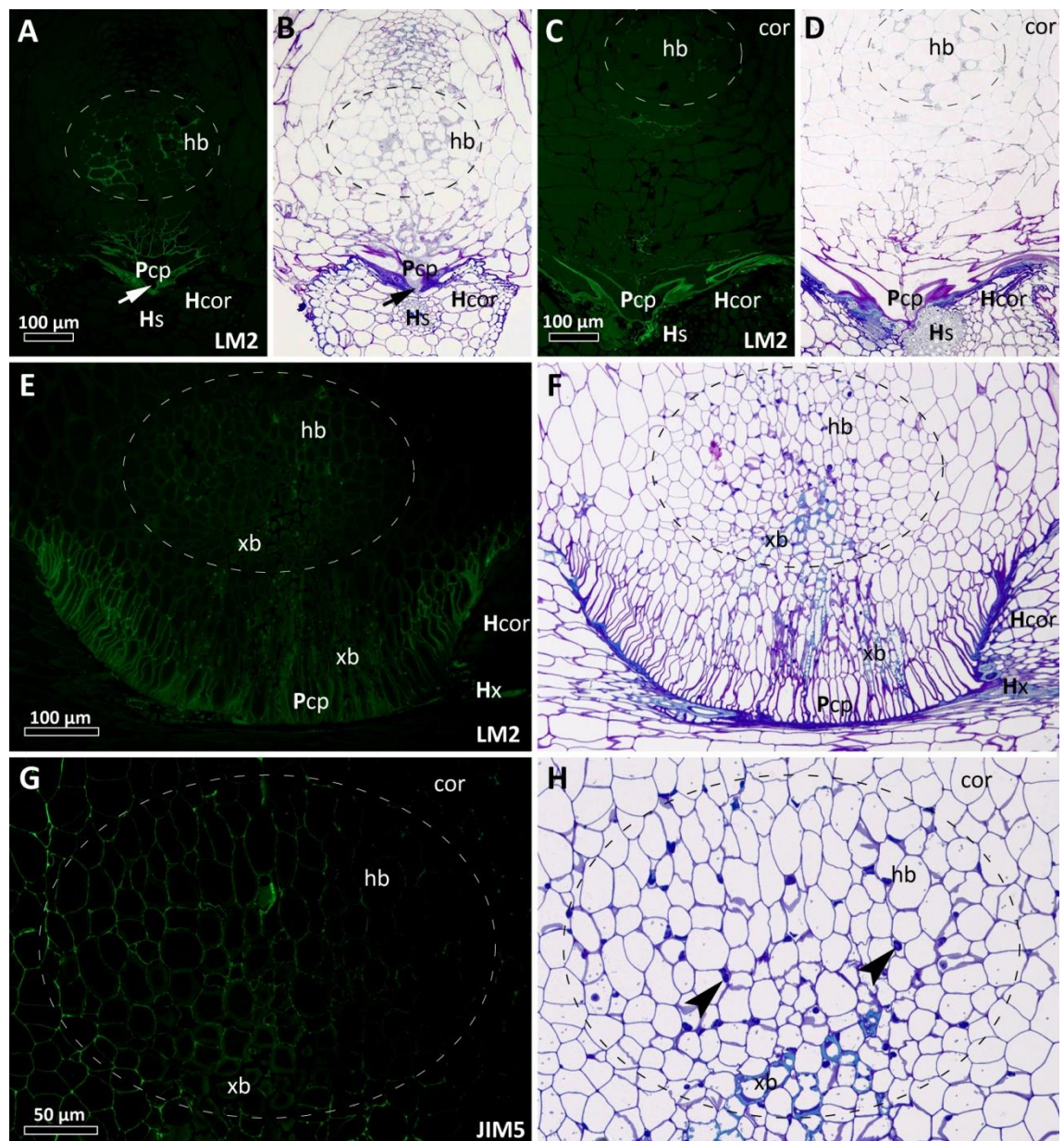


Figure 6.5: Structure and immunocytochemistry of three different haustoria of *R. minor* attached to *P. lanceolata*. Initially, the haustoria develop normally with LM2 labelling present in the hyaline body (◀) and contact parenchyma of the parasite (Pcp) (A and B). Haustorium depicted in figures A and B appears to have been still growing at the time of collection as evidenced by a highly protoplasmic contact cell aiming for the host stele (Hs). In mature haustoria (C–H), labelling of the hyaline body with LM2 is much weaker than in the interfacial peranchyma (C and E) and de-esterified pectin epitopes are detected (G). This is true for haustoria that do (F and H) and do not (D) develop a xylem bridge. The hyaline bodies display enlarged nuclei (◀) but are not highly protoplasmic.

6.3.2 Histology and immunocytochemistry of host responses

Scarcity of early stage haustoria did not allow investigations of any potential defence responses localised at the epidermis or hypodermis during early stages of penetration. Therefore only defences mounted at the cortex and stele are described. Table 6.3 summarises host responses and haustorial features examined in this study.

Table 6.2: Summary of anatomical and immunohistochemical features of *Rhinathus minor* haustoria and parasitised host roots.

feature	grasses					legumes				non-legume eudicots				<i>R. minor</i>
	<i>A. stol</i>	<i>A. elat</i>	<i>C. cris</i>	<i>H. lana</i>	<i>L. pere</i>	<i>A. vuln</i>	<i>L. prat</i>	<i>M. lupu</i>	<i>V. sepi</i>	<i>D. caro</i>	<i>P. majo</i>	<i>P. lanc</i>	<i>P. vulg</i>	
access to stele	✓	✓	✓	✓	✓	✓	✓	✓	✓	✓	✓	✓	✓	✓
xylem bridge	✓	✓	✓	✓	✓	✓	✓	✓	✓	✓	✓	✓/—	✓	✓
vessel abutment	✓	✓	✓	✓	✓	✓	✓	✓	✓	✓	✓	✓	✓	✓
luminal continuity	n/i	✓	n/i	✓	✓	—	✓	✓	✓	✓	✓	✓/—	—	—
distinctive hyaline body	✓	✓	✓	✓	✓	✓	✓	✓	✓	✓	✓	✓/—	✓/—	✓
AGPs in contact parenchyma	n/i	✓	n/i	✓	✓	✓	✓	n/i	✓	✓	✓	✓	✓	✓
phenolic-rich interfacial layer (PRIR)	✓	✓	✓	✓	✓	✓	✓	✓	✓	✓	✓	✓	✓	✓
AGPs and extensins in crushed cells and PRIR	n/i	✓	n/i	n/i	n/i	n/i	✓	n/i	n/i	n/i	✓	✓	n/i	n/i
crushed cortex parenchyma	✓	✓	✓	✓	✓	✓	✓	✓	✓	✓	✓	✓	✓	✓
crushed stele parenchyma	n/i	✓	n/i	✓	✓	✓	✓	✓	✓	✓	✓	✓	✓	✓
necrotic host cells at interface	—	—	—	—	—	✓	—	—	✓	✓	—	✓	—	—
necrotic parasite cells at interface	—	—	—	—	—	—	—	—	—	—	—	✓	—	—
occluded vessels	n/i	+	n/i	+	+	++	—/+	+	+/++	+/++	+/++	++	++	—

n/i not investigated, ✓ present, — absent or not observed, + scarce (within individual samples), ++ abundant

A number of defence responses were identified histologically in different hosts, although they were generally insufficient in stopping the penetration of tissues by the haustorium. No evidence for physical blocking of the parasite by a mechanically reinforced encapsulation layer of lignin, suberin or callose was seen in any of the examined haustoria and the penetrating cells of the endophyte managed to reach host xylem on all hosts (Fig. 6.2 and 6.3) even in those samples where extensive host cell death had taken place at the interface (Fig. 6.6).

Similar to the findings described in the previous chapter, a layer of extramural interfacial deposits of thickness similar to parasite contact cell walls was found in all parasite-host combinations examined. It formed a line of light blue staining with toluidine blue O, clearly seen at high magnifications in some haustoria (Fig. 6.4E and 6.8B), while not being apparent in others. Presence of these extramural interfacial phenolics was generally not correlated with host quality and might have functions other than host defence, as further discussed in chapter 6. In general, phenolics were found lining the interfacial space or filling host necrotic cells but lignification of host walls was almost never apparent. In fact, it was the parasite contact parenchyma that in some cases displayed very pronounced lignification (Fig. 6.6C–F). One of a few rare examples of host wall reinforcement through thickening and lignification was observed in the root of an apparently good host *Pimpinella major* (Fig. 6.4C and D).

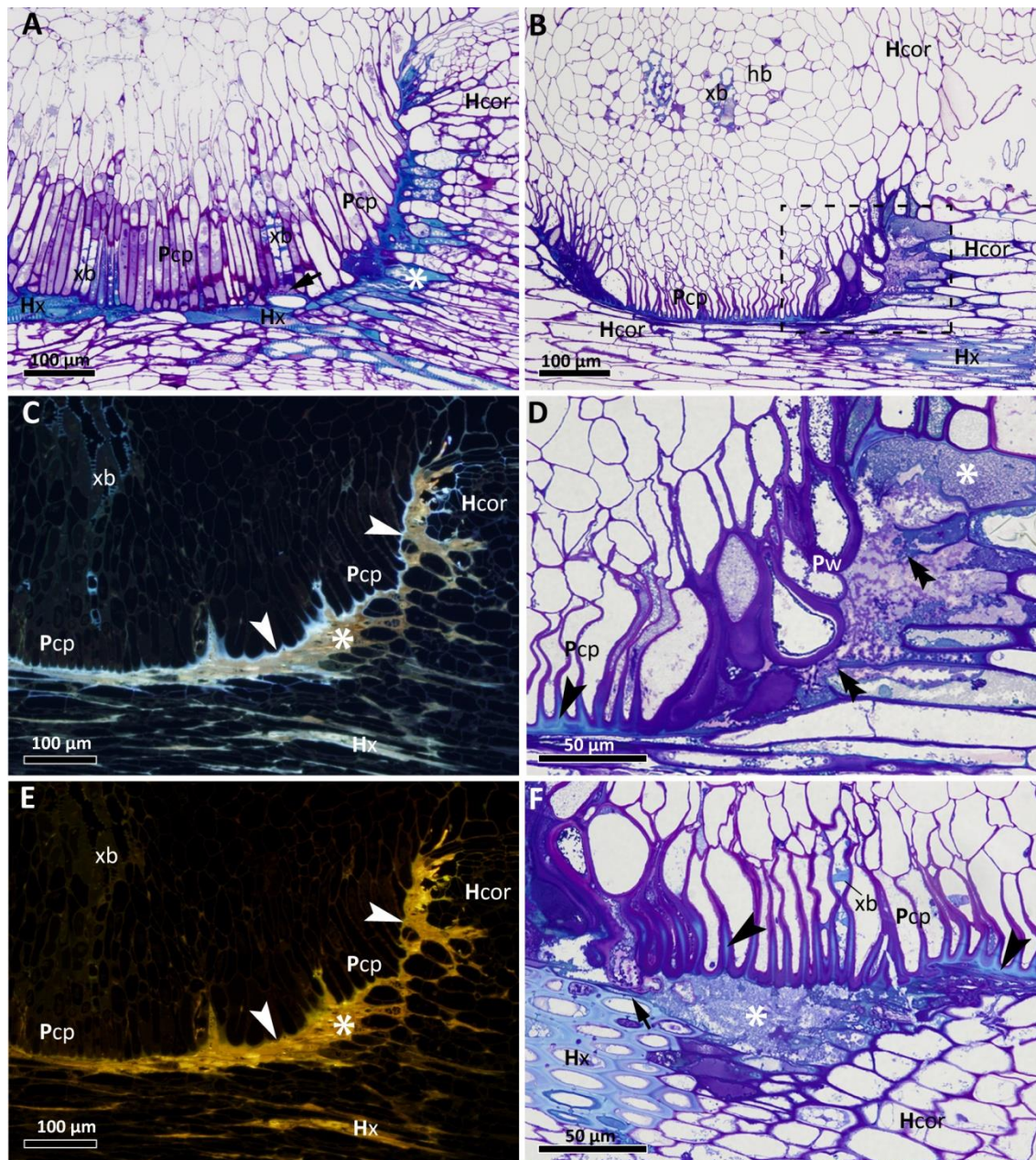


Figure 6.6: Cell death in roots of *D. carota* (A, C and E) and *P. lanceolata* (B, D and F) parasitized by *R. minor*. Sections were taken longitudinally to *D. carota* root and slightly obliquely to *P. lanceolata* root axis. Samples in figures A, B, D and F are stained with toluidine blue O. Images in figures C and E depict one unstained section taken from the same haustorium as the section in figure A, excited by UV light (blue channel) and blue light (green channel). Figure D shows a magnified region of figure 1 as indicated by the dashed line. Figure F depicts a section taken from a haustorium attached to a root with secondary growth. A layer of dead cells and their debris (\ast) lines most of the interface in *D. carota* while occurring in patches in *P. lanceolata*. Interruption of host walls (\blackleftarrow) is evident. Walls of the parasite contact parenchyma (Pcp) are lignified (\blackleftarrow) as seen by light blue autofluorescence in the blue channel (C) and light blue staining with toluidine blue O (D and F). Parasite xylem bridge (xb) vessels are in contact (\blackleftarrow) with host xylem (Hx) in *D. carota* (A) while very scarce xylem is present in the endophyte penetrating *Plantago lanceolata* (F). A parasite's necrotic parenchyma cell abuts (\blackleftarrow) the xylem of this host.

Dead cells were seen in the interfacial regions of all hosts. Most consistently, a layer of mechanically crushed, necrotic cells could be observed, particularly at the lateral interface, compressed by the clasping folds (Fig. 6.9B, D, F, H and J). The disintegrated protoplasts of crushed interfacial cells were often labelled with anti-AGP

and anti-extensin probes (Fig. 6.10A–C, Fig. 9A and B). Below this layer, healthy cortex cells occurred. However, below the layer of compressed cells in *Daucus* and *Plantago* roots, dead but not compressed cells with some cell wall interruptions were seen, suggesting programmed cell death rather than necrosis. This was seen only on larger host roots and in case of *Plantago* it had a localised character, often occurring in patches rather than surrounding the endophyte in a continuous layer. Although appearing very severe, these changes did not prevent access of penetrating *Rhinanthus* cells to host vasculature as endophyte cells were always able to establish contact. In a sample of *R. minor* attached to *Plantago* with highest levels of necrosis the endophyte still reached the host xylem (Fig. 6F) although no xylem bridge was present. Nevertheless, the interface with young (primary growth) *Plantago* roots was typically clear of disintegrating cells and the only visible defence was the occlusion of some vessels (Fig. 6.11D). In some roots with secondary growth, the interface was similarly clean, at least in parts (Fig. 6.5D).

In *Daucus carota* the phenolics filling these dead cells appeared to be of a different character than found in other hosts as evidenced by unsuccessful quenching with toluidine blue O and strong residual autofluorescence (Fig. 6.3C and chapter 3, Fig. 3.4G–I). They also fluoresced bright yellow when viewed under blue excitation and with a long pass filter applied (Fig. 6.6C and E), suggesting flavonoids (Valette *et al.*, 1998). In haustoria attached to this host, endophyte parenchyma and flange-like parenchyma associated with the axial strand of the xylem bridge often possessed vacuoles which stained very dark blue or purple with toluidine blue O (Fig. 6.3D, 6.4B and 6.11C). These appeared to be tannin vacuoles with a possible role in detoxifying phenolics from carrot.

Anthyllis vulneraria roots displayed a very conspicuous modification at and several millimetres from the points of haustorial attachment. Isolated, regularly scattered parenchyma cells of the cortex were filled with phenolics, most likely tannins, which gave the cells a striking brown-red colouration, readily observable under the stereomicroscope (not shown). In sectioned material, these cells stained blue-green with toluidine blue O (Fig. 6.7).

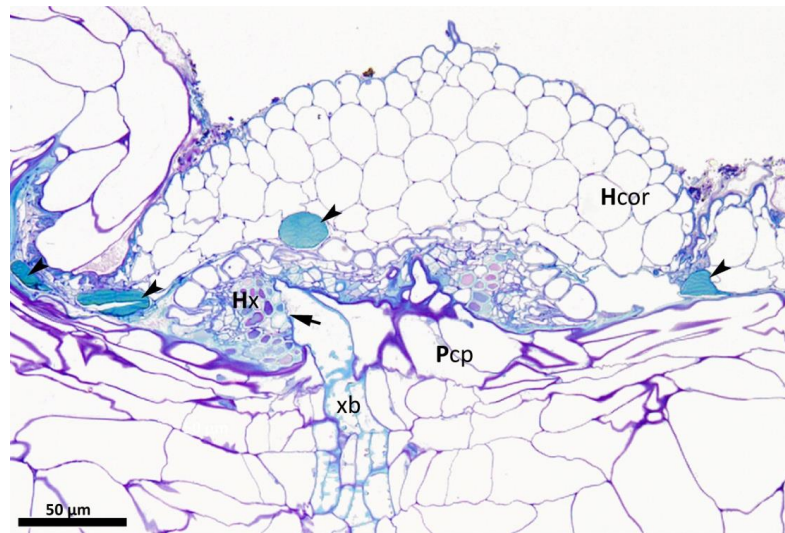


Figure 6.7: Tanniferous idioblasts (◄) in the cortex (**Hcor**) of *A. vulneraria* parasitized by *R. minor*. Some of the idioblasts had been pulled away with the cortex by the claspings folds and crushed. Parasite contact parenchyma (**Pcp**) has penetrated host xylem (**Hx**) and a xylem bridge (**xb**) vessel is in direct contact (◄) with a host vessel.

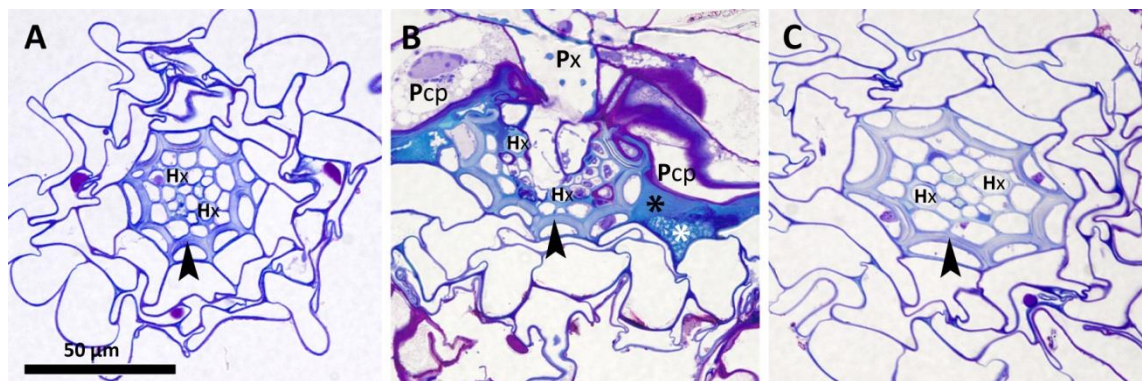


Figure 6.8: Tertiary endodermis (◄) of *A. elatius* at the point of (B) and several millimeters from each side of (A and C) the point of haustorial attachment. Structure of the endodermis is not different at the point of attachment. **Pcp** — parasite contact parenchyma, **Hx** — host xylem, * — necrotic cell, * — extramural phenolic deposits

In all grass-hosts examined, the tertiary 3° endodermis had developed at the point of penetration. However, this feature was not specific to the site of haustorial attachment and occurred several millimeters away from both sides of the haustorium, even in thin roots (Fig. 6.8). Roots of uninfected control plants of comparable size also possessed tertiary endodermis (not shown). The inner periclinal and anticlinal walls of 3° endodermis were thickened via a series of suberised and lignified lamellae. In all cases, this barrier was successfully overcome by penetration between two endodermal cells at the level of middle lamella, as previously explained in chapter 4. The two cells which were peeled off were pushed to the side and often compressed. Their lumina were filled with phenolic compounds as well as extensins as evidenced by light blue staining with toluidine blue O (Fig. 6.9H) and immunogold labelling (Fig. 6.9E

and Fig. 6.10D and E). These cell contents coincided with good infiltration with resin, which was not observed in other endodermal cells. None of the eudicot species developed a thickened endodermis. There was also no increase in constitutive mechanical tissues in the stele, namely sclerenchymal bundles in the roots of *Vicia sepium* and collenchymateous tissue in the roots of *Pimpinella major* (data not shown).

Occlusion of vessels was found in good and bad hosts alike, although generally a greater proportion displayed such modifications in eudicot hosts, especially non-hosts, with more occasional occlusions present in grasses (Fig. 6.11). The occluding material usually stained light blue with toluidine blue, suggesting phenolics, although in some cases pink or dark blue staining characteristic of carbohydrates was noted (Fig. 6.11). In grasses, phenolic occluding materials were more common while carbohydrates were seen much more often in eudicot vessels. Levels of occlusion ranged from apposition layers to full obstruction of the lumen. In several cases, an inner wall layer and, occasionally, also lumina of grass xylem vessels close to the endophyte were stained with the LM1 antibody against extensins (Fig. 6.7E) and JIM8 antibody against AGPs (Fig. 6.9 G).

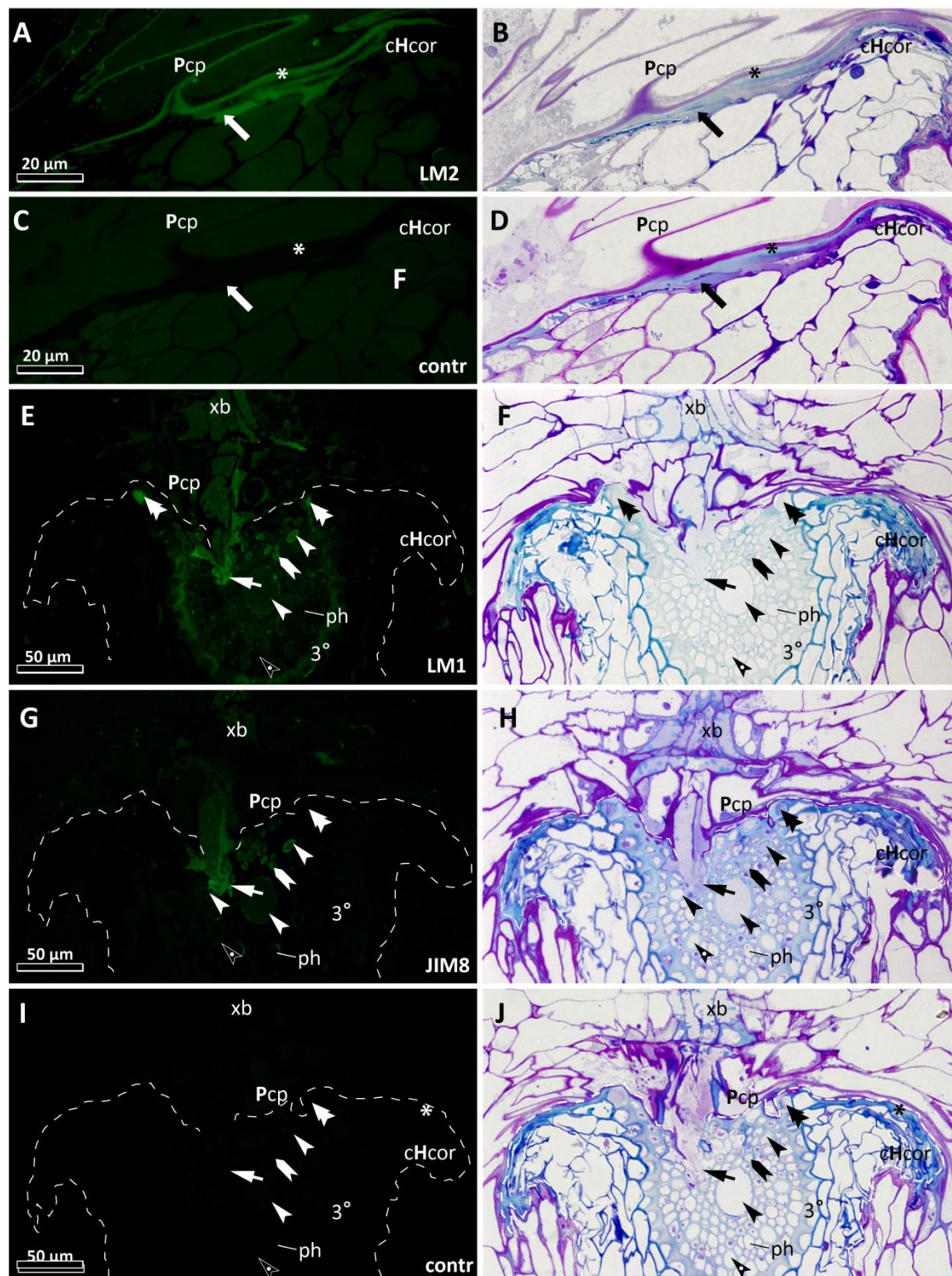


Figure 6.9: Interfaces between *R. minor* and *P. major* (A–D) as well as *A. elatius* (E–I) immunolabelled with monoclonal antibodies against AGPs (LM2 and JIM8) and extensins (LM1) and stained with toluidine blue O. In addition to the typical labelling of parasite contact parenchyma (Pcp) walls and the disintegrating protoplasts of partly differentiated xylem bridges (xb), labelling with LM2 is induced in *A. elatius* vessels (◄) and several other cells (◄) only near the endophyte but not in the vessels away from the endophyte (◄) (B), as well as in some (◄) crushed cortex cells (cHcor) of *P. major* and adjacent extramural deposits (*) (F). Controls (contr) are included to show that the fluorescence is a result of labelling rather than upregulation of phenolics which might autofluoresce. LM1 labelling of the grass host largely overlaps with LM2 labelling, with additional signal detected in the cells of tertiary endodermis (3°), including the protoplasts (◄) of its cells peeled off by the endophyte. Both antibodies label a small area (◄) between the dissolving tip of the endophyte and host cells.

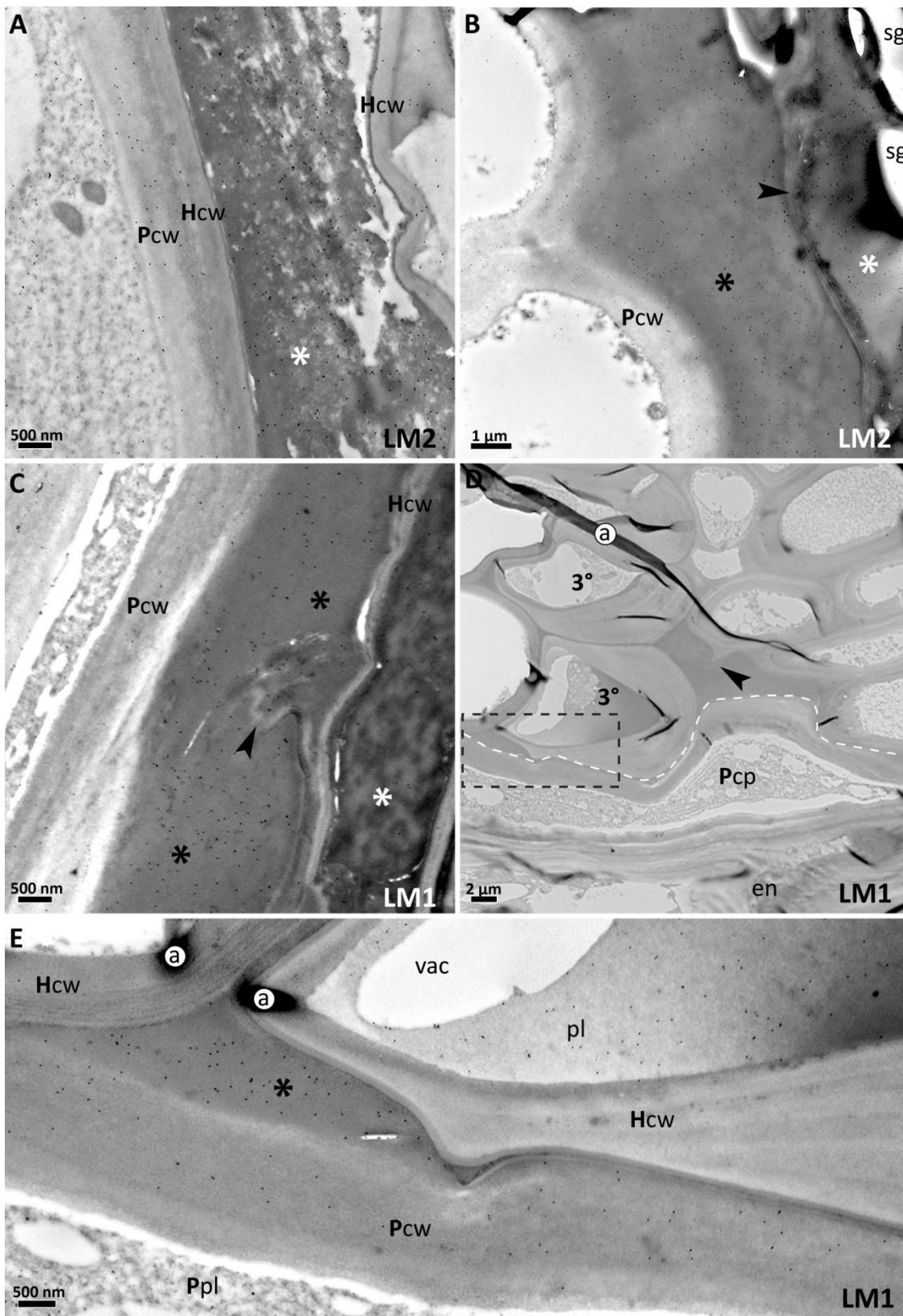


Figure 6.10: Ultrastructural detail of interfaces between *R. minor* and *A. elatius* (A, C–E) as well as *L. pratensis* labelled with LM2 mAb against AGPs (A and B) and LM1 mAb against extensins (C–D). Both antibodies label the extramural interfacial deposits (*) as well as the content of necrotic host cells (◄) but no deposition is observed in host cell walls (Hcw), debris of which can be seen (◄) embedded in the layer of extramural deposits. Parasite cell walls (Pcw) label with both antibodies. Figure E shows the magnified region of the interface (white dashed line) between parasite contact parenchyma (Pcp) with tertiary grass endodermis (3°) indicated by the box in image D. Extensin epitopes are present in the protoplast (pl) but not the vacuole (vac) of the peeled endodermal cell.

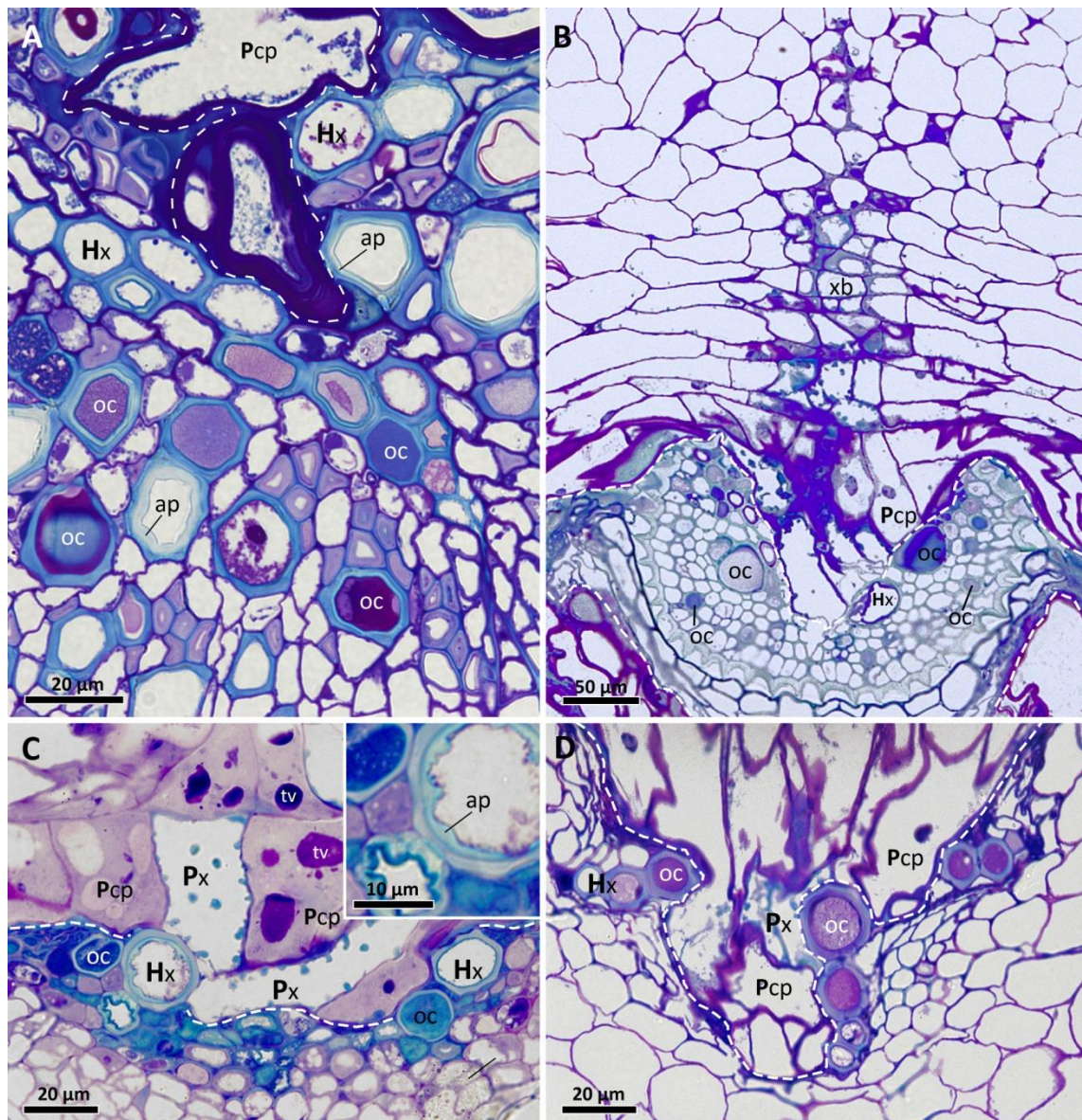


Figure 6.11: A variety of anatomical vessel modifications found in the xylem (Hx) of *R. minor* hosts *A. vulneraria* (A), *A. elatius* (B), *D. carota* (C) and *P. lanceolata* (D). Modifications include apposition layers (ap) uniform (A) and heterogenous (C) in thickness as well as complete lumen occlusions (oc) with phenolic (blue), carbohydrate (purple) and mixed materials. Occlusions with carbohydrates are more common in eudicots (A and D) while grass vessels are filled predominantly with phenolics. Pcp — parasite contact parenchyma, Px — parasite xylem, tv — tannin vacuole. Dashed line indicates the interface.

6.3.4 Auto-parasitic haustoria

In addition to haustoria attached to host roots, haustoria attached to the parasite's own roots were occasionally found. These auto-parasitic haustoria had developed similar to normal haustoria. A continuous xylem bridge with graniferous elements and in contact with invaded root xylem was developed although no luminal continuity was observed (Fig. 6.12A). Xylem apposition layers were also developed in the portion of the stele near the endophyte (Fig. 6.12A) and LM2 labelling was induced in cells near the endophyte, but not several millimeters away from it (Fig. 6.12B). The hyaline body was present and showed the characteristic immunolabelling pattern of AGP

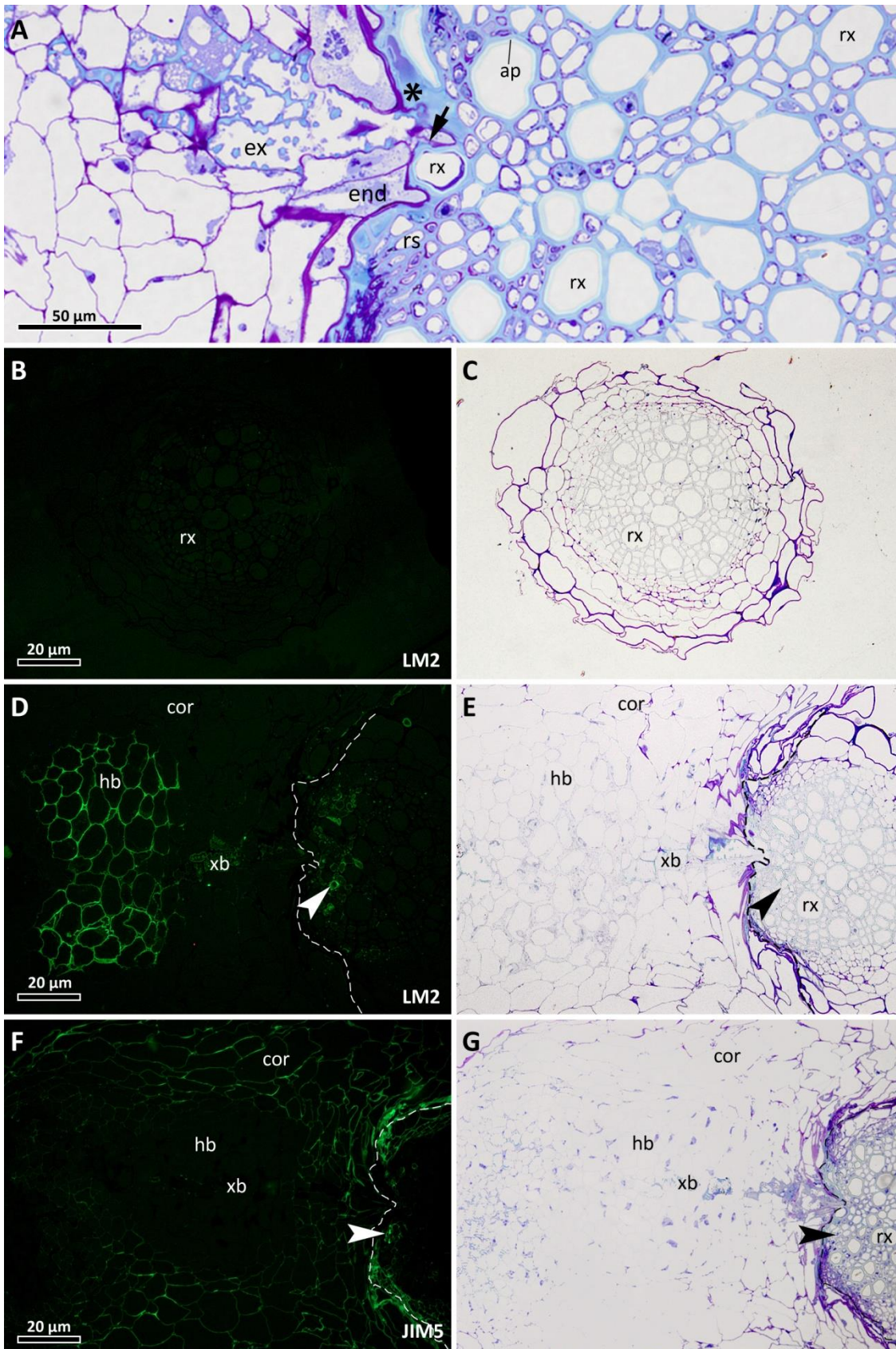


Figure 6.12: Anatomy and immunocytochemistry of haustoria of self-parasitising *R. minor*. Contact (◄) between endophyte (end) xylem (ex) and parasitized root xylem (rx) without luminal continuity is visible (A). Root xylem near the endophyte has developed inner apposition layers (ap). An interfacial layer of phenolics is present (*). Labelling with LM2 shows that the relevant AGP glycan epitopes are absent from the parasitized root immediately beyond the haustorium (B) while being upregulated (◄) near the endophyte (B). The hyaline body is characterised by LM2 and JIM5-detected epitope distribution typical of associations with real hosts, i.e. the hyaline body labels with LM2 (D) but not JIM5 (F). Interfacial parenchyma is not labelled with LM2 (D).

enrichment correlated with a lack of detection of de-esterified pectins (Fig. 6.12D–G). However, AGP labelling was absent from the endophyte parenchyma while being specifically present in the stele cells next to the endophyte.

6.4 Discussion

Post-penetration resistance determines certain eudicots as non-hosts

Previous anatomical studies of *Rhinanthus minor* haustorial connections showed that host defences localised at interfaces with haustoria determined whether vascular continuity between the parasite and the host could be established. Non-hosts (*Plantago lanceolata* and *Leucanthemum vulgare*) prevented parasite from accessing the root stele by what was referred to as “encapsulation” in a layer of lignin, suberin and/or dead cells (Cameron *et al.*, 2006; Cameron & Seel, 2007; Rümer *et al.*, 2007). Susceptible hosts (grasses and legumes) did not mount sufficient defences and therefore the endophyte was able to reach host vasculature and differentiate into xylem. Together with experimental data from several growth and ecological studies, these findings suggested that three major functional groups of hosts for *Rhinanthus minor* existed, i.e. 1) grasses and 2) legumes (good hosts) as well as 3) non-leguminous eudicot hosts (non-hosts).

Histological evidence from this study provides further anatomical data in support of the good hosting quality of grasses and legumes, as evidenced by fully developed haustoria on 3 previously unexamined legume species; *Lathyrus pratensis*, *Medicago lupulina* and *Vicia sepium*, and 3 grass species *Arrhenatherum elatius* var. *bulbosum*, *Holcus lanatus* and *Lolium perenne*. However, a higher degree of non-host root penetration was found than reported in the literature. Fully developed haustoria formed on eudicot hosts *Daucus carota* and *Pimpinella major*, which supported normal growth of the parasite. While relatively scarce haustorial connections between *Rhinanthus minor* and *Daucus carota* had been previously identified (Gibson & Watkinson, 1989), they were not investigated in anatomical detail, whereas *Pimpinella major* was examined as a host for the first time in this study. This is, therefore, the first histological account of haustorial success on non-legume eudicots in *Rhinanthus*. Whereas biomass data for *Daucus* was obtained from few plants, this rough estimation together with morphological features summarised in table 6.1 indicates that carrot is capable of supporting relatively good growth of the parasite. It is more difficult to make conclusions about the hosting quality of *Pimpinella* as the parasites died prematurely as a result of fungal infection. However, normal growth prior to infection suggests that this species can also benefit *Rhinanthus* and, most importantly, it supports haustorial development.

In addition to these two eudicot hosts supporting both haustorial development and parasite growth, two other eudicots — *Prunella vulgaris* and *Plantago lanceolata*

allowed relatively advanced haustorial development with continuous xylem bridge formation, while resulting in poor parasite growth. What is most surprising is that *Plantago lanceolata*, a host previously determined to be exceptionally incompatible with *R. minor* in physiological and anatomical studies (Seel *et al.*, 1993; Cameron *et al.*, 2006; Cameron & Seel, 2007; Rümer *et al.*, 2007), is capable of supporting relatively advanced development of some haustoria. While in the previous studies the endophyte was typically stopped in the *P. lanceolata* root cortex, xylem bridges were scarce and endophytic xylem was never observed (Cameron *et al.*, 2006; Cameron & Seel, 2007; Rümer *et al.*, 2007) — in this study, the majority of haustoria had penetrated the stele and developed some interfacial xylem in contact with host vessels. This was only true for young host plants and mostly for those roots that had not begun secondary growth, although occasional cases of host secondary xylem penetration with scarce endophytic xylem suggest that a degree of susceptibility is possible. Although endophytic xylem was not abundant and lumen-lumen connections were not seen in the samples examined, some of the endophyte xylem abutted host xylem pits. Therefore, uptake of some nutrients is a possibility, especially when one considers that lack of direct lumen to lumen contact between parasite and susceptible hosts vessel has been previously reported from *Olex phyllanthi* (Pate *et al.*, 1990), *Ileostylus micranthus* (Condon & Kuijt, 1994), *Santalum acuminatum* (Tennakoon *et al.*, 1997) or *Santalum album* (Tennakoon & Cameron, 2006). Additionally, a range of compatible parasite-host associations is possible when the parasite side of the interface is formed exclusively by parenchyma (Kuo *et al.*, 1989; Condon & Kuijt, 1994). While the xylem bridge is considered the primary path of solute uptake in *R. minor*, apoplastic transfer across endophytic parenchyma walls has not been investigated and might be a possibility as low levels of nutrient abstraction by encapsulated haustoria of *Plantago lanceolata* without xylem bridges has been observed (Cameron & Seel, 2007).

Penetration of non-hosts was not prevented in the majority of examined haustoria and xylem was scarcer and made of less well developed cells in haustoria on the two bad hosts than in those on good hosts. This suggests that rather than a mechanical factor being the main determinant, an element of haustorial development stimulation is either missing or tampered with. Whether potential stimulatory substances from the host or parasite are inhibited, not produced, delivered or perceived can be only a matter of speculation until convincing experimental data is obtained. However, suggestions of Rümer and colleagues (2007) that phytotoxic effects of the secondary metabolite acetosid, which is abundant in *Plantago*, could contribute to resistance might be of importance. Similarly, *Prunella vulgaris* accumulates high amounts of rosmarinic acid (Psotova *et al.*, 2006), a phenolic derivative that is a constitutive defence compound in plants (Petersen & Simmonds, 2003) and is induced by methyl jasmonate as well as fungal and bacterial elicitors (Szabo *et al.*, 1999; Bais *et al.*, 2002; Yan *et al.*, 2006). If these compounds were implicated, it would not be the first time and not the only way that secondary metabolites from a host are demonstrated

to affect the physiology of the parasite. Remarkably, alkaloids taken up from *Lupinus albus* L. by *Castilleja indivisa* reduced insect herbivory performed on the parasite and increased the numbers of visits from pollinators (Adler, 2000). Examples more relevant for this study include phytoalexins and coumarins produced by *Helianthus annuus* in response to *Orobancha cumana* attack and resulting in the oppressor's death (Serghini et al. 2001; Echevarría-Zomeño et al. 2006). In a non-host *Medicago truncatula* inoculated with *Orobancha crenata* phytoalexins were identified using thin-layer chromatography (Lozano-Baena et al., 2007). In this case the host stele was reached but phytoalexins inhibited normal development of the primary haustorium resulting in the early death of the parasite.

Further evidence for a host-derived inhibiting factor comes from an example of post-penetrative resistance found in a non-host grass *Tripsacum dactyloides* (eastern gamagrass) parasitized by *Striga hermonthica* (Gurney et al., 2001, 2003). Similar to my findings with non-hosts *Plantago lanceolata* and *Prunella vulgaris*, xylem connections were achieved between the haustoria of *Striga* and *T. dactyloides* roots but did not guarantee physiological success of the parasite. The parasites' progress was stopped after vascular connections developed but before the hyaline bodies differentiated fully, and the plants did not advance beyond tubercle morphology characteristic of early post-attachment stages (Hiraoka & Sugimoto, 2008). Lack of developmental cues was hypothesised to cause tubercle development arrest in an incompatible *Striga gesneroides*-blackeye pea association (Botanga & Timko 2005). However, application of a haustorial inducing factor (HIF), syringic acid, or synthetic germination stimulant, GR-24, to the *Striga-Tripsacum* association did not induce further differentiation of haustoria and parasites' development although it did increase the number of tubercles. While it cannot be ruled out that other HIFs could have had a stimulatory effect if applied, a strong case for the presence of inhibitory compounds from *T. dactyloides* was further presented in the study. *Striga hermonthica* plants that had successfully attached to *Zea mays* (susceptible host) were subsequently manipulated to attach to *Tripsacum dactyloides* and not only developed poorly differentiated haustoria on *Tripsacum* but any haustoria that subsequently developed on maize were also poorly differentiated. This suggested that inhibitory factors from *Tripsacum* were either exuded into the soil and taken up by the parasite or transported within the parasite-graminoid root system (Gurney et al., 2003).

Xylem links were found between other parasites and their non-hosts. *Vigna unguiculata* and *Arabidopsis* allowed vascular continuity with *Striga hermonthica* (Yoshida & Shirasu, 2009) although no specific mode of post vascular connection resistance was suggested. Mistletoes *Amyema preissii* and *Lysiana exocarpi* developed xylem links with incompatible hosts, while further differentiation of haustoria was poor (Press, 1993). Presence of xylem-xylem contact in incompatible interactions is therefore likely to be relatively common and post-penetration defence mechanisms

applied by hosts may well include exudation of toxic compounds into the solutes stolen by the parasite or diffusion across cell walls into the parasites' tissues.

As AGPs strongly labelled endophyte parenchyma in most pairings except those with *Daucus carota*, *Prunella vulgaris* and auto-parasitic haustoria, presence of AGPs in this region cannot be used as a marker of host quality. Similar to the findings of Gurney *et al.* (2001, 2003), my results suggest that a well functioning hyaline body might offer a more confident indication of good haustorial development than the presence of a xylem bridge or AGP abundance in the endophyte. However, it is somewhat more difficult in case of *Rhinanthus*. While the function of this tissue is generally not well understood, hyaline bodies of *Striga*, for instance, are extremely cytoplasmically rich and stain very darkly with histological dyes such as toluidine blue O in well developed haustoria on favourable hosts (Dörr, 1997; Gurney *et al.*, 2003, 2006). Their lack, or poor differentiation, is therefore very apparent in histological preparations. In contrast, mature hyaline bodies of *Rhinanthus* can often be very vacuolated and therefore do not stain conspicuously. A trained eye will be able to distinguish the tissue in question by a smaller cell size and isodiametric cell shape, although it is not easy in all haustoria. While labelling with LM2 is a very reliable marker of the hyaline body location in such cases, the mere extent of the tissue is not informative enough to conclude its function. It is not clear if and how the functioning of the hyaline body changes after vacuolation in good hosts and how this compares with well vacuolated hyaline bodies in haustoria attached to non-hosts.

A hyaline body is not absent in those haustoria attached to *Plantago lanceolata* that are devoid of a xylem bridge, which, again, is in contrast with the findings of Cameron and Seel (2007). Nevertheless, in general the hyaline body is less apparent when attached to non-hosts. Its anatomy is never as organelle-rich as on good hosts and the characteristic AGP/de-esterified pectin immunofluorescence pattern is not as clear. AGP labelling is weaker and de-esterified pectin epitopes are usually detected. Further comparative studies of hyaline body ultrastructure on different hosts might reveal organelles consistently absent or infrequent in the hyaline bodies in haustoria attached to non-hosts and help elucidate their functions.

Two major conclusions can be drawn from these results. Firstly, access to host stele and physical contact with host vasculature was not a determining factor for host quality in this study. Parasitic success appears to be reflected more accurately in the abundance and structure of xylem in the endophyte in addition to good differentiation of the hyaline body. Secondly, host quality is likely to vary greatly within at least one of the functional groups (non-legume dicots) previously proposed for *Rhinanthus*. Intraspecies differences are also likely to be common. This variation has supposedly more bearing on the associations with non-legume eudicots as good hosting quality of grasses and legumes appears much more consistent. However, Mutikainen *et al.* (2000) found that *Rhinanthus serotinus* performed differently

on different populations of *Agrostis capillaris*, while successfully developing haustoria on all 4 populations examined. Furthermore, *Galium verum* (a eudicot) was shown to be a better host than certain grasses and worse than others (Seel *et al.*, 1993). This suggests that post-penetration resistance mechanisms of varying strength might be in place even within the functional groups generally thought to have a positive effect on the parasite. The differences might also be a consequence of varying degrees of tolerance.

Histology of host and non-host responses is similar

In this study, no particular histological response mechanism could be identified as a consistent element of resistance. Even though resistance can be successfully implemented as early as at parasite germination, development on hosts and non-hosts can often follow a similar initial pathway with defence being expressed at later developmental stages (Hood *et al.*, 1998). Furthermore, quantitative rather than qualitative differences may form the basis of resistance. In a resistant cultivar of poplar, for instance, it was production of more abundant inner periderm and flavonoids than in a susceptible one that accounted for resistance to *Viscum album* (Hariri *et al.*, 1991).

The host cortex is typically the first line of induced mechanical defence during root parasitism. This has been demonstrated in several studies to be associated with some changes to host walls in contact with the parasite. Thickening of cortex walls in contact with the endophyte was recorded in resistant *Helianthus* roots (Dörr *et al.*, 1994). In *Tagetes erecta* L. cv. Crackerjack (marigold) — a non-host to *Striga asiatica*, cortical cells in contact with the parasite developed distinctive wall appositions followed by cell necrosis 144 hours post inoculation (Hood *et al.*, 1998; Gowda *et al.*, 1999). Lignification of *Phleum bertolonii* cortices was observed at the point of attachment of *Rhinanthus minor* (Rümer *et al.*, 2007). Cortex cell wall reinforcement was observed only in one sample of *R. minor* attached to *Pimpinella major* in this study. This finding would ideally require more detailed confirmation at the ultrastructural level although it is surprising that no apparent changes were seen with light microscopy. However, a number of mechanisms undetected by histological techniques are also likely to be in place. Defensins (a type of PR proteins) secreted to the apoplast have been demonstrated as a successful resistance factor against *Orobanche cumana* in *Helianthus annuus*, where it was proposed to interfere with parasite membrane sphingolipids (De Zélicourt *et al.*, 2007).

Although cortex cell wall reinforcement does not appear to contribute considerably to host resistance, cortex-localised mechanical resistance has in many cases been attributed to what is referred to by several authors as a darkly-staining interfacial “encapsulation layer” (Visser *et al.*, 1990; Labrousse, 2001; Zehhar *et al.*, 2003; Rümer *et al.*, 2007; Yoshida & Shirasu, 2009). It is generally assumed that this layer, formed either of extramural polyphenolics and/or dead cells, is created by the host as

an active mean of defence. However, upon close examination of the relevant published figures it becomes obvious that 1) the encapsulation layer is often not much different from a layer of debris found at the interfaces of successful haustoria (compare figure III.F in Visser *et al.* (1990) with figures of a range of compatible pairings in this and previous chapter and 2) one can only assume that the phenolics are secreted exclusively by the host. Data presented in chapter 6 suggests a significant proportion of this material might in fact be produced by the parasite.

No encapsulation layers were identified in this study, which is in strong contrast with previously published findings (Cameron *et al.*, 2006; Cameron & Seel, 2007; Rümer *et al.*, 2007). Although Cameron *et al.* (2006) mention dark staining only at the interfaces of *Rhinanthus minor* with bad hosts, close examination of the relevant figures reveals that some dark staining is present along the interfaces with good hosts as well. This might be attributed to mechanically crushed host cells and extramural phenolics which were present in all pairings examined in this study and were, therefore, not related to host quality. Cell death in the cortices of grasses and legumes as well as *Pimpinella major* and *Prunella vulgaris* was always associated with compression by the parasite and therefore did not appear to form part of an active defence response. However, in *Daucus carota* and *Plantago lanceolata*, dying but not crushed cells filled with phenolics were found, suggesting the possibility of an active, hypersensitive-like response. In either case, however, the endophyte reached host vasculature and the dead tissue never formed a continuous layer encapsulating the endophyte. These results vary from previously published findings where the central interface region was sealed off by a layer of dead cells in *Plantago lanceolata* (Cameron *et al.*, 2006). Although not investigated in much detail, it is worth noting that haustoria attached to *Daucus carota* often possessed darkly stained vacuoles. Their function might be to detoxify interfacial phenolics from carrot that appear to be different than those produced by other hosts as their autofluorescence is not quenched by toluidine blue O. Yellow autofluorescence is indicative of flavonoids (Valette *et al.*, 1998).

Neumann *et al.* (1999) found that in response to haustorial intrusion, LM1-recognised epitopes were accumulating in host interfacial walls and occasionally filled entire parenchyma cells in contact with the parasite endophyte. In this study, AGP and extensin epitopes were found primarily in the extramural, phenolic-rich layer and the disintegrating protoplasts, without enrichment in the cell walls. There are no known implications of AGPs and extensins in cell necrosis and it is unclear why the epitopes are abundant in the protoplast. While influx of soluble carbohydrate fractions of AGPs could explain this at least partly, the distribution is quite uniform across the protoplast. Furthermore, extensins are not soluble and therefore it is more likely that they cross-link the disintegrating cell contents, as is typically found in cell walls during plant pathogenesis (Brisson *et al.*, 1994). In *Anthyllis vulneraria*, *Vicia sepium* and *Lathyrus pratensis*, a large proportion of root parenchyma labelled with

LM2. Time constraints of this project did not allow comparison with roots of uninfected control plants although sections from the host root taken several millimetres away from the haustorium showed similar labelling.

Tannin-filled cells in the cortices of *Anthyllis vulneraria* represent another type of induced response. They are known as tanniferous idioblasts or tannin sacs and are a common and normal element of different tissues and organs in legumes and several other families (Evert, 2006) where they are known to participate in heavy metal chelation and detoxification (Davis *et al.*, 2001). Although localized at and around the point of haustorial attachment, these modified cells were not concentrated at the interface. Therefore, while they are known to participate in plant defences against pathogens and herbivores, they are unlikely to act in the “poisoning” of the haustorium and might represent a more general, unspecific type of response. To my best knowledge, such cells are not known to be induced during pathogenesis or parasitic plant attack, while pre-existing sacs have been previously observed to be penetrated by fungal hyphae (Dow & Lumsden, 1975).

Thickening of the endodermis, which was responsible for the lack of host susceptibility to *Striga* (Maiti *et al.*, 1984; Cissoko *et al.*, 2011) or *Orobanche* (Goldwasser *et al.*, 2000; Pérez-de-Luque *et al.*, 2005, 2007) was not induced in any of the examined hosts. In fact, tertiary endodermis that was observed to form locally and asymmetrically in *Phleum bertolonii* and *Hordeum vulgare* at the point of *Rhinanthus minor* penetration while remaining at secondary stage at the opposite side of the stele (Rümer *et al.*, 2007), was in this study found to be a constitutive element of grass anatomy rather than an induced feature. Nevertheless, a number of unsuccessful cortex and stele-localised host responses were observed. This highlights the multilayered and potentially cumulative nature of host defence responses to attack by *Rhinanthus minor* and raises the question of physiological post-penetrational incompatibility versus mechanical barrier building.

While Cameron & Seel (2007) found vessel occlusion only in eudicot hosts, in this study it was identified in bad and good hosts alike but was more prominent in eudicots. Although typically associated with non-hosts, localised plugging of vessels did not disrupt the general flow of solutes from *Chamaecytisus palmensis* parasitized by *Ileostylus micranthus* (Condon & Kuijt, 1994). The structure of occlusions varied and was reminiscent of other examples of plant parasitism. Similar to the finding of Labrousse (2001) during *Orobanche cumana* Wallr.-*Helianthus* interactions — uniformly occluding phenolic material staining green-blue with toluidine blue O was identified in some vessels. Much less commonly, pink/purple stained carbohydrates were also found. Similarly, carbohydrate-based materials were found in the vessels of *Vicia sativa* attacked by *Orobanche crenata* (Pérez-de-Luque *et al.*, 2006). They were believed to be formed by mucilage secreted by the parasite and products of host wall digestion. Partly-occluding apposition layers of uniform thickness were also identified in this study. They resembled coating layers of lamellate, lignified architecture seen

in the vessels of *Helianthus annuus* roots parasitised by *Orobanche cumana* primary haustoria (Dörr *et al.*, 1994) or thickenings found in *Medicago truncatula* parasitized by *Orobanche crenata* (Lozano-Baena *et al.*, 2007).

Another resistance mechanism identified in the host steles was the upregulation of AGP and extensin epitopes in host cells, notably vessels. This was demonstrated in *Arrhenatherum elatius*, *Plantago lanceolata* and infected roots of autoparasitic *Rhinanthus minor*. This is in agreement with the findings of Wydra & Beri (2007) who found that both resistant and susceptible strains of tomato responded to infection by a fungal pathogen *Ralstonia solanaceum* with AGP upregulation in vessel walls. However, in this study the labelling was mainly present in the lumina. AGPs were suggested to have a cross-linking function in mechanical strengthening of vessels during infection. This is likely for two reasons. Firstly, AGP cross-linking has been demonstrated previously during leaf excision (Kjellbom *et al.*, 1997). Secondly, AGPs in host vessels co-localised with extensins, which are commonly involved in crosslinking within cell walls during pathogenesis (Brisson *et al.*, 1994). Whether this can also be true for xylem lumina remains to be established.

Plantago lanceolata was the only host that caused death of endophyte cells. This was observed in one haustorium only. Endophyte death was much more common on this host in previous studies and was also found in *Striga asiatica* (Hood *et al.*, 1998) and *Orobanche crenata* (Rubiales *et al.*, 2003) interacting with non-hosts. Hood *et al.* (1998) found that in associations with non-hosts the cytoplasm of the palisade interfacial tissue of *Striga asiatica* appeared degenerated, endophyte cell walls were thickened and the endophyte did not reach the endodermis or stele, except for less than 1% of connections examined. Extremely thickened cell walls were also found in the lateral parts of *Rhinanthus minor* endophyte parasitizing a *Plantago lanceolata* root with secondary growth, as well as a large root of *Anthyllis vulneraria*, also with secondary growth.

Are taxonomic differences in cell wall composition an important factor?

Although our knowledge of how cell wall composition affects pathogenic attacks is limited (Vorwerk *et al.*, 2004) the potential for differences in signalling and subsequent defence mechanisms is enormous as a result of considerable diversity not only between different plant groups but also within individual plants, organs and tissues. In chapter 3 it was hypothesised that cell wall diversity at the taxonomic level might affect host susceptibility to parasitic attack and that it might be advantageous to parasitise taxonomically distant hosts as part of enzymatic self-damage prevention. This seems appealing as host functional groups for generalistic plant parasites often follow the graminoid versus eudicot distinction. As *Rhinanthus minor* represents an elegant example of preference for graminoids at both anatomical and ecological level, it is possible that the former are better facilitators of parasitism because of their different cell walls. Cell walls of Poales

are known to have cell walls very distinctive from those of eudicots and other monocots (Carpita, 1996; Vogel, 2008). The characteristic features include high abundance of glucuronoarabinoxylan and mixed linkage glucan in parallel with low amounts of xyloglucans, pectins and structural proteins. Additionally, primary, non-lignified walls are enriched in aromatic substances, mainly the hydroxycinnamates ferulic acid and *p*-coumaric acid, esterified and etherified forms of which participate in links between hemicelluloses as well as between hemicelluloses and lignin. As components of the middle lamellae they participate in intercellular adhesion (Roberts & Gonzalez-Carranza 2007). Phenolics largely replace structural proteins of other groups of plants in their carbohydrate-crosslinking function. Furthermore, those extensins that are found in grasses, are of different structure (Carpita, 1996). All these differences could affect cell wall degradation and separation of host cells by the endophyte.

However, as convenient as the idea of taxonomically different grass walls facilitating parasitism may seem, it is not clear how exactly that would be achieved. Considering the intercellular mode of endophyte penetration, low content of pectins in middle lamellae might contribute to decreased adhesion. In this study, no pectins were detected in grass middle lamellae. However, phenolic cross-linking which participates in cell adhesion in grasses is also a known and persistent contributor to grass cell wall recalcitrance (Jeffries *et al.*, 1990; Himmel *et al.*, 2007). It cannot therefore be simply assumed that lower content of pectins allows easier cell separation, because phenolics might easily compensate for this difference. As it is not clear if the primary and secondary walls are enzymatically loosened to facilitate infection or disintegrate mainly after the cells have been crushed, it is difficult to make any conclusions as to whether and how their composition might affect penetration.

Furthermore, many inconsistencies in terms of taxonomically-correlated resistance have to be considered. First of all, although grasses are common hosts, eudicots are generally parasitized more often (Heide-Jørgensen, 2008) and *Orobanche*, for instance, parasitises eudicots (Udayakumar *et al.*, 1996). It could be argued that different parasites are enzymatically adapted for the decomposition of walls of different taxonomically homogenous functional groups. However, *Rhinanthus* itself shows that there are exceptions. First of all, in addition to grasses, legumes are well known hosts of *Rhinanthus*. This could be explained by their relatively low recalcitrance when compared to other eudicots (Jung & Allen, 1995). However, as it has been shown for the first time in this study, some non-leguminous eudicot hosts are also successfully parasitized while non-host eudicots can still be penetrated without a very apparent histological reaction. Examples of other parasite-host interactions further prove that within-group variation is common. Poales can show a great degree of interspecific variability. Eleven native African grasses showed varying resistance to *Striga hermonthica* (Del.) Benth., *Striga aspera* (L.) Kuntze, with hosts ranging from full resistance (parasite termination shortly after attachment) to complete

susceptibility (Kuiper *et al.*, 1998). Even during parasitism by *R. minor*, lignification of the stele and cortex was much more pronounced in *Phleum bertolonii* than in *Hordeum vulgare* although it did not prevent successful attachment (Rümer *et al.*, 2007). *Alectra vogelii* was found to distinguish between different species of legumes and connected to *Vigna unguiculata* while cortex-localised resistance in *Pisum sativum* and *Vicia faba* caused haustorial arrest (Visser *et al.*, 1990). While *Parentucellia viscosa*, a close relative of *R. minor*, was shown to display similar general preference for grasses and legumes (Suetsugu *et al.*, 2012), parasites from within the same genus can have contrasting preferences. While *Striga gesneroides* prefers dicots, other species of *Striga* parasitise grasses (Mohamed *et al.*, 2001). Finally, there are parasite species closely related to *Rhinanthus minor* that display no clear patterns of coarse taxonomical host preference. *Plantago coronopus* and *Trifolium repens* were the best, while *Festuca ovina* and *Potentilla erecta*, the worst hosts to four species of *Euphrasia* (Wilkins, 1963).

Self parasitizing haustoria found in this study provide further evidence that similarity between haustorial and parasitized organ cell wall structure is not a determinant of incompatibility. The phenomenon of autoparasitism was also found in *Triphysaria* and found to be at least partly determined by genetic inheritance, i.e. occurrence of autoparasitism in parents increased the chances of autoparasitism in the progeny (Yoder, 1997). Furthermore, autohaustoria were induced by the parasites' own exudates but were less numerous than normal haustoria, suggesting qualitative interspecific differences in stimulants. Autoparasitism is common among Orobanchaceae (Musselman & Dickison, 1975). However, as the precise mechanisms underlying this phenomenon are far from clear, it is at this stage impossible to tell whether it further negates the implications of wall diversity in recognition or whether it is a mere consequence of such putative system being or becoming faulty in intraspecific interactions.

All these points considered, resistance does not appear to be related to the coarse taxonomical diversity of host cell walls. It is either that subtle differences are more important or that cell-wall determinants are outweighed by other factors. Nevertheless, preference for grasses and legumes is rather consistent in *Rhinanthus minor* and the implications of host wall diversity in host recognition and penetration are definitely worth pursuing further for this and other species that do show a relatively defined preference. Analysis of the interfacial exoproteome of *R. minor* would show whether its enzymes are qualitatively and/or quantitatively tuned for modification of particular cell walls. Similarly, different cell wall material preparations could be tested for their ability to induce and maintain haustorial development.

What might be the cause of the intraspecific variability ?

This study shows that there is anatomical variation in attachment success even within one host plant and it is dependent on host root age. Although *Plantago lanceolata* has been previously found to be a non-host that prevents endophyte penetration beyond cortex (Cameron *et al.*, 2006; Rümer *et al.*, 2007), the variation discovered in this study leaves a window of opportunity for full penetration resulting in xylem to xylem contact. While in case of *Plantago* as a host this variation in penetrative scope cannot be related to physiological success of the parasite, the observation raises a question whether it might in other parasite-host associations.

Existence of strains, also termed pathotypes by Timko *et al.* (2012), of the same parasite species with different host specificities has been reported for *Alectra vogelii* (Polniaszek & Parker, 1987), *Striga* sp. (Mohamed *et al.*, 2001) *Orobanche* sp. (Musselman & Parker, 1982) and *Orobanche minor* (Thorogood *et al.*, 2009) and at least seven races of *Striga gesneroides* are known (Li *et al.*, 2009). Curiously, sequence differences between the chloroplast DNA (cpDNA) and nuclear ribosomal DNA (nrDNA) internal transcribed spacer (ITS) of the long-recognised three subspecies of *Viscum album* are minute (Zuber & Widmer, 2000). Genetic variation in the host has also been demonstrated as being an important factor. In addition to the already mentioned study by Mutikainen *et al.* (2000) where biomass reduction of *Agrostis capillaris* by *Rhinanthus serotinus* varied between host genotypes, *Urtica dioica* showed varying resistance and tolerance (again, expressed as biomass measurements rather than histological investigations of haustoria) to parasitism by *Cuscuta europaea* (Koskela *et al.*, 2002). That was attributed to genetic differences between maternal families as well as host sex. Similarly, genetic variation in *Rhinanthus minor* and *R. angustifolius* as well as their host *Hordeum vulgare* was found to affect the outcome of parasitism (biomass and seed production of the parasite and host) (Rowntree *et al.*, 2011). However, Houston and Wolff (2012) found no significant differences when using local population seeds of *Rhinanthus minor* in grassland restoration. This suggests that such genetic differences might have different bearing on the general, cumulative effect of parasitism than on host species-level interactions. It would be of interest to test the haustorial development of *R. minor* on *Plantago lanceolata* using combinations of seeds of different provenances and carrying out genetic analyses.

Environmental factors may also affect haustorial development. Temperatures below 18°C were necessary for *Orobanche crenata* and *O. aegyptiaca* to parasitise *Daucus carota* (Eizenberg *et al.*, 2001) while *Helianthus annuus* expressed higher levels of resistance to *O. aegyptiaca* and *O. cumana* in higher temperature regimes (Ish-Shalom-Gordon *et al.*, 1994; Eizenberg, 2003). However, resistance of *Vicia* genotypes to *O. aegyptiaca* was unaffected under different temperatures (Goldwasser *et al.*, 2000).

Ecological implications

One of the biggest challenges in relating histological studies of haustoria to the ecological consequences of parasitism is the fact that the interaction dynamics are much more complicated in the natural environments. Immunocytochemical or histological features may therefore be modified in an environment-dependant manner or their effect observed in the lab might be of a different magnitude in the field. For instance, it is not known at present whether the eudicot hosts *Daucus carota* and *Pimpinella major* identified here as “good” are also parasitized in the field in the presence of other hosts and to what extent. As *Galium verum* was demonstrated by Seel and *et al.* (1993) to be a better host than *Poa alpina*, *Festuca ovina* and *Brachypodium pinnatum*, it is possible that the effect of *Rhinanthus* on dicots in the wild is not always as positive as assumed. Interestingly, *Pimpinella major* and *Vicia sepium*, both attracting successful haustorial attachments, are species of hedgerows and grassland-hedgerow boundaries (Grime *et al.*, 1988; Stace, 2010). The results suggest that *Rhinanthus* can form haustorial connections with species from outside of its grassland habitat optimum, further supporting its flexibility in terms of host selection and possible variations in effects on communities.

It is rather unlikely that the higher degree of *Plantago lanceolata* penetration found in this study has considerable bearing on community structure. Although host biomass was not measured, no detrimental effects of parasitism on this host were observed and *Rhinanthus minor* performed poorly, suggesting that the haustorial connections are probably not functional. However, the gradation of resistance in *Plantago lanceolata* makes it a potentially important species for researching various levels of incompatibility in parasite-host interactions. Inconsistency in the relationship between apparently full haustorial penetration and physiological success of the parasite make it difficult to quickly determine ‘good hosts’ in the field.

6.3.5 Conclusions

Results presented in this chapter highlight the complex and multi-layered nature of plant defences against angiosperm parasites. *Rhinanthus minor* hosts mount various histological defences in different regions of the parasitized roots, without preventing vascular links in most cases. The quality of a host can therefore be determined only using a range of ecological, histological and physiological techniques and has to be interpreted with care. Non-leguminous dicots might be of more importance as hosts than previously assumed. As immunocytochemical features of haustoria, particularly the distribution of AGPs, are highly preserved yet affected by low host quality, they must be of fundamental importance to the functioning of these highly specialised structures. Advances in AGP research will be helpful in the verification of their precise functions in interactions with different hosts.

7 Lignin as a contributor to virulence rather than defence? — novel-insights from metahaustoria

7.1 Abstract

Non-infecting metahaustoria developed on roots of *Rhinanthus minor* and *Odontites vernus* when they come into contact with pot surface. Within this chapter, a previously unreported layer of extramural deposits secreted in contact with the wall of the pot was described. It is enriched in lignin-like phenolic substances co-occurring with xyloglucans which I have termed the **phenolic-rich interfacial secretion complex** (PhISC). It bears considerable resemblance to contact secretions at the equivalent interfacial area between normal attached haustoria and parasitized host roots, which were compared histochemically and immunocytochemically, as well as chemometrically using Raman spectroscopy.

Metahaustorial PhISC morphologically resembles cuticle and is stratified while the secretions in contact with a host are not clearly layered. Interfacial parenchyma cells walls which are most likely to produce the PhISC, are thickened. This feature is particularly pronounced in metahaustoria, where cell lumina are often narrower than spongy cell walls with swollen middle lamellae.

Pectins are the main structural components of interfacial parenchyma walls detected by immunolabeling, they were not observed in the PhISC, in which xyloglucan was the main structural carbohydrate detected. AGP epitopes were detected with LM2 and JIM8 antibodies in the cell walls as well as the PhISC. The PhISC was strongly autofluorescent under UV, blue and green excitation and stained positively for lignin with Wiesner reagent, Maüle reagent and toluidine blue O, which quenched the intrinsic fluorescence. Classic lipophilic stains (Sudan III, Sudan IV, Sudan black and Oil Blue N) did not stain the PhISC. Immunogold labelling with three polyclonal antibodies against guaiacyl (H), *p*-hydroxyphenyl (H) and syringyl (S) lignin showed a high concentration of the latter in the PhISC. The cell walls also labelled, even though this was not always correlated with histochemical staining. Raman spectroscopy confirmed a high concentration of phenolics in the PhISC and a lower concentration of phenolics in the interfacial parenchyma cell walls. A single-peak Raman shift into a spectral region characteristic for phenolics was detected. Host xylem cell walls were represented by a double peak typical of lignins.

Together, these results suggest that at least some of the extramurally deposited phenolics-rich deposits commonly found at haustorial interfaces with host tissues and assumed to contribute to host defence are synthesised by and beneficial to the parasite. Consequently, reinterpretation of the role of interfacial lignin in parasitic plant-host interactions is required.

7.2 Introduction

Successful parasitism and its wider impacts result from the interplay between host defensive abilities and parasites' adaptations to overcome them, as discussed in detail in chapter 4. Just as wide an array of intrusive mechanisms is used by parasitic plants, host responses are very complex and multilayered. Host defences aimed at preventing haustorial penetration take the form of programmed cell death or physical strengthening of cell walls and are major contributors to the net host resistance. In common with responses to fungal infections (Mayer, 2006) and wounding (Rittinger *et al.*, 1987), strengthening of cell walls with lignin, suberin, callose or protein cross-links in order to prevent haustorial penetration have been reported in parasitic plant hosts (Pérez-de-Luque *et al.*, 2006a; Echevarría-Zomeño *et al.*, 2006; Rümer *et al.*, 2007). In addition to the cell wall specifically being impregnated, a number of authors referred to a more structurally vague, darkly-staining interfacial "encapsulation layer" (Visser *et al.*, 1990; Labrousse, 2001; Zehhar *et al.*, 2003; Rümer *et al.*, 2007; Yoshida & Shirasu, 2009). While the precise structure, composition and assembly of encapsulation layers are poorly characterised, interfacial lignins have frequently been suggested as a crucial component (Maiti *et al.*, 1984; Pérez-de-Luque *et al.*, 2006a; Cameron *et al.*, 2006; Rümer *et al.*, 2007). In some cases, osmiophilic and/or phenolic-rich apoplastic deposits were specified to fill the narrow space between the mature haustorium and host cells (Piehl, 1963; Musselman & Dickison, 1975), while in others, for example during parasitism of *Plantago lanceolata* by *Rhinanthus minor*, dead host cells also contribute to the physical blocking of the haustorium (Cameron *et al.*, 2006; Rümer *et al.*, 2007). Because of this association of interfacial phenolics substances with the site of mechanical resistance expression, and because they are a typical defence compound in pathogenic interactions with plants, they are generally believed to be a defensive product of host organs penetrated by haustoria. Although several authors cautiously suggested that the parasite might participate in synthesising these substances (Neumann *et al.*, 1999; Rümer *et al.*, 2007), literature focusing on pursuing this argument is lacking. Furthermore, the cementing secretions of root parasite haustoria aiding adhesion have typically been observed to be carbohydrate-based, as detected by PAS and Alcian blue staining of *Orobancha cumana* and *O. aegyptiaca* (Joel & Losner-Goshen, 1994), or by JIM5 labelling of de-esterified pectins in *Cuscuta* haustorial cement (Vaughn, 2002), indirectly supporting the notion that interfacial phenolics are derived from the host. However, PATAg staining of *Rhamphicarpa fistulosa* and pearl millet mature interfaces has been observed (Neumann *et al.*, 1998). A cuticle-like adhesive secretion complex has also been described for *Viscum minimum* (Heide-Jørgensen, 1988). In some cases, both lipids and carbohydrates are present (Joel & Losner-Goshen, 1994).

Most studies of interface-localised interactions are characterised by a common approach — they are based on samples of haustoria attached to their hosts. Although this might seem to be the obvious approach, its major limitation is that once

attachment has occurred, it is difficult to pinpoint the origin of substances sandwiched between the host and the parasite to either of them. Careful ultrastructural studies including immunogold labelling of material fixed to high standard can provide snapshots of the secretion processes in the form of epitopes detected in vesicles (Ripper *et al.*, 2008). However, few immunocytochemical studies of parasitic plant haustoria exist (Reiss & Bailey, 1998; Losner-Goshen, 1998; Neumann *et al.*, 1999; Vaughn, 2002, 2003, 2006; Pérez-de-Luque *et al.*, 2006b) and they focus on host cell wall modification *in muro* by the searching tip of endophyte rather than the synthesis or composition of substances filling lateral parts of the interface. Early developmental stages of haustoria can provide some information on the origin of such secretions, which was demonstrated for a shoot parasite mistletoe *Viscum minimum* (Heide-Jørgensen, 1988). However, this method is much harder to apply to root parasites as the haustoria occur below the soil surface, making it very difficult to follow successive stages of development and collect samples at high temporal resolution. While soil-free culture protocols have been developed for some parasites, in particular *Triphysaria* (Tomilov *et al.*, 2004), these require specialised, sterile conditions and high maintenance, and have not been tested on non-model taxa. Furthermore, as a result of the compositional diversity of interfacial materials and the very tight physical contact between both organisms, even a comprehensive set of developmental stages at a researcher's disposal might not prove helpful in identifying which side of the interface secreted the substance in question.

An alternative and largely unexplored system that allows exclusion of the potential host factor is offered by non-functional haustoria that develop without contact with a host organ and have received rather little academic attention. These may be haustoria clasping around small stones (Piehl 1963, figure 14), dead organic matter such as dead roots (Piehl, 1963) or twigs (Ren *et al.*, 2010) as well as non-clasping metahaustoria. The term was coined by Weber (1976) and where the prefix meta- was presumably used to mean "related to", in analogy to its application in chemistry. Metahaustoria were subsequently mentioned in some detail in the work of Kuijt (1977) as well as Attawi and Weber's manuscript on *Orobanche* (1980). These authors describe metahaustoria as large (up to 3.5mm wide) but non-parasitising haustoria that lost contact with host root after initiation but develop many features characteristic of normal attached haustoria, for example a secondary xylem strand. They should not be mistaken for very small (up to 0.1mm) wart haustoria which usually develop in higher parts of parasites' roots and in contact with a host root, however, lack the penetrative endophyte peg. In addition to these three key publications, other authors have used different terms describing (usually very briefly) non-functional haustoria that develop without contact with a host. These include "pseudo-haustoria" of *Cuscuta campestris* (Hong *et al.* 2011) and hormone-induced and thigmotropic pseudo-haustoria of *Triphysaria* grown in Hoagland medium (Tomilov *et al.*, 2005); "pre-haustoria" formed by *Cuscuta reflexa* on wooden sticks (Löffler *et al.*, 1999) and on filter paper (Ramasubramanian *et al.*, 1988) or by *Krameria lappacea* collected

in the wild; “spontaneous haustoria” developed by *Orthocarpus purpurascens* in Petri dishes with no germinations stimulants added (Atsatt *et al.*, 1978) and by *Agalinis purpurea* grown on nutrient agar (Riopel and Musselman 1979, Steffens *et al.* 1982). Haustoria attaching to pot surface have been observed in *Santalum album* (Tennakoon and Cameron 2006). Werth and Riopel (1979) found unattached haustoria with a smooth distal surface on *Aureolaria pedicularia* excavated in the wild. These haustoria differed from other ones which bore signs of previous attachment.

In this study, metahaustoria were commonly formed by pot-grown *Rhinanthus minor* and *Odontites vernus* in contact with container walls. They were also observed to produce phenolic-rich substances, which coated their pot-appressed facets, i.e the surfaces homologous to the interfacial zone in host-infecting haustoria. A study combining histology, immunocytochemistry and Raman spectroscopy was undertaken in order to characterise the architecture of these deposits in metahaustoria and infective haustoria. The ultimate aim was to provide insights into the origin of these phenolic-rich substances during infection of hosts, i.e. their deposition by the host versus the parasite.

7.3 Results

7.3.1 Morphology and anatomy of metahaustoria

Metahaustoria were developed by *Rhinanthus minor* and *Odontites vernus* grown with and without hosts. They were particularly abundant on *Rhinanthus minor* grown in cavity inserts in a greenhouse, with up to 23 large (2 mm) metahaustoria produced per plant. These plants were typically smaller than those grown with hosts but occasionally flowered. *O. vernus* grown in a half-size propagator also developed apparently normally and flowered (Fig. 7.1A), producing many metahaustoria on the outer surface of the soil (Fig. 7.1B). Plants grown in round pots with bad and good hosts typically produced up to five large metahaustoria (Fig. 7.1C). It was in only very few instances that no metahaustoria were produced. Additionally, both species produced haustoria when kept in Petri dishes in the fridge for 3–4 weeks after germination. They attached to filter paper and in one instance, already described in chapter 5, a haustorium was found appressed to the side of the dish.

When viewed under a stereomicroscope, the contact surface of a metahaustorium is smooth, with a narrow slit running through the centre of the haustorial face (Fig. 7.1C). A series of rib-like, elongated structures perpendicular to the slit is also visible (Fig. 7.1D). Serial sectioning revealed that these were elongated epidermal cells, homologous to the contact parenchyma of normal, attached haustoria. The interface-spanning, elongated shape of these cells is illustrated in figure 7.2. It corresponds with that of parasite contact parenchyma cells that stretch across the lateral parts of interface into the host stele in normal attached haustoria, when observed in

a cross-section view. Examples of these elongated interfacial cells in attached haustoria are shown in figures 7.6A–C or in figure 6.11B. Metahaustoria also possess tissue folds apparently homologous with clasping folds in attached haustoria. Despite these similarities, no cases of epidermal cell differentiation into xylem were observed in any of the analysed metahaustoria and few xylem bridge elements were detected in only one metahaustorium (data not shown). However, an early-stage hyaline body was found in several samples and labelled with LM2 (Fig. 7.3), similar to the hyaline bodies of attached haustoria. The contact parenchyma also labelled. These results show a considerable degree of similarity between metahaustoria and infective haustoria i.e. haustoria attached to hosts.

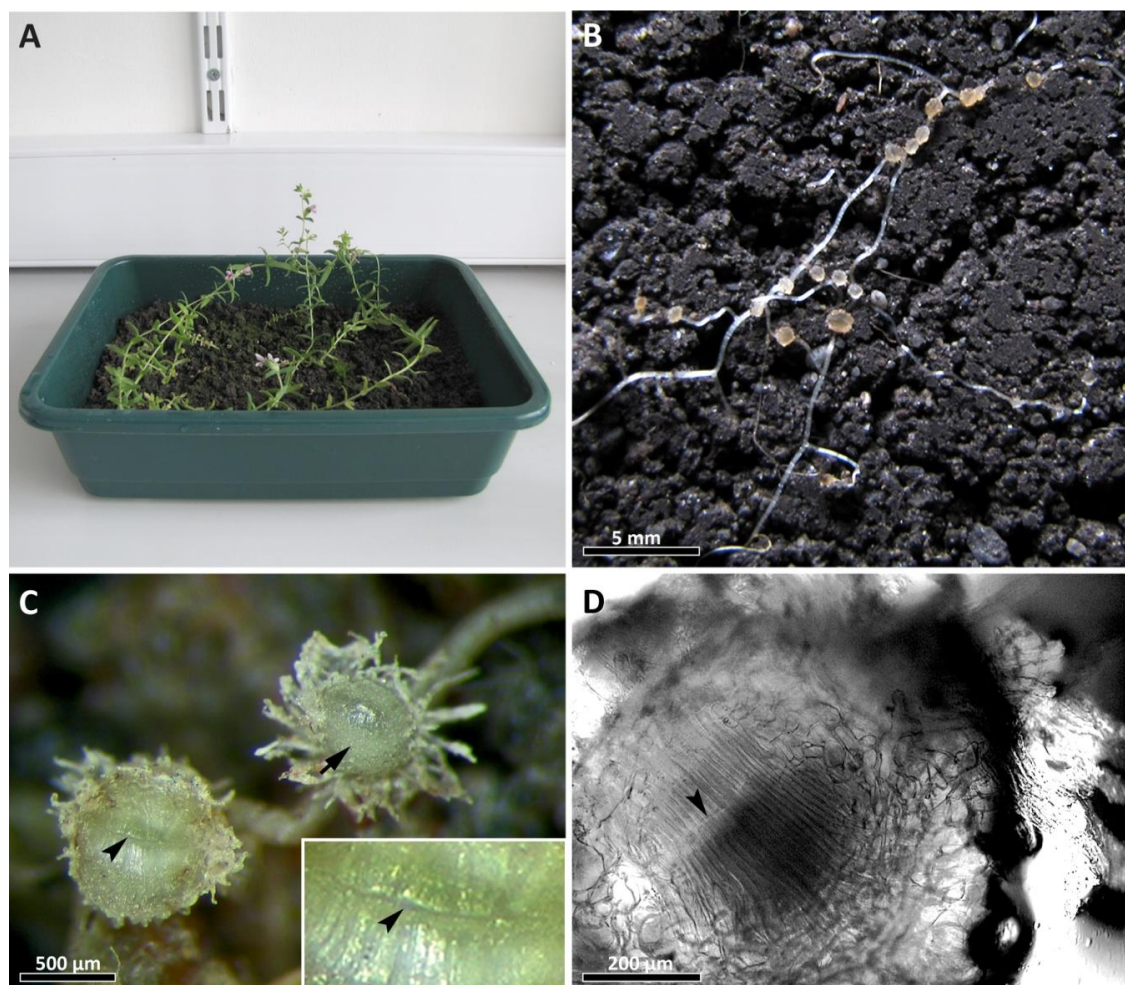


Figure 7.1: Morphology of metahaustoria. **A)** *Odontites vernus* grown in a half-size propagator without a host. Plants developed normally and flowered. **B)** Metahaustoria produced by *O. vernus* plants shown in image A. They appear as bead-like structures located along the roots, on the outside of the root ball, where they faced the wall of the pot. **C)** A stereomicrograph of metahaustoria of *Rhinanthus minor* grown with *Arrhenatherum elatius* var. *bulbosum*. Metahaustoria shown developed in addition to normal, infective haustoria. A fringe of haustorial hairs is visible. The smooth face (◄) of the haustorium is divided by a narrow slit (◄). **D)** A light micrograph of a metahaustorial face. Under the smooth haustorial face, a series of elongated cells, appearing as rib-like lines perpendicular to the slit (◄), is visible.

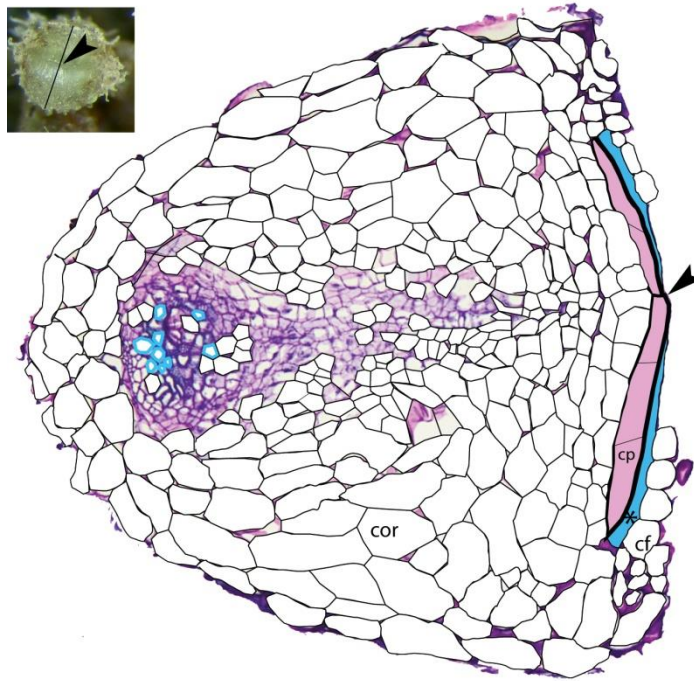


Figure 7.2: A diagram illustrating the anatomy of a metahaustorium in a plane corresponding to a cross section through a normal attached haustorium, as explained in figure 3.2. Inset image shows section orientation. In this view, contact parenchyma (**cp**) cells are elongated and possess scarce, thin cross walls. A layer of PhISC (*) is the thickest under the clasp folds (**cf**) which are appressed to the haustorial face. It gradually narrows towards the centre of the haustorial face, where two elongated cells of contact parenchyma meet (◄). This interruption in PhISC and site of cell contact is visible as the central slit illustrated in figure 7.1C. It corresponds with the site of endophyte cell descent into the host root in normal, infecting haustoria. A strand of small, cambium-like cells is visible in the centre but no axial xylem strand has formed.

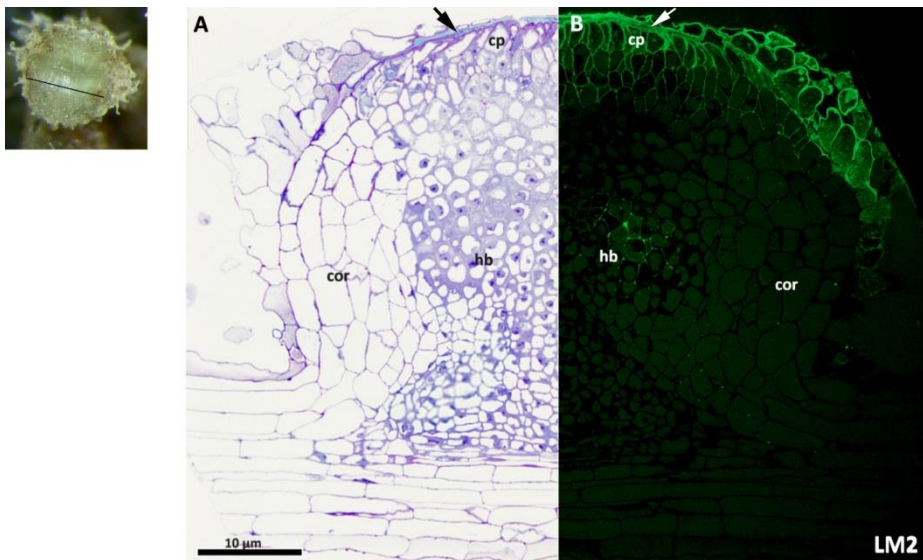


Figure 7.3: An example of a metahaustorium with developmentally advanced anatomy in a plane corresponding with a longitudinal section of an attached haustorium (Fig. 3.2). Inset image shows section orientation. Contact parenchyma (**cp**) cells are narrow and elongated towards the interface in this view. **A)** A distinct hyaline body (**hb**) region is present but a xylem bridge has not formed. **B)** The sample shows labelling with LM2 analogous to that seen in normal, attached haustoria, i.e. the hyaline body and contact parenchyma (**cp**) label strongly, whereas the cortex (**cor**) does not. Light-blue stained PhISC (◄) coats the pot-facing surface of contact parenchyma. This colour of staining indicates polyphenolics such as lignin.

The haustorial face is covered with a layer of material morphologically resembling cuticle. This layer does not, however, appear to be of lipidic nature but is phenolic-rich, as discussed in further parts of the results section, and is from now on referred to as **phenolic-rich interfacial secretion complex (PhISC)**. PhISC is the thickest in the lateral parts of the haustorial face, under the tissue folds, and gradually narrows and disappears at the central slit (Fig. 7.2). The slit corresponds with the site of parasite's cell intrusion into the host in host-infecting haustoria.

7.3.2 The architecture of the PhISC and contact parenchyma cell walls

Contact parenchyma cell walls often display an exaggerated degree of thickening in comparison with that typically observed in host-infecting haustoria (Fig. 7.4). Distal periclinal walls in contact with the PhISC are the thickest and the thickness gradually decreases in the direction proximal to parasite root. The proximal periclinal walls are therefore the thinnest (Fig. 7.4B and C). Several cell layers adjacent to contact epidermis also possess thickenings, although they are much less pronounced (Fig. 7.4B). Tissue folds covering the secretion often display similar wall thickening, which takes the form of more irregular flanges (Fig. 7.4B and C) with occasional ovoid areas of loosely fibrillar material (Fig. 7.4 C and E). The middle lamellae of tissue fold cells and epithelial cells are often swollen and very loosely fibrillar (Fig. 7.4D), resembling the ovoid structures in their supramolecular organisation. This swelling of middle lamellae is similar to that occasionally seen in normal haustoria (Fig. 5.15H). Vesicles (Fig. 7.4F and G) are often associated with contact parenchyma walls. Some of them appear to be filled with membraneous material, which might indicate endocytotic membrane recycling associated with intensive secretion (Stahelin & Chapman, 1987).

While the cell walls are clearly fibrillar (Fig. 7.4D and F), the extramural layer of PhISC shows a range of apparently non-fibrillar textures (Fig. 7.5). The layering can be very regular with smooth-textured, parallel strata (Fig. 7.5 A), or more complex, whereby the strata are of less uniform thickness, interlock in places and are differently textured (Fig. 7.5B–D). The fibrillar fraction of the wall can occasionally be seen interlocking with the innermost layer of the PhISC in a form of curved strands (Fig. 7.5A and 7.13B). Bacterial endospores are occasionally found in the PHISC of both metahaustoria and infecting haustoria (data not shown).

At light microscopy level, the interfacial substance of attached haustoria spanned from the flanks of the lateral interface to the sites of endodermis and pericycle separation (Fig. 7.6A–F). The blue staining with toluidine blue O occasionally gradually changed into purple away from the interface (Fig. 7.6B and E). At ultrastructural level, the PhISC of attached haustoria resembled that of metahaustoria in that no fibrillar structure was observed (Fig. 7.6G and H, Fig. 11D and E, Fig. 13A and C). However, the textured layering distinctive in the metahaustorial PhISC was not seen either. Additionally, a globular secretion structure was identified in areas that appear to be either still filling

with the deposits or had become torn/interrupted during sample processing (Fig. 7.6H).

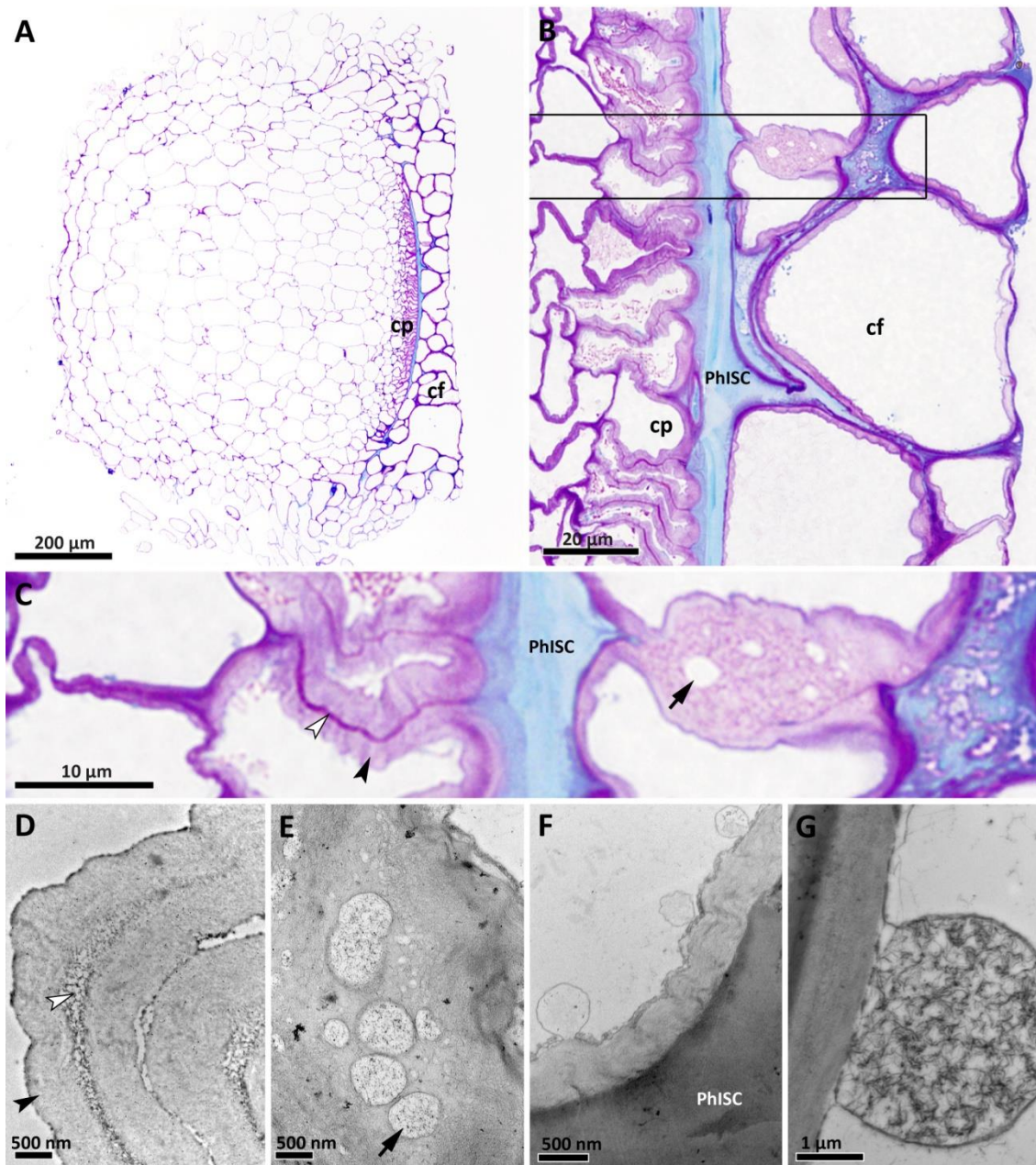


Figure 7.4: Structure of cell walls of the metahaustorial contact parenchyma (cp) and clasp ing fold (cf) parenchyma in *Rhinanthus minor* (A–D and F) and *Odontites vernus* (E and G). **A)** An overview image showing a longitudinal section taken some distance away from the central slit, where PhISC is covered by the cells of a clasp ing fold. **B)** A high magnification image showing the contact parenchyma, PhISC and clasp ing fold cells. While the cell walls of contact parenchyma and clasp ing fold parenchyma stain pink, indicative of pectins, PhISC stains bright blue, which is a colour characteristic of polyphenolics, such as lignin. The blue staining extends between the clasp ing fold cells where it co-occurs with irregular areas with pink-stained edges **C)** A higher magnification of the area indicated by the black outline in image B. Cell walls of contact parenchyma (◄) are considerably thickened (up to 4 μm from the middle lamella (◄) to the inner face of the thickened wall). The clasp ing fold cell wall thickenings are even more pronounced (up to 10 μm), and display swollen, spongy appearance with unstained oval areas (◄) often present. **D)** Detail of a cell wall thickening in contact parenchyma. The middle lamellae, which stained darkly with TBO (image C) are composed of loosely dispersed fibrils, similar to **E)** the oval areas which are found in clasp ing fold cell walls and do not visibly stain with toluidine blue O. **F)** Fibrils within the cell wall of metahaustorial contact parenchyma show a considerable degree of convolution. PhISC displays no apparent fibrillar structure. Plasmalemma-associated vesicles are common. **G)** occasionally contain what appears to be fragmented membrane material.

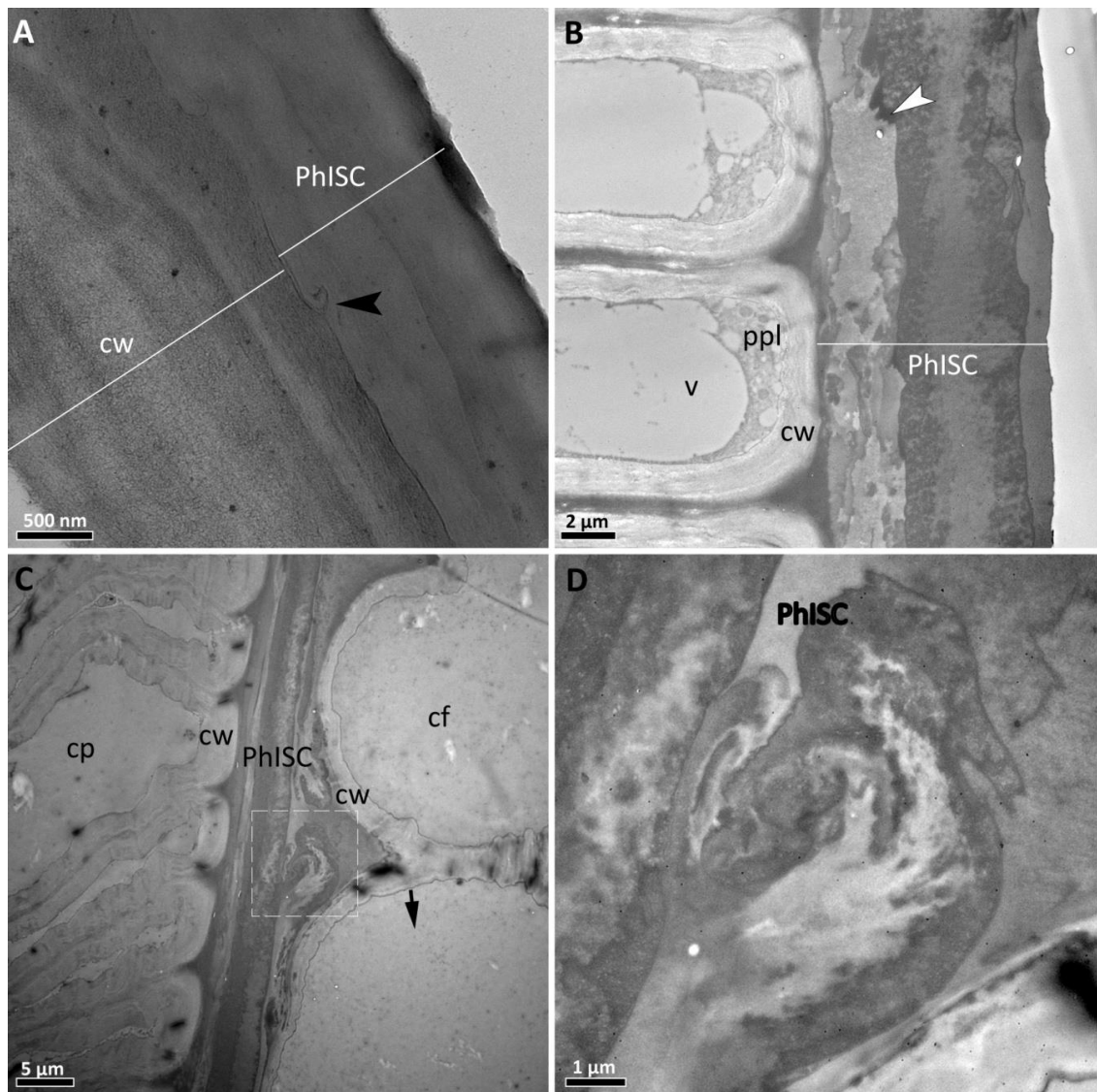


Figure 7.5: Ultrastructure of metahaustorial the PhISC in *Odontites vernus* (A) and *Rhinanthus minor* (B–D). Only sample shown in image A was osmicated and stained with uranyl acetate. Samples shown in B–D were not osmicated and are unstained. **A)** In its simplest form, the PhISC is composed of one or two layers of smooth-textured deposits with no apparent fibrillar component similar to that seen in the pecto-cellulosic cell walls (**cw**) of contact parenchyma (**cp**). Curved strands (\blacktriangleleft) of the regular cell wall interlocking with the PhISC are occasionally present. **B)** In many metahaustoria, the PhISC displays more complex layering with distinct texturing differing in electron-lucence. Contact parenchyma cells are sronly vacuolated (**v**) with protoplasts (**ppl**) concentrated at the tips. The layers often interlock (\blacktriangleleft) forming more irregular, angled edges boundaries than those seen in image A. **C and D)** The complex, textured layering and interlocking of the PhISC layers can also occur along more curved lines, displaying appearance reminiscent of partly-mixed, set liquid. **cf** — clasp cell

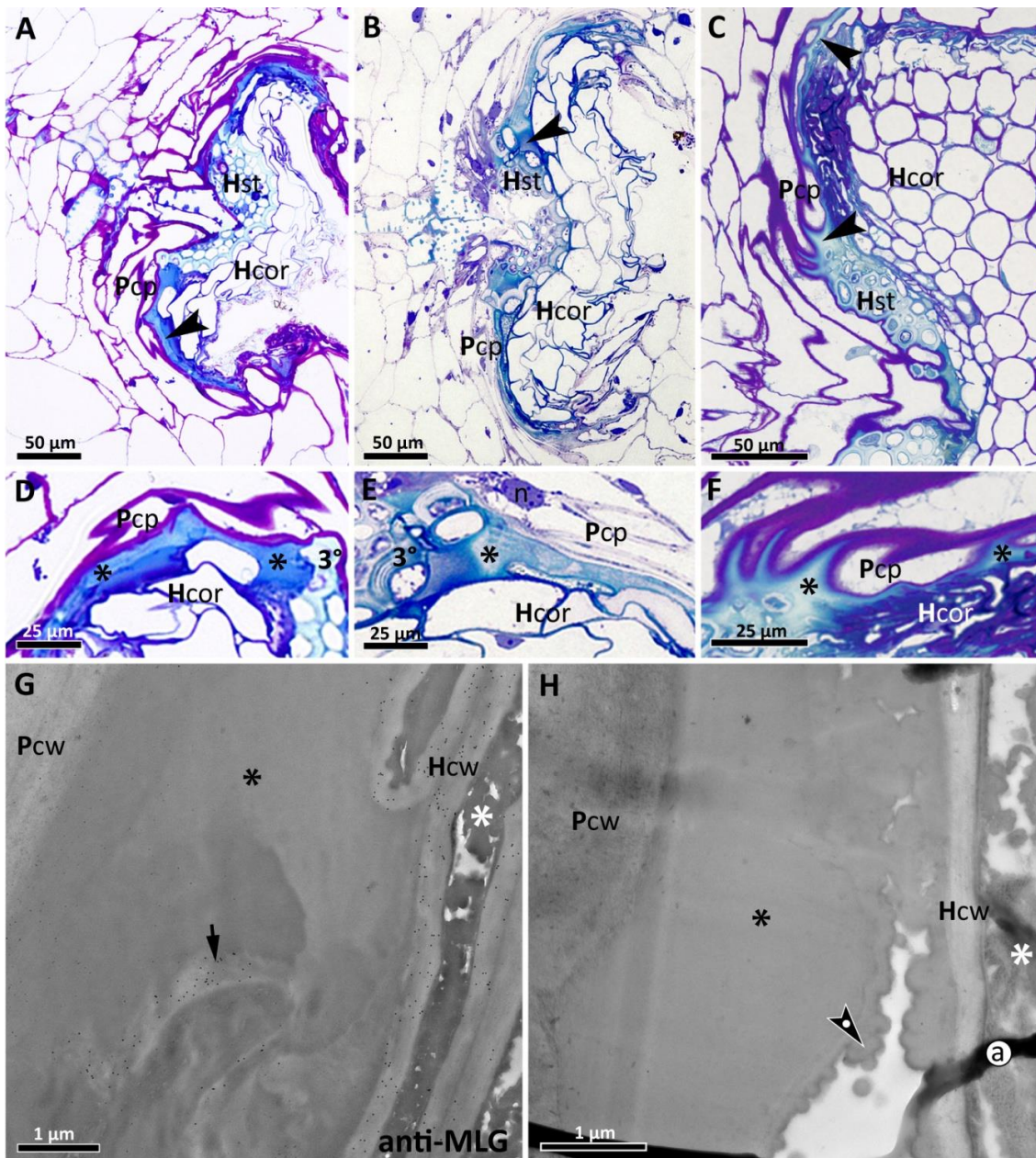


Figure 7.6: PhISC at the interfaces between normal attached haustoria of *Rhinanthus minor* and its non-host (a eudicot *Plantago lancolata*; images C and F) and a host (a grass *Arrhenatherum elatius* ssp. *bulbosum*; remaining images). **A, B and C)** Light blue staining (◄) indicative of polyphenolics is present along the lateral interfaces between parasite contact parenchyma (Pcp) and the cortices (Hcor) of the hosts as well as the non-host. In either case, access to the host stele (Hst) is gained. Thickness of PhISC is similar in all pairings. **D, E and F)** PhISC tightly fills the interfacial space between parasite contact parenchyma and host cortex, as well as the spaces between the peeled off tertiary endodermis (3°) and host cortex (D and E). E) PhISC staining shows a gradient, with blue staining gradually changing into purple away from the interface. **G and H)** The ultrastructure of PhISC (*) at lateral interfaces with *Arrhenatherum elatius* ssp. *bulbosum*. The secretion appears smooth and surrounds remnants of host cell walls (Hcw) which appear partly dissolved and are easily distinguished from parasite's walls after immunogold labelling with an anti-Mixed linkage glucan monoclonal antibody. Where PhISC does not fill the interfacial space completely, globular structure (◄) can be observed on the edges of the secretion. Disintegrated host protoplasts (⊛) show a coagulated structure.

Unstained PhISC was very strongly autofluorescent in blue and green channel (Fig. 7.7F and H and 7.8A). Strong red autofluorescence was observed as well, but is not shown. Autofluorescence was also found at the interfaces of attached haustoria and

in haustorial xylem (Fig. 7.7 E and G). Blue, green and red autofluorescence was also seen in lignified thickenings of haustorial xylem. This, in particular blue autofluorescence, suggests the presence of lignin in the PhISC. Intrinsic blue fluorescence overlaps with the calcofluor emission spectrum making it impossible to use it as an indication of cellulose presence within this layer, particularly as post-staining with toluidine blue O quenches the autofluorescence but interferes with calcofluor staining.

In addition to light blue staining with toluidine blue O, histochemical staining with Weisner reagent (Fig. 7.7 A and B, Fig. 7.8B) and Maüle reagent (Fig. 7.7C and D, Fig. 7.8D) and specific for lignin, resulting in dark brown and deep magenta colour respectively, suggests the presence of this compound in the metahaustorial PhISC. Again, this staining was also found at contact sites between infecting haustoria and their hosts, where it filled the lateral part of the interface and cracks in host root effected during intrusion (Fig. 7.9). Lipophilic fluorochromes Rhodamine B and Auramine O stain the PhISC but also the xylem and therefore are not useful in distinguishing a possible lipid component such as suberin (data not shown). Lipophilic dyes Oil Blue N, Oil Red O, Sudan III, IV and Black did not stain any metahaustorial walls (data not shown).

Comparison of toluidine blue O, Maüle reagent, Weisner reagent and Rhodamine B staining and quenching effect showed heterogeneity in the metahaustorial PhISC (Fig. 7.8). Toluidine blue staining occurred in light blue and pink parallel bands within the PhISC while quenching of autofluorescence was uniform. Maüle reagent stained the entire layer in banded patterns of varying intensities and quenched all autofluorescence. The PhISC stained dark brown and xylem was coloured light brown, whereas all remaining cell walls stained light yellowish brown. Neither extended washing in 3% HCl, nor increasing the concentration of HCl to 10%, resulted in the removal of parenchyma staining or caused a change of PhISC staining colour to red, which is typically indicative of syringyl-rich lignin (Iiyama *et al.*, 1988; Guo *et al.*, 2001; Shadle *et al.*, 2007), detected in the PhISC with polyclonal antibodies (see later parts of this section). Phloroglucinol stained strongly most of the PhISC, leaving a thin outer band unstained and autofluorescent. Rhodamine B resulted in the most uniform staining and quenching, saturating the entire extent of the secretion and leaving no residual autofluorescence.

The staining with all of the above dyes showed that the PhISC was also sandwiched between the distal parts of anticlinal walls of contact epidermis by means of extensions resembling anticlinal pegs of cuticles. The fibrillar epidermal walls stained pink or purple with toluidine blue O, indicating the presence of pectins. While strong birefringence was seen in the walls of xylem, contact parenchyma and many other parenchyma cells, the PhISC is non-birefringent (Fig. 7.10). In infecting haustoria non-birefringent PhISC is in contrast with strongly birefringent lignified cells of the host stele.

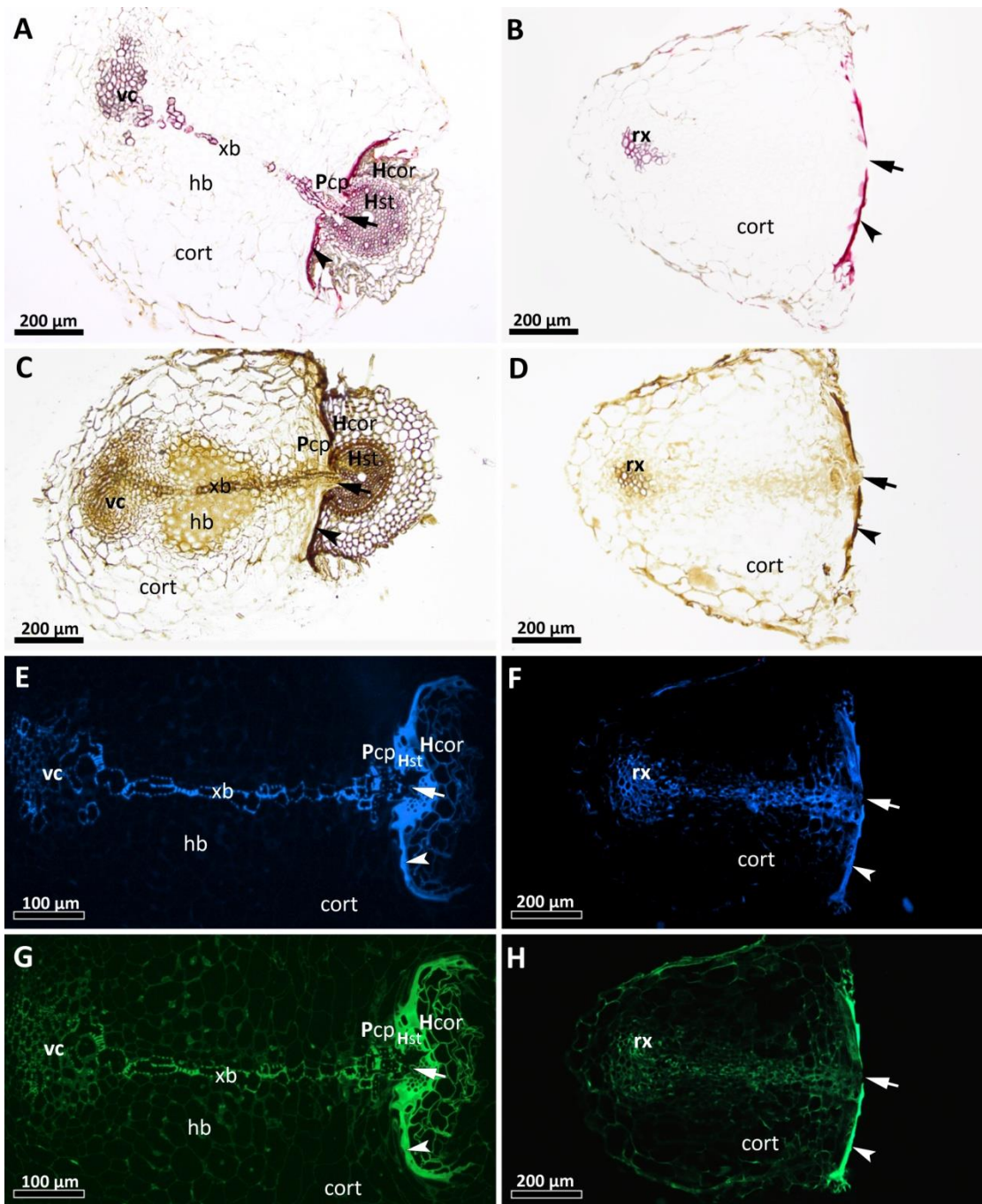


Figure 7.7: Autofluorescence and histochemical detection of lignin in PhISC. Figures A–D illustrate sections obtained from Steedman’s wax-embedded samples. **A)** Weisner reagent staining of lignins in a haustorial graft between *Rhinanthus minor* and *Lolium perenne*. Lignin is detected in the xylem bridge (xb) and host stele. Additionally, a line of dark staining is present at the interface (◄). **B)** A layer of Weisner reagent-positive material lines the metahaustorial face, i.e. in the region analogous to the interface in attached haustoria. An unstained “opening” (◄) is present at the centre of the face, corresponding with the site of enophytic cell intrusion into the host in attached haustoria. Similarity between the interfacial region of attached haustoria and metahaustorial faces is further confirmed with Maüle reagent staining (**C and D**) as well as blue (**E and F**) and green (**G and H**) autofluorescence. All of these detection methods also highlight the similarity of the PhISC to xylem, further suggesting the presence of lignin.

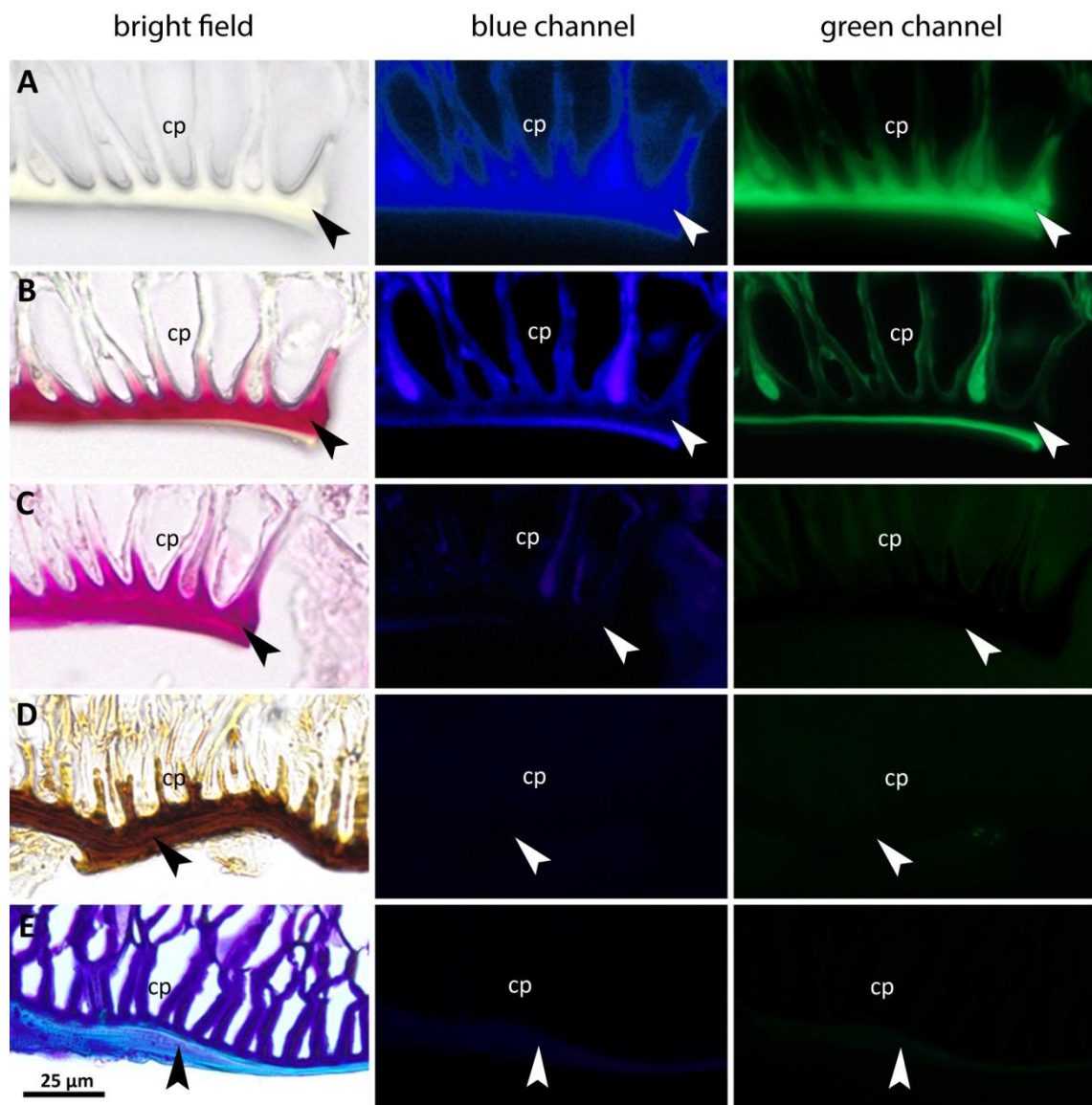


Figure 7.8: Autofluorescence quenching by histochemical dyes. **A)** unstained; **B)** Weisner reagent; **C)** Rhodamine B; **D)** Maüle reagent; **E)** Toluidine blue O. Sections were obtained from Steedman's wax-embedded samples. Stains specific for lignin, Weisner reagent and Maüle reagent stain PhISC strongly and also react with the distal parts of cell walls in contact parenchyma. Maüle reagent quenches all autofluorescence while Weisner reagent quenches a thick band of PhISC, while leaving a thin, unstained outer strip and cell walls of contact parenchyma (**cp**) unquenched. Toluidine blue O, which stains PhISC light blue indicating polyphenolics, leaves only extremely faint autofluorescence. Staining with Rhodamine B, which is a lipophilic fluorochrome, is, in this case, unusual in that it quenches autofluorescence and effects no secondary fluorescence. It also stains xylem (not shown) and therefore is not specific for lipids. It quenches autofluorescence more effectively than Weisner reagent.

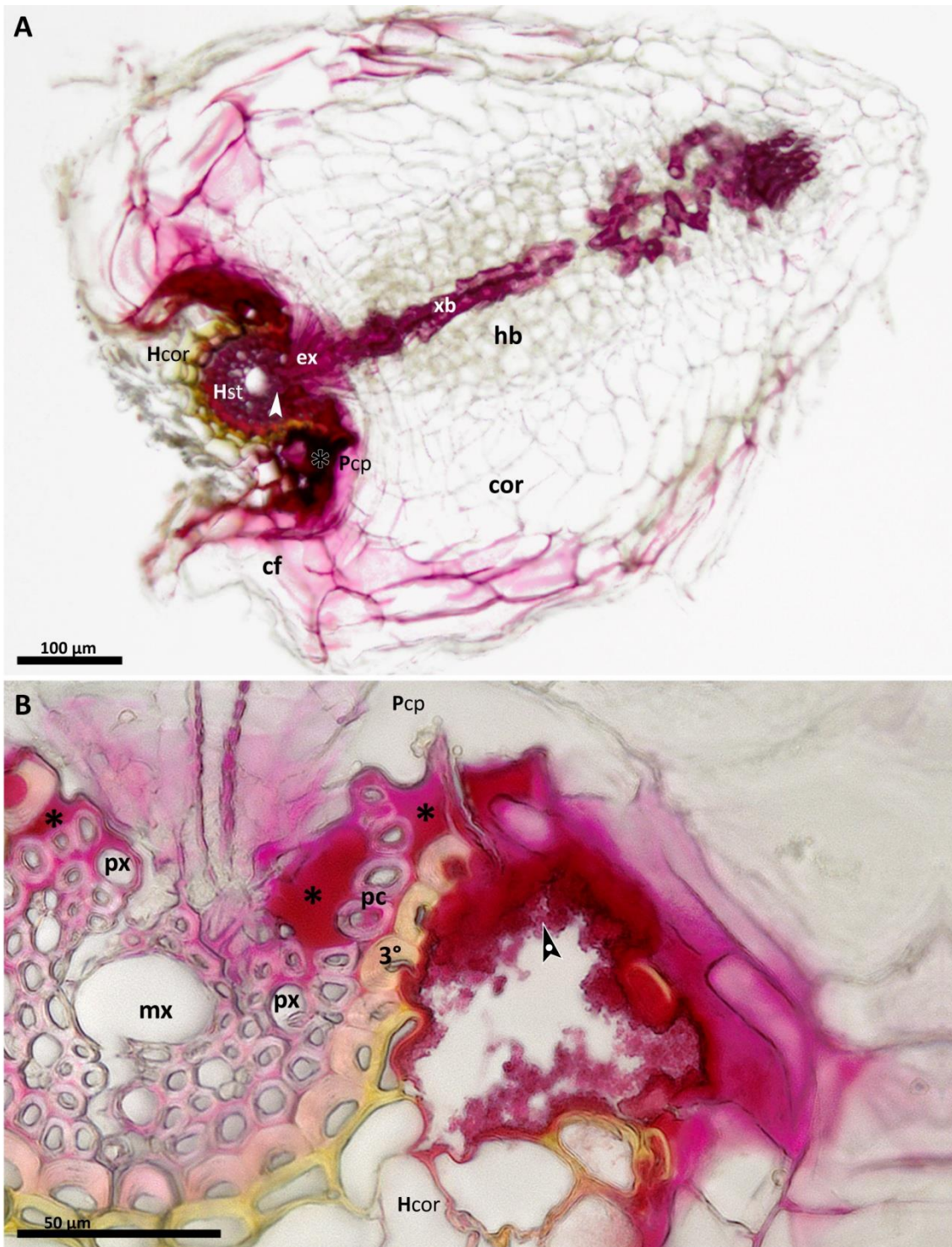


Figure 7.9 Weisner reagent staining of lignin in a haustorium of *Odontites vernus* attached to a host *Arrhenatherum elatius* var *bulbosum*. Sections were obtained from Steedman's wax-embedded samples. **A)** The reagent stains the vasculature of the xylem bridge (**xb**) but also reacts with parenchyma cells of the clasp folds (**cf**) and distal outer parts of the cortex (**cor**) as well as the interfacial contact parenchyma (**Pcp**). Host stele (**Hst**) also stains. The endophyte tip (**▲**) has penetrated the host stele and its cells have differentiated into xylem (**ex**). **B)** Detail of the interfacial region in a section taken from the same haustorium as in image A. Darkly stained PhISC (*****) fills the spaces between the parasite's contact parenchyma (**Pcp**) and peeled off layers of pericycle (**pc**) and tertiary endodermis (**3°**). At the interface with the host cortex (**Hcor**), PhISC does not fill the entire interfacial space and displays globular structure on the edges (**▲**). Parasite contact parenchyma has partly grown between the tertiary endodermis and pericycle.

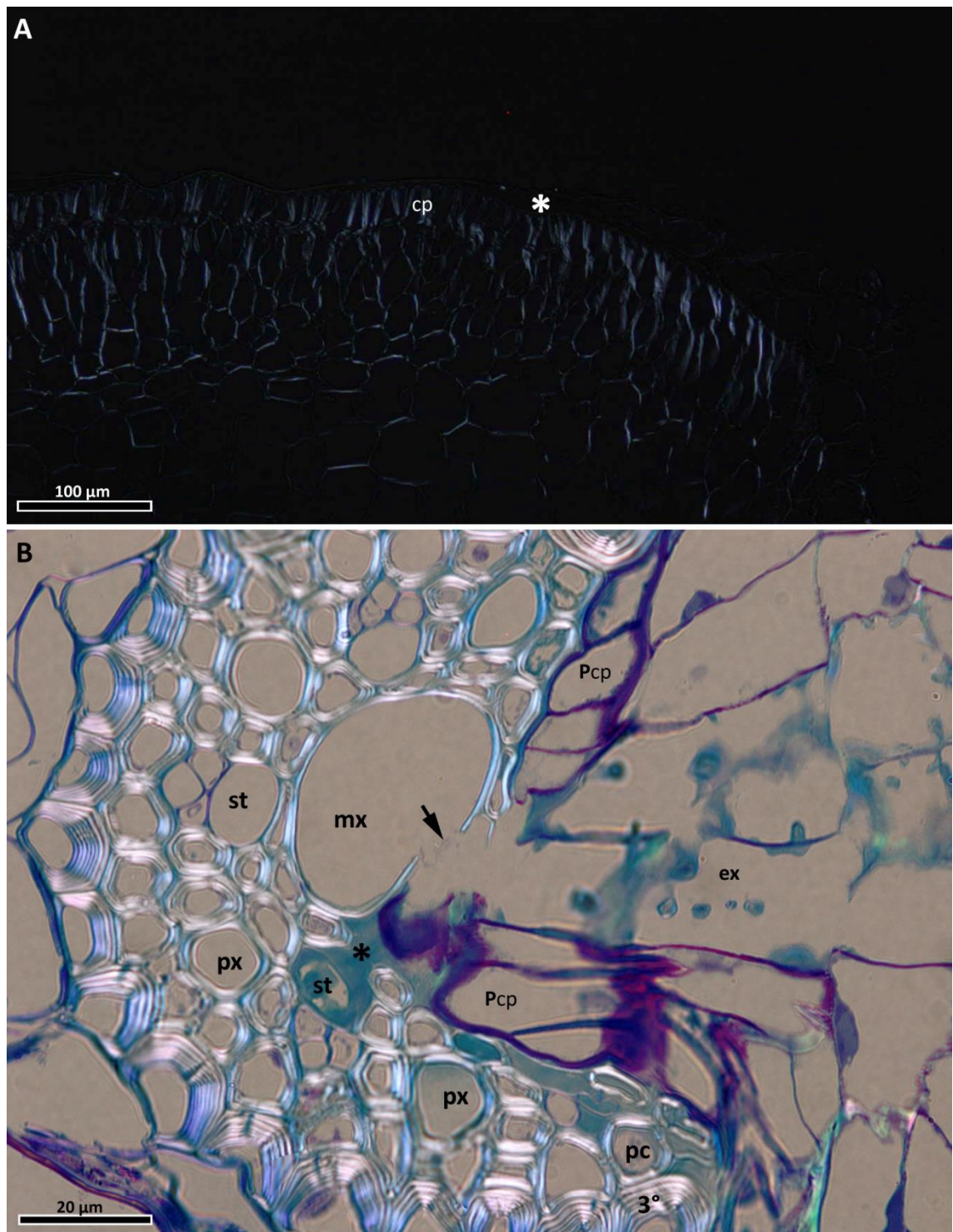


Figure 7.10: Cell wall birefringence in a metahaustorium of *Rhinanthus minor* (A) and at the interface between *Rhinanthus minor* and *Arrhenatherum elatius* var *bulbosum*. In the metahaustorium, contact parenchyma (cp) is birefringent but PhISC (*) is not. In the attached haustorium contact parenchyma (Pcp) is not birefringent and endophyte xylem (ex) cell walls are only weakly birefringent. The strongest birefringence is seen in the lignified cells of the host stele. PhISC shows no birefringence. **st** — sieve tube, **px** — protoxylem, **mx** — metaxylem, **3°** — tertiary endodermis, **←** — site of metaxylem wall interruption and luminal continuity between the parasite and host

Immunolabelling with antibodies JIM5 and JIM7 confirmed the presence of pectins in contact parenchyma cell walls but not PhISC (Fig. 7.11A and B). Xyloglucan epitopes detected by monoclonal antibodies LM15 and LM25 were abundant in the secretion and scarce elsewhere (Fig. 7.11E–G). Labelling was generally denser and more uniform with LM25. Additionally, low levels of xylans and mannans were detected using LM11 and LM22, respectively (data not shown). LM2-detected arabinogalactan protein epitopes were very abundant in the interfacial parenchyma walls (Fig. 7.11D) and up to 3 adjacent layers of cells (Fig. 7.2). The labelling was also dense in the PhISC. In analogy to metahaustorial labelling, AGP immunodetection was pronounced in the parasite contact cells during infection of a host and in the PhISC, where gold particles often occurred at highest density.

At immunofluorescence level, the polyclonal antibodies against lignin bound to virtually all walls of the haustorium, showing the strongest immunofluorescence signal in the contact parenchyma (data not shown). Of the three probes used, anti-S antibody produces the broadest immunogold binding to parenchymal walls, while also showing the most pronounced increase in the labelling of the PhISC. Immunogold labelling resulted in the highest particle density in the PhISC (Fig. 7.12A and D), while the contact parenchyma cell walls (Fig. 7.12A and B) and, to a lesser extent, protoplasts, also labelled. The spongy cell walls and fibrillar content often seen in the cells of the clasping folds also labelled (Fig. 7.12C). As this binding within parenchyma did not correspond with light blue staining with TBO, a degree of non-specificity of the antibodies is possible. Controls excluding the primary antibody were devoid of particles (Fig. 12 E and F). G and H lignin amounts were usually detected at much lower densities (results not shown).

Raman spectroscopy point measurements within the PhISC, centred at $1500 \text{ wavenumbers/cm}^{-1}$ resulted in a distinctive band in the region of $1600 \text{ wavenumbers/cm}^{-1}$ (data not shown). This peak was not detected in epidermal cell walls. Subsequent heat maps analysed by means of principle component analysis (PCA) and multivariate curve resolution (MCR) resulted in clear distinction of a component characterised by a phenolic-specific peak around $1600 \text{ wavenumbers/cm}^{-1}$ and localized in the PhISC (Fig. 7.13 and 7.14). Weaker intensity was also observed in the interfacial parenchyma cell walls (Fig. 7.13 PC1 and comp1). Additionally, differentiation of phenolics into different components was achieved with MCR in samples of infecting haustoria (Fig. 7.14). Phenolics in the host xylem are separated from those in the cell contents of a crushed tertiary endodermis cell and the PhISC. They are characterized by a double peak, typical of lignins (Schmidt *et al.*, 2010; Gordon Allison, *pers. comm.*).

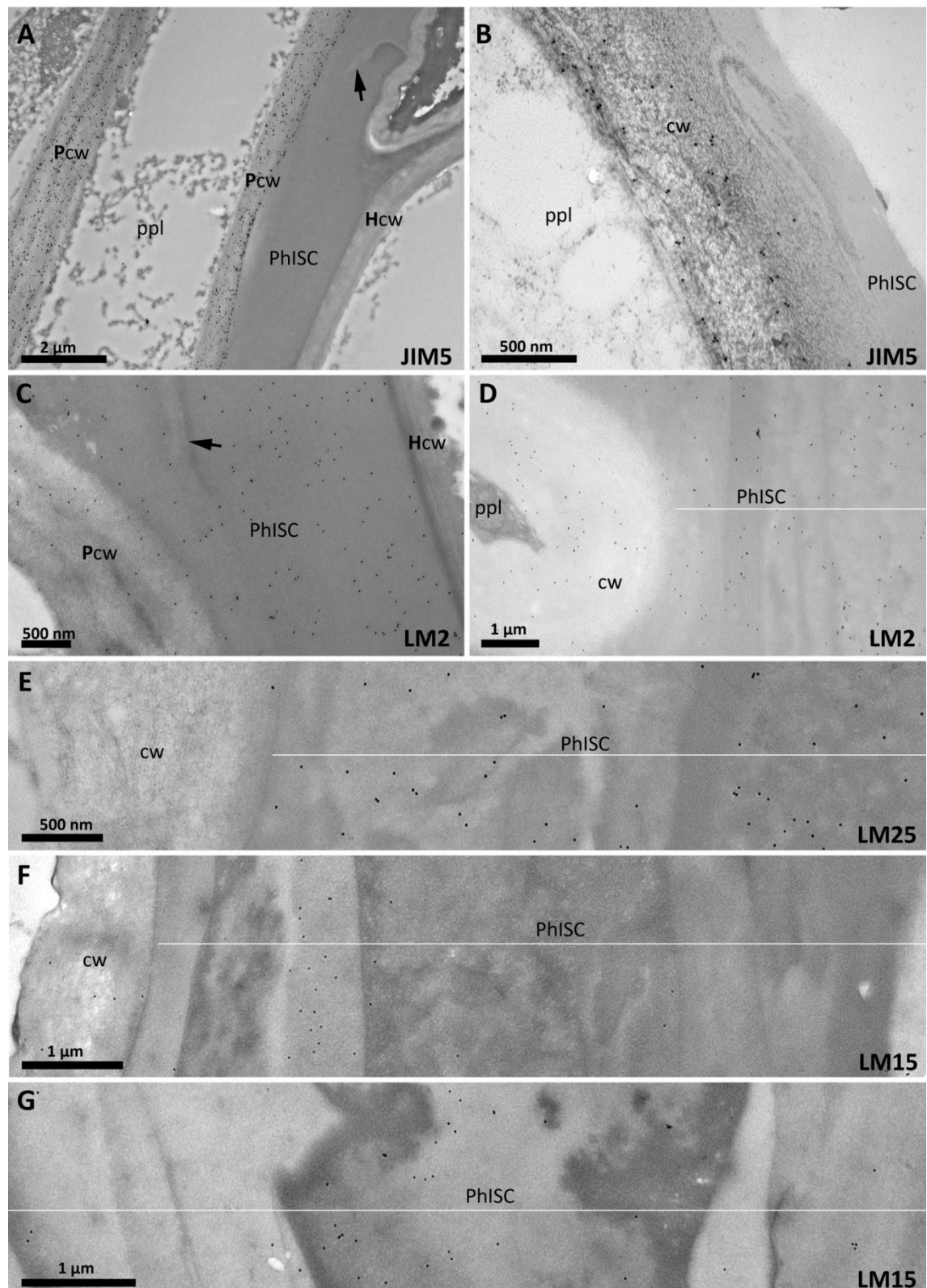


Figure 7.11: Immunogold detection of glycan epitopes in the PhISC (extent indicated with white a white line). **A)** JIM5 homogalacturonan labeling is absent from the PhISC and host (*Arrhenatherum elatius* var. *bulbosum*) cell walls, while being dense in the parasite contact parenchyma cell walls (**Pcw**). Host cell wall delamination is also seen, with a partly dissolved cell wall fragment (◄) embedded in the PhISC. **B)** Similar to the interfacial PhISC, the meta-haustorial PhISC does not label with JIM5, while the cell wall does. A curved area of the cell wall and the PhISC interlocking is present. **C and D)** The interfacial (C) and the meta-haustorial (D) PhISC immunogold label densely for AGPs with LM2. **E)** Xyloglucan labeling with LM25 mAb is present across the entire thickness of the PhISC, while **F and G)** LM15-recognised epitopes are found in isolated layers within the PhISC.

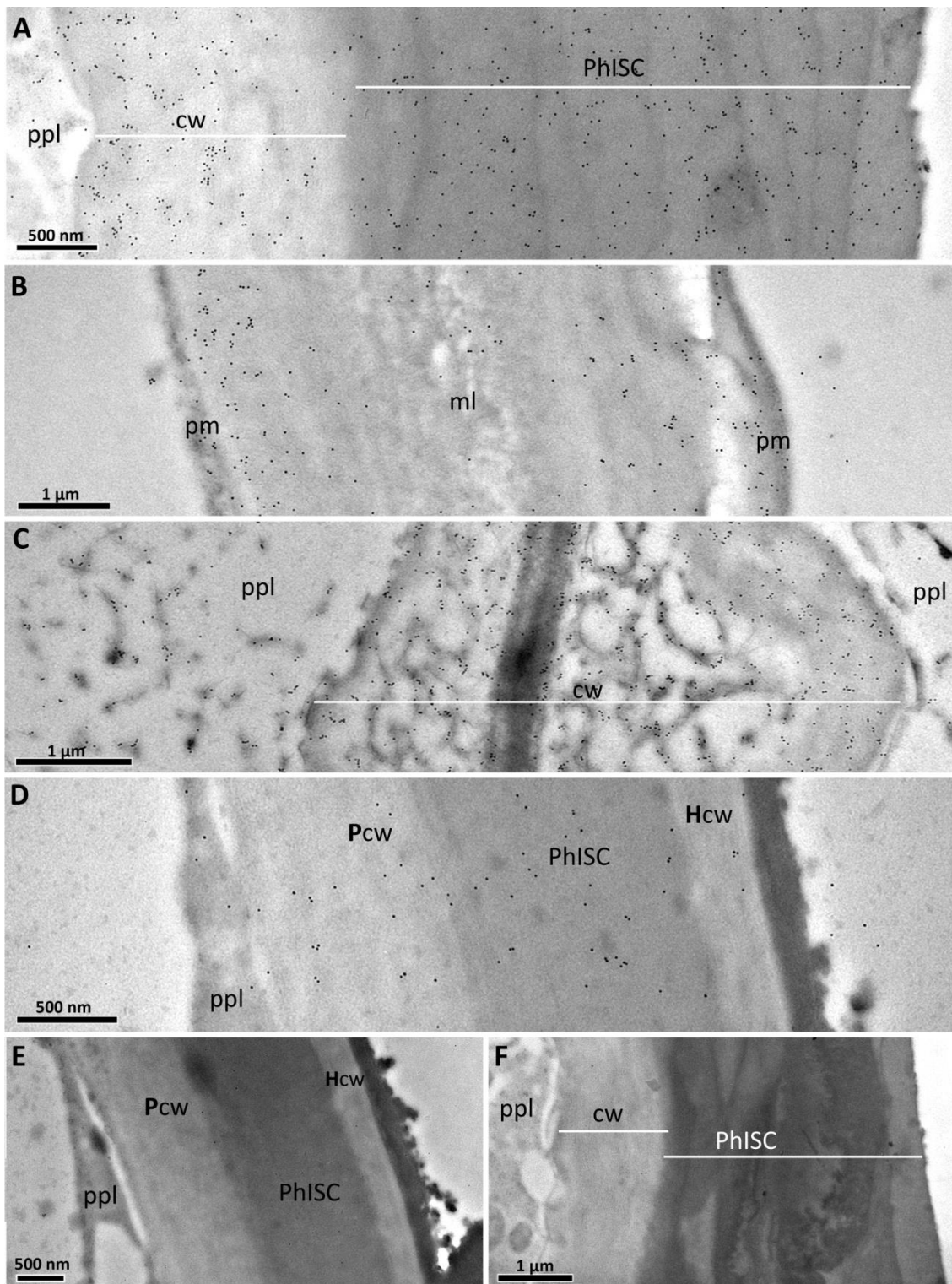


Figure 7.12: Immunogold labelling of haustorial and metahaustorial cell walls and PhISC with a polyclonal antibody against syringyl sub-units of lignin. **A)** Gold particles can be observed in the protoplast (**ppl**) and increase in density in the cell wall (**cw**). Labelling is also positive across the entire thickness of PhISC. **B)** Labelling of the anticlinal cell walls of metahaustorial contact parenchyma. Gold particles show highest density in close to the protoplast but are also present in the middle lamella (**ml**). **C)** Labelling within a clasping fold cell is distributed across the entire thickness of the swollen cell wall (extent indicated with a white line), including the loosely fibrillar portion as well as more compact layers. Labelled fibrils are also present within the protoplast. **D)** Labelling at the interface between *Rhinanthus minor* and *Arrhenatherum elatius* var. *bulbosum* involves cell walls of the host (**Hcw**) and parasite (**Pcw**) as well as PhISC, with scarce particles also found in the protoplast. **E and F)** Control images of the interface between *Rhinanthus minor* and *Arrhenatherum elatius* var. *bulbosum* (E) and *R. minor* metahaustorium.

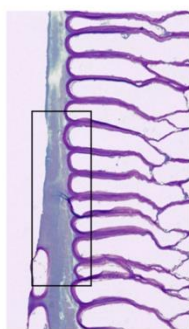
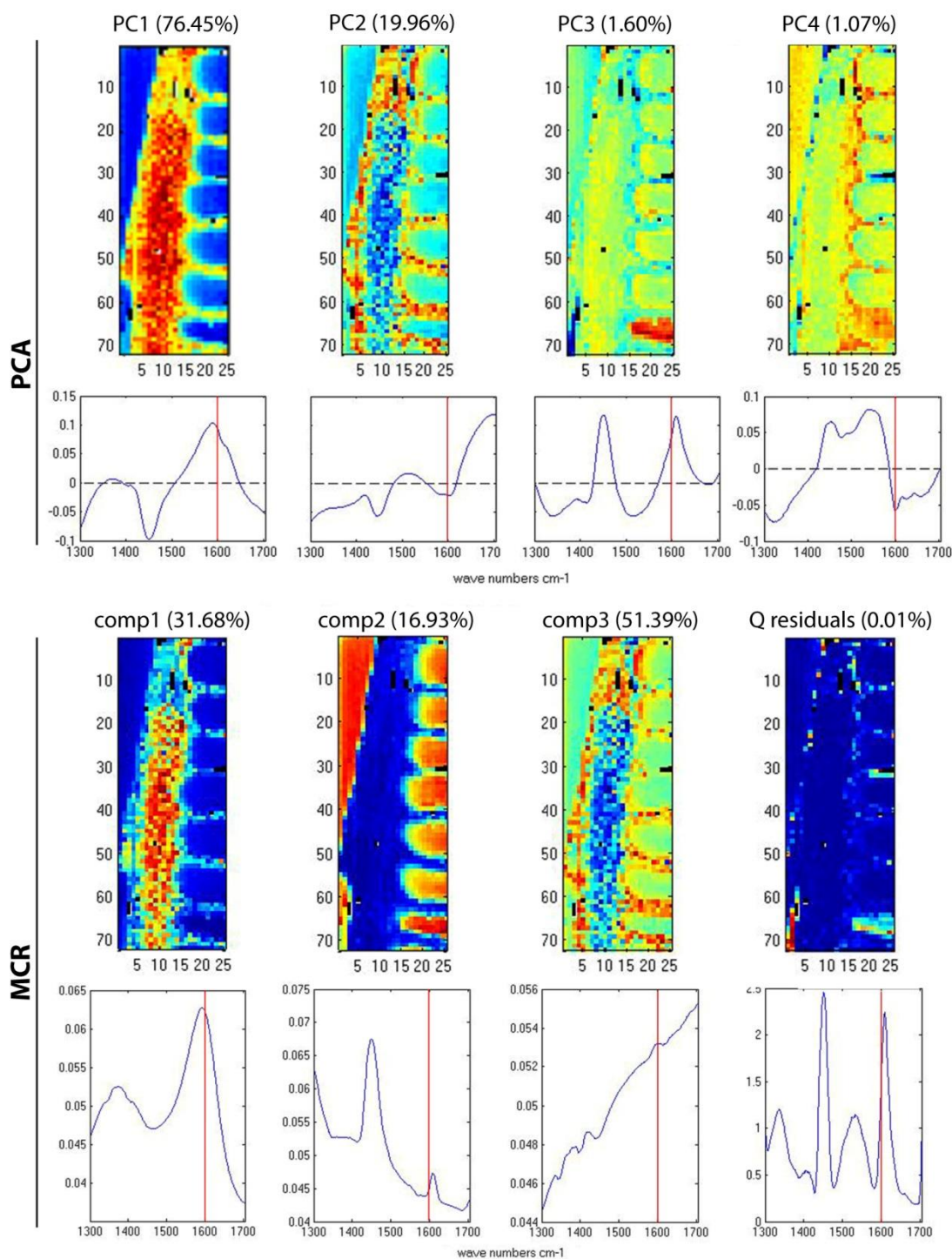


Figure 13: Raman spectroscopy of phenolic compounds in metahaustorial PhISC. A peak at 1450 wavenumbers $\times \text{cm}^{-1}$ represents background signal from the protoplasts (comp2). Both PCA component one and MCR component 1 recognise a single peak around 1600 wavenumbers $\times \text{cm}^{-1}$, confined to the PhISC and, at a lower intensity, contact parenchyma cell walls (red and orange scores on PC1 and comp 1). A degree of heterogeneity is present within the PhISC and might reflect the ultrastructural (textural and compositional) differences seen with immunogold labelling and histochemical staining. Inset image to the left depicts a serial section taken immediately after the mapped section and stained with toluidine blue O toluidine blue. The extent of the mapped area is indicated by the box.

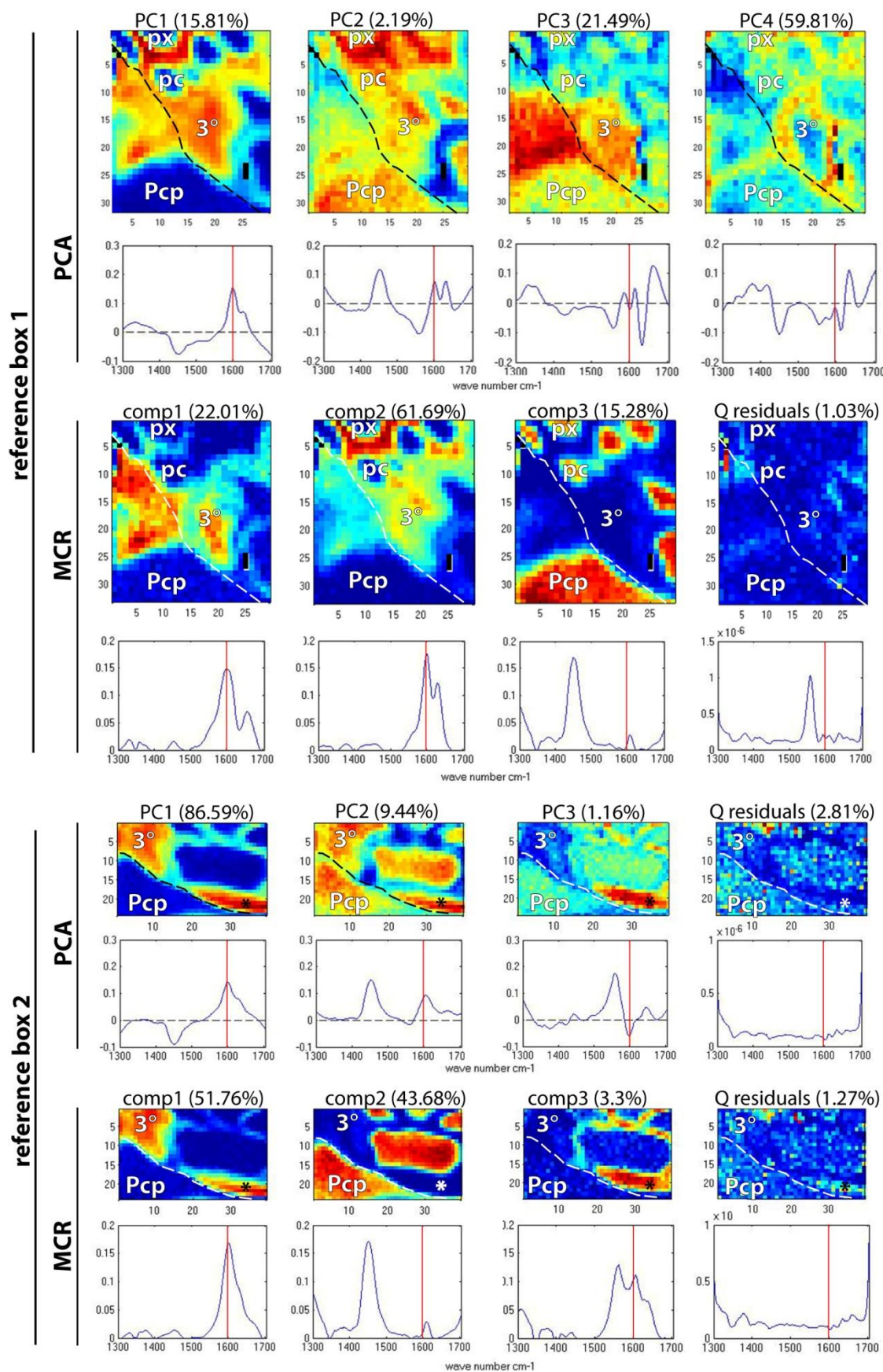
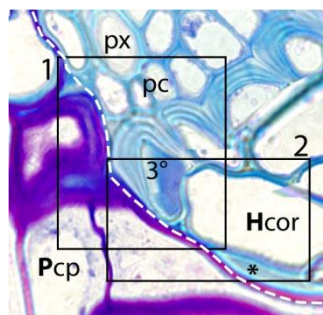


Figure 7.14 (continued with an overview image on the next page): Raman spectroscopy of lignin and lignin-like polyphenolics at the interface between *Rhinanthus minor* and *Arrhenatherum elatius* var *bulbosum*.

Figure 7.14 (continued from the previous page): The overview image illustrates a section taken very close to those mapped. Therefore the layout of cells might not be exactly the same. All tissue to the bottom left of the dashed line is the parasite's contact parenchyma (**Pcp**). Peaks near 1450 wavenumbers $\times \text{cm}^{-1}$ (comp 3 and comp 2) represent background signal from the protoplast. **A)** Both, principle component analysis (PCA) and multivariate curve resolution (MCR) show that the cell walls of host protoxylem (**px**) display a double peak around 1600 wavenumbers $\times \text{cm}^{-1}$, characteristic of lignins. This is illustrated as intense red scores for principle component 1 (**PC1**) and component 2 (**comp2**). This peak is to a lesser extent recorder from the cell walls of tertiary (**3°**) endodermis (yellow and orange scores for comp2). Lignin-like substance characterised by a single peak at 1600 wavenumbers $\times \text{cm}^{-1}$ is identified as MCR component 1 (**comp1**). It is localised in the protoplast of the crushed endodermal cell and in one of the contact parenchyma (**Pcp**) cell walls. **B)** Mapping of the interface immediately above the endodermis, where no xylem is present, returns no typical, lignin-specific double bands. PhISC present in contact with host cortex is characterised by the same, lignin-like, single peak as the contents of the crushed endodermal cell (PC1 and comp1), similar to that seen in the metahaustorial PhISC.



7.4 Discussion

A previously unreported layer of lignin-like extracellular deposits covering the contact face of metahaustoria was described in this study and termed phenolics-rich interfacial secretion complex (PhISC). Its discovery provides novel insights into the origination of cell wall phenolic substances at the interfaces of host-infecting haustoria. Lignin (Vance *et al.*, 1980; Nicholson & Hammerschmidt, 1992; Rümer *et al.*, 2007; Bhuiyan *et al.*, 2009) as well as suberin (Kamula *et al.*, 1994; Lulai, 1998), callose (Brown *et al.*, 1998; Letousey *et al.*, 2007) and extensins (Pérez-de-Luque *et al.*, 2006a; Deepak *et al.*, 2010) are molecules known to undergo crosslinking, contributing to cell wall reinforcement during wounding and pathogenesis, as well as prevention of the progress of fungal and angiosperm haustoria. It is, therefore, understandable that any such substances found at haustorial interfaces are expected to be a product of the host. Further, it is difficult to imagine that a phenolic-incrusted layer separating the host from its invader could serve the latter in its offensive efforts. However, this study demonstrates that the contact cells of *Rhinanthus minor* and *Odontites vernus* are able to secrete large amounts of phenolic-rich substances, when they come into contact with inorganic objects, and that similar substances occur in the equivalent regions of the infecting haustoria. This is in accord with the findings presented in chapter 6, which stated that cell walls of various hosts were not found to respond to infection by cell wall lignification, while a distinct layer of a phenolic-rich interfacial secretion complex (PhISC) was found at the interface with hosts and non-hosts. A similar observation was made for interfaces between *Striga hermonthica* and its wheat and sorghum hosts, where a layer of phenolics was also present, but not successful in stopping the parasite (Vasey *et al.*, 2005).

In addition to filling the space between the parasite and the host, the PhISC was also tightly associated with parasite contact cells and was anchored between their distal ends. Presence of lignins in distal periclinal walls of contact cells in the haustoria

of members of the Orobanchaceae was demonstrated for *Triphysaria* (Heide-Jørgensen and Kuijt 1993) and *Buchnera hispida* (Neumann *et al.*, 1999) where it was hypothesised to benefit the parasite by strengthening the infective cells to prevent microbial infection or to cross-link the parasite to host cell walls for better grip. Furthermore, Tennakoon and Cameron (2006) found dark-staining materials in the space between the searching cells of *Santalum album* and the host and proposed that they might be produced by the invader to facilitate adhesion. Rümer *et al.* (2007) suggested that similar interfacial materials could be implicated in sealing to prevent water loss during abstraction by the parasite. Piehl (1963) observed globular interfacial material in *Pedicularis canadensis* and suggested it was parasite-derived and facilitated attachment and breakdown of host cells. Nwoke (1982) proposed interfacial deposits staining dark brown with Safranin to be debris of host cells digested by *Alectra vogelii*. However, he had previously suggested that they had been secreted by the parasite and may have contained enzymes facilitating loosening of middle lamellae and, ultimately, infiltration and dissolution of host cells (Nwoke & Okonkwo 1978). While no evidence to support these theories was demonstrated, Losner-Goshen (1998 — figure 2) observed that osmiophilic coating on the lateral haustorial surface of *Orobanche aegyptiaca* extended to regions not in contact with host tissues. Unfortunately, this finding was not further investigated or discussed, although it suggested that phenolic substances in the interfacial region were produced not only by the host, but also the parasite. Considering the findings presented in this chapter, these substances, only briefly mentioned by other authors, might have represented a type of material similar to the PhISC.

Metahaustoria and metahaustoria-like structures are likely to be common but overlooked in different families. Non-attached haustoria of a shrubby root hemiparasite *Krameria lappacea* (Krameriaceae) termed as “pre-haustoria” (Brokamp *et al.*, 2012) are covered by a layer of periderm with an opening at the distal surface, in analogy with the central slit in the PhISC.

Metahaustoria are presumed to be of thigmotropic character and, as previously found for *Santalum album* (Tennakoon and Cameron 2006), they were formed by *Rhinanthus* and *Odontites* on the outside of the root ball, facing the wall of the pot. The examined metahaustoria share more features with mature than with young infecting haustoria and therefore provide a useful and justified system for comparative studies. Certain examples reach dimensions larger than those of fully developed infecting haustoria but usually lack a xylem bridge, while a well defined hyaline body is a relatively common feature. Clasping folds, also known as mantel lobes (Kuijt 1977), which normally clasp around host root, are present. They are appressed to the contact parenchyma, from which they are separated by the PhISC. As metahaustoria develop in the absence of a host and care was taken in this study to collect haustoria appressed to the pot, presence of clasping folds does not support the view of Weber (1976) that they

are characteristic of those metahaustoria that once clasped around a host root. It also highlights the low level of dependence on, or specificity of, inducing factors from the host to develop a structure which evolved to hold an infected organ. The relatively large amount of the PhISC is another feature shared by metahaustoria and mature infective haustoria, but not early stage attached haustoria. A several-days old metahaustorium that developed on the wall of a Petri dish had not yet deposited any PhISC, suggesting that it is secreted at later developmental stages. As shown in chapter 5, an immature haustorium before host endodermal penetration possesses a relatively thin layer of deposits, clearly visible only when using electron microscopy. Bacterial endospores are occasionally embedded in PhISC of both metahaustoria and normal haustoria, as previously found by Losner-Goshen (1998) and Joel and Losner-Goshen (1994). Additionally, hyaline bodies of several haustoria labelled with anti-AGP probes. Hyaline body labelling of infective haustoria appears during endodermal penetration and is not present in the hyaline body meristems. Therefore, its labeling in metahaustoria suggests their relatively advanced anatomical development.

Composition

Overall, the results presented in this chapter suggest, that the PhISC represents a type of sequentially deposited, lignin-like material with hemicellulosic and AGP glycan components. Histological staining with toluidine blue O, Weisner reagent and Maüle reagent give the first hints of the presence of polyphenolics. The first two stain the PhISC and xylem in the same way, while the Maüle reaction is much stronger in the PhISC than in any other area of the metahaustorium. Weisner reaction is aldehyde-specific (Clifford, 1974; Pomar *et al.*, 2002). While aldehydes are common precursors of monolignols, their association with the polymeric fractions of lignin is not well understood as they remain extractable (Ralph *et al.*, 1998). Phenolic aldehydes not typically found in polymeric lignin, such as vanillin, can give a positive reaction (Black *et al.*, 1951; Hartley & Keene, 1984).

Immunogold labelling showed an increasing gradient of particles into the PhISC, which was most pronounced for S lignin (and, to a lesser extent, G and H lignin). This is surprising as the Maüle reaction does not produce the red colour typical of syringyl lignins. These inconsistencies might imply an unusual composition for lignins present in the PhISC. A lignin-like substance rather than typical lignin seems to be further indicated by Raman spectroscopy results, in particular the atypical single peak detected separately from the double peak of xylem lignins.

A degree of non-specificity associated with polyclonal probes is to be expected and could explain binding to some of the parenchyma tissues. However, Ligrone *et al.* (2007) also reported binding to parenchyma cell walls in bryophytes labelled with polyclonal probes against G and GS lignin. They argued that the pure character of the antigens used to raise the antibodies and negative controls make the possibility of binding to compounds unrelated to lignin highly unlikely. They also refer

to “phenolic compounds immunologically related to lignin” as the target of these antibodies in bryophytes. This might be the case in this study and monomers not recognized by histological stains might be the cause of antibody binding.

Toluidine Blue stains thickened parenchyma walls pink (typical of pectins), indicating the presence of pectins. Layers of light pink staining can be seen in the PhISC at high magnifications in some samples, suggesting the involvement of a pectic component (O’Brien *et al.*, 1964; Parker *et al.*, 1982). However, immunogold labelling suggests that homogalacturonans are present only in the epithelial walls and disappear at the boundary with the PhISC. Presence of hemicelluloses is confirmed by immunogold labelling. Abundant xyloglucan epitopes are detected by mAbs LM15 and LM25. These antibodies localise more abundantly to layers that appear more mottled, further highlighting architectural heterogeneity of the PhISC. Xylan and mannan are also present as detected with antibodies LM11 and LM22 but occur in lower amounts.

Birefringence, which is commonly observed in lignified and suberised walls (Vaughn 1987) was recorded in xylem and some parenchyma walls including epithelial walls but not in the PhISC or flanges. As the property results from the orientation order and crystallinity of cellulose in the walls rather than incrustation with lignin or suberin (Pate & Gunning, 1972; Yu *et al.*, 2005; Nakagawa *et al.*, 2012), the PhISC is likely to lack a highly organized, crystalline carbohydrate component. Cellulose to lignin ratio may also be too low to be detected in cross polarized light (Seth, 2003).

A possible lipidic component is suggested by the globular structure of PhISC observed in some haustoria. However, globular arrangement has also been reported for lignins (Terashima *et al.*, 2012). Although cuticles are typically a feature of plant aerial organs, they are also known from subterranean structures, for example *Psilotum* gametophytes (Whittier & Peterson, 1995). It is theoretically possible that the histological staining is based on phenolics embedded in lipidic matrix, for example phenolics in suberin. Cuticles can also autofluoresce (Fernández *et al.*, 1999) or stain with Weisner reagent (Griffith & Brown, 1982) when it contains phenolic and flavonoid compounds. Cutin autofluorescence was observed under UV and blue excitation in *Humulus lupulus* (Fortes *et al.*, 2002) and under blue excitation in grape *Vitis vinifera* (Considine & Knox, 1979). However, none of the histological tests specific for lipids confirmed the presence of lipids. Rhodamine B, which is typically used to detect mitochondria but has also been applied to study cuticles (Salanenka *et al.*, 2009), stained both xylem and PhISC and was therefore not useful for distinguishing between lignin and lipids. Additionally, the strong staining did not produce characteristic fluorescence, while quenching autofluorescence. Sudan dyes, Oil blue N and Oil Red O did not produce appreciable staining either. It is possible that part of the potential lipid component was extracted during processing for wax embedding. However, samples of fresh haustoria did not absorb Sudan dyes. Furthermore, Oil Blue N has been previously demonstrated to stain suberin in dewaxed material (Rümer *et al.*, 2007).

Secretion

Lignin polymerization is removed from the plasma membrane and its deposition is preceded by the synthesis and deposition of a carbohydrate frame which is then incrustated with lignin (Lewis & Yamamoto, 1990; Donaldson, 2001). Depending on the carbohydrate matrix type, the supramolecular structure of deposited lignin varies (Donaldson, 1994). In secondary walls with highly organized carbohydrate structure, lignin deposition occurs in distinct layers (or lamellae) corresponding to the direction of cellulose microfibrils and parallel to the cell surface. On the other hand, its synthesis in middle lamellae and primary walls, which possess a more random carbohydrate network, starts in roughly spherical patches that spread and merge in all directions as lignification proceeds. The metahaustorial PhISC shows layered structure displaying various levels and types of layer interlocking. At the point of its deposition between the endodermis and the endophyte and pericycle by attached haustoria, banding parallel to the interface can be observed, with a gradient of decreasing light blue staining with toluidine blue O, replaced by purple staining indicative of carbohydrates. This suggests that a carbohydrate scaffold might be laid first and subsequently incrustated with parasite-secreted polyphenolics, resulting in the staining gradient. No secretory pockets resembling fibrillar inclusions as described by Joel and Losner-Goshen (1994) for *Orobanch* cuticle or cystoliths in *Viscum minimum* cuticular adhesive substance (Heide-Jørgensen, 1988) could be identified.

In host-infecting haustoria the PhISC is often separated from healthy host tissues by two or three layers of necrotic host cells and adheres tightly to the surface of the parasite. It is unlikely that crushed host cells produce these relatively large amounts of deposits, especially if compression occurs rapidly. Another question that needs to be asked is whether cells of parasitized host cortex are equipped with secretory machinery capable of synthesizing and exporting the PhISC even before they become crushed. Host root cortex cells in contact with the haustorium are filled with large vacuoles and possess a very thin layer of protoplast. This is in stark contrast with parasite contact cells filled with organelle-dense cytoplasm with very large nuclei. Given this juxtaposition, it seems more likely that the secretion is synthesised by the parasite. Furthermore, the success of penetration into the xylem of good and bad hosts was not related to PhISC presence, as similar amounts of the secretion were found in contact with all hosts. This suggests that production of the PhISC is part of a mechanism independent of host cell lignification and may not be defence-related.

No open ducts between the contact cell protoplasts and the PhISC were observed. This suggests that secretion occurs through putative pores in the fibrillar cell wall. However, no such structures or trans-wall vesicles were observed. It is not possible to determine with certainty why contact parenchyma cell walls are much thicker and more 'spongy' in metahaustoria than in infective haustoria before differentiation into xylem, although transfer cells can differentiate as a result of nutrient deficiency (Schikora & Schmidt, 2002). An interesting example is that of the C-type transfer walls induced

by developmental stress in *Cuscuta* xylem-abutting parenchyma when grown on an incompatible host or in agar culture (Christensen *et al.*, 2003). This was interpreted as a compensation mechanism. Presence of AGPs in the PhISC highlights the ability of AGPs to move across the thick cellulosic wall. Although the exact mechanism of this transport is not known, the proteoglycan module can be cleaved off via the action of phospholipases and may diffuse through the pores in the wall (4–5 nm in primary walls) as the AGP molecule (approximately 5 nm in diameter) (Ellis *et al.*, 2010). Furthermore, Lamport and Kieliszewski (2005) as well as Knox (2006) suggested that since AGPs may modify the properties of cell wall polymers by plasticizing pectins through decreasing their cross-linking (Lamport & Kieliszewski, 2005; Lamport *et al.*, 2006) and affecting the action of xyloglucan transglycosylases (Takeda & Fry, 2004), they might be able to facilitate their own progress across the wall by modifying the physical obstacles within it.

Possible functions

As shown in figure 7.9, the amount of the PhISC at haustorium-host interfaces can be very large even when the parasite is attached to a good host and gains access to its vasculature. This indicates that production of the PhISC by the host as a defence response would be an energetically extravagant, yet ineffective venture. On the other hand, there are several possible functions beneficial to the parasite that the PhISC might serve.

Firstly, the PhISC might act adhesive implicated in early stages of attachment and further involved in the mechanics of haustorial penetration. Metahaustoria were easily removed from pots and the outer layer stayed intact making it unlikely that the secretion is “sticky” in a viscous sense. However, attachment might occur via oxidative crosslinking of the PhISC, parasite and host cell walls, as previously suggested for intramural interfacial lignins by Neumann *et al.* (1999). This might, in turn, substantially aid penetration by holding the host root in place while mechanical pressure is exerted and would prevent a) the host root from being pushed away from the haustorial face during the action of clasping folds, especially where they are small b) the cells peeled from cortex from sliding along the interface. Presence of AGPs in the PhISC might contribute to intermolecular binding, as this class of molecules has been previously shown to be prone to peroxidase-mediated crosslinking (Kjellbom *et al.*, 1997). On the other hand they could possibly act as plasticisers of PhISC, as previously suggested for AGPs interaction with pectins (Lamport *et al.*, 2006; Moore *et al.*, 2013). This would be particularly important during endophyte growth. Another putative function that has been previously suggested is the ordering of polyphenolic deposition and formation of nucleation sites in secondary wall deposition (Kieliszewski & Lamport, 1994). While the former function was suggested for plasma-membrane bound AGPs, the latter agrees with their uniform distribution across the entire extent of the PhISC, which suggests that the glycan epitopes are incorporated in its architecture as a structural element.

The PhISC localized in areas of cell separation often appears wedge-shaped. This, intuitively, leads to a hypothesis that its likely rapid buildup and hardening in this part of the interface, might further mechanically aid the process of penetration between these cell layers.

As the PhISC, typically, tightly fills the spaces between tissue layers peeled off the host, it might act as a sealant, preventing 1) complete disintegration of host root; 2) leakage of abstracted nutrients, which has been previously hypothesised for interfacial lignins (Rümer *et al.*, 2007); and 3) embolism. The latter seem particularly likely as parasite vessels typically open into a common space abutting host vessels. This space needs to remain filled with xylem sap in order for the transpiration-effected movement to occur. It seems that the path of radial liquid escape is blocked by the PhISC, which typically continues from the lateral interface into the central interface, immediately above the gap, and, where the PhISC does not reach, by the intact cells of the stele.

Additionally, the PhISC could play a role of a physical and biochemical shield to recognition by a host. A layer rich in phenolics, which are one of the main defense-related compounds produced by the host, is likely to be perceived by the attacked organ as native and safe. Furthermore release of potential signaling molecules from parasite structural polysaccharides is more difficult in such a modified environment as substrates of signal-generating enzymes are likely to be masked. This hypothesis is in accord with the fact that a layer of PhISC thinner than that at lateral interfaces is often sandwiched between the parasite and host cells even at the central interface, where endophyte cells need to elongate towards the host stele. While the contact surface area between an invader and a host theoretically does not need to be large to trigger off defences, keeping it to the necessary minimum might limit host responses.

It is not unlikely that the PhISC additionally fulfills a role of a “graveyard”, where cell debris are buried in the secretion and the effects of any toxic compounds that otherwise might be released towards the parasite are captured and/or neutralized. Dying parenchyma cells are known to form fungitoxic and fungistatic compounds (Kemp & Burden, 1986) and phenolics, most likely tannins or flavonoids were seen abundantly in the cortical cell of *Daucus carota* in this study.

The presence of bacterial endospores in the PhISC of parasite-host interfaces poses the question as to whether an additional function is to protect the site of intrusion from microbial attack. It is not clear if endospores that are encountered by chance become surrounded by the secretion or whether the bacteria actively enter it. The possibility of a symbiotic interaction has not been previously addressed.

7.5 Conclusions

It might have been assumed in recent years that, as non-functional structures, metahaustoria do not deserve academic scrutiny. This study proves that this is not

Chapter 7

the case and that metahaustoria can provide valuable information which can be compared with, and extrapolated to, a typical system of a fully functional haustorium attached to a host. The results presented in this chapter likely form the most direct evidence that interfacial phenolic substances typically assumed to be produced by the host, are in fact secreted by the parasite. This calls for reinterpretation of the role of lignins and related polymers at haustorial interfaces.

It will be important to determine how deposition of the PhISC is harmonised with the rapid cell elongation, secretion of enzymes and reception of cues. While lignin, and even cuticle, allow some diffusion of substances (Nawrath, 2006), it is likely that the PhISC significantly hampers exchange of signals between the two organisms. Another challenge will be to elucidate when and how the PhISC deposition is initiated what the mode of its deposition is. In relation to this question, the mechanisms coordinating lignification of endophyte parenchyma associated with differentiation into xylem elements, as opposed to the PhISC deposition, will need to be addressed.

Extracellularly deposited lignin-like substances are yet another part of the puzzle of the complicated virulence/resistance relationships between parasitic angiosperms and their hosts. As the precise functions and mechanisms of PhISC deposition emerge, they can become subject to genetic engineering of avirulence.

8 General discussion

Approximately 1% of all plants have evolved to be parasitic on other plants (Westwood *et al.*, 2010). They develop specialised grafting organs called haustoria to attach to, and infiltrate, host organs for nutrients (Heide-Jørgensen, 2008). This life strategy has profound economic consequences in tropical and sub-tropical agrosystems, where parasitic plants cause extensive crop losses every year (Parker, 2009, 2012). In temperate regions, including Ireland, parasitic plants are often confined to semi-natural systems, where their ecological impact is of significant importance (Press & Phoenix, 2005). This is a consequence of their ability to alter community structure by modulating the competitive balance between plants susceptible to parasitism (hosts) and resistant species (non-hosts) (Press & Phoenix, 2005; Watson, 2009). *Rhinanthus minor* (yellow rattle), a hemiparasitic annual herb, is particularly well researched with regard to host preference and typically reduces the growth of grasses, allowing eudicot herbs to compete (Gibson & Watkinson, 1991). This generally leads to increased floral diversity of the occupied grasslands (Davies, 1997; Pywell *et al.*, 2004; Bullock & Pywell, 2005; Westbury *et al.*, 2006).

The results of the community survey carried out for this project extend the details regarding distribution and community associations of two native Irish hemiparasites, *Rhinanthus minor* and *Odontites vernus*, allowing for their comparison. Field observations and a review of published reports from the Irish Semi-natural Grassland survey (Martin *et al.*, 2007; O'Neill *et al.*, 2009, 2010) confirm that *Rhinanthus minor* is associated with high species richness. They also show that it is strongly associated with higher eudicot to graminoid ratio and lower nitrogen values than *Odontites vernus*, a rather poorly researched native annual hemiparasite, considered a species of marginal habitats such as road sides and waste ground, which are associated with low floral diversity (Grime *et al.*, 1988). My study confirmed that *Odontites vernus* also appears in species-rich grasslands as a result of habitat deterioration caused by soil disturbance or trampling, in agreement with previous findings for calcareous grasslands in England (Hirst *et al.*, 2005). At one of the surveyed sites (Berneens in the high Burren) it was found in extremely species-rich areas. Therefore, *Odontites vernus* cannot be universally associated with low species diversity, although it is not expected to contribute in the same way as *Rhinanthus minor*. In fact, in addition to the appearance of *Odontites vernus* being an indicator of habitat deterioration, its impact on the ecological dynamics of grasslands during post-disturbance recovery is not known. While this might not be a nationally important aspect of grassland conservation, my personal observations indicate that this species is relatively widespread in the Burren and a better understanding of its biology might contribute to management of floral diversity in Burren winterages, in places where overgrazing and trampling can be of concern.

The ecological processes outlined above are largely determined at haustorial interfaces, where the tissues of the parasite and the host meet. Histochemical studies have previously shown that resistance of non-leguminous eudicots *Plantago lanceolata* and *Leucanthemum vulgare* to *R. minor* is primarily determined by mechanical resistance within haustorial tissues (Cameron *et al.*, 2006; Cameron & Seel, 2007; Rümer *et al.*, 2007). This mechanical resistance was reported to involve reinforcement of host cell walls with lignin and suberin, which, together with dead host cells resulting from the hypersensitive response, contribute to the formation of encapsulation layers preventing haustorial access to host root stele. Inclusion in my studies of a wider range of non-leguminous eudicots lead to a discovery that fully developed haustorial connections can be formed between *Rhinanthus minor* and some non-legume eudicot species. For instance, luminal continuity was achieved with the xylem of *Daucus carota* and *Pimpinella major* (both in the Apiaceae) and was associated with good haustorial differentiation. Vessel abutment was also seen at interfaces with *Prunella vulgaris* and *Plantago lanceolata*, although in these cases luminal continuity was not seen. These observations are the first report of xylem abutment between *Rhinanthus minor* and *Plantago lanceolata*, which is a well documented non-host for this hemiparasite (Seel *et al.*, 1993; Cameron & Seel, 2007; Rümer *et al.*, 2007). Attachment to all hosts, except *Prunella vulgaris* and *Plantago lanceolata* was found to stimulate the parasite's growth. Therefore, non-leguminous eudicots might prove to be suitable hosts under natural field conditions as well as the reported laboratory growth experiments. However, confirmation of parasitism of non-leguminous eudicots under natural conditions is needed.

Cell walls form the initial site of direct contact, as well as signaling, between the host and the parasite during haustorial attachment and penetration. However, studies of haustorial cell walls are scarce and have typically focused on characterisation of the defence compounds produced at the interfacial region (Pérez-de-Luque *et al.*, 2006; Echevarría-Zomeño *et al.*, 2006; Cameron *et al.*, 2006; Rümer *et al.*, 2007). My research identified conspicuous cell wall modifications at the interface as well as in the central part of *Rhinanthus minor* and *Odontites vernus* haustoria. In addition to the lignified cell walls of the xylem bridge, which participates directly in the abstraction of nutrients, a range of cell wall specific characteristics were found in the cells of haustorial parenchymatous tissues. Cell walls of the interfacial parenchyma display considerable acropetal thickening and are rich in pectins and arabinogalactan proteins (AGPs) from early stages of attachment and penetration until conversion into xylem. Cell walls of flange-like parenchyma are thickened in contact with the xylem bridge vessels and have a conspicuous layered structure which occasionally includes xylem-like lignified thickenings. Hyaline body cell walls are immunocytochemically different from the cell walls of the surrounding cortex. They are often enriched in AGPs and show reduced immunolabelling for de-esterified

pectins. They are, furthermore, associated with abundant paramural deposits, while ergastic inclusions of cell wall materials are also found within the cytoplasm. This diversity in cell wall composition and structure as well as differentiation in response to the infection process must be justified by important physiological and structural roles which await discovery.

These findings lend support to the theories of Fineran (1987), who was of the opinion that, if the sole roles of haustoria were nutrient abstraction and transport, it would be reflected by haustoria being of only very basic structure focused on establishing luminal continuity. Instead, the complexity of tissues and associated cell walls seen in this, and other, studies, highlights the sophistication of haustorial differentiation and suggests additional roles in the processing of stolen nutrients. Organelle-rich cytoplasm coupled with the existence of paramural deposits and ergastic inclusions implies active processing and deposition of abstracted solutes and suggests that the hyaline body might be the metabolic brains of the parasitic operation at haustorial level. For this reason, and in addition to the findings of this and previously published research (Gurney *et al.*, 2003) indicating that its structure reflects the quality of infected hosts, the hyaline body deserves more academic attention than it has so far received. Studies utilising apoplastic tracers could indirectly verify whether the unique cell walls of the hyaline body and flange-like parenchyma are a form of adaptation for apoplastic transport.

The presence of thickened and/or swollen cell walls in specialised regions of the haustoria certainly supports their involvement in multiple functions previously suggested for the haustorial apoplast, including transport (Fineran, 1987, 1996; Kuo *et al.*, 1989) and storage (Visser *et al.*, 1984). The fact that the thick-walled contact parenchyma might participate in solute transfer is indirectly indicated by the exaggerated morphology of the homologous tissue in metahaustoria, where extremely thickened cell walls and swollen middle lamellae might represent a compensation mechanism in response to lack of a host. Such a putative compensation mechanisms were suggested as the reason for development of transfer cell wall morphology in *Cuscuta* during parasitism of non-hosts (Christensen *et al.*, 2003).

One of the most exciting findings of this project was the discovery that AGP glycan epitopes are found specifically in the areas of the haustoria key to their functioning. In addition to the walls of the hyaline body and interfacial parenchyma, the phenolic-rich interfacial secretion complex (PhISC) is labelled. Furthermore, AGPs appear transiently in xylem lumina during protoplast disintegration associated with programmed cell death. This spatio-temporal specificity suggests that a diversity of functions essential to parasitism of host species could be fulfilled by AGPs. Furthermore, their presence in the haustoria of both investigated species and on most investigated hosts implies their involvement in fundamental processes

Dissection and immunolabeling of haustoria on a diversity of hosts showed that intense immunolabeling of AGPs in the three distinct areas of haustoria was conserved among all pairings tested, except with the non-hosts *Prunella vulgaris* and *Plantago lanceolata*. However, even parasitism on these species was associated with the detection of some AGPs. Together, these results suggest that AGPs play fundamental roles in the development and functioning of haustoria and that their presence might be regulated and stimulated by the same factors that underlie full differentiation of haustoria. If that was the case and AGPs played roles in modification of cell wall rheology and, therefore, apoplastic transport, there would be no need for their synthesis and secretion into the ECM; hence they would be found in lower abundance or be absent from haustoria without apparent xylem continuity with the host. This scenario seems plausible as AGPs were immunolocalised with particularly high fluorescence intensity in the young hyaline bodies of *Rhinanthus minor* haustoria attached to good hosts, whereas those attached to *Plantago lanceolata* were typically labelled much more weakly for AGPs. Alternatively, AGPs might participate in the regulation of development and their absence or low abundance could be one of the reasons behind poor differentiation of hyaline bodies on *Prunella vulgaris* and *Plantago lanceolata*.

The conspicuous presence of AGPs in haustoria was contrasted with the rather unexpected finding that no very distinct immunocytochemical changes to host cell walls were observed at light microscopy level. This is most likely a result of the haustorial tissues being largely unprepared for large scale synthesis and restructuring. Cortical cells of all examined hosts were strongly vacuolated, with small amounts of protoplast, while endophyte cells prior to conversion into xylem are densely-cytoplasmic, with large nuclei, abundant mitochondria, ER and ribosomes. I did not observe strong upregulation of extensins or accumulation of callose in host cell walls at the infection site. However, the protoplasts of crushed cells were often rich in extensin, AGP and lignin epitopes, in graminoid, legume and non-leguminous eudicot hosts. Such an occurrence might be widespread as LM1 labeling of crushed interfacial cells of the host has previously been observed during parasitism of *Pennisetum americanum* (graminoid) by *Buchnera hispida*; *Vigna unguiculata* (legume) by *Rhamphicarpa fistulosa* and *Sorghum bicolor* (graminoid) by *Striga hermonthica* (Neumann *et al.*, 1999). However, AGPs (and extensins) were often localised in host vessel lumina and occasionally all parenchyma tissues in host roots labelled with then anti-AGP antibody LM2. A study focused on host defences is needed to confirm whether the concentrations and types of AGPs are increased in host roots in response to parasitism.

Perhaps the most unexpected finding of this study was that 1) interfacial lignified compounds occurred mainly in a thin layer tightly filling the interfacial space rather than being increased in host cell walls during attack, 2) they were not related to host quality and that 3) they are most likely synthesised by the parasite. Host phenolics

are known to induce virulence in fungi (Spencer & Towers, 1989) and parasitic plants (Chang & Lynn, 1986; Yoder *et al.*, 2009). The most fully described example of the latter is the release of a haustorial inducing factor (HIF) 2,6-dimethoxy-1,4-benzo-quinone (DMBQ) from phenolic esters of pectins in the presence of hydrogen peroxide from the parasite (Kim *et al.*, 1998; Keyes *et al.*, 2000). However, to my best knowledge, production of lignin to aid virulence has not been previously reported from any other organism. Although Heide-Jørgensen & Kuijt (1993) as well as Neumann *et al.* (1999) have previously observed intramural lignification of contact parenchyma cell walls in other species of Orobanchaceae, extramural deposition of lignin into the interface by parasitic plants has not been reported. Characterisation of the phenolics-rich interfacial secretion complex (PhISC) in this study and its similarity in normal attached haustoria and non-infective metahaustoria suggests that the role of interfacial lignins during the parasitic process needs to be re-evaluated. As parasite vessels often open to a common space abutting host vessels, it is likely that PhISC participates in sealing of cracks in the tissue to avoid leakage and prevent embolism. PhISC at lateral interfaces might aid attachment and subsequent mechanical penetration, preventing slippage of host tissues against the haustorial interface, particularly where clasping folds are small.

Future work and closing remarks

This project involved the first extensive antibody screen of angiosperm haustoria and allowed to determine AGPs as molecules of potentially high importance to haustorial development and functioning. Therefore, it is important that follow-up studies focusing on the elucidation of their precise functions are pursued. In order to achieve this, various approaches should be undertaken. At the anatomical level, it is important to confirm the plasma membrane versus cell wall localisation of AGP glycans, as this will indirectly assist discrimination between their potential signalling versus structural or rheology-modifying function. Cryofixation, in particular, might reveal features that are generally sensitive to fixation, especially membranes, including vesicles (Haas & Otegui, 2007; Ripper *et al.*, 2008), which participate in the trafficking of AGPs to the apoplast and their recycling. Additionally, tissue prints could be applied if loss of soluble AGPs is a concern.

With a view to experimentally testing the functions of AGPs in haustoria, it would be extremely valuable to identify the protein backbone, or backbones, which the AGP epitopes detected in this study are associated with, specifically in haustoria. Furthermore, identification of enzymes participating in AGP glycosylation would open up fascinating opportunities for genetic manipulation and testing of functions of individual epitopes. However, these are general milestone advancements awaited by cell wall research and posing considerable difficulties (Tan *et al.*, 2012) and it might take quite some time for them to be applied to parasitic plant research. In the meantime, the efforts should concentrate on AGP glycan epitope screening, with a wide variety of probes at high developmental resolution, and on structural

characterisation, involving extractions. The latter also poses problems as many procedures require cell wall alcohol insoluble residue (AIR) to be obtained in amounts in the order of tens of milligrams. Large haustoria of *Rhinanthus minor* are approximately 1 mm³ and assuming mass similar to that of water, a large haustorium weighs approximately 1 milligram. As the mass ratio of fresh tissue to alcohol-insoluble residue is often in the range of 100 to 1 (Fry, 1988), obtaining sufficient amounts of haustorial material is difficult. For instance, Sørensen & Willats (2011) recommend 10 mg of AIR for carbohydrate microarrays. As it would be preferable to isolate contact parenchyma and hyaline body tissues, which in itself could pose specific difficulties, and analyse them separately, the issue of minimal sample weight considerably limits the number of biochemical analysis techniques that can be applied.

As the β -linked glucuronic acid epitope recognised by LM2 monoclonal antibody was a particularly consistent marker of xylem maturation, as well as of the hyaline bodies and interfacial parenchyma, this antibody and epitope might prove particularly important when comparing different developmental stages and different species. Systems allowing collection of early developmental stages would be of great value. Such systems include *Cuscuta*, which produces a series of haustoria at its shoot tips, allowing regular observation and collection at preferred stages of development. *In vitro* root cultures of *Triphysaria* (Tomilov *et al.*, 2004) have already proven useful for investigating many aspects of root parasitism and this might be extended to include AGP distribution in haustoria. Another possibility is the use of the recently developed transparent soil (Downie *et al.*, 2012). On the other hand, field-collected plants should be included in the immunocytochemical screens, to confirm that the AGP distributions seen in this study are a feature of parasitic plants grown in a variety of environmental conditions.

LM2 screening could also be applied with a phylogenetic focus. As in this thesis two closely related species were shown to be enriched in AGPs in the same tissues, it would be of interest to investigate if this is a general feature and therefore also the case in parasites from other clades and families.

Although genetic studies have considerable limitations with respect to researching AGPs, they have provided some insights into cell wall molecules undetectable histologically, notably expansins, genes of which are upregulated during hypertrophy in haustorial initials of *Striga asiatica* (O'Malley & Lynn, 2000). It is important to consider other molecules that might interact with AGPs at specific stages of haustorial development and functioning. Therefore, while genetic studies cannot always be applied to investigate AGPs directly, integration of molecular results concerning other molecules is of high importance.

The discovery of the phenolics-rich interfacial secretion complex (PhISC), warrants further investigation. As currently a finite supply of only 4 polyclonal antibodies, which

are not commercially available, against synthetic S, G, mixed S/G and H lignins exists (Ruel *et al.*, 1994; Joseleau & Ruel, 1997; Zeier *et al.*, 1999), the potential for their future use is limited. Generation of commercially-available monoclonal antibodies against native plant lignins would greatly contribute to this aspect of parasitic plant research, as well as more generally to many other aspects of plant cell wall research. This includes the mechanisms of lignin secretion, which could contribute to better understanding of its involvement in parasitism. Spectroscopy techniques have the potential to show differences in lignin composition when polyclonal anti-lignin antibodies are not available or do not display satisfactory specificity. As demonstrated by results presented in chapter 7, Raman spectroscopy offers a relatively easy and rapid way of identifying lignin and related polyphenolics. While Raman spectra for lignin are characterised, with key peaks falling between 1550 and 1700 wavenumbers $\times \text{cm}^{-1}$ (Schmidt *et al.*, 2010), other cell wall components present in the PhISC, notably hemicelluloses, are not well documented in terms of the relevant bands. Therefore, further immunogold labelling with a wider range of antibodies and using more samples might provide insights into the biochemical basis of the structural heterogeneity of the PhISC. Identification of a potential lipidic component, such as suberin, will require characterisation of the relevant Raman spectra or using, for example the more established FT-IR spectroscopy (Smith-Moritz *et al.*, 2011). Isolation and chemical analysis of PhISC using pyrolysis-GCMS might also be feasible (John Ralph, *pers. comm.*).

Since haustorial AGPs and lignins provided the most important highlights of this project, it is intriguing that their distribution overlaps in the interfacial region. Therefore, another possible future research direction could focus in the interactions between AGPs and polyphenolics in PhISC. As the interfacial region is likely to be very dynamic in terms of signalling between the parasite and the host, as well as intrusive growth through host tissues, a multitude of functions played jointly by these two classes of cell wall molecules is possible. One of these could be the maintenance of the balance between the fluidity of the PhISC during penetration and its subsequent setting, possibly via oxidative crosslinking.

Finally more efforts into integrating the laboratory-based findings with the ecological outcomes of parasitism should be undertaken. Previous studies on *Rhinanthus minor* (Cameron *et al.*, 2006; Cameron & Seel, 2007; Rümer *et al.*, 2007) showed great potential towards explaining ecological processes through cell wall-focused histochemical approaches, while the work presented in this thesis demonstrated variable resistance within functional groups of hosts, notably non-leguminous eudicots. This highlights the need to include a wider diversity of host species, as extrapolations from a small number of taxa can lead to false generalisations.

A considerable amount of structural and immunocytochemical diversity of haustorial cell walls in *Rhinanthus minor* and *Odontites vernus* was demonstrated in this study. As my results suggest that AGPs are likely to be crucial in haustorial functioning, while

Chapter 8

remaining the subject of cutting-edge cell wall research, it is my hope that this data provokes more detailed, immunocytochemical studies of angiosperm haustoria, particularly with respect to elucidating the precise functions that AGPs play in the different haustorial tissues. In conclusion, this study shows several novel aspects of the parasitic interactions between plants at ecological and biochemical level, with cell walls contributing greatly to the interplay between parasites, their hosts and the surrounding environment.

Literature cited:

- Adler L. 2000.** Alkaloid uptake increases fitness in a hemiparasitic plant via reduced herbivory and increased pollination. *The American Naturalist* **156**: 92–99.
- Van Aelst AC, Van Went JL. 1992.** Ultrastructural immuno-localization of pectins and glycoproteins in *Arabidopsis thaliana* pollen grains. *Protoplasma* **168**: 14–19.
- Afzal AJ, Wood AJ, Lightfoot DA. 2008.** Plant receptor-like serine threonine kinases: roles in signaling and plant defense. *Molecular Plant-Microbe Interactions* **21**: 507–17.
- Albersheim P, Darvill AG. 1985.** Oligosaccharins: novel molecules that can regulate growth, development, reproduction, and defense against disease in plants. *Scientific American* **253**: 58–64.
- Albersheim P, Darvill A, Augur C, Cheong J-J, Eberhard S, Hahn MG, Marfa V, Mohnen D, O'Neill MA, Spiro MD, et al. 1992.** Oligosaccharins: oligosaccharide regulatory molecules. *Accounts of Chemical Research* **25**: 77–83.
- Albersheim P, Darvill A, Roberts K, Sederoff R, Staehelin A. 2011.** *Plant Cell Walls*. New York: Garland Science.
- Albert M, Belastegui-Macadam X, Kaldenhoff R. 2006.** An attack of the plant parasite *Cuscuta reflexa* induces the expression of attAGP, an attachment protein of the host tomato. *The Plant Journal* **48**: 548–556.
- Albert M, Van der Krol S, Kaldenhoff R. 2010.** *Cuscuta reflexa* invasion induces Ca²⁺ release in its host. *Plant Biology* **12**: 554–557.
- Albert M, Werner M, Proksch P, Fry SC, Kaldenhoff R. 2004.** The cell wall-modifying xyloglucan endotransglycosylase/hydrolase LeXTH1 is expressed during the defence reaction of tomato against the plant parasite *Cuscuta reflexa*. *Plant Biology* **6**: 402–407.
- Albinsson B, Li S, Lundquist K, Stomberg R. 1999.** The origin of lignin fluorescence. *Journal of Molecular Structure* **508**: 19–27.
- Albrecht H, Anderlik-Wesinger G, Kühn N, Matthies A, Pfadenhauer J. 2007.** Effects of land use changes on the plant species diversity in agricultural ecosystems. In: Schröder P, Pfadenhauer J, Munch JC, eds. Perspectives for agroecosystem management: balancing environmental and socio-economic demands. Amsterdam: Elsevier Science, 203–235.
- Almagro L, Gómez Ros L V, Belchi-Navarro S, Bru R, Ros Barceló A, Pedreño MA. 2009.** Class III peroxidases in plant defence reactions. *Journal of Experimental Botany* **60**: 377–90.
- Alosi MC. 1980.** Morphological and cytological studies on *Arceuthobium* (Viscaceae) in relationship to host phloem with studies on the healthy phloem in *Pinus sabiniana* (Pinaceae). PhD Thesis. Oregon: Portland State University
- Ameloot E. 2007.** Impact of hemiparasitic *Rhinanthus* spp. on vegetation structure and dynamics of semi-natural grassland. *Landschap*: 240. PhD Thesis. Leuven: Katholieke Universiteit
- Ameloot E, Verheyen K, Bakker JP, De Vries Y, Hermy M. 2006.** Long-term dynamics of the hemiparasite *Rhinanthus angustifolius* and its relationship with vegetation structure. *Journal of Vegetation Science* **17**: 637–646.
- Ameloot E, Verheyen K, Hermy M. 2005.** Meta-analysis of standing crop reduction by *Rhinanthus* spp. and its effect on vegetation structure. *Folia Geobotanica* **40**: 289–310.
- Anderson CM, Wagner TA, Perret M, He ZH, He D, Kohorn BD. 2001.** WAKs: cell wall-associated kinases linking the cytoplasm to the extracellular matrix. *Plant Molecular Biology* **47**: 197–206.
- Ángeles Castillejo M, Amiour N, Dumas-Gaudot E, Rubiales D, Jorrín J V. 2004.** A proteomic approach to studying plant response to crenate broomrape (*Orobancha crenata*) in pea (*Pisum sativum*). *Phytochemistry* **65**: 1817–1828.
- Annis SL, Goodwin PH. 1997.** Recent advances in the molecular genetics of plant cell wall-degrading enzymes produced by plant pathogenic fungi. *European Journal of Plant Pathology* **103**: 1–14.

9. Literature cited

- Atera E, Itoh K. 2011.** Evaluation of ecologies and severity of *Striga* weed on rice in sub-Saharan Africa. *Agriculture and Biology Journal of North America* **2**: 752–760.
- Atsatt P. 1973.** Parasitic Flowering Plants: How Did They Evolve? *The American Naturalist* **107**: 502–510.
- Atsatt PR, Hearn TF, Nelson RL, Heineman RT. 1978.** Chemical induction and repression of haustoria in *Orthocarpus purpurascens* (Scrophulariaceae). *Annals of Botany* **42**: 1177–1184.
- Attawi FAJ, Weber HC. 1980.** Parasitism, morphology and anatomy of the secondary haustoria in *Orobanche* species (Orobanchaceae). *Flora* **169**: 55–83.
- Avci U, Pattathil S, Hahn MG. 2012.** Immunological approaches to plant cell wall and biomass characterization: immunolocalization of glycan epitopes. In: Himmel ME, ed. Biomass conversion: methods and protocols, methods in molecular biology. Totowa, NJ: Humana Press, 73–82.
- Averis AM, Averis ABG, Birks HJB, Horsfield D, Thompson DBA, Yeo MJM. 2004.** *An illustrated guide to British upland vegetation*. Peterborough: Joint Nature Conservation Committee.
- Ba AT. 1983.** Evidence of enzyme activities in the haustorium of *Striga gesneroides* (Scrophulariaceae). In: Ramaiah K V, Vasudeva Rao MJ, eds. Proceedings of the Second International Workshop on *Striga*. Ouagadougou, Upper Volta: ICRISAT, 39–42.
- Baba K. 2006.** Models of plant cell walls. In: Hayashi T, ed. The science and lore of the plant cell wall: biosynthesis, structure and function. Boca Raton: Brown Walker Press, 3–10.
- Bai L, Zhang G, Zhou Y, Zhang Z, Wang W, Du Y, Wu Z, Song C-P. 2009.** Plasma membrane-associated proline-rich extensin-like receptor kinase 4, a novel regulator of Ca²⁺ signalling, is required for abscisic acid responses in *Arabidopsis thaliana*. *The Plant Journal* **60**: 314–327.
- Bais HP, Walker TS, Schweizer HP, Vivanco JM. 2002.** Root specific elicitation and antimicrobial activity of rosmarinic acid in hairy root cultures of *Ocimum basilicum*. *Plant Physiology and Biochemistry* **40**: 983–995.
- Baldwin TC, McCann MC, Roberts K. 1993.** A novel hydroxyproline-deficient arabinogalactan protein secreted by suspension-cultured cells of *Daucus carota* (purification and partial characterisation). *Plant Physiology* **103**: 115–123.
- Balestrini R, Hahn MG, Faccio A, Mendgen K, Bonfante P. 1996.** Differential localization of carbohydrate epitopes in plant cell walls in the presence and absence of arbuscular mycorrhizal fungi. *Plant Physiology* **111**: 203–213.
- Bar-Nun N, Mayer AM. 2009.** Possible function of isoleucine in the methyl jasmonate response of *Arabidopsis* to *Phelipanche aegyptiaca*. *Phytoparasitica* **37**: 485–488.
- Barcelona JF, Pelsler PB, Balet DS, Co LL. 2009.** Taxonomy, ecology, and conservation status of Philippine *Rafflesia* (Rafflesiaceae). *Blumea - Biodiversity, Evolution and Biogeography of Plants* **54**: 77–93.
- Barkman TJ, Lim S-H, Salleh KM, Nais J. 2004.** Mitochondrial DNA sequences reveal the photosynthetic relatives of *Rafflesia*, the world's largest flower. *Proceedings of the National Academy of Sciences* **101**: 787–792.
- Bar-Nun N, Mayer AM. 2008.** Methyl jasmonate and methyl salicylate, but not cis-jasmone, evoke defenses against infection of *Arabidopsis thaliana* by *Orobanche aegyptiaca*. *Weed Biology and Management* **8**: 91–96.
- Baron-Epel O, Gharyal PK, Schindler M. 1988.** Pectins as mediators of wall porosity in soybean cells. *Planta* **175**: 389–395.
- Bar-Peled M, O'Neill M a. 2011.** Plant nucleotide sugar formation, interconversion, and salvage by sugar recycling. *Annual Review of Plant Biology* **62**: 127–155.
- Battaglia M, Solórzano RM, Hernández M, Cuéllar-Ortiz S, García-Gómez B, Márquez J, Covarrubias AA. 2007.** Proline-rich cell wall proteins accumulate in growing regions and phloem tissue in response to water deficit in common bean seedlings. *Planta* **225**: 1121–1133.
- Becraft PW. 2002.** Receptor kinase signaling in plant development. *Annual Review of Cell and Developmental Biology* **18**: 163–192.

- Beliën T, Van Campenhout S, Robben J, Volckaert G. 2006.** Microbial endoxylanases: effective weapons to breach the plant cell-wall barrier or, rather, triggers of plant defense systems? *Molecular Plant-Microbe Interactions* **19**: 1072–1081.
- Ben-Hod G, Nun NB, Tzaban S, Mayer AM. 1997.** Inhibitors of polygalacturonase in calli of *Orobanchae aegyptiaca*. *Phytochemistry* **45**: 1115–1121.
- Bennett J, Mathews S. 2006.** Phylogeny of the parasitic plant family Orobanchaceae inferred from phytochrome A. *American Journal of Botany* **93**: 1039–1051.
- Berlyn GP, Miksche JP. 1976.** *Botanical microtechnique and cytochemistry*. Ames: The Iowa State University Press.
- Bernards MA. 2002.** Demystifying suberin. *Canadian journal of botany* **80**: 227–240.
- Bessire M, Chassot C, Jacquat A-C, Humphry M, Borel S, Petétot JM-C, Métraux J-P, Nawrath C. 2007.** A permeable cuticle in *Arabidopsis* leads to a strong resistance to *Botrytis cinerea*. *The European Molecular Biology Organization* **26**: 2158–2168.
- Bhuiyan NH, Selvaraj G, Wei Y, King J. 2009.** Role of lignification in plant defense. *Plant Signaling & Behavior* **4**: 158–159.
- Bidartondo MI, Redecker D, Hijri I, Wiemken A, Bruns TD, Domínguez L, Sérsic A, Leake JR, Read DJ. 2002.** Epiparasitic plants specialized on arbuscular mycorrhizal fungi. *Nature* **419**: 389–392.
- Bindschedler L V, Dewdney J, Blee KA, Stone JM, Asai T, Plotnikov J, Denoux C, Hayes T, Gerrish C, Davies DR, et al. 2006.** Peroxidase-dependent apoplastic oxidative burst in *Arabidopsis* required for pathogen resistance. *The Plant Journal* **47**: 851–863.
- Birschwilks M, Sauer N, Scheel D, Neumann S. 2007.** *Arabidopsis thaliana* is a susceptible host plant for the holoparasite *Cuscuta spec.* *Planta* **226**: 1231–1241.
- Björkman E. 1960.** *Monotropa hypopitys* L. - an epiparasite on tree roots. *Physiologia Plantarum* **13**: 308–327.
- Black RA, Rosen AA, Adams SL. 1951.** The chromatographic separation of hardwood extractive components giving color reactions with phloroglucinol. *Journal of the American Chemical Society* **75**: 5344–5346.
- Bleischwitz M, Albert M, Fuchsbauser H-L, Kaldenhoff R. 2010.** Significance of *Cuscutain*, a cysteine protease from *Cuscuta reflexa*, in host-parasite interactions. *BioMed Central Plant Biology* **10**: 227–238.
- Boerjan W, Ralph J, Baucher M. 2003.** Lignin biosynthesis. *Annual Review of Plant Biology* **54**: 519–546.
- Bolwell GP. 1993.** Dynamic aspects of the plant extracellular matrix. *International Review of Cytology* **146**: 261–324.
- Bonilla I, Mergold-Villaseñor C, Campos ME, Sánchez N, Pérez H, López L, Castrejón L, Sánchez F, Cassab GI. 1997.** The aberrant cell walls of boron-deficient bean root nodules have no covalently bound hydroxyproline-/proline-rich proteins. *Plant Physiology* **115**: 1329–1340.
- Bootten TJ, Harris PJ, Melton LD, Newman RH. 2011.** Using solid state ¹³C NMR spectroscopy to study the molecular organisation of primary plant cell walls. In: Popper ZA, ed. *The Plant Cell Wall. Methods and Protocols*. Totowa, NJ: Humana Press, 179–196.
- Ter Borg SJ. 2005.** Dormancy and germination of six *Rhinanthus* species in relation to climate. *Folia Geobotanica* **40**: 243–260.
- Borner GHH, Lilley KS, Stevens TJ, Dupree P. 2003.** Identification of glycosylphosphatidylinositol-anchored proteins in *Arabidopsis*. A proteomic and genomic analysis. *Plant Physiology* **132**: 568–577.
- Bosch M, Knudsen JS, Derksen J, Mariani C. 2001.** Class III pistil-specific extensin-like proteins from tobacco have characteristics of arabinogalactan proteins. *Plant Physiology* **125**: 2180–2188.
- Bossy A, Blaschek W, Classen B. 2009.** Characterization and immunolocalization of arabinogalactan-proteins in roots of *Echinacea purpurea*. *Planta Medica* **75**: 1526–1533.

9. Literature cited

- Botanga CJ, Timko MP. 2005.** Genetic structure and analysis of host and nonhost interactions of *Striga gesnerioides* (Witchweed) from central Florida. *Phytopathology* **95**: 1166–1173.
- Bouwmeester HJ, Matusova R, Zhongkui S, Beale MH. 2003.** Secondary metabolite signalling in host-parasitic plant interactions. *Current Opinion in Plant Biology* **6**: 358–364.
- Bouwmeester HJ, Roux C, Lopez-Raez JA, Bécard G. 2007.** Rhizosphere communication of plants, parasitic plants and AM fungi. *Trends in Plant Science* **12**: 224–230.
- Bradley DJ, Kjellbom P, Lamb CJ. 1992.** Elicitor- and wound-induced oxidative cross-linking of a proline-rich plant cell wall protein: a novel, rapid defense response. *Cell* **70**: 21–30.
- Brady KP, Darvill AG, Albersheim P. 1993.** Activation of a tobacco glycine-rich protein gene by a fungal glucan preparation. *The Plant Journal* **4**: 517–524.
- Braun-Blanquet J, Tüxen R. 1952.** Irische Pflanzengesellschaften. In: Lüdi W, ed. Die Pflanzenwelt Irlands. Zürich: Veröffentlichung Geobotanisches Institute, 224–415.
- Braybrook SA, Hofte H, Peaucelle A. 2012.** Probing the mechanical contributions of the pectin matrix. Insights for growth. *Plant Signalling and Behavior* **7**: 1037–1041.
- Brett C. 1983.** Cell walls do not a prison make. *New Scientist* **99**: 693–695.
- Brett CT, Waldron K. 1996.** *Physiology and Biochemistry of Plant Cell Walls*. London: Chapman and Hall.
- Brewin NJ. 2004.** Plant Cell Wall Remodelling in the Rhizobium–Legume Symbiosis. *Critical Reviews in Plant Sciences* **23**: 293–316.
- Brewin N, Khodorenko A, Tsyganov VE, Borisov AY, Tikhonovich IA, Rathbun E. 2008.** Legume agglutinins in *Rhizobium* infection. *Biological nitrogen fixation: towards poverty alleviation through sustainable agriculture*. **42**: 185–187.
- Brisson LF, Tenhaken R, Lamb C. 1994.** Function of oxidative cross-linking of cell wall structural proteins in plant disease resistance. *The Plant Cell* **6**: 1703–1712.
- Brokamp G, Dostert N, Cáceres-H F, Weigend M. 2012.** Parasitism and haustorium anatomy of *Krameria lappacea* (Dombey) Burdet & B.B. Simpson (Krameriaceae), an endangered medicinal plant from the Andean deserts. *Journal of Arid Environments* **83**: 94–100.
- Brown I, Trethowan J, Kerry M, Mansfield J, Bolwell GP. 1998.** Localization of components of the oxidative cross-linking of glycoproteins and of callose synthesis in papillae formed during the interaction between non-pathogenic strains of *Xanthomonas campestris* and French bean mesophyll cells. *The Plant Journal* **15**: 333–343.
- Bullock JM, Pywell RF. 2005.** *Rhinanthus*: a tool for restoring diverse grassland? *Folia Geobotanica* **40**: 273–288.
- Burgert I, Fratzl P. 2009.** Plants control the properties and actuation of their organs through the orientation of cellulose fibrils in their cell walls. *Integrative and Comparative Biology* **49**: 69–79.
- Busch S, Schmitt K, Erhardt C, Speck T. 2010.** Analysis of self-repair mechanisms of *Phaseolus vulgaris* var. *saxa* using near-infrared surface-enhanced Raman spectroscopy. *Journal of Raman Spectroscopy* **41**: 490–497.
- Byrne C. 1996.** Semi-natural grassland communities in Eastern Ireland: classification, conservation and management. PhD Thesis. Dublin: Trinity College.
- Caffall KH, Mohnen D. 2009.** The structure, function, and biosynthesis of plant cell wall pectic polysaccharides. *Carbohydrate Research* **344**: 1879–1900.
- Calvin CL, Wilson CA. 1996.** Endophytic System. In: Wiens HF& D, ed. Agriculture handbook 709. Dwarf mistletoes: biology, pathology, and systematic. Washington, DC.: United States Department of Agriculture Forest Service, 113–122.
- Cameron DD, Coats AM, Seel WE. 2006.** Differential resistance among host and non-host species underlies the variable success of the hemi-parasitic plant *Rhinanthus minor*. *Annals of Botany* **98**: 1289–1299.

- Cameron DD, Geniez J-M, Seel WE, Irving LJ. 2008.** Suppression of host photosynthesis by the parasitic plant *Rhinanthus minor*. *Annals of Botany* **101**: 573–578.
- Cameron DD, Hwangbo J-K, Keith AM, Geniez J-M, Kraushaar D, Rowntree J, Seel WE. 2005.** Interactions between the hemiparasitic angiosperm *Rhinanthus minor* and its hosts: from the cell to the ecosystem. *Folia Geobotanica* **40**: 217–229.
- Cameron DD, Seel WE. 2007.** Functional anatomy of haustoria formed by *Rhinanthus minor*: linking evidence from histology and isotope tracing. *New Phytologist* **174**: 412–419.
- Cannesan MA, Durand C, Burel C, Gangneux C, Lerouge P, Ishii T, Laval K, Follet-Gueye M-L, Driouich A, Vitré-Gibouin M. 2012.** Effect of arabinogalactan proteins from the root caps of pea and *Brassica napus* on *Aphanomyces euteiches* zoospore chemotaxis and germination. *Plant Physiology* **159**: 1658–1670.
- Cannon MC, Terneus K, Hall Q, Tan L, Wang Y, Wegenhart BL, Chen L, Lampport DT a, Chen Y, Kieliszewski MJ. 2008.** Self-assembly of the plant cell wall requires an extensin scaffold. *Proceedings of the National Academy of Sciences of the United States of America* **105**: 2226–2231.
- Cantu D, Vicente AR, Labavitch JM, Bennett AB, Powell ALT. 2008.** Strangers in the matrix: plant cell walls and pathogen susceptibility. *Trends in Plant Science* **13**: 610–617.
- Carol M, Calvin L. 1985.** The ultrastructure of dwarf mistletoe (*Arceuthobium* spp.) sinker cells in the region of the host secondary vasculature. *Canadian Journal of Botany* **63**: 889–898.
- Carpita NC. 1996.** Structure and biogenesis of the cell walls of grasses. *Annual Review of Plant Physiology and Plant Molecular Biology* **47**: 445–476.
- Carpita NC, Gibeaut DM. 1993.** Structural models of primary cell walls in flowering plants: consistency of molecular structure with the physical properties of the walls during growth. *The Plant Journal* **3**: 1–30.
- Casadevall A, Nosanchuk JD, Williamson P, Rodrigues ML. 2009.** Vesicular transport across the fungal cell wall. *Trends in Microbiology* **17**: 158–162.
- Casero PJ, Casimiro I, Knox JP. 1998.** Occurrence of cell surface arabinogalactan-protein and extensin epitopes in relation to pericycle and vascular tissue development in the root apex of four species. *Planta* **204**: 252–259.
- Cassab GI. 1998.** Plant cell wall proteins. *Annual Review of Plant Physiology and Plant Molecular Biology* **49**: 281–309.
- Chang M, Lynn DG. 1986.** The haustorium and the chemistry of host recognition in parasitic angiosperms. *Journal of Chemical Ecology* **12**: 561–579.
- Chasan R. 1994.** Arabinogalactan-proteins: getting to the core. *The Plant Cell* **6**: 1519–1521.
- Chebli Y, Kaneda M, Zerkour R, Geitmann A. 2012.** The cell wall of the *Arabidopsis thaliana* pollen tube — spatial distribution, recycling and network formation of polysaccharides. *Plant Physiology* **160**: 1940–1955.
- Chen X, Kim J. 2009.** Callose synthesis in higher plants. *Plant Signalling and Behaviour* **4**: 489–492.
- Chen F, Tobimatsu Y, Jackson L, Nakashima J, Ralph J, Dixon R a. 2012.** Novel seed coat lignins in the Cactaceae: structure, distribution and implications for the evolution of lignin diversity. *The Plant Journal* **73**: 201–211.
- Cheng TC. 1991.** Is parasitism symbiosis? A definition of terms and the evolution of concepts. In: Toft CA, Aeschlimann A, Bolis L, eds. Parasite-host associations. Coexistence or conflict? Oxford University Press, 15–36.
- Cheung AY, Wu H-M. 1999.** Arabinogalactan proteins in plant sexual reproduction. *Protoplasma* **208**: 87–98.
- Christensen NM, Dörr I, Hansen M, Van der Kooij T a W, Schulz A. 2003.** Development of *Cuscuta* species on a partially incompatible host: induction of xylem transfer cells. *Protoplasma* **220**: 131–142.

9. Literature cited

- Cissoko M, Boissard A, Rodenburg J, Press MC, Scholes JD. 2011.** New Rice for Africa (NERICA) cultivars exhibit different levels of post-attachment resistance against the parasitic weeds *Striga hermonthica* and *Striga asiatica*. *New Phytologist* **192**: 952–963.
- Clarke AE, Anderson RL, Stone BA. 1979.** Review of form and function of arabinogalactans and arabinogalactan-proteins. *Phytochemistry* **18**: 521–540.
- Clausen MH, Willats WGT, Knox JP. 2003.** Synthetic methyl hexagalacturonate hapten inhibitors of anti-homogalacturonan monoclonal antibodies LM7, JIM5 and JIM7. *Carbohydrate Research* **338**: 1797–1800.
- Clifford M. 1974.** Specificity of acidic phloroglucinol reagents. *Journal of Chromatography* **94**: 321–324.
- Collmer A, Keen NT. 1986.** The role of pectic enzymes in plant pathogenesis. *Annual Review of Phytopathology* **24**: 383–409.
- Condon J, Kuijt JOB. 1994.** Anatomy and ultrastructure of the primary endophyte of *Ileostylus micranthus* (Loranthaceae). *International Journal of Plant Sciences* **155**: 350–364.
- Considine JA, Knox RB. 1979.** Development and histochemistry of the cells, cell walls, and cuticle of the dermal system of fruit of the grape, *Vitis vinifera* L. *Protoplasma* **365**: 347–365.
- Cook CE, Whichard LP, Turner B, Wall ME, Egley GH. 1966.** Germination of witchweed (*Striga lutea* Lour.): isolation and properties of a potent stimulant. *Science* **154**: 1189–1190.
- Cosgrove DJ. 1993.** Tansley Review No. 46 Wall extensibility: its nature, measurement and relationship to plant cell growth. *New Phytologist* **124**: 1–23.
- Cosgrove DJ. 1997.** Assembly and enlargement of the primary cell wall in plants. *Annual Review of Cell and Developmental Biology* **13**: 171–201.
- Cosgrove DJ. 2000.** Expansive growth of plant cell walls. *Plant Physiology and Biochemistry* **38**: 109–124.
- Cosgrove DJ. 2005a.** Plant cell enlargement and the action of expansins. *BioEssays* **18**: 533–540.
- Cosgrove DJ. 2005b.** Growth of the plant cell wall. *Nature Reviews. Molecular Cell Biology* **6**: 850–861.
- Currie HA, Perry CC. 2007.** Silica in plants: biological, biochemical and chemical studies. *Annals of Botany* **100**: 1383–1389.
- Daayf F, Schmitt A, Belanger RR. 1997.** Evidence of phytoalexins in cucumber leaves infected with powdery mildew following treatment with leaf extracts of *Reynoutria sachalinensis*. *Plant Physiology* **113**: 719–727.
- Dahiya P, Brewin NJ. 2000.** Immunogold localization of callose and other cell wall components in pea nodule transfer cells. *Protoplasma* **214**: 210–218.
- Davies D. 1997.** The impact of *Rhinanthus* spp. on sward productivity and composition: Implications for the restoration of species-rich grasslands. *Biological Conservation* **82**: 87–93.
- Davis CC, Latvis M, Nickrent DL, Wurdack KJ, Baum DA. 2007.** Floral gigantism in Rafflesiaceae. *Science* **315**: 1812–1812.
- Davis MA, Pritchard SG, Boyd RS, Prior SA. 2001.** Developmental and induced responses of nickel-based and organic defences of the nickel-hyperaccumulating shrub, *Psychotria douarrei*. *New Phytologist* **160**: 49–58.
- Dean RA, Timberlake WE. 1989.** Production of cell wall-degrading enzymes by *Aspergillus nidulans*: a model system for fungal pathogenesis of plants. *The Plant Cell* **1**: 265–273.
- Decreux A, Messiaen J. 2005.** Wall-associated kinase WAK1 interacts with cell wall pectins in a calcium-induced conformation. *Plant Cell Physiology* **46**: 268–278.
- Deenihan A, Donlan J, Breen J, Moles R. 2009.** Mid-term impacts of excluding large grazing animals on a Burren grass/scrubland patch. *Biology & Environment: Proceedings of the Royal Irish Academy* **109**: 107–113.
- Deepak S, Shailasree S, Kini RK, Muck A, Mithöfer A, Shetty SH. 2010.** Hydroxyproline-rich glycoproteins and plant defence. *Journal of Phytopathology* **593**: 585–593.

- DeWitt G, Richards J, Mohnen D, Jones AM. 1999.** Comparative compositional analysis of walls with two different morphologies: archetypical versus transfer-cell-like. *Protoplasma* **209**: 238–245.
- Die JV, Dita MA, Krajinski F, González-Verdejo CI, Rubiales D, Moreno MT, Román B. 2007.** Identification by suppression subtractive hybridization and expression analysis of *Medicago truncatula* putative defence genes in response to *Orobanche crenata* parasitization. *Physiological and Molecular Plant Pathology* **70**: 49–59.
- Ding S-Y, Himmel ME. 2006.** The maize primary cell wall microfibril: a new model derived from direct visualization. *Journal of Agricultural and Food Chemistry* **54**: 597–606.
- Ding L, Zhu JK. 1997.** A role for arabinogalactan-proteins in root epidermal cell expansion. *Planta* **203**: 289–294.
- Dita M a, Die J V, Román B, Krajinski F, Küster H, Moreno MT, Cubero JI, Rubiales D. 2009.** Gene expression profiling of *Medicago truncatula* roots in response to the parasitic plant *Orobanche crenata*. *Weed Research* **49**: 66–80.
- Dolan L, Linstead P, Roberts K. 1995.** An AGP epitope distinguishes a central metaxylem initial from other vascular initials in the *Arabidopsis* root. *Protoplasma* **189**: 149–155.
- Dolan L, Linstead P, Roberts K. 1997.** Developmental regulation of pectic polysaccharides in the root meristem of *Arabidopsis*. *Journal of Experimental Botany* **48**: 713–720.
- Domon J-M, Neutelings G, Roger D, David A, David H. 2000.** A basic chitinase-like protein secreted by embryogenic tissues of *Pinus caribaea* acts on arabinogalactan proteins extracted from the same cell lines. *Journal of Plant Physiology* **156**: 33–39.
- Donaldson LA. 1994.** Mechanical constraints on lignin deposition during lignification. *Wood Science and Technology* **28**: 111–118.
- Donaldson LA. 2001.** Lignification and lignin topochemistry — an ultrastructural view. *Phytochemistry* **57**: 859–873.
- Van Doorn WG, Beers EP, Dangl JL, Franklin-Tong VE, Gallois P, Hara-Nishimura I, Jones a M, Kawai-Yamada M, Lam E, Mundy J, et al. 2011.** Morphological classification of plant cell deaths. *Cell Death and Differentiation* **18**: 1241–1246.
- Dörr I. 1997.** How *Striga* parasitizes its host: a TEM and SEM study. *Annals of Botany* **79**: 463–472.
- Dörr I, Kollman R. 1995.** Symplasmic sieve element continuity between *Orobanche* and its host. *Botanica acta* **108**: 47–55.
- Dörr I, Kollmann R. 1976.** Strukturelle Grundlagen des Parasitismus bei *Orobanche*. III. Die Differenzierung des Xylemanschlusses bei *O. crenata*. *Protoplasma* **89**: 235–249.
- Dörr I, Staack A, Kollmann R. 1994.** Resistance of *Helianthus* to *Orobanche* — histological and cytological studies. Proceedings of the Third International Workshop on *Orobanche* and related *Striga* Research, Amsterdam. Amsterdam: Royal Tropical Institute, 276–289.
- Dow L, Lumsden D. 1975.** Histopathology of infection of bean with *Pythium myriotylum* compared with infection with other *Pythium* species. *Canadian Journal of Botany* **53**: 1786–1795.
- Downie H, Holden N, Otten W, Spiers AJ, Valentine T a, Dupuy LX. 2012.** Transparent soil for imaging the rhizosphere. *PLOS ONE* **7**: e44276.
- Doyle GJ. 1993.** *Cuscuta epithimum* (L) L (Convolvulaceae), its hosts and associated vegetation in a limestone pavement habitat in the Burren lowlands in county Clare (H9), Western Ireland. *Biology and Environment: Proceedings of the Royal Irish Academy* **93B**: 61–67.
- Du H, Clarke AE, Bacic A. 1996.** Arabinogalactan-proteins: a class of extracellular matrix proteoglycans involved in plant growth and development. *Trends in Cell Biology* **6**: 411–414.
- Dunnett NP, Willis AJ, Hunt R, Grime JP. 1998.** A 38-year study of relations between weather and vegetation dynamics in road verges near Bibury, Gloucestershire. *Journal of Ecology* **86**: 610–623.

9. Literature cited

- Dvoráková L, Srba M, Opatrný Z, Fischer L. 2012.** Hybrid proline-rich proteins: novel players in plant cell elongation? *Annals of Botany* **109**: 453–462.
- Dyakov Y, Dzhavakhiya V, Korpela T (Eds.). 2007.** *Comprehensive and molecular phytopathology*. Amsterdam: Elsevier.
- Echevarría-Zomeño S, Pérez-de-Luque A, Jorrín J, Maldonado AM. 2006.** Pre-haustorial resistance to broomrape (*Orobancha cumana*) in sunflower (*Helianthus annuus*): cytochemical studies. *Journal of Experimental Botany* **57**: 4189–4200.
- Eigenbrode SD, Espelie KE. 1995.** Effects of plant epicuticular lipids on insect herbivores. *Annual Review of Entomology* **40**: 171–194.
- Eizenberg H. 2003.** Resistance to broomrape (*Orobancha spp.*) in sunflower (*Helianthus annuus* L.) is temperature dependent. *Journal of Experimental Botany* **54**: 1305–1311.
- Eizenberg H, Tanaami Z, Jacobsohn R, Rubin B. 2001.** Effect of temperature on the relationship between *Orobancha spp.* and carrot (*Daucus carota* L.). *Crop Protection* **20**: 415–420.
- Ejeta G, Butler LG. 1993.** Host-parasite interactions throughout the *Striga* life cycle, and their contributions to *Striga* resistance. *African Crop Science Journal* **1**: 75–80.
- Ellis M, Egelund J, Schultz CJ, Bacic A. 2010.** Arabinogalactan-proteins: key regulators at the cell surface? *Plant Physiology* **153**: 403–419.
- Enkerli J, Felix G, Boller T. 1999.** The enzymatic activity of fungal xylanase is not necessary for its elicitor activity. *Plant Physiology* **121**: 391–397.
- Eraso F, Hartley RD. 1990.** Monomeric and dimeric phenolic constituents of plant cell walls -possible factors influencing wall biodegradability. *Journal of the Science of Food and Agriculture* **51**: 163–170.
- Esquerré-Tugayé M-T, Boudart G, Dumas B. 2000.** Cell wall degrading enzymes, inhibitory proteins, and oligosaccharides participate in the molecular dialogue between plants and pathogens. *Plant Physiology and Biochemistry* **38**: 157–163.
- Estabrook EM, Yoder JJ. 1998.** Plant-plant communications: rhizosphere signaling between parasitic angiosperms and their hosts. *Plant Physiology* **116**: 1–7.
- Evert RF (Ed.). 2006.** *Esau's Plant Anatomy*. Hoboken, NJ: John Wiley & Sons.
- Fangel JU, Ulvskov P, Knox JP, Mikkelsen MD, Harholt J, Popper ZA, Willats WGT. 2012.** Cell wall evolution and diversity. *Frontiers in Plant Science* **3**: 1-8.
- Federici L, Di Matteo A, Fernandez-Recio J, Tsernoglou D, Cervone F. 2006.** Polygalacturonase inhibiting proteins: players in plant innate immunity? *Trends in Plant Science* **11**: 65–70.
- Feehan J. 2003.** *Farming in Ireland — history, heritage and environment*. Dublin: University College Dublin Press.
- Fernández S, Osorio S, Heredia A. 1999.** Monitoring and visualising plant cuticles by confocal laser scanning microscopy. *Plant Physiology and Biochemistry* **37**: 789–794.
- Fernández-Aparicio M, Moral A, Kharrat M, Rubiales D. 2012.** Resistance against broomrapes (*Orobancha* and *Phelipanche* spp.) in faba bean (*Vicia faba*) based in low induction of broomrape seed germination. *Euphytica* **186**: 897–905.
- Field RA. 2009.** Oligosaccharide signalling molecules. In: Osbourn AE, Lanzotti V, eds. *Plant-derived natural products. Synthesis, function and application*. New York, NY: Springer US, 349–359.
- Fincher GB, Stone BA. 1983.** Arabinogalactan-proteins: structure, biosynthesis, and function. *Annual Review of Plant Physiology* **34**: 47–70.
- Fineran BA. 1987.** A structural approach towards investigating transport systems between host and parasite, as exemplified by some mistletoes and root parasites. In: Weber HC, Forstreuter W, eds. *Proceedings of the 4th International Symposium on Parasitic Flowering Plants, Marburg 1987*. 201–220.
- Fineran BA. 1996.** Flange-type parenchyma cells: occurrence and structure in the haustorium of the dwarf mistletoe *Korthalsella* (Viscaceae). *Protoplasma* **194**: 40–53.

- Fineran BA, Calvin CL. 2000.** Transfer cells and flange cells in sinkers of the mistletoe *Phoradendron macrophyllum* (Viscaceae), and their novel combination. *Protoplasma* **211**: 76–93.
- Fitter A. H, Peat HJ. 1994.** The Ecological Flora Database. *Journal of Ecology* **82**: 415–425.
- Flanders DJ, Rawlins DJ, Shaw PJ, Lloyd CW. 1990.** Nucleus-associated microtubules help determine the division plane of plant epidermal cells: avoidance of four-way junctions and the role of cell geometry. *The Journal of Cell Biology* **110**: 1111–1122.
- Florentino LH, Santos A a, Fontenelle MR, Pinheiro GL, Zerbini FM, Baracat-Pereira MC, Fontes EPB. 2006.** A PERK-like receptor kinase interacts with the geminivirus nuclear shuttle protein and potentiates viral infection. *Journal of Virology* **80**: 6648–6656.
- Fortes AM, Testillano PS, Del Carmen Risueño M, Pais MS. 2002.** Studies on callose and cutin during the expression of competence and determination for organogenic nodule formation from internodes of *Humulus lupulus* var. Nugget. *Physiologia Plantarum* **116**: 113–120.
- Fossitt JA. 2000.** *A guide to habitats in Ireland*. Kilkenny: The Heritage Council.
- Franke R, Schreiber L. 2007.** Suberin — a biopolyester forming apoplastic plant interfaces. *Current Opinion in Plant Biology* **10**: 252–9.
- Frühling M, Hohnjec N, Schröder G, Küster H, Pühler A, Perlick A. 2000.** Genomic organization and expression properties of the VfENOD5 gene from broad bean (*Vicia faba* L.). *Plant Science* **155**: 169–178.
- Fry SC. 1983.** Feruloylated pectins from the primary cell wall: their structure and possible functions. *Planta* **157**: 111–123.
- Fry SC. 1988.** *The Growing Plant Cell Wall: Chemical and Metabolic Analysis*. New York: John Wiley and Sons.
- Fry SC. 1989.** Cellulases , hemicelluloses and auxin-stimulated growth: a possible relationship. *Physiologia Plantarum* **75**: 532–536.
- Fry SC. 1995.** Polysaccharide-modifying enzymes in the plant cell wall. *Annual Review of Phytopathology* **46**: 497–520.
- Fry SC. 2011.** Cell wall polysaccharide composition and covalent crosslinking. *Annual Plant Reviews* **41**: 1–42.
- Fry SC, Nesselrode BHW a, Miller JG, Mewburn BR. 2008.** Mixed-linkage (1→3, 1→4)-beta-D-glucan is a major hemicellulose of Equisetum (horsetail) cell walls. *New Phytologist* **179**: 104–15.
- Fujita M, Kinoshita T. 2012.** GPI-anchor remodeling: potential functions of GPI-anchors in intracellular trafficking and membrane dynamics. *Biochimica et Biophysica Acta* **1821**: 1050–1058.
- Fukuda H. 1997.** Tracheary element differentiation. *The Plant Cell* **9**: 3–7.
- Fukuda H. 2004.** Signals that control plant vascular cell differentiation. *Nature Reviews. Molecular Cell Biology* **5**: 379–391.
- Fukushima K, Terashima N. 1990.** Heterogeneity in formation of lignin. XIII. Formation of *p*-hydroxyphenyl lignin in various hardwoods visualized by microautoradiography. *Journal of Wood Chemistry and Technology* **10**: 413–433.
- Fukushima K, Terashima N. 1991.** Heterogeneity in formation of lignin. *Wood Science and Technology* **25**: 371–381.
- Ganguly A, Lee SH, Cho M, Lee OR, Yoo H, Cho H-T. 2010.** Differential auxin-transporting activities of PIN-FORMED proteins in *Arabidopsis* root hair cells. *Plant Physiology* **153**: 1046–1061.
- Gao M, Kieliszewski MJ, Lampert DT, Showalter a M. 1999.** Isolation, characterization and immunolocalization of a novel, modular tomato arabinogalactan-protein corresponding to the LeAGP-1 gene. *The Plant Journal* **18**: 43–55.
- Gao M, Showalter AM. 2000.** Immunolocalization of LeAGP-1, a modular arabinogalactan-protein, reveals its developmentally regulated expression in tomato. *Planta* **210**: 865–874.

9. Literature cited

- Gaspar Y, Johnson KL, McKenna J a, Bacic A, Schultz CJ. 2001.** The complex structures of arabinogalactan-proteins and the journey towards understanding function. *Plant Molecular Biology* **47**: 161–176.
- Gaspar YM, Nam J, Schultz CJ, Lee L, Gilson PR, Gelvin SB, Bacic A. 2004.** Characterization of the *Arabidopsis* lysine-rich arabinogalactan-protein AtAGP17 mutant (rat1) that results in a decreased efficiency of *Agrobacterium* transformation. *Plant Physiology* **135**: 2162–2171.
- Gavnholt B, Larsen K. 2002.** Molecular biology of plant laccases in relation to lignin formation. *Physiologia Plantarum* **116**: 273–280.
- Geitmann A. 2010.** How to shape a cylinder: pollen tube as a model system for the generation of complex cellular geometry. *Sexual Plant Reproduction* **23**: 63–71.
- Geitmann A. 2011.** Generating a cellular protuberance: mechanics of tip growth. In: Wojtaszek P, ed. *Mechanical Integration of Plant Cells and Plants*. Berlin, Heidelberg: Springer Berlin Heidelberg, 117–132.
- Geitmann A, Ortega JKE. 2009.** Mechanics and modeling of plant cell growth. *Trends in Plant Science* **14**: 467–478.
- Gens JS, Fujiki M, Pickard BG. 2000.** Arabinogalactan protein and wall-associated kinase in a plasmalemmal reticulum with specialized vertices. *Protoplasma* **212**: 115–134.
- Gibeaut DM, Carpita NC. 1991.** Tracing cell wall biogenesis in intact cells and plants: selective turnover and alteration of soluble and cell wall polysaccharides in grasses. *Plant Physiology* **97**: 551–561.
- Gibson CC, Watkinson AR. 1989.** The host range and selectivity of a parasitic plant: *Rhinanthus minor* L. *Oecologia* **78**: 401–406.
- Gibson C, Watkinson A. 1991.** Host selectivity and the mediation of competition by the root hemiparasite *Rhinanthus minor*. *Oecologia* **86**: 81–87.
- Gibson C, Watkinson A. 1992.** The role of the hemiparasitic annual *Rhinanthus minor* in determining grassland community structure. *Oecologia* **89**: 62–68.
- Gilbert HJ. 2010.** The biochemistry and structural biology of plant cell wall deconstruction. *Plant Physiology* **153**: 444–55.
- Gilbert HJ, Stålbrand H, Brumer H. 2008.** How the walls come crumbling down: recent structural biochemistry of plant polysaccharide degradation. *Current Opinion in Plant Biology* **11**: 338–348.
- Goldwasser Y, Plakhine D, Kleifeld Y, Zamski E, Rubin B. 2000.** The differential susceptibility of Vetch (*Vicia* spp.) to *Orobanche aegyptiaca*: anatomical studies. *Annals of Botany* **85**: 257–262.
- Golovchenko V V, Ovodova RG, Shashkov AS, Ovodov YS. 2002.** Structural studies of the pectic polysaccharide from duckweed *Lemna minor* L. *Phytochemistry* **60**: 89–97.
- Goodrum LJ, Patel A, Leykam JF, Kieliszewski MJ. 2000.** Gum arabic glycoprotein contains glycomodules of both extensin and arabinogalactan-glycoproteins. *Phytochemistry* **54**: 99–106.
- Goriely A, Tabor M. 2006.** Estimates of biomechanical forces in *Magnaporthe grisea*. *Mycological Research* **110**: 755–759.
- Gothandam KM, Nalini E, Karthikeyan S, Shin JS. 2010.** OsPRP3, a flower specific proline-rich protein of rice, determines extracellular matrix structure of floral organs and its overexpression confers cold-tolerance. *Plant Molecular Biology* **72**: 125–35.
- Govier R, Brown J, Pate J. 1968.** Hemiparasitic nutrition in angiosperms. II. Root haustoria and leaf glands of *Odontites verna* (Bell.) Dum. and their relevance to the abstraction of solutes from the host. *New Phytologist* **67**: 963–972.
- Govier R, Nelson MD, Pate J. 1967.** Hemiparasitic nutrition in angiosperms. I. The transfer of organic compounds from host to *Odontites verna* (Bell.) Dum. (Scrophulariaceae). *New Phytologist* **66**: 285–297.
- Gowda BS, Riopel JL, Timko MP. 1999.** NRSA-1: a resistance gene homolog expressed in roots of non-host plants following parasitism by *Striga asiatica* (witchweed). *The Plant Journal* **20**: 217–230.

- Grandin U. 2006.** PC-ORD version 5: A user-friendly toolbox for ecologists. *Journal of Vegetation Science* **17**: 843–844.
- Green III F, Kuster TA, Highley TL. 1996.** Pectin degradation during colonization of wood by brown-rot fungi. *Recent Research Developments in Plant Pathology* **1**: 83–93.
- Grewell BJ. 2008.** Parasite facilitates plant species coexistence in a coastal wetland. *Ecology* **89**: 1481–1488.
- Griffith M, Brown GN. 1982.** Cell wall deposits in winter rye *Secale cereale* L. “Puma” during cold acclimation. *Botanical Gazette* **143**: 486–490.
- Grime JP, Hodgson JG, Hunt R. 1988.** *Comparative Plant Ecology. A functional approach to common British species*. London: Chapman and Hall.
- Guo D, Chen F, Inoue K, Blount JW, Dixon RA. 2001.** Downregulation of caffeic acid 3-*O*-methyltransferase and caffeoyl CoA 3-*O*-methyltransferase in transgenic alfalfa. impacts on lignin structure and implications for the biosynthesis of G and S lignin. *The Plant Cell* **13**: 73–88.
- Gurney A, Grimanelli D, Kanampiu F, Hoisington D, Scholes J, Press M. 2001.** Can wild relatives of cereals provide new sources of resistance to the parasitic angiosperm *Striga hermonthica*? Proceedings of the Seventh International Parasitic Weed Symposium, Nantes, France, 4-8 June. 247.
- Gurney AL, Grimanelli D, Kanampiu F, Hoisington D, Scholes JD, Press MC. 2003.** Novel sources of resistance to *Striga hermonthica* in *Tripsacum dactyloides*, a wild relative of maize. *New Phytologist* **160**: 557–568.
- Gurney AL, Press MC, Scholes JD. 2002.** Can wild relatives of sorghum provide new sources of resistance or tolerance against *Striga* species? *Weed Research* **42**: 317–324.
- Gurney AL, Slate J, Press MC, Scholes JD. 2006.** A novel form of resistance in rice to the angiosperm parasite *Striga hermonthica*. *New Phytologist* **169**: 199–208.
- Haas TJ, Otegui MS. 2007.** Electron tomography in plant cell biology. *Journal of Integrative Plant Biology* **49**: 1091–1099.
- Hamann T. 2012.** Plant cell wall integrity maintenance as an essential component of biotic stress response mechanisms. *Frontiers in Plant Science* **3**: 1–5
- Hamann T, Denness L. 2011.** Cell wall integrity maintenance in plants: lessons to be learned from yeast? *Plant Signaling & Behavior* **6**: 1706–1709.
- Harholt J, Suttangkakul A, Vibe Scheller H. 2010.** Biosynthesis of pectin. *Plant Physiology* **153**: 384–395.
- Hariri EB, Sallé G, Andary C. 1991.** Involvement of flavonoids in the resistance of two poplar cultivars to mistletoe (*Viscum album* L.). *Protoplasma* **162**: 20–26.
- Harker FR, Hallett IC. 1992.** Physiological changes associated with development of mealiness of apple fruit during cool storage. *Horticultural Science* **27**: 1291–1294.
- Harris PJ. 2005.** Diversity in plant cell walls. In: Henry RJ, ed. *Plant Diversity and Evolution: Genotypic and Phenotypic Variation in Higher Plants*. CABI Publishing, 201–227.
- Harris PJ, Hartley RD. 1976.** Detection of bound ferulic acid in cell walls of the Graminae by ultraviolet fluorescence microscopy. *Nature* **259**: 508–510.
- Harris PJ, Kelderman MR, Kendon MF, Mckenzie RJ. 1997.** Monosaccharide compositions of unlignified cell walls of monocotyledons in relation to the occurrence of wall-bound ferulic acid. *Biochemical Systematics and Ecology* **25**: 167–179.
- Harris PJ, Trethewey JAK. 2009.** The distribution of ester-linked ferulic acid in the cell walls of angiosperms. *Phytochemistry Reviews* **9**: 19–33.
- Hartley RD, Keene AS. 1984.** Aromatic aldehyde constituents of graminaceous cell walls. *Phytochemistry* **23**: 1305–1307.

9. Literature cited

- Hartley RD, Morrison WH. 1991.** Monomeric and dimeric phenolic acids released from cell walls of grasses by sequential treatment with sodium hydroxide. *Journal of the Science of Food and Agriculture* **55**: 365–375.
- Hatakka PA. 2001.** Biodegradation of lignin. In: Hofrichter M SA, ed. Biopolymers: lignin, humic substances and coal. Weinheim: Wiley-VCH, 129–180.
- He ZH, He D, Kohorn BD. 1998.** Requirement for the induced expression of a cell wall associated receptor kinase for survival during the pathogen response. *The Plant Journal* **14**: 55–63.
- Heery S. 1996.** Callows and floodplains. In: Otte ML, ed. Wetlands of Ireland. Distribution, ecology, uses and economic value. Dublin: University College Dublin Press, 109–123.
- Heide-Jørgensen HS. 1988.** Development and ultrastructure of the haustorium of *Viscum minimum*. I. The adhesive disk. *Canadian Journal of Botany* **67**: 1161–1173.
- Heide-Jørgensen H. 1995.** The haustorium of the root parasite *Triphysaria* (Scrophulariaceae), with special reference to xylem bridge ultrastructure. *American Journal of Botany* **82**: 782–797.
- Heide-Jørgensen HS. 2008.** Parasitic flowering plants. Leiden: Brill Academic Publishing.
- Heide-Jørgensen HS, Kuijt J. 1993.** Epidermal derivatives as xylem elements and transfer cells: a study of the host-parasite interface in two species of *Triphysaria* (Scrophulariaceae). *Protoplasma* **174**: 173–183.
- Heller A, Thines M. 2009.** Evidence for the importance of enzymatic digestion of epidermal walls during subepidermal sporulation and pustule opening in white blister rusts (Albuginaceae). *Mycological Research* **113**: 657–667.
- Hématy K, Cherk C, Somerville S. 2009.** Host-pathogen warfare at the plant cell wall. *Current Opinion in Plant Biology* **12**: 406–413.
- Van Hengel AJ, Tadesse Z, Immerzeel P, Schols H, Kammen A Van, De Vries SC. 2001.** N-acetylglucosamine and glucosamine-containing arabinogalactan proteins control somatic embryogenesis. *Plant Physiology* **125**: 1880–1890.
- Hepler PK, Vidali L, Cheung AY. 2001.** Polarized cell growth in higher plants. *Annual Review of Cell and Developmental Biology* **17**: 159–187.
- Hervé C, Marcus SE, Knox JP. 2011.** Monoclonal antibodies, carbohydrate-binding molecules, and the detection of polysaccharides in plant cell walls. In: Popper ZA, ed. The Plant Cell Wall. Methods and Protocols. New York: Humana Press, 103–113.
- Hervé C, Rogowski A, Gilbert HJ, Paul Knox J. 2009.** Enzymatic treatments reveal differential capacities for xylan recognition and degradation in primary and secondary plant cell walls. *The Plant Journal* **58**: 413–422.
- Higuchi M, Pischke MS, Mähönen AP, Miyawaki K, Hashimoto Y, Seki M, Kobayashi M, Shinozaki K, Kato T, Tabata S, et al. 2004.** In planta functions of the *Arabidopsis* cytokinin receptor family. *Proceedings of the National Academy of Sciences of the United States of America* **101**: 8821–8826.
- Hill MO, Mountford JO, Roy DB, Bunce. RGH. 1999.** *Ellenberg's indicator values for British plants*. Huntingdon: Centre for Ecology & Hydrology.
- Himmel ME, Ding S-Y, Johnson DK, Adney WS, Nimlos MR, Brady JW, Foust TD. 2007.** Biomass recalcitrance: engineering plants and enzymes for biofuels production. *Science* **315**: 804–807.
- Hiraoka Y, Sugimoto Y. 2008.** Molecular responses of Sorghum to purple witchweed (*Striga hermonthica*) parasitism. *Weed Science* **56**: 356–363.
- Hirsch AM, Bauer WD, Bird DM, Cullimore J, Tyler B, Yoder JI. 2003.** Molecular signals and receptors: controlling rhizosphere interactions between plants and other organisms. *Ecology* **84**: 858–868.
- Hirst R, Pywell RF, Marrs RH, Putwain PD. 2005.** The resilience of calcareous and mesotrophic grasslands following disturbance. *Journal of Applied Ecology* **42**: 498–506.
- Hoch G. 2007.** Cell wall hemicelluloses as mobile carbon stores in non-reproductive plant tissues. *Functional Ecology* **21**: 823–834.

- Hoffman M, Jia Z, Peña MJ, Cash M, Harper A, Blackburn AR, Darvill A, York WS. 2005.** Structural analysis of xyloglucans in the primary cell walls of plants in the subclass Asteridae. *Carbohydrate Research* **340**: 1826–1840.
- Hong L, Shen H, Chen H, Li L, Hu X, Xu X, Ye W, Wang Z. 2011.** The morphology and anatomy of the haustoria of the holoparasitic angiosperm *Cuscuta campestris*. *Pakistan Journal of Botany* **43**: 1853–1859.
- Hood ME, Condon JM, Timko MP, Riopel JL. 1998.** Primary haustorial development of *Striga asiatica* on host and nonhost species. *Phytopathology* **88**: 70–75.
- Hooper NM. 1997.** Glycosyl-phosphatidylinositol anchored membrane enzymes. *Clinica Chimica Acta* **266**: 3–12.
- Houston K, Wolff K. 2012.** *Rhinanthus minor* population genetic structure and subspecies: Potential seed sources of a keystone species in grassland restoration projects. *Perspectives in Plant Ecology, Evolution and Systematics* **14**: 423–433.
- Hückelhoven R. 2007.** Cell wall-associated mechanisms of disease resistance and susceptibility. *Annual Review of Phytopathology* **45**: 101–127.
- Van Hulst R, Shipley B, Thériault A. 1987.** Why is *Rhinanthus minor* (Scrophulariaceae) such a good invader? *Canadian Journal of Botany* **65**: 2373–2379.
- Humphrey T V, Bonetta DT, Goring DR. 2007.** Sentinels at the wall: cell wall receptors and sensors. *New Phytologist* **176**: 7–21.
- Hwangbo J-K, Seel WE. 2002.** Effects of light availability on attached *Rhinanthus minor* (L.), an angiospermatic root hemiparasite. *Journal of Plant Biology* **45**: 102–106.
- Hwangbo J-K, Seel WE, Woodin SJ. 2003.** Short-term exposure to elevated atmospheric CO² benefits the growth of a facultative annual root hemiparasite, *Rhinanthus minor* (L.), more than that of its host, *Poa pratensis* (L.). *Journal of Experimental Botany* **54**: 1951–1955.
- Iiyama K, Pant R, Dun D. 1988.** The mechanism of the Maüle colour reaction. Introduction of methylated syringyl nuclei into softwood lignin. *Wood Science and Technology* **22**: 167–175.
- Ikegawa T, Mayama S, Nakayashiki H, Kato H. 1996.** Accumulation of diferulic acid during the hypersensitive response of oat leaves to *Puccinia coronata* f. sp. *avenae* and its role in the resistance of oat tissues to cell wall degrading enzymes. *Physiological and Molecular Plant Pathology* **48**: 245–255.
- Ikezawa H. 2002.** Glycosylphosphatidylinositol (GPI)-anchored proteins. *Biological & Pharmaceutical Bulletin* **25**: 409–417.
- Immerzeel P, Eppink MM, De Vries SC, Schols HA, Voragen AGJ. 2006.** Carrot arabinogalactan proteins are interlinked with pectins. *Physiologia Plantarum* **128**: 18–28.
- Irving LJ, Cameron DD. 2009.** You are what you eat: interactions between root parasitic plants and their hosts. *Advances in Botanical Research* **50**: 87–138.
- Ishii T, Hiroi T. 1990.** Linkage of phenolic acids to cell-wall polysaccharides of bamboo shoot. *Carbohydrate Research* **206**: 297–310.
- Ish-Shalom-Gordon N, Jacobsohn R, Cohen Y. 1994.** Seasonal fluctuations in sunflower's resistance to *Orobanche cumana*. Proceedings of the Third International Workshop on *Orobanche* and related *Striga* research, Amsterdam. 351–355.
- Ivimey-Cook RB, Proctor MCF. 1966.** The plant communities of the Burren, Co. Clare. *Proceedings of the Royal Irish Academy. Section B: Biological, Geological and Chemical Science* **64**: 211–302.
- Jamil M, Rodenburg J, Charnikhova T, Bouwmeester HJ. 2011.** Pre-attachment *Striga hermonthica* resistance of New Rice for Africa (NERICA) cultivars based on low strigolactone production. *New Phytologist* **192**: 964–975.
- Jarvis MC. 1984.** Structure and properties of pectin gels in plant cell walls. *Plant, Cell and Environment* **7**: 153–164.

9. Literature cited

- Jarvis MC, Briggs SPH, Knox JP. 2003.** Intercellular adhesion and cell separation in plants. *Plant, Cell and Environment* **44**: 977–989.
- Jauh GY, Lord EM. 1996.** Localization of pectins and arabinogalactan-proteins in lily (*Lilium longitlorum* L.) pollen tube and style, and their possible roles in pollination. *Planta* **199**: 251–261.
- Jeffree CE. 2006.** The Fine Structure of the Plant Cuticle. In: Riederer M, Mller C, eds. *Biology of the Plant Cuticle*. Oxford, UK: Blackwell Publishing Ltd, .
- Jeffrey DW, Jones MB, McAdam JH. 1995.** Irish grasslands in perspective. In: Jeffrey DW, Jones MB, McAdam JH, eds. *Irish Grasslands — their biology and management*. Dublin: Royal Irish Academy, 1–5
- Jeffries TW, Gifford O, Drive P. 1990.** Biodegradation of lignin-carbohydrate complexes. *Biodegradation* **1**: 163–176.
- Jeon J, Goh J, Yoo S, Chi M-H, Choi J, Rho H-S, Park J, Han S-S, Kim BR, Park S-Y, et al. 2008.** A putative MAP kinase kinase kinase, MCK1, is required for cell wall integrity and pathogenicity of the rice blast fungus, *Magnaporthe oryzae*. *Molecular Plant-Microbe Interactions* **21**: 525–534.
- Jiang F. 2004.** Water, mineral nutrient and hormone flows and exchanges in the hemiparasitic association between root hemiparasite *Rhinanthus minor* and the host *Hordeum*. PhD Thesis. Würzburg: Bayerischen Julius-Maximilians-Universität
- Jiang F, Dieter Jeschke W, Hartung W. 2005.** Contents and flows of assimilates (mannitol and sucrose) in the hemiparasitic *Rhinanthus minor*/*Hordeum vulgare* association. *Folia Geobotanica* **40**: 195–203.
- Jiang F, Jeschke WD, Hartung W. 2003.** Water flows in the parasitic association *Rhinanthus minor*/*Hordeum vulgare*. *Journal of Experimental Botany* **54**: 1985–1993.
- Jiang F, Jeschke WD, Hartung W. 2004.** Abscisic acid (ABA) flows from *Hordeum vulgare* to the hemiparasite *Rhinanthus minor* and the influence of infection on host and parasite abscisic acid relations. *Journal of Experimental Botany* **55**: 2323–2329.
- Jiang F, Jeschke WD, Hartung W, Cameron DD. 2008a.** Does legume nitrogen fixation underpin host quality for the hemiparasitic plant *Rhinanthus minor*? *Journal of Experimental Botany* **59**: 917–925.
- Jiang F, Jeschke WD, Hartung W, Cameron DD. 2008b.** Mobility of boron-polyol complexes in the hemiparasitic association between *Rhinanthus minor* and *Hordeum vulgare*: the effects of nitrogen nutrition. *Physiologia Plantarum* **134**: 13–21.
- Jiang F, Jeschke WD, Hartung W, Cameron DD. 2010.** Interactions between *Rhinanthus minor* and its hosts: A review of water, mineral nutrient and hormone flows and exchanges in the hemiparasitic association. *Folia Geobotanica* **45**: 369–385.
- Joel DM, Losner-Goshen D. 1994a.** Early host-parasite interaction: models and observations of host root penetration by the haustorium of *Orobancha*. In: Pieterse AH, Verkleij JAC, Borg SJ, eds. *Proceedings of The Third International Workshop on Orobancha and Related Striga Research*, Amsterdam. Amsterdam: Royal Tropical Institute, 237–247.
- Joel DM, Losner-Goshen D. 1994b.** The attachment organ of the parasitic angiosperms *Orobancha cumana* and *O. aegyptiaca* and its development. *Canadian Journal of Botany* **72**: 564–574.
- Joel DM, Portnoy VH. 1998.** The angiospermous root parasite *Orobancha* L. (Orobanchaceae) induces expression of a pathogenesis related (PR) gene in susceptible tobacco roots. *Annals of Botany* **81**: 779–781.
- Johnson KL, Jones BJ, Bacic A, Schultz CJ. 2003.** The fasciclin-like arabinogalactan proteins of *Arabidopsis*. A multigene family of putative cell adhesion molecules. *Plant Physiology* **133**: 1911–1925.
- Johnson MA, Lord E. 2006.** Extracellular guidance cues and intracellular signaling pathways that direct pollen tube growth. *Plant Cell Monographs* **3**: 223–242.
- Jones L, Seymour GB, Knox JP. 1997.** Localization of pectic galactan in tomato cell walls using a monoclonal antibody specific to (1->4)-[beta]-D-galactan. *Plant Physiology* **113**: 1405–1412.

- Jongedijk E, Tigelaar H, Roekel JSC Van, Bres-vloemans SA, Dekker I, Elzen PJM Van Den, Cornelissen BJC, Melchers LS. 1995.** Synergistic activity of chitinases and β -1,3-glucanases enhances fungal resistance in transgenic tomato plants. *Euphytica* **85**: 173–180.
- Joseleau J. 2004.** A polyclonal antibody directed against syringylpropane epitopes of native lignins? *Comptes Rendus Biologies* **327**: 809–815.
- Joseleau JP, Ruel K. 1997.** Study of lignification by noninvasive techniques in growing maize internodes. *Plant Physiology* **114**: 1123–1133.
- Joshi J, Matthies D. 2000.** Root hemiparasites and plant diversity in experimental grassland communities. *Journal of Ecology* **88**: 634–644.
- Juge N. 2006.** Plant protein inhibitors of cell wall degrading enzymes. *Trends in Plant Science* **11**: 359–367.
- Jung HG, Allen MS. 1995.** Characteristics of plant cell walls affecting intake and digestibility of forages by ruminants. *Journal of Animal Science* **73**: 2774–2790.
- Kakimoto T. 2003.** Perception and signal transduction of cytokinins. *Annual Review of Plant Biology* **54**: 605–627.
- Kamisaka S, Takeda S, Takahashi K, Shibata K. 1990.** Diferulic and ferulic acid in the cell wall of *Avena* coleoptiles Their relationships to mechanical properties of the cell wall. *Physiologia Plantarum* **78**: 1–7.
- Kamula SA, Peterson CA, Mayfield CI. 1994.** Impact of the exodermis on infection of roots by *Fusarium culmorum*. *Plant and Soil* **167**: 121–126.
- Kauss H, Seehaus K, Franke R, Gilbert S, Dietrich R a, Kröger N. 2003.** Silica deposition by a strongly cationic proline-rich protein from systemically resistant cucumber plants. *The Plant Journal* **33**: 87–95.
- Keegstra K, Talmadge KW, Bauer WD, Albersheim P. 1973.** The structure of plant cell walls. *Plant Physiology* **51**: 188–196.
- Keith AM, Cameron DD, Seel WE. 2004.** Spatial interactions between the hemiparasitic angiosperm *Rhinanthus minor* and its host are species-specific. *Functional Ecology* **18**: 435–442.
- Keller T, Damude HG, Werner D, Doerner P, Dixon RA, Lamb C. 1998.** A plant homolog of the neutrophil NADPH oxidase gp91phox subunit gene encodes a plasma membrane protein with Ca^{2+} binding motifs. *The Plant Cell* **10**: 255–266.
- Keller B, Templeton MD, Lamb CJ. 1989.** Specific localization of a plant cell wall glycine-rich protein in protoxylem cells of the vascular system. *Proceedings of the National Academy of Sciences of the United States of America* **86**: 1529–1533.
- Kelly CK, Venable DL, Zimmerer K. 1988.** Host specialisation in *Cuscuta costaricensis*: an assessment of host use relative to host availability. *Oikos* **53**: 315–320.
- Kemp MS, Burden RS. 1986.** Phytoalexins and stress metabolites in the sapwood of trees. *Phytochemistry* **25**: 1261–1269.
- Kent M, Coker P. 1994.** *Vegetation description and analysis: A practical approach*. Chichester: John Wiley.
- Keyes WJ, O'Malley RC, Kim D, Lynn DG. 2000.** Signaling organogenesis in parasitic angiosperms: xenognosin generation, perception, and response. *Journal of Plant Growth Regulation* **19**: 217–231.
- Kieliszewski MJ, Lampport DTA. 1994.** Extensin: repetitive motifs, functional sites, post-translational codes, and phylogeny. *The Plant Journal* **5**: 157–172.
- Kim D, Kocz R, Boone L, Keyes WJ, Lynn DG. 1998.** On becoming a parasite: evaluating the role of wall oxidases in parasitic plant development. *Chemistry and Biology* **5**: 103–117.
- Kim H, Ralph J, Lu F, Ralph S a, Boudet AM, MacKay JJ, Sederoff RR, Ito T, Kawai S, Ohashi H, et al. 2003.** NMR analysis of lignins in CAD-deficient plants. Part 1. Incorporation of hydroxycinnamaldehydes and hydroxybenzaldehydes into lignins. *Organic & Biomolecular Chemistry* **1**: 268–281.

9. Literature cited

- Kjellbom P, Snogerup L, Stöhr C, Reuzeau C, McCabe PF, Pennell RI. 1997.** Oxidative cross-linking of plasma membrane arabinogalactan proteins. *The Plant Journal* **12**: 1189–1196.
- Klaren CH, Janssen G. 1978.** Physiological changes in the hemiparasite *Rhinanthus serotinus* before and after attachment. *Physiologia Plantarum* **42**: 151–155.
- Knox JP. 1992.** Cell adhesion, cell separation and plant morphogenesis. *The Plant Journal* **2**: 137–141.
- Knox JP. 1997.** The use of antibodies to study the architecture and developmental regulation of plant cell walls. *International Review of Cytology* **171**: 79–120.
- Knox JP. 2006.** Up against the wall: arabinogalactan-protein dynamics at cell surfaces. *New Phytologist* **169**: 443–445.
- Knox JP. 2008.** Revealing the structural and functional diversity of plant cell walls. *Current Opinion in Plant Biology* **11**: 308–313.
- Knox JP, Day S, Roberts K. 1989.** A set of cell surface glycoproteins forms an early marker of cell position, but not cell type, in the root apical meristem of *Daucus carota* L. **56**: 47–56.
- Knox JP, Linstead P, King J, Cooper C, Roberts K. 1990.** Pectin esterification is spatially regulated both within cell walls and between developing tissues of root apices. *Planta* **181**: 512–521.
- Knox JP, Linstead PJ, Peart J, Cooper C, Roberts K. 1991.** Developmentally regulated epitopes of cell surface arabinogalactan proteins and their relation to root tissue pattern formation. *The Plant Journal* **1**: 317–326.
- Kohorn BD. 2001.** WAKs; cell wall associated kinases. *Current Opinion in Cell Biology* **13**: 529–533.
- Kohorn BD, Kohorn SL. 2012.** The cell wall-associated kinases, WAKs, regulate cell expansion and the stress response (F Tax and B Kemmerling, Eds.). *Signalling and Communication in Plants* **13**: 109–124.
- Konieczny R, Swierczyńska J, Czaplicki AZ, Bohdanowicz J. 2007.** Distribution of pectin and arabinogalactan protein epitopes during organogenesis from androgenic callus of wheat. *Plant Cell Reports* **26**: 355–363.
- Koskela T, Puustinen S, Salonen V, Mutikainen P. 2002.** Resistance and tolerance in a host plant-holoparasitic plant interaction: genetic variation and costs. *Evolution* **56**: 899–908.
- Kosuta S, Chabaud M, Loughon G, Gough C, De J, Barker DG, Bécard G. 2003.** A diffusible factor from arbuscular mycorrhizal fungi induces symbiosis-specific MtENOD11 expression in roots of *Medicago truncatula*. *Plant Physiology* **131**: 952–962.
- Koutecký P, Tuleu G, Baďurová T, Košnar J, Štech M, Těšitel J. 2012.** Distribution of cytotypes and seasonal variation in the *Odontites vernus* group in central Europe. *Preslia* **84**: 887–904.
- Krause K. 2011.** Piecing together the puzzle of parasitic plant plastome evolution. *Planta* **234**: 647–656.
- Kreuger M, Van Holst GJ. 1996.** Arabinogalactan proteins and plant differentiation. *Plant Molecular Biology* **30**: 1077–1086.
- Kuijt J. 1969.** The biology of parasitic flowering plants. Berkeley: University of California Press.
- Kuijt J. 1977.** Haustoria of phanerogamic parasites. *Annual Review of Phytopathology* **17**: 91–118.
- Kuiper E, Groot A, Noordover ECM, Pieterse AH, Verkleij JAC. 1998.** Tropical grasses vary in their resistance to *Striga aspera*, *Striga hermonthica*, and their hybrids. *Canadian Journal of Botany* **76**: 2131–2144.
- Kunst L, Samuels AL. 2003.** Biosynthesis and secretion of plant cuticular wax. *Progress in Lipid Research* **42**: 51–80.
- Kuo J, Pate JS, Davidson NJ. 1989.** Ultrastructure of the haustorial interface and apoplastic continuum between host and the root hemiparasite *Olax phyllanthi* (Labill.) R . Br . (Olacaceae). *Protoplasma* **150**: 27–39.
- Kusumoto D, Goldwasser Y, Xie X, Yoneyama K, Takeuchi Y, Yoneyama K. 2007.** Resistance of red clover (*Trifolium pratense*) to the root parasitic plant *Orobancha minor* is activated by salicylate but not by jasmonate. *Annals of Botany* **100**: 537–544.

- Labrousse P. 2001.** Several mechanisms are involved in resistance of *Helianthus* to *Orobanche cumana* Wallr. *Annals of Botany* **88**: 859–868.
- Lafferty KD. 2008.** Parasites. In: Jorgensen SE, Fath B, eds. Reference Module in Earth Systems and Environmental Sciences. Encyclopedia of Ecology. Amsterdam: Elsevier, 2640–2644.
- Lamport D, Kieliszewski M. 2005.** Stress upregulates periplasmic arabinogalactan-proteins. *Plant Biosystems — An International Journal Dealing with all Aspects of Plant Biology* **139**: 60–64.
- Lamport DTA, Kieliszewski MJ, Chen Y, Cannon MC. 2011.** Role of the extensin superfamily in primary cell wall architecture. *Plant Physiology* **156**: 11–9.
- Lamport DTA, Kieliszewski MJ, Showalter AM. 2006.** Salt stress upregulates periplasmic arabinogalactan proteins: using salt stress to analyse AGP function. *New Phytologist* **169**: 479–492.
- Langan KJ, Nothnagel EA. 1997.** Cell surface arabinogalactan-proteins and their relation to cell proliferation and viability. *Protoplasma* **196**: 87–98.
- Laschimke R. 1989.** Investigation of the wetting behaviour of natural lignin — a contribution to the cohesion of water transport in plants. *Thermochimica Acta* **151**: 35–56.
- Lay FT, Anderson MA. 2005.** Defensins — components of the innate immune system in plants. *Current Protein & Peptide Science* **6**: 85–101.
- Leake JR. 2004.** Myco-heterotroph/epiparasitic plant interactions with ectomycorrhizal and arbuscular mycorrhizal fungi. *Current Ppinion in Plant Biology* **7**: 422–428.
- Leake JR. 2005.** Plants parasitic on fungi: unearthing the fungi in myco-heterotrophs and debunking the “saprophytic” plant myth. *Mycologist* **19**: 113–122.
- Lee KB. 2008.** Anatomy and ultrastructure of epidermal cells in the haustorium of a parasitic flowering plant, *Cuscuta japonica*, during attachment to the host. *Journal of Plant Biology* **51**: 366–372.
- Lee KJD, Marcus SE, Knox JP. 2011.** Cell wall biology: perspectives from cell wall imaging. *Molecular Plant* **4**: 212–219.
- Lejeune A, Constant S, Delavault P, Simier P, Thalouarn P, Thoiron S. 2006.** Involvement of a putative Lycopersicon esculentum wall-associated kinase in the early steps of tomato-*Orobanche ramosa* interaction. *Physiological and Molecular Plant Pathology* **69**: 3–12.
- Lemaitre AB, Troncoso AJ, Niemeyer HM. 2012.** Host preference of a temperate mistletoe: Disproportional infection on three co-occurring host species influenced by differential success. *Austral Ecology* **37**: 339–345.
- Leroux O. 2012.** Collenchyma: a versatile mechanical tissue with dynamic cell walls. *Annals of Botany* **110**: 1083–1098.
- Letousey P, De Zélicourt A, Vieira Dos Santos C, Thoiron S, Monteau F, Simier P, Thalouarn P, Delavault P. 2007a.** Molecular analysis of resistance mechanisms to *Orobanche cumana* in sunflower. *Plant Pathology* **56**: 536–546.
- Lewis NG, Yamamoto E. 1990.** Lignin: occurrence, biogenesis and biodegradation. *Annual Review of Plant Physiology and Plant Molecular Biology* **41**: 455–496.
- Li Y, Faleri C, Geitmann A, Zhang H, Cresti M. 1995.** Immunogold localization of arabinogalactan proteins, unesterified and esterified pectins in pollen grains and pollen tubes of *Nicotiana tabacum* L. *Protoplasma* **189**: 26–36.
- Li J, Lis KE, Timko MP. 2009a.** Molecular genetics of race-specific resistance of cowpea to *Striga gesnerioides* (Willd.). *Pest Management Science* **65**: 520–527.
- Li D-M, Staehelin C, Wang W-T, Peng S-L. 2010.** Molecular cloning and characterization of a chitinase-homologous gene from *Mikania micrantha* infected by *Cuscuta campestris*. *Plant Molecular Biology Reporter* **28**: 90–101.

9. Literature cited

- Li D-M, Staehelin C, Zhang Y-S, Peng S-L. 2009b.** Identification of genes differentially expressed in *Mikania micrantha* during *Cuscuta campestris* infection by suppression subtractive hybridization. *Journal of Plant Physiology* **166**: 1423–1435.
- Li J, Timko MP. 2009.** Gene-for-gene resistance in *Striga*-cowpea associations. *Science* **325**: 1094.
- Ligrone R, Carafa A, Duckett JG, Renzaglia KS, Ruel K. 2007.** Immunocytochemical detection of lignin-related epitopes in cell walls in bryophytes and the charalean alga *Nitella*. *Plant Systematics and Evolution* **270**: 257–272.
- Lind JL, Bacic A, Clarke AE, Anderson MA. 1994.** A style-specific hydroxyproline-rich glycoprotein with properties of both extensins and arabinogalactan proteins. *The Plant Cell Wall. Methods and Protocols* **6**: 491–502.
- Lionetti V, Cervone F, Bellincampi D. 2012.** Methyl esterification of pectin plays a role during plant-pathogen interactions and affects plant resistance to diseases. *Journal of Plant Physiology* **169**: 1623–1630.
- Liu C, Mehdy MC. 2007.** A nonclassical arabinogalactan protein gene highly expressed in vascular tissues, AGP31, is transcriptionally repressed by methyl jasmonic acid in *Arabidopsis*. *Plant Physiology* **145**: 863–874.
- Löffler C, Czygan F, Proksch P. 1999.** Role of indole-3-acetic acid in the interaction of the phanerogamic parasite *Cuscuta* and host plants. *Plant Biology* **1**: 613–617.
- Long HC. 1924.** Plants poisonous to livestock. Cambridge University Press.
- Van Loon LC, Rep M, Pieterse CMJ. 2006.** Significance of inducible defense-related proteins in infected plants. *Annual Review of Phytopathology* **44**: 135–162.
- Loopstra C a, Sederoff RR. 1995.** Xylem-specific gene expression in loblolly pine. *Plant Molecular Biology* **27**: 277–291.
- López-Curto L, Márquez-Guzmán J, Díaz-Pontones DM. 2006.** Invasion of *Coffea arabica* (Linn.) by *Cuscuta jalapensis* (Schlecht): *in situ* activity of peroxidase. *Environmental and Experimental Botany* **56**: 127–135.
- Losner-Goshen D. 1998.** Pectolytic activity by the haustorium of the parasitic plant *Orobanche* L. (Orobanchaceae) in host roots. *Annals of Botany* **81**: 319–326.
- Lozano-Baena MD, Prats E, Moreno MT, Rubiales D, Pérez-de-Luque A. 2007.** *Medicago truncatula* as a model for nonhost resistance in legume-parasitic plant interactions. *Plant Physiology* **145**: 437–449.
- Lu H, Chen M, Showalter AM. 2001.** Developmental expression and perturbation of arabinogalactan-proteins during seed germination and seedling growth in tomato. *Physiologia Plantarum* **112**: 442–450.
- Lulai E. 1998.** Differential deposition of suberin phenolic and aliphatic domains and their roles in resistance to infection during potato tuber (*Solanum tuberosum* L.) wound-healing. *Physiological and Molecular Plant Pathology* **53**: 209–222.
- Maiti RK, Ramaiah K V, Bisen SS, Chidley VL. 1984.** A comparative study of the haustorial development of *Striga asiatica* (L.) Kuntze on *Sorghum cultivars*. *Annals of Botany* **54**: 447–457.
- Majewska-Sawka A, Nothnagel EA. 2000.** The multiple roles of arabinogalactan proteins in plant development. *Plant Physiology* **122**: 3–10.
- Mallaburn PS, Stewart GR. 1987.** Haustorial function in *Striga*: comparative anatomy of *S. asiatica* (L.) Kuntz and *S. hermonthica* (Del.) Benth. (Scrophulariaceae). In: HC W, Forstreuter, eds. Proceedings of the 4th International Symposium on Parasitic Flowering Plants, Marburg 1987.523–536.
- Mangeon A, Junqueira RM, Sachetto-Martins G. 2010.** Functional diversity of the plant glycine-rich proteins superfamily. *Plant Signaling & Behavior* **5**: 99–104.
- Marcus SE, Blake AW, Benians T a S, Lee KJD, Poyser C, Donaldson L, Leroux O, Rogowski A, Petersen HL, Boraston A, et al. 2010.** Restricted access of proteins to mannan polysaccharides in intact plant cell walls. *The Plant Journal* **64**: 191–203.
- Marcus A, Greedberg J, Averyhart-Fullard V. 1991.** Repetitive proline-rich proteins in the extracellular matrix of the plant cell. *Physiologia Plantarum* **81**: 273–279.

- Marcus SE, Verhertbruggen Y, Hervé C, Ordaz-Ortiz JJ, Farkas V, Pedersen HL, Willats WGT, Knox JP. 2008.** Pectic homogalacturonan masks abundant sets of xyloglucan epitopes in plant cell walls. *BMC Plant Biology* **8**: 60–72.
- Martin WL. 1991.** Survey of hay meadows in the area of West Corrib, Co. Galway. *Irish Naturalists Journal* **23**: 365–371.
- Martin JR, Gabbett M, Perrin PM, Delaney A. 2007.** *Semi-natural grasslands survey of counties Roscommon and Offaly*. Dublin: Unpublished report for National Parks & Wildlife Service.
- Martin JR, Perrin PM, Delaney AM, O'Neill FH, McNutt KE. 2008.** *Irish semi-natural grasslands survey. annual report No. 1: Counties Cork and Waterford*. Dublin: Unpublished report for National Parks & Wildlife Service.
- Martinez Del Rio C, Hourdequin M, Silva A, Medel R. 1995.** Short note The influence of cactus size and previous infection on bird deposition of mistletoe seeds. : 571–576.
- Marvier MA. 1998.** Parasite impacts on host communities: Plant parasitism in a California coastal prairie. *Ecology* **79**: 2616–2623.
- Marvier MA, Smith DL. 1997.** Conservation implications of host use for rare parasitic plants. *Conservation Biology* **11**: 839–848.
- Mashiguchi K, Asami T, Suzuki Y. 2009.** Genome-wide identification, structure and expression studies, and mutant collection of 22 early nodulin-like protein genes in *Arabidopsis*. *Bioscience, Biotechnology, and Biochemistry* **73**: 2452–2459.
- Mashiguchi K, Urakami E, Hasegawa M, Sanmiya K, Matsumoto I, Yamaguchi I, Asami T, Suzuki Y. 2008.** Defense-related signaling by interaction of arabinogalactan proteins and beta-glucosyl Yariv reagent inhibits gibberellin signaling in barley aleurone cells. *Plant & Cell Physiology* **49**: 178–190.
- Mashiguchi K, Yamaguchi I, Suzuki Y. 2004.** Isolation and identification of glycosylphosphatidylinositol-anchored arabinogalactan proteins and novel beta-glucosyl Yariv-reactive proteins from seeds of rice (*Oryza sativa*). *Plant & Cell Physiology* **45**: 1817–1829.
- Matsuyama T, Satoh H, Yamada Y, Hashimoto T. 1999.** A maize glycine-rich protein is synthesized in the lateral root cap and accumulates in the mucilage. *Plant Physiology* **120**: 665–674.
- Matusova R, Rani K, Verstappen FWA, Franssen MCR, Beale MH, Bouwmeester HJ. 2005.** The strigolactone germination *Striga* and *Orobanch* spp. are derived from the carotenoid pathway. *Plant Physiology* **139**: 920–934.
- Mauricio R, Rausher MD, Burdick DS. 1997.** Variation in the defense strategies of plants: are resistance and tolerance mutually exclusive? *Ecology* **78**: 1301–1311.
- Mauseth JD, Montenegro G, Walckowiak AM. 1985.** Host infection and flower formation by the parasite *Tristerix aphyllus* (Loranthaceae). *Canadian Journal of Botany* **63**: 567–581.
- Mayer AM. 2006.** Pathogenesis by fungi and by parasitic plants: Similarities and differences. *Phytoparasitica* **34**: 3–16.
- Mazeau K, Heux L. 2003.** Molecular dynamics simulations of bulk native crystalline and amorphous structures of cellulose. *The Journal of Physical Chemistry B* **107**: 2394–2403.
- McCabe PF, Valentine TA, Forsberg LS, Pennell RI. 1997.** Soluble signals from cells identified at the cell wall establish a developmental pathway in carrot. *The Plant Cell* **9**: 2225–2241.
- McCann MC, Knox JP. 2011.** Plant cell wall biology: polysaccharides in architectural and developmental contexts. *Annual Plant Reviews* **41**: 343–366.
- McCann MC, Roberts K. 1991.** Architecture of the primary cell wall. In: Lloyd C, ed. *The Cytoskeletal Basis of Plant Growth and Form*. Academic Press, 109–129.
- McCartney L, Marcus SE, Knox JP. 2005.** Monoclonal antibodies to plant cell wall xylans and arabinoxylans. *The Journal of Histochemistry and Cytochemistry* **53**: 543–546.

9. Literature cited

- McCune B, Grace JB. 2002.** Analysis of ecological communities. Oregon: MJM Software Design.
- McCune B, Mefford MJ. 2006.** PC-ORD. Multivariate analysis of ecological data In Version 5.1.MJM Software.
- McDonagh J. 1992.** The geomorphology of the Moycullen-Oughterard lowlands. PHD Thesis. Galway: University College
- McGough HN. 1984.** *A report on the grasslands and closely related vegetation types of the Burren Region of western Ireland.* Unpublished report to The National Parks and Wildlife Service, Dublin.
- Medel R. 2001.** Assessment of correlational selection on tolerance and resistance traits in a host plant—parasitic plant interaction. *Evolutionary Ecology* **15**: 37–52.
- Meikle PJ, Bonig I, Hoogenraad NJ, Clarke AE, Stone BA. 1991.** The location of (1→3)- β -glucans in the walls of pollen tubes of *Nicotiana glauca* using a (1→3)- β -glucan-specific monoclonal antibody. *Planta* **185**: 1–8.
- Mescher MC, Smith J, De Moraes CM. 2009.** Host location and selection by holoparasitic plants. In: Baluška F, ed. *Plant-Environment Interactions From Sensory Plant Biology to Active Plant Behavior.* Berlin, Heidelberg: Springer-Verlag, 101–118.
- De Mesy Jensen K, Di Sant’Agnese P. 1992.** Large block embedding and “pop-off” technique for immunoelectron microscopy. *Ultrastructural Pathology* **16**: 51–59.
- Micali CO, Neumann U, Grunewald D, Panstruga R, O’Connell R. 2011.** Biogenesis of a specialized plant-fungal interface during host cell internalization of *Golovinomyces orontii* haustoria. *Cellular Microbiology* **13**: 210–226.
- Misas-Villamil JC, Van der Hoorn R a L. 2008.** Enzyme-inhibitor interactions at the plant-pathogen interface. *Current Opinion in Plant Biology* **11**: 380–388.
- Mohamed KI, Musselman LJ, Riches CR. 2001.** The genus *Striga* (Scrophulariaceae) in Africa. *Annals of the Missouri Botanical Garden* **88**: 60–103.
- Mohnen D. 2008.** Pectin structure and biosynthesis. *Current Opinion in Plant Biology* **11**: 266–277.
- Mollet J-C, Kim S, Jauh G-Y, Lord EM. 2002.** Arabinogalactan proteins, pollen tube growth, and the reversible effects of Yariv phenylglycoside. *Protoplasma* **219**: 89–98.
- Moore JP, Nguema-Ona EE, Vitré-Gibouin M, Sørensen I, Willats WGT, Driouich A, Farrant JM. 2013.** Arabinose-rich polymers as an evolutionary strategy to plasticize resurrection plant cell walls against desiccation. *Planta* **237**: 739–754.
- Morand S, Gonzalez E. 1997.** Is parasitism a missing ingredient in model ecosystems? *Ecological Modelling* **95**: 61–74.
- Morris ER, Walker JC. 2003.** Receptor-like protein kinases: the keys to response. *Current Opinion in Plant Biology* **6**: 339–342.
- Motose H, Fukuda H, Sugiyama M. 2001a.** Involvement of local intercellular communication in the differentiation of *Zinnia* mesophyll cells into tracheary elements. *Planta* **213**: 121–131.
- Motose H, Sugiyama M, Fukuda H. 2001b.** An arabinogalactan protein(s) is a key component of a fraction that mediates local intercellular communication involved in tracheary element differentiation of zinnia mesophyll cells. *Plant & Cell Physiology* **42**: 129–137.
- Motose H, Sugiyama M, Fukuda H. 2004.** A proteoglycan mediates inductive interaction during plant vascular development. *Nature* **429**: 873–878.
- Müller C. 2008.** Resistance at the Plant Cuticle. In: Schaller A, ed. *Induced Plant Resistance to Herbivory.* Berlin: Springer, 107–129.
- Müsel G, Schindler T, Bergfeld R, Ruel K, Jacquet G, Lapierre C, Speth V, Schopfer P. 1997.** Structure and distribution of lignin in primary and secondary cell walls of maize coleoptiles analyzed by chemical and immunological probes. *Planta* **201**: 146–159.
- Musselman LJ, Dickison WC. 1975.** The structure and development of the haustorium in parasitic Scrophulariaceae. *Botanical Journal of the Linnean Society* **70**: 183–212.

- Musselman LJ, Parker C. 1982.** Preliminary host ranges of some strains of economically important broomrapes. *Economic Botany* **36**: 270–273.
- Mutikainen P, Salonen V, Puustinen S, Koskela T. 2000.** Local adaptation, resistance, and virulence in a hemiparasitic plant-host plant interaction. *Evolution* **54**: 433–440.
- Nagar R, Singh M, Sanwal GG. 1984.** Cell wall degrading enzymes in *Cuscuta reflexa* and its hosts. *Journal of Experimental Botany* **35**: 1104–1112.
- Nakagawa K, Yoshinaga A, Takabe K. 2012.** Anatomy and lignin distribution in reaction phloem fibres of several Japanese hardwoods. *Annals of Botany* **110**: 897–904.
- Nawrath C. 2006.** Unraveling the complex network of cuticular structure and function. *Current Opinion in Plant Biology* **9**: 281–287.
- Neumann U, Salle G, Weber H. 1998.** Development and structure of the haustorium of the parasite *Rhamphicarpa fistulosa* (Scrophulariaceae). *Botanica Acta* **111**: 354–365.
- Neumann U, Vian B, Weber HC, Sallé G. 1999.** Interface between haustoria of parasitic members of the Scrophulariaceae and their hosts: A histochemical and immunocytochemical approach. *Protoplasma* **207**: 84–97.
- Nguema-Ona E, Coimbra S, Vicré-Gibouin M, Mollet J-C, Driouich A. 2012.** Arabinogalactan proteins in root and pollen-tube cells: distribution and functional aspects. *Annals of Botany* **110**: 383–404.
- Nicholson RL, Hammerschmidt R. 1992.** Phenolic compounds and their role in disease resistance. *Annual Review of Phytopathology* **30**: 369–389.
- No E-G, Loopstra CA. 2000.** Hormonal and developmental regulation of two arabinogalactan-proteins in xylem of loblolly pine (*Pinus taeda*). *Physiologia Plantarum* **110**: 524–529.
- Noda J, Brito N, González C. 2010.** The *Botrytis cinerea* xylanase Xyn11A contributes to virulence with its necrotizing activity, not with its catalytic activity. *BMC Plant Biology* **10**: 38.
- Novo-Uzal E, Pomar F, Gómez Ros L V, Espiñeira JM, Barcelo AR. 2012.** Evolutionary history of lignins. *Advances in Botanical Research* **61**: 311–350.
- NPWS. 2011.** Conservation objectives for Moneen Mountain SAC [000054]. Generic Version 3.0. Available at: <http://www.npws.ie/media/npwsie/content/images/protectedsites/conservationobjectives/CO000054.pdf> [accessed 16.01.13]
- Nwoke FIO. 1982.** The initiation of the secondary haustorium in *Alectra vogelii* Benth. *Ann. Bot.* **49**: 669–676.
- Nwoke FIO, Okonkwo SNC. 1978.** Structure and development of the primary haustorium in *Alectra vogelii* Benth. (Scrophulariaceae). *Annals of Botany* **42**: 447–454.
- O'Brien TP, Feder N, McCully ME. 1964.** Polychromatic staining of plant cell walls by toluidine blue O. *Protoplasma* **59**: 368–373.
- O'Brien VJ, Leach SS. 1983.** Investigations into the mode of resistance of potato tubers to *Fusarium roseum* "Sambucinum". *American Potato Journal* **60**: 227–233.
- O'Connell RJ, Brown IR, Mansfield JW, Bailey JA, Mazau D, Rumeau D, Esquerré-Tugayé M-T. 1990.** Immunocytochemical localization of hydroxyproline-rich glycoproteins accumulating in melon and bean at sites of resistance to bacteria and fungi. *Molecular Plant-Microbe Interactions* **3**: 33–40.
- O'Malley RC, Lynn DG. 2000.** Expansin message regulation in parasitic angiosperms: marking time in development. *The Plant Cell* **12**: 1455–1465.
- O'Mara F. 2008.** *Country pasture/forage resource profile, Ireland*. Available at <http://www.fao.org/ag/AGP/AGPC/doc/Counprof/Ireland/Ireland.htm>. [accessed 27.02.13]
- O'Neill MA, Ishii T, Albersheim P, Darvill AG. 2004.** Rhamnogalacturonan II: structure and function of a borate cross-linked cell wall pectic polysaccharide. *Annual Review of Plant Biology* **55**: 109–139.

9. Literature cited

- O'Neill FH, Martin JR, Devaney FM, McNutt KE, Perrin PM, Delaney A. 2010. *Irish semi-natural grasslands survey. Annual report No. 3: Counties Donegal, Dublin, Kildare and Sligo*. Dublin: Unpublished report for National Parks & Wildlife Service.
- O'Neill FH, Martin JR, Perrin PM, Delaney A, McNutt KE, Devaney FM. 2009. *Irish semi-natural Grasslands Survey. Annual report No. 2: Counties Cavan, Leitrim, Longford and Monaghan*. Dublin: Unpublished report for National Parks & Wildlife Service.
- O'Sullivan AM. 1982. The lowland grasslands of Ireland. In: White J, ed. *Studies on Irish Vegetation*. Dublin: Royal Irish Academy, 131–142.
- Oda Y, Fukuda H. 2012. Secondary cell wall patterning during xylem differentiation. *Current Opinion in Plant Biology* 15: 38–44.
- Offler CE, McCurdy DW, Patrick JW, Talbot MJ. 2003. Transfer cells: cells specialized for a special purpose. *Annual Review of Plant Biology* 54: 431–454.
- Okonkwo SNC, Nwoke FIO. 1978. Initiation, development and structure of the primary haustorium in *Striga gesnerioides* (Scrophulariaceae). *Annals of Botany* 42: 455–463.
- Olivier A, Benhamou N, Leroux GD. 1991. Cell surface interactions between sorghum roots and the parasitic weed *Striga hermonthica*: cytochemical aspects of cellulose distribution in resistant and susceptible host tissues. *Canadian Journal of Botany* 69: 1679–1690.
- Osakabe Y, Maruyama K, Seki M, Satou M, Shinozaki K, Yamaguchi-Shinozaki K. 2005. Leucine-rich repeat receptor-like kinase1 is a key membrane-bound regulator of abscisic acid early signaling in *Arabidopsis*. *The Plant Cell* 17: 1105–1119.
- Osafune T, Schwartzbach SD. 2010. Serial section immunoelectron microscopy of algal cells. *Methods in Molecular Biology* 657: 259–274.
- Otypková Z, Chytrý M. 2006. Effects of plot size on the ordination of vegetation samples. *Journal of Vegetation Science* 17: 465–472.
- Palin R, Geitmann A. 2012. The role of pectin in plant morphogenesis. *BioSystems* 109: 397–402.
- Park YB, Cosgrove DJ. 2012. Changes in cell wall biomechanical properties in the xyloglucan-deficient xxt1/xtt2 mutant of *Arabidopsis*. *Plant Physiology* 158: 465–475.
- Parker C. 2009. Observations on the current status of *Orobanch*e and *Striga* problems worldwide. *Pest Management Science* 65: 453–459.
- Parker C. 2012. Parasitic weeds: a world challenge. *Weed Science* 60: 269–276.
- Parker AJ, Haskins EF, Deyrup-Olsen I. 1982. Toluidine blue: a simple, effective stain for plant tissues. *The American Biology Teacher* 44: 487–489.
- Parnell J, Curtis T. 2012. *Webb's an Irish Flora*. Cork University Press.
- Parr AJ, Ng A, Waldron KW. 1997. Ester-linked phenolic components of carrot cell walls. *Journal of Agricultural and Food Chemistry* 45: 2468–2471.
- Parr S, O'Donovan G, Ward S, Finn J. 2009. Vegetation analysis of upland burren grasslands of conservation interest. *Biology & Environment: Proceedings of the Royal Irish Academy* 109: 11–33.
- Passardi F, Cosio C, Penel C, Dunand C. 2005. Peroxidases have more functions than a Swiss army knife. *Plant Cell Reports* 24: 255–265.
- Passardi F, Penel C, Dunand C. 2004. Performing the paradoxical: how plant peroxidases modify the cell wall. *Trends in Plant Science* 9: 534–540.
- Pate JS, Gunning BES. 1972. Transfer cells. *Annual Review of Plant Physiology* 23: 173–196.
- Pate JS, Ireland N. 1969. "Transfer cells". Plant cells with wall ingrowths, specialized in relation to short distance transport of solutes — their occurrence, structure, and development. *Protoplasma* 133: 107–133.
- Pate JS, Kuo J, Davidson NJ. 1990. Morphology and anatomy of the haustorium of the root hemiparasite *Oxalophyllanthi* (Oxalaceae), with special reference to the haustorial interface. *Annals of Botany* 65: 425–436.

- Pattathil S, Avci U, Baldwin D, Swennes AG, McGill JA, Popper Z, Bootten T, Albert A, Davis RH, Chennareddy C, et al. 2010.** A comprehensive toolkit of plant cell wall glycan-directed monoclonal antibodies. *Plant Physiology* **153**: 514–525.
- Pauly M, Scheller HV. 2000.** O-Acetylation of plant cell wall polysaccharides: identification and partial characterization of a rhamnogalacturonan O-acetyl-transferase from potato suspension-cultured cells. *Planta* **210**: 659–667.
- Pavlova ZN, Loskutova NA, Vnuchkova VA, Muromtsev GS, Usov AI, Shibaev VN. 1996.** Xyloglucan oligosaccharins as elicitors of plant defense responses. *Russian Journal of Plant Physiology* **43**: 242–246.
- Peaucelle A, Louvet R, Johansen JN, Höfte H, Laufs P, Pelloux J, Mouille G. 2008.** *Arabidopsis* phyllotaxis is controlled by the methyl-esterification status of cell-wall pectins. *Current Biology* **18**: 1943–1948.
- Pedersen HL, Fangel JU, McCleary B, Ruzanski C, Rydahl MG, Ralet M-C, Farkas V, Von Schantz L, Marcos SE, Andersen MCF, et al. 2012.** Versatile high-resolution oligosaccharide microarrays for plant glycobiology and cell wall research. *The Journal of Biological Chemistry* **287**: 39429–39438.
- Pelegrini PB, Franco OL. 2005.** Plant gamma-thionins: novel insights on the mechanism of action of a multi-functional class of defense proteins. *The International Journal of Biochemistry & Cell Biology* **37**: 2239–2253.
- Pennell RI, Janniche L, Kjellbom P, Scofield GN, Peart JM, Roberts K. 1991.** Developmental regulation of a plasma membrane arabinogalactan protein epitope in oilseed rape flowers. *The Plant Cell* **3**: 1317–1326.
- Pennell RI, Knox PJ, Scofield GN, Selvendran RR, Roberts K. 1989.** A family of abundant plasma membrane-associated glycoproteins related to the arabinogalactan proteins is unique to flowering plants. *The Journal of Cell Biology* **108**: 1967–1977.
- Pérez-de-Luque A, González-Verdejo CI, Lozano MD, Dita M a, Cubero JI, González-Melendi P, Risueño MC, Rubiales D. 2006a.** Protein cross-linking, peroxidase and beta-1,3-endoglucanase involved in resistance of pea against *Orobanche crenata*. *Journal of Experimental Botany* **57**: 1461–1469.
- Pérez-de-Luque A, Lozano MD, Cubero JI, González-Melendi P, Risueño MC, Rubiales D. 2006b.** Mucilage production during the incompatible interaction between *Orobanche crenata* and *Vicia sativa*. *Journal of Experimental Botany* **57**: 931–942.
- Pérez-de-Luque A, Lozano MD, Moreno MT, Testillano PS, Rubiales D. 2007.** Resistance to broomrape (*Orobanche crenata*) in faba bean (*Vicia faba*): cell wall changes associated with prehaustorial defensive mechanisms. *Annals of Applied Biology* **151**: 89–98.
- Pérez-de-Luque A, Moreno MT, Rubiales D. 2008.** Host plant resistance against broomrapes (*Orobanche* spp.): defence reactions and mechanisms of resistance. *Annals of Applied Biology* **152**: 131–141.
- Pérez-de-Luque A, Rubiales D, Cubero JI, Press MC, Scholes J, Yoneyama K, Takeuchi Y, Plakhine D, Joel DM. 2005.** Interaction between *Orobanche crenata* and its host legumes: unsuccessful haustorial penetration and necrosis of the developing parasite. *Annals of Botany* **95**: 935–942.
- Perrin PM, Martin JR, Barron SJ, Roche JR. 2006.** A cluster analysis approach to classifying Irish native woodlands. *Biology and Environment: Proceedings of the Royal Irish Academy* **106B**: 261–275.
- Petersen M, Simmonds MSJ. 2003.** Rosmarinic acid. *Phytochemistry* **62**: 121–5.
- Peterson CA, Cholewa E. 1998.** Structural modifications of the apoplast and their potential impact on ion uptake. *Zeitschrift für Pflanzenernährung und Bodenkunde* **161**: 521–531.
- Pickard BG, Fujiki M. 2005.** Ca²⁺ pulsation in BY-2 cells and evidence for control of mechanosensory Ca²⁺-selective channels by the plasmalemmal reticulum. *Functional Plant Biology* **32**: 863–879.
- Piehl M. 1963.** Mode of attachment, haustorium structure, and hosts of *Pedicularis canadensis*. *American Journal of Botany* **50**: 978 – 985.
- Pilcher J, Hall V. 2001.** *Flora Hibernica*. Cork: Collins Press.

9. Literature cited

- Plantureaux S, Peeters A, McCracken D. 2005** Biodiversity in intensive grasslands: effect of management, improvement and challenges. *Agronomy Research* **3**: 153–164
- Pollard M, Beisson F, Li Y, Ohlrogge JB. 2008.** Building lipid barriers: biosynthesis of cutin and suberin. *Trends in Plant Science* **13**: 236–246.
- Polniaszek TI, Parker C. 1987.** Variation in host specificity of *Alectra vogelii* Benth. (Scrophulariaceae). In: HC W, Forstreuter, eds. Proceedings of the 4th International Symposium on Parasitic Flowering Plants, Marburg 1987.613–619.
- Pomar F, Merino F, Barceló AR. 2002.** O-4-Linked coniferyl and sinapyl aldehydes in lignifying cell walls are the main targets of the Wiesner (phloroglucinol-HCl) reaction. *Protoplasma* **220**: 17–28.
- Popper ZA. 2008.** Evolution and diversity of green plant cell walls. *Current Opinion in Plant Biology* **11**: 286–292.
- Popper ZA, Fry SC. 2005.** Widespread occurrence of a covalent linkage between xyloglucan and acidic polysaccharides in suspension-cultured angiosperm cells. *Annals of Botany* **96**: 91–99.
- Popper ZA, Michel G, Hervé C, Domozych DS, Willats WGT, Tuohy MG, Kloareg B, Stengel DB. 2011.** Evolution and diversity of plant cell walls: from algae to flowering plants. *Annual Review of Plant Biology* **62**: 567–590.
- Postel S, Küfner I, Beuter C, Mazzotta S, Schwedt A, Borlotti A, Halter T, Kemmerling B, Nürnberger T. 2010.** The multifunctional leucine-rich repeat receptor kinase BAK1 is implicated in *Arabidopsis* development and immunity. *European Journal of Cell Biology* **89**: 169–174.
- Poulin R, Morand S. 2000.** The diversity of parasites. *The Quarterly Review of Biology* **75**: 277–293.
- Press M, Graves J (Eds.). 1995.** 1995. *Parasitic plants*. London: Chapman and Hall.
- Press MC, Phoenix GK. 2005.** Impact of parasitic plants on natural communities. *New Phytologist* **166**: 737–751.
- Preston CD, Pearman DA, Dines TD. 2002.** *Atlas of the British and Irish flora*. Oxford: Oxford University Press.
- Price PW. 1980.** *Evolutionary biology of parasites*. Princeton: Princeton University Press.
- Prinsloo LC, Du Plooy W, Van der Merwe C. 2004.** Raman spectroscopic study of the epicuticular wax layer of mature mango (*Mangifera indica*) fruit. *Journal of Raman Spectroscopy* **35**: 561–567.
- Psotova J, Svobodova A, Kolarova H, Walterova D. 2006.** Photoprotective properties of *Prunella vulgaris* and rosmarinic acid on human keratinocytes. *Journal of Photochemistry and Photobiology. B, Biology* **84**: 167–174.
- Puhlmann J, Bucheli E, Swain MJ, Dunning N, Albersheim P, Darvill AG, Hahn MG. 1994.** Generation of monoclonal antibodies against plant cell-wall polysaccharides. *Plant Physiology* **104**: 699–710.
- Pywell RF, Bullock JM, Walker KJ, Coulson SJ, Gregory SJ, Stevenson MJ. 2004.** Facilitating grassland diversification using the hemiparasitic plant *Rhinanthus minor*. *Journal of Applied Ecology* **41**: 880–887.
- Qi W, Fong C, Lampert DTA. 1991.** Gum arabic glycoprotein is a twisted hairy rope. A new model based on O-galactosylhydroxyproline as the polysaccharide attachment site. *Plant Physiology* **96**: 848–855.
- Ralet M-C, Tranquet O, Poulain D, Moïse a, Guillon F. 2010.** Monoclonal antibodies to rhamnogalacturonan I backbone. *Planta* **231**: 1373–1383.
- Ralph J. 1986.** An unusual lignin from Kenaf. *Journal of Natural Products* **59**: 341–342.
- Ralph J, Kim H, Lu F, Sally A, Landucci LL, Ito T. 1999.** Incorporation of hydroxycinnamaldehydes into lignins. Proceedings of the 10th International Symposium on Wood and Pulping Chemistry, Yokohama, Japan. 58–63.
- Ralph J, Peng J, Lu F, Hatfield RD, Helm RF. 1999.** Are lignins optically active? *Journal of Agricultural and Food Chemistry* **47**: 2991–2996.
- Ramaiah BK V, Chidley VL, House LR. 1991.** A time-course study of early establishment stages of parasitic angiosperm *Striga asiatica* on susceptible sorghum rootst. *Annals of Applied Biology* **118**: 403–410.

- Ramasubramanian TS, Paliyath G, Rajagopal I, Maheshwari R, Mahadevan S. 1988.** Hormones and *Cuscuta* development: In vitro induction of haustoria by cytokinin and its inhibition by other hormones. *Journal of Plant Growth Regulation* **7**: 133–144.
- Ranathunge K, Thomas RH, Fang X, Peterson CA, Gijzen M, Bernards MA. 2008.** Soybean root suberin and partial resistance to root rot caused by *Phytophthora sojae*. *Phytopathology* **98**: 1179–1189.
- Rank C, Rasmussen LS, Jensen SR, Pierce S, Press MC, Scholes JD. 2004.** Cytotoxic constituents of *Alectra* and *Striga* species. *Weed Research* **44**: 265–270.
- Reddy AS, Komariah M, Reddy SM. 1980.** Cellulase activity in haustoria of *Cassytha filiformis* L. *Current Science* **49**: 670–671.
- Reddy A, Komraiah M, Reddy S. 1981.** Production of pectic enzymes by *Cassytha filiformis* L. *Current Science* **50**: 283–284.
- Reed JD. 1995.** Nutritional toxicology polyphenols in of tannins and related forage legumes. *Journal of Animal Science* **73**: 1516–1528.
- Reguera M, Abreu I, Brewin NJ, Bonilla I, Bolaños L. 2010.** Borate promotes the formation of a complex between legume AGP-extensin and rhamnogalacturonan II and enhances production of *Rhizobium* capsular polysaccharide during infection thread development in *Pisum sativum* symbiotic root nodules. *Plant, cell & environment* **33**: 2112–2120.
- Rehker J, Lachnit M, Kaldenhoff R. 2012.** Molecular convergence of the parasitic plant species *Cuscuta reflexa* and *Phelipanche aegyptiaca*. *Planta* **236**: 557–566.
- Reid JSG. 1985.** Cell wall storage carbohydrates in seeds — biochemistry of the seed “gums” and “hemicelluloses”. *Advances in Botanical Research* **11**: 125–155.
- Reiss GC, Bailey JA. 1998.** *Striga gesnerioides* parasitising cowpea: development of infection structures and mechanisms of penetration. *Annals of Botany* **81**: 431–440.
- Ren Y-Q, Guan K-Y, Li A-R, Hu X-J, Zhang L. 2010.** Host dependence and preference of the root hemiparasite, *Pedicularis cephalantha* Franch. (Orobanchaceae). *Folia Geobotanica* **45**: 443–455.
- Renard CMG., Jarvis M. 1999.** Acetylation and methylation of homogalacturonans 1: optimisation of the reaction and characterisation of the products. *Carbohydrate Polymers* **39**: 201–207.
- Reymond P, Grünberger S, Paul K, Müller M, Farmer EE. 1995.** Oligogalacturonide defense signals in plants: large fragments interact with the plasma membrane *in vitro*. *Proceedings of the National Academy of Sciences of the United States of America* **92**: 4145–4149.
- Reynolds S. C. P 2002** *A Catalogue of Alien Plants in Ireland*. National Botanic Gardens Glasnevin occasional Papers 14: 1–414
- Ringli C, Keller B, Ryser U. 2001.** Glycine-rich proteins as structural components of plant cell walls. *Cellular and Molecular Life Sciences* **58**: 1430–1441.
- Riopel JL, Musselman LJ. 1979.** Experimental initiation of haustoria in *Agalinis purpurea* (Scrophulariaceae). *American Journal of Botany* **66**: 570–575.
- Riopel JL, Timko MP. 1995.** Haustorial initiation and differentiation. In: Press MC, Graves JD, eds. *Parasitic Plants*. London: Chapman and Hall, 39–79.
- Ripper D, Schwarz H, Stierhof Y-D. 2008.** Cryo-section immunolabelling of difficult to preserve specimens: advantages of cryofixation, freeze-substitution and rehydration. *Biology of the Cell* **100**: 109–123.
- Rittinger PA, Biggs AR, Peirson DR. 1987.** Histochemistry of lignin and suberin deposition in boundary layers found after wounding in various plant species and organs. *Canadian Journal of Botany* **65**: 1886–1892.
- Robards AW, Lucas WJ. 1990.** Plasmodesmata. *Annual Review of Plant Physiology* **41**: 369–419.

9. Literature cited

- Robbins CT, Mole S, Hagerman AE, Hanley TA. 1987.** Role of tannins in defending plants against ruminants: reduction in dry matter digestion? *Ecology* **68**: 1606–1615.
- Roberts K. 1994.** The plant extracellular matrix: in a new expansive mood. *Current Opinion in Cell Biology* **6**: 688–694.
- Roberts JA, Gonzalez-Carranza Z. 2007.** *Plant Cell Separation and Adhesion*. Oxford: Blackwell Publishing.
- Rodenburg J, Bastiaans L. 2011.** Host-plant defence against *Striga* spp.: reconsidering the role of tolerance. *Weed Research* **51**: 438–441.
- Rodwell JS. 1992.** *British plant communities. Volume 3. Grasslands and montane communities*. Cambridge: Cambridge University Press.
- Rodwell JS. 2000.** *British plant communities. Vol.5 Maritime communities and vegetation of open habitats*. Cambridge: Cambridge University Press.
- Roland J, Reis D. 1982.** Cell wall texture along the growth gradient of the mung bean hypocotyl: ordered assembly and dissipative processes. *Journal of Cell Science* **56**: 303–318.
- Rost FWD. 1995.** Autofluorescence in plants, fungi and bacteria. In: Rost FWD, Fluorescence Microscopy. Vol. II. Cambridge University Press, 16–39.
- Roussel H, Bruns S, Gianinazzi-Pearson V, Hahlbrock K, Franken P. 1997.** Induction of a membrane intrinsic protein-encoding mRNA in arbuscular mycorrhiza and elicitor-stimulated cell suspension cultures of parsley. *Plant Science* **126**: 203–210.
- Roux M, Schwessinger B, Albrecht C, Chinchilla D, Jones A, Holton N, Malinovsky FG, Tör M, De Vries S, Zipfel C. 2011.** The *Arabidopsis* leucine-rich repeat receptor-like kinases BAK1/SERK3 and BKK1/SERK4 are required for innate immunity to hemibiotrophic and biotrophic pathogens. *The Plant Cell* **23**: 2440–2455.
- Rowntree JK, Cameron DD, Preziosi RF. 2011.** Genetic variation changes the interactions between the parasitic plant-ecosystem engineer *Rhinanthus* and its hosts. *Philosophical transactions of the Royal Society of London. Series B, Biological sciences* **366**: 1380–1388.
- Roy BA, Kirchner JW. 2000.** Evolutionary dynamics of pathogen resistance and tolerance. *Evolution* **54**: 51–63.
- Rubiales D, Fernández-Aparicio M. 2012.** Innovations in parasitic weeds management in legume crops. A review. *Agronomy for Sustainable Development* **32**: 433–449.
- Rubiales D, Pérez-de-luque A, Joel DM, Alcántara C, Sillero JC. 2003.** Characterization of resistance in chickpea to crenate broomrape (*Orobanche crenata*). *Weed Science* **51**: 702–707.
- Ruel K, Faix O, Joseleau JP. 1994.** New immunogold probes for studying the distribution of the different lignin types during plant cell wall biogenesis. *Journal of Trace and Microprobe Techniques* **12**: 247–265.
- Rümer S, Cameron D, Wacker R, Hartung W, Jiang F. 2007.** An anatomical study of the haustoria of *Rhinanthus minor* attached to roots of different hosts. *Flora* **202**: 194–200.
- Runyon JB, Mescher MC, De Moraes CM. 2010.** Plant defenses against parasitic plants show similarities to those induced by herbivores and pathogens. *Plant Signaling & Behavior* **5**: 929–931.
- Ruyter-Spira C, Al-Babili S, Van der Krol S, Bouwmeester H. 2012.** The biology of strigolactones. *Trends in Plant Science* **18**: 72–83.
- Ruzin S. 1999.** *Plant microtechnique and microscopy*. Oxford: Oxford University Press.
- Ryser U, Schorderet M, Zhao GF, Studer D, Ruel K, Hauf G, Keller B. 1997.** Structural cell-wall proteins in protoxylem development: evidence for a repair process mediated by a glycine-rich protein. *The Plant Journal* **12**: 97–111.
- Sachs IB, Nair MG, Kuntz JE. 1970.** Penetration and degradation of cell walls in oaks infected with *Ceratocystis fagacearum*. *Phytopathology* **60**: 1399–1404.
- Salaneka YA, Goffinet MC, Taylor AG, Sciences H, Street WN. 2009.** Structure and histochemistry of the micropylar and chalazal regions of the perisperm — endosperm envelope of cucumber seeds

associated with solute permeability and germination. *Journal of the American Society for Horticultural Science* **134**: 479–487.

Salcedo G, Sánchez-Monge R, Barber D, Díaz-Perales A. 2007. Plant non-specific lipid transfer proteins: an interface between plant defence and human allergy. *Biochimica et Biophysica Acta* **1771**: 781–91.

Salonen V, Puustinen S. 1996. Success of a root hemiparasitic plant is influenced by soil quality and by defoliation of its host. *Ecology* **77**: 1290–1293.

Šamaj J, Šamajová O, Peters M, Baluška F, Lichtscheidl I, Knox JP, Volkmann D. 2000. Immunolocalization of LM2 arabinogalactan protein epitope associated with endomembranes of plant cells. *Protoplasma* **212**: 186–196.

Sanchez F, Padilla JE, Perez H, Lara M. 1991. Control of nodulin genes in root-nodule development and metabolism. *Annual Review of Plant Physiology and Plant Molecular Biology* **42**: 507–528.

Sbrana C, Giovannetti M. 2005. Chemotropism in the arbuscular mycorrhizal fungus *Glomus mosseae*. *Mycorrhiza* **15**: 539–545.

Scheller HV, Ulvskov P. 2010. Hemicelluloses. *Annual Review of Plant Biology* **61**: 263–289.

Schikora A, Schmidt W. 2002. Formation of transfer cells and H(+)-ATPase expression in tomato roots under P and Fe deficiency. *Planta* **215**: 304–311.

Schindler T, Bergfeld R, Schopfer P. 1995. Arabinogalactan proteins in maize coleoptiles: developmental relationship to cell death during xylem differentiation but not to extension growth. *The Plant Journal* **7**: 25–36.

Schmidt M, Schwartzberg AM, Carroll A, Chaibang A, Adams PD, Schuck PJ. 2010. Raman imaging of cell wall polymers in *Arabidopsis thaliana*. *Biochemical and Biophysical Research Communications* **395**: 521–523.

Schneider DS, Ayres JS. 2008. Two ways to survive infection: what resistance and tolerance can teach us about treating infectious diseases. *Nature* **8**: 889–895.

Schofield P, Mbugua DM, Pell AN. 2001. Analysis of condensed tannins: a review. *Animal Feed Science and Technology* **91**: 21–40.

Schopfer P. 1990. Cytochemical identification of arabinogalactan protein in the outer epidermal wall of maize coleoptiles. *Planta* **183**: 139–142.

Schuetz M, Smith R, Ellis B. 2013. Xylem tissue specification, patterning and differentiation mechanisms. *Journal of Experimental Botany* **64**: 11–31.

Schultz C, Gilson P, Oxley D, Youl J, Bacic A. 1998. GPI-anchors on arabinogalactan-proteins: implications for signalling in plants. *Trends in Plant Science* **3**: 426–431.

Schulz S, Hussani MA, Kling JG, Berner DK, Ikie FO. 2003. Evaluation of integrated *Striga hermonthica* control technologies under farmer management. *Experimental Agriculture* **39**: 99–108.

Seel W. 1996. Effects of repeated parasitism by *Rhinanthus minor* on the growth and photosynthesis of a perennial grass, *Poa alpina*. *New Phytologist* **134**: 495–502.

Seel WE, Cooper RE, Press MC. 1993. Growth, gas exchange and water use efficiency of the facultative hemiparasite *Rhinanthus minor* associated with hosts differing in foliar nitrogen concentration. *Physiologia Plantarum* **89**: 64–70.

Seel W, Jeschke W. 1999. Simultaneous collection of xylem sap from *Rhinanthus minor* and the hosts *Hordeum* and *Trifolium*: hydraulic properties, xylem sap composition and effects of attachment. *New Phytologist* **143**: 281–298.

Seel W, Parsons A. 1993. Do inorganic solutes limit growth of the facultative hemiparasite *Rhinanthus minor* L. in the absence of a host? *New Phytologist* **124**: 283–289.

Seel WE, Press MC. 1994. Influence of the host on three sub-Arctic annual facultative root hemiparasites II. Gas exchange characteristics and resource use-efficiency. *New Phytologist* **127**: 37–44.

9. Literature cited

- Seifert GJ, Blaukopf C. 2010.** Irritable walls: the plant extracellular matrix and signaling. *Plant Physiology* **153**: 467–478.
- Seifert GJ, Roberts K. 2007.** The biology of arabinogalactan proteins. *Annual Review of Plant Biology* **58**: 137–461.
- Serghini K, Pérez-de-Luque A, Castejon-Muñoz M, García-Torres L, Jorrín J V. 2001** Sunflower (*Helianthus annuus* L.) response to broomrape (*Orobancha cernua* Loefl.) parasitism: induced synthesis and excretion of 7-hydroxylated simple coumarins. *J. Exp. Bot.* **52**: 2227–2234.
- Serpe MD, Muir AJ, Driouich A. 2002.** Immunolocalization of beta-D-glucans, pectins, and arabinogalactan-proteins during intrusive growth and elongation of nonarticulated laticifers in *Asclepias speciosa* Torr. *Planta* **215**: 357–370.
- Serpe MD, Nothnagel EA. 1999.** Arabinogalactan-proteins in the multiple domains of the plant cell surface. *Advances in Botanical Research* **30**: 207–289.
- Seth BRS. 2003.** and significance Their addition to pulp improves sheet consolidation. **2**: 47–50.
- Shadle G, Chen F, Srinivasa Reddy MS, Jackson L, Nakashima J, Dixon R a. 2007.** Down-regulation of hydroxycinnamoyl CoA: shikimate hydroxycinnamoyl transferase in transgenic alfalfa affects lignification, development and forage quality. *Phytochemistry* **68**: 1521–1529.
- Shailasree S, Kini KR, Deepak S, Kumudini BS, Shetty HS. 2004.** Accumulation of hydroxyproline-rich glycoproteins in pearl millet seedlings in response to *Sclerospora graminicola* infection. *Plant Science* **167**: 1227–1234.
- Sheng J, D'Ividio R, Mehdy MC. 1991.** Negative and positive regulation of a novel proline-rich protein mRNA by fungal elicitor and wounding. *The Plant Journal* **1**: 345–354.
- Sherrier DJ, Vandenbosch KA. 1994.** Localization of repetitive proline-rich proteins in the extracellular matrix of pea root nodules. *Protoplasma* **183**: 148–161.
- Shimwell DW. 1971.** *Festuco-Brometea* Br.-Bl. & R. Tx. 1943 in the British Isles: The phytogeography and phytosociology of limestone grasslands. *Vegetatio* **23**: 29–60.
- Shinohara N, Demura T, Fukuda H. 2000.** Isolation of a vascular cell wall-specific monoclonal antibody recognizing a cell polarity by using a phage display subtraction method. *Proceedings of the National Academy of Sciences of the United States of America* **97**: 2585–2590.
- Shomer-Ilan A. 1994.** Enzymes that degrade cell wall components are excreted by the haustorium of *Orobancha aegyptiaca* Pers. Proceedings of the Third International Workshop on Orobancha and Related Striga Research, Amsterdam. 255–260.
- Showalter a M. 1993.** Structure and function of plant cell wall proteins. *The Plant Cell* **5**: 9–23.
- Showalter AM. 2001.** Arabinogalactan-proteins: structure, expression and function. *Cellular and Molecular Life Sciences* **58**: 1399–1417.
- Showalter AM, Keppler B, Lichtenberg J, Gu D, Welch LR. 2010.** A bioinformatics approach to the identification, classification, and analysis of hydroxyproline-rich glycoproteins. *Plant Physiology* **153**: 485–513.
- Shpak E, Barbar E, Leykam JF, Kieliszewski MJ. 2001.** Contiguous hydroxyproline residues direct hydroxyproline arabinosylation in *Nicotiana tabacum*. *The Journal of Biological Chemistry* **276**: 11272–11278.
- Silanikove N, Nitsan Z, Perevolotsky A. 1994.** Effect of a daily supplementation of polyethylene glycol on intake and digestion of tannin-containing leaves (*Ceratonia siliqua*) by sheep. *Journal of Agricultural and Food Chemistry* **42**: 2844–2847.
- Silva NF, Goring DR. 2002.** The proline-rich, extensin-like receptor kinase-1 (PERK1) gene is rapidly induced by wounding. *Plant Molecular Biology* **50**: 667–685.
- Singh A, Singh M. 1997.** Incompatibility of *Cuscuta* haustoria with the resistant hosts — *Ipomoea batatas* L. and *Lycopersicon esculentum* Mill. *Journal of Plant Physiology* **150**: 592–596.

- Skamnioti P, Henderson C, Zhang Z, Robinson Z, Gurr SJ. 2007.** A novel role for catalase B in the maintenance of fungal cell-wall integrity during host invasion in the rice blast fungus *Magnaporthe grisea*. *Molecular Plant-Microbe Interactions* **20**: 568–580.
- Smallwood M, Beven A, Donovan N, Neill SJ, Peart J, Roberts K, Knox JP. 1994.** Localization of cell wall proteins in relation to the developmental anatomy of the carrot root apex. *The Plant Journal* **5**: 237–246.
- Smallwood M, Martin H, Knox JP. 1995.** An epitope of rice threonine- and hydroxyproline-rich glycoprotein is common to cell wall and hydrophobic plasma-membrane glycoproteins. *Planta* **196**: 510–522.
- Smallwood M, Yates EA, Willats WGT, Martin H, Knox JP. 1996.** Immunochemical comparison of membrane-associated and secreted arabinogalactan-proteins in rice and carrot. *Planta* **198**: 452–459.
- Smart MG, Aist JR, Israel HW. 1986.** Structure and function of wall appositions. 2. Callose and the resistance of oversize papillae to penetration by *Erysiphe graminis* f. sp. hordei. *Canadian Journal of Botany* **64**: 802–804.
- Smith JL, De Moraes CM, Mescher MC. 2009.** Jasmonate- and salicylate-mediated plant defense responses to insect herbivores, pathogens and parasitic plants. *Pest Management Science* **65**: 497–503.
- Smith PL, Stewart GR. 1987.** *Striga gesneroides* (Willd.) Vatke (*S. orobanchoides* Benth.) (Scrophulariaceae). Haustorial ontogeny and a role for ergastic substances in the maintenance of physiological integrity. In: Weber HC, Forstreuter W, eds. Parasitic Flowering Plants. Proceedings of the 4th International Symposium on Parasitic Flowering Plants, Marburg 1987.763–774.
- Smith-Moritz AM, Chern M, Lao J, Sze-To W, Heazlewood JL, Ronald PC, Vega-Sánchez ME. 2011.** Combining multivariate analysis and monosaccharide composition modeling to identify plant cell wall variations by Fourier Transform Near Infrared spectroscopy. *Plant Methods* **7**: 26–29.
- Snogerup B. 1982.** Host influence on northwest European taxa of *Odontites* (Scrophulariaceae). *Annales Botanici Fennici* **19**: 17–30.
- Somerville C, Bauer S, Brininstool G, Facette M, Hamann T, Milne J, Osborne E, Paredez A, Persson S, Raab T, et al. 2004.** Toward a Systems Approach to Understanding Plant Cell Walls. *Science* **306**: 2206–2211.
- Sommer-Knudsen J, Bacic A, Clarke AE. 1998.** Hydroxyproline-rich plant glycoproteins. *Phytochemistry* **47**: 483–497.
- Sonneveld C, Voogt W. 2009.** *Plant nutrition of greenhouse crops*. Dordrecht: Springer Netherlands.
- Sørensen I, Domozych D, Willats WGT. 2010.** How have plant cell walls evolved? *Plant Physiology* **153**: 366–372.
- Sørensen I, Pettolino FA, Bacic A, Ralph J, Lu F, O'Neill MA, Fei Z, Rose JKC, Domozych DS, Willats WGT. 2011.** The charophycean green algae provide insights into the early origins of plant cell walls. *The Plant Journal* **68**: 201–211.
- Sørensen I, Pettolino FA, Wilson SM, Doblin MS, Johansen B, Bacic A, Willats WGT. 2008.** Mixed-linkage (1→3),(1→4)-beta-D-glucan is not unique to the Poales and is an abundant component of *Equisetum arvense* cell walls. *The Plant Journal* **54**: 510–521.
- Sørensen I, Willats WGT. 2011.** Screening and characterization of plant cell walls using carbohydrate microarrays. In: Popper ZA, ed. The Plant Cell Wall. Methods and Protocols. Humana Press, 115–121.
- Spencer PA, Towers GHN. 1989.** Virulence-inducing phenolic compounds detected by *Agrobacterium tumefaciens*. Plant cell wall polymers. American Chemical Society, 283–298.
- Spurr AR. 1969.** A low-viscosity epoxy resin embedding medium for electron microscopy. *Journal of Ultrastructure Research* **26**: 31–43.
- Stace CA. 2010.** *New Flora of the British Isles*. Cambridge University Press.

9. Literature cited

- Stacey NJ, Roberts K, Carpita NC, Wells B, McCann MC. 1995.** Dynamic changes in cell surface molecules are very early events in the differentiation of mesophyll cells from *Zinnia elegans* into tracheary elements. *The Plant Journal* **8**: 891–906.
- Stahelin LA, Chapman RL. 1987.** Secretion and membrane recycling in plant cells: novel intermediary structures, visualized in ultrarapidly frozen sycamore and carrot suspension-culture cells. *Planta* **171**: 43–57.
- Stark-Urnau M, Mendgen K. 1995.** Sequential deposition of plant glycoproteins and polysaccharides at the host-parasite interface of *Uromyces vignae* and *Vigna sinensis*. Evidence for endocytosis and secretion. *Protoplasma* **186**: 1–11.
- Štech M, Wesselingh RA. 2010.** The biology of non-weedy hemiparasitic Orobanchaceae: the second symposium. *Folia Geobotanica* **45**: 345–346.
- Stintzi A, Heitza T, Prasad V, Kauffmann S, Geoffroy P, Legrand M, Fritiga B. 1993.** Plant “pathogenesis-related” proteins and their role in defense against pathogens. *Biochimie* **75**: 687–706.
- Stranger A, Corbett JM, Dunn MJ, Totty NF, Sterling A, Bolwell GP. 1999.** Identification of developmentally-specific markers in germinating and haustorial stages of *Striga hermonthica* (Del.) Benth. seedlings. *Journal of Experimental Botany* **50**: 269–274.
- Suetsugu K, Kawakita A, Kato M. 2008.** Host range and selectivity of the hemiparasitic plant *Thesium chinense* (Santalaceae). *Annals of Botany* **102**: 49–55.
- Suetsugu K, Takeuchi Y, Futai K, Kato M. 2012.** Host selectivity, haustorial anatomy and impact of the invasive parasite *Parentucellia viscosa* on floodplain vegetative communities in Japan. *Botanical Journal of the Linnean Society* **170**: 69–78.
- Sullivan C a., Skeffington MS, Gormally MJ, Finn J. 2010.** The ecological status of grasslands on lowland farmlands in western Ireland and implications for grassland classification and nature value assessment. *Biological Conservation* **143**: 1529–1539.
- Sweeney J. 1997.** Ireland. In: Wheeler, D. & Mayes J, ed. *Regional Climates of the British Isles*. London: Routledge, 254–275.
- Szabo E, Thelen A, Petersen M. 1999.** Fungal elicitor preparations and methyl jasmonate enhance rosmarinic acid accumulation in suspension cultures of *Coleus blumei*. *Plant Cell Reports* **18**: 485–489.
- Takeda T, Fry SC. 2004.** Control of xyloglucan endotransglucosylase activity by salts and anionic polymers. *Planta* **219**: 722–732.
- Talbot MJ, Offler CE, McCurdy DW. 2002.** Transfer cell wall architecture: a contribution towards understanding localized wall deposition. *Protoplasma* **219**: 197–209.
- Tan L, Showalter AM, Egelund J, Hernandez-Sanchez A, Doblin MS, Bacic A. 2012.** Arabinogalactan-proteins and the research challenges for these enigmatic plant cell surface proteoglycans. *Frontiers in Plant Science* **3**: 1–10.
- Taylor LP, Hepler PK. 1997.** Pollen germination and tube growth. *Annual Review of Plant Physiology and Plant Molecular Biology* **48**: 461–491.
- Tennakoon KU, Cameron DD. 2006.** The anatomy of *Santalum album* (Sandalwood) haustoria. *Canadian Journal of Botany* **84**: 1608–1616.
- Tennakoon KU, Pate J, Arthur D. 1997.** Ecophysiological aspects of the woody root hemiparasite *Santalum acuminatum* (R. Br.) A. DC and its Common Hosts in South Western Australia. *Annals of Botany* **80**: 245–256.
- Terashima N, Yoshida M, Hafrén J, Fukushima K, Westermark U. 2012.** Proposed supramolecular structure of lignin in softwood tracheid compound middle lamella regions. *Holzforschung* **66**: 907–915.
- Těšitel J, Plavcová L, Cameron DD. 2010.** Heterotrophic carbon gain by the root hemiparasites, *Rhinanthus minor* and *Euphrasia rostkoviana* (Orobanchaceae). *Planta* **231**: 1137–1144.
- Thomas R, Fang X, Ranathunge K, Anderson TR, Peterson C a, Bernardis M a. 2007.** Soybean root suberin: anatomical distribution, chemical composition, and relationship to partial resistance to *Phytophthora sojae*. *Plant Physiology* **144**: 299–311.

- Thordal-Christensen H. 2003.** Fresh insights into processes of nonhost resistance. *Current Opinion in Plant Biology* **6**: 351–357.
- Thorogood CJ, Rumsey FJ, Hiscock SJ. 2009.** Host-specific races in the holoparasitic angiosperm *Orobanche minor*: implications for speciation in parasitic plants. *Annals of Botany* **103**: 1005–1014.
- Timko MP, Huang K, Lis KE. 2012.** Host resistance and parasite virulence in *Striga*–host plant interactions: a shifting balance of power. *Weed Science* **60**: 307–315.
- Toft C, Aeschlimann A. 1991.** *Parasite-host associations. Coexistence or conflict?* Oxford University Press.
- Tomilov AA, Tomilova NB, Abdallah I, Yoder JI. 2005.** Localized hormone fluxes and early haustorium development in the hemiparasitic plant *Triphysaria versicolor*. *Plant Physiology* **138**: 1469–1480.
- Tomilov A, Tomilova N, Yoder JI. 2004.** *In vitro* haustorium development in roots and root cultures of the hemiparasitic plant *Triphysaria versicolor*. *Plant Cell, Tissue and Organ Culture* **77**: 257–265.
- Tubridy M. 2006.** *Laois Esker survey 2005*. Unpublished Report for Laois County Council.
- Tubridy M, Meehan R. 2006a.** *County Offaly Esker Survey 2006*. Unpublished Report for Offaly County Council.
- Tubridy M, Meehan R. 2006b.** Study to establish the extent, location of eskers and associated habitats in Co. Westmeath: Phase 2. An Action of the Westmeath Heritage Plan. Unpublished report produced for Westmeath Heritage Forum and Westmeath County Council.
- Udayakumar M, Sciences A, Krishi G, Kendra V, State K, Struik PC, Timmermans PCJM, Agricultural W. 1996.** Management of broomrape (*Orobanche* spp.) — A review. *Journal of Agronomy and Crop Science* **175**: 335–359.
- Uehlein N, Fileschi K, Eckert M, Patrick G, Bertl A, Kaldenhoff R. 2007.** Arbuscular mycorrhizal symbiosis and plant aquaporin expression. *Phytochemistry* **68**: 122–129.
- Usacheva MN, Teichert MC, Usachev YM, Sievert CE, Biel MA. 2008.** Interaction of the photobactericides methylene blue and toluidine blue with a fluorophore in *Pseudomonas aeruginosa* cells. *Lasers in Surgery and Medicine* **40**: 55–61.
- USDA. 2013.** Plants Profile: *Odontites vernus* (Bellardi) Dumort, red bartsia. Available at <http://plants.usda.gov/java/profile?symbol=ODVE>. [accessed 08.03.13]
- Valette C, Andary C, Geiger JP, Sarah JL, Nicole M. 1998.** Histochemical and cytochemical investigations of phenols in roots of banana infected by the burrowing nematode *Radopholus similis*. *Phytopathology* **88**: 1141–1418.
- Van Buuren ML, Maldonado-Mendoza IE, Trieu AT, Blaylock LA, Harrison MJ. 1999.** Novel genes induced during an arbuscular mycorrhizal (AM) symbiosis formed between *Medicago truncatula* and *Glomus versiforme*. *Molecular Plant-Microbe Interactions* **12**: 171–181.
- Vance C, Kirk T, Sherwood R. 1980.** Lignification as a mechanism of disease resistance. *Annual Review of Phytopathology* **180**: 259–288.
- Vandenbosch KA, Bradley DJ, Knox JP, Perotto S, Butcher GW, Brewin NJ. 1989.** Common components of the infection thread matrix and the intercellular space identified by immunocytochemical analysis of pea nodules and uninfected roots. *The European Molecular Biology Organization Journal* **8**: 335–341.
- Vanholme R, Demedts B, Morreel K, Ralph J, Boerjan W. 2010.** Lignin biosynthesis and structure. *Plant Physiology* **153**: 895–905.
- Vasey RA, Scholes JD, Press MC. 2005.** Wheat (*Triticum aestivum*) is susceptible to the parasitic angiosperm *Striga hermonthica*, a major cereal pathogen in Africa. *Phytopathology* **95**: 1294–1300.
- Vaughn KC. 1987.** *CRC handbook of plant cytochemistry. Volume II: Other cytochemical staining procedures*. Boca Raton: CRC Press.
- Vaughn KC. 2002.** Attachment of the parasitic weed dodder to the host. *Protoplasma* **219**: 227–237.

9. Literature cited

- Vaughn KC. 2003.** Dodder hyphae invade the host: a structural and immunocytochemical characterization. *Protoplasma* **220**: 189–200.
- Vaughn KC. 2006.** Conversion of the searching hyphae of dodder into xylem and phloem hyphae: A cytochemical and immunocytochemical investigation. *International Journal of Plant Sciences* **167**: 1099–1114.
- Vaughn KC, Talbot MJ, Offler CE, McCurdy DW. 2007.** Wall ingrowths in epidermal transfer cells of *Vicia faba* cotyledons are modified primary walls marked by localized accumulations of arabinogalactan proteins. *Plant & Cell Physiology* **48**: 159–168.
- Verhertbruggen Y, Marcus SE, Haeger A, Ordaz-Ortiz JJ, Knox JP. 2009.** An extended set of monoclonal antibodies to pectic homogalacturonan. *Carbohydrate Research* **344**: 1858–1862.
- Veronesi C, Bonnin EF, Benharrat H, Fer A, Thalouarn P. 2005.** Are pectinolytic activities of *Orobancha cumana* seedlings related to virulence towards sunflower? *Israel Journal of Plant Sciences* **53**: 19–27.
- Vicré M, Santaella C, Blanchet S, Gateau A, Driouich A. 2005.** Root border-like cells of *Arabidopsis*. Microscopical characterization and role in the interaction. *Plant Physiology* **138**: 998–1008.
- Vieira Dos Santos C, Delavault P, Letousey P, Thalouarn P. 2003a.** Identification by suppression subtractive hybridization and expression analysis of *Arabidopsis thaliana* putative defence genes during *Orobancha ramosa* infection. *Physiological and Molecular Plant Pathology* **62**: 297–303.
- Vieira Dos Santos C, Letousey P, Delavault P, Thalouarn P. 2003b.** Defense gene expression analysis of *Arabidopsis thaliana* parasitized by *Orobancha ramosa*. *Genetics and Resistance* **93**: 451–457.
- Vignols F, José-Estanyol M, Caparrós-Ruiz D, Rigau J, Puigdomènech P. 1999.** Involvement of a maize proline-rich protein in secondary cell wall formation as deduced from its specific mRNA localization. *Plant Molecular Biology* **39**: 945–952.
- Visser JH, Dörr I, Kollmann R. 1984.** The “hyaline body” of the root parasite *Alectra orobanchoides* Benth. (Scrophulariaceae)—Its anatomy, ultrastructure and histochemistry. *Protoplasma* **121**: 146–156.
- Visser JH, Dörr I, Kollmann R. 1990.** Compatibility of *Alectra vogelii* with different leguminous host species. *Journal of Plant Physiology* **135**: 737–745.
- Vleeshouwers VG, Van Dooijeweert W, Govers F, Kamoun S, Colon LT. 2000.** The hypersensitive response is associated with host and nonhost resistance to *Phytophthora infestans*. *Planta* **210**: 853–864.
- Vogel J. 2008.** Unique aspects of the grass cell wall. *Current Opinion in Plant Biology* **11**: 301–307.
- Vorwerk S, Somerville S, Somerville C. 2004.** The role of plant cell wall polysaccharide composition in disease resistance. *Trends in Plant Science* **9**: 203–209.
- Wagner TA, Kohorn BD. 2001.** Wall-associated kinases are expressed throughout plant development and are required for cell expansion. *The Plant Cell* **13**: 303–318.
- Walsh S. 2012.** *Climatological note no. 14. A summary of climate averages for Ireland 1981–2010.* Available at <http://www.met.ie/climate-ireland/SummaryClimAvg.pdf>. [accessed 21.03.13]
- Wang SY, Wu JH, Ng TB, Ye XY, Rao PF. 2004.** A non-specific lipid transfer protein with antifungal and antibacterial activities from the mung bean. *Peptides* **25**: 1235–1242.
- Watkinson A, Davy A. 1985.** Population biology of salt marsh and sand dune annuals. *Vegetatio* **62**: 487–497.
- Watson DM. 2009.** Parasitic plants as facilitators: more Dryad than Dracula? *Journal of Ecology* **97**: 1151–1159.
- Webb DA, Scannell MJP. 1983.** *Flora of Connemara and the Burren.* Dublin and Cambridge: Royal Dublin Society and Cambridge University Press.
- Weber HC. 1976.** Studies on new types of haustoria in some Central European Rhinanthoideae (Scrophulariaceae). *Plant Systematics and Evolution* **125**: 223–232.
- Weber HC. 1987.** Evolution of the secondary haustoria to a primary haustorium in the parasitic Scrophulariaceae/Orobanchaceae. *Plant Systematics and Evolution* **156**: 127–131.

- Wei G, Shirsat AH. 2006.** Extensin over-expression in *Arabidopsis* limits pathogen invasiveness. *Molecular Plant Pathology* **7**: 579–592.
- Werner M, Uehlein N, Proksch P, Kaldenhoff R. 2001.** Characterization of two tomato aquaporins and expression during the incompatible interaction of tomato with the plant parasite *Cuscuta reflexa*. *Planta* **213**: 550–555.
- Werth CR, Riopel JL. 1979.** A Study of the host range of *Aureolaria pedicularia* (L.) Raf. (Scrophulariaceae). *American Midland Naturalist* **102**: 300–306.
- Westbury DB. 2004.** *Rhinanthus minor* L. *Journal of Ecology* **92**: 906–927.
- Westbury DB, Davies A, Woodcock BA, Dunnett NP. 2006.** Seeds of change: The value of using *Rhinanthus minor* in grassland restoration. *Journal of Vegetation Science* **17**: 435–446.
- Westbury DB, Dunnett NP. 2007.** The impact of *Rhinanthus minor* in newly established meadows on a productive site. *Applied Vegetation Science* **10**: 121–129.
- Westwood JH, DePamphilis CW, Das M, Fernández-Aparicio M, Honaas L a., Timko MP, Wafula EK, Wickett NJ, Yoder JI. 2012.** The Parasitic Plant Genome Project: new tools for understanding the biology of *Orobanche* and *Striga*. *Weed Science* **60**: 295–306.
- Westwood JH, Yoder JI, Timko MP, De Pamphilis CW. 2010.** The evolution of parasitism in plants. *Trends in Plant Science* **15**: 227–235.
- Whetten R, Sederoff R. 1995.** Lignin biosynthesis. *The Plant Cell* **7**: 1001–1013.
- Whittier DP, Peterson RL. 1995.** The cuticle on *Psilotum gametophytes*. *Canadian Journal of Botany* **73**: 1283–1288.
- Wieczorek K, Seifert GJ. 2012.** Plant cell wall signaling in the interaction with plant-parasitic nematodes. In: Witzany G, Baluška F, eds. *Biocommunication of Plants*. Berlin, Heidelberg: Springer Berlin Heidelberg, 139–155.
- Wilkins DA. 1963.** Plasticity and establishment in *Euphrasia*. *Annals of Botany* **27**: 533–552.
- Willats WGT, Knox JP. 1996.** A role for arabinogalactanproteins in plant cell expansion: evidence from studies on the interaction of b-glucosyl Yariv reagent with seedlings of *Arabidopsis thaliana*. *Plant J* **9**: 919–925.
- Willats W, Knox J, Mikkelsen J. 2006.** Pectin: new insights into an old polymer are starting to gel. *Trends in Food Science & Technology* **17**: 97–104.
- Willats WGT, Marcus SE, Knox JP. 1998.** Generation of a monoclonal antibody specific to (1-5)- α -L-arabinan. *Carbohydrate Research* **308**: 149–152.
- Willats WG, McCartney L, Mackie W, Knox JP. 2001a.** Pectin: cell biology and prospects for functional analysis. *Plant Molecular Biology* **47**: 9–27.
- Willats WGT, McCartney L, Steele-King CG, Marcus SE, Mort A, Huisman M, Van Alebeek G-J, Schols H a, Voragen AGJ, Le Goff A, Bonnin E, Thibault J-F, Knox JP. 2004.** A xylogalacturonan epitope is specifically associated with plant cell detachment. *Planta* **218**: 673–681.
- Willats WG, Orfila C, Limberg G, Buchholt HC, Van Alebeek GJ, Voragen a G, Marcus SE, Christensen TM, Mikkelsen JD, Murray BS, Knox JP. 2001b.** Modulation of the degree and pattern of methyl-esterification of pectic homogalacturonan in plant cell walls. Implications for pectin methyl esterase action, matrix properties, and cell adhesion. *The Journal of Biological Chemistry* **276**: 19404–19413.
- Winship LJ, Obermeyer G, Geitmann A, Hepler PK. 2011.** Pollen tubes and the physical world. *Trends in Plant Science* **16**: 353–355.
- Wolf S, Mouille G, Pelloux J. 2009.** Homogalacturonan methyl-esterification and plant development. *Molecular Plant* **2**: 851–860.

9. Literature cited

- Wood TM, McCrae SI. 1996.** Arabinoxylan-degrading enzyme system of the fungus *Aspergillus awamori*: purification and properties of an alpha-L-arabinofuranosidase. *Applied Microbiology and Biotechnology* **45**: 538–545.
- Woodward JR, Fincher GB, Stone BA. 1983.** Water-soluble (1→3), (1→4)-β-D-Glucans from barley (*Hordeum vulgare*) endosperm. II. Fine structure. *Carbohydrate Polymers* **3**: 207–225.
- Wyatt RE, Nagao RT, Key JL. 1992.** Patterns of soybean proline-rich protein gene expression. *The Plant Cell* **4**: 99–110.
- Wydra K, Beri H. 2007.** Immunohistochemical changes in methyl-ester distribution of homogalacturonan and side chain composition of rhamnogalacturonan I as possible components of basal resistance in tomato inoculated with *Ralstonia solanacearum*. *Physiological and Molecular Plant Pathology* **70**: 13–24.
- Xie D, Ma L, Samaj J, Xu C. 2011.** Immunohistochemical analysis of cell wall hydroxyproline-rich glycoproteins in the roots of resistant and susceptible wax gourd cultivars in response to *Fusarium oxysporum* f. sp. *Benincasae* infection and fusaric acid treatment. *Plant Cell Reports* **30**: 1555–1569.
- Yan Z. 1993.** Resistance to haustorial development of two mistletoes, *Amyema preissii* (Miq.) Tieghem and *Lysiana exocarpi* (Behr.) Tieghem ssp. *Exocarpi* (Loranthaceae), on host and nonhost species. *International Journal of Plant Sciences* **154**: 386–394.
- Yan Q, Shi M, Ng J, Wu JY. 2006.** Elicitor-induced rosmarinic acid accumulation and secondary metabolism enzyme activities in *Salvia miltiorrhiza* hairy roots. *Plant Science* **170**: 853–858.
- Yang S, Pfister DH. 2006.** *Monotropa uniflora* plants of eastern Massachusetts form mycorrhizae with a diversity of russulacean fungi. *Mycologia* **98**: 535–540.
- Yariv J, Rapport MM, Graf L. 1962.** The interaction of glycosides and saccharides with antibody to the corresponding phenylazo glycosides. *The Biochemical Journal* **85**: 383–388.
- Yates EA, Valdor JF, Haslam SM, Morris HR, Dell A, Mackie W, Knox JP. 1996.** Characterization of carbohydrate structural features recognized by anti-arabinogalactan-protein monoclonal antibodies. *Glycobiology* **6**: 131–139.
- Ye Z-H, Song Y-R, Marcus A, Varner JE. 1991.** Comparative localization of three classes of cell wall proteins. *The Plant Journal* **1**: 175–183.
- Yin C, Hulbert S. 2011.** Prospects for functional analysis of effectors from cereal rust fungi. *Euphytica* **179**: 57–67.
- Yoder JI. 1997.** A species-specific recognition system directs haustorium development in the parasitic plant *Triphysaria* (Scrophulariaceae). *Planta* **202**: 407–413.
- Yoder JI. 2001.** Host-plant recognition by parasitic Scrophulariaceae. *Current Opinion in Plant Biology* **4**: 359–65.
- Yoder J, Gunathilake P, Jamison-McClung D. 2009.** Hemiparasitic plants: exploiting their host's inherent nature to talk. In: Baluska F, Vivanco J, eds. *Plant-Environment Interactions*. Berlin, Heidelberg: Springer Berlin Heidelberg, 85–100.
- Yoneyama K, Xie X, Sekimoto H, Takeuchi Y, Ogasawara S, Akiyama K, Hayashi H, Yoneyama K. 2008.** Strigolactones, host recognition signals for root parasitic plants and arbuscular mycorrhizal fungi, from Fabaceae plants. *New Phytologist* **179**: 484–494.
- Yoshida S, Shirasu K. 2009.** Multiple layers of incompatibility to the parasitic witchweed, *Striga hermonthica*. *New Phytologist* **183**: 180–189.
- Yoshida S, Shirasu K. 2012.** Plants that attack plants: molecular elucidation of plant parasitism. *Current Opinion in Plant Biology*: 1–6.
- Yu H, Liu R, Shen D, Jiang Y, Huang Y. 2005.** Study on morphology and orientation of cellulose in the vascular bundle of wheat straw. *Polymer* **46**: 5689–5694.
- Yun HS, Kwon C. 2012.** Trafficking at the host cell surface during plant immune responses. *Journal of Plant Biology* **55**: 185–190.

- Zandleven J, Sørensen SO, Harholt J, Beldman G, Schols H a, Scheller H V, Voragen AJ. 2007.** Xylogalacturonan exists in cell walls from various tissues of *Arabidopsis thaliana*. *Phytochemistry* **68**: 1219–1226.
- Zehhar N, Labrousse P, Arnaud M. 2003.** Study of resistance to *Orobancha ramosa* in host (oilseed rape and carrot) and non-host (maize) plants. *European Journal of Plant Pathology* **109**: 75–82.
- Zeier J, Ruel K, Ryser U, Schreiber L. 1999.** Chemical analysis and immunolocalisation of lignin and suberin in endodermal and hypodermal/rhizodermal cell walls of developing maize (*Zea mays* L.) primary roots. *Planta* **209**: 1–12.
- De Zélicourt A, Letousey P, Thoiron S, Campion C, Simoneau P, Elmorjani K, Marion D, Simier P, Delavault P. 2007.** Ha-DEF1, a sunflower defensin, induces cell death in *Orobancha* parasitic plants. *Planta* **226**: 591–600.
- Zelmer DA. 1998.** An evolutionary definition of parasitism. *International Journal for Parasitology* **28**: 531–533.
- Zhang Y, Brown G, Whetten R, Loopstra CA, Neale D, Kieliszewski MJ, Sederoff RR. 2003.** An arabinogalactan protein associated with secondary cell wall formation in differentiating xylem of loblolly pine. *Plant Molecular Biology* **52**: 91–102.
- Zhang X, Teixeira da Silva J a, Duan J, Deng R, Xu X, Ma G. 2012.** Endogenous hormone levels and anatomical characters of haustoria in *Santalum album* L. seedlings before and after attachment to the host. *Journal of Plant Physiology* **169**: 859–866.
- Zhong R, Ye Z-H. 2009.** Secondary Cell Walls. *Encyclopedia of Life Sciences*. Chichester: John Wiley & Sons, 1–9.
- Zhou XL, Stumpf M a, Hoch HC, Kung C. 1991.** A mechanosensitive channel in whole cells and in membrane patches of the fungus *Uromyces*. *Science* **253**: 1415–1417.
- Zuber D, Widmer A. 2000.** Genetic evidence for host specificity in the hemi-parasitic *Viscum album* L. (Viscaceae). *Molecular Ecology* **9**: 1069–1073.
- Zwanenburg B, Mwakaboko AS, Reizelman A, Anilkumar G, Sethumadhavan D. 2009.** Structure and function of natural and synthetic signalling molecules in parasitic weed germination. *Pest Management Science* **65**: 478–491.

9. Literature cited

Appendix 1: Results of the first count of *Rhinanthus minor* seed germination

SEED STRATIFICATION START: 16.12.2009																	
dish no	germinated	root length of germinated seeds [mm]											St. Dev. within p. dish	St. Dev. for the lot	Average	Av. for the lot	
0/4 °C - recorded 25/02/10																	
1	11	20	6	8	6	2	8	4	5	3.5	7.5	3		4.88		6.64	
2	10	10	13	13	14	7	9	10	2	3	1.5			4.70		8.25	
3	8	17	7	15	1	6	4.5	8	14					5.59		9.00	
4	10	5.5	13	5	9	10	10	2.5	10	1.5	6			3.71		7.25	
5	6	11	6	6	18	6	13							4.92		9.92	
6	8	20	2.5	11	4	4	7	12	17					6.44		9.69	
7	10	4	12	8	10	7	2	15	17	4	14			5.03		9.20	
8	12	1	29	13	8	10	11	2.5	7.5	14	14	15	14	7.12		11.50	
9	9	3.5	20	10	14	2.5	7.5	11	2	13				6.02		9.28	
10	13	14	13	4	16	22	6.5	14	3	3	13	4	9	5.87		10.27	
11	11	6	7.5	5	23	3	2	9	11	14	11	12		5.83		9.27	
12	11	18	4	12	11	1.5	15	1	13	5.5	3.5	7		5.65		8.23	
13	7	10	3	2.5	3	4.5	13	7						3.91		6.07	
14	8	1	7	6	4	3	7	12	11					3.78		6.38	
15	8	15	20	8	7.5	5	7	8.5	10					4.95		10.13	
16	13	0.5	8	10	13	5	19	9.5	13	16	12	11	6	4.87	4.85	10.08	8.59
17	10	1	7.5	10	3	12	5	7.5	11	13	8.5			3.91		7.85	
18	12	4	6	8	11	3.5	10	6.5	13	15	8.5	8.5	14	3.65		8.92	
19	10	14	3.5	10	7	5	13	5	3	14	5			4.40		7.95	
20	6	9.5	2	10	15	2	2							5.55		6.75	
21	8	17	12	12	7	3	14	4	3					5.39		8.94	
22	10	4	12	10	6.5	8	9	6	12	6	8			2.65		8.15	
23	9	2	2	3	11	10	8	12	10	7				3.96		7.22	
24	10	7	4	1.5	12	13	15	19	12	3	11			5.60		9.65	
25	13	3	5	10	11	7	18	2	6	5	11	15	6	4.86		7.85	
26	13	2	5	5	7	9	3	8	8.5	12	3.5	13	16	4.04		7.58	
27	12	8	7	5.5	5.5	5	7	8	11	4	14	15	3	3.71		7.71	
28	7	20	10	2	9	17	8	12						5.96		11.14	
29	13	1.5	3.5	4	15	4	11	8	9	6	3	10	10	3.79		7.04	
30	8	11	10	7	3	14	9	15	12					3.78		10.06	
4 °C - recorded 26/02/10																	
31	0																
32	0																
33	5	7	5	7	6.5	5								1.02		6.10	
34	10	6	4.5	7	4.5	6.5	6.5	5	3.5	2.5	6			1.46		5.20	
35	6	2	4.5	5	6	5	3							1.47		4.25	
36	8	5	10	13	8	4.5	9	10	12					3.03		8.94	
37	0																
38	0																
39	1	3.5															
40	8	1.5	5	4	1.5	3	4	3	4					1.25		3.25	
41	5	4	3	2	6.5	4								1.67		3.90	
42	1	4														4.00	
43	5	8	6	4.5	3	5	5							1.67		5.25	
44	0																
45	3	2.5	1	5										2.02		2.83	
46	1	2.5															
47	2	4.5	9											3.18		6.75	
48	1	5.5															
49	3	8	4.5	2										3.01		4.83	
50	0																
51	0																
52	2	4	6											1.41		5.00	
53	1	5.5															
54	2	4	5											0.71		4.50	
55	0																
56	8	7	4.5	5	7.5	9	9	5	1.5					2.56		6.06	
57	0																
58	2	7	5											1.41		6.00	
59	2	5.5	5											0.35		5.25	
60	0																

